ELECTRONIC TRANSPORT PROCESSES IN SOME HIGHLY INSULATING AND SEMI-CONDUCTING POLYMERS

By

NABIL AMIN-PETER HILAL

Bachelor Of Science
American University Of Beirut
Beirut, Lebanon
1970

Master Of Science
American University Of Beirut
Beirut, Lebanon
1973

Submitted to the Faculty of the
Graduate College of the
Oklahoma State University
in partial fulfillment of
the requirements for
the Degree of
DOCTOR OF PHILOSOPHY
May, 1988

ELECTRONIC TRANSPORT PROCESSES IN SOME

HIGHLY INSULATING AND SEMI-

CONDUCTING POLYMERS

Thesis Approved:

James P. Wicksted

Thesis Advisor

[illegible]

J Paul Devlin

Warren T Ford

Norman N. Durham

Dean of the Graduate College

DEDICATION

To my mother Nuha, and my sister Nabila

ACKNOWLEDGMENTS

The author is indebted to many individuals and friends without whose support and encouragement this project would have never materialized. As such, the order of crediting the various persons and groups of people who contributed to this work bears no relevance on the highest esteem in which they are held.

The author wishes to express his endless and sincere thanks to thesis advisor Dr. James Wicksted who took on the challenging task of directing this research, and contributed to the financing of the printing costs from his own grants, after Dr. Herb Pohl, who initiated this project in august of 1982, and presided over it till march 1986, had to leave for M.I.T in pursuit of a new position at the National Magnet Labs; and his subsequent and untimely death on june 22, 1986.

Special thanks go to: Dr. Paul Westhause who coordinated the transition procedures between Dr. Pohl and Dr. Wicksted, and to Dr. Larry Scott who assumed the chairmanship responsibilities of the advisory committee as of july 1986.

Many thanks are extended to Dr. Bill Hughes head of the Engineering Energy Lab. for providing financial support for this research during the academic year 1982-83, and to the U.S. Army Special Grants Fund for providing research money during the summers of 1984 and 1985.

Numerous thanks are given to Dr. Warren Ford and Dr. Lee Dunn of the Chemistry Department, for their preparation and synthesis of the polymer samples, and to distinguished committee member Dr. Paul Devlin of the Chemistry Department for his accepting to replace former committee member Dr. Bruce Ackerson who had to go on sabbatical leave, (and to whom the warmest thanks are forwarded).

Deepest gratitude and appreciation go to two very dear friends of mine Mr. Gary Berman of Texas Instruments, and Mrs. Willis D. Gallup of Stillwater who provided much needed moral support and love, and financed this research during the periods from july 1986 to the present, and from october 1983 - october 1985 during which period, the then chairman of the physics department Jeffry Summers, "could not afford" to provide financial assistance for this work, despite the fact that graduate students from the engineering school were being hired at the time to fill in the vacancies for lab. instruction positions. I am so grateful to the Lord Jesus for bringing Gary and Mrs. Gallup into my life, for His miracles never cease.

Last but not least, very special thanks are given to machine shop personnel Mr. Mike Lucas and Mr. David Fisher for their professional dedication and excellent craftsmanship, and to machine shop director Mr. Heinz Hall for his helpful hints and innovation. Generous thanks are awarded to Mr. Doug West and Mr. Warren Grider of the electronics shop for their help and prompt servicing of the equipment.

Finally, I take pleasure in thanking my mother and my sister for patiently bearing with me this ten thousand-mile journey under the most severe hardships a human life can endure in the war-torn city of Beirut, Lebanon. And for sacrificing their life-savings so that I could stay financially sound and secure during the years 1983-85.

To all of you, I thank you wholeheartedly and extend my best wishes and gratitude for helping me make this dream a reality, and for helping me achieve a goal planned long time ago, despite the sweat, the pain, and the tears.

I thank you all because you've made me smile at last.

TABLE OF CONTENTS

LIST OF TABLES

LIST OF FIGURES

Figure Page

CHAPTER I

GENERAL REVIEW AND BASIC PRINCIPLES

Introduction

A) Historical Background

Long-chain organic materials, commonly referred to as polymers, comprise a wide variety of physical properties, especially the electrical and the electro-active (1) aspects. From the highly conductive polyacetylene and the superconducting polysulfur nitride (SN)x; to the highly polar semiconducting polyacene quinone radicals (7), exists a large group of synthesizable materials that might be tailored to the specific needs of electronics and space industries.

What common features abound in a given category and what distinguish them from the rest, has been a subject of great concern and research interest for the past twenty five years or so. Numerous multi-disciplinary fields of science and engineering have contributed to this very fascinating and important branch of chemical physics.

The interest in organic solids dates back as far as 1906 when Pocchetino (10) studied the photo-conducting properties of anthracene. In 1941 Szent-Gyorgi (11) claimed that biological processes could be understood by studying organic chem-

ical structures having semi-conducting characteristics.

Two years later, the collected works of R. Fuoss appeared in "The Chemistry Of Large Molecules" (12), a major treatise on polymers mainly devoted to the study of relaxation times distributions of polar polymers in dilute solution of non-polar solvents. The works of Kirkwood & Fuoss (13-17) provided most of the material subject of the book. The following year, "Tables Of Dielectric Materials" was published by M.I.T; a three-volume compendium considered the first of its kind on the subject, and characterizing such polymers as: poly(ethylene), poly(styrene), poly(vinyl chloride) etc..over a wide frequency range from 100 to 10^{10} Hz.(18).

In 1949 Fujishiro and Kotera (19) investigated the loss factor as a function of the (average) molecular weight of polymers and found that it decreased with increasing molecular weight. Now since the degree of polymerization (D.P) is defined as the ratio of the molecular weight of a polymer to the molecular weight of the basic monomer unit, it follows that D.P may be regarded as a measure of the average or effective molecular length of the polymer molecule. Thus the above study provided one of the first correlation effects between loss and molecular length. A related work by Wurstlin (20) was done with poly(vinyl acetate) and he found that increasing the molecular weight, raises the temperature at which maximum absorption (loss) occurs.

In the early fifties, Akamatsu and Inokuchi (21) studied the effect of pressure on the conductivity of iso-violanthr-

one and found that compression lowers the activation energy of the polymer. By the late fifties, serious and concentrated efforts were being made to study and characterize polymers.

Among the early pioneers, Many et al. (22) was the first to draw attention to the fact that in low molecular weight organic crystals, a quasi-linear relationship exists between the activation energy Ea and the logarithm of the pre-exponential factor appearing in the Arrhenius law governing the conductivity : $\sigma = \sigma_0 \exp(-Ea/kT)$. Four years later, Eley (23,24) discovered similar correlation patterns in certain groups of polymers. The patterns separated distinctly into two groups; Those corresponding to highly insulating polymers displayed very well-defined linearity and a correlation coefficient of about unity, while the semi-conducting species showed a rather erratic behaviour and very poor correlation.

In the early sixties, things took on a full swing: An extensive review of polar and non-polar polymers (both amorphous & crystalline) documented by A.J. Curtis of the National Bureau of Standards was published (25). It covered topics on the temperature dependence of relaxation and dispersion for such materials as poly-{ethylene, isobutylene, tetrafluoroethylene, vinyl acetate, vinyl ethers, vinyl chloride, esters, amides}, and rubber. The report centered around the works of Mikhailov & co-workers (26-30), Hoff, Robinson, and Willbourn (31), Nakajima, Saito, & Ishikawa (32,33), Gibbs & De Marzio (34), Reddish (35), and Kirkwood & Fuoss (13-17).

Pohl & co-workers at Princeton (36-48), and others (49 -

53), followed a systematic research program oriented towards the characterization and synthesis of some special class of materials, mainly those of the Poly(acene quinone) radical type (PAQR). Other chemical species considered were the poly (acetylenes), poly(benzimidazole), and pyropolymers. Conductivities ranging from 10^{-11} to 10 S/cm under various pressures were observed. Further studies of correlation effects followed in succession: Pohl & Chartoff (47), Pohl and Opp (43) investigated the dependence of the conductivity on the unpaired electron spins. Extensive study of the effects of pressure & temperature was done by Pohl, Rembaum & Henry (42).

Pohl & Rosen (1) investigated the unusually high dielectric constant of anthroquinone & pyromellitic dianhydride as well as the effects of D.C bias electric field on this parameter. They also studied the properties of metal-doped pyropolymers (44). Dielectric relaxation studies on (PAQR) polymers were done by Pohl & Hartman (2,54), and by Pohl & Wyhof (55), while the conductivity dependence on pressure, temperature & electric field were explored by Pohl & Englehardt (3) and by Pohl (56).

An empirical relationship between the dielectric constant and the D.C.electric field bias was determined and verified by Pohl & Wyhof (7). This and the previous advancements helped formulate a model theory for polymeric conduction and polarisation which became known as the Pohl-Pollak theory & model (1975-77), (8-9). Among the many predictions of the theory, was one that is unique to polymeric materials: the existence

of "cross-over" frequencies Wc for which the dielectric constant K increases with respect to the D.C. electric field bias (over a certain range of bias values) for frequencies above Wc, as contrasted to the normal decrease in K for frequencies below Wc. This prediction was observed by Pethig & Pohl (57) in '76 and by Vijayakumar and Pohl (58-59) in 1981-83.

The effect of radiation on polymers has also been of great interest due to its defense oriented nature, and has been under study since 1938. Notable works in this field include: Charlesby, Alexander, and Black (60-63); Bopp and Sisman (64); Fowler & Farmer (65-69); and Chapiro (70-72).

As one might expect, polymers can be extremely susceptible to radiation (be it rays or particles), the reason being that a slight alteration in the chemical structure of a side group or a terminal group of atoms in the polymer chain, can mean a completely different material having different physical, chemical, and electrical properties. Irradiated polymer materials have been found to undergo either one or both of two types of change: they may cross-link to form an insoluble gel-type material, or undergo molecular degradation through chain scission to form substances of lower molecular weight.

Finally, the possibility of super-conducting polymers having elevated transition temperatures has been an active research subject for many years. The first to propose such a possibility was W.A.Little in 1964 (73-75). Criteria for the existence of superconductivity in polymer systems have been sought by Cohen (76),who showed that a polymer must exhibit a

very large dielectric constant as one of four sufficient conditions, the other three being a high carrier concentration, a large effective mass of carriers (polaron type), and a multi-valley energy band structure in momentum space.

B) Present-Day Status of Dielectric Theory

In recent years attention has been focused on the attempts towards a "grand unification" theory; the so-called "universality approach" for the treatment of dielectric phenomena is being promoted by Jonscher (77), Cole (78), and others (79-81) as the "better" alternative to the understanding of this subject .

Jonscher and his proponents argue that because the dielectric response in solids displays a universal character regardless of the detailed microscopic structure of the particular material, (namely the power law dependence of the de-polarization current[1]), then a higher-order theory must be sought that would fit the data of any type material under any frequency range without having to resort to the existing "patchwork" theories which, in most cases, are not based on true physical grounds. A classic example of this is the distribution function for the relaxation times of materials exhibiting deviation (and almost all do) from the single relaxation Debye model (applicable to non-interacting dipoles or, charge carriers only.)

---

1) $i(t) \propto t^{-s}$ where $0<s<1$ or $1<s<2$

Further, there are instances where many researchers have developed strong convictions about specific conduction mechnisms without sufficiently cut-proof evidence. For example, the power law relationship for the A.C. conductivity in amorphous semiconductors, glassy materials, and ionic solids, (which follows an w^s dependence where $s \sim 0.8$) has frequently been taken as proof for hopping electronic-only, conduction.

This kind of practice was widespread in the 1960's when studies on amorphous semiconductors were popular. What seems to have eluded many[1] is the fact that a hopping charge (be it electronic or ionic) can give rise to dielectric behaviour similar to what one might expect from permanent dipoles. In fact, a hopping charge confined to hop between two preferred positions is indistinguishable from a permanent dipole; while the situation would be completely different if the charge is allowed to hop over several molecular sites or even rove over finite distances, as in the case of certain polymers.

At present, the Dissado-Hill theory (79,80) has been successfully applied to polar materials employing an all-new universal approach based on a two-level double potential interaction describing the energy of many individual systems within the dielectric medium. However, it has not been tested on polymeric systems, and the future awaits such an advance-

---

1) A noteworthy exception to this are the works of Dr. Herb Pohl who carried out Hall effect measurements in order to determine the sign of the charge carriers (3,82).

ment and what it might reveal about the nature of co-operative phenomena in polymeric solids.

C) Statement of The Problem

The present work is primarily intended to explore whatever channels are available for the enhancement and improvement of dielectric quality, which will hopefully allow us to engineer polymers with specific electrical properties.

Whether it is possible at least in principle, to match the dielectrical qualities of $BaTiO_3$ remains an open question considering the host of theory that is needed from a multitude of scientific disciplines. However, as the present work shows there is ample evidence to make us believe that a polymeric equivalent to $BaTiO_3$ can be realized.

In order to achieve our goal, we shall carry dielectric and conductivity measurements on some 10 samples under a variety of macroscopic conditions: pressure, temperature, and electric field bias over a frequency range extending from D.C (100 Hz.for K) to 10^5 Hz. Information from the above data on other relevant quantities such as average molecular length, relaxation times, and activation energies will be obtained and correlated to σ', K, molecular sructure, and method of synthesis. Conclusions and recommendations will be made regarding the prospects of optimization of the polymer characteristics.

1.1) Rudiments of Dielectric Theory

A) Types of Polarisation and Dielectric Spectra

As is well known, matter is not uniform in its dipole moment constituency. There are many varieties arising from differences in the molecular structure of a given material. Thus an ionic solid is expected to have a large contribution in its dielectric response from permanent dipoles, while a simple atomic substance will display most of its response from the induced dipoles formed by the outermost shell (valence) electrons. Moreover since each particular type of polarisation has its own characteristic natural frequency of oscillation (or relaxation) then in a given frequency regime, only those "aggregates" whose natural frequencies match or are close to the excitation frequency will contribute.

Because of the relatively small masses of the charge carriers, inertial effects do not appear until short microwave frequencies (10^{12}) are attained. This is because the mass impedance term "iwm" is much smaller than the elastance term "H/iw" (where H is "Hooke's law" constant of elasticity) at low frequencies $<< \sqrt{H/m}$ ($\simeq 10^{12}$ for atomic nuclei bound in crystals or macromolecules, to 10^{16} for electrons bound in atoms).

Consequently at low frequencies, a dielectric is expected to portray a behaviour similar to a damped spring system or a capacitive-resistive combination. In this regime, the frequencies at which maximum absorption of energy occurs are

precisely the inverse of the decay constant time(s) characteristic of the system (also known as "relaxation" time(s)).

It is for this reason that these frequencies of maximum absorption are usually referred to as "relaxation" spectra.

Fig.1(a) shows the response of a typical dielectric material over the entire observable frequency range up to 10^{20} Hz. At the extreme left of the diagram is the contribution from space-charge polarisation which exists in materials containing carriers that do not recombine at the electrodes, thereby behaving like a macroscopic dipole which can only follow the field variation as long as the frequency is very low (few cycles per second). A similar response also occurs in heterogeneous systems such as a two-layer capacitor, this is known as Maxwell-Wagner interfacial polarisation.

Next comes the contribution of the so-called orientational polarisation arising from permanent dipoles that may exist in ionic crystals having lattice defects; or polar molecules in gaseous and liquid substances. Generally speaking this type of polarisation is characterized by inelastic restoring forces with properties akin to those of viscosity in fluids. Thus energy is continuously dissipated in the system as heat, due to irreversible thermodynamic processes. Due to its great variety in size and type of structure, orientational polarisation has the widest spectrum of all the other kinds reaching as much as nine decades.

At frequencies above 10^{11} Hz. resonances of atomic vibrations start appearing. These are followed by resonances of the

Fig.(1) - Spectral characteristics of the real and imaginary parts of the dielectric permittivity arbitrary scales), for: (a) Ordinary dielectric materials (including non-ekaconjugated polymer systems), and (b) Long-chain ekaconjugated polymers. The polaron resonance in (b) is only speculative at this stage.

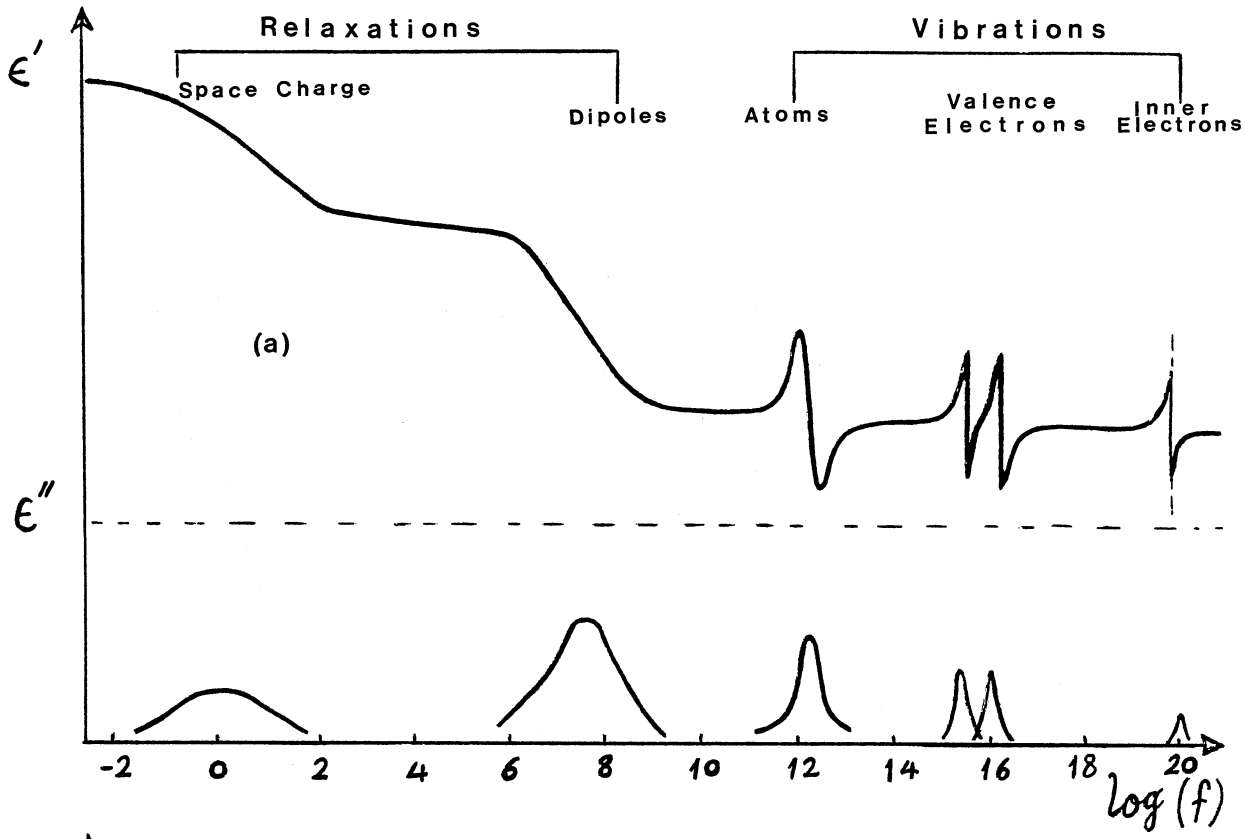
Relaxations
Vibrations
Space Charge
Dipoles
Atoms
Valence Electrons
Inner Electrons
ε'
ε''
(a)
-2
0
2
4
6
8
10
12
14
16
18
20
log (f)

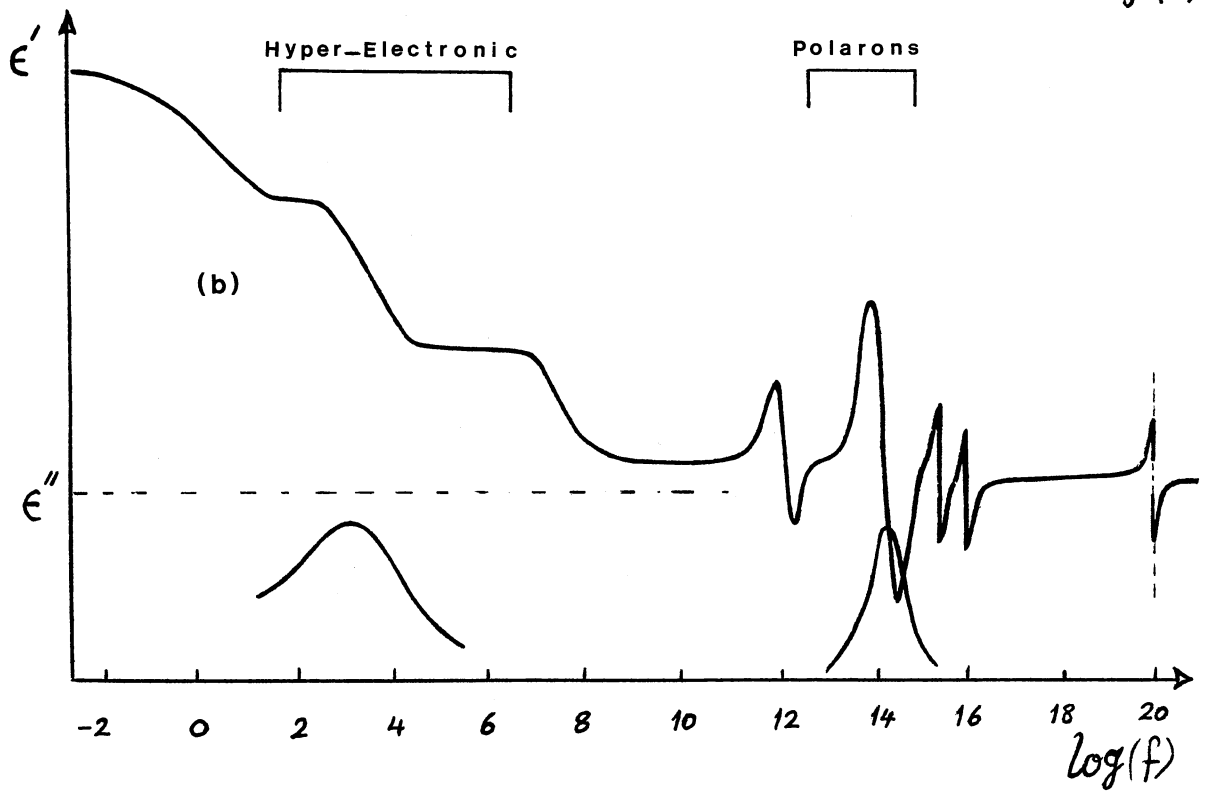
Hyper-Electronic
Polarons
ε'
ε''
(b)
-2
0
2
4
6
8
10
12
14
16
18
20
log(f)

Fig.(1)

valence electrons around 10^{15} Hz. and ultimately by the resonances of the "inner core" electrons at X-ray or γ- ray frequencies.

In contrast to the above, a typical polymer is expected to display a response similar to what is shown in Fig.1(b). Here, there exists a characteristic absorption at much lower frequencies than in ordinary-materials. Thus for example, a ralaxation absorption may occur around 10^{3} to 10^{4} Hz. as compared with 10^{6} to 10^{8} for conventional materials, while resonance absorption may occur around 10^{10} to 10^{13} Hz. for the so-called "eka-conjugated" type polymers exhibiting polaronic conduction.

For the time being let us dwell on some basic notions underlying the general principles of dielectric conduction and polarisation in matter.

B) Relaxation Response of Dielectrics

This type of response is best analyzed by considering first, the action of a D.C. electric field :

$$E(t) = EoU(t) \qquad 1.1.1$$

where U(t) is the unit step function : $= \begin{cases} 0 & \text{for } t < 0 \\ +1 & \text{for } t \geqslant 0 \end{cases}$

When the above D.C field is applied to a dielectric medium the polarisation P does not become established to its final steady value instantaneously. This delayed response is due to the "sluggish" nature of the restoring forces making up the dipoles or acting between them in such a manner as to always counteract their tendency to align with the direction of the field.

If D_∞ and D_s are the values of the electric displacement D at t = 0+, and t = ∞ respectively, then the value of D at any instant > 0 may be written as :

$$D(t) = D_\infty + (D_s - D_\infty).f(t) \qquad 1.1.2$$

where f(t) is a "growth" function characterizing the manner in which D(t) approaches its equilibrium value. For the time being, specific forms of f(t) are not relevant to our discussion, and so they will not be detailed. We do require however, that f(t) sati-

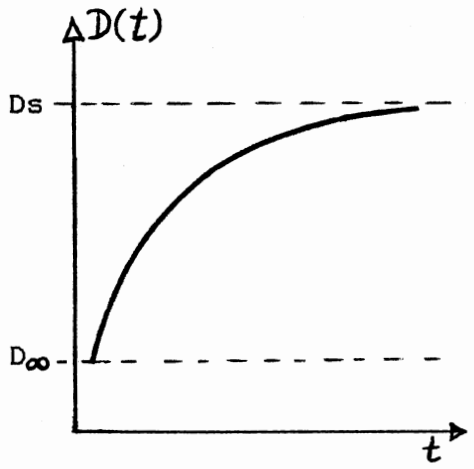

Fig.(2)

fies the boundary conditions:

$f(t) = 0$ for $t < 0$, and $f(t) = 1$ for $t \longrightarrow \infty$. Now D represents the "instantaneous" contribution to D(t) and can be physically traced to electronic effects; it usually gets established within 10^{-17} sec.

From the definitions of the dielectric permittivity, we may write :

$$D_\infty = \epsilon_\infty E(t) \quad \text{and} \quad D_s = \epsilon_s E(t) \qquad 1.1.3$$

Here, the permittivity ϵ_s represents the static value that is observed when one has waited a "long" time after the field has been switched on. We remark in this context that "long" time does not necessarily mean "infinite"; all that is implied is that t >> some characteristic time of the system.

For a linear medium the response to any general excitation may be obtained from the above by the superposition principle. Thus for example, the response to a D.C. pulse such as the one shown in Fig.(3) may be obtained by noting that E'(t) can be written as :

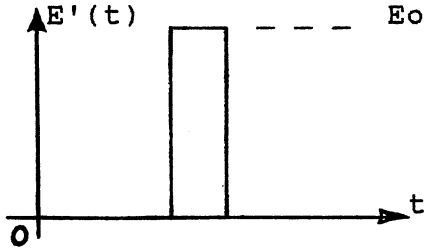

Fig.(3)

$$E'(t) = EoU(t-\theta) - EoU(t-\theta-d\theta)$$
$$= E_1(t) + E_2(t)$$

Hence we may write : $D'(t) = D_1(t) + D_2(t)$

or $D'(t) = \epsilon_\infty E'(t) + (\epsilon_s - \epsilon_\infty) E_1(t-\theta) f(t-\theta) - (\epsilon_s - \epsilon_\infty) . E_2(t-\theta-d\theta) f(t-\theta-d\theta)$.

Rearranging gives:

$$D(t) = \epsilon_\infty E(t) + (\epsilon_s - \epsilon_\infty) Eo \phi(t-\theta)d\theta \qquad 1.1.4$$

where $\phi(t)$ is the derivative of $U(t)f(t)$ for $t > 0$, and is necessarily a monotone decreasing function approaching zero as $t \longrightarrow \infty$.

It should be noted that although $\phi(t)$ is ∞ at $t = 0$, we shall implicitly assume that the product $\phi(t-\theta)d\theta$ remains finite as $d\theta \longrightarrow 0$, ($t$ approaching θ that is.)

Following the same lines of thought, it is now an easy matter to generalize to the case of a train of pulses each having a duration $d\theta$ but "fired" at times θ_K , $k = 1,2,3...$ and with amplitudes Eo_K etc.. For such an excitation, D may be written as:

$$D(t) = \epsilon_\infty E(t) + (\epsilon_s - \epsilon_\infty) \sum_{K:\theta_K \leqslant t} Eo \phi(t-\theta_K)d\theta_K \qquad 1.1.5$$

$$\text{Where } E(t) = \sum_K E_K(t) \qquad 1.1.6$$

Finally since any continuous excitation may be broken up into an infinite sum of discrete pulses whose widths are $\longrightarrow$ arbitrarily small numbers, then by the Fundamental Theorem of integral calculus we have :

$$D(t) = \epsilon_\infty E(t) + (\epsilon_s - \epsilon_\infty) \int_{-\infty}^{t} E(\theta) \phi(t-\theta)d\theta$$

which can be rearranged through a change of variable into:

$$D(t) = \epsilon_\infty E(t) + (\epsilon_s - \epsilon_\infty) \int_{0}^{+\infty} E(t-\xi) \phi(\xi)d\xi \qquad 1.1.7$$

The integral in eq.(1.1.7) is recognized as the convolution of $E(t)$ with $\phi(t)$.

As a simple application to eq.(1.1.7) we consider the case of a harmonic electric field:

$$E(t) = E_o \exp(iwt) \qquad 1.1.8$$

we get for D(t) the integral:

$$D(t) = \epsilon_\infty E(t) + (\epsilon_s - \epsilon_\infty) \int_0^\infty E_o \exp\left[iw(t - \xi)\right] \phi(\xi) d\xi$$

$$= E(t)\left\{\epsilon_\infty + (\epsilon_s - \epsilon_\infty) \int_0^\infty \exp(-iw\xi)\, \phi(\xi) d\xi\right\} \qquad 1.1.9$$

The quantity in braces is recognized as the permittivity of the system. It is generally a complex number indicating that D and E are not in phase. Thus we have :

$$\epsilon^* = \epsilon_\infty + (\epsilon_s - \epsilon_\infty) \int_0^\infty \exp(-iw\xi)\, \phi(\xi) d\xi \qquad 1.1.10$$

If we split ϵ^* into real and imaginary parts according to $\epsilon^* = \epsilon' - i\epsilon''$, then we get:

$$(\epsilon' - \epsilon_\infty)/(\epsilon_s - \epsilon_\infty) = \int_0^\infty \phi(\xi) \cos(w\xi) d\xi \qquad 1.1.11$$

$$\epsilon'' /(\epsilon_s - \epsilon_\infty) = \int_0^\infty \phi(\xi) \sin(w\xi) d\xi \qquad 1.1.12$$

This shows that both ϵ' and ϵ'' are essentially the Fourier cosine and sine transforms of the same function $\phi(u)$. Between eqs.(1.1.11 & 12) the function $\phi(\xi)$ may be eliminated by inverting the Fourier transform from one and then substituting in the other yielding:

$$\epsilon' = \epsilon_\infty + (2/\pi) \int_0^\infty \frac{u\,\epsilon''(u)}{(u^2 - w^2)}\,du \qquad 1.1.13$$

Likewise :

$$\epsilon'' = -(2w/\pi) \int_0^\infty \frac{\epsilon'(u) - \epsilon_\infty}{(u^2 - w^2)}\,du \qquad 1.1.14$$

Eqs.(1.1.13-14) are known as the Kramers-Krönig relations They provide all the mathematical framework needed to study dielectric relaxation spectra. An important consequence of the inter-relation between the real and imaginary parts of ϵ^* is that a knowledge of either one over the entire frequency range guarantees knowledge of the other through eqs.(1.1.13) & eq. (1.1.14). Moreover, an important physical insight is provided by observing that ϵ' and ϵ'' are always related in the same manner irrespective of what the form of the relaxation function $\phi(\xi)$ might be. This is an extermely important hint in support of the "universality" notion in dielectric processes.

In order to obtain explicit expressions for ϵ' and ϵ'' we need to propose a specific, physically acceptable form for the function $\phi(t)$. This topic will be covered in the next section in conjunction with the Debye equations.

C) The Debye Equations and Cole-Cole Plots

In most mechano-electrical systems the dissipative term can be shown to be proportional to the velocity of the mass involved (neutral or charged), be it frictional or radiation damping. For a spring-damper combination having an elastic constant H and damping constant b, the equation of motion is

$$H.x + b.dx/dt = F(t) \qquad 1.1.15$$

where F(t) is the impressed force. The case of a unit-step excitation F(t) = FoU(t) gives by eq.(1.1.15), with x(0) = 0

$$x(t) = (Fo/H).\{ 1 - \exp[-t/\tau] \} \qquad 1.1.16$$

where τ = b/H is a characteristic time constant.

The quantity $f(t) = 1 - \exp(-t/\tau)$ is identifiable as the "growth" function introduced in the beginning of sec.1.1B as it satisfies the requirements at t = 0 and t = ∞. It follows that the relaxation function of the system is:

$$\phi(t) = (1/\tau) \exp[-t/\tau] \qquad 1.1.17$$

Eq.(1.1.15) describes equally well the motion of a point charge experiencing damping due to visco-elastic forces in the material. Thus setting F(t) = q.E(t) and writing the polarization P as Nq.x(t) where N is the number of dipoles q.x per unit volume, we find again:

$$H.P + b.dP/dt = N.q^2.E(t) \qquad 1.1.18$$

Thus P is also governed by the same relaxation function as given in eq(1.1.17). Finally since $D = \epsilon_o E + P$, it follows that D is also governed by eq.(1.1.17) and so is the dielectric permittivity ϵ^* in eq(1.1.10). Substituting from (1.1.17) into eq(1.1.10) gives:

$$\epsilon^* - \epsilon_\infty = (\epsilon_s - \epsilon_\infty)(1/\tau)\int_0^\infty \exp(-iw\xi - \xi/\tau)\,d\xi \qquad 1.1.19$$

$$(\epsilon^* - \epsilon_\infty)/(\epsilon_s - \epsilon_\infty) = 1/(1 + iw\tau) \qquad 1.1.20$$

Solving for the real and imaginery parts we arrive at:

$$\epsilon' = \epsilon_\infty + \frac{(\epsilon_s - \epsilon_\infty)}{1 + (w\tau)^2} \qquad 1.1.21$$

$$\epsilon'' = (\epsilon_s - \epsilon_\infty)\frac{(w\tau)}{1 + (w\tau)^2} \qquad 1.1.22$$

The above are called the Debye equations. Debye first obtained them in connection with his "Polar Molecules" theory of liquids (83) in 1929. He arrived at his results simply by solving eq.(1.1.18) in which E(t) was a harmonic excitation without resorting to the kind of elaborations we had.

Fig.(4) shows a plot of ϵ' & ϵ'' as function of frequency. We note that the point at which ϵ'' reaches its maximum value is precisely $1/\tau$, thus systems having short relaxation times will display higher-frequency absorption spectra.

A useful way of presenting the Debye equations is by means

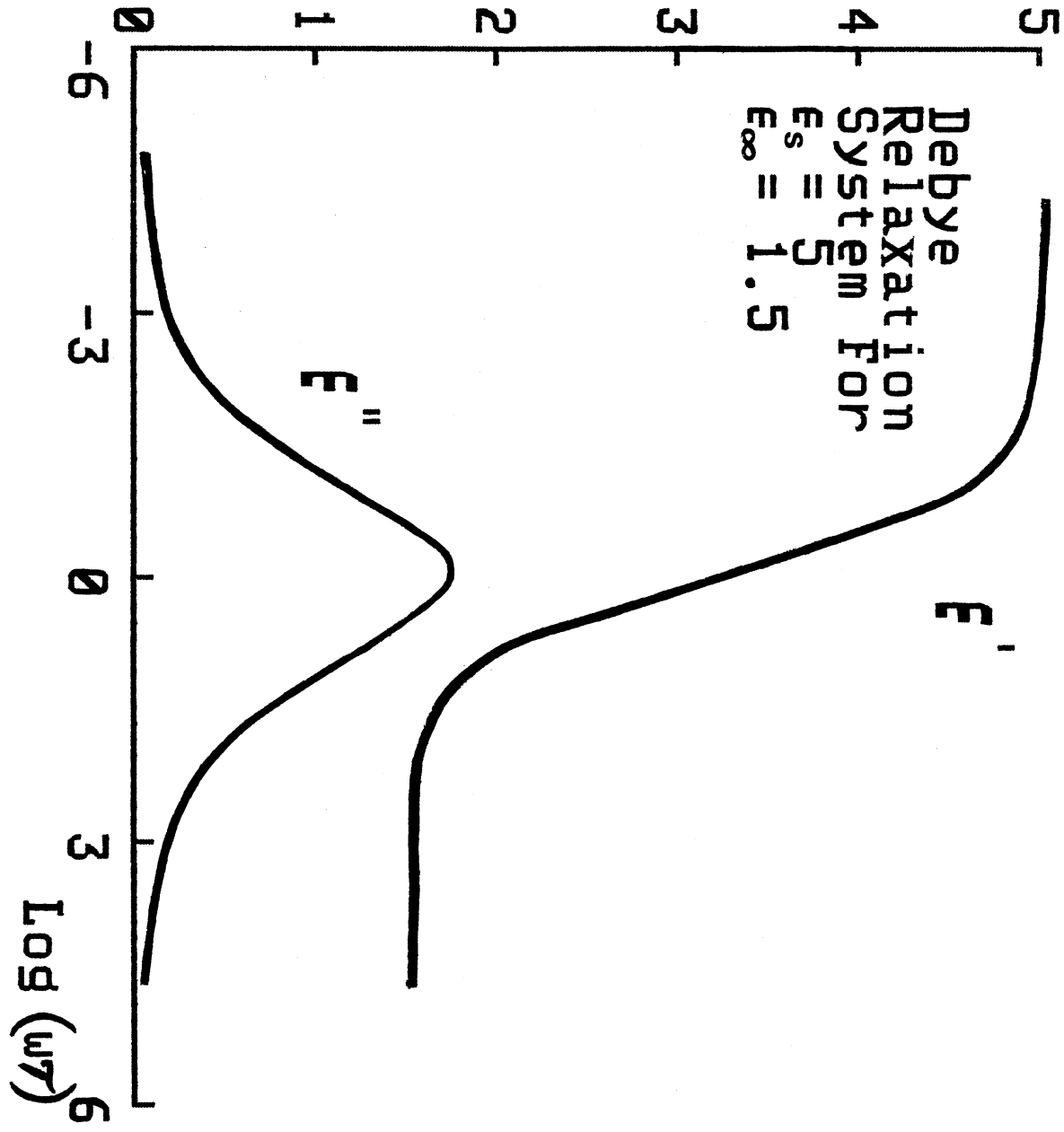
Debye
Relaxation
System For
$\varepsilon_s = 5$
$\varepsilon_\infty = 1.5$
ε''
ε'
$\log_{10}(\omega\tau)$
-6
-3
0
3
0
1
2
3
4
5

Fig. (4)

of the Argand diagram. As may be noted from eq.(1.1.21 & 22) they represent the parametric equations of a circle in the ϵ' - ϵ'' plane. Simple algebra shows that the circle is centered at $\epsilon' = (\epsilon_s + \epsilon_\infty)/2$ and $\epsilon'' = 0$, with a radius of:

$(\epsilon_s - \epsilon_\infty)/2$, see Fig.(5). These results may also be obtained by noting that in the complex plane, the vectors:

$$Y = \frac{1}{1 + iw\tau} \quad \text{and} \quad V = 1 - Y = (iw\tau)Y$$

vary in the lower half plane (as w goes from 0 to ∞), in such a way that they remain orthogonal to each other, and such that Y + V = 1, which means that the vertex at their intersection describes a circle whose equation may be determined from the condition:

$$|Y|^2 + |V|^2 = 1 \qquad \text{(recall that Y.V = 0) etc...}$$

The $\epsilon''(\epsilon')$ representation shown in Fig.(5) is known as the Cole-Cole plot (84). Only the upper (positive) portion of the circle has physical meaning as it corresponds to positive ϵ''. The advantage of this plot is that it provides a practical way of determining the extreme values of ϵ' and ϵ'' from relatively fewer data points than what might be needed using the more conventional plots of Fig.(4).

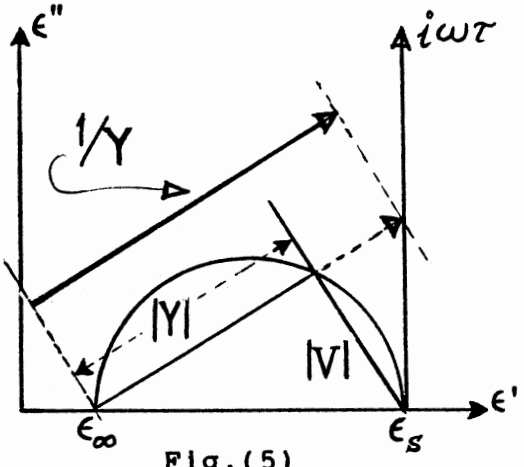

Fig.(5)

$\{ \epsilon_s - \epsilon_\infty = 1 \}$

We remark at this stage that the loss term ϵ'' does not include the contribution of the free charge (ohmic) conductivity. This contribution can be appreciable in materials containing high concentrations of free charge carriers where σ can be large. The point to keep in mind is that the loss which is measured experimentally includes the contribution of σ, and therefore has to be modified accordingly should the need arise in the analysis of the results, (refer to Sec.2.1).

Some further comments on the Debye model are in order at this point. First, only a handful of materials actually obey the simplified picture presented above. These are mostly the anhydrous alcohol groups, and dilute solutions of symmetrical polar molecules (such as chlorobenzene) in non-polar solvents (e.g. benzene, alkanes,..). In reality most materials show a deviation from the Debye model in two ways: The $\epsilon''(\epsilon')$ plot may not be a full semi-circle but an arc of a circle, in which case the maximum value of ϵ'' would be less than $(\epsilon_s - \epsilon_\infty)/2$. Secondly the actual plot may be a skewed arc with out any axis of symmetry.These deviations are attributed to an over simplification inherent in the Debye model which is based on an ideal non-interacting set of dipoles all having the same relaxation time and sharing identical surroundings.

More realistic models take account of the above by invoking a distribution of relaxation times, which corresponds physically to the realization that dipoles in a given material can be of different kinds as well as possessing multiple axes of symmetry none of which are aligned with their perma-

nent dipole moment u. This results in unequal components of (u) along these axes causing the molecule to experience unequal torques in the presence of an external electric field and hence result in different alignment times.

If we break the polarization P into several contributions P_1 , P_2 , etc.. ,each relaxing with characteristic time τ_1, τ_2 ,.., the dielectric permittivity becomes:

$$\epsilon^* = \epsilon_\infty + \epsilon_1 + \epsilon_2 + - - -$$

where $\epsilon_r = (\epsilon_{sr} - \epsilon_\infty)/(1 + iw\tau_r)$

then it follows that the most general case of a continuous distribution of relaxations takes the form:

$$\epsilon^* = \epsilon_\infty + \int (\epsilon_s(\tau) - \epsilon_\infty) \cdot \frac{R(\tau)d\tau}{(1 + iw\tau)} \qquad 1.1.23$$

From here on it becomes a matter of finding a suitable function $R(\tau)$ that best fits the data on a given material. However, because of the mathematical complexity that may arise in practice, other, more direct methods of approach have been proposed. For example Cole & Cole suggested using an empirical fit of the form:

$$\epsilon^* = \epsilon_\infty + \frac{(\epsilon_s - \epsilon_\infty)}{1 + (iw\tau)^{1-h}} \qquad 1.1.24$$

This is only suitable for data that forms arcs of a perfect circle ,with the parameter h characterizing the degree of the flattening from the ideal semi-circle shape .

In order to account for skewed arcs, Davison & Cole (85) proposed a somewhat different form to the above:

$$\epsilon^* = \epsilon_\infty + \frac{(\epsilon_s - \epsilon_\infty)}{(1 + iw\tau)^\beta} \qquad 1.1.25$$

where β is a parameter taking values between zero and one. Historically, eq.(1.1.25) was used to fit the data of Glycerol at -50 C. Further techniques relating to the methods of determining ϵ_s, ϵ_∞ from Cole-Cole plots will be taken up in chapters two and four.

D) Resonance Absorption and The Dispersion Relations

As the frequency of the impressed electric field goes up beyond 10^{10} Hz. the masses of the charges can no longer be ignored. In the classical approach a typical equation taking into account inertial effect has the form:

$$d^2X/dt^2 + 2\alpha\, dX/dt + w_o^2 X = f \qquad 1.1.26$$

where f is the impressed force per unit mass. For instance, if E' is the local value of the externally applied electric field then f = eE'/m where "e" is the charge carried by the particle of mass "m". The simplest possible form of E' is that given by the Mosotti approximation $E' = E + \epsilon_o P/3$, however due to its limited applicability we shall restrict ourselves to E' = E. Now from P = NeX (where N is the no. of dipoles

per unit volume) we see that P also satisfies eq.(1.1.26) in which the right-hand term is given by $(Ne^2/m)E$.

This means that for the case of a harmonic electric field: $E = Eo.\exp(iwt)$ the polarization is given by:

$$P = Po.\exp(iwt + \varphi) \qquad 1.1.27$$

where :

$$Po.\exp(i\varphi) = \frac{(Ne^2/m)Eo}{w_o^2 - w^2 + 2i\alpha w} \qquad 1.1.28$$

From the above, one deduces the dielectric "constant" to be

$$K^* = 1 + \frac{(Ne^2/\epsilon_o m)}{w_o^2 - w^2 + 2i\alpha w} \qquad 1.1.29$$

In general a given material may contain a variety of dipoles having different masses, elastic constants, and damping factors. Thus, the most general form of eq.(1.1.29) would be:

$$K^* = 1 + \sum_s \frac{(Nse^2/\epsilon_o m_s)}{(w_{os})^2 - w^2 + 2i\alpha_s w} \qquad 1.1.30$$

Eq(1.1.30) is the general dispersion formula of classical physics. It explains why the index of refraction depends on the frequency of light, as well as why certain wavelengths

are more readily absorbed than others. Although a quantum mechanical treatment is required to explain the anomalies that do arise in practice, the above description can be considered generally adequate for presenting the main ideas.

For values of w around a given resonance w_{or} , eq(1.1.30) can be re-written as:

$$K^{*} = A + \frac{B}{\Delta w + i\alpha_r} \qquad 1.1.31$$

where A & B are constants independent of frequency, and Δw is $w_{or} - w$. The real and imaginary parts of K^{*} are sketched in Fig.(6). Note that as we pass through the resonance, the value of K' swings from a mximum of $A + B/2\alpha_r$ at $w_{or} - \alpha_r$ to a minimum of $A - B/2\alpha_r$ at $w_{or} + \alpha_r$. while K" reaches its peak value of B/α_r at w_{or} . The bandwidth of the resonance is $BW = 2\alpha_r$ and can be used to characterize the system.
The sketches in Fig.(6) correspond to A = 10, B = $4X10^{12}$, and $\alpha_r^2 = 9.5X10^{22}$.

++++++++++++++++++++

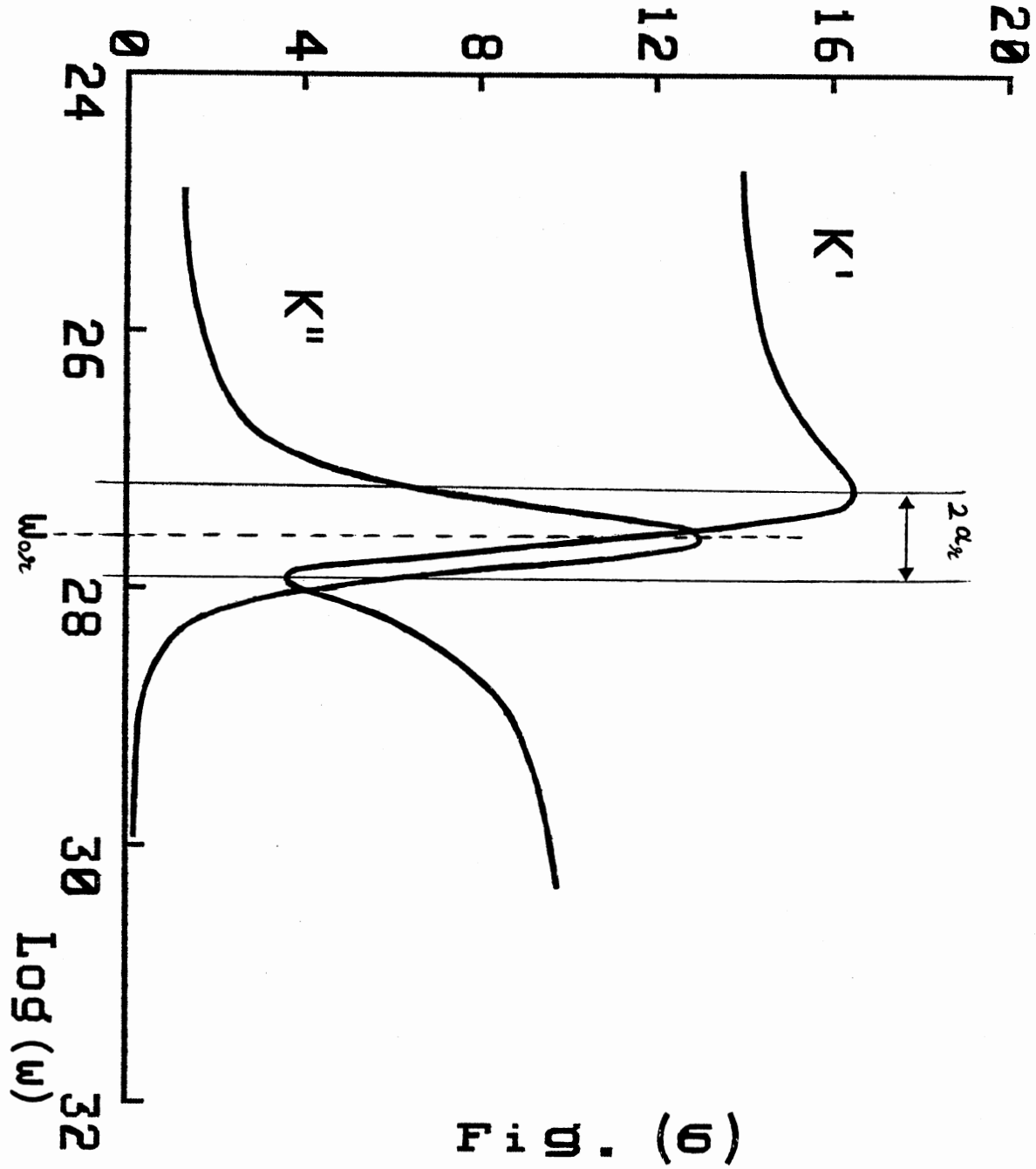

Fig. (6)

The real and imaginary parts of the dielectric constant K^* given by eq.(1.1.31), drawn to scale.

1.2) General Exposition of Polymer Characteristics

It has been found by Pohl and co-workers (2,7,54) that polymers may be classified according to their type of conjugation (alternation between double and single bonds): those with long-range electronic orbital delocalization are called eka-conjugated and are supposed to have, ideally, a perfect interlinking between the atomic pi-orbitals along the chain; while those suffering from defects, molecular or otherwise, are called rubi-conjugated, and generally, have a broken sequence of atomic pi-orbital delocalization which usually suppresses or hinders carrier transport and other electronic processes along the chain.

The above two types are also very different in their spectra, electrical properties, and chemical activity. Unless otherwise noted, it will be implicitly assumed that all polymers under study are of the eka-conjugated type.

Electro-active, nomadically (54) polarizable polymers exhibit remarkably different characteristics than most conventional materials. These features may be summarized in terms of the effects of few macroscopic parameters on the dielectric constant K , the loss factor tan(δ), and the conductivity σ (D.C. and A.C.).

It has been observed (1-3,7) that: 1) Ln(σ) increases approximately linearly with the square root of the applied pressure P, as does Ln(K). 2) Both σ and K strongly increase with temperature according to $\sim \exp(-Ea / k_B T)$.

where Ea is an activation energy and k_B is Boltzmann's constant. 3) The D.C. conductivity increases exponentially with the D.C. electric field bias E. 4) There exist frequencies Wc above which the dielectric constant K increases with the E-field bias (over some range of bias values) instead of decreasing as it always does at lower frequencies. The value of Wc determines the range of E-field interval over which the reversal takes place. The lowest possible frequency Wc for which this happens is referred to as the "cross-over" frequency of the system. 5) Eka-conjugated polymers exhibit unusually long relaxation times of the order of 10^{-3} to 10^{-4} sec. (52,53) as compared to those of regular materials which are of the order of 10^{-6} to 10^{-7} sec. Detailed account of the above features will be explored in secs.(1.3) & (1.4) .

For the moment, however, we just wish to point out that the aforementioned properties are rather unique to polymeric solids on account of their physical and chemical structure.

Besides this, polymers offer the widest range in their electrical/ dielectric character of all known semi-conducting materials, as a result of special doping and synthesis. Recent work on poly(acetylene) has shown that conductivities as high as $1.2X10^{3}$ S/cm are attainable (86), while tetracyanoquinodimethane (TCNQ) salts can be made to exhibit both donor and acceptor properties depending on whether the dopant is a metal or non-metal ions (87).

1.3) Dynamic Aspects of Hyper-Electronic Conduction and Polarisation

A) Introduction

In conventional solids and other materials, polarization is brought about by one or more of the following mechanisms:

1) The alignment of permanent dipoles under the influence of an external electric field (orientational polarization).

2) The creation of dipoles due to the action of an external electric field (induced polarization); this latter type can be electronic as well as atomic in nature.

3) Space-charge polarization due to trapping of charge carriers at the interface separating the material and the electrode.

When it comes to polymer materials, the above mentioned mechanisms are practically negligible compared to other phenomena pertaining to polymers; besides, none of them can explain the unusually high dielectric constant, the low-field saturation of the polarization, and the many other effects reviewed in sec.(1.2). Since existing evidence indicates that these effects are usually of electronic origin rather than protonic, Pohl et al.(1,2,37) introduced the term "hyper-electronic" to emphasize the concept of charge carrier delocalization as being a primary cause behind this phenomena that is practically unique to polymeric solids.

In 1975 H. Pohl and M. Pollak (8) proposed a model based on the so called "Domain Theory" whose essence is that in a

polymeric substance there exists an appreciable number of dissociated charge pairs arising as thermally or field generated excitons[1], with each member of the pair existing on separate molecules. These carriers are able to rove along a one dimensional molecular "spine" over great distances of the order of thousands Å, thereby giving rise to huge dipole moments several hundred to thousand times larger than those of induced electronic origin. The theory suggests a "polaronic" - type[2] motion along the molecular spine, and a "hopping" motion between consecutive chains. Of course, the availability of long molecular domains, along which, delocalized charges can move unobstructedly, is a crucial assumption of the theory. There is ample evidence however, to support this presumption for numerous types of polymers notably the (PAQR) group as revealed by E.S.R studies, mobility measurements, and other dielectric behaviour (1-3,7).

---

1) A (Wannier) exciton is a loosely coupled electron-hole pair, in which the electron has been lifted to an orbital above the ground state (88-90).

2) In ionic crystals or charge-complex polymers, an electron trapped on a lattice site can become surrounded by other negative ions which due to repulsion, give rise to lattice distortion. As the electron travels, the distortion follows it, thereby creating the illusion of a more massive particle - the polaron.

We have mentioned earlier that the roving charges arise as excitons. These are of two kinds: Inter-molecular (Mott) excitons, and intra-molecular (Frenkel) excitons

For this topic of study, Mott excitons are the more dominant kind. In this type of polarisation, the dissociated charge pairs have each of their members lying on different molecules separated by thousands of Å (weak binding case). The term "nomadic polarization" has been introduced by Pohl et al.(54) to describe the effortless motion with which the charges move along the main "spine" of the molecule, as contrasted with the more difficult motion across the "gap" separating two given molecules.

Thermally-activated "hopping" between molecular chains has been shown to predict with relative success the experimentally observed data on "H.E.P" as affected by pressure, temperature, E-field, and frequency (1-3,7,41,42).

B) Statistics of Mott Excitons

As far as their statistical behaviour is concerned, Mott excitons may be treated as electron-hole pairs. It is well known from solid state theory (Kittel (91)), regarding the statistics of electrons and holes that the Fermi level is given by:

$$u = (1/2)Eg + (3/4)k_B T.\ln[M_h / M_e] \qquad 1.3.1$$

where Eg is the energy gap separating the valence and the

conduction bands, M_h and M_e refer to the masses of hole and electron respectively, k_B is Boltzmann's constant, and T is the absolute temperature.

Because of the shallow energy bands in polymers, it will be assumed that for these excitons, M_h and M_e are equal, and so u is just Eg/2. Further, the energy gap Eg may be identified with the dissociation energy W (the energy needed to overcome the electron-hole affinity in a given domain (molecule) minus the ionization energy).

Following Fermi-Dirac statistics we may therefore write for the number of occupied (single particle) exciton states at temp. T and dissociation energy W:

$$N(W) = \frac{Z(W)}{\exp[-(u-W)/k_B T] + 1} \qquad 1.3.2$$

where Z(W) is the number of states available at energy W . With u=(1/2)W it follows that the probability of occupation of a state with given energy level W (namely N(W)/Z(W)) is given by :

$$P(W) = \frac{1}{\exp[W/2k_B T] + 1} \qquad 1.3.3$$

****

C) Form of The Effective (Internal) Potential Acting on a Charge Carrier

It has been shown by Wyhof (92) that the dependence of the static dielectric constant K on the action of an external D.C. electric field can be described by an empirical formula of the form:

$$Ko/K = 1 + (E/Eh) \qquad 1.3.4$$

where Ko is the value of K at zero electric field, Eh is the value of E when K drops to half its value at zero field, Ko. It is important to observe that in the above relation E is just the magnitude of the electric field.

In a naive picture we may imagine an elementary dipole being formed by the displacement of a charge carrier "e" a distance $\vec{x}$ from its equilibrium position under the action of the external field $\vec{E}$, thereby giving rise to an elementary dipole moment $e\vec{x}$. Let us remark here that if $\vec{E}$ is positive then e end $\vec{x}$ will both have the same sign, while if $\vec{E}$ is negative, e and $\vec{x}$ will have opposite signs.

We denote by $\vec{E}'$ the internal electric field acting on a charge carrier as a result of the neighboring molecular forces, and without loss of generality we may assume $\vec{E}'$ to be a function of the displacement $\vec{x}$.

Under equilibrium conditions the resultant forces acting on the charge "e" will be zero and so we may write:

$$e\vec{E}'(x) + e\vec{E} = 0 \quad \text{or} \quad \vec{E}'(x) = -\vec{E} \qquad 1.3.5$$

Now the polarization vector $\vec{P}$ is given by N.e.$\vec{x}$, where N is the number of elementary dipoles per unit volume.

Further, we have from the definition of the dielectric constant:

$$\vec{P} = \epsilon_o(K-1).\vec{E} \qquad 1.3.6$$

We may now express $\vec{E}'(\vec{x})$ purely as a function of x and a few parameters, as follows:

First, to avoid confusion let us rewrite E which appears in eq.(1.3.4) as |E| to emphasize that it stands for absolute value of the component of $\vec{E}$, the symbols E and x will be retained for the components of these vectors along the unit x-axis vector $\vec{i}$.

Thus $\vec{E} = E\vec{i}$ and $\vec{x} = x\vec{i}$ etc.. Next, we solve for K from eq.(1.3.4) and substitute in (1.3.6) to get:

$$Ne\vec{x} = \left[\left(\frac{Ko.Eh}{|E| + Eh}\right) - 1\right]\vec{E} \qquad 1.3.7$$

From here on we must consider two separate cases:

1) When $\vec{E}$ is in the positive x-direction, |E| = E, and we obtain: (neglecting "1" in comparison with Ko, which is reasonable for long-chain polymers)

$$E = \frac{Eh.(N.ex)}{Ko.Eh - N.ex} \qquad E > 0 \qquad 1.3.8$$

With E' = - E, we get for the corresponding internal potential :

$$\frac{\partial V'}{\partial x} = -E' = \frac{Eh.(N.ex)}{Ko.Eh - N.ex} \qquad 1.3.9$$

This may be integrated to give :

$$V' = \pm\, Eh.[\, |x| + Lo.\ln(1 - |x|/Lo)\,] \qquad 1.3.10$$

depending on whether e is (-) or (+) respectively. Lo is given by :

$$Lo = \frac{Ko.Eh}{N.|e|} \qquad 1.3.11$$

and may be considered a characteristic "half-length" of the polymer molecule .

2) When E is in the negative x - direction, $|E| = -E$ and so eq.(1.3.7) becomes :

$$E = \frac{Eh.(Nex)}{Ko.Eh + N.ex} \qquad E < 0 \qquad 1.3.12$$

again we find that V' is given by eq.(1.3.10)

The physical significance of Lo may be further appreciated if one considers the case for which E is along the positive x - axis:

With $E > 0$ and $ex > 0$ eq.(1.3.8) implies $Ko.Eh - N.ex > 0$

or: $x < Ko.Eh/Ne$, assuming "e" to be (+).

hence $x < Lo$.

Similarly, if $\vec{E}$ is along the negative x -axis then x is necessarily negative since ex < 0. In this case eq.(1.3.12) gives:

$Ko.Eh + N.ex > 0$ or $-x < Ko.Eh/Ne$ that is to say:

$$|x| < Ko.Eh/Ne \quad ===> \quad |x| < Lo$$

Thus x is always bounded by Lo. Identical conclusions may be drawn if we had assumed a negative charge. Consequently Lo can be regarded as the extent to which the restoring field E' acts, and which in turn, may be identified with the extension of the molecular chain on both sides of the origin in Fig.(7).

Under equilibrium conditions, the total potential which the charge carrier finds itself in, will be the sum of what is given by eq.(1.3.10) and the external field potential Vo. (Vo = -Ex), thus:

$$Vtot = -Ex \pm Eh.(|x| + Lo .ln[1 - |x|/Lo]) \qquad 1.3.13$$

This function is sketched for E = 0.25 Eh, 1Eh, and 4Eh respectively in Figs.(8 - 10), for negative "e".

It should be noted that the foregoing treatment was somewhat over-simplified since we completely neglected the effect of the local value of the external field. In reality,it's Eloc that acts on a charge carrier displacing it a distance

x and so the balance equation at equilibrium between E' and the external field should have been written as :

$$\vec{E}' + \vec{E}loc = 0 \qquad 1.3.14$$

In general Eloc can be very difficult to calculate, therefore we will just be content with the simplification Eloc = E.

We also remark that eqs.(1.3.8) & (1.3.12) are unaffected by either choice we make, however eq.(1.3.13) would be modified in a local-field approach .

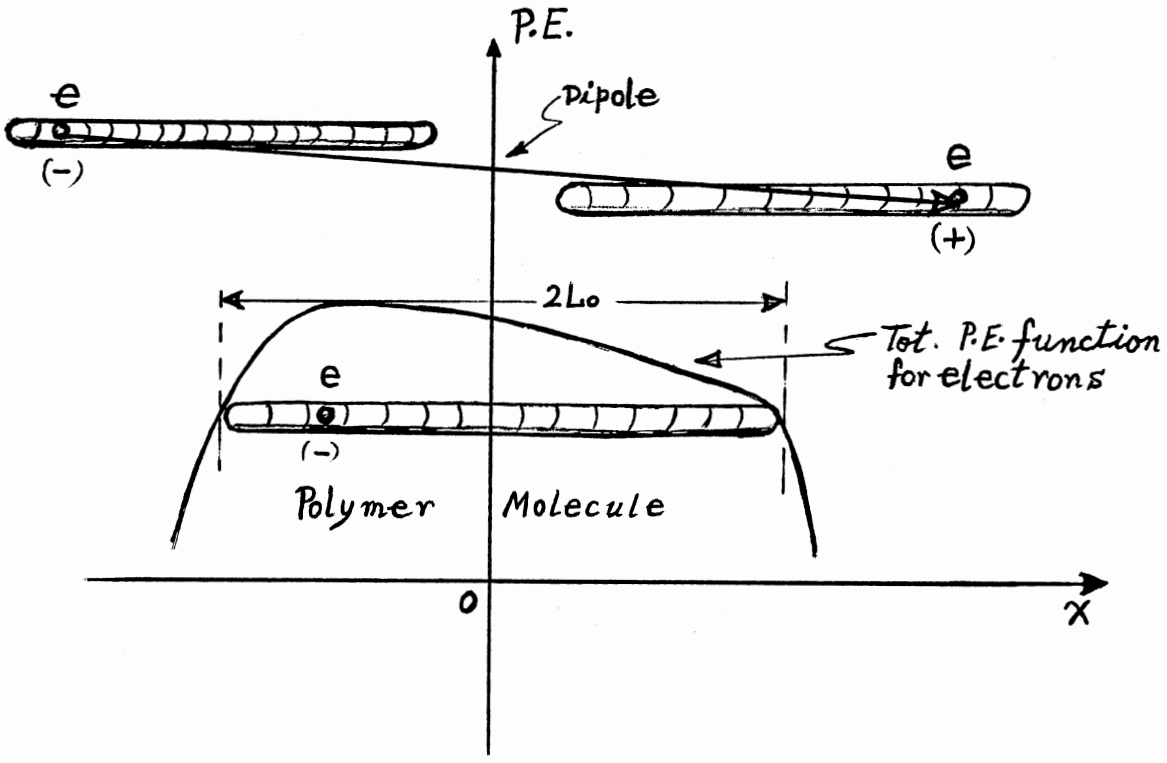

Fig.(7)

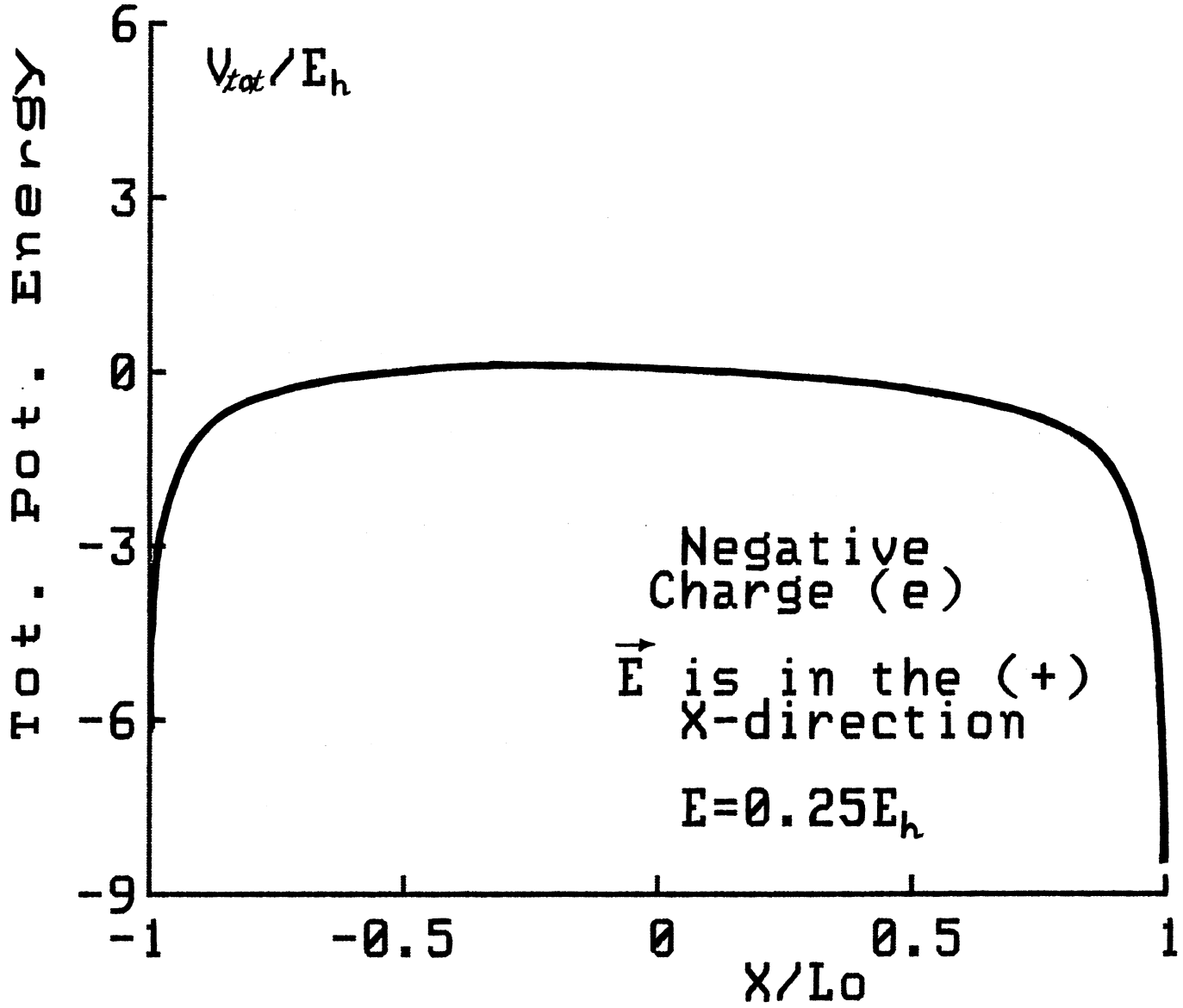
6
3
0
-3
-6
-9
-1
-0.5
0
0.5
1
X/Lo
Tot. Pot. Energy
V_{tot}/E_h
Negative
Charge (e)
$\vec{E}$ is in the (+)
X-direction
$E=0.25E_h$

Fig. (8)

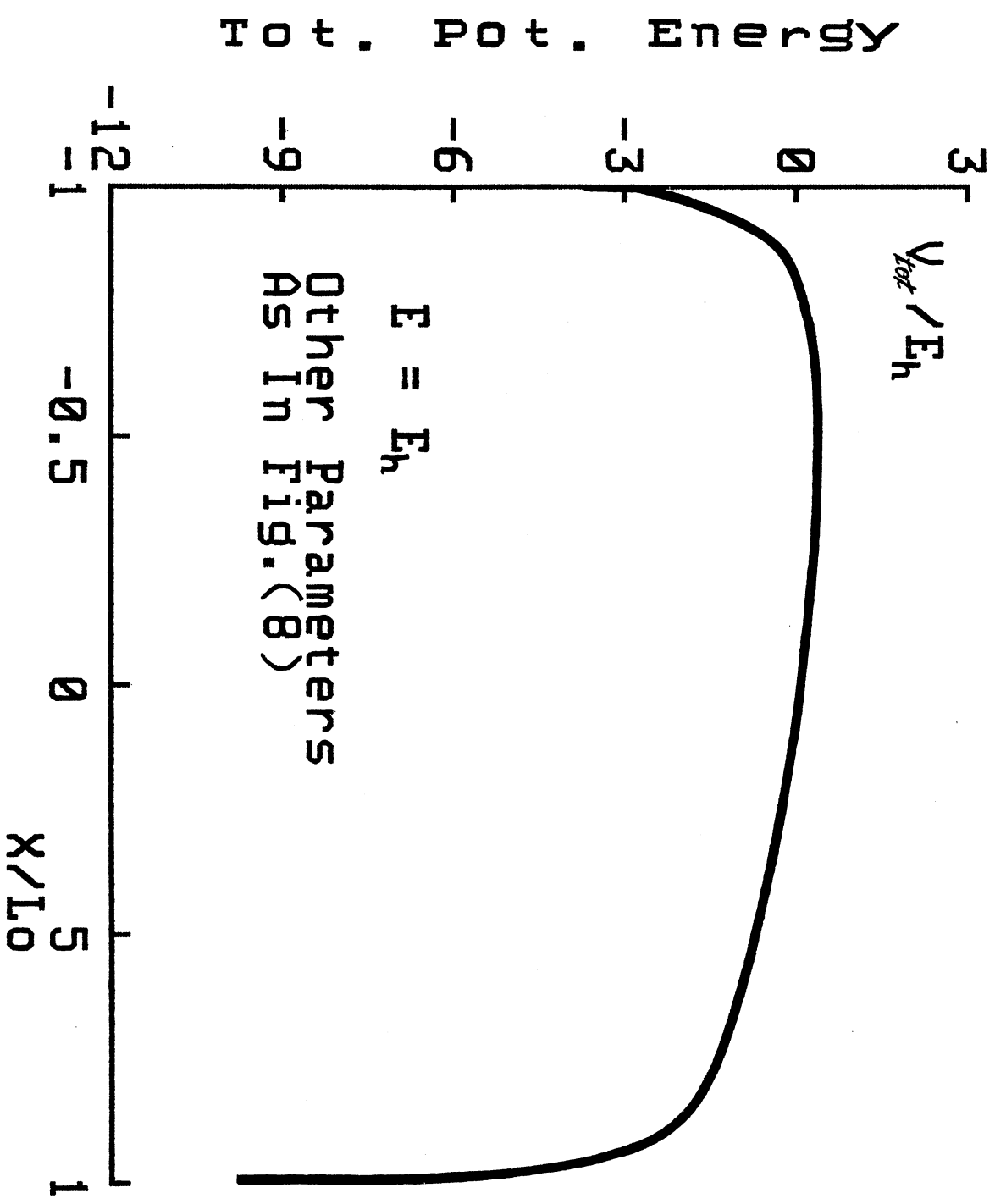
Tot. Pot. Energy
-12
-9
-6
-3
0
3
V_{tot}/E_h
1
0.5
0
-0.5
-1
X/Lo
E = E_h
As in Fig.(8)
Other parameters

Fig. (9)

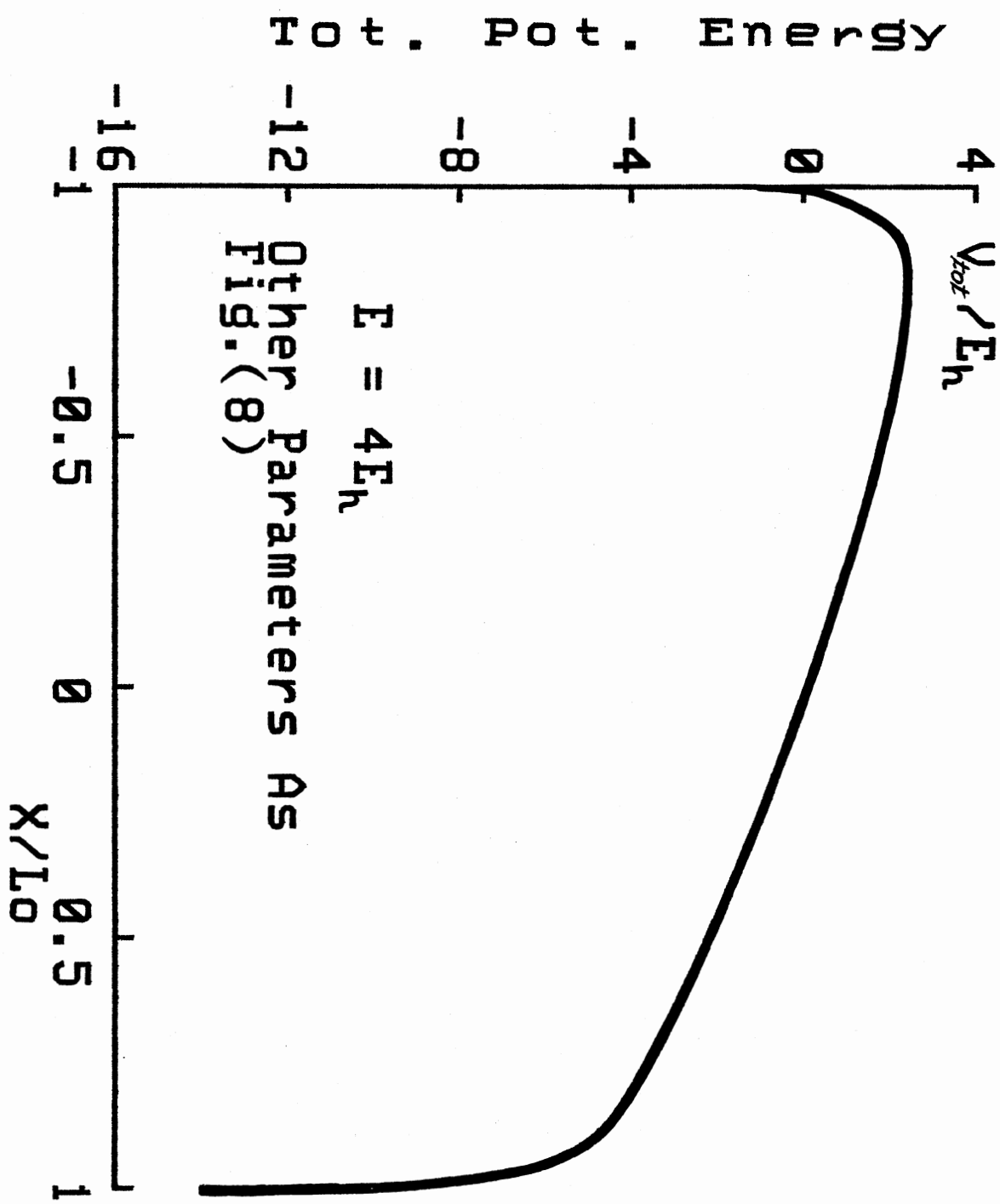
Tot. Pot. Energy
-16
-12
-8
-4
0
4
V_{tot}/E_h
E = $4E_h$
Other Parameters As
Fig.(8)
-1
-0.5
0
0.5
1
X/Lo

Fig. (10)

D) Low-Field Saturation Effect in Nomadic Polarisation

Let's consider a polymer chain made of "n" basic units (mers), each having length "a_o" giving a total length Lo = na_o for the molecular chain.

According to the hypothesis of polaronic type conduction it is legitimate to assume that the wave function of a given charge carrier is localized on a given unit site. This is valid if the molecules have narrow bands (about 0.1eV or less)

In the absence of an external electric field, all sites are equally likely to be occupied with probability fs = 1/n for any site "s". In this simplified picture the number of sites per monomer is taken to be unity.

When an external electric field is applied, the energy levels available to the charge carriers are changed and so are the occupation probabilities. From classical statistical mechanics the probability to occupy a state with energy level U is $\sim \exp[-U/k_B T]$ where U is measured relative to the ground state. Now when an electric field is switched on, it creates an energy level $(-\vec{p}.\vec{E})$ relative to the initial "ground" state, $\vec{p}$ being the induced dipole moment created by the displacement of the charge carrier a distance $\vec{x}$ from the equilibrium, namely $e\vec{x}$. It follows that the probability of the occupation of a site "s" is:

$$fs = fo.\exp[+\vec{p}.\vec{E}/k_B T] = fo.\exp[+e\vec{x}.\vec{E}/k_B T] \qquad 1.3.15$$

Where fo is a normalization constant. Worth noting from

eq.(1.3.15) is the fact that fs is greater when $\vec{p}$ is in the direction of the electric field and is much smaller when $\vec{p}$ is opposite to $\vec{E}$.

For our purposes we shall consider the site coordinate x to be a continuous variable s, this is reasonable for long polymer chains of a thousand units or more. Thus we let fs ——> f(s).

The constant fo is determined from the normalization condition :

$$1 = \int_{-Lo/2}^{+Lo/2} fo \exp[+eEs/k_B T]\, ds$$

Which gives :

$$fo = (\eta)/Lo.\sinh(\eta) \ , \quad \text{where } \eta = eELo/2k_B T \qquad 1.3.16$$

For a molecule with a single charge carrier "e", the linear charge density is $\lambda = ef(s)$. This means that at a given site position s, there is an elemental charge λds giving rise to an elemental, induced, dipole moment ef(s).sds. Hence the average induced dipole moment of the molecule is:

$$\langle p \rangle = \int_{-Lo/2}^{+Lo/2} ef(s).sds = \frac{eLo}{2}\left[\coth(\eta) - \frac{1}{\eta}\right] \qquad 1.3.17$$

We note again, that for (1.3.17) to be strictly correct the electric field appearing in it must be considered to be the local field Eloc. However for the purpose of illustrating

the basic concepts involved,we shall adhere to the simplified picture chosen here. For details on local field theories the interested reader is referred to the literature (93-95). We remark briefly in this context that the usual way of approach is to regard "E" in eq.(1.3.17) as the local field, compute the differential polarizability $\alpha_d = d\langle p\rangle/dE$ (if large fields are being used), or the tangential polarizability $\alpha_t = \langle p\rangle/E$, (if the fields are small), and then try to evaluate the sum of all the polarizabilities over a unit volume, taking into account the random orientations of the molecules as well as the fact that the field E is not constant any more but varies from one molecule to the next. Due to the complexity of the procedure, Pollak (96) has introduced a so-called "mean field" theory in which the contribution from each polarizable center is found by averaging the induced polarization field over the volume of the polarizable center (a whole molecule in this case). The method requires computational help, and gives rise to divergencies unless a limitation on the "distance" variable is imposed. In any case, graphical plots of the approximate expressions show that the actual shape of the polarization is not really that much different from the "Langevin" form, but the absolute magnitude can be off by as much as 20% (especially at large electric fields).

In order to get the polarization P we need to know N the number of equivalent sites (charge centers) per unit volume This is obtained as follows: In the presence of an electric field, a given molecule will have "n" distinct, non - degen-

erate sites available for occupation. This means that the volume associated with a given state (site) at energy level W is that of the molecule itself.

If we imagine the polymer molecule to be made up of "n" cylindrical blocks each of diameter "$2a_o$", then the volume of the whole molecule will be :

$$Zo = n.\pi a_o^3 \qquad 1.3.18$$

so the number of available sites per unit volume at energy level W is :

$$No = 1/Zo = 1/n.\pi a_o^3 = 1/ALo \qquad 1.3.19$$

where A is the cross-sectional area πa_o^2 . It follows from eq(1.3.3) and (1.3.19) that the number of occupied sites per unit volume at energy level W is:

$$N(W) = \frac{No}{\exp[W/2k_B T] + 1} \qquad 1.3.20$$

Consequently the polarization P may now be written as:

$$P = \langle p \rangle . N(W) = \frac{(e/2A)[\coth(\eta) - 1/(\eta)]}{\exp[W/2k_B T] + 1} \qquad 1.3.21$$

In the above derivation we assumed that all the polymer molecules are aligned along the same axis as that of the electric field, and that they all have the same length Lo. The statistics for the real situation where, a distribution of molecular lengths and random orientations arises, can be extremely involved since not all sites corresponding to the

same energy level occupy the same (relative) position along the molecular spine. For the time being, however, we will not consider the effect of length distribution; as for the distribution of orientations one can suppose that for low field strengths, the molecular orientations are completely random and each direction is equally probable. Thus by averaging the molecular number N over a solid angle of 4π steradians we obtain a factor of (1/3).

Hence eq.(1.3.21) becomes :

$$P = \frac{(e/2A)[\coth(\eta) - 1/(\eta)]}{3\,(\exp[W/2k_BT] + 1)} \qquad 1.3.22$$

At low fields , $eELo/2k_BT$ is $<<$ 1 , $\coth(\eta) - 1/\eta \equiv L(\eta)$, reduces to $\eta/3$, (obtained by taking the limit when $L(\eta)$ is in integral form), so that eq.(1.3.22) becomes:

$$P = \left(\frac{eLo}{Zo}\right)\left(\frac{eELo}{36k_BT}\right)\left(\frac{1}{\exp[W/2k_BT] + 1}\right) \qquad 1.3.23$$

From this one obtains the dielectric constant K :

$$K = 1 + \frac{(eLo)^2/(36k_BT.\,\epsilon_o Zo)}{\exp[W/2k_BT] + 1} \qquad 1.3.24$$

It is seen from the above, that K is practically a constant independent of the field intensity E, as long as the condi-

tion: $|e|ELo << 2k_BT$ holds. Equation (1.3.22) is plotted as a function of the parameter η for W = 0.5 eV & 0.05 eV at two different temperatures: 300°K, 500°K, in Figs.(11-12). Note the saturation effect implied by the Langevin function:

$$L(x) = \coth(x) - 1/x \qquad 1.3.25$$

which appears in the numerator of (1.3.22). As seen from the plots, saturation starts only around a few thousand volts/cm.

A full expression for K from eq.(1.3.22) may also be developed using the relation $\epsilon_o(K - 1)\, E = P$, we have :

$$K = 1 + \frac{\{No(eLo)^2/12\,\epsilon_o k_B T\}}{(\exp[W/2k_BT] + 1)} \cdot \frac{L(\eta)}{\eta} \qquad 1.3.26$$

It should be pointed out that the foregoing analysis, and especially eq.(1.3.22) and (1.3.26) are valid only at very low frequencies (< 100 Hz.), and strictly speaking, should only be considered to hold under static conditions .

Plots of eq.(1.3.26) are shown in Figs.(13-14) for the same parameters values listed after eq.(1.3.24).

We should point out that although the curves in Figs.(11-14) always display the "knee" bend at the same value of η , they do correspond to different values of electric field by virtue of eq.(1.3.16), assuming the length "Lo" is the same. Further, the shape of these plots is not affected by the temperature T (they merely become rescaled as T varies), however, the influence of W grows less and less as T increases. The quantities (e/6A) in eq.(1.3.22), and $No(eLo)^2/12\,\epsilon_o k_B T$ in eq.(1.3.26) are taken to be unity in the plots (Figs.11-14).

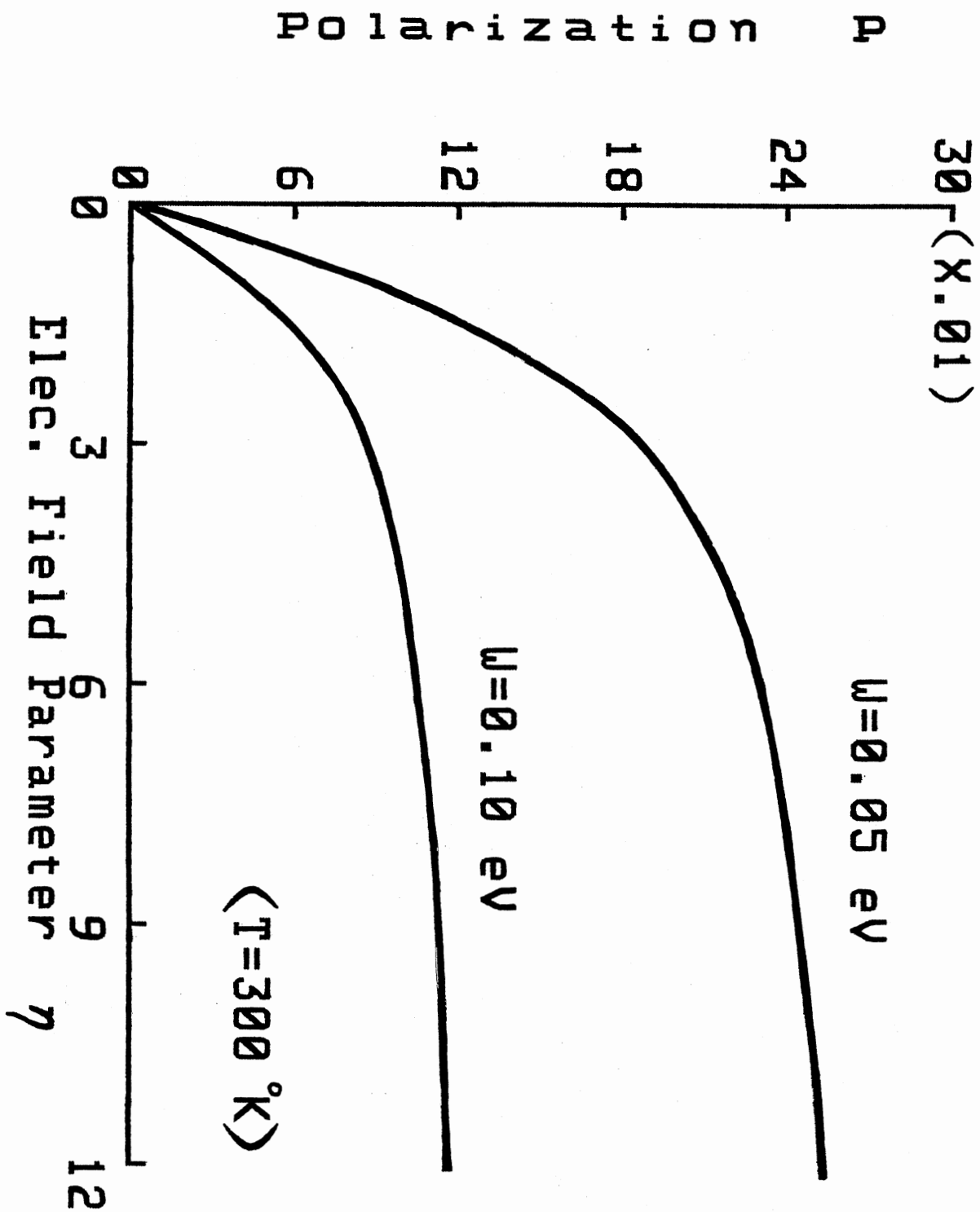
Polarization P
(X.01)
0
6
12
18
24
30
Elec. Field Parameter η
0
3
6
9
12
U=0.05 eV
U=0.10 eV
(T=300°K)

Fig. (11)

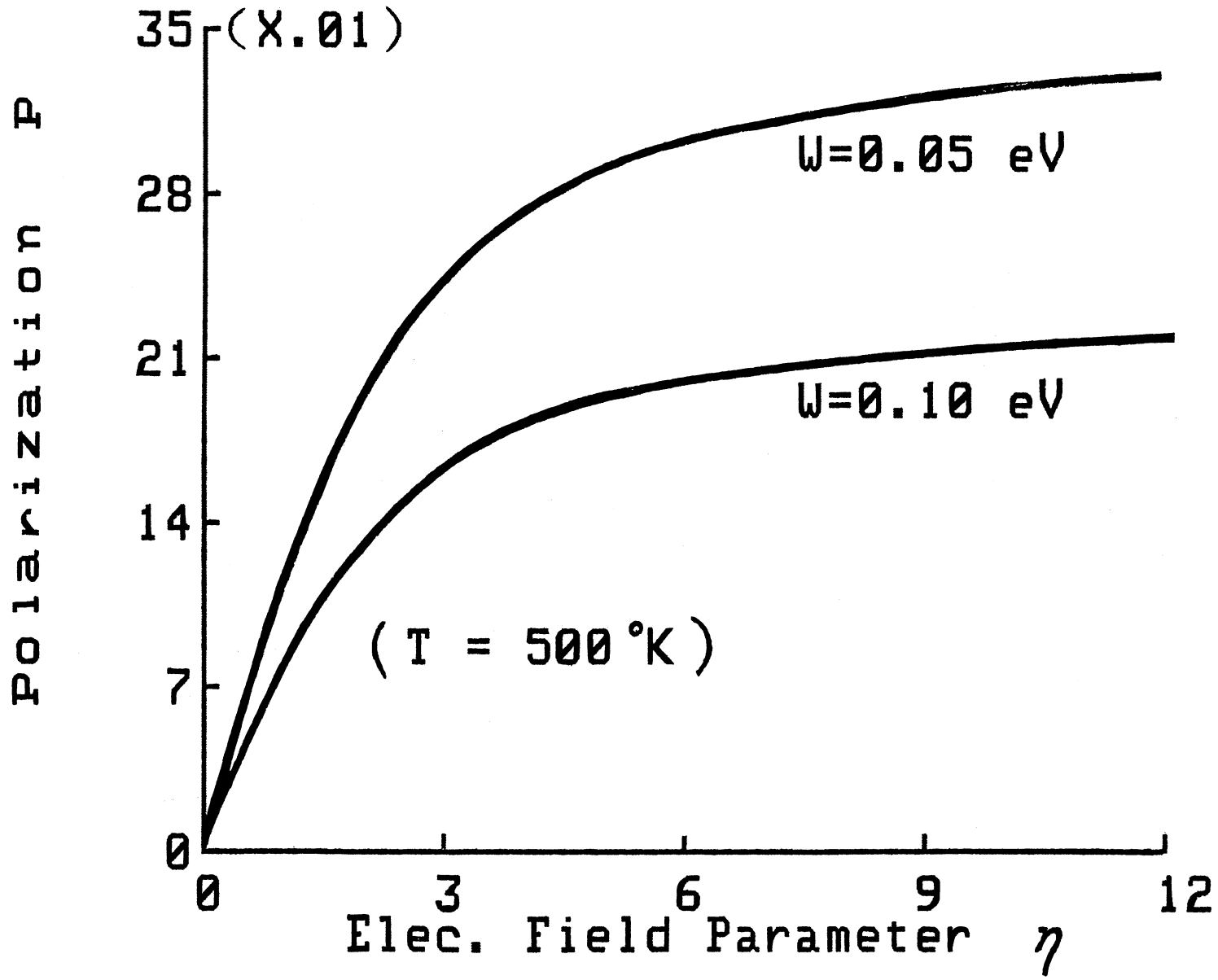
35
(X.01)
28
21
14
7
0
Polarization P
W=0.05 eV
W=0.10 eV
(T = 500 °K)
0
3
6
9
12
Elec. Field Parameter η

Fig. (12)

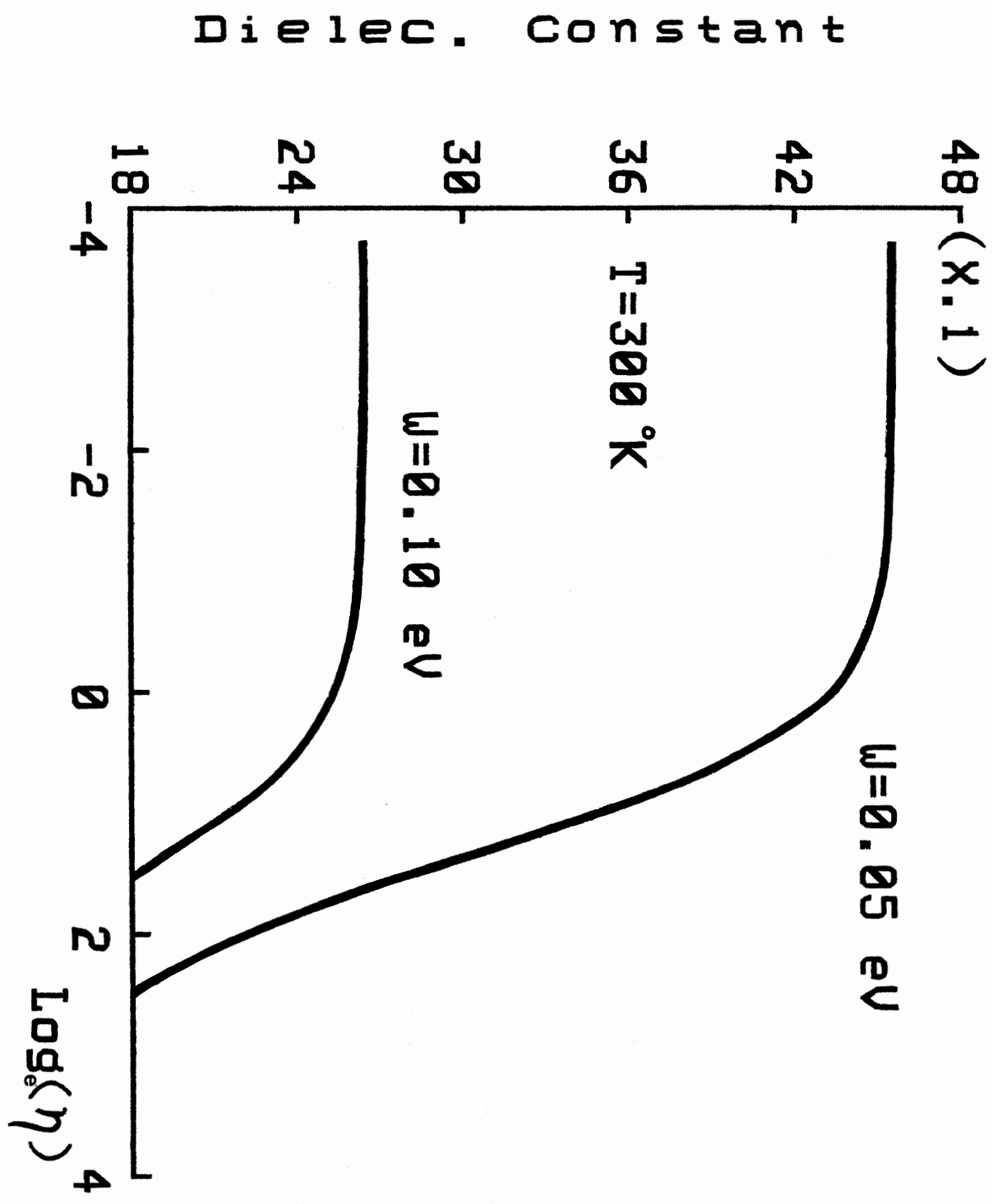
Dielec. Constant
18
24
30
36
42
48
(X.1)
-4
-2
0
2
4
Log$_e$(η)
T=300 °K
W=0.10 eV
W=0.05 eV

Fig. (13)

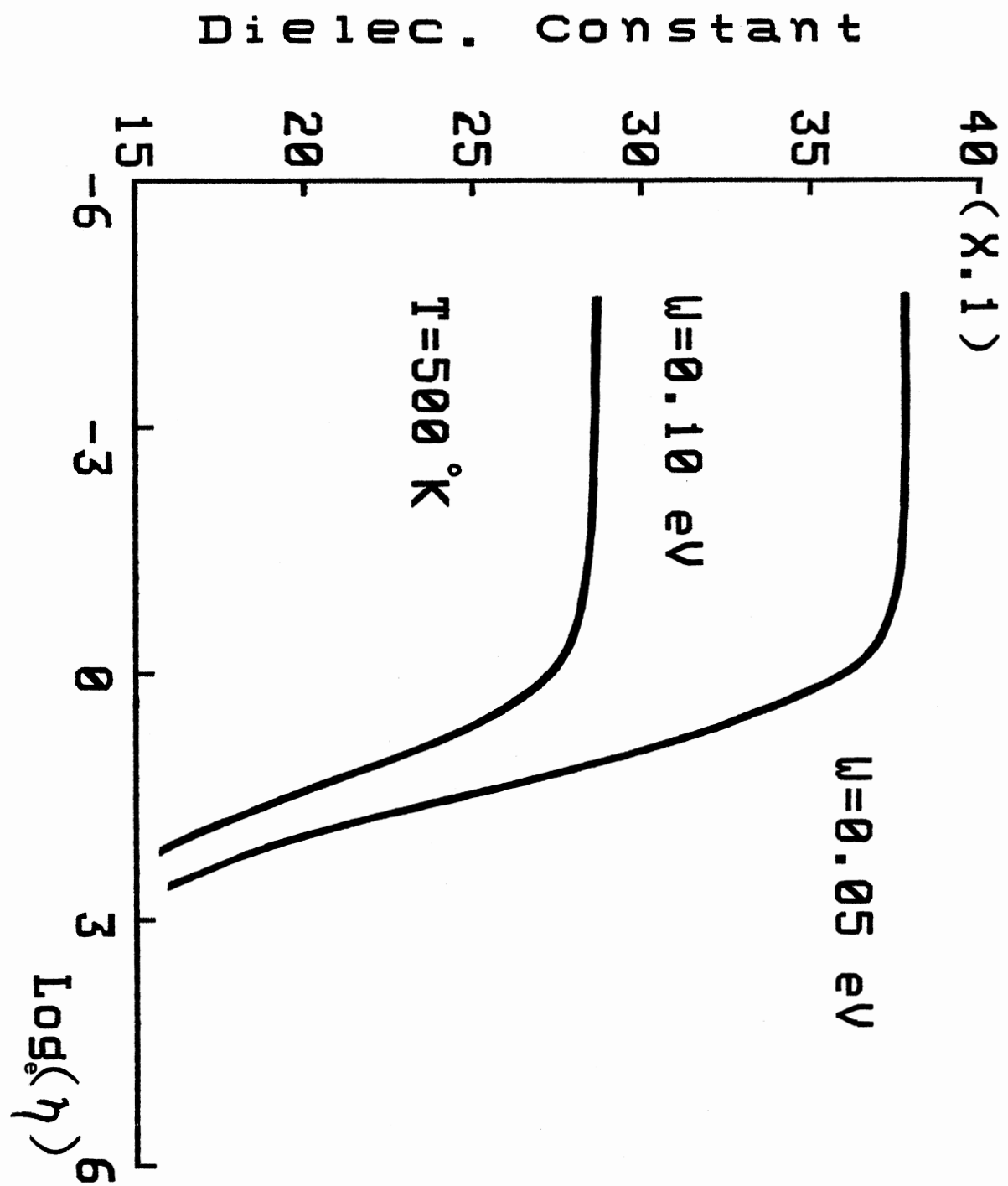
Dielec. Constant
15
20
25
30
35
40
(X.1)
-6
-3
0
3
6
Log(η)
T=500°K
U=0.10 eV
U=0.05 eV

Fig.(14)

1.4) The Pohl-Pollak Theory and Model

In 1975 Pohl and Pollak (8) proposed a model for A.C. conduction in long chain eka-conjugated polymers using a ladder-type RC network Fig.(15).

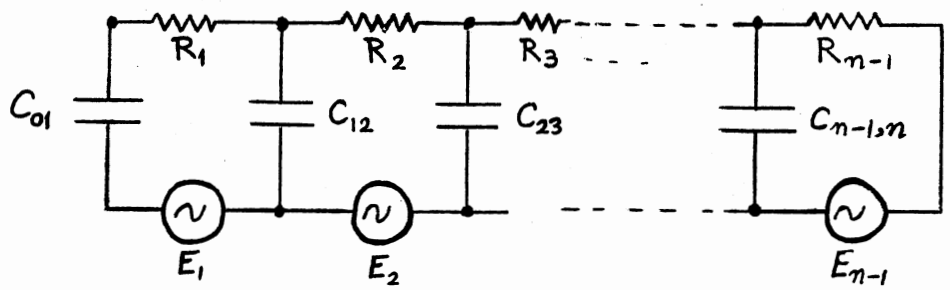

Fig.(15)

The RC values and those of the voltages are chosen to simulate the proposed physical model of the polymer chain namely a linear aggregate of n basic units "mers" along which a charge carrier moves from site to site by means of thermally activated hopping (polaron type motion), while the transport between macromolecules is assumed to be much more difficult.

The model is based on the well-known Boltzmann equation relating the rate of change of probability of finding a carrier on a given site j to the transition rates between nearest neighbors, namely :

$$df_j/dt = f_{j-1}\,p_{j-1,j} - f_j\,.\,(p_{j,j-1} + p_{j,j+1}) + f_{j+1} + p_{j+1,j} \qquad 1.4.1$$

where p_{KS} is the rate of transition from k ——> s and is assumed to be frequency independent, and such that for zero DC bias $p_{j,j-1} = p_{j,j+1}$. Moreover in the presence of a uniform external D.C. field, the $p_{j,j+1}$ are all equal to each other in view of the assumed regularity of the polymer molecule.

According to Miller & Abrahams (97) the impedance representation of the Boltzmann equation takes the form :

$$C_{j-1,j} = e^2 p_j / K_B T$$

$$R_j = K_B T/e^2 . (\vec{p} f_j + \overleftarrow{p} f_{j+1}) \qquad 1.4.2$$

where $\vec{p} = p_{j,j+1}$ and $\overleftarrow{p} = p_{j,j-1}$, the voltages E_j are all equal and given by $E.a_o$ where E is the externally applied field (strictly, must be considered to be the local value) which could be simultaneously A.C.& D.C.and "a_o" is the length of the monomer unit. Pohl & Pollak suggest a solution in terms the normal modes of the impedance matrix relating the loop currents I_j to the generator voltages.

In order to faithfully represent the voltage values at the end points and for negative coordinates, semi-periodic boundary conditions are invoked by replacing the finite macromolecule by an infinite one along which the field is given by:

$$E_j = E.a_o \quad \text{for} \quad (2m-1)n > j > 2mn$$

$$E_j = 0 \quad \text{for} \quad j = mn \qquad 1.4.3$$

$$E_j = -E.a \quad \text{for} \quad 2mn > j > (2m+1)n$$

Where m takes integral values from $-\infty$ to $+\infty$.

The actual physical current density J is related to the average polarization <P> by : $J = d\langle P\rangle/dt$ where <P> is given by (1/3)N.p, "N" being the number of dipoles per unit volume, and p is the dipole moment of a single macromolecule. We have :

$$p = \sum_j x_j q_{j,j+1} = a_o \cdot \sum_j j q_{j,j+1}$$

Hence $J = (1/3)N.a_o \sum_j j.\dot{q}_{j,j+1}$, which by Kirchhoff's

rules becomes :

$$J = (1/3)N.a_o \sum_j j.(I_{j+1} - I_j) = (1/3)N.a_o \sum_j I_j \quad \text{(since Io = In = 0)} \qquad 1.4.4$$

Next the loop currents I_j are calculated by solving the matrix equation E = Z.I in a representation where Z is diagonal, in which case the currents I will be simply the eigenvectors of Z etc..For brevity we shall only give the main results. For the case of zero bias and small amplitude A.C. field, the impedance network has identical elements given by

$$R = nk_BT/2p_o e^2 \qquad C = e^2/nk_BT \quad \text{for all sites j}$$

and the current density is related to the electric field E by :

$$J = (2n/3)(Nea_o^2/\pi^2R).E \sum_{\alpha=1,3,5\ldots} (1/\alpha^2)\left(\frac{(w\tau_\alpha)^2 + iw\tau_\alpha}{1 + (w\tau_\alpha)^2}\right) \qquad 1.4.5$$

From which the real part of the conductivity $\sigma'(w)$ is obtained as Re(J/E):

$$\sigma'(w) = (2nNea_o^2/3\pi^2R). \sum_{\alpha=1,3,5\ldots} \frac{(w\tau_\alpha)^2/\alpha^2}{[1 + (w\tau_\alpha)^2]} \qquad 1.4.6$$

Eq.(1.4.6) contains, in principle, all the relevant information on the system, since $\sigma^* = iw\epsilon^*$, and the real and imaginary parts of ϵ^* are connected through the Kramers-Krönig relations eq.(1.1.13 & 14). Fig.(16) shows a plot of eq(1.4.6) for two values of RC, where $\tau_\alpha = RC/2q_\alpha$, $q_\alpha = 1 - \cos(\pi\alpha/n)$.

The main implication of eq.(1.4.6) is the existence of an infinite number of relaxation times. However, only the $\alpha = 1$ mode contributes the most (89% of the total), which, as will be apparent later, is to the disadvantage of the theory.

The general case where a D.C. bias is present can be treated similarly keeping in mind that the probabilities f_j are no longer equal nor are the transition rates $\vec{p}$ and $\overleftarrow{p}$. The algebra is rather cumbersome and will not be discussed. The results are given as follows:

$$\sigma'(w) = (Ne^2 p a_0^2 n/6\pi^2 k_B T)\{\coth(\eta/4).A + \tanh(\eta/4).B\}\eta \qquad 1.4.7$$

where :

$$A\ ,\ B = \sum_{\substack{\alpha\ odd,\\ even}} \frac{\alpha^2\ [(w\tau_\alpha)^2 + iw\tau_\alpha)]}{[\bar{\eta}^2 + \alpha^2]^2.[1 + (w\tau_\alpha)^2]} \qquad 1.4.8$$

$$\text{and}\quad \tau_\alpha = n/(\alpha^2 + \bar{\eta}^2).p_0\pi \qquad 1.4.9$$

$$\text{with}\quad \bar{\eta} = \eta/2\pi \quad \text{and} \quad p_0 = p.\exp(-\mathcal{E}_A/K_B T) \qquad 1.4.10$$

In this case it is observed that the relaxation times are shifted (decreased) in the presence of a D.C. bias. But more important, however, is the fact that the $\alpha = 1$ mode no more dominates the dispersion spectrum; in fact the largest contribution now comes from the mode for which:

$$(d/d\alpha)[\alpha^2/(\bar{\eta}^2 + \alpha^2)^2] = 0 \implies \alpha = \eta/2\pi$$

The physical meaning of this is that the effective length of the molecule is decreased by the application of the D.C. field.

Similarly the dielectric constant is given by :

$$K' = (Ne^2 L_o^2/6\pi^4 k_B T)\cdot\{\coth(\eta/4).G + \tanh(\eta/4).H\}\eta \qquad 1.4.11$$

where :

$$G\ ,\ H = \sum_{\substack{\alpha\ odd,\\ even}} \frac{\alpha^2}{[\bar{\eta}^2 + \alpha^2]^3.[1 + (w\tau_\alpha)^2]} \qquad 1.4.12$$

One important consequence of eq.(1.4.11 & 12) is the prediction

that after a certain frequency Wc, K' starts increasing with the electric field bias over a certain range of field values as can be obsereved from the plots of eq.(1.4.11) as function of frequency in Figs.(17-18).

As seen from the plots the frequency Wc is not unique and depends on the range of the E-field bias used. However, it's evident from the graphs that a minimum frequency exists, and is called the "cross-over" frequency. Below that frequency, K' always decreases with E-field bias for any field value, but above it there will be range of values for which K' increases.

Although it is a formidable task to try to determine the frequency Wc analytically it is evident from the graphs that it exists. Physically speaking, as the frequency is raised higher and higher, the polarization P would require stronger D.C. bias to achieve the same state of saturation as what can be attained at lower frequency (and hence lower fields).

Despite its success in explaining relaxation times and electric field bias effects, the Pohl-Pollak theory has some serious drawbacks the most important of which is the fact that the exponent in the power law for the increase of σ' with frequency always has a fixed value that cannot be related in any way to the polymer characteristics. Besides, the value of the exponent is > 1 (see Fig.16) whereas, in actually observed systems the value of the exponent is < 0.7 and varies from one species to the next. In addition to the above, the theory completely neglects the effects of D.C conduction which can be appreciable in some cases.

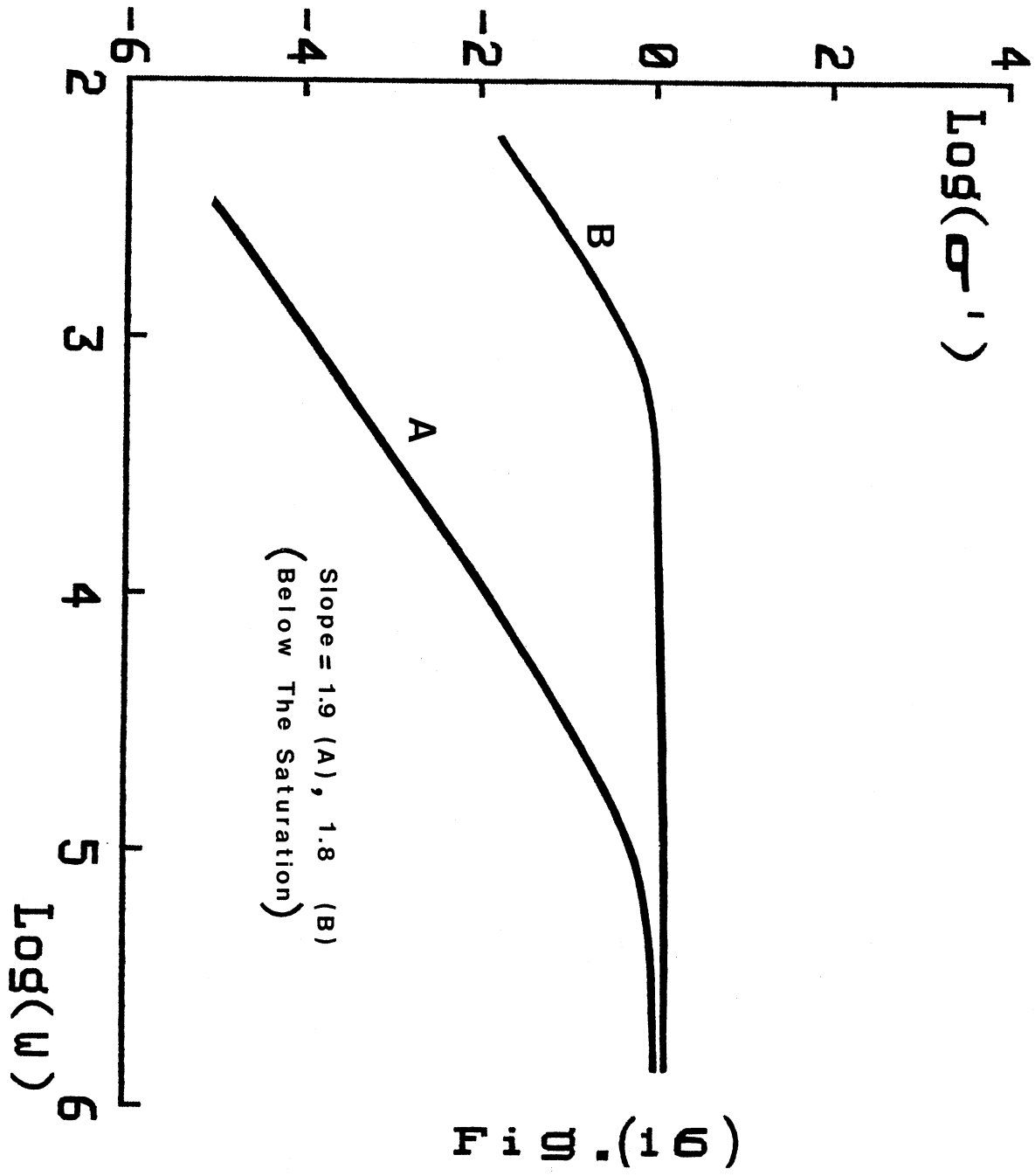

Fig.(16)

The A.C. conductivity according to the Pohl-Pollak theory, calculated for the first 10 values of α in eq.(1.4.6). RC = 1E-10 for curve (A), = 8E-9 for (B). n = 1000 for both The factor $(2nNea_o^2/3\pi^2R)$ is taken to be unity.

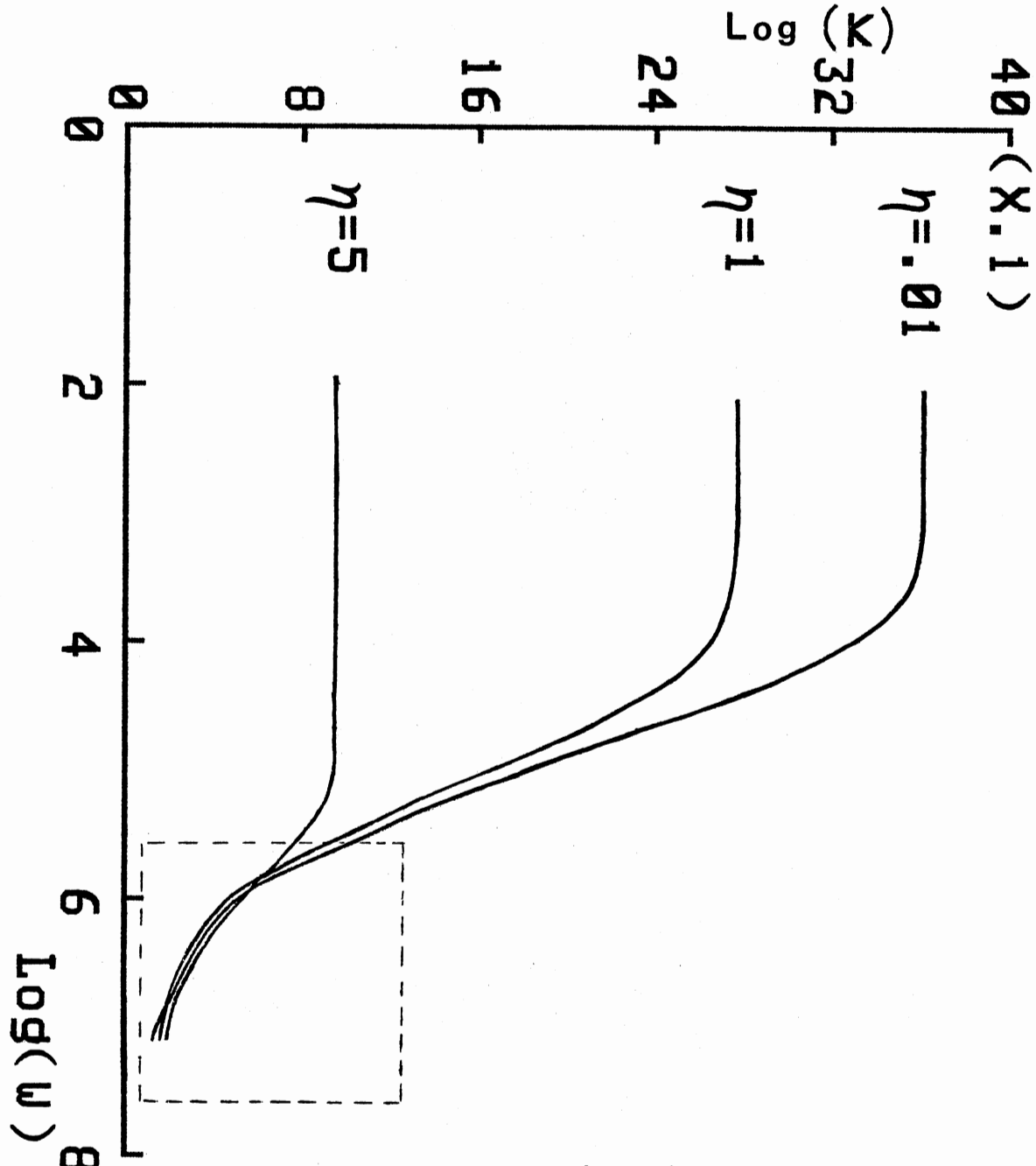

Fig.(17)

The dielectric constant as a function of the frequency for different D.C. electric field biases. The cross-over point depends on the pair of electric field values considered. Fig.(18) shows detail of the cross-over region. The factor $N(eLo)^2/6\pi^4 k_B T$ is taken to be 1000.

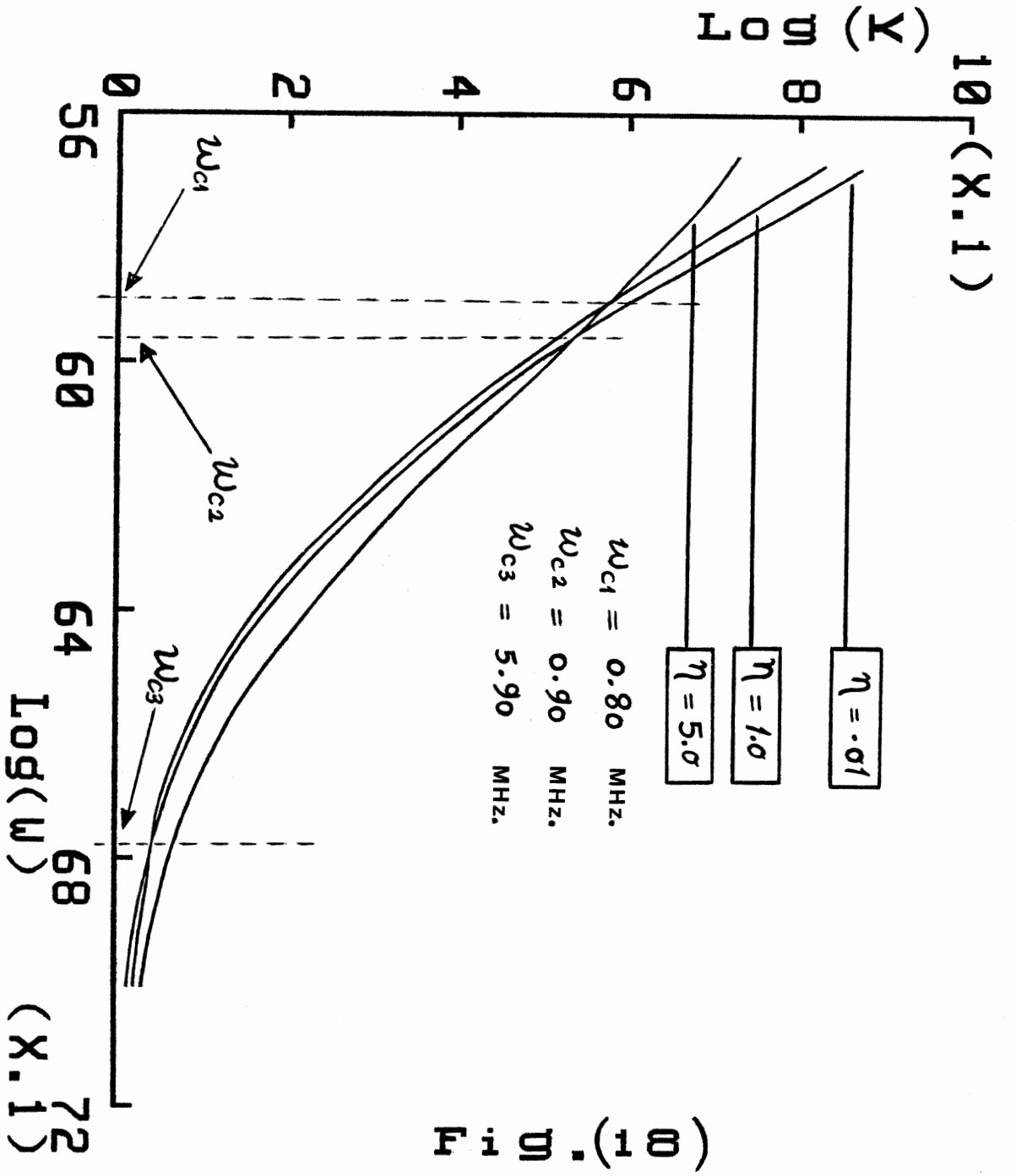

Fig.(10)

Detail of the cross-over frequency region. The value of Wc is much higher for pairs of curves corresponding to low D.C. bias and vice versa.

CHAPTER II

EXPERIMENTAL TECHNIQUES AND PROCEDURES, ERROR ANALYSIS

2.1) Representation of Dielectrics by Equivalent Impedance

We consider a parallel plate capacitor whose plate separation "s" is $<< \sqrt{A}$, (where A is the plate area) so that within the error allowance of our measurements, the capacitance in air (vaccuo) is appropriately given by:

$$Co = \epsilon_o A/s \qquad 2.1.1$$

Next we fill the space between the plates with a dielectric material having permittivity ϵ^* and conductivity σ defined by

$$D = \epsilon^* E \quad \text{and} \quad J = \sigma E + \partial D/\partial t \qquad 2.1.2$$

where E is the instantaneous electric field across the capacitor plates (within the dielectric), and J is the total current density. In general D is not in phase with E (refer to sec.(1.1), and so ϵ^* is a complex number $\epsilon' - i\epsilon''$. This also implies that J and E are not in phase with each other by virtue of the polarisation current term $\partial D/\partial t$. Thus we are naturally led to the concept of the complex conductivity defined by :

$$J = \sigma^* E \qquad 2.1.3$$

Using this definition and eq.(2.1.2) we obtain: (for the case when E = Eo.exp(iwt))

$$\sigma^* = \sigma + iw\epsilon^* \equiv \sigma' + i\sigma'' \qquad 2.1.4$$

$$\text{where } :\sigma' = \sigma + w\epsilon'' \ , \sigma'' = w\epsilon' \qquad 2.1.5$$

Now for a perfectly insulating material (σ = 0), we have: $J = iw\epsilon^* E$, hence in order to preserve the mathematical symmetry in the general case when σ is $\neq$ 0 , we introduce a "fictitious" permittivity ϵ_1 such that :

$$J = iw\epsilon_1 E \qquad 2.1.6$$

Comparison with eq.(2.1.3) yields :

$$\sigma^* = iw\epsilon_1 \text{ or } \epsilon_1 = \sigma''/w - i\sigma'/w = \epsilon' - i\sigma'/w \qquad 2.1.7$$

That ϵ_1 is more than a mere mathematical convenience may be realized by noting that since it relates two directly observable quantities J and E, then it must itself be an observable quantity. We may convert eq.(2.1.3) into a relation between the total current I and the voltage V by setting I = J.A = J.(ϵ_oA/s).(s/ϵ_o) = J.Co.(s/ϵ_o) and using eq.(2.1.6) gives :

$$I = Co.iw\epsilon_1 E.(s/\epsilon_o) = iw(\epsilon_1/\epsilon_o)Co.V = V/Z \qquad 2.1.8$$

where Z = 1/(iwCo.ϵ_1/ϵ_o), which has the standard form 1/iwC if we identify (ϵ_1/ϵ_o).Co as the capacitance C in the presence of the dielectric. The fact that C is a complex number indicates that the dielectric is not ideal but has losses of several kinds, including the loss from the free-charge conduction. We may define a "complex" dielectric constant K^* by K^* = C/Co, whose physical significance is seen as follows:

If we let $K^* = K' - iK''$ 2.1.9

then $1/Z = iwK^*.Co = iw(K'-iK'').Co$

$\Longrightarrow$ $1/Z = iwK'Co + wK''Co$ 2.1.10

This is equivalent to a lumped impedance network (Fig.19) made up of an ideal capacitor Cp (no losses) in parallel with a conductance G, the values of which are given by :

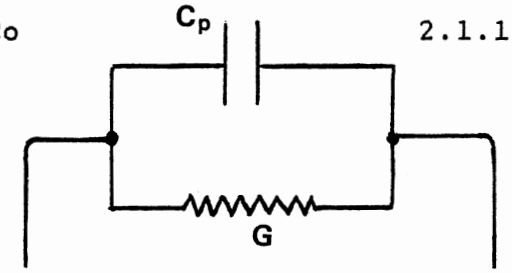

Fig.(19)

$$Cp = K'Co \quad \text{and} \quad G = wK''Co \qquad 2.1.11$$

Likewise, eq.(2.1.10) may be equally represented by a series equivalent network whose values are given by:

$$Rs = RpD^2/(1 + D^2) \quad \text{and} \quad Cs = D/wR = Cp(1 + D^2) \qquad 2.1.12$$

where : $Rp = 1/G$, and $D = 1/wRpCp$ 2.1.13

It can be shown (using the parallel equivalent representation), that over a quarter cycle, the ratio of the energy dissipated in the system to the energy stored in it is given by :$(\pi/2)/wRpCp$. For this reason the quantity $1/wRpCp = D$ is called the loss factor; and often referred to as the "loss tangent", since $D = k''/k'$ is simply the tangent of the angle that Z makes with the imaginary axis. We remark that the above result is independent of the particular representation used. Indeed, for the series case, the quarter-cycle energy ratio is $(\pi/2)wRsCs$, which by virtue of eq.(2.1.12) is identical to the parallel case. Consequently "D" is an "invariant"

of the series - to - parallel transformation .

In conclusion, the problem of measuring the parameters of a given dielectric has been reduced to that of measuring any general R-C type impedance. This topic will be taken up in the next section .

2.2) Methods of Impedance Measurements at Intermediate Frequencies

A) Introduction

At frequencies between 10 to 10^8 s^{-1} the most commonly used methods are those employing resonant circuits, or those making use of impedance bridges. Although each method offers certain virtues not found in the other, it is best to employ either one interchangeably depending on what is dictated by a given specific situation. For example, resonant circuits can be more accurate than bridges in the frequency regime over 1 MHz especially when low-loss materials are under study. The reason is due to the fact that at these frequencies it becomes increasingly difficult to account for the inductive effects and capacitive coupling between the various elements making up the bridge, thereby resulting in considerable and unnecessary error.

In order not to delve into areas beyond our immediate scope of interest the reader is referred to the literature on bridges and resonant systems. A particularly outstanding review by W.E. Vaughan appears in "Dielectric Properties and Molecular Behaviour" ed. T.M Sugden, Van Nostrand & Co. London 1969, p.108; other excellent treatments are given by Scaife (95), and Boyd (98). For our purposes, we shall focus the attention on the specific type of bridge used in our own measurements, with detail.

B) <u>The Schering Impedance Bridge</u>

The measurements presented in this work were done using a General Radio model 716-C Schering bridge and guard circuit. This type of bridge is considered ideal for the frequency range (100-500K) Hz. and is especially suitable for high voltage work. A schematic diagram of a Schering - type bridge (without the guard circuit) is shown in Fig.(20).

The bridge is operated in the "direct mode", whereby the unknown impedance Zx is balanced internally by the use of a pair of precision air capacitances C_N and C_A which have been calibrated to give the values of the series equivalent network for Zx at balance.

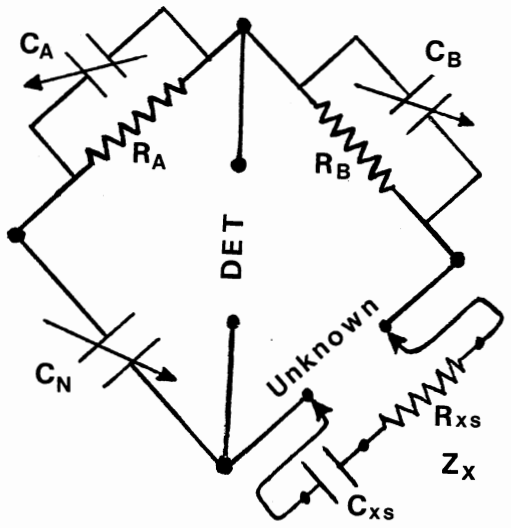

Fig.(20)

C_N is calibrated to give C_{xs} directly while C_A gives the loss factor $wR_{xs}C_{xs}$. The precision resistors R_A and R_B are varied through a range selector dial in order to balance the bridge at higher loss values. By solving the basic balancing condition of the bridge namely:

$$Z_A . Zx = Z_B . Z_N \qquad 2.2.1$$

we get: $C_{xs} = (R_A/R_B)C_N$ and $R_{xs} = (C_A/C_N)R_B$ 2.2.2

from which the loss tangent Dx is given by :

$$Dx = wR_AC_A \qquad 2.2.3$$

Thus C_{xs} is proportional to C_N while Dx is proportional to C_A

The range of capacitance for C_N is from 100 to 1050 pf. in divisions of 0.20 pf, but can be read to within an accuracy of 0.10 pf. The range of the loss factor dial is from about 0.0001 to 0.55, which at 1 KHz. and 150 pf. for C_{xs}, corresponds to a range of resistance from about 10^4 M.Ohms to 2.50 M.Ohms (parallel equivalents). Because of the particular way in which the bridge is built, there are additional correction factors involved. For Dx > 0.01, the true value for C_{xs} is given by :

$$C_{tr} = C_{xs} .(1 - 0.026Dx.(f/fo)) \qquad 2.2.4$$

where f is the operating frequency and fo is the "selector dial" frequency which is adjustable in decade steps from 0.1 to 100 KHz. The bridge will have optimal sensitiviy when the selector dial value fo is closest to the actual operating frequency f.

Similarly when Dx is > 0.1, its true value is given by:

$$D = Dx.(1 - 0.026Dx.(f/fo)) \qquad 2.2.5$$

The above corrections are intrinsic to the bridge and have to be carried consistently. Even so, there may be other calibrations needed to insure maximum accuracy. In our case we found that the loss dial of the bridge is skewed by about 20% for values of Dx $\leqslant$ 0.035, and by about 5% for Dx > 0.035 even after taking eq.(2.2.5) into account. For this reason the "D" appearing in eq.(2.2.5) will be referred to as the "nominal" D, while the real (correct) D will be the one called the true D, and denoted by D_{tr} . This will be discussed with more detail in sec.(2.5B) and Appendix (A)

C) Effects of The Leads and Sample Holder

In practice, the specimen to be measured is contained in a special cell or sample holder Fig.(21), which in turn is connected to the bridge via a coaxial cable.The sample holder consists of two parts: a main body whose structure and geometry are fixed, and a detachable module consisting of two plates designed to hold the polymer sample between them. This means that the impedance values read off the bridge include the contribution of the cable(s) as well as the sample holder. In order to account for this, one first balances the bridge with the cable and the main body of the sample holder attached to it but without the module containing the specimen. We let C_L , D_L be the dial readings (parallel equivalents) of the balanced bridge, after having done all the necessary corrections etc.. Now since the cable (leads), the main body of the sample holder, and the module are physically in parallel with each other, then the bridge readings (parallel equivalents) when the module is attached; namely C_T , D_T will be related to the initial set of values by :

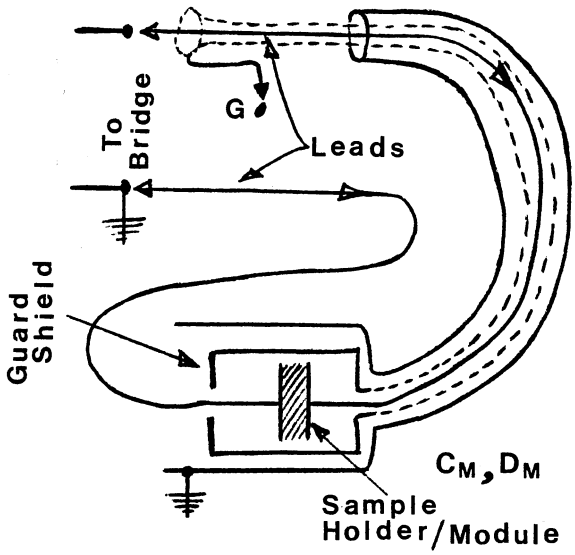

Fig.(21)

$$C_T = C_L + C_M \qquad 2.2.6$$

$$D_T\ C_T = D_L\ C_L + D_M\ C_M \qquad 2.2.7$$

where C_M is the capacitance of the module when filled with

the dielectric material to be measured, and D_M is the loss factor of that material. In practice the cable/sample holder losses D_L are negligible and of the order of 0.0005, so they can be neglected when dealing with high-loss materials whose D_M is > 1 (provided C_M is comparable to C_L). But when low-loss (insulating) materials are being measured it is imperative to retain all terms in eq.(2.2.7). The air value Co of the capacitance of the module is usually calculated from the geometry of the plates and their separation (as determined by the thickness of the specimen used). Consequently we have

$$C_M = C_T - C_L \quad \text{and} \quad D_M = (1/C_M).(D_T C_T - D_L C_L) \qquad 2.2.8$$

from which the dielectric constant of the material is found using the definition: $K' = C_M / Co$ (see eq.(2.1.11)).

D) <u>The Guard Circuit</u>

In a real-life situation, the grounded terminal of the bridge may not be at earth's potential; thus there exists a virtual (stray) capacitance to earth from the "high" terminal electrode holding the sample as well as from the "low" electrode. These capacitances combine in series, and their equivalent, Ce, appears in parallel with the specimen module. This may cause appreciable fluctuations in the readings since the capacitance Ce is a function of the surroundings. In order to circumvent this problem, the module containing the sample is enclosed within a shield whose potential can be controlled.

By bringing the potential of the shield to that of the ground electrode, the "high" terminal will always "see" the same identical surrounding and thereby more stable and reproducible readings are assured. To see how this is accomplished we consider a three-terminal bridge system shown schematically in Fig.(22). This is called a guarded bridge system. Suppose that a third point G is created with respect to the terminal module and is electrically insulated from either one of its electrodes. Point G is connected to point 3 as shown. The bridge is balanced if points 1,2, & G are at the same potential. Simple algebra shows that balance is achieved if either one of the following conditions holds:

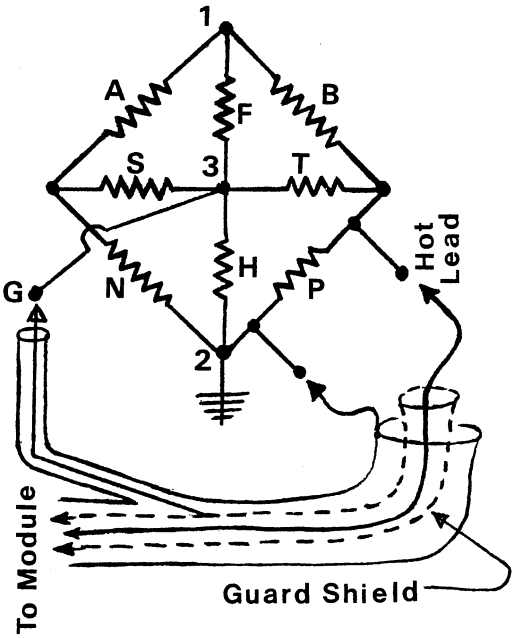

Fig.(22)

$$A/B = N/P = S/T \qquad \text{or} \qquad A/B = N/P = F/H \qquad 2.2.9$$

Thus by varying the impedances until a minimum is observed in the detector, we can be assured that the potential of the "guard" G is the same as that of the "ground" electrode.

The guard circuit employed in the experiments is a General Radio model 716-P4 system. Detailed layout of the complete guard and bridge systems is shown in Fig.(23). In practice the guarded bridge system is balanced iteratively in three-step cycles: First the "coupling" resistance F is varied un-

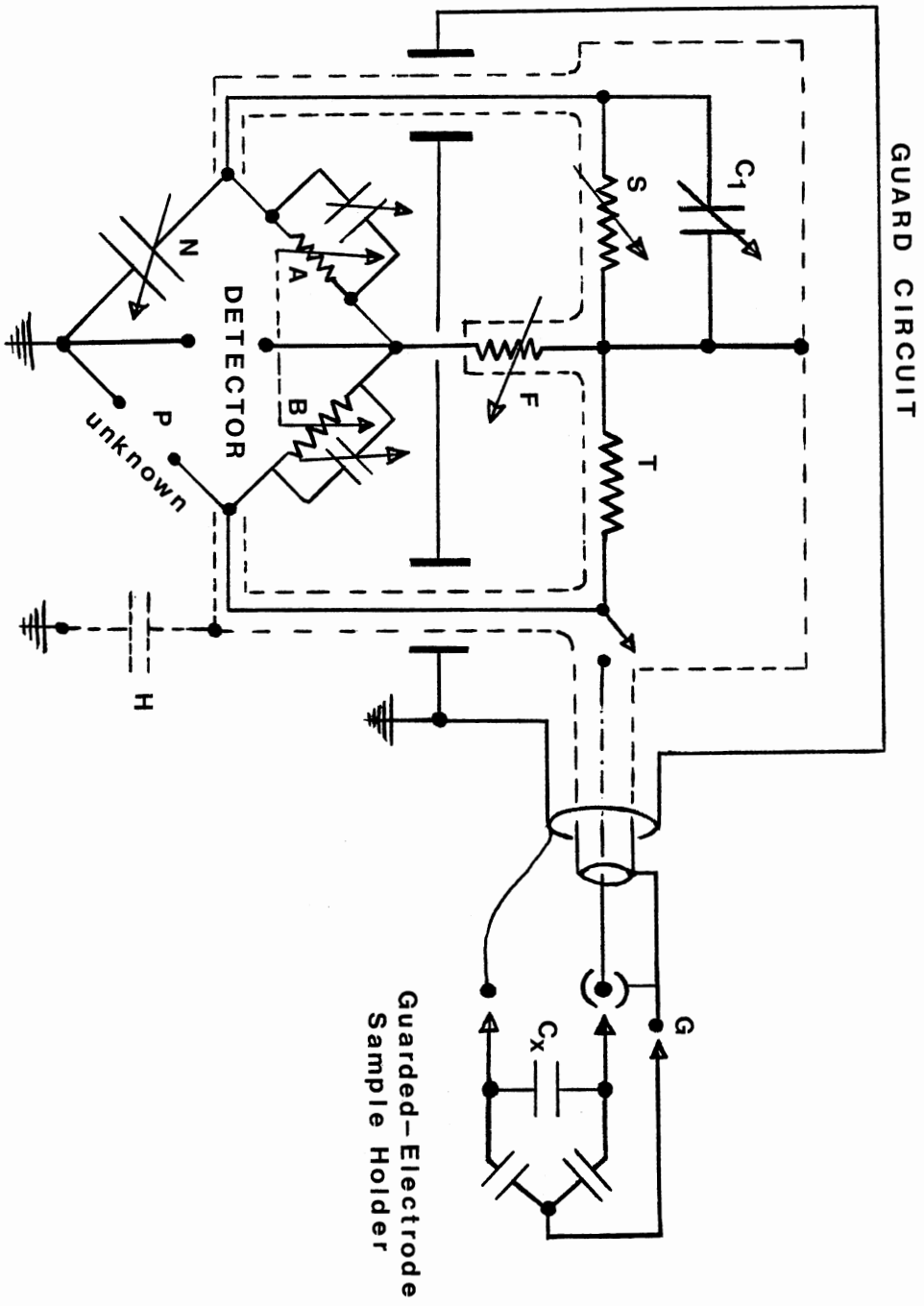

Schering Bridge With Guard Circuit Attachment And The Equivalent Schematic Of The Guarded Sample Holder.

Fig.(23)

til a minimum is reached, then the guard impedance S is varied in both its parts, and finally the bridge capacitances are varied till a minimum is reached. This process is repeated over and over until no further reduction in the signal is observed. The procedure is lengthy, laborious and requires between 3 to 5 iteration rounds to obtain a good balance.

2.3) D.C. Measurements

In this section we discuss the problems involved in the study of the DC response of a given material. Since DC observations are an integral part of the correlation analysis no study would be complete without them. We shall be concerned only with the measurement techniques for the (ohmic) conductivity. Techniques relating to the static dielectric constant measurements will not be discussed in this work due to our having to delete this topic from our program for lack of time and funding. Those interested are referred to the appropriate sources (99-102).

Measurement of The Ohmic Conductivity

Since highly insulating materials require appreciable voltage across them in order to produce measurable currents and since the conductivity of the materials under study are known to change drastically with high voltages, it is anticipated that we shall be dealing with small currents of the order of 10^{-8} amperes in order not to exceed the voltage limits beyond which begins to depend strongly on the electric field. According to the model discussed in chap. one, a given voltage is "safe" if the corresponding electric field does not exceed 400 V/cm. For a sample of 20 mil thickness, this translates into a max. of 20 Volts. However, in order to get a good working range with samples that might be as thin as 10 mils, we elected to use a half-way value of 10 Volts for most

of the samples. Only a couple required some 30 Volts across them for a measurable current.

A standard set-up for conductivity measurements is shown in Fig.(24). The μ-ammeter is in series with the sample and the 10 V source is a regulated power supply. The resistance of the ammeter can be as high as 100 M ohms depending on the sensitivity scale being used, and as such, must be accounted for in the results. This calls for an accurate calibration of the μ-ammeter at each setting (see Appendix A). If Rg is the resistance of the ammeter at a given setting, the resistance of the sample is given by:

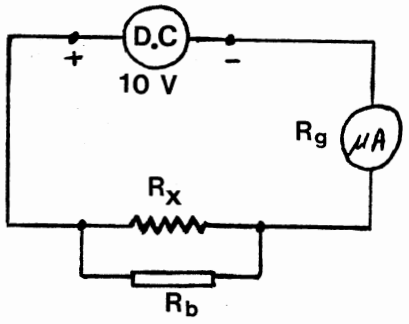

Fig.(24)

$$Rx = V/I - Rg \quad \text{where } V = 10 \text{ Volts} \qquad 2.3.1$$

The conductivity is then computed from knowledge of the sample geometry according to $\sigma = (d/A \cdot Rx)$ 2.3.2

where "d" is thickness and "A" the cross-sectional area.

In practice the sample holder itself may have "leakage" resistance comparable to that of the material tested and so it must be accounted for in the results. This "background" conduction can be estimated by taking a reading of the current without any material in the sample holder. This yields a resistance R_b . Now the value of Rx appearing in (2.3.1) is in reality the parallel equivalent of R_b and the true sample resistance Rs, therefore we get for the correct sample resist-

ance Rs :

$$Rs = R_b Rx/(R_b - Rx) \qquad 2.3.3$$

and $$\sigma \text{ (true)} = d/(A \cdot Rs) \qquad 2.3.4$$

Usually the above correction is necessary only in extremely insulating materials, and for our situation it was only needed on two occasions as our sample holder has a practically infinite leakage resistance (better than 10^{12} ohms).

2.4) Measurements Under Varied Macroscopic Conditions

A) Pressure Dependence

To observe the dielectric parameters as a function of pressure the powdered material is placed in a constraining ring made out of teflon, and is pressed between two carborandum/steel anvils as illustrated in Fig.(25).The outer cylindrical shell is present for reasons of safety, and to help prevent lateral slippage of the anvils. Electrical contact to the sample is provided through the anvils themselves via a pair of leads at the top and the bottom as shown. A 1.5-ton Pasedena Hydraulics model 7-4664 press was used to provide pressures up to 3.5 Kbars. In order to insure proper molding of the formed pellet, the sample has to be compressed two or three times to about 2.4 Kbars before any readings can be taken. Measurements must be made from low pressure upwards and not the reverse. Data for both D.C. and A.C. measurements should be taken concurrently and in the shortest possible time to obtain good reproducibility. The pressure has to be monitored continuously since the press valves relax over extended

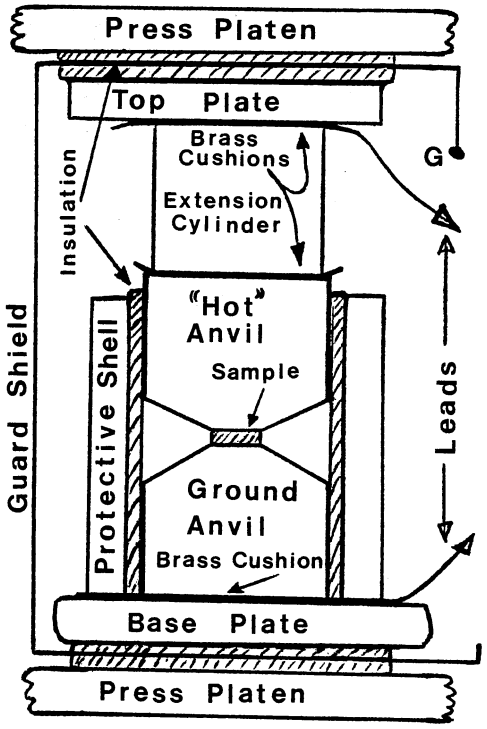

Fig.(25)

periods causing erroneous pressure readings, particularly in polymers having large coefficients of variation. Furthermore, since humidity can be a very critical factor in affecting polymer properties (103-105), and since in our case it was not possible to enclose the whole press in a moisture free environment, we had to take our data on dry days, which according to The Weather Bureau, should have a relative humidity below 65% .

Most of the polymers in this study were easily pelletable and did not fracture while being removed from the press. The only exceptions were LD-52B and LD-106 which were very brittle, and presented great difficulty in obtaining a full circular pellet.

B) Temperature Dependence: The Constant Pressure Cell

The principle of the constant-pressure sample holder has been discussed by Hottman and Pohl (106). Their idea is based on the famous C - section clamp developed by Chester & Jones (107) shown in Fig.(26).

We present here a somewhat different treatment than either of the above references in order to bring out the more subtle points of the theory, and to help assess how far off the system is from being ideal.

For simplicity, we shall assume that the expansion takes place along the longitudinal direction only. By choice, metal B has a greater expansion coefficient than metal A. From the

figure we see that as the A-side expands "outwards" at a rate α , the B-side expands "inwards" at a larger rate β . So by a proper choice of the parameters, we should be able to keep the gap size constant or allow it to acquire a pre-determined size (if the specimen to be held in the gap is also known to expand appreciably). After the expansion, the gap size S, becomes S' such that:

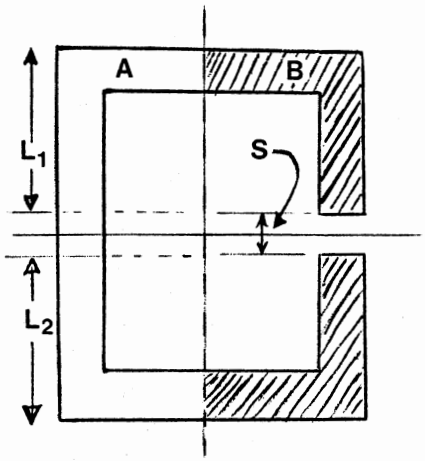

Fig.(26)

$$S' + (1+\beta).(L1 + L2) = (1+\alpha).(S + L1 + L2) \qquad 2.4.1$$

or :

$$S' = (1 + \alpha)S + (\alpha - \beta).(L1 + L2) \qquad 2.4.2$$

Without loss of generality, we may suppose that the specimen in the gap also expands to a new size $d' = (1 + \gamma).d$ (where initially $d = S$). Hence if there is to be no differential pressure on the sample as a result of the expansions we must have :

$S' = d' = (1 + \gamma)\ S$, which by eq.(2.4.2) translates into:

$$(\alpha - \gamma).S = (\beta - \alpha).L \quad , \quad \text{where } L = L1 + L2 \qquad 2.4.3$$

In practice it is the length L that is chosen to suit the gap size in accordance with eq.(2.4.3) and not the other way around. More sophisticated clamps provide "variable L" modification to accommodate different gap sizes. Since typical values of L/S are of the order of 100 , then for ($\gamma \ll \alpha$),

the above theory will work only if α and β are in very close proximity with a difference of no more than 0.01. This stringent demand is not met by most pure metals, and so the only way around this is to use different alloys of the same metal with highly controlled percentages. In the case when γ is as large as α, or extremely close to it, it is better to use the same metal all around; that is: take $\alpha = \beta$.

The above conditions can be very hard to realize in practice, and also very costly. So we had to settle for a chamber whose design is well within our means. The shortcut contemplated in this regard is backed by the fact that for most familiar metals α is of the order of $10^{-6}/°K$, and so the relative % change in the gap size for a homogeneous clamp (for which $\alpha = \beta$), will be about 0.0001%. The real fractional change will be even smaller, since the specimen itself may expand slightly and help close the gap.

Consequently with our relatively wide margin of error the above approximation should be very adequate without any fear of yielding erroneous results. It should be pointed out however, that at temperatures above 75 °C our chamber did not accommodate the fast expansion rate of the compressed-powder pellets, which showed about 10% change in thickness, resulting in excessive squeezing of the sample. Because of this we decided to limit our operating temperatures to those between liquid air and room temperature, for most of the samples, as there was no apparent squeezing effects within this range.

For our particular needs we had to design a chamber that

will not only accommodate temperature measurements, but also the D.C. electric field case as well; and at the same time provides guard-shielded measurements for maximum protection against fluctuations. These demands are met in the design of the special chamber shown in Fig.(27).

The inner insulation lining (I) is made of a special glass-filled phenol acrylic substance, which is capable of withstanding over 20000 volts/cm, and has a high-temperature capabilty up to 350 ^{o}C. This material also has other ideal features such as a low loss factor, and an ability to endure repeated mechanical stresses without becoming brittle at low temperatures. It is also very resistant to moisture.

A copper-constantan thermocouple (E) is located on the side of the bottom anvil (X) to monitor the temperature effectively. Four, equally spaced windows (not shown), are cut in the inner lining to help increase the heat transfer and insure a uniform distribution of temperature throughout the chamber body. This is needed since neither electrode has any metallic contact with the main guard shield body (G) around which the heater wire (F) is wrapped. The movable plate electrode (A) is attached to the "advancement" screw (B) by means of a shoe-mount type accessory (O) which allows its easy removal or installation. The shoe is precisely machined to the size of the mount to prevent any displacement along the vertical direction (which can be crucial at large D.C. elctric fields), while at the same time it allows for a smooth rotation of the plate around the vertical axis, which is essential

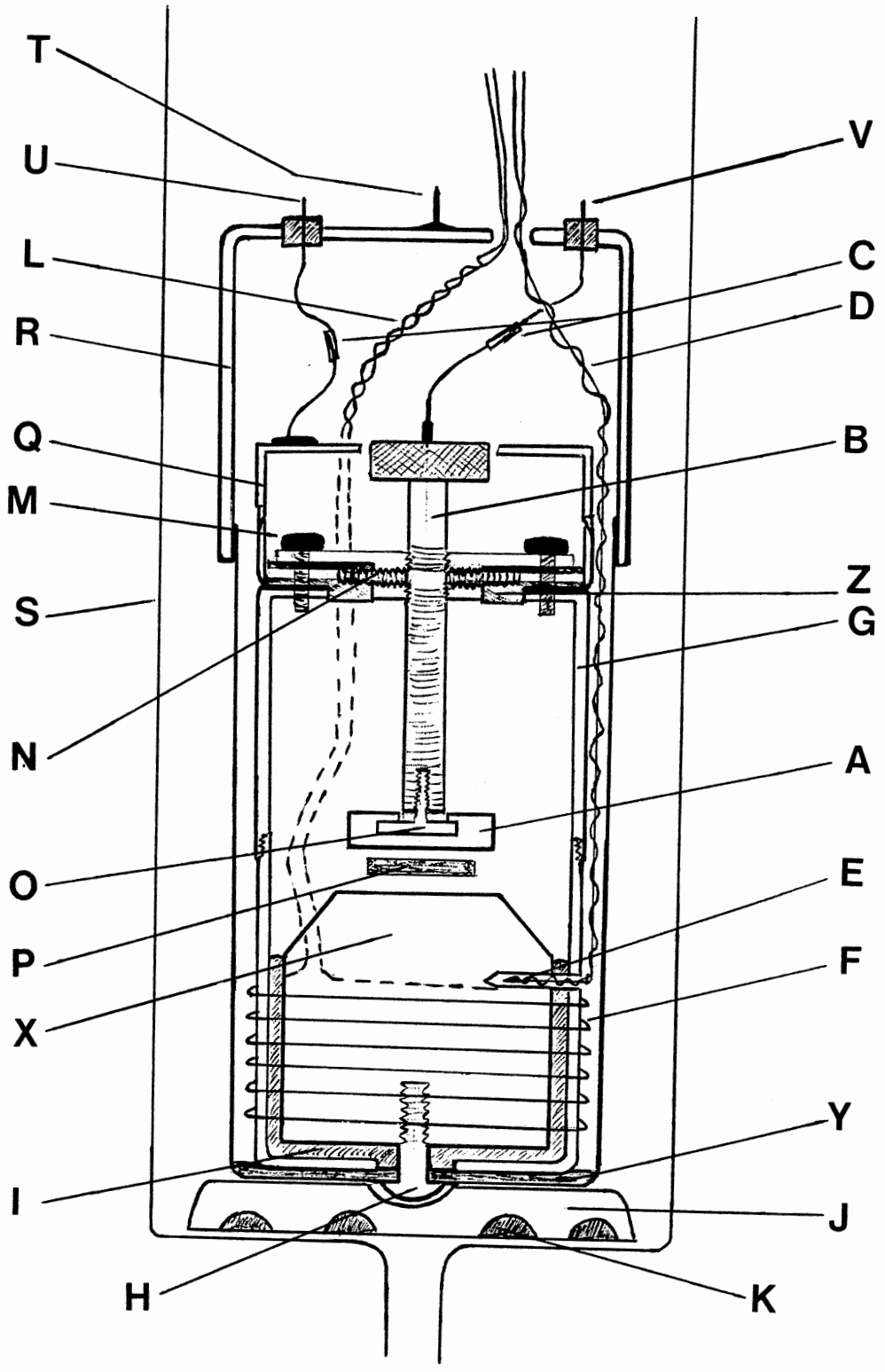

Fig.(27)

in preventing shear while the plates are being tightened onto the sample (P). The heater is made from an 8-mil diameter tungsten wire, having a total resistance of about 11 ohms. The wire is wrapped around the guard shield chamber as shown. The heater current is provided by a 35 volt D.C. power supply and a 10 - Ohm / 5 amperes rheostat. For a long service life of the heater it is recommended to cast the wire in an epoxy having a wide temperature range. The bottom anvil (ground electrode) (X) is electrically connected to the ground shield (R) via a screw (H) at the bottom end. Two steel screws (N) provide a tight clamp around the shaft of the main "advancement" screw (B). The portion where this clamp presses is left unthreaded. The top (cap) section (Q) of the guard shield (G) is attached to the main (bottom) part by means of three special heat resistant plastic screws (M). An insulating washer (Z) that fits like a collar around the thread mount holding (B) keeps the guard electrically insulated from the "hot" electrode (A). Detachable gold pins (C) and (T,U,V) provide the necessary electrical connections to the outside.

The chamber rests on a special hard teflon seat (J) equipped with vents (K) to provide efficient venting of gases into or out of the chamber's Pyrex glass enclosure (S). This enclosure allows us to control the environment of the sample for either a nitrogen bath or a vacuum surrounding. The top portion of the guard shield (G) has three circular windows (not shown) for rapid venting and heat transfer. A teflon pad (Y) insulates the guard (G) from the ground housing (R).

C) Measurements Under D.C. Electric Field

For observing the ohmic conductivity under large D.C. electric field, the circuit arrangement used is the same as the one shown in Fig.(24) except that an ammeter or a milli-ammeter is substituted to accommodate the larger currents.

Because of the special cell design there is no effect of pressure from the electrostatic force created by the high voltage (which can be as much as 15 PSI at 20,000 V/cm). The high voltage regulated power supply is a North-East Scientific Co. model RE 1602 with a continuous range of 300 V. to 1,500 V. A 250-K.Ohm potentiometer is used to obtain low voltages below 300 V.

When it comes to A.C. measurements there are two circuit arrangements to provide high D.C. voltage on the sample without interfering with the bridge operation. These are sketched in Fig.(28 a & b). Configuration "a" has the advantage of providing higher D.C. voltage without having to worry about the bridge elements since the whole bias circuit is external to the bridge. Its main drawbacks however, are that both plates of the sample holder are "floating" with respect to D.C which makes it difficult to eliminate fluctuations using the guard circuit. Further it is very difficult to account for the shunting effect of the power supply when calculating the sample capacitance and loss, since its parameters fluctuate with the 57 cycle line voltage conditions. Attempting to reduce the fluctuations by using a value for R1 >> Rs will only create

more problems since Rs depends critically on the voltage across it, which means that the true voltage across the sample cannot be known because the charging current in the loop satisfies a non-linear equation. In fact the only way to be sure of what the voltage across the sample is, is to keep R1 << Rs.

Thus to avoid potentially serious problems we elected to use configuration "b". This arrangement eliminates all the problems associated with circuit "a" since the power supply appears in parallel with the A.C. source and therefore has no bearing whatsoever on the condition of balance. The only limitation is that we are restricted in the high voltage to no more than 900 volts so as not to surpass the bridge ratings.

The blocking capacitor C_B is chosen to be large enough that it is effectively an A.C. short even at 10 cycles. It is actually a set of three capacitors in series each of which is rated to withstand 600 volts, so that the series combination can carry as much as 1,200 V.

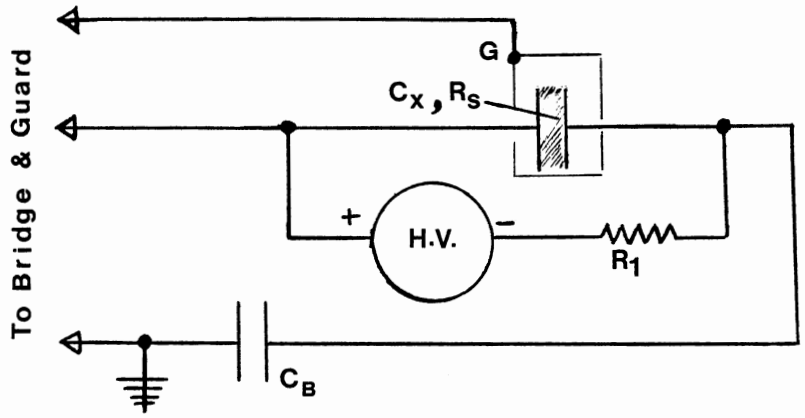
To Bridge & Guard
G
C_X, R_S
+
H.V.
−
R_1
C_B

(a)

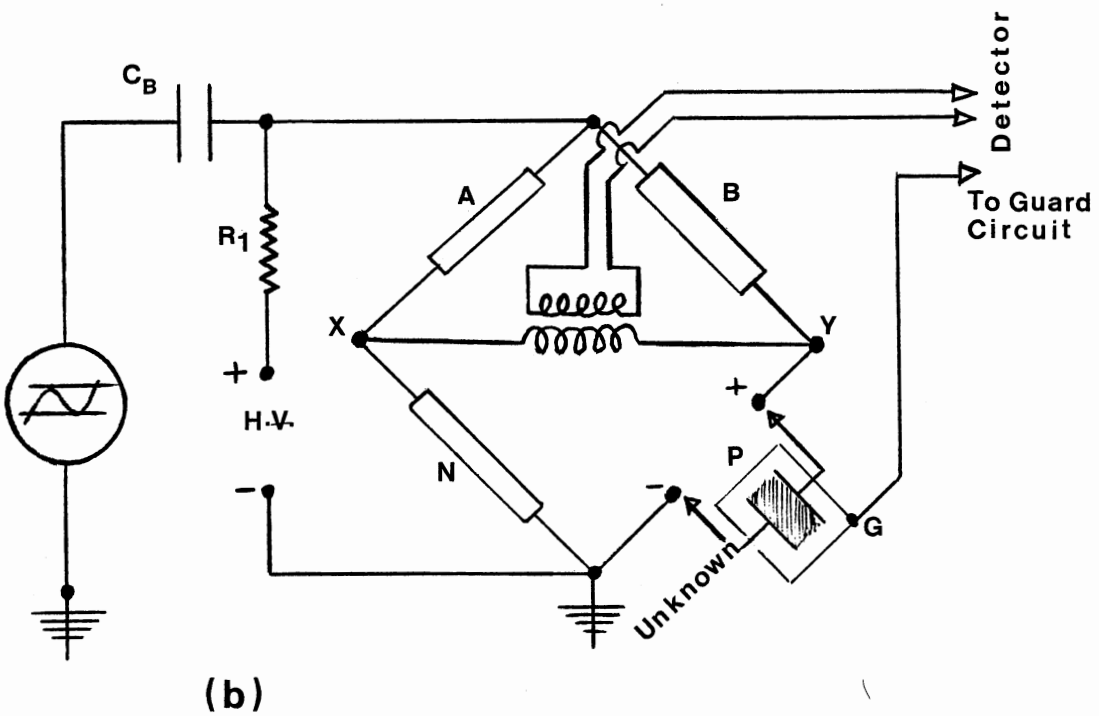
C_B
R_1
+
H.V.
−
A
B
X
Y
N
P
+
−
G
Unknown
Detector
To Guard Circuit

(b)

Fig (28)

2.5) Some Graphical Techniques, Error Analysis and Reproducibility of Measurements

A) Graphical Methods Relating to The Extraction of ϵ'' From The K" - Data

It was mentioned earlier, (Sec.(1.1 C)) that the analysis of experimental results on $\epsilon'(w)$ and $\epsilon''(w)$ cannot be done unless the value of σ has been accounted for. According to Sec.(2.1) the imaginary part of the permittivity ϵ_1 defined in eq.(2.1.6) is given by: $-\epsilon_o K''$ (since $K^* = \epsilon_1/\epsilon_o = K' - iK''$). Thus by eq.(2.1.7), $\epsilon_o K'' = \sigma'/w = \epsilon'' + \sigma/w \equiv Y$ 2.5.1

Thus a Cole-Cole plot of the experimentally determined (Y) will look as in Fig.(29) (based on a simple Debye model).

It is clear that the larger the ohmic conductivity, the larger is the departure from the circular shape.

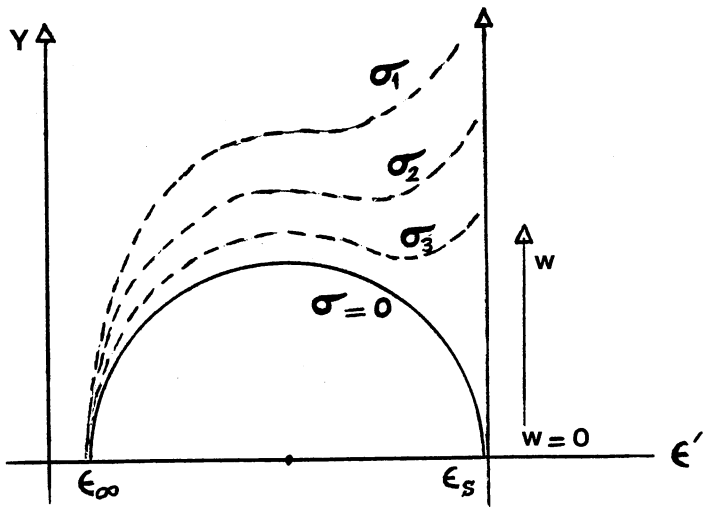

Fig.(29)

Now according to eq.(1.1.22), $\epsilon_0 K''$ may be approximated suitably over the w - domain as follows:

For $w\tau << 1$, $Y \approx \sigma/w$ 2.5.2

$w\tau >> 1$, $Y \approx (\epsilon_s - \epsilon_\infty)/w\tau$ 2.5.3

$w\tau \approx 1$, $Y \approx (1/2).(\epsilon_s - \epsilon_\infty)w\tau + \sigma\tau$ 2.5.4

If we denote by I ,II and III the respectively defined regions then we may write for the corresponding values of $\epsilon_0 K''$:

$\log(YI) = \log\sigma - \log w$ (region I) 2.5.5

$\log(YII) = \log[(\epsilon_s - \epsilon_\infty)/\tau] - \log w$ (region II) 2.5.6

It follows (treating YI ,YII as legitimate functions for all w) that:

$$\log(YII) = \log[(\epsilon_s - \epsilon_\infty)/\tau] + \log(YI) - \log\sigma$$

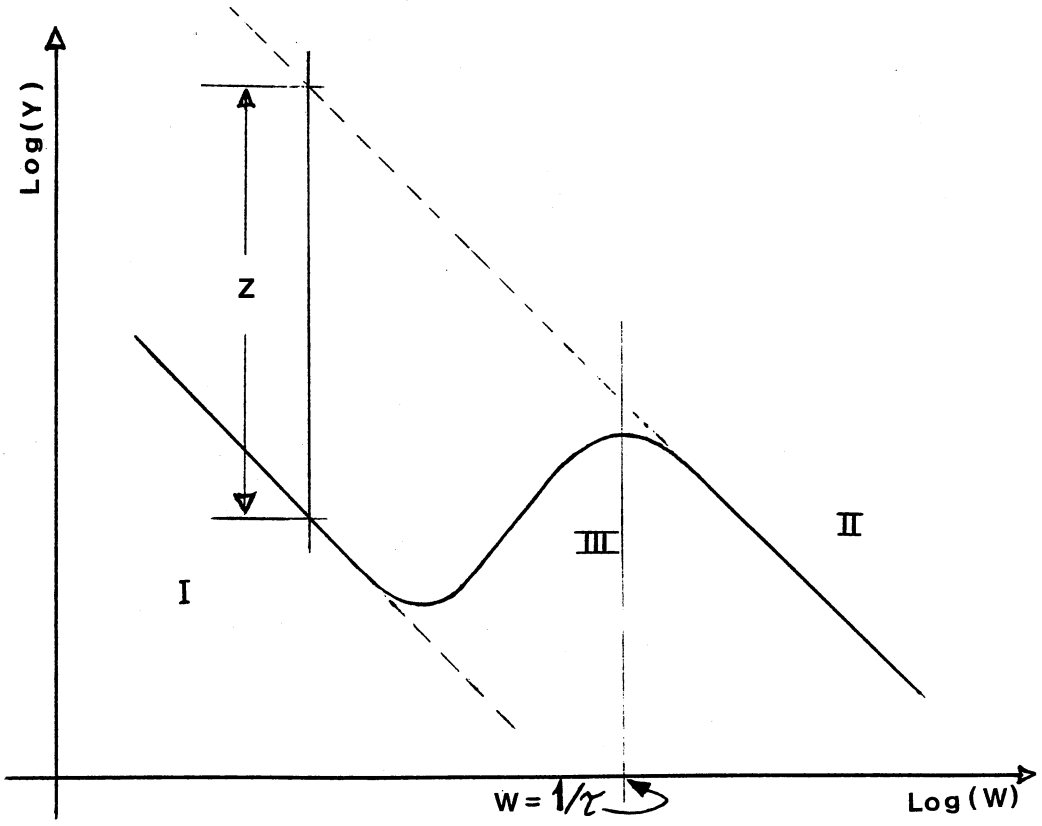

Fig.(30)

or $Z \equiv \log(YII) - \log(YI) = \log[(\epsilon_s - \epsilon_\infty)/\sigma\tau]$ 2.5.7

Eq.(2.5.7) gives us a versatile tool in the manipulation of experimental data: Since Z is determinable from the graph in Fig.(30) as the vertical shift between YI and YII in region I, τ can be obtained from the inverse frequency at maximum Y (= YIII).

It follows that (2.5.7) provides a direct link between the ohmic conductivity σ and the dielectric range $(\epsilon_s - \epsilon_\infty)$. Thus if σ is known from D.C. measurement, $(\epsilon_s - \epsilon_\infty)$ may be readily computed. This is a much easier alternative to the Cole-Cole plots, which requires a much wider frequency range In fact if $\epsilon''(w)$ is known over the "entire" spectrum, we can make use of eq.(1.1.13) to calculate $\epsilon''(0) \equiv \epsilon_s$ to get :

$$\epsilon_s - \epsilon_\infty = (2/\pi) \int_0^\infty \epsilon''(v)\, d(\log v) \qquad 2.5.8$$

The integral on the right-hand side of eq.(2.5.8) is nothing but the area under the graph of $\epsilon''(w)$ plotted versus log(w). Thus by numerical integration, the area A can be obtained and we get :

$$\epsilon_s - \epsilon_\infty = (2/\pi).A \qquad 2.5.9$$

Of course the validity of (2.5.9) rests on how extensive our knowledge of $\epsilon''(w)$ is. Polymers in general, display a broad loss peak and more often the maximum of $\epsilon''(w)$ is very flat and barely noticeable, which means that if eq(2.5.9) is to be of any use, $\epsilon''(w)$ has to be known over 12 decades of frequency. This in itself can be a formidable task!

B) Getting a Hand on Errors

1) Sources of Systematic Errors. These types of errors may be traced to three major contributions:
a) Accuracy of the impedance bridge dials. b) Stability and control of the environment surrounding the mounted sample. c) Non-ideal geometry and finiteness of the sample size. Relating to the first issue, it has been found that the particular bridge in use showed a systematic difference in its "loss factor" dial readings when compared against a standard set of precision resistors which had been precisely measured (to within 0.1%) using a Hewlett-Packard model HP-3468A digital multimeter. The calibration of the loss dial was carried out under guarded shielding conditions including a special guarded box for the standard resistors. This kept the error in the capacitance readings at a minimal value of about 0.5%. Otherwise, stray capacitance created by the variation in the resistors' geometry and the number of elements present in the box holder may cause as much as a 10% increase in the capacitance values especially at the higher end of the "loss-dial".

The results of the loss-dial calibration are given in appendix (A) along with the graphs and the computer programs used to obtain them. The calibration's standard estimate of the error is very precise and is between (1-2)% .

The calibration was done for eight different frequencies ranging from 100 Hz.- 100 KHz.

As far as the environmental surroundings of the sample are concerned, they may be divided into two parts:

b1) Making contact with the sample.

b2) Effects of the atmospheric conditions.

In (b1), the initial arrangement was to clamp the pressed pellet between the plates of the capacitor module at a minimal constant pressure of 2 to 3 PSI using a special spring mechanism of known stiffness. However the above set-up did not provide a means to "lock" the movable plate of the module in a specific desirable position; a demand which can be very crucial when working at high D.C. bias voltages. For example at 20,000 V/cm. the pressure arising from the attractive coulomb force between the plates is $\approx$ 15 PSI, which could produce some error (as much as 50%) in the D.C. conductivity values. Due to this and other reasons connected with part (b2), the spring-type clamping device was abandoned and a new chamber/ sample holder was designed with the above considerations in mind.

The module of the new chamber has been described in sec. (2.4)/ Fig.(27). It suffices to mention here that the movable plate of the capacitance module was held in position by employing a shoe-mount at the end terminal of the main "advancement" screw (B), upon which the movable plate rides. Contact pressure with the sample is set at a fixed value by referencing it to the pressure created by a pre-determined standard weight, employing D.C.- type current measurements similar to those described in sec.(2.3).

The advancement screw was locked in place at the correct pressure via two tiny screws (N) that were fitted to the collar piece mount holding the shaft of the advancement screw. Great care being exercised to avoid the possibility of electrical shorts.

Due to practical considerations the background capacitance was measured in the absence of the module's movable plate (A). This caused the "hot" pin (main advancement screw shaft) to intercept a wider solid angle at the position of the ground (fixed) plate, over what it would if the movable plate was in place. The error involved although very small, was accounted for by comparing measurements on standard materials having low dielectric constant (such as teflon and plexiglas), with their accepted literature values. The correction factor so obtained was found to be (0.81 ± 0.2) pf.

(b2) Early in the program it was observed that the humidity of the atmosphere as well as its ionic content, had an appreciable effect on the loss-factor data. This observation has been well documented by numerous authors particularly in relation to polymer materials (103-105).

Because of this, it was decided to place the whole chamber system containing the guard shield and the module, in a specially designed vacuum enclosure as in Fig.(27). This helped stabilize the readings and greatly improved the reproducibility of the data. Of course, since the main body of the Schering Bridge could not be accommodated into a vacuum housing due to a variety of reasons, we had to take into considera-

tion the fluctuation in its open-terminal readings on a daily and sometimes on an hourly basis. The corrections were reflected as adjustments in the Y - intercepts of the loss - dial calibration graphs (Appendix A)

Coming to the third source of error, we note that this issue relates mostly to the dielectric constant and the D.C conductivity of the material. It's completely irrelevant as far as the loss factor is concerned, since the latter is an intrinsic property of the material, and is not dependent on the sample geometry.

Perhaps the greatest error contribution of geometrical origin comes from the non-uniformity in the thickness of the specimen causing wedge-like gaps to exist between it and the capacitor plates. In our case, the pressed, disc-shaped pellets showed a bulging effect around the central region of about 0.5 to 1.5 mils thicker than at the edges for a typical sample thickness of 20-30 mils. According to appendix (B) the error in the dielectric constant resulting from such an imperfection (relative to the ideal situation when the dielectric fills the whole space), is in the range of (8-15)% depending on what the dielectric constant is.
The pressure while forming the pellets was limited to 1,200 PSI in order to prevent the cusping of the anvil heads and thereby reduce the chance of formation of a central bulge.

Geometrical imperfections presented yet a more serious error in the D.C. conductivity measurements where in some cases the surface irregularity prevented us from determining

what the true area of contact was, thereby resulting in a less-than-average reproducibility. In order to combat this problem, we had to grind the powdered polymers into ultra-fine particles. It should be pointed out, however, that reproducing the grain size to the same degree each time is an impossible task, but we kept the grinding time length fixed, figuring that it affects the grain fineness proportionally. The powder was crushed inside a paper folder using the same steel block weight each time.

The effect of coarse-grain and fine-grain sizes on the conductivity (D.C. to 100 K.Hz), and the dielectric constant is shown in tables (3.2-3.4), and the corresponding graphs in Figs.(32-38) for LD-105, 104, and 97.

The area of the sample (which may not necessarily be that of electrical contact) was always measured with a high degree of precision (to within 0.5%) and therefore paused no major problem as such, since it was accounted for within the error analysis computations.

The effects of the edge corrections due to the finite size of the capacitor plates has been studied by Wintle and Kurylowicz (108), who showed that for a typical aspect ratio (plate's dimension / plate separation) of 10 there is about 14% relative error. However, the above does not apply to the case of guarded electrodes since in that situation the lines of force from the exterior faces of the capacitor plates do not meet due to their diversion by the guard electrode.

Finally, when taking readings as function of pressure while the sample is between the press anvils, one must correct for the change in the sample thickness as the pressure increases. Observations on the sample thickness at the highest gauge pressure used (namely 1200 PSI), revealed very small compression, no more than 8% of the original thickness at zero pressure. However, in order to be on the safe side, an error analysis was made to see how much the difference between a corrected reading and an uncorrected one would influence the values of K and σ, assuming as much as 10% relative compression in the sample thickness at 1200 PSI. The thickness as a function of the lower pressure values being scaled linearly. The results indicate that only the high pressure readings are important; with K showing 8% relative deviation while σ was off by $\simeq$ 7% for the polymer LD-105 at 700 PSI. Consequently for the sake of consistency, we elected to incorporate the correction at all pressure values so as to reduce our chance of propagating undesirable errors.

2) Sources of Random Errors. There are three main sources of random errors:

a) The electronic hum (60 cycle line signal); and the S/N ratio as the bridge approaches balance.

b) Random fluctuations in the background characteristics of the bridge due to changes in the surroundings: temperature, humidity & ionic content.

c) The D.C. electrometer readings for the measurement of current.

The first problem was taken care of rather remarkably by using two highly selective, low-noise tuned amplifiers with a total gain better than 140 dB. The sensitivity so obtained, allowed us to detect variations around the minimum values as small as 0.05 pf in the capacitance and to within (1-10)% in the loss factor dial depending on the frequency being used. The worst cases being at the 100-200 Hz. range; improving as we go up in frequency. The tuned amplifiers were: a P.A.R model 113 and General Radio model 1232A.

As for the random fluctuations in the bridge characteristics, the cable from the bridge to the chamber, being the main contributor of error, was double-shielded, with the inner shield acting as the "guard" electrode. This insured a great deal of stability against electrical surges and random changes in the capacitance between the "hot" lead and ground. Nevertheless, the bridge characteristics (open-terminal readings) were monitored on a daily basis (and sometimes between hours during the humid summer days) prior to the start of

taking data.

It is to be noted that the open-terminal capacitance readings showed no observable fluctuations after the double-shielded cable was installed, but the loss-dial showed measurable shifts between dry days and damp ones; this, however paused no problem as it was monitored regularly.

Finally, the D.C. current measurements were read accurately to one part in 100 (apart from fluctuations resulting from from changes in the contact pressure), which amounted to a net relative error of (1.5-3)% in the sample conductance. This, as noted, represents the smallest error possible from the instrument, and in practice, errors as much as 10% due to the other sources mentioned can be expected.

The internal resistance Rg of the D.C electrometer was also calibrated against the same precision set of resistors used in the bridge loss dial calibration to optimize our accuracy. The results of these calibrations are given in Appendix (A) part (2).

A summary of the main sources of error for each of the three basic quantities observed is given in table (2.1): K is the dielectric constant, DM is the loss factor, σ is the D.C conductivity. The total conductivity σ' , being proportional to the product of K and DM, is not listed, but it should be clear that any errors in K and DM will propagate on to σ'.

TABLE (2.1)

SUMMARY OF THE MAIN SOURCES OF ERRORS AFFECTING A GIVEN QUANTITY

Observable	Error Sources And Description
K	: Bridge Dials (Reading & Calibration), Surroundings, Background Fluctuations, And Geometry.
DM	: Bridge Dials At Low Values, Background Fluctuations, And Surroundings.
σ	: DC Electrometer Calibration, Scale Fluctuations Geometry, And surroundings.

C) Reproducibility of A.C. (Bridge) Measurements on Standard Materials

We present in this section the results of measurements conducted on poly(tetrafluoroethylene) and poly(methyl methacrylate), commercially known as teflon and plexiglas, at 1KHz. under vacuum using our specially designed guarded chamber & sample holder.

The data, taken on several different occasions, weeks or months apart, and always using the same sample of each material, are shown in table (2.2), and the corresponding results are in table (2.3). It is evident that the reproducibility is well within the error quoted from the literature values

(109,110). The error in the powdered polymer samples can be of course, considerably larger since these materials are much more sensitive to the numerous factors discussed before.

TABLE (2.2)

DATA FOR THE DIELECTRIC CONSTANT AND LOSS IN TEFLON AND PLEXIGLAS UNDER ROOM CONDITIONS, AT 1 KHz.

MATERIAL	DATE	Cx ,	Dx	CL ,	DL
TEFLON	7/11/86	141.5 ,	-0.0045	133.4 ,	0.014
"	7/20/86	141.9 ,	0.019	133.8 ,	0.015
"	7/28/86	142.5 ,	0.017	134.4 ,	0.037
"	9/05/86	133.7 ,	0.0055	125.4 ,	0.028
"	9/12/86	134.1 ,	0.24	125.8 ,	0.27
"	9/25/86	155.3 ,	-0.004	146.9 ,	0.015
"	10/4/86	133.7 ,	-0.002	125.6 ,	0.02
PLEXIGLAS	7/25/86	139.8 ,	0.22	134.1 ,	0.038
"	7/28/86	139.5 ,	0.26	134.4 ,	0.055
"	9/10/86	131.6 ,	0.47	125.7 ,	0.17
"	9/12/86	131.8 ,	0.53	125.8 ,	0.27
"	9/25/86	152.5 ,	0.17	146.9 ,	0.015
"	10/7/86	132.0 ,	0.19	125.6 ,	0.025

* The underlined numbers are estimates from interpolation.

between scale divisions. The variations in the lead capacitance values were deliberately created, by attaching extra cables to the "load" terminals of the bridge, in order to insure that the final results are statistically independent of the background readings. (CL,DL) are the capacitance and loss dial readings when the chamber is attached to the bridge without the module that carries the material, they are referred to as the "background". (Cx,Dx) are the same set of readings but with the module carrying the sample attached.

The geometrical factors for the two samples are:

t/A = 10/1.227 (mil/cm2) for teflon

t/A = 22.7/1.227 (mil/cm2) for plexiglas

Where t is the thickness and A is the area .

The literature (109,110) values for the dielectric constant and loss of teflon and plexiglas at 1 KHz. are :

2.01 < K < 2.1 , and 2E-5 < DM < 4E-4 (Teflon)

3.2 < K < 3.4 , and 0.05 < DM < 0.06 (Plexiglas)

TABLE (2.3)

DIELECTRIC CONSTANT AND LOSS OF TEFLON AND PLEXIGLAS AS DETERMINED FROM THE DATA OF TABLE (2.2)

MATERIAL	K	DM
TEFLON	2.13	5.9E-04
"	2.05	7.1E-04
"	2.13	8.9E-04
"	2.08	6.4E-04
"	2.08	2.5E-04
"	2.15	5.8E-04
"	2.08	5.2E-04
Ave.	2.1	6E-04
Std. Dev.	± 0.03	± 2E-04
PLEXIGLAS	3.45	0.041
"	3.16	0.044
"	3.40	0.038
"	3.64	0.043
"	3.58	0.047
"	3.58	0.052
Ave.	3.5	0.044
Std. Dev.	±0.2	±0.005

CHAPTER III

PRESENTATION OF THE EXPERIMENTAL RESULTS

3.1) Exposition of The Polymers Studied in This Research

Poly-acene quinone radical (PAQR) polymers are prepared from aromatic hydrocarbons or their derivatives by their catalyzed condensation with aromatic anhydrides using catalysts such as ZnCl2 at temperatures ranging from about 200 - 450 °C (111).

The specific aromatic compounds used include pyrene, anthracene, quinone, anthrone, acridine, violanthrone, etc..After the reaction is completed the products are kept in the heat bath for an extended time period, as much as 30 hours to insure that most of the product has polymerized.

The by-products of the reaction are removed by extraction with HCl, ethyl alcohol, and methyl alcohol.

Typical composition by weight of PAQR polymers is about 65%-85% carbon, 5% hydrogen, plus other elements present in the starting materials, including small amounts of ZnCl2. Reliable analyses are difficult to obtain because of difficulty in attaining complete combustion of the samples. Also it is often difficult to produce identical specimens starting

from the same ingredients, because of the heterogeneous preparation conditions.

Most of the specimens we dealt with showed excellent moldability, and were pressed into pellets when subjected to a modest pressure of 2.5 Kbars. However in a couple cases the polymer did not mold and retained its sand-like characteristic. This made it quite difficult to handle especially when measuring the sample's dimensions.

Table (3.1) lists the various polymers under their code name as well as the monomer unit from which they are derived. Information relevant to their method of synthesis is given in the right-hand column. Fig.(31) shows the molecular structure of the various monomers as well as their dimensions.

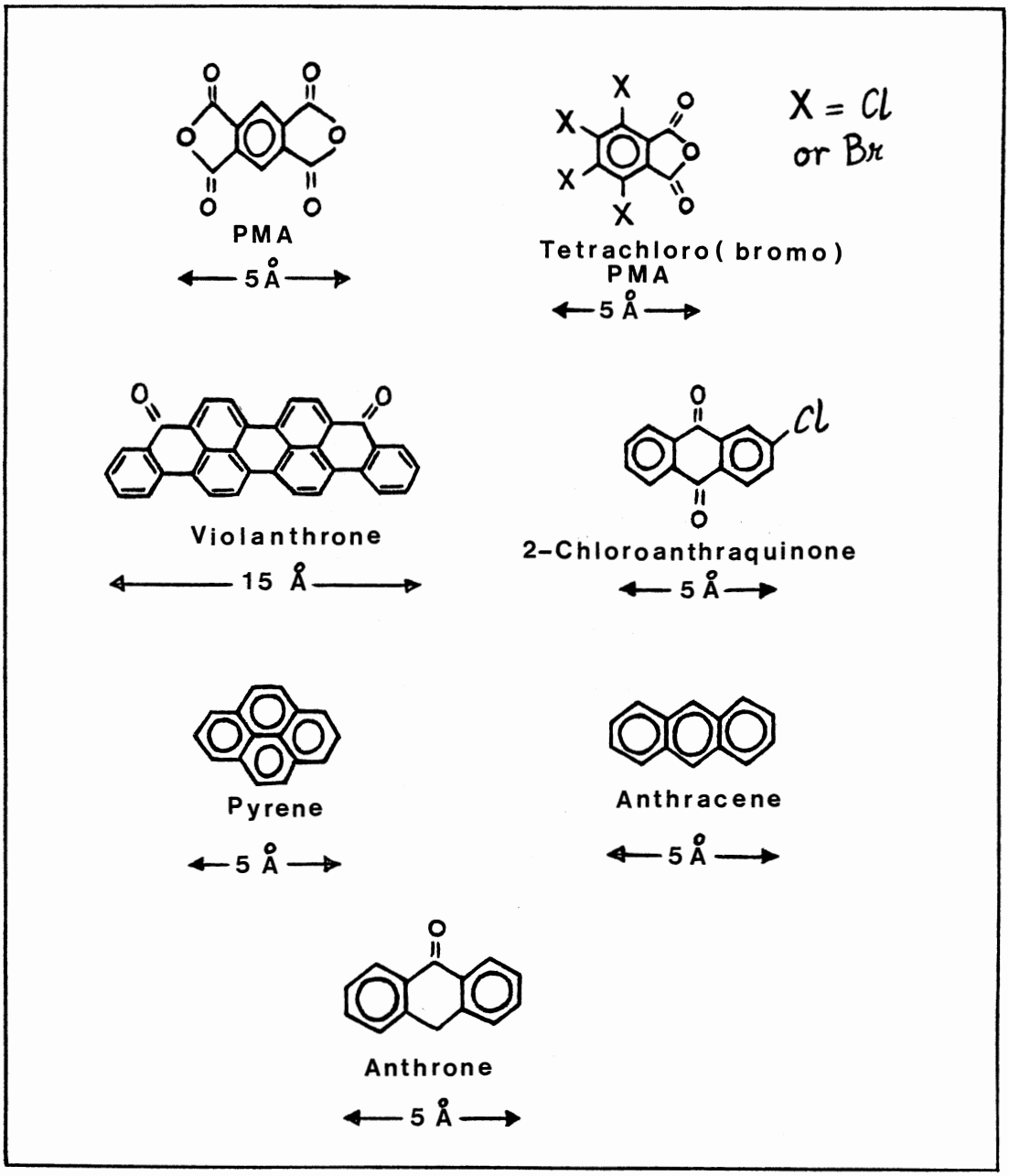

Monomer structure of the various polymers and co-polymers studied. All dimensions are approximate.

Fig.(31)

TABLE (3.1)

IDENTIFICATION OF THE POLYMERS BY THEIR CODE NAME

CODE #	BASIC MONOMER UNIT
LD-105	Violanthrone / PMA / $ZnCl_2$(solution), 306 °C & 15 h. Mole Ratio 1 : 1 : 6
LD-104	Violanthrone / PMA / $ZnCl_2$(solution), 310 °C & 15 h. Mole Ratio 1 : 1 : 2
LD-97	Violanthrone / PMA / $ZnCl_2$(solution), 307 °C & 15 h. Mole Ratio 1 : 1 : 2
LD-95	Anthracene / PMA / $ZnCl_2$ (solution), 307 °C & 15 h. Mole Ratio 1 : 1 : 2
LD-94	Pyrene / PMA / $ZnCl_2$(solution), 307 °C & 15 h. Mole Ratio 1 : 1 : 2
LD-14A	Anthrone / Polyphosphoric acid , 140 °C & 25h 19.42 g, 300 g,
LD-6A	2-Chloro Anthraquinone /Tetrabromo PA/$ZnCl_2$ Mole Ratio 1 : 1 : 2 , At 440 °C & 15h
LD-54	Violanthrone / PMA / $AlCl_3$,Mole Ratio 1:1:1 At 210 °C in Nitrobenzene, 15 h.
LD-52B	Violanthrone /Tetrachloro PA / $AlCl_3$(solution) At 210 °C & (?) h. Mole Ratio 1 : 1 : 2
LD-106	Violanthrone / PMA / $AlCl_3$(solution), 210 °C & (?) h. Mole Ratio 1 : 1 : 2

3.2) The Results of Measurements

Introduction

In the following sections we present our experimental findings on the polymer samples under three different macroscopic conditions: pressure, temperature, and D.C electric field bias, plus a frequency dependence study under room conditions. There are essentially two basic quantities of interest being studied: The dielectric constant and the (total) conductivity $\sigma'(w)$ defined by Re(J/E). Here J is the total current density in the medium. It is made up of an ohmic contribution J_Ω, and a polarisation current term Jp. By their very definition, Jp —> 0 when w = 0, while J_Ω —> $J_{D.C.}$ at zero frequency. It should be noted that for polymer systems J_Ω may become frequency - dependent at frequencies as low as 10^7 or 10^8 (see chap.4), and so in practice there is no way to identify the frequency - dependent terms making up J(w). For this reason it has become customary to lump the frequency - dependent parts in a single term, called the A.C. current density J_{AC}. All quantities related to it will be labeled in the same way (σ_{AC} is Re(J_{AC}/E etc...)

Thus we write :

$$J(w) = J_{DC} + J_{AC} \qquad 3.2.1$$

with the understanding that J_{AC} may contain ohmic contributions above certain frequencies, and such that it —> 0 at w = 0. The loss factor of the material generally decreases with frequency at high frequencies, but usually displays a

rather erratic behaviour at lower frequencies. For this reason the loss factor will not be displayed graphically, but only tabulated in most of the cases. We remark that the loss factor reported in the tables includes the effect of the D.C. conductivity, that is: DM = $\sigma' / \epsilon_o w K'$. This differs from the loss factor for a perfectly insulating material (σ = 0), by the term $\sigma / \epsilon_o w K'$. The D.C conductivity is tabulated as the value of $\sigma'(w)$ at w = 0.

As it turned out, the D.C. conductivity of the polymers is a negligible part of the total conductivity even at frequencies as low as 100 Hz. This means that for all practical purposes, the total conductivity at non-zero frequencies may be taken equal to the A.C. conductivity for these polymers, and the experimental loss factor DM may be considered approx. equal to tan(δ) = K"/K' $\equiv$ K"/K . We shall start by presenting the frequency response under room conditions.

A) Frequency Response at Room Temperature

Throughout this section and the ones that follow (except for section (B)), the contact pressure on the sample was maintained at $\simeq$27 PSI (0.065 K.bars) according to the procedures described in chap.(2).

The dielectric constant, the (total) conductivity, and the loss factor are tabulated in tables (3.2 - 3.11) and the resulting graphs are shown in Figs.(32 - 52). The plots display at least two independent measurements done on pellets from the same polymer,and prepared from powder of the "same"

degree of fineness. In several cases, coarse-grained specimens were also included and the corresponding results were shown for the purpose of comparisons. The loss factor is not plotted.

Coarse-grained specimens consistently yielded lower conductivity and lower loss at all frequencies (including D.C.) for all the cases observed, this supports the speculation that coarse-grained pellets contain sizable voids due to poor packing, resulting in poorer conduction and lower loss. Also, for the same grade powder, certain polymers reproduced better than others, with LD-95 being the best while LD-105 and LD-97 among the worst. Finally since the discrepancy in some cases is greater than what could be accounted for on the basis of the error analysis of sec(2.5B) it is believed that the large fluctuations at lower frequencies are mainly due to possible inhomogeneity in the polymer: either due to structural differences (e.g. a wide distribution of molecular lengths), or impurity content. The evidence stems from the fact that while the D.C. conductivities of the different trials (of a given polymer) are fairly close to each other, the loss factor and hence the dielectric constant, are not. Moreover the various data points are not randomly distributed but follow a systematic pattern whereby for a given pair of samples, the observed values of K are always either smaller or larger (below a given frequency) in one sample than in the other, and tending to a common value at higher frequencies - an indication that not all the samples from a given polymer share the same distribution of relaxation times - which suggests that the poly-

mers have a non-uniform distribution of lengths and a variety of cross-links. The above also explains why some trials "seem" to agree better at say, 1 KHz, rather than at another frequency. It is simply because that frequency may not always be the "cross-over" point for these samples.

Unless otherwise noted, and throughout secs.(3.2A-D) all samples are prepared from fine-grain powder. The conductivities listed are given in $(\text{ohm} - \text{cm})^{-1}$. The maximum experimental and computational error on all the values given in tbls. (3.2-3.41) is between (8-12)%, except those polymers whose loss factor is below 0.20 (at frequencies < 500 Hz), these carry an error between (15-22)% over that range of frequencies due to the low sensitivity of the system at the "low - end" of the loss dial.

The graphs display the A.C. conductivity which is $\sigma' - \sigma$ where, of course, σ is just σ_{DC}, the ohmic conductivity at zero frequency. The total conductivity at zero value of some other parameter "x" will be denoted by σ_o' (i.e. $\sigma_o' = \sigma' \Big\}_{X=0}$) while the D.C conductivity at x = 0 will be written as σ_o. Occasionally, σ and σ_{DC} are used interchangeably. Logarithms to base 10 of any quantity "f", are written as: "log(f)". The natural logarithm of a given quantity "X" is written "$\log_e(X)$". In cases where the results on different samples are fairly close, only an average is reported for the parameters defining the linear fit. Throughout this chapter, "room conditions" will be understood to mean: <u>room temperature and an "ambient" pressure of 27 PSI</u>.

TABLE (3.2)

FREQUENCY RESPONSE OF LD-105 UNDER ROOM CONDITIONS

		<=== f (KHz) ===>						
		0	1	1.5	2	3.5	10	100
Sample								
# C	σ'	3.7E-8	4.2E-6	---	---	7.5E-6	1.2E-5	4.3E-5
	K	--	61	---	---	37	27	11.5
	DM	--	1.3	---	---	1.1	0.75	0.67
# S	σ'	1.1E-7	---	8.8E-6	7.4E-6	1.3E-5	1.7E-5	5.0E-5
	K	--	---	76	77	38	26	11.7
	DM	--	---	1.4	0.86	1.8	1.1	0.77
# Q	σ'	9.7E-8	---	9.4E-6	7.6E-6	1.1E-5	1.3E-5	4.6E-5
	K	--	---	52	56	33	22	11.6
	DM	--	---	2.2	1.2	1.8	1.1	0.71

cont'd

σ': Total Conductivity, K : Dielectric Constant, DM : Loss Factor

C is pressed out of coarse - grained powder

TABLE (3.2) Cont'd

# J	σ' | 1.1E-7	---	---	---	1.4E-5	1.7E-5	5.0E-5
	K | --	---	---	---	37	26	11.9
	DM | --	---	---	---	1.9	1.2	0.75
# K	σ' | 1.2E-7	---	---	---	1.3E-5	1.8E-5	6.3E-5
	K | --	---	---	---	43	35	14.1
	DM | --	---	---	---	1.6	0.92	0.81
# L	σ' | 9.6E-8	---	---	---	9.5E-6	1.1E-5	4.5E-5
	K | --	---	---	---	23	21	11.4
	DM | --	---	---	---	2.1	0.91	0.71
# N	σ' | 9.5E-8	---	---	---	1.3E-5	1.2E-5	3.5E-5
	K | --	---	---	---	32	18	9.7
	DM | --	---	---	---	2.1	1.2	0.65

cont'd

TABLE (3.2) Cont'd

# G	σ'	1.1E-7	---	---	---	1.1E-5	1.3E-5	4.1E-5
	K	--	---	---	---	24	20	9.5
	DM	--	---	---	---	2.4	1.2	0.77
# H	σ'	9.6E-8	---	---	---	1.0E-5	1.2E-5	4.4E-5
	K	--	---	---	---	24	20	11.2
	DM	--	---	---	---	2.2	1.1	0.71
Ave.	σ'	1.0E-7	---	8.7E-6	7.0E-6	1.2E-5	1.4E-5	4.7E-5
	K	--	---	64	65	32	24	11.4
	DM	--	---	1.7	0.97	2.0	1.1	0.73
St.dev.								
	σ'	$\pm$0.1E-7	---	$\pm$0.5E-6	$\pm$0.2E-6	$\pm$0.1E-5	$\pm$0.3E-5	$\pm$0.8E-5
	K	--	---	$\pm$12	$\pm$10	$\pm$7	$\pm$5	$\pm$1.3
	DM	--	---	$\pm$0.4	$\pm$0.2	$\pm$0.3	$\pm$0.05	$\pm$0.05

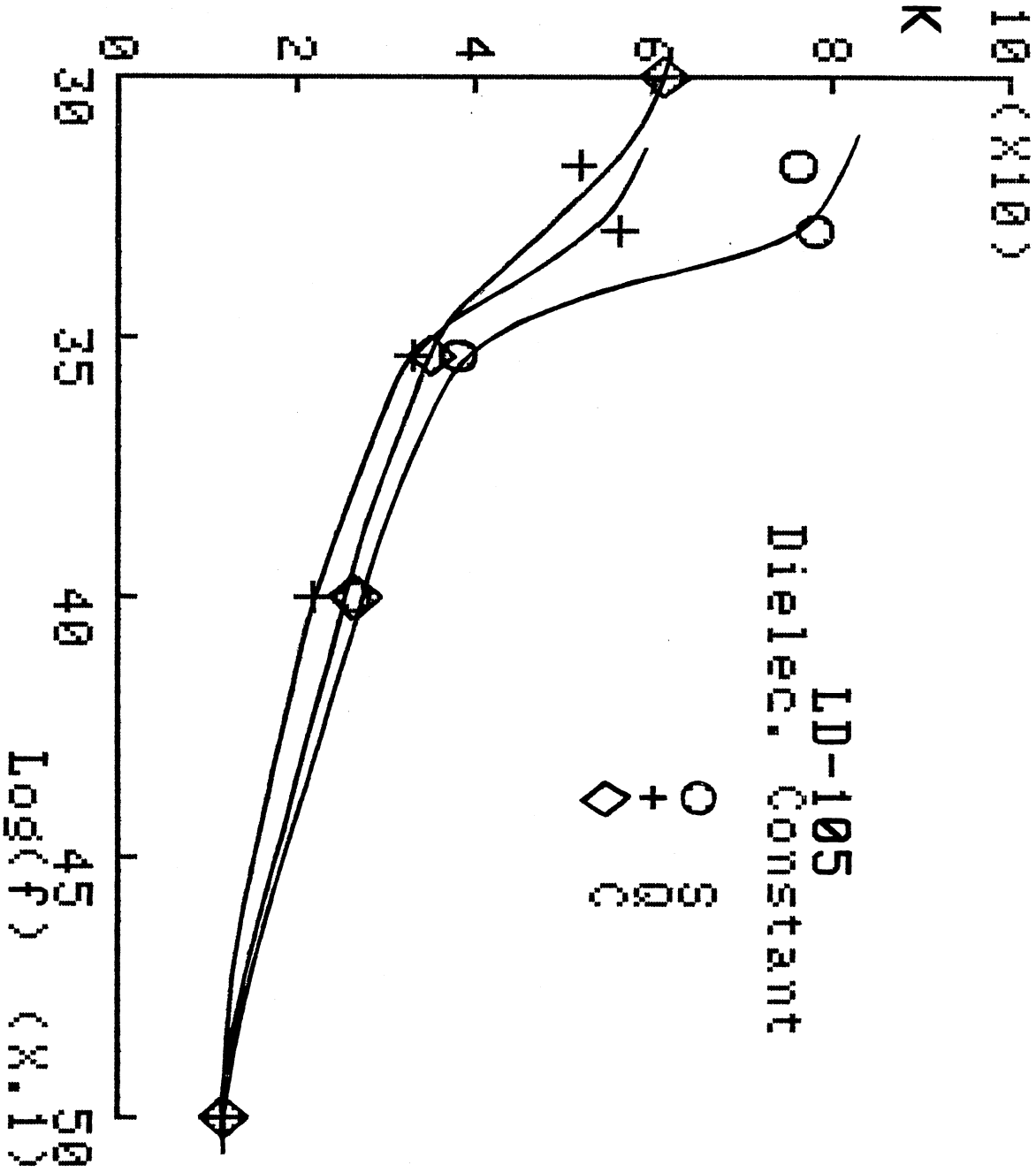

Fig.(32)

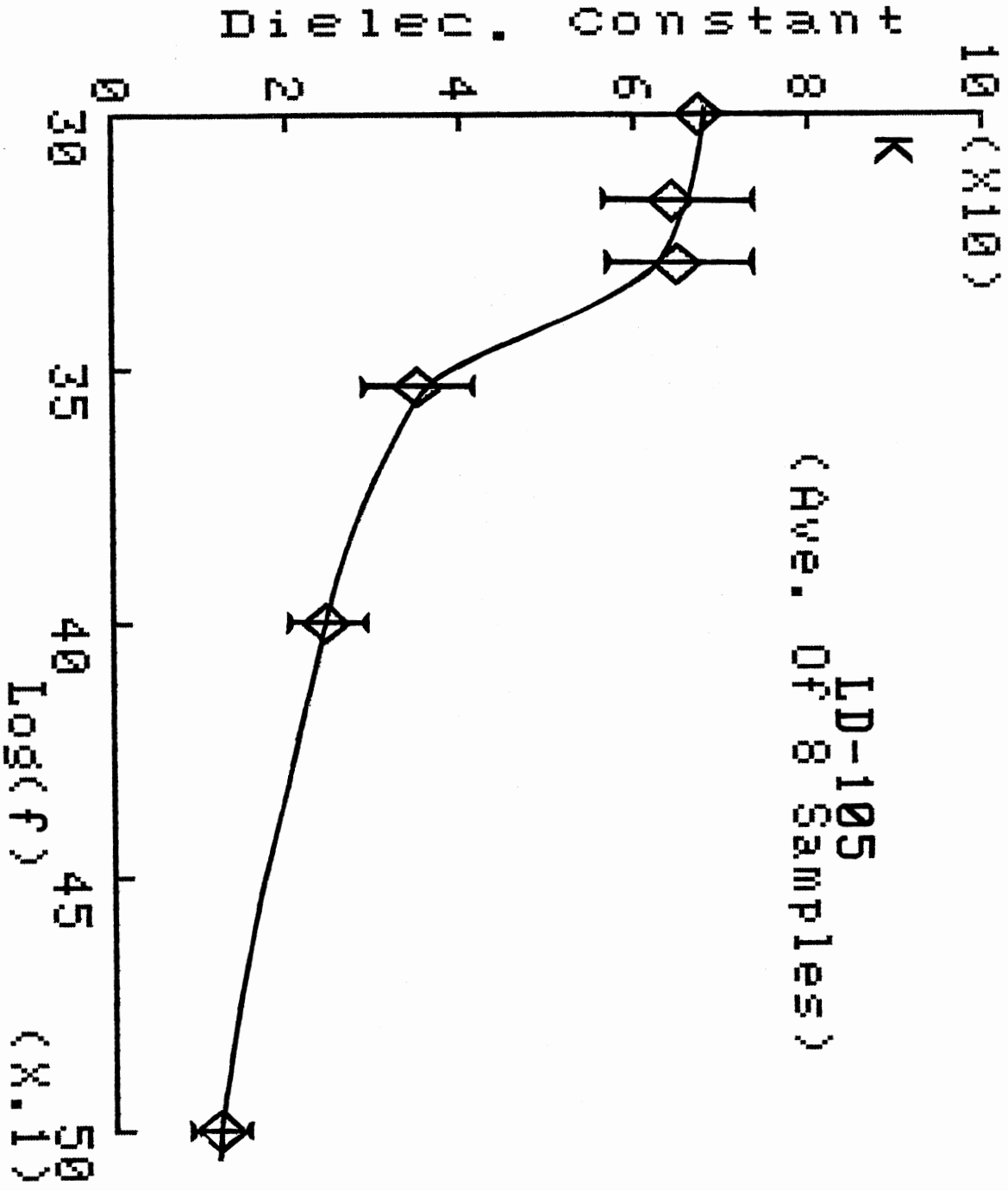
Dielec. Constant
0
2
4
6
8
10
(X10)
K
20
25
30
35
40
45
50
Log(f) (X-1)
LD-105
Of 8 samples
(Ave. of 8 samples)

Fig.(33)

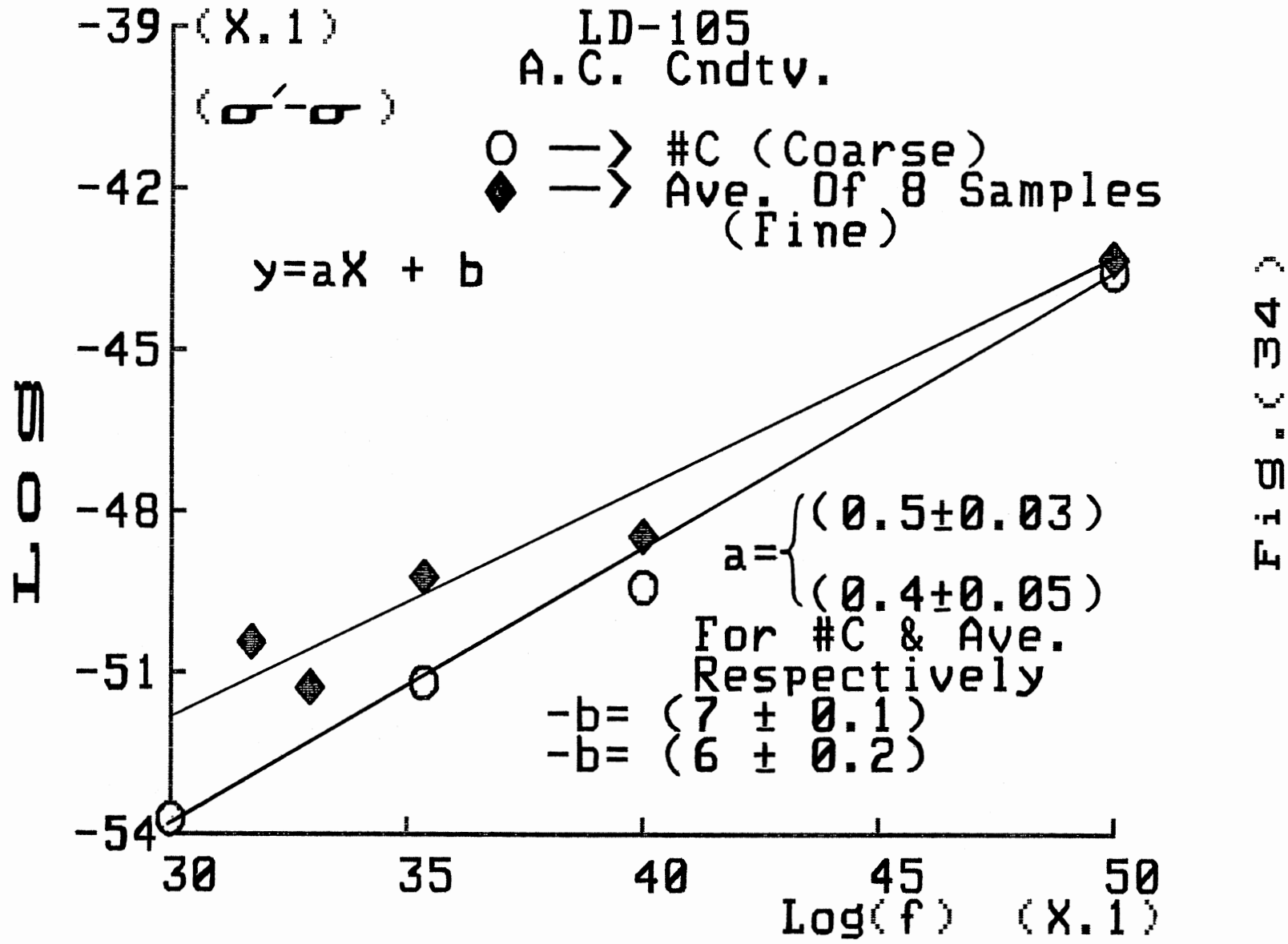
LD-105
A.C. Cndtv.
(X.1)
(σ′-σ)
O —> #C (Coarse)
♦ —> Ave. Of 8 Samples (Fine)
y=aX + b
-39
-42
-45
-48
-51
-54
Log
30
35
40
45
50
Log(f) (X.1)
a={(0.5±0.03) (0.4±0.05)
For #C & Ave. Respectively
-b= (7 ± 0.1)
-b= (6 ± 0.2)

Fig. (34)

TABLE (3.3)

FREQUENCY RESPONSE OF LD-104 UNDER ROOM CONDITIONS

	<=== f (KHz) ===>							
	0	0.1	0.2	0.5	1	3.5	10	100
Sample								
# A σ'	1.5E-9	8.6E-8	1.4E-7	2.2E-7	4.1E-7	1.0E-6	1.9E-6	5.6E-6
K	--	34	20	18	15	12	9.1	5.8
DM	--	0.45	0.62	0.44	0.48	0.45	0.38	0.17
# G σ'	1.7E-9	2.6E-7	3.4E-7	5.4E-7	8.8E-7	2.0E-6	3.6E-6	9.8E-6
K	--	53	46	31	23	14	10	6.5
DM	--	0.88	0.65	0.63	0.67	0.71	0.64	0.27
# H σ'	1.6E-9	1.6E-7	2.2E-7	4.4E-7	8.1E-7	1.9E-6	3.7E-6	9.5E-6
K	--	51	45	28	24	14	9.7	5.9
DM	--	0.55	0.43	0.57	0.59	0.72	0.68	0.29

A is pressed out of coarse - grained powder

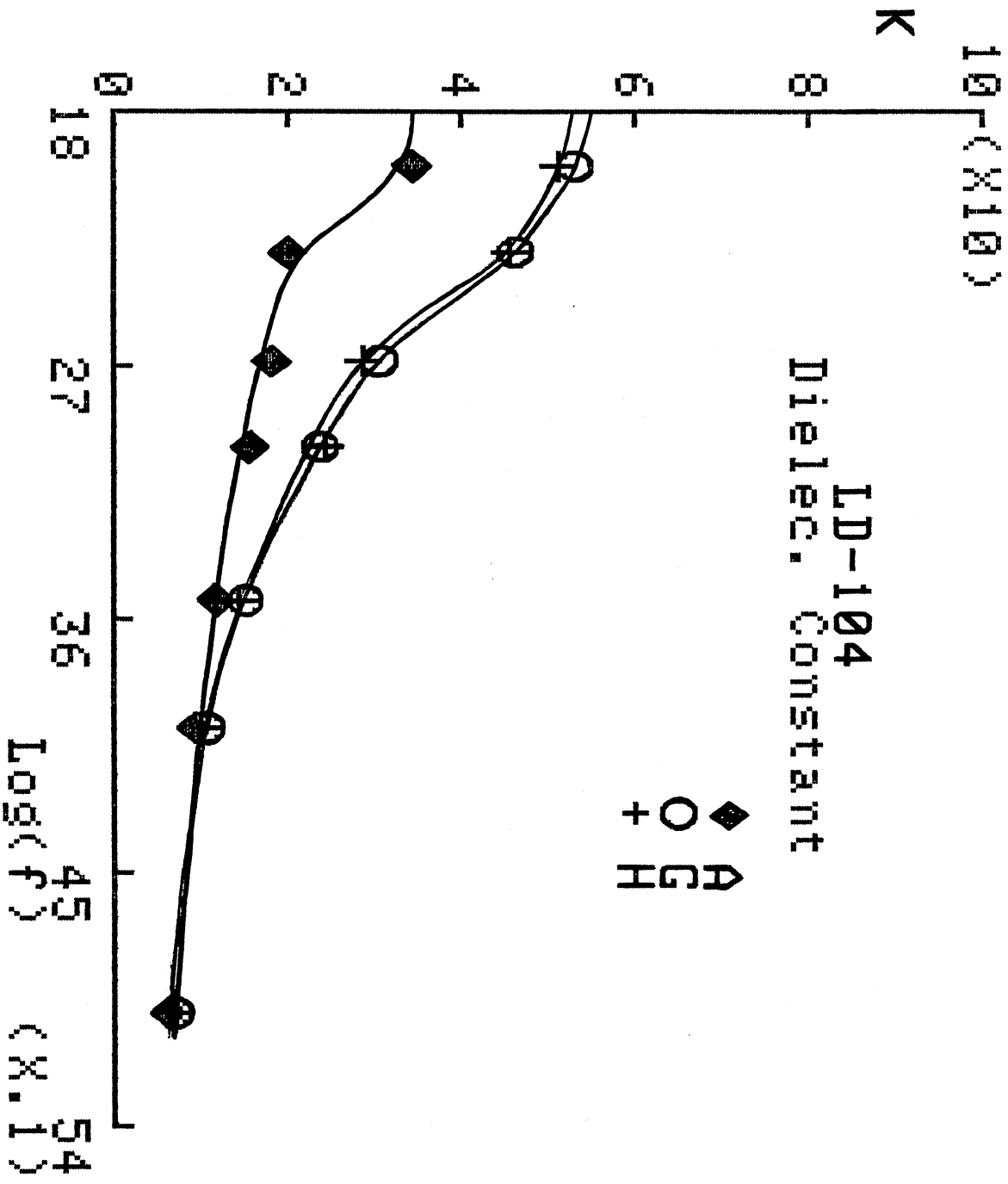

Fig.(35)

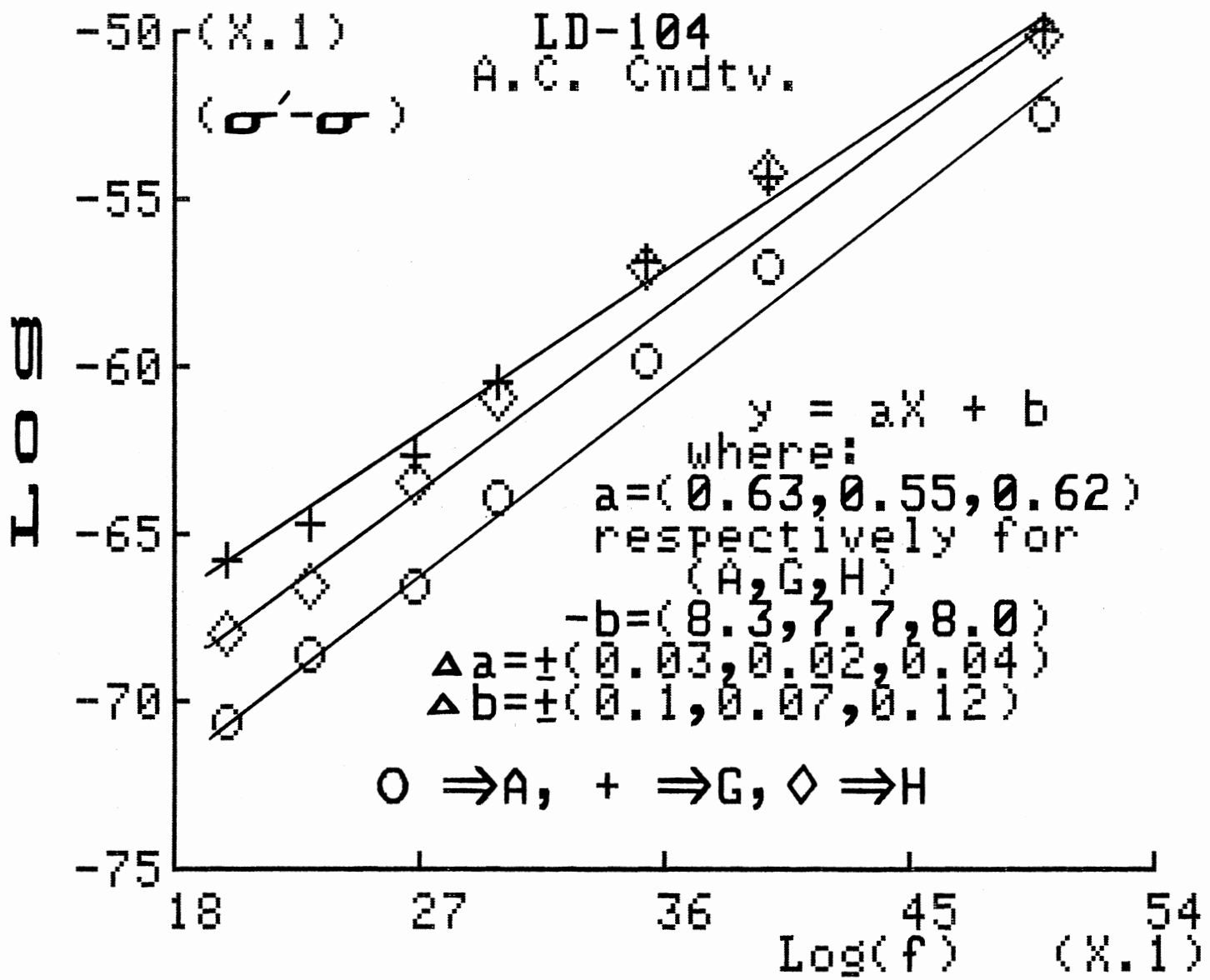
LD-104
A.C. Cndtv.
(σ′-σ)
(X.1)
-50
-55
-60
-65
-70
-75
Log
18
27
36
45
54
Log(f) (X.1)
y = aX + b
where:
a=(0.63,0.55,0.62)
respectively for
(A,G,H)
-b=(8.3,7.7,8.0)
△a=±(0.03,0.02,0.04)
△b=±(0.1,0.07,0.12)
O ⇒A, + ⇒G, ◇ ⇒H

Fig.(36)

TABLE (3.4)

FREQUENCY RESPONSE OF LD-97 UNDER ROOM CONDITIONS

	<=== f (KHz) ===>							
	0	0.1	0.2	0.5	1	3.5	10	100
Sample								
# A o	1.6E-9	2.2E-7	2.6E-7	4.2E-7	6.3E-7	1.5E-6	2.5E-6	7.7E-6
K	--	50	39	32	28	21	18	15
DM	--	0.78	0.59	0.47	0.41	0.35	0.25	0.09
# S o	3.2E-9	3.4E-7	4.1E-7	7.0E-7	1.0E-6	2.8E-6	4.8E-6	1.4E-5
K	--	72	59	36	32	20	13	7.9
DM	--	0.84	0.62	0.69	0.58	0.71	0.65	0.32
# T o	3.4E-9	4.0E-7	4.7E-7	6.9E-7	9.1E-7	1.9E-6	3.3E-6	9.1E-6
K	--	46	34	23	20	14	9.9	6.4
DM	--	1.6	1.2	1.1	0.81	0.71	0.61	0.25

A is pressed out of coarse grained powder

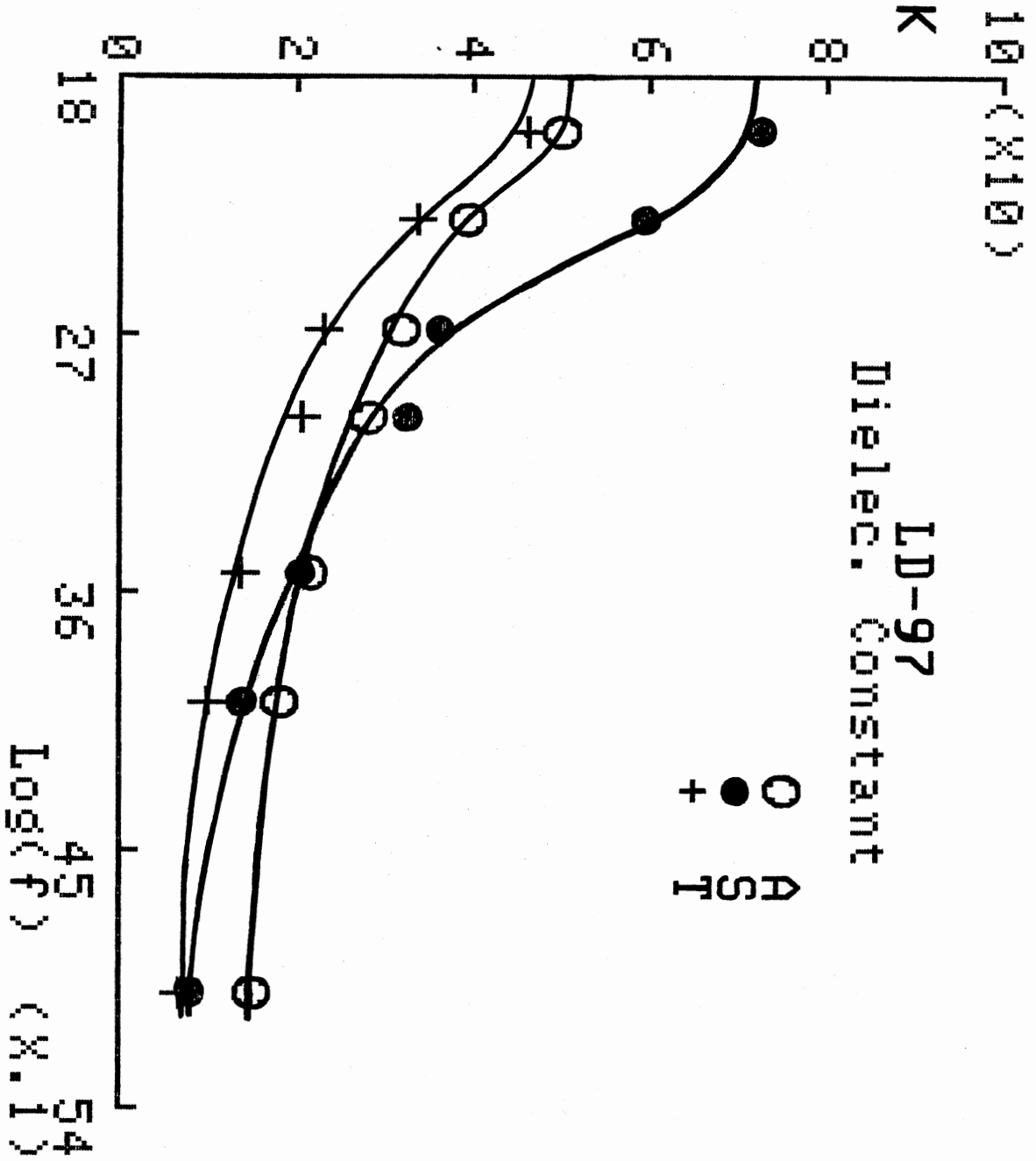
10(x10)
K
0
2
4
6
8
18
27
36
45
54
Log(f) (x.1)
LD-97
Dielec. Constant
ASET
+ ● O

Fig.(37)

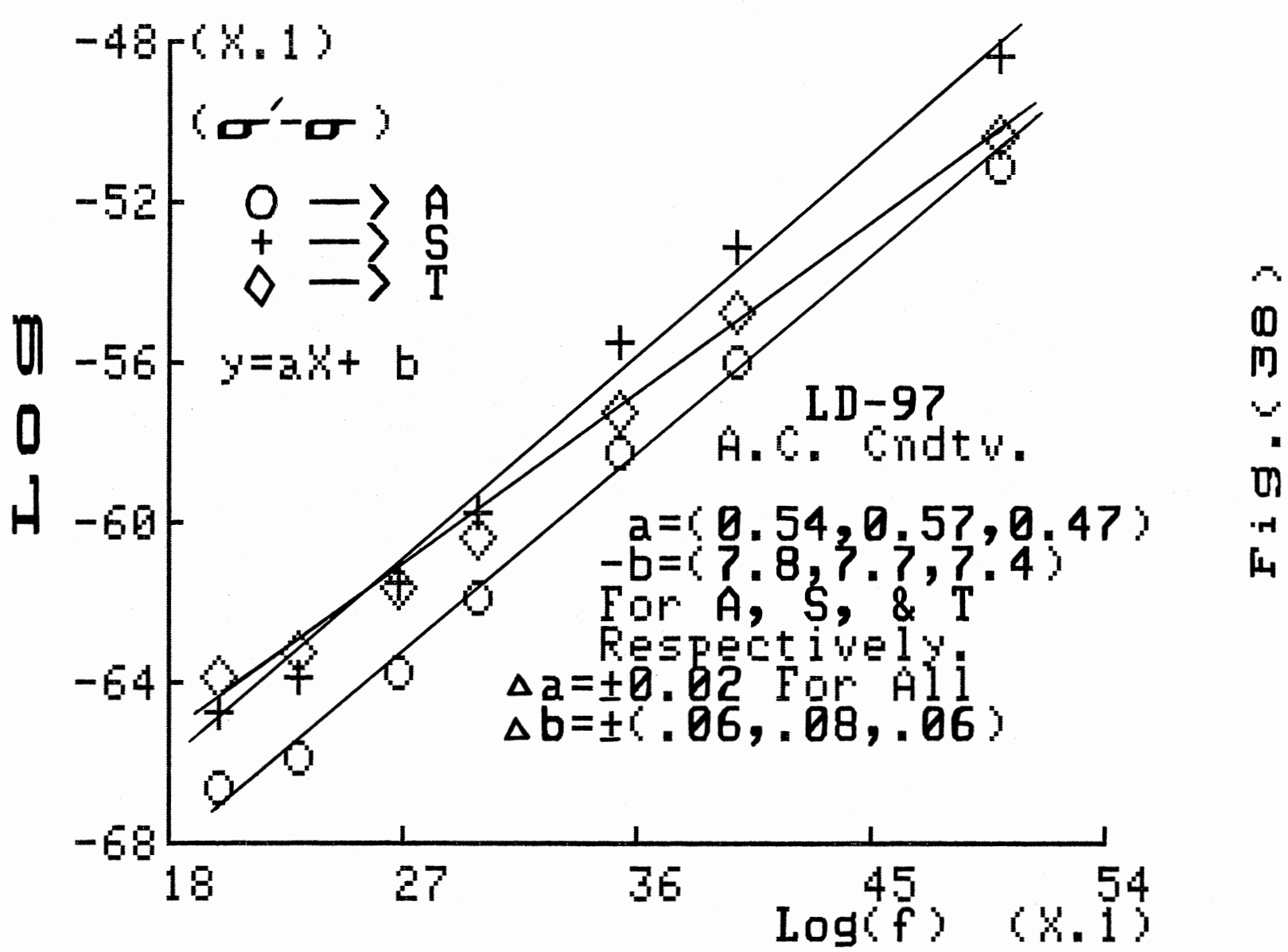
-48
(X.1)
(σ′-σ)
O —> A
+ —> S
◇ —> T
y=aX+ b
-52
-56
-60
-64
-68
Log
LD-97
A.C. Cndtv.
a=(0.54,0.57,0.47)
-b=(7.8,7.7,7.4)
For A, S, & T
Respectively.
Δa=±0.02 For All
Δb=±(.06,.08,.06)
18
27
36
45
54
Log(f) (X.1)

Fig. (38)

TABLE (3.5)

FREQUENCY RESPONSE OF LD-95 UNDER ROOM CONDITIONS

	<=== f (KHz) ===>							
	0	0.1	0.2	0.5	1	3.5	10	100
Sample								
# A σ'	3.4E-9	3.4E-7	4.6E-7	6.8E-7	1.0E-6	1.7E-6	2.5E-6	6.2E-6
K	--	54	36	24	18	11	7.9	5.3
DM	--	1.1	1.2	1.0	1.0	0.81	0.56	0.21
# B σ'	3.7E-9	3.6E-7	4.3E-7	7.2E-7	1.0E-6	1.7E-6	3.1E-6	6.7E-6
K	--	52	38	22	18	11	8.1	5.3
DM	--	1.3	1.0	1.2	1.0	0.85	0.68	0.22

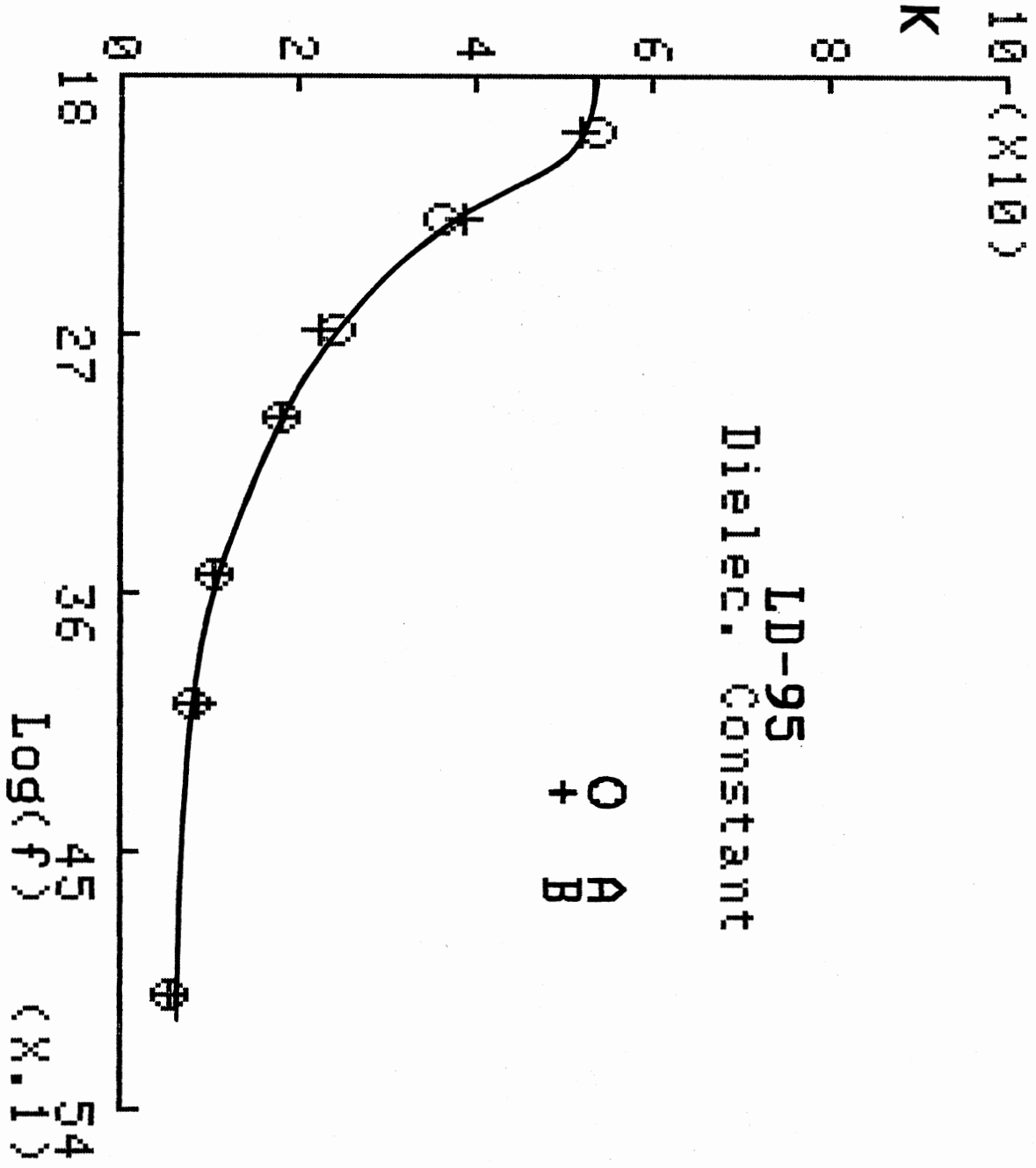

Fig.(39)

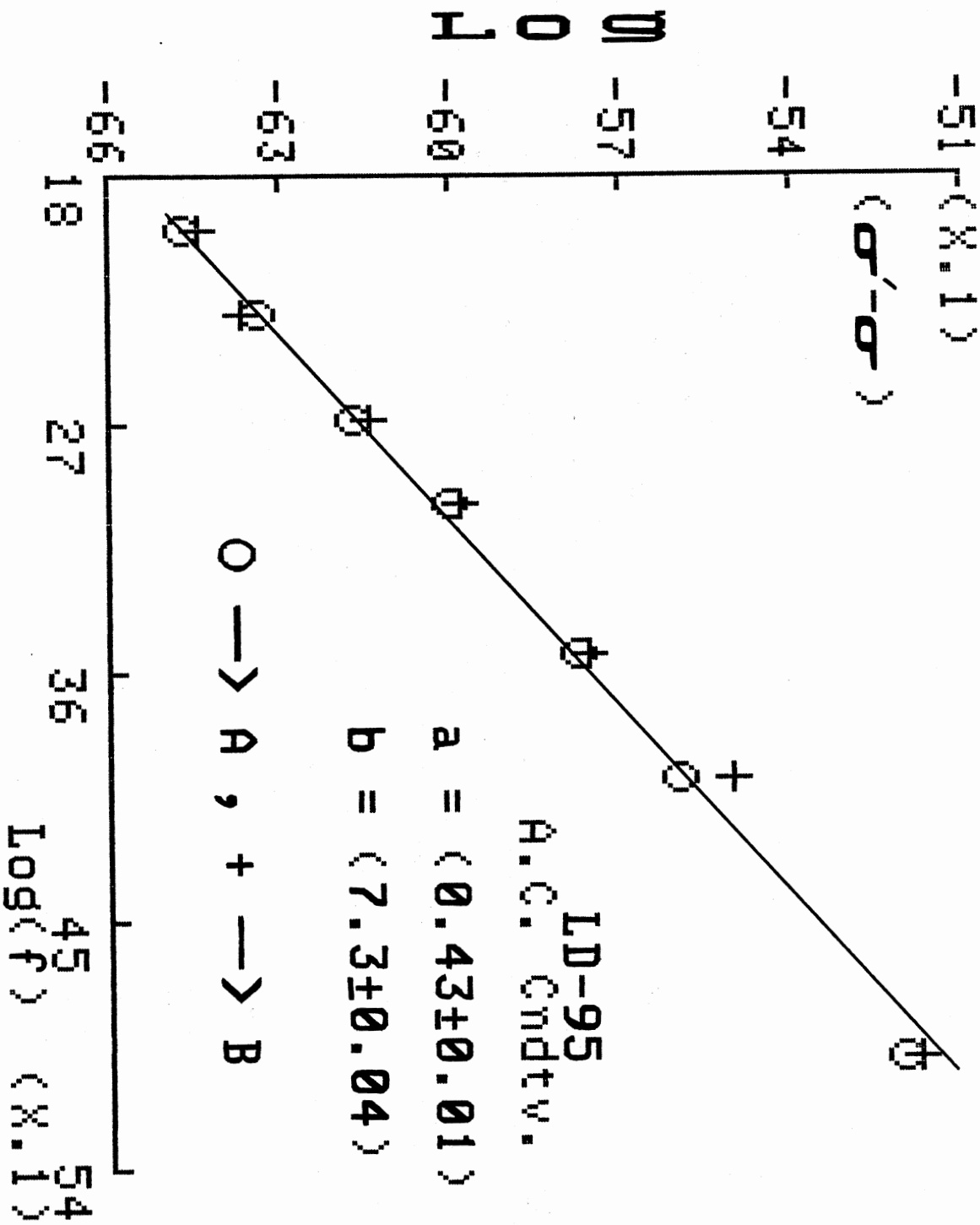
LOG
(x.1)
-51
-54
-57
-60
-63
-66
18
27
36
45
54
Log(f) (x.1)
LD-95
A.C. Cndtv.
a = (0.43±0.01)
b = (7.3±0.04)
O —< A , + —< B

Fig.(40)

TABLE (3.6)

FREQUENCY RESPONSE OF LD-94 UNDER ROOM CONDITIONS

	<=== f (KHz) ===>							
	0	0.1	0.2	0.5	1	3.5	10	100
Sample								
# A σ'	1.8E-8	--	8.4E-7	1.3E-6	2.7E-6	4.0E-6	5.3E-6	1.8E-5
K	--	--	80	64	31	19	15	6.8
DM	--	--	0.96	0.74	1.6	1.1	0.64	0.48
# B σ'	2.5E-8	--	2.1E-6	2.5E-6	2.8E-6	4.3E-6	5.5E-6	1.7E-5
K	--	--	36	30	25	17	13	6.2
DM	--	--	5.2	3.0	2.0	1.3	0.77	0.52

#A is pressed out of coarse grained powder

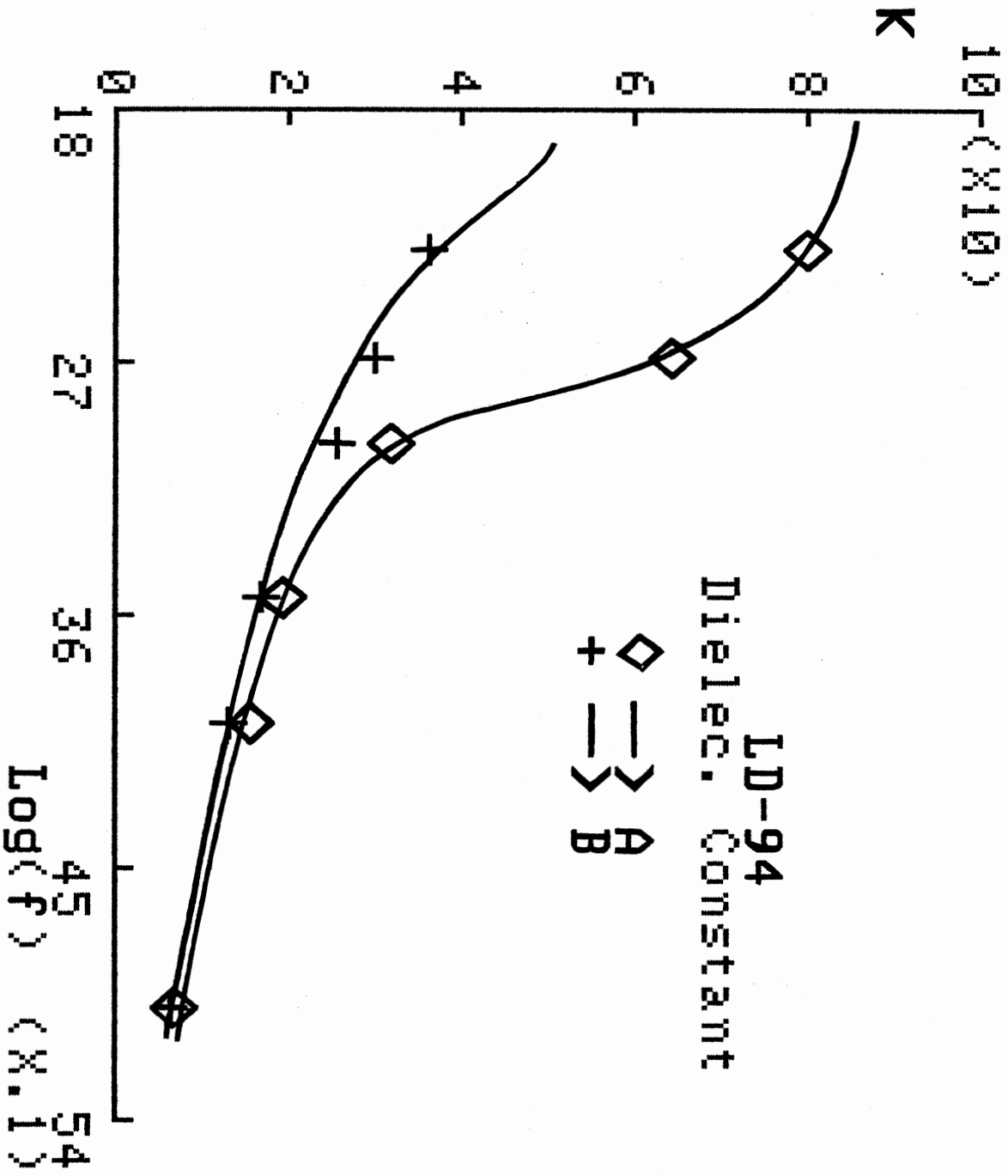

Fig.(41)

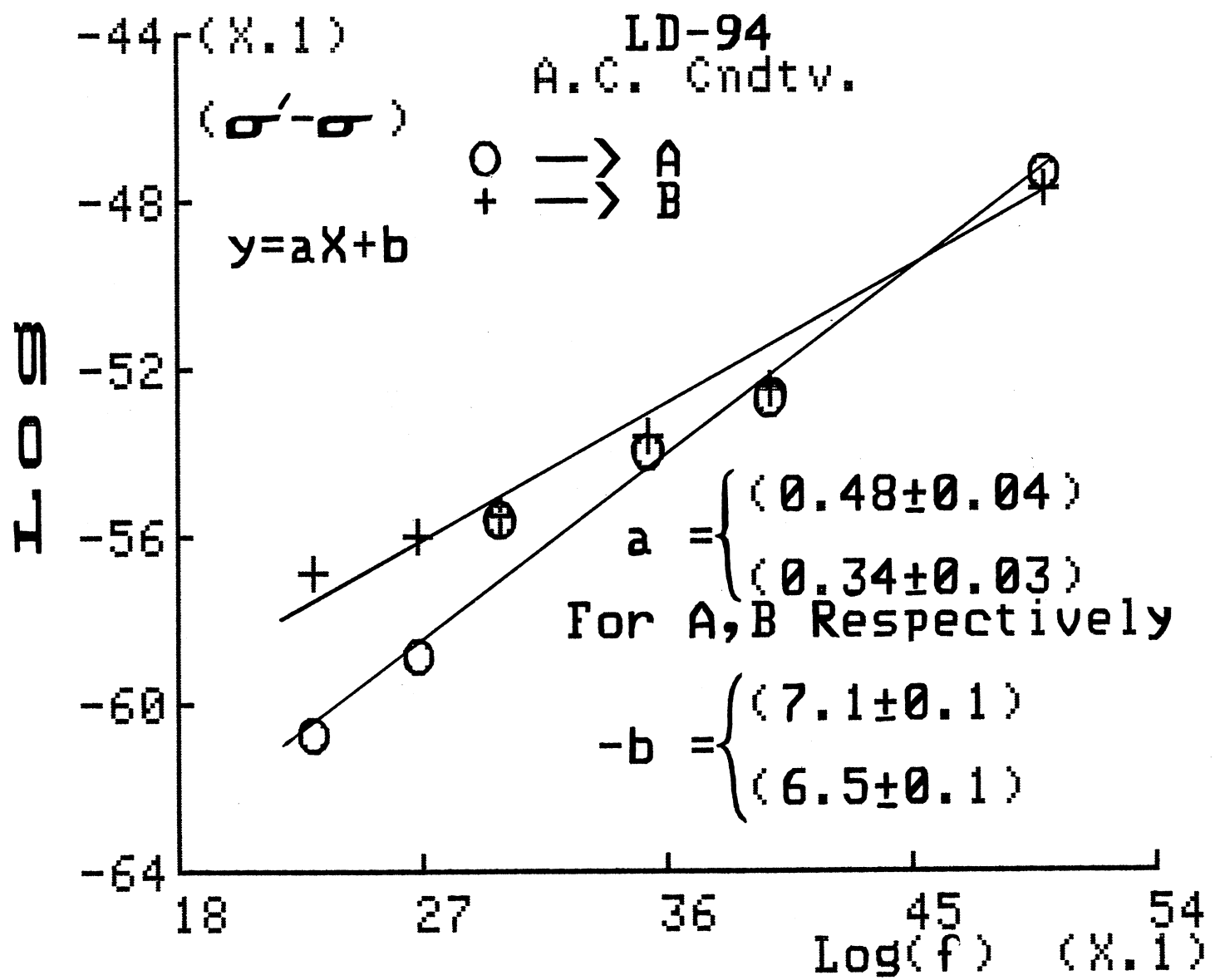
LD-94
A.C. Cndtv.
(X.1)
(σ′-σ)
y=aX+b
O ⟶ A
+ ⟶ B
Log
-44
-48
-52
-56
-60
-64
18
27
36
45
54
Log(f) (X.1)
a = {(0.48±0.04) (0.34±0.03)
For A,B Respectively
-b = {(7.1±0.1) (6.5±0.1)

Fig.(42)

TABLE (3.7)

FREQUENCY RESPONSE OF LD-14A UNDER ROOM CONDITIONS

	<=== f (KHz) ===>							
	0	0.1	0.2	0.5	1	3.5	10	100
Sample								
# E σ'	9.0E-10	1.6E-7	2.2E-7	4.2E-7	5.8E-7	1.1E-6	1.5E-6	3.3E-6
K	--	46	28	18	13	8.5	6.2	5.6
DM	--	0.63	0.70	0.83	0.78	0.67	0.42	0.11
# V σ'	6.8E-10	1.0E-7	1.5E-7	2.9E-7	5.1E-7	8.0E-7	1.1E-6	2.8E-6
K	--	71	24	14	11	7.1	5.6	5.0
DM	--	0.26	0.54	0.71	0.82	0.57	0.34	0.10

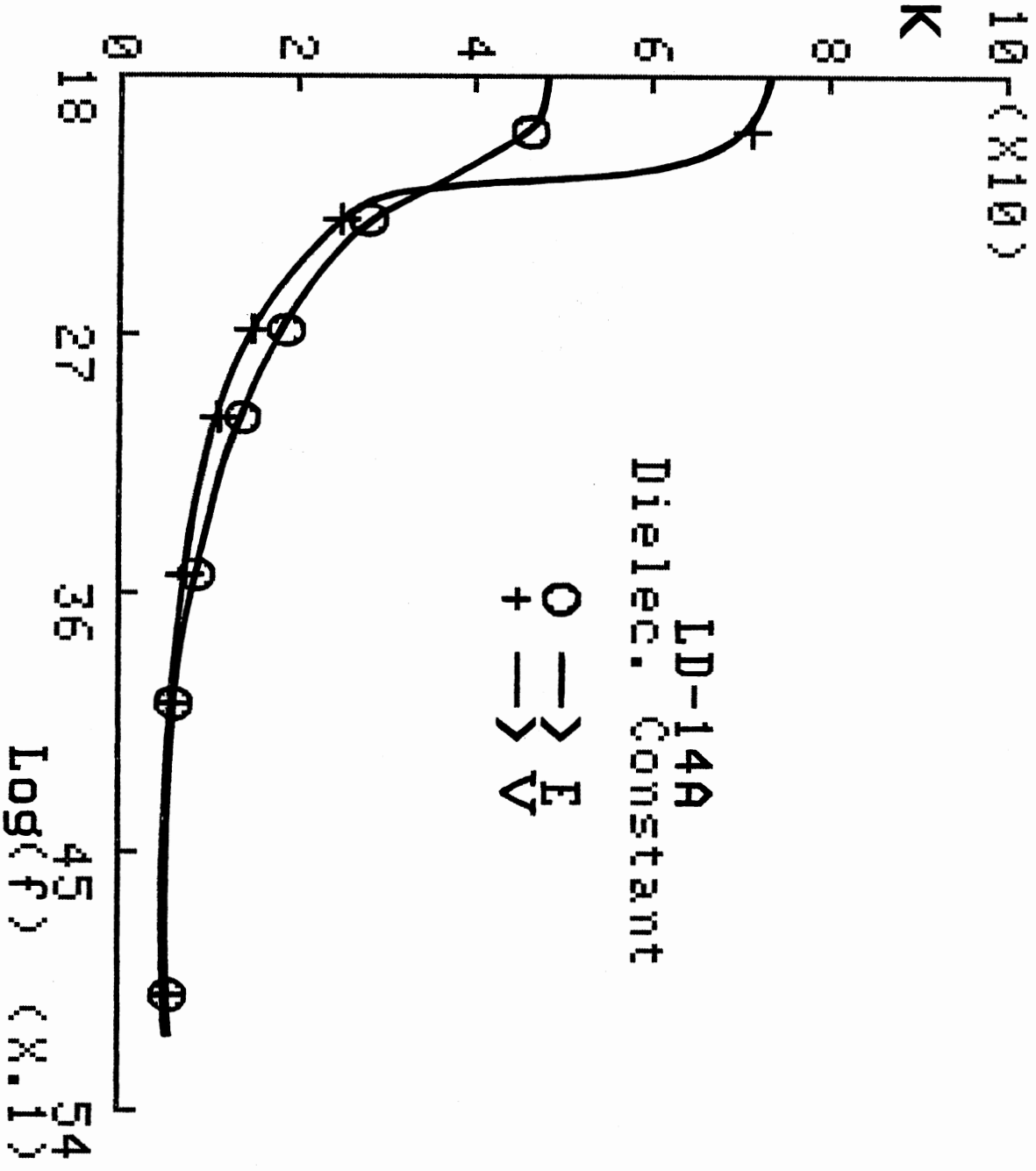

Fig.(43)

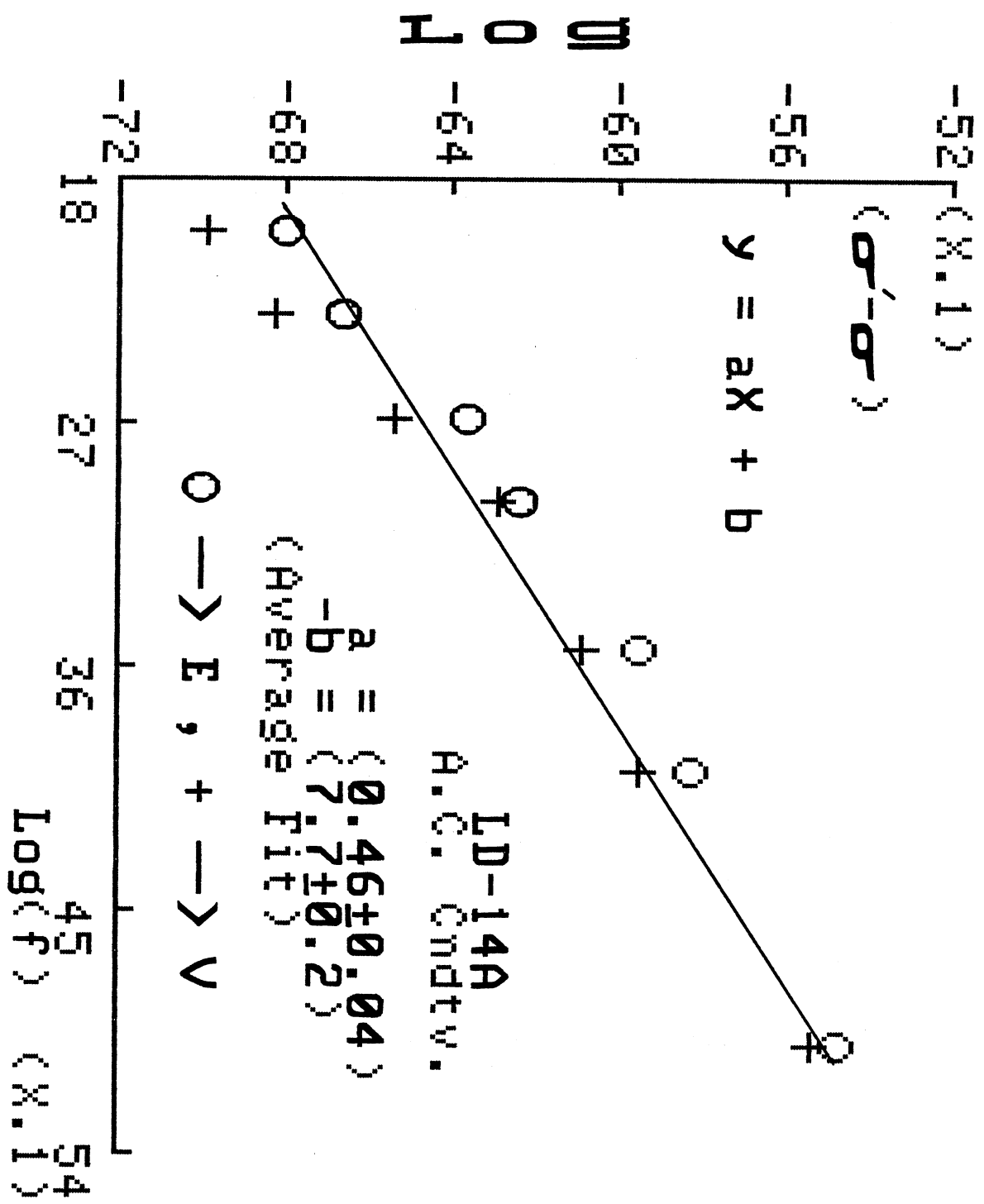
Log
(x.1)
(q'-q)
y = ax + b
LD-14A
P.C. Cndtv.
a = (0.46±0.04)
b = (-2.2±0.2)
(Average Fit)
O — E, + — V
Log(fj) (x.1)
54
45
36
27
18
-72
-68
-64
-60
-56
-52

Fig.(44)

TABLE (3.8)

FREQUENCY RESPONSE OF LD-6A UNDER ROOM CONDITIONS

	<=== f (KHz) ===>							
	0	0.1	0.2	0.5	1	3.5	10	100
Sample								
# F σ'	5.6E-9	5.1E-7	5.8E-7	7.9E-7	8.9E-7	1.7E-6	2.9E-6	1.3E-5
K	--	37	24	20	20	16	13	8.2
DM	--	2.5	2.2	1.4	0.82	0.55	0.41	0.29
# G σ'	6.4E-9	7.5E-7	7.2E-7	8.7E-7	1.1E-6	1.9E-6	3.4E-6	1.5E-5
K	--	83	37	27	22	17	14	8.0
DM	--	1.7	1.8	1.2	0.92	0.58	0.45	0.33

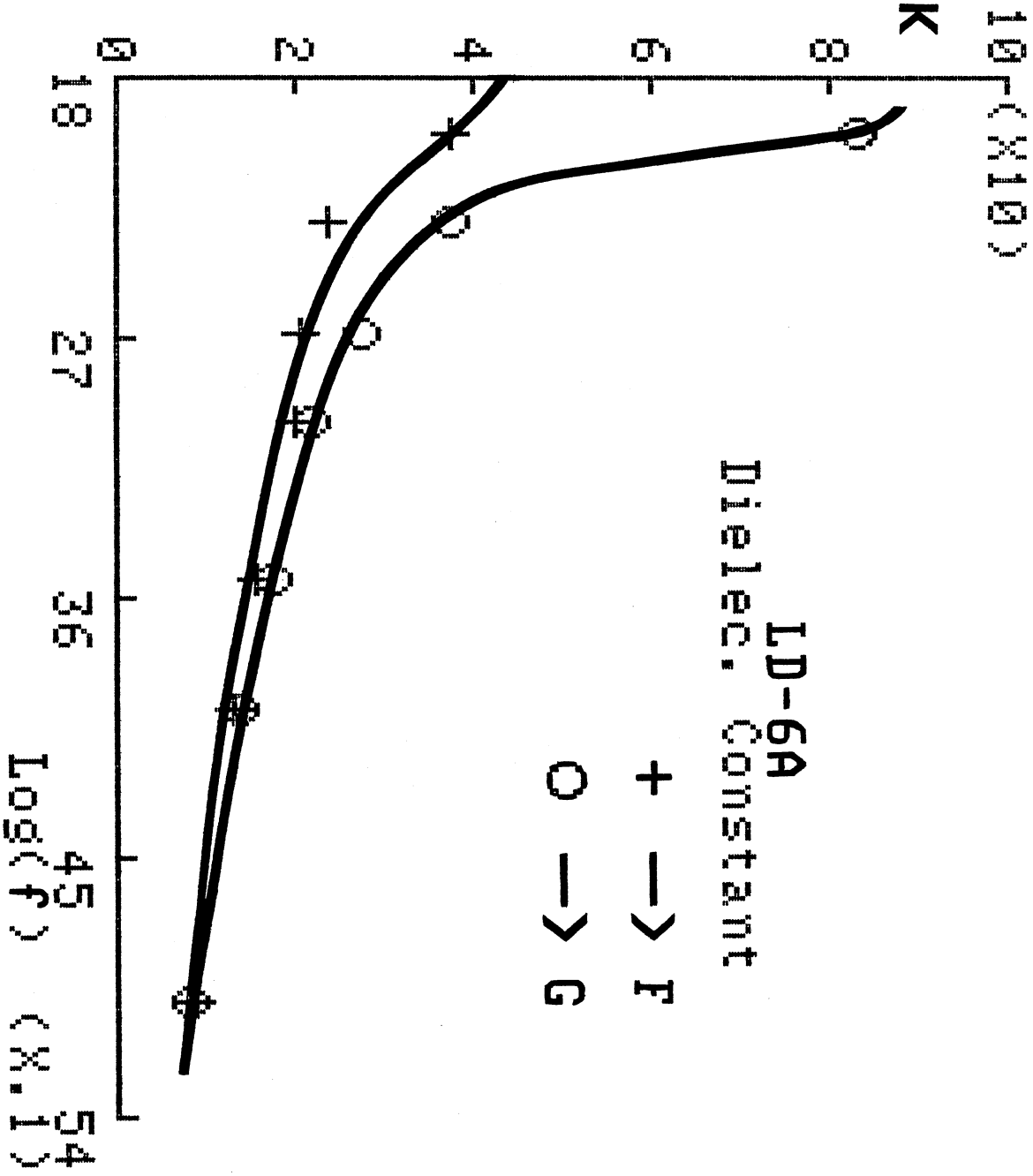

Fig.(45)

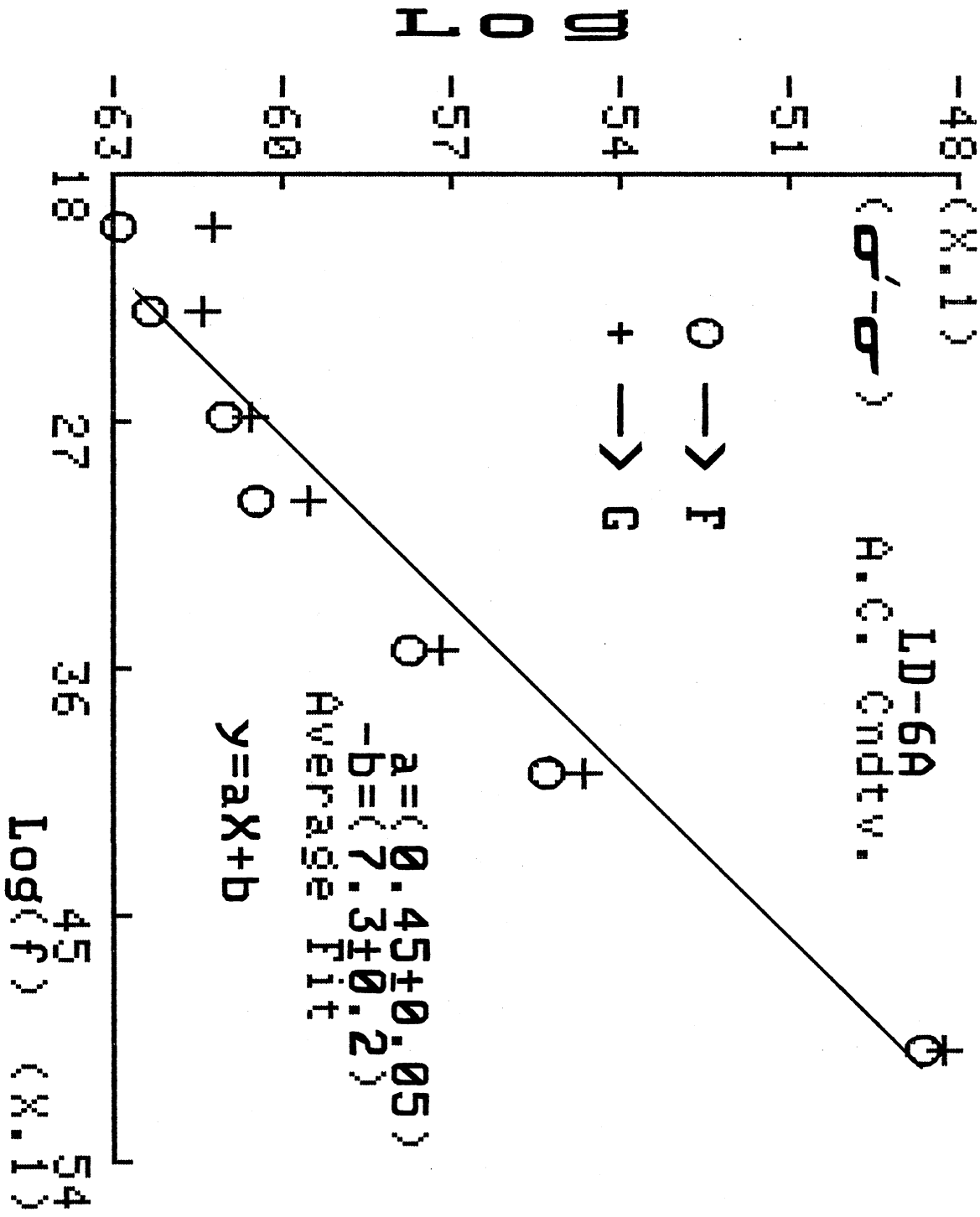
Log
-48 (x.1)
-51
-54
-57
-60
-63
18
22
26
30
45
54
Log(f) (x.1)
(q'-q")
O → F
+ → G
LD-6A
R.C.: Cndtv.
a=(0.45±0.05)
b=(7.3±0.2)
Average Fit
y=aX+b

Fig.(46)

TABLE (3.9)

FREQUENCY RESPONSE OF LD-54 UNDER ROOM CONDITIONS

	<=== f (KHz) ===>							
	0	0.1	0.2	0.5	1	3.5	10	100
Sample								
#A σ'	7.3E-13	2.0E-9	5.1E-9	3.7E-9	2.0E-8	2.2E-8	4.9E-8	3.3E-7
K	--	8.1	5.8	5.3	4.7	5.0	4.9	4.8
DM	--	0.045	0.078	0.025	0.075	0.022	0.018	0.012
#B σ'	9.5E-13	--	6.4E-9	4.7E-9	2.1E-8	3.0E-8	3.0E-8	2.8E-7
K	--	--	6.0	5.6	5.2	5.2	5.1	5.2
DM	--	--	0.097	0.030	0.072	0.030	0.010	0.010

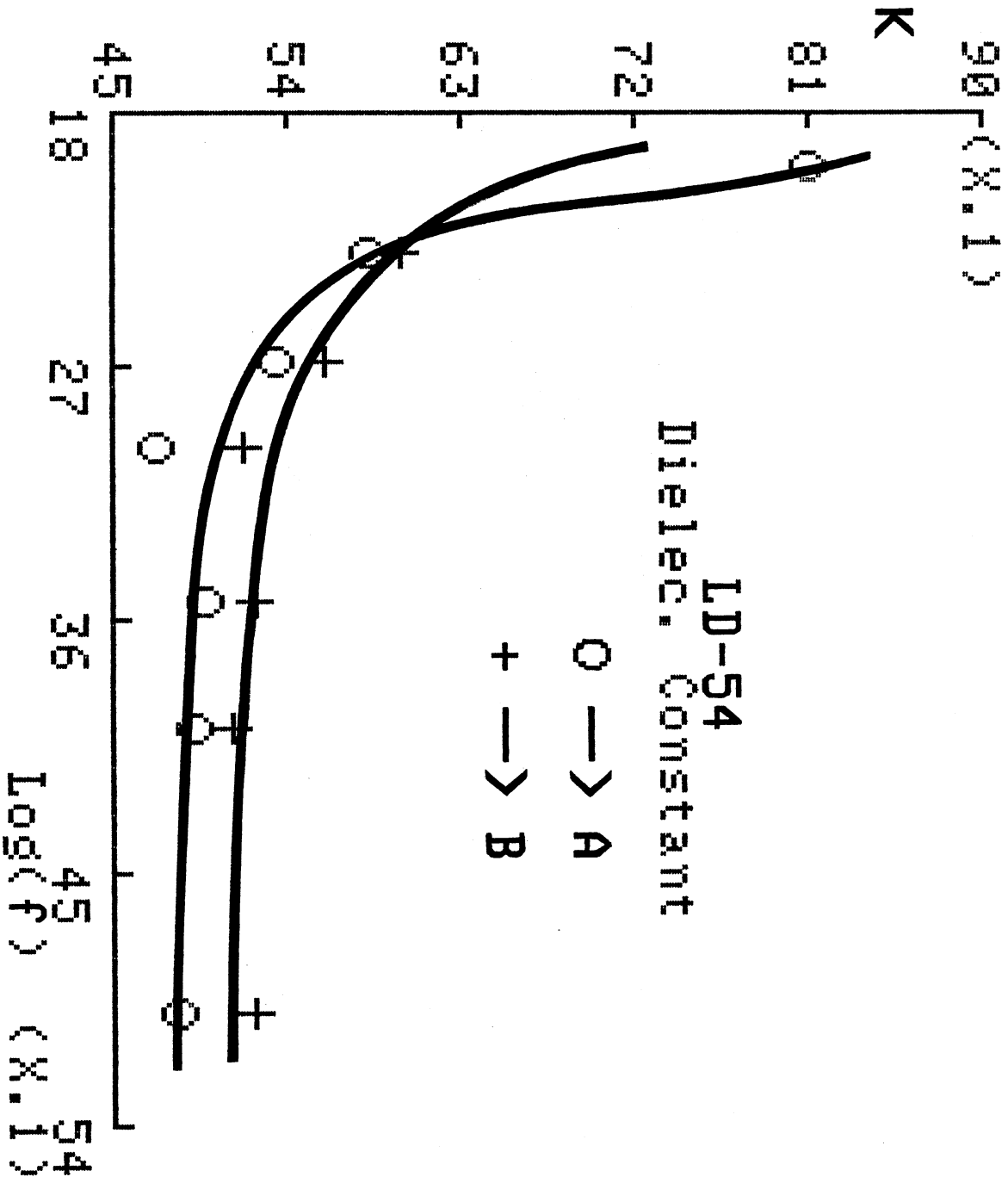
K
(x.10)
99
81
63
54
45
18
27
36
45
54
Log(f) (x.10)
LD-54
Dialac. Constant
O —V A
+ —V B

Fig.(47)

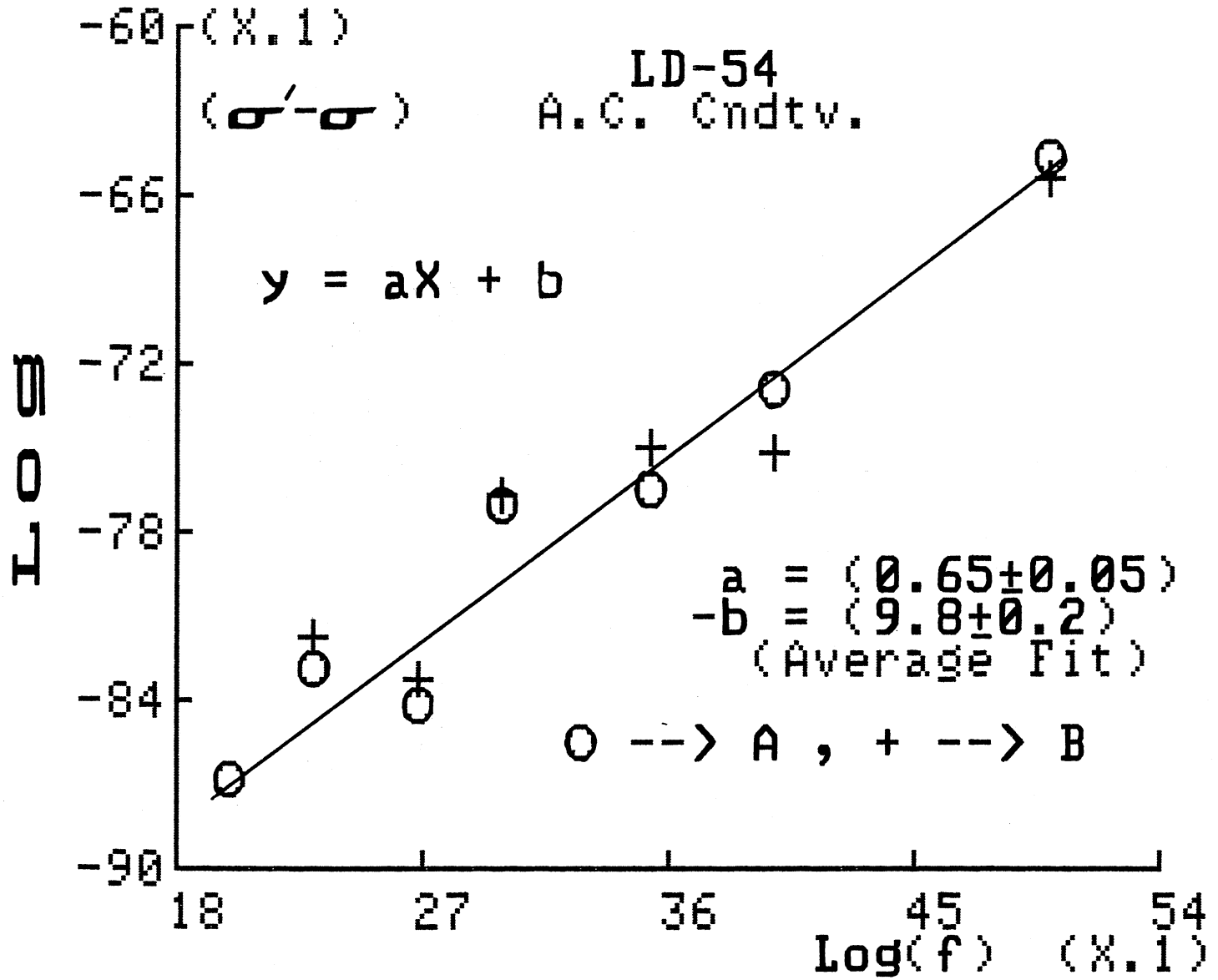
-60 (X.1)
LD-54
(σ'-σ) A.C. Cndtv.
-66
y = aX + b
-72
Log
-78
a = (0.65±0.05)
-b = (9.8±0.2)
(Average Fit)
-84
O --> A , + --> B
-90
18
27
36
45
54
Log(f) (X.1)

Fig.(48)

TABLE (3.10)

FREQUENCY RESPONSE OF LD-52B UNDER ROOM CONDITIONS

	<=== f (KHz) ===>							
	0	0.1	0.2	0.5	1	3.5	10	100
Sample								
#A o	5.2E-12	3.2E-9	6.5E-9	1.1E-8	1.7E-8	3.5E-8	7.0E-8	4.4E-7
K	---	10.2	6.4	5.4	5.3	5.1	5.0	4.9
DM	---	0.057	0.093	0.077	0.056	0.035	0.025	0.016
#H o	5.4E-12	.86E-9	3.7E-9	1.5E-8	2.0E-8	7.2E-8	1.5E-7	1.1E-6
K	---	8.2	6.3	6.5	5.8	5.7	5.5	5.4
DM	---	0.019	0.052	0.086	0.051	0.065	0.050	0.035

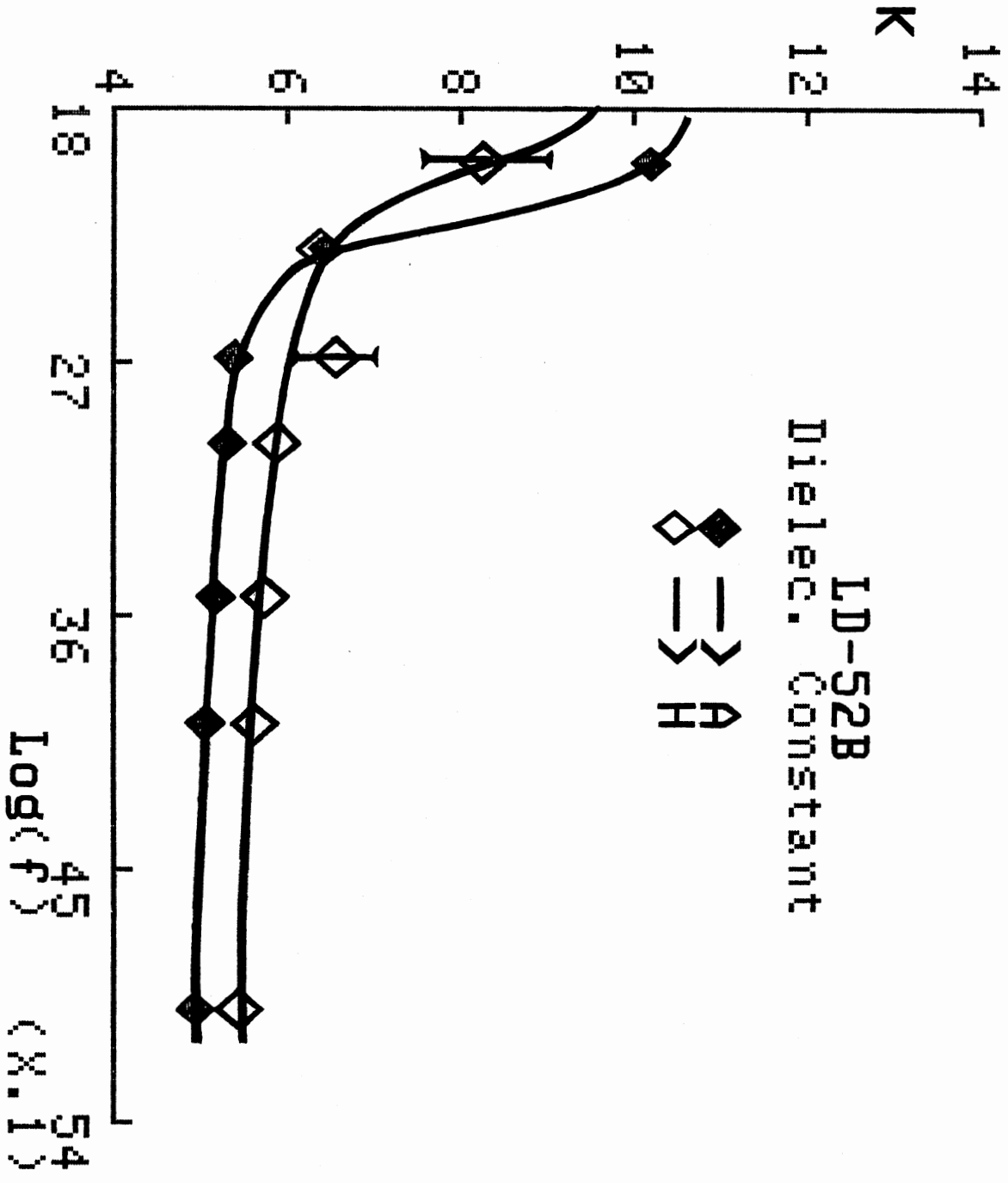

Fig.(49)

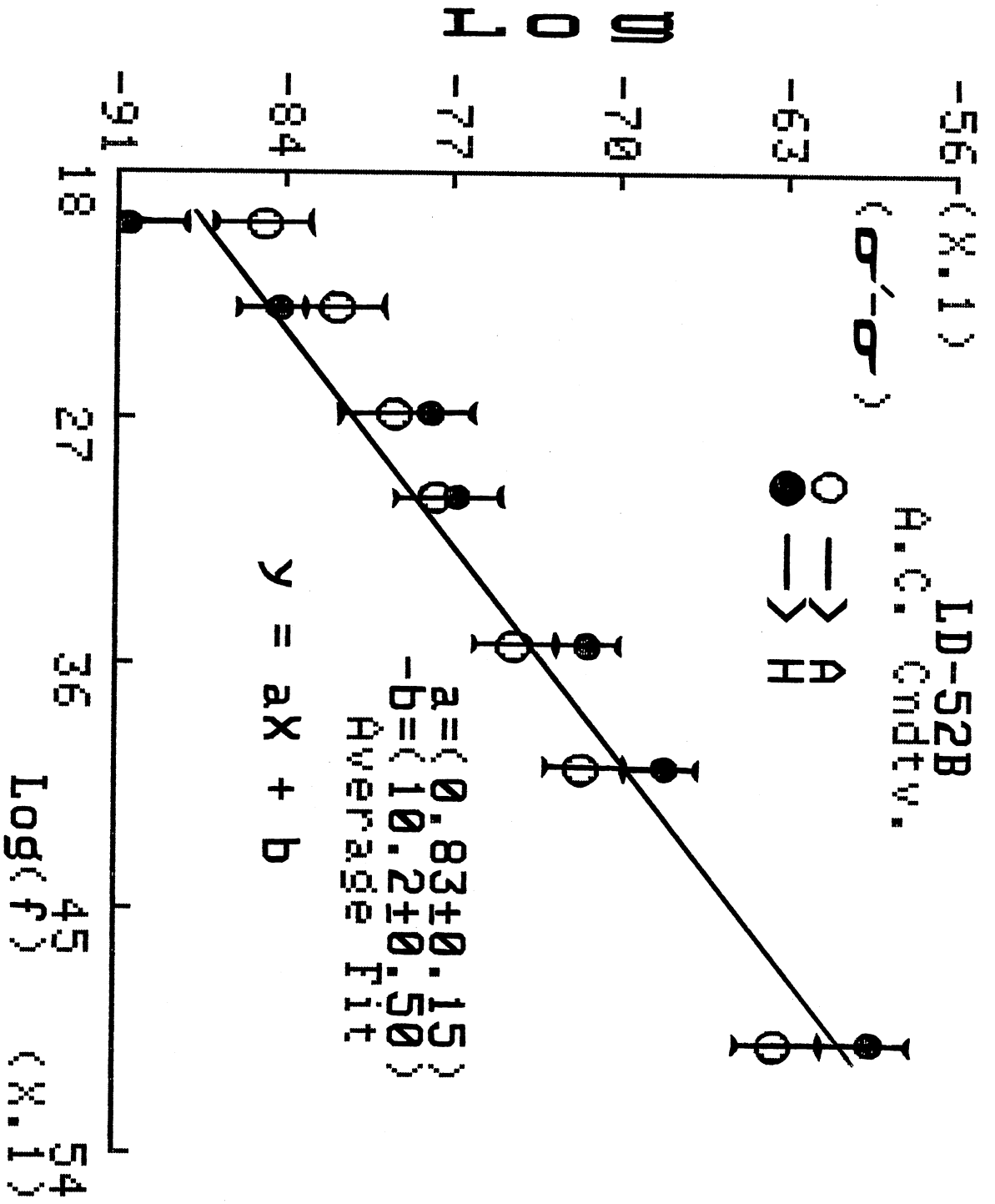
Log
-56 (x.1)
-63
-70
-77
-84
-91
18
22
26
30
34
Log(f)
(x.1)
LD-52B
A.C. Cndtv.
(q'-q)
A
H
y = ax + b
a=(0.82±0.15)
b=(10.2±0.50)
Average Fit

Fig.(50)

TABLE (3.11)

FREQUENCY RESPONSE OF LD-106 UNDER ROOM CONDITIONS

	<=== f (KHz) ===>							
	0	0.1	0.2	0.5	1	3.5	10	100
Sample								
#C σ'	1.0E-10	1.9E-8	3.9E-8	1.9E-8	9.1E-8	1.9E-7	3.2E-7	1.3E-6
K	--	11.4	9.5	8.1	7.5	6.7	6.3	5.8
DM	--	0.31	0.38	0.082	0.22	0.15	0.089	0.039
#E σ'	2.3E-10	2.1E-8	3.7E-8	1.8E-8	1.3E-7	2.7E-7	4.7E-7	1.9E-6
K	--	11.1	8.5	7.3	6.1	5.1	4.5	4.0
DM	--	0.35	0.39	0.090	0.38	0.28	0.19	0.087

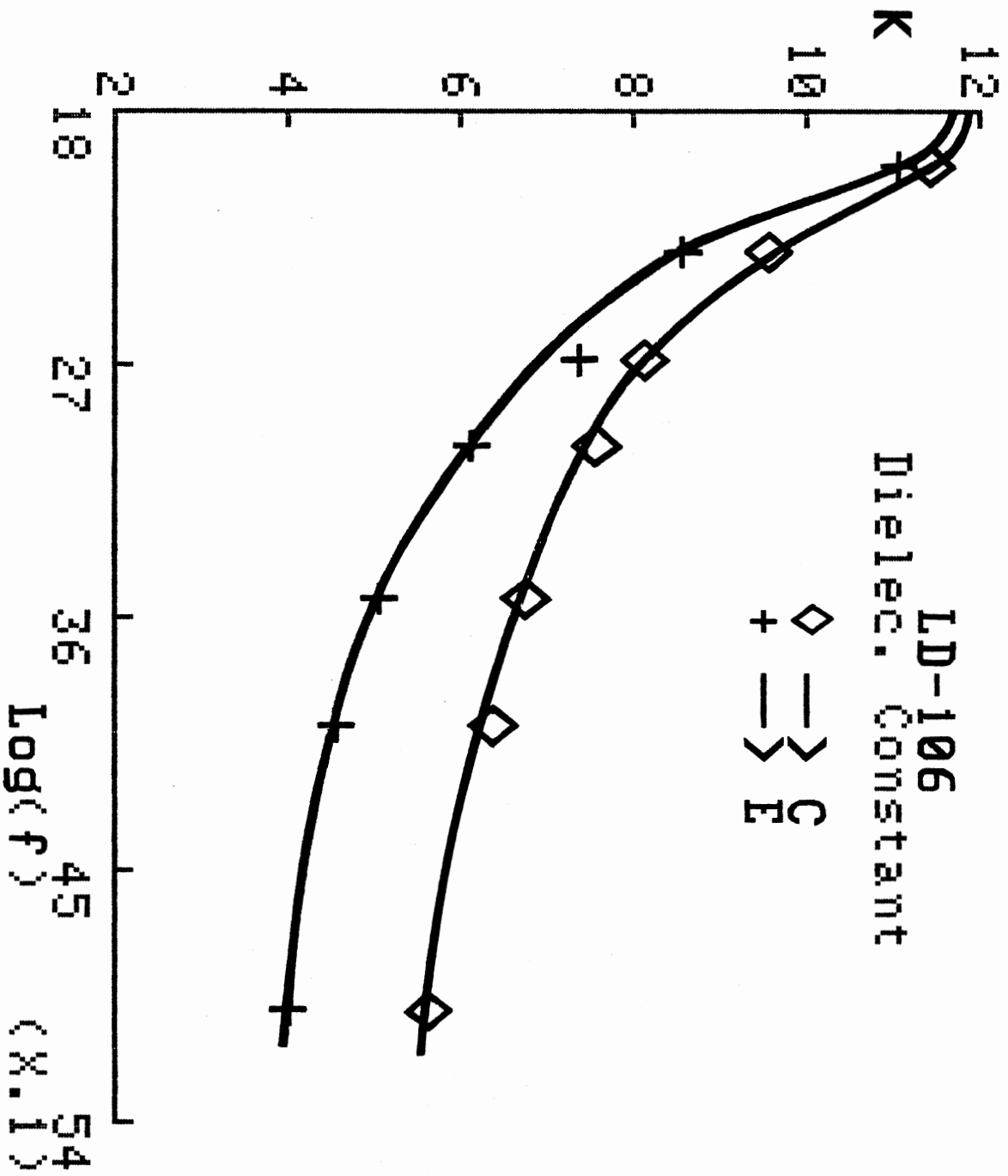

Fig.(51)

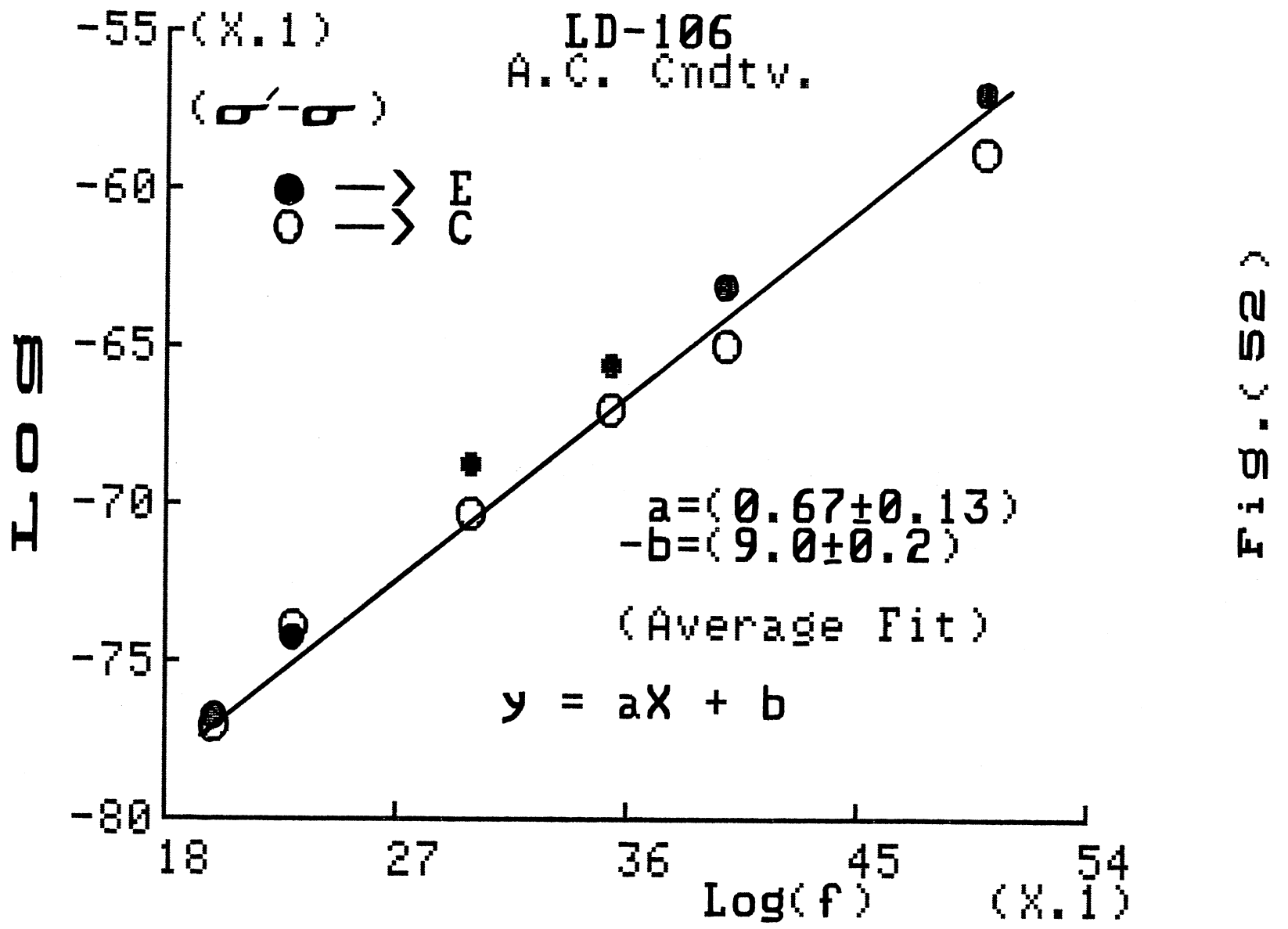
LD-106
A.C. Cndtv.
(σ'-σ)
(X.1)
-55
-60
-65
-70
-75
-80
● → E
○ → C
a=(0.67±0.13)
-b=(9.0±0.2)
(Average Fit)
y = aX + b
18
27
36
45
54
Log(f)
(X.1)
Log σ

Fig.(52)

B) The Effects of Pressure on Polymer Characteristics

The polymer species under study showed quite a diversity in their characteristics when subjected to pressure. Only a few displayed the "normal" pattern, namely, the logarithmic increase of the conductivity and dielectric constant in proportion to the square-root of the pressure. In most cases it was found that both σ' and the D.C. conductivity σ, rather than their logarithm, displayed a better linear fit with P, or the square-root of P. Similarly, "K" instead of $\text{Log}_e(K)$, showed an approximate linear increase with P or $\sqrt{P}$ in most cases. The only exception was (LD-14A) where "K" actually decreased with $\sqrt{P}$. It is also noted that the higher the frequency, the greater the "saturation" pressure becomes.

The fact that "K" decreases with $\sqrt{P}$ for LD-14A shows that for this particular polymer the loss factor DM increases at a higher rate than the usual $P^{1/2}$ - law.

Tables (3.12)-(3.21) summarize the dependence of K, σ', DM, and σ on the applied pressure. The piezo-capacitive and piezo-conductive coefficients are evaluated off the graphs in Figs.(53)-(88). The units of these coefficients are sometimes omitted for lack of space. The symbols "a" and "b" are defined through the linear fit equation: y = ax + b in all cases. For brevity, the abbreviation "Cndtv." is sometimes used in place of the full word "Conductivity". Unless otherwise noted, all measurements in this section were taken at room temperature.

Due to the limited range of the Schering bridge loss-factor dial, several polymers had to be observed at 10 KHz. and 100 KHz.

All quantities are presented to two significant figures, except in some cases where it was deemed necessary to retain three digits in order to make appear the fineness of the variations in certain slowly varying quantities. In general the third figure is not significant and should only be regarded as a convenience in graphical fitting.

The pressure guage readings were corrected for the shift in the zero-point, due to the weight of the upper anvil and the backing plate. The correction was to add 0.0405 K.Bars to all pressure readings.

TABLE (3.12)

THE EFFECTS OF PRESSURE ON LD-105 AT 100 KHz.

	<===$\sqrt{}$PRESSURE (K.Bars)$^{1/2}$===>								
Sample	0.23	0.27	0.31	0.39	0.51	0.69	0.96	1.25	1.49
K : σ'	1.4	1.5	1.7	1.8	2.7	4.0	6.3	9.7	--
K	13.3	13.2	13.2	13.0	14.4	14.7	14.6	12.8	--
DM	1.8	2.0	2.3	2.5	3.4	4.9	7.7	13.6	--
σ	8.5	9.3	11	15	21	33	54	88	115
L : σ'	1.6	1.7	1.8	2.2	2.8	4.0	6.2	--	--
K	13.9	13.7	13.6	13.0	13.1	14.3	15.0	--	--
DM	2.1	2.2	2.4	3.1	3.9	5.0	7.4	--	--
σ	8.7	11	12	15	20	31	52	79	107

Two Samples (K) And (L) Are Shown For Verifying The Reproducibility Of The Measurements. All Values Of σ' Are (X1E-4), While Those Of σ Are (X1E-7).

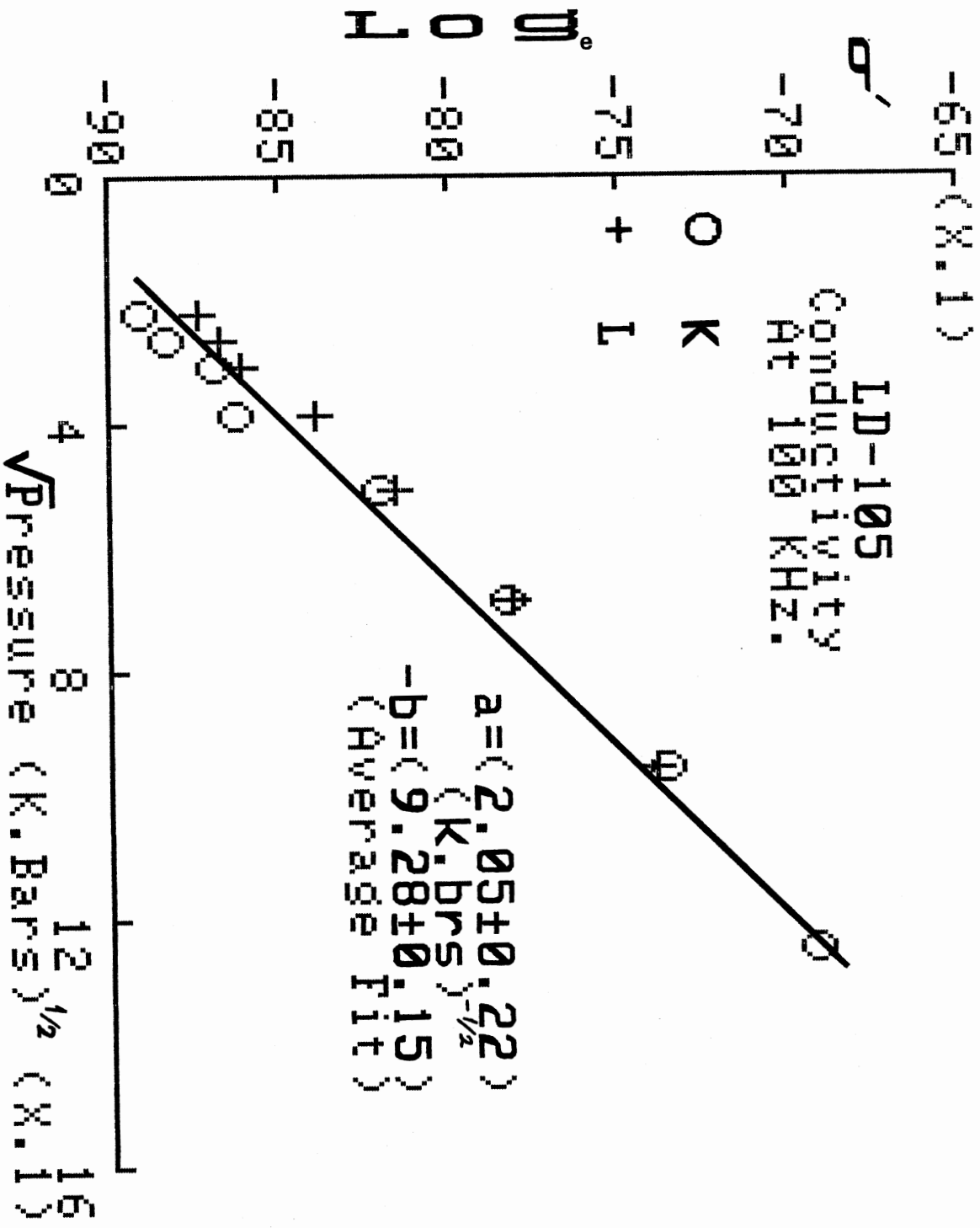
Log e
q´
-65 (x.1)
-70
-75
-80
-85
-90
0
4
8
12
15 (x.1)
√Pressure (K.Bars)½ (x.1)
LD-105
Conductivity
At 100 KHz.
T
K
O
+
a=(2.05±0.22)
(K.bars)-½
-b=(9.28±0.15)
(Average Fit)

Fig.(53)

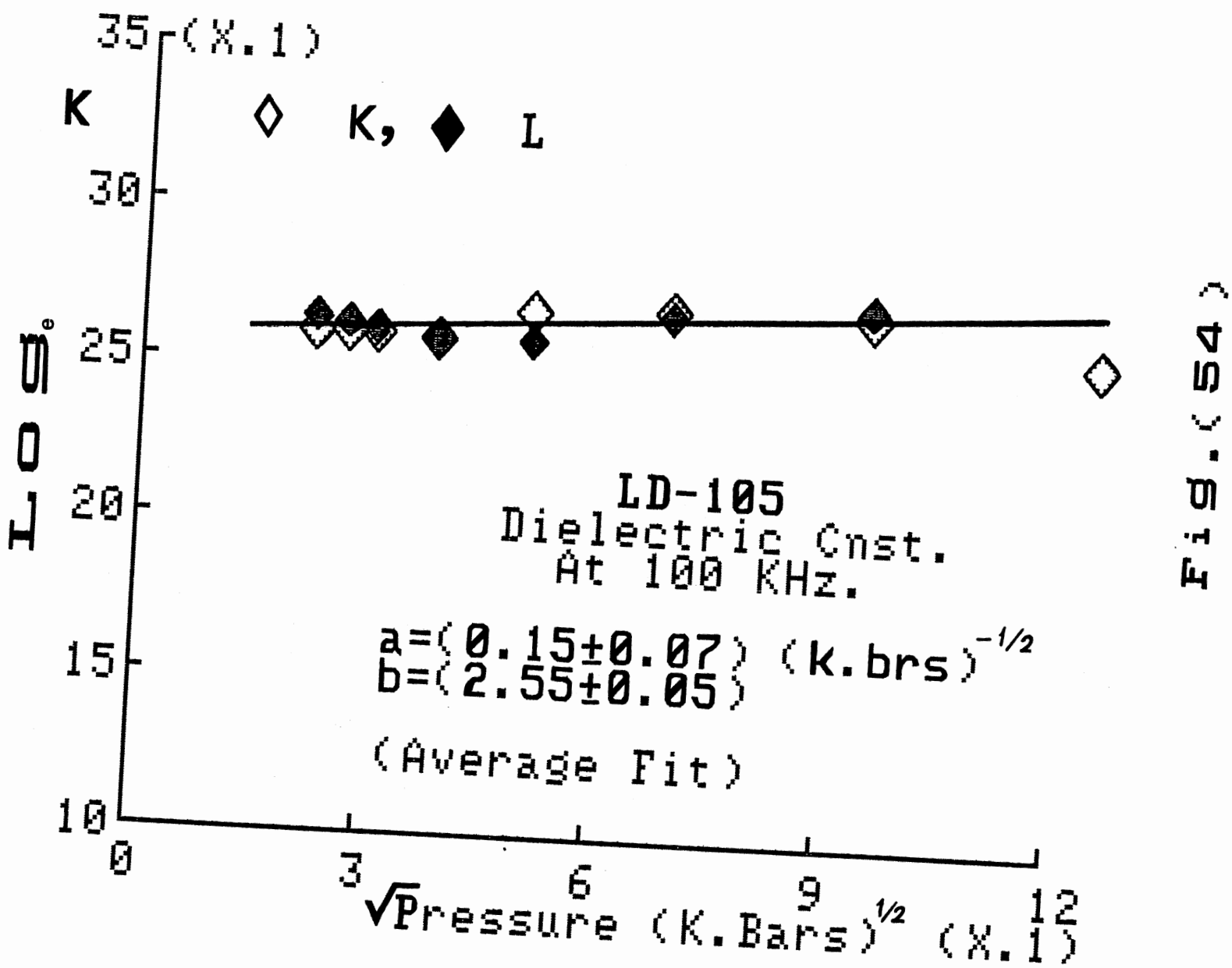
35 (X.1)
K
◇ K, ◆ L
30
25
20
15
10
0
3
6
9
12
Log$_e$
LD-105
Dielectric Cnst.
At 100 KHz.
a=(0.15±0.07) (k.brs)$^{-1/2}$
b=(2.55±0.05)
(Average Fit)
$\sqrt{P}$ Pressure (K.Bars)$^{1/2}$ (X.1)

Fig.(54)

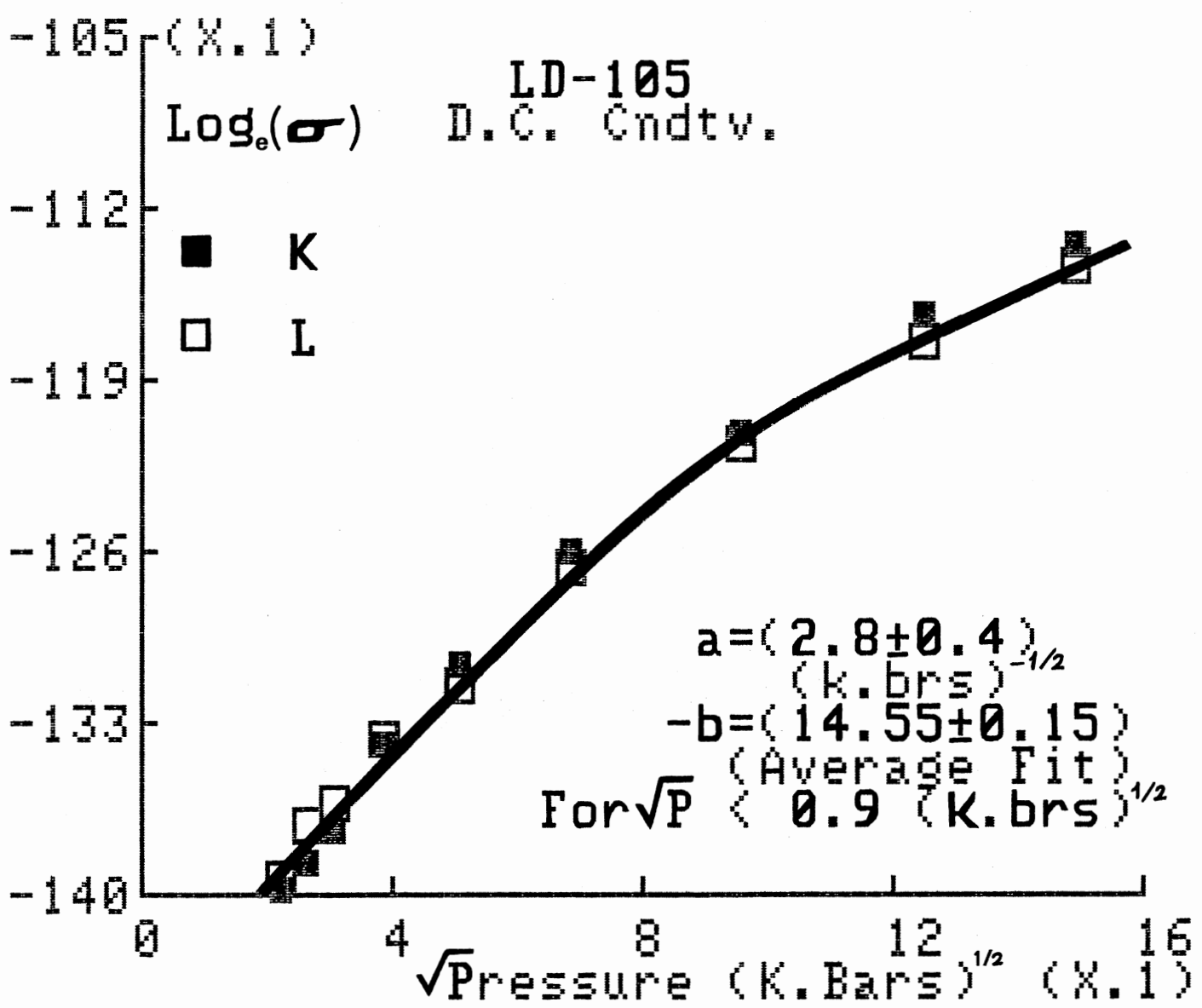
-105 (X.1)
LD-105
Log$_e$(σ) D.C. Cndtv.
-112
K
L
-119
-126
-133
-140
a=(2.8±0.4)$^{-1/2}$ (k.brs)
-b=(14.55±0.15)
(Average Fit)
For $\sqrt{P}$ < 0.9 (K.brs)$^{1/2}$
0
4
8
12
16
$\sqrt{P}$ Pressure (K.Bars)$^{1/2}$ (X.1)

Fig.(55)

TABLE (3.13)

THE EFFECTS OF PRESSURE ON LD-104 AT 1 KHz.

	<===$\sqrt{P}$RESSURE (K.Bars)$^{1/2}$===>								
Sample	0.23	0.27	0.31	0.39	0.51	0.69	0.96	1.25	1.49
G : σ'	0.97	1.4	2.2	3.3	4.4	6.0	7.8	--	--
K	25	27	29	29	30	32	33	--	--
DM	0.70	0.94	1.3	2.1	2.6	3.4	4.6	--	--
σ	2.9	5.0	7.0	14	16	28	43	56	68
H : σ'	0.83	1.1	2.0	3.7	5.3	7.3	--	--	--
K	21	24	30	32	34	36	--	--	--

cont'd

TABLE (3.13) Cont'd

	DM	0.72	0.80	1.2	2.1	2.8	3.7	--	--	--
	σ	1.5	2.7	7.8	13	22	38	50	63	78
H :	σ'	7.0	7.2	7.7	8.7	9.8	12	14	16	17
	K	13.3	13.3	13.4	13.8	14.7	16	18	19	20
	DM	0.95	0.98	1.03	1.13	1.2	1.3	1.4	1.5	1.5

The Listings For Sample (H) At The Bottom (3rd Section) Were Taken At 10 KHz. All Values of σ' Are (X1E-6), While Those Of σ (DC) Are (X1E-9).

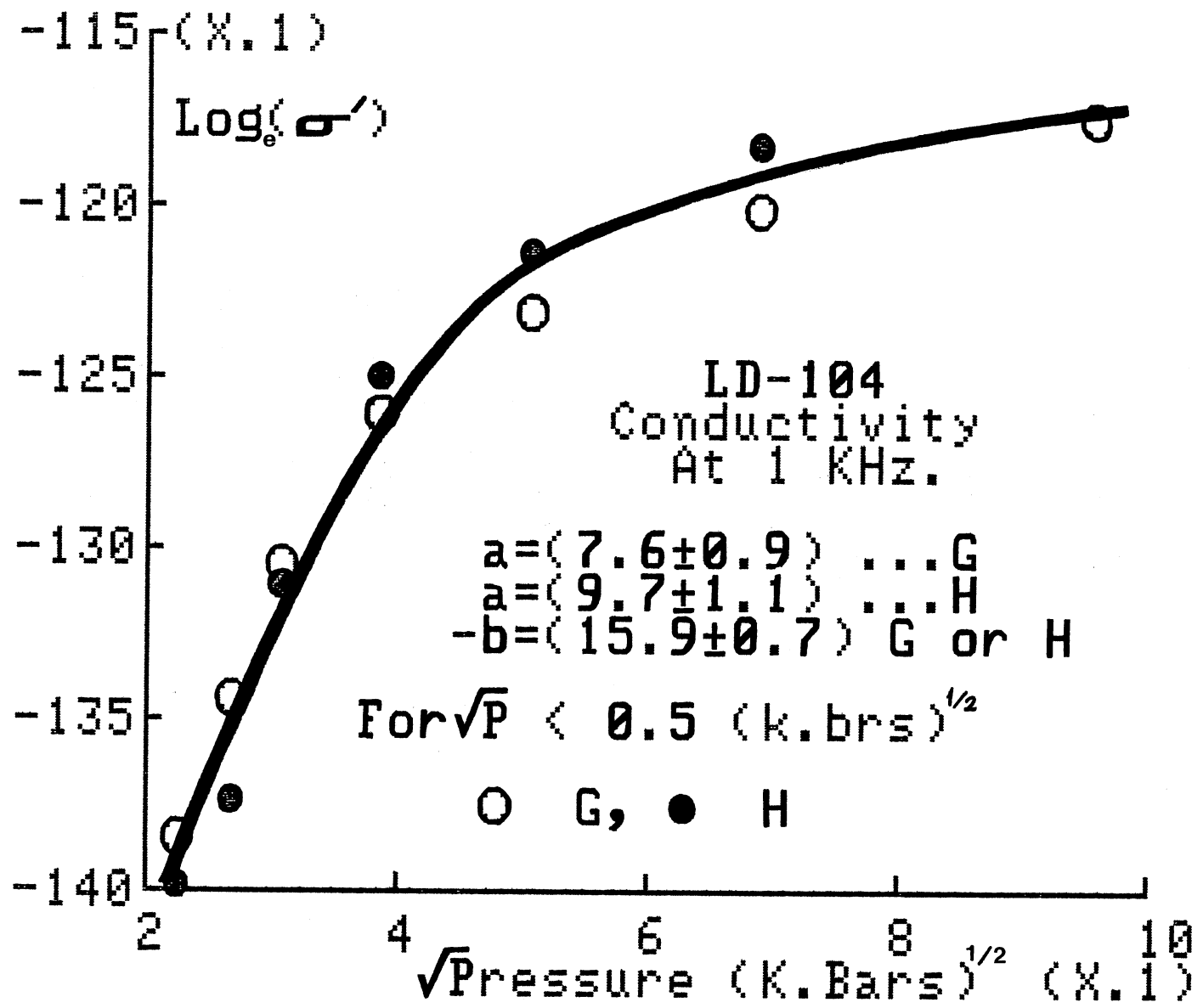
-115 (X.1)
Log$_e$(σ′)
-120
-125
-130
-135
-140
2
4
6
8
10
√Pressure (K.Bars)$^{1/2}$ (X.1)
LD-104
Conductivity
At 1 KHz.
a=(7.6±0.9) ...G
a=(9.7±1.1) ...H
-b=(15.9±0.7) G or H
For√P < 0.5 (k.brs)$^{1/2}$
O G, ● H

Fig. (56)

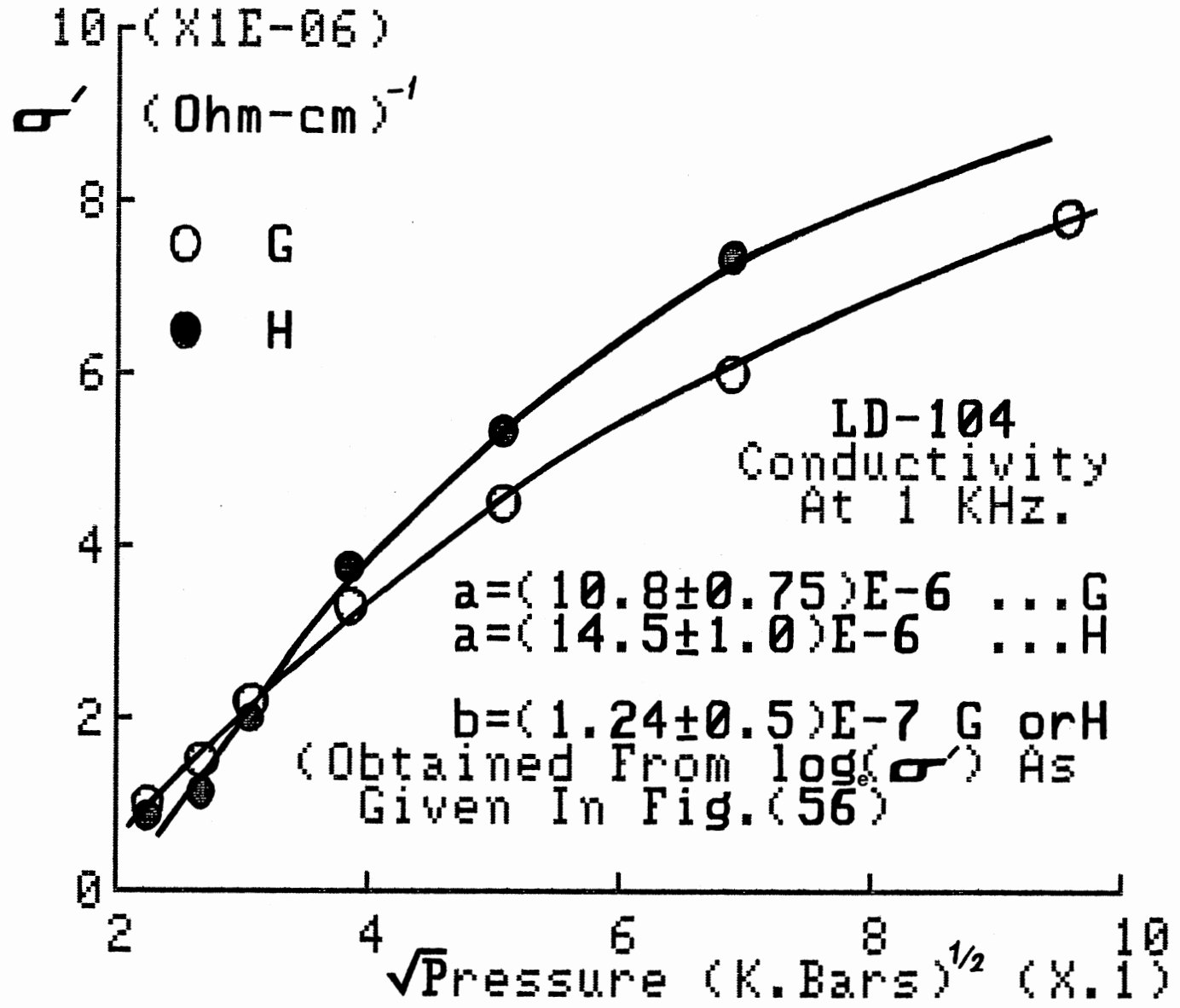
10
(X1E-06)
σ′
(Ohm-cm)⁻¹
8
6
4
2
0
O G
● H
LD-104
Conductivity
At 1 KHz.
a=(10.8±0.75)E-6 ...G
a=(14.5±1.0)E-6 ...H
b=(1.24±0.5)E-7 G orH
(Obtained From log(σ′) As
Given In Fig.(56)
2
4
6
8
10
√Pressure (K.Bars)^1/2 (X.1)

Fig.(57)

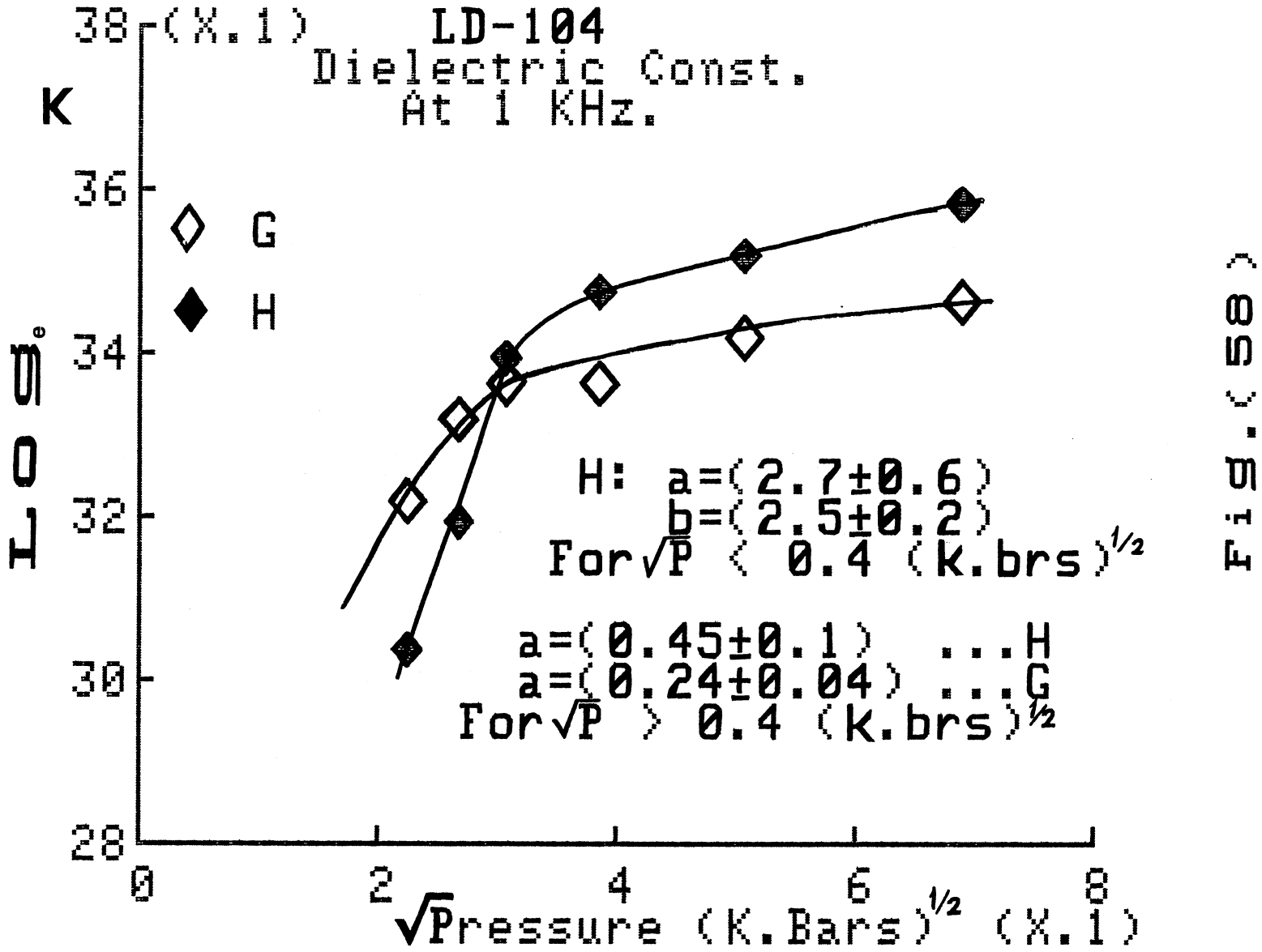
(X.1)
LD-104
Dielectric Const.
At 1 KHz.
K
38
36
34
32
30
28
0
2
4
6
8
G
H
H: a=(2.7±0.6)
b=(2.5±0.2)
For √P < 0.4 (k.brs)^1/2
a=(0.45±0.1) ...H
a=(0.24±0.04) ...G
For √P > 0.4 (k.brs)^1/2
√Pressure (K.Bars)^1/2 (X.1)

Fig. (58)

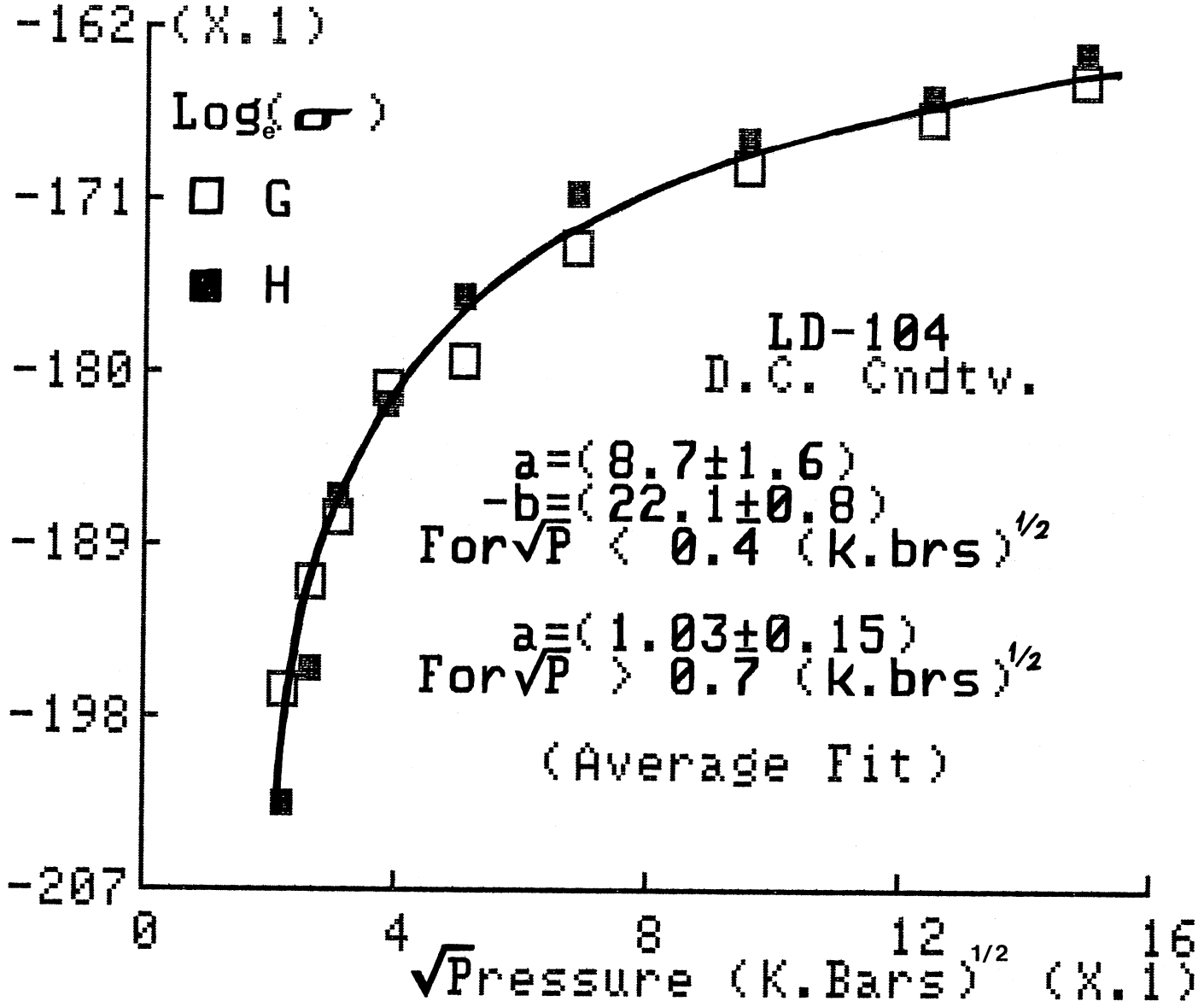
-162 (X.1)
Log$_e$(σ)
-171
-180
-189
-198
-207
G
H
LD-104
D.C. Cndtv.
a=(8.7±1.6)
-b=(22.1±0.8)
For√P < 0.4 (k.brs)$^{1/2}$
a=(1.03±0.15)
For√P > 0.7 (k.brs)$^{1/2}$
(Average Fit)
0
4
8
12
16
√Pressure (K.Bars)$^{1/2}$ (X.1)

Fig. C 59

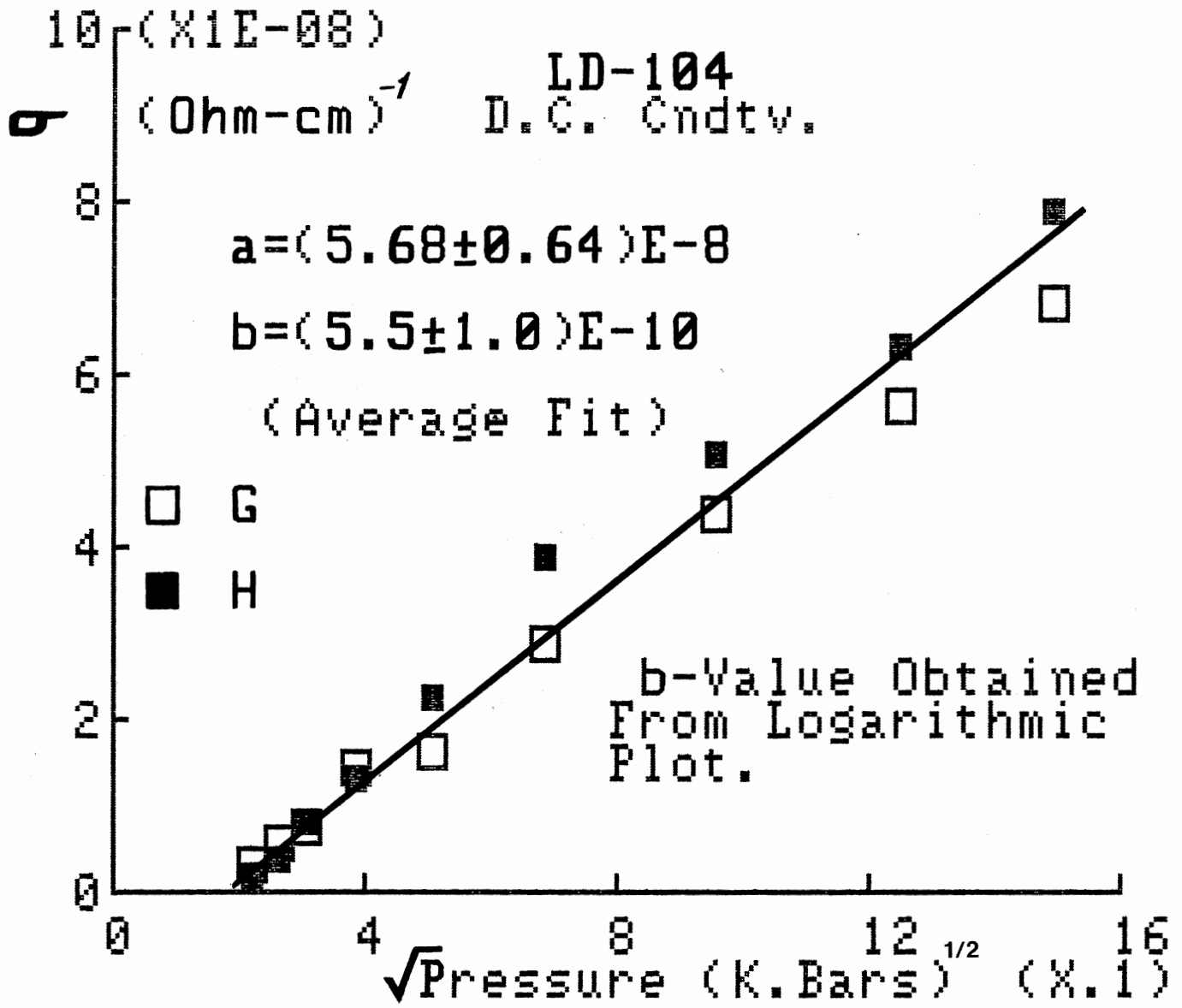
10
(X1E-08)
σ
(Ohm-cm)^-1
LD-104
D.C. Cndtv.
8
a=(5.68±0.64)E-8
6
b=(5.5±1.0)E-10
(Average Fit)
G
H
4
2
0
b-Value Obtained
From Logarithmic
Plot.
0
4
8
12
16
√Pressure (K.Bars)^1/2 (X.1)

Fig. (60)

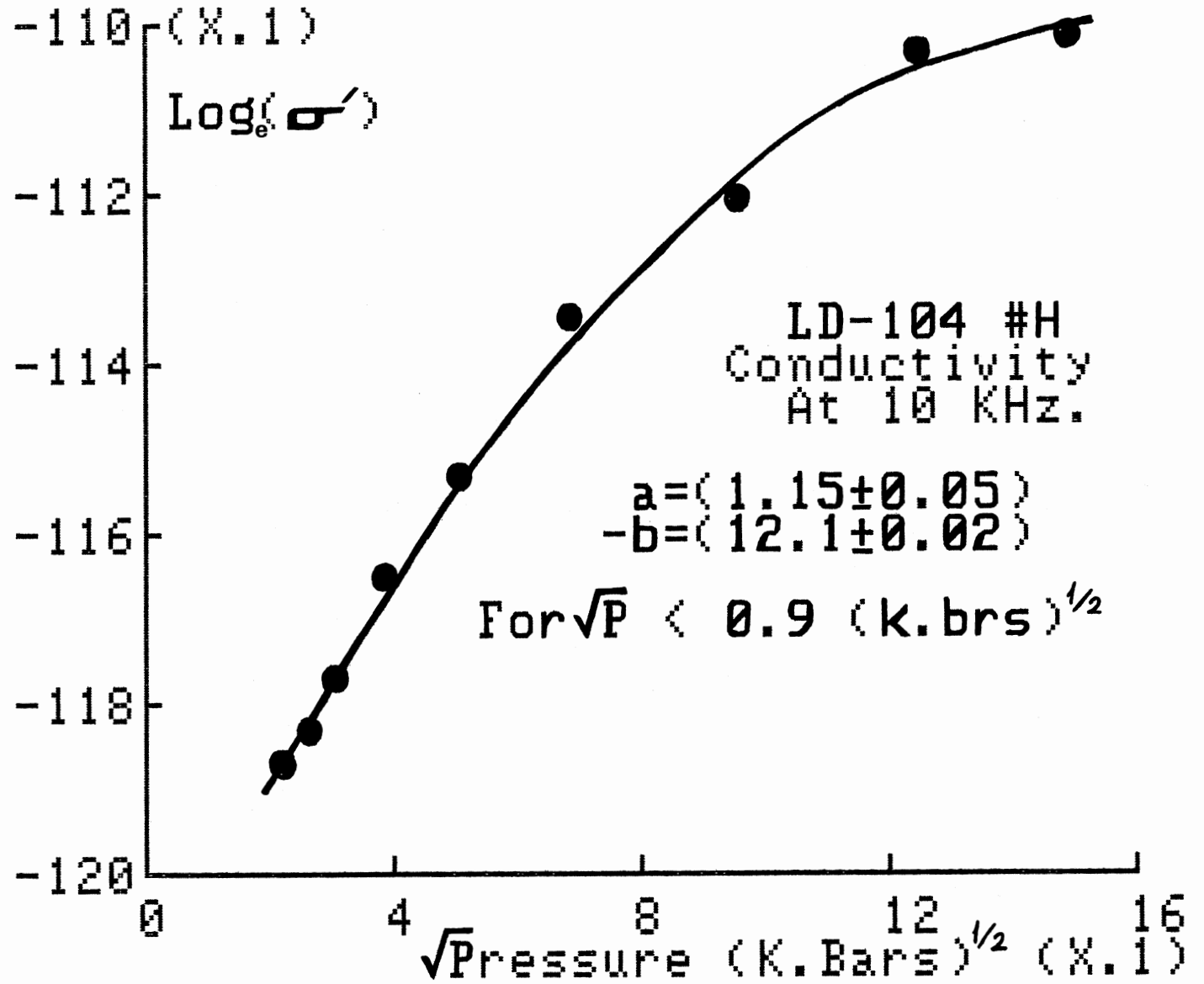
-110 (X.1)
Log$_e$(σ′)
-112
-114
-116
-118
-120
0
4
8
12
16
√P Pressure (K.Bars)$^{1/2}$ (X.1)
LD-104 #H
Conductivity
At 10 KHz.
a=(1.15±0.05)
-b=(12.1±0.02)
For √P < 0.9 (k.brs)$^{1/2}$

Fig.(61)

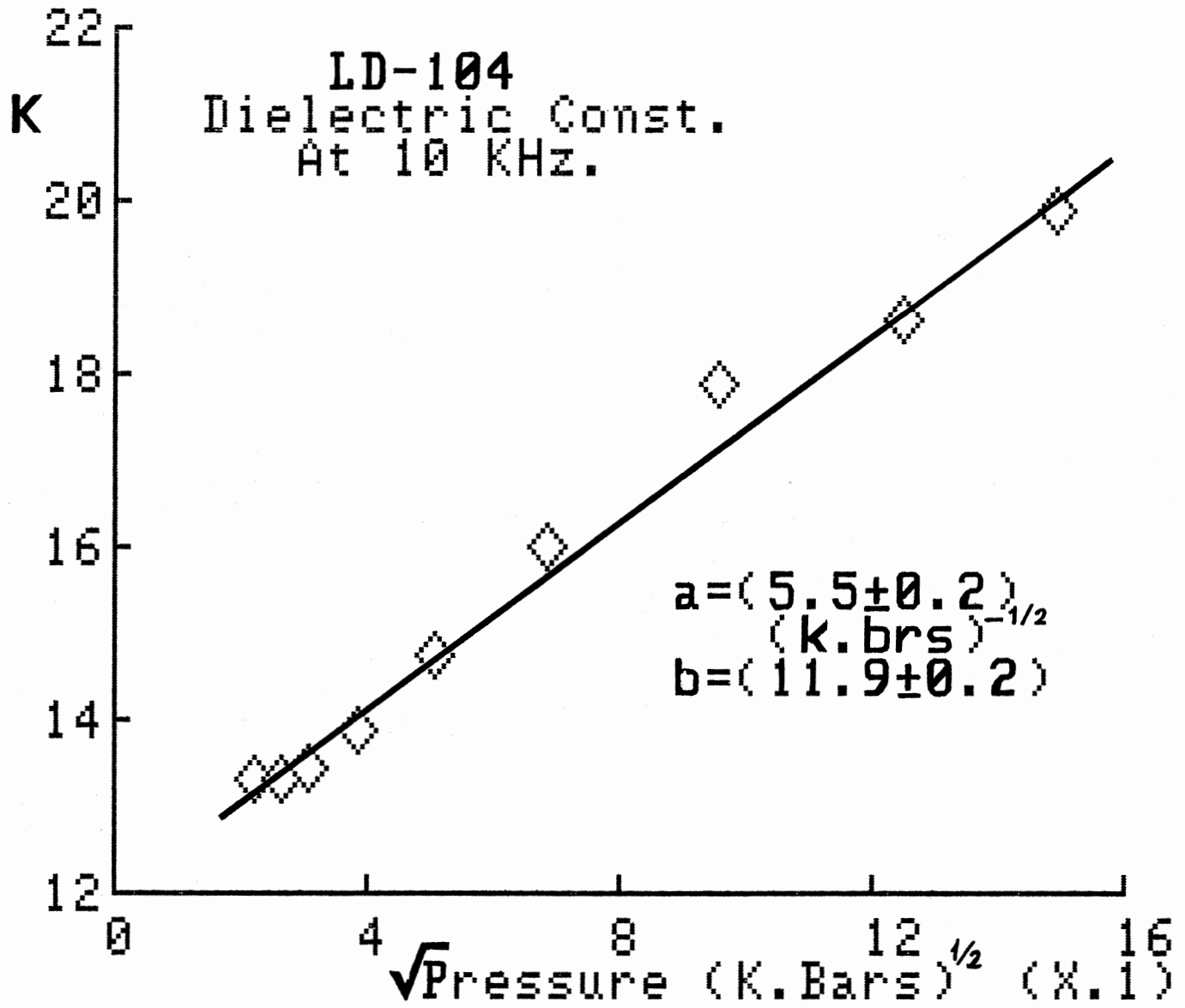
LD-104
Dielectric Const.
At 10 KHz.
K
22
20
18
16
14
12
0
4
8
12
16
√Pressure (K.Bars)^1/2 (X.1)
a=(5.5±0.2) (k.brs)^-1/2
b=(11.9±0.2)

Fig.(62)

TABLE (3.14)

THE EFFECTS OF PRESSURE ON LD-97 AT 10 KHz.
AND 100 KHz. RESPECTIVELY

	<===$\sqrt{\text{PRESSURE}}$ (K.Bars)$^{1/2}$===>								
Sample	0.23	0.27	0.31	0.39	0.51	0.69	0.96	1.25	1.49
S : σ'	1.5	1.6	1.8	2.1	2.6	3.2	3.8	4.2	4.4
K	23.6	23.7	23.9	25.3	27.0	28.5	29.7	31.0	30.4
DM	1.17	1.23	1.4	1.5	1.7	2.0	2.3	2.4	2.6
σ	4.1	5.0	5.3	7.5	8.5	12	15	18	18
T : σ'	1.1	1.3	1.4	2.0	2.6	3.4	4.1	4.6	4.6
K	20.5	22.6	22.8	24.5	27.2	31.0	32.4	33.6	32.6

cont'd

TABLE (3.14) Cont'd

	DM	0.94	1.1	1.1	1.5	1.7	1.9	2.3	2.5	2.6
	σ	2.5	3.6	4.2	6.9	8.4	13	16	19	19
S :	σ'	4.3	4.4	4.7	5.2	6.0	6.8	7.8	8.4	8.4
	K	10.1	10.2	10.4	10.8	11.6	12.5	13.5	13.9	13.9
	DM	0.76	0.78	0.81	0.86	0.93	0.99	1.03	1.08	1.08
T :	σ'	3.25	3.34	3.70	5.1	6.1	7.2	8.5	9.1	--
	K	9.50	9.80	10.3	11.2	12.1	13.5	14.8	15.3	--
	DM	0.62	0.61	0.65	0.81	0.90	0.96	1.03	1.07	--

Two Samples S and T Are Shown To Verify Reproducibility. All Values Of σ' are (X1E-5), While Those Of σ Are (X1E-8).

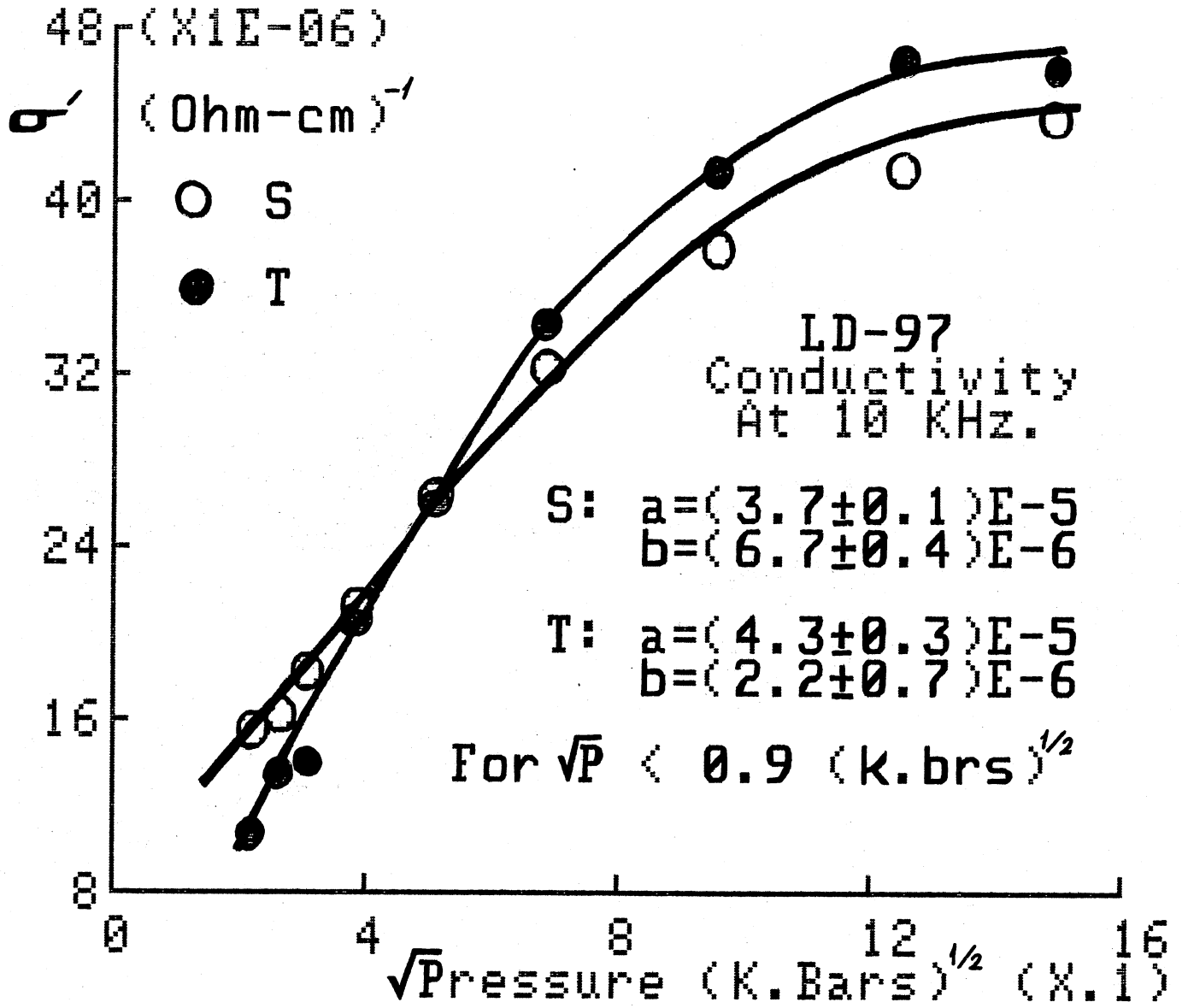
48
40
32
24
16
8
(X1E-06)
σ′
(Ohm-cm)⁻¹
O S
● T
LD-97
Conductivity
At 10 KHz.
S: a=(3.7±0.1)E-5
b=(6.7±0.4)E-6
T: a=(4.3±0.3)E-5
b=(2.2±0.7)E-6
For √P < 0.9 (k.brs)^1/2
0
4
8
12
16
√Pressure (K.Bars)^1/2 (X.1)

Fig. 63

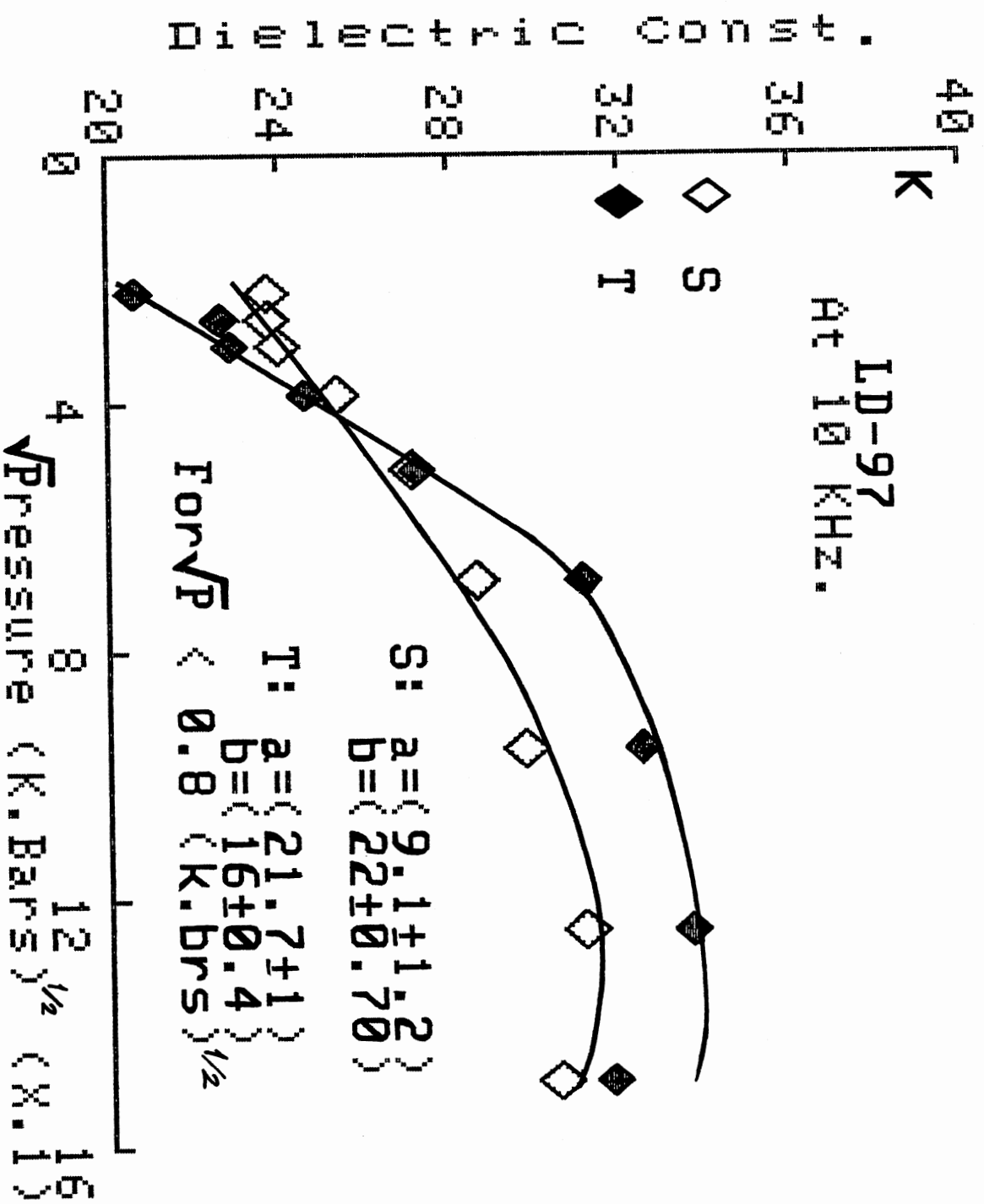
Dielectric Const.
K
S
T
LD-97
At 10 kHz.
For √P < 0.8 (K.brs)^1/2
S: a=(9.1±1.2)
b=(22±0.70)
T: a=(21.7±1)
b=(16±0.4)
√Pressure (K.Bars)^1/2 (x.10)

Fig.(64)

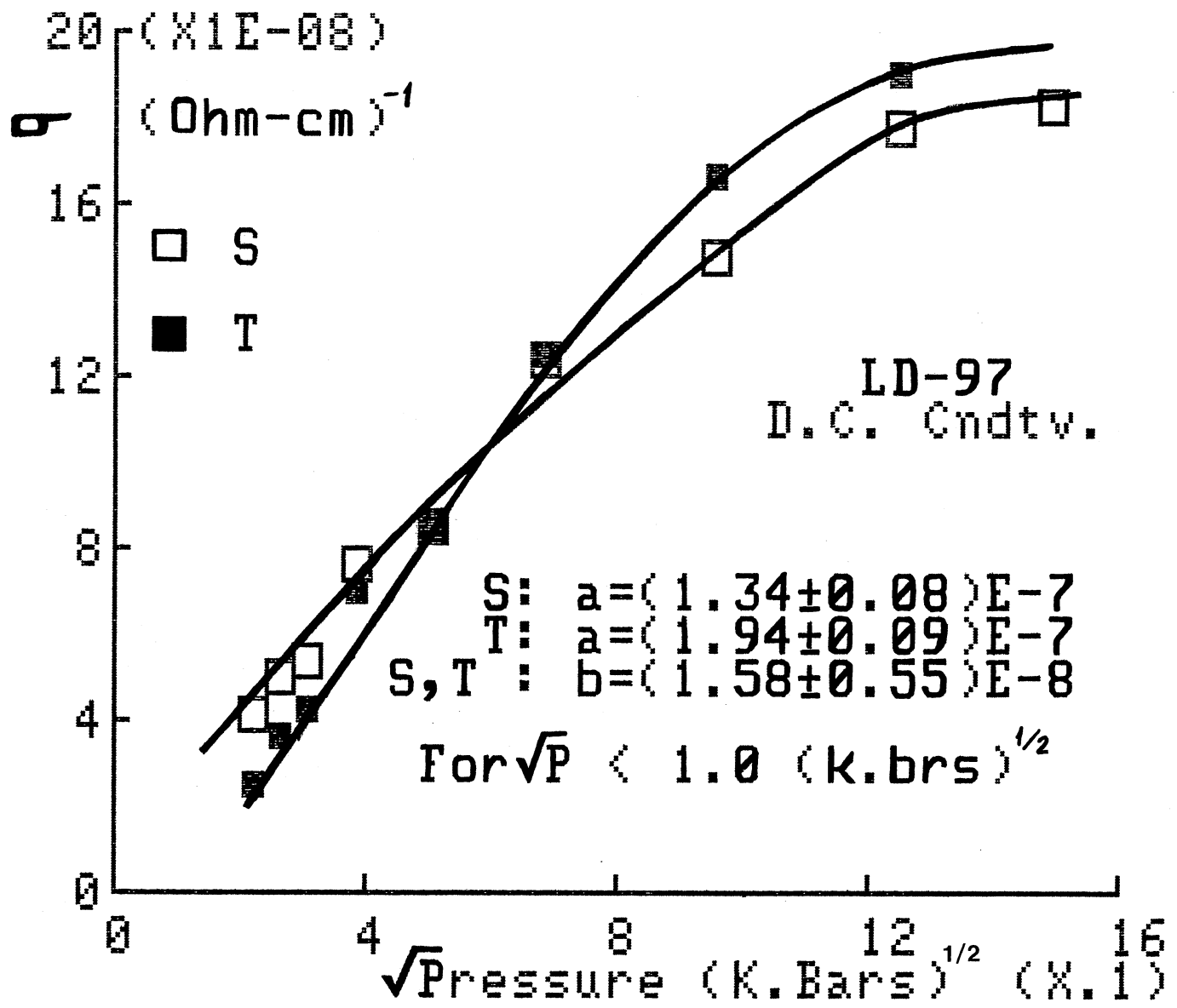
20
(X1E-08)
σ
(Ohm-cm)$^{-1}$
16
S
T
12
LD-97
D.C. Cndtv.
8
S: a=(1.34±0.08)E-7
T: a=(1.94±0.09)E-7
S,T : b=(1.58±0.55)E-8
4
For√P < 1.0 (k.brs)$^{1/2}$
0
0
4
8
12
16
√Pressure (K.Bars)$^{1/2}$ (X.1)

Fig. (65)

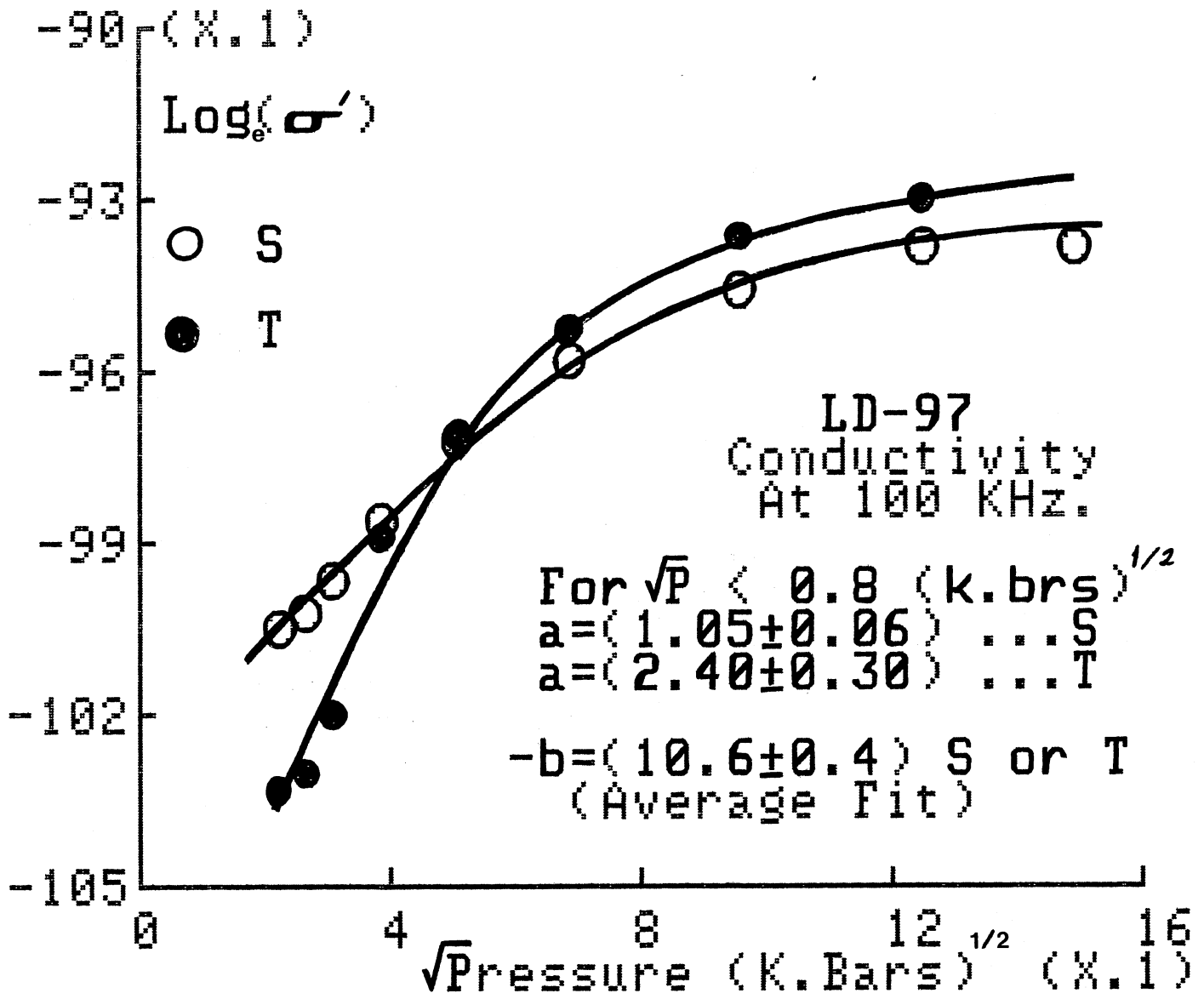
-90 (X.1)
Log$_e$(σ')
-93
-96
-99
-102
-105
O S
● T
LD-97
Conductivity
At 100 KHz.
For √P < 0.8 (k.brs)$^{1/2}$
a=(1.05±0.06) ...S
a=(2.40±0.30) ...T
-b=(10.6±0.4) S or T
(Average Fit)
0
4
8
12
16
√Pressure (K.Bars)$^{1/2}$ (X.1)

Fig. (66)

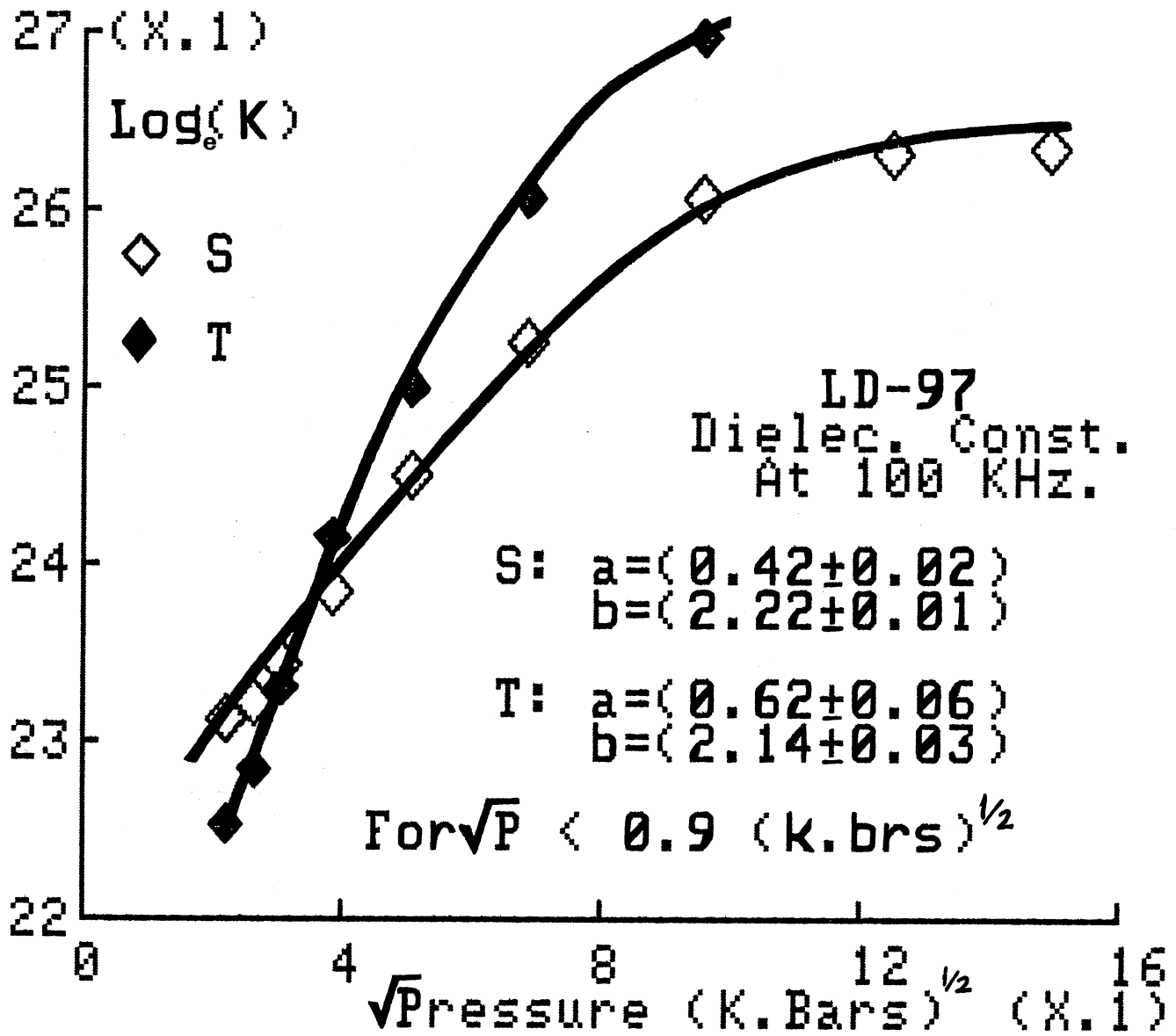
27 (X.1)
Log$_e$(K)
26
25
24
23
22
◇ S
◆ T
LD-97
Dielec. Const.
At 100 KHz.
S: a=(0.42±0.02)
b=(2.22±0.01)
T: a=(0.62±0.06)
b=(2.14±0.03)
For $\sqrt{P}$ < 0.9 (k.brs)$^{1/2}$
0
4
8
12
16
$\sqrt{P}$ Pressure (K.Bars)$^{1/2}$ (X.1)

Fig. (67)

TABLE (3.15)

THE EFFECTS OF PRESSURE ON LD-95 AT 10 KHz.

	<===√PRESSURE (K.Bars)$^{1/2}$===>								
Sample	0.23	0.27	0.31	0.39	0.51	0.69	0.96	1.25	1.49
B : σ'	3.8	5.5	6.7	8.2	9.8	13	18	27	42
K	6.2	7.0	8.1	9.1	11	13	17	20	23
DM	1.1	1.4	1.5	1.6	1.6	1.8	2.0	2.5	3.2
σ	1.2	2.1	2.9	3.4	5.4	8.1	13	19	25

All Values Of σ' Are (X1E-6), While Those Of σ Are (X1E-8).

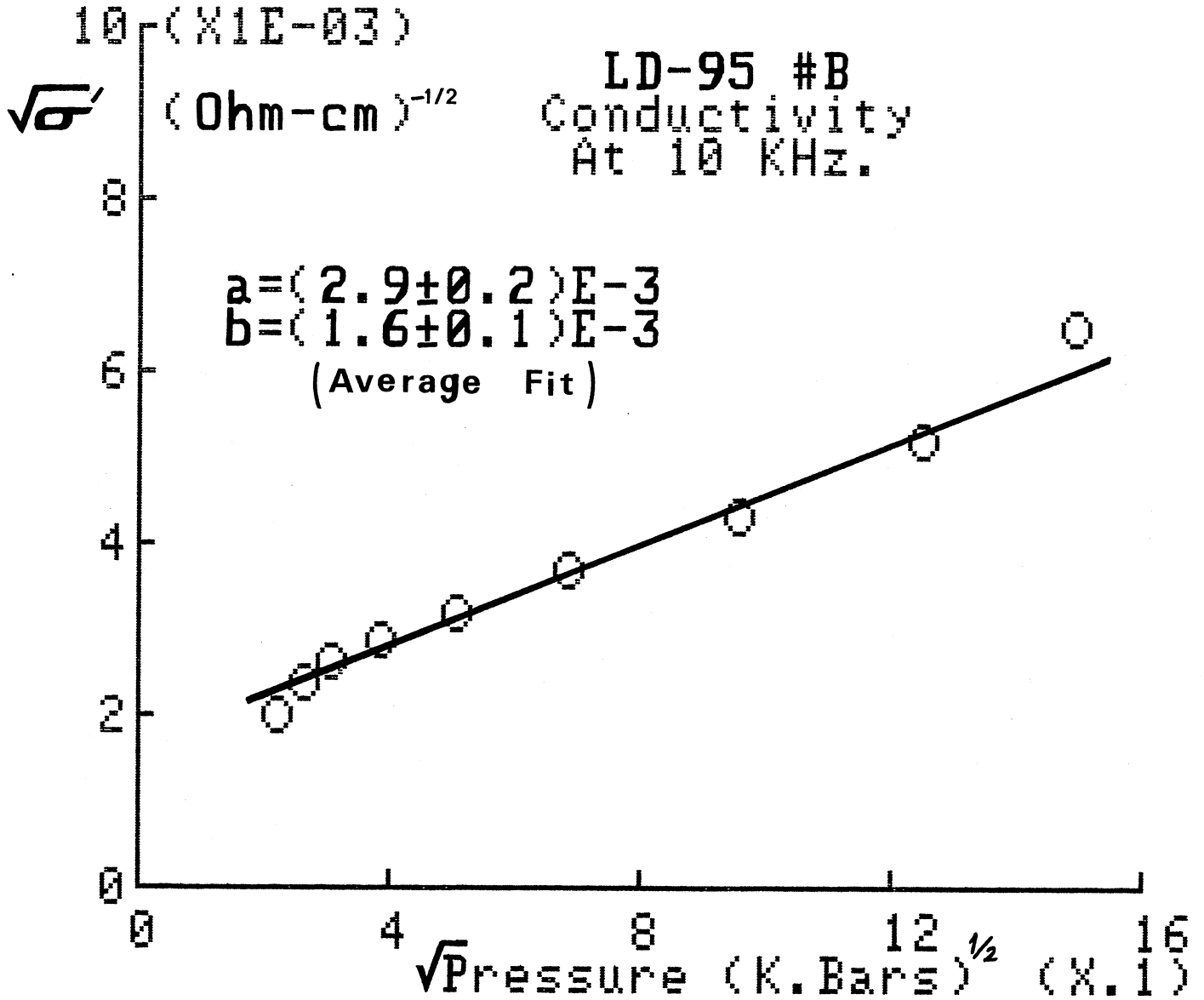
10
(X1E-03)
√σ′
(Ohm-cm)^-1/2
LD-95 #B
Conductivity
At 10 KHz.
a=(2.9±0.2)E-3
b=(1.6±0.1)E-3
(Average Fit)
8
6
4
2
0
0
4
8
12
16
√Pressure (K.Bars)^1/2 (X.1)

Fig. 6(c)

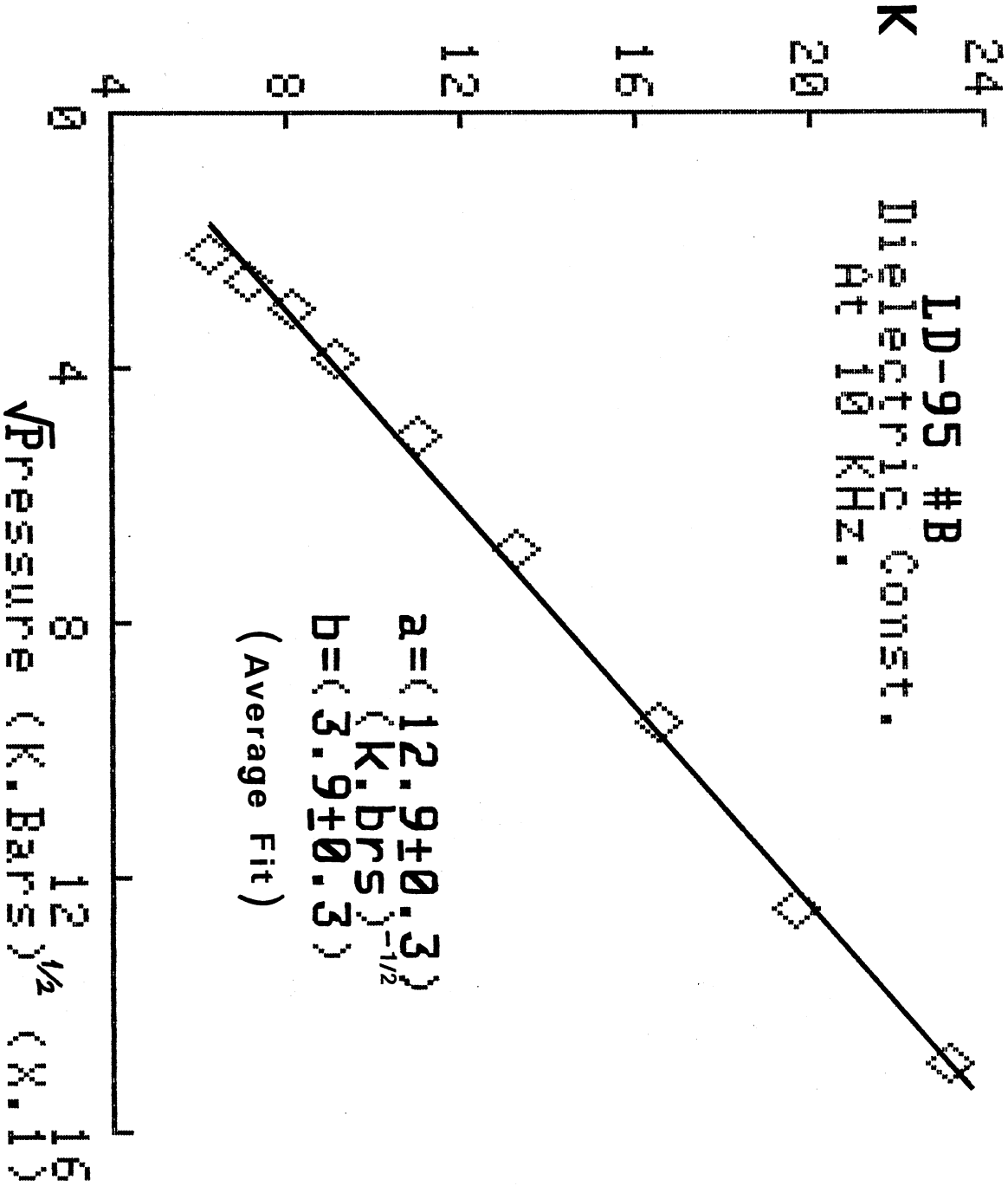
LD-95 #B
Dielectric Const.
At 10 KHz.
K
24
20
16
12
8
4
0
4
8
12
16
√Pressure (K. Bars)^1/2 (X.1)
a=(12.9±0.3)
(K.brs)^-1/2
b=(3.9±0.3)
(Average Fit)

Fig.(69)

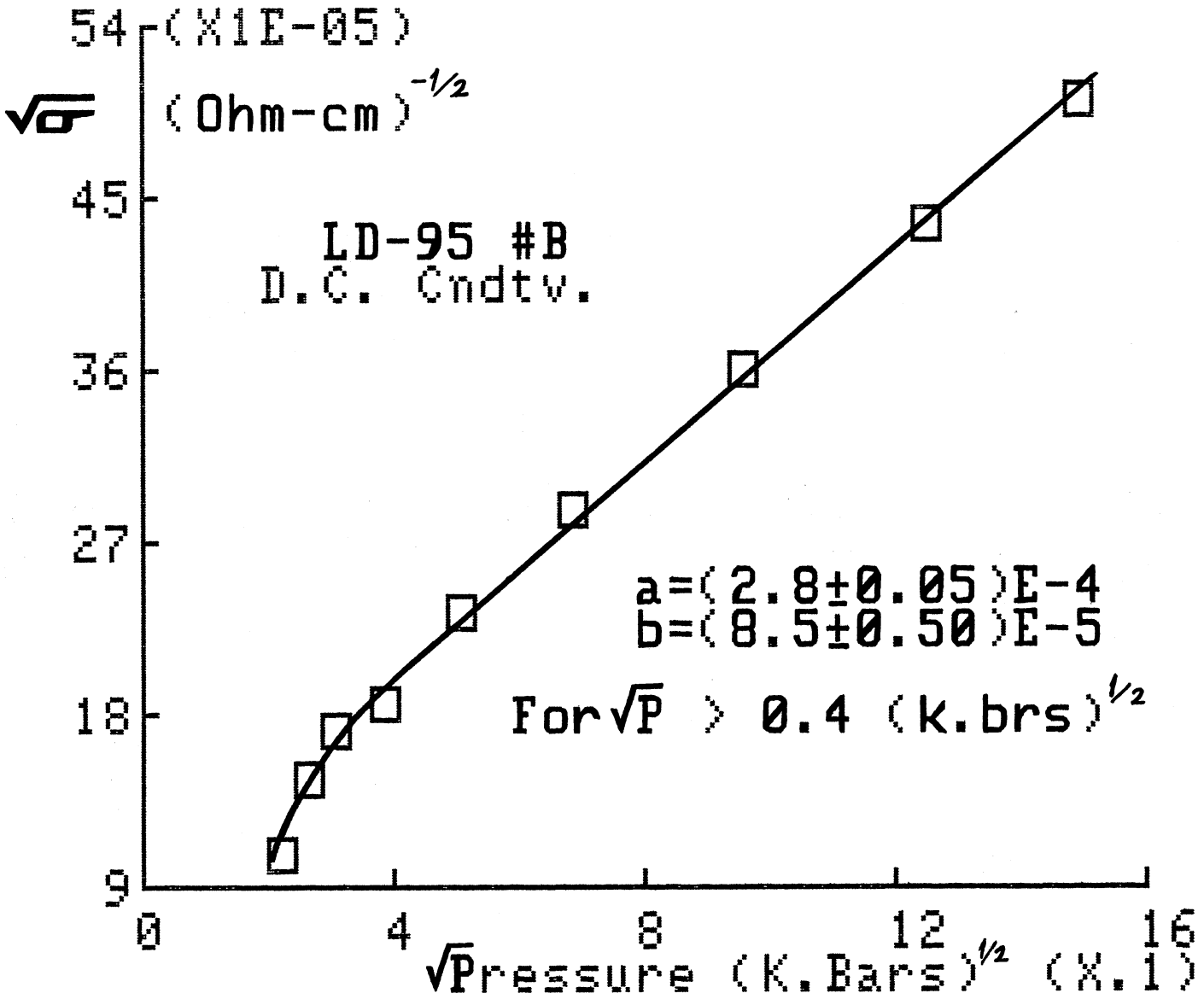
54
(X1E-05)
√σ
(Ohm-cm)^-1/2
45
36
27
18
9
LD-95 #B
D.C. Cndtv.
a=(2.8±0.05)E-4
b=(8.5±0.50)E-5
For √P > 0.4 (k.brs)^1/2
0
4
8
12
16
√Pressure (K.Bars)^1/2 (X.1)

Fig. V-20

TABLE (3.16)

THE EFFECTS OF PRESSURE ON LD-94 AT 10 KHz.

	<===$\sqrt{P}$RESSURE (K.Bars)$^{1/2}$===>								
Sample	0.23	0.27	0.31	0.39	0.51	0.69	0.96	1.25	1.49
B : σ'	1.98	2.12	2.7	3.5	4.6	6.5	--	--	--
K	17	18	18	20	23	25	--	--	--
DM	2.1	2.1	2.7	3.2	3.7	4.7	--	--	--
σ	1.4	1.6	2.1	2.8	3.7	5.5	8.0	11	15

All Values Of σ' Are (1XE-5), While Those Of σ Are (X1E-7).

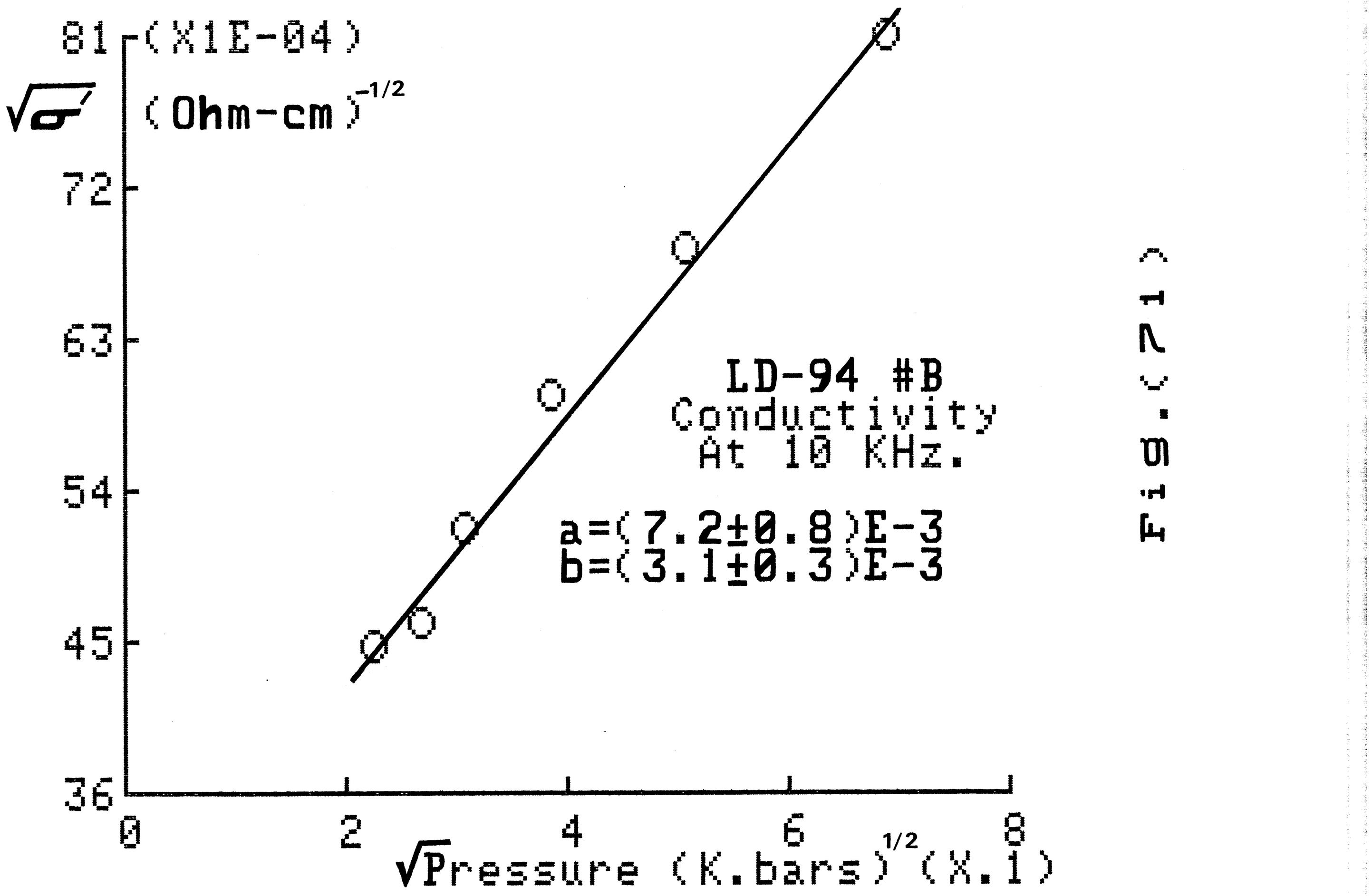
81
72
63
54
45
36
(X1E-04)
$\sqrt{\sigma'}$ (Ohm-cm)$^{-1/2}$
LD-94 #B
Conductivity
At 10 KHz.
a=(7.2±0.8)E-3
b=(3.1±0.3)E-3
0
2
4
6
8
$\sqrt{P}$ressure (K.bars)$^{1/2}$ (X.1)

Fig. 6.(21)

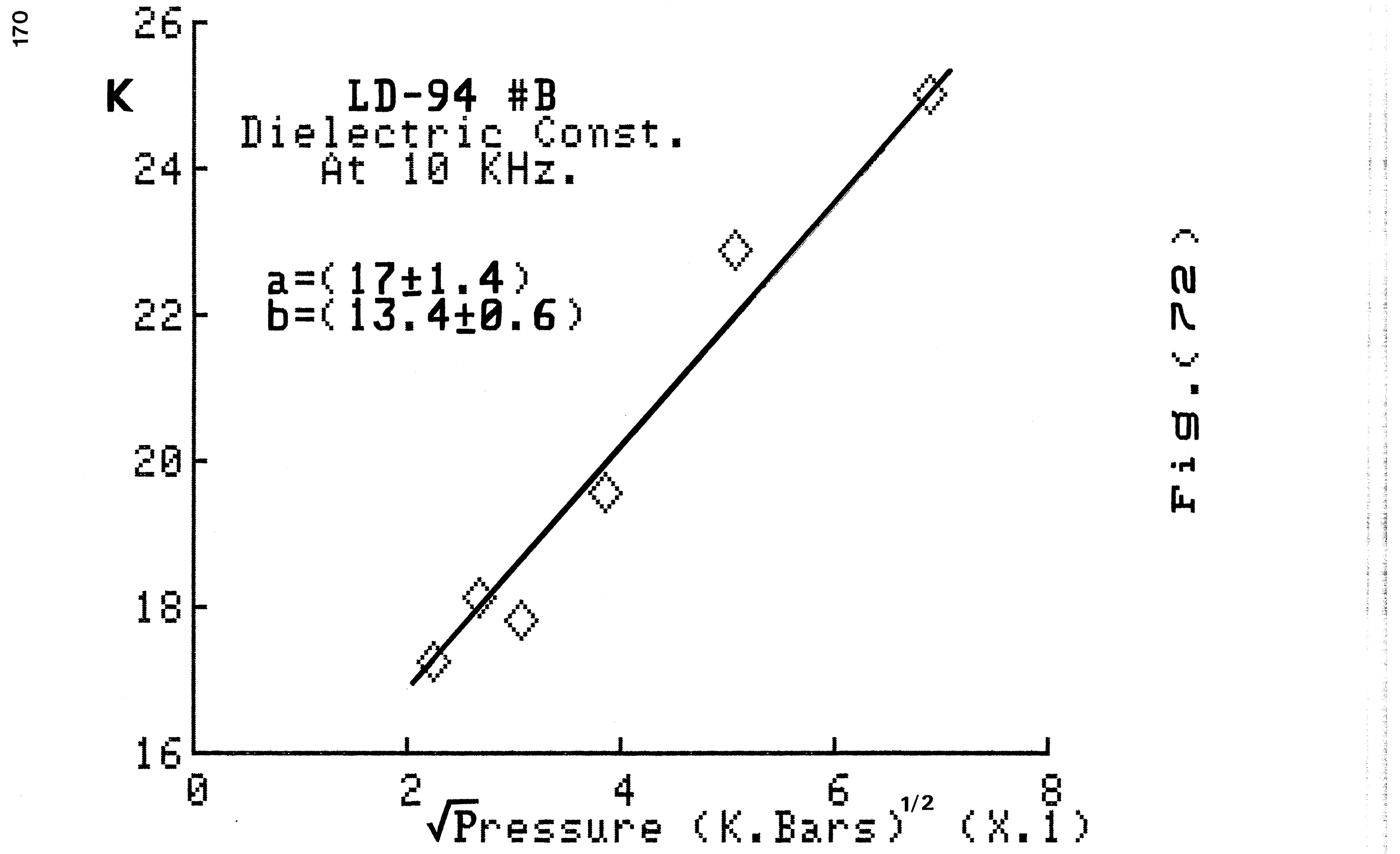
K
LD-94 #B
Dielectric Const.
At 10 KHz.
a=(17±1.4)
b=(13.4±0.6)
26
24
22
20
18
16
0
2
4
6
8
√Pressure (K.Bars)^1/2 (X.1)

Fig. 5.22

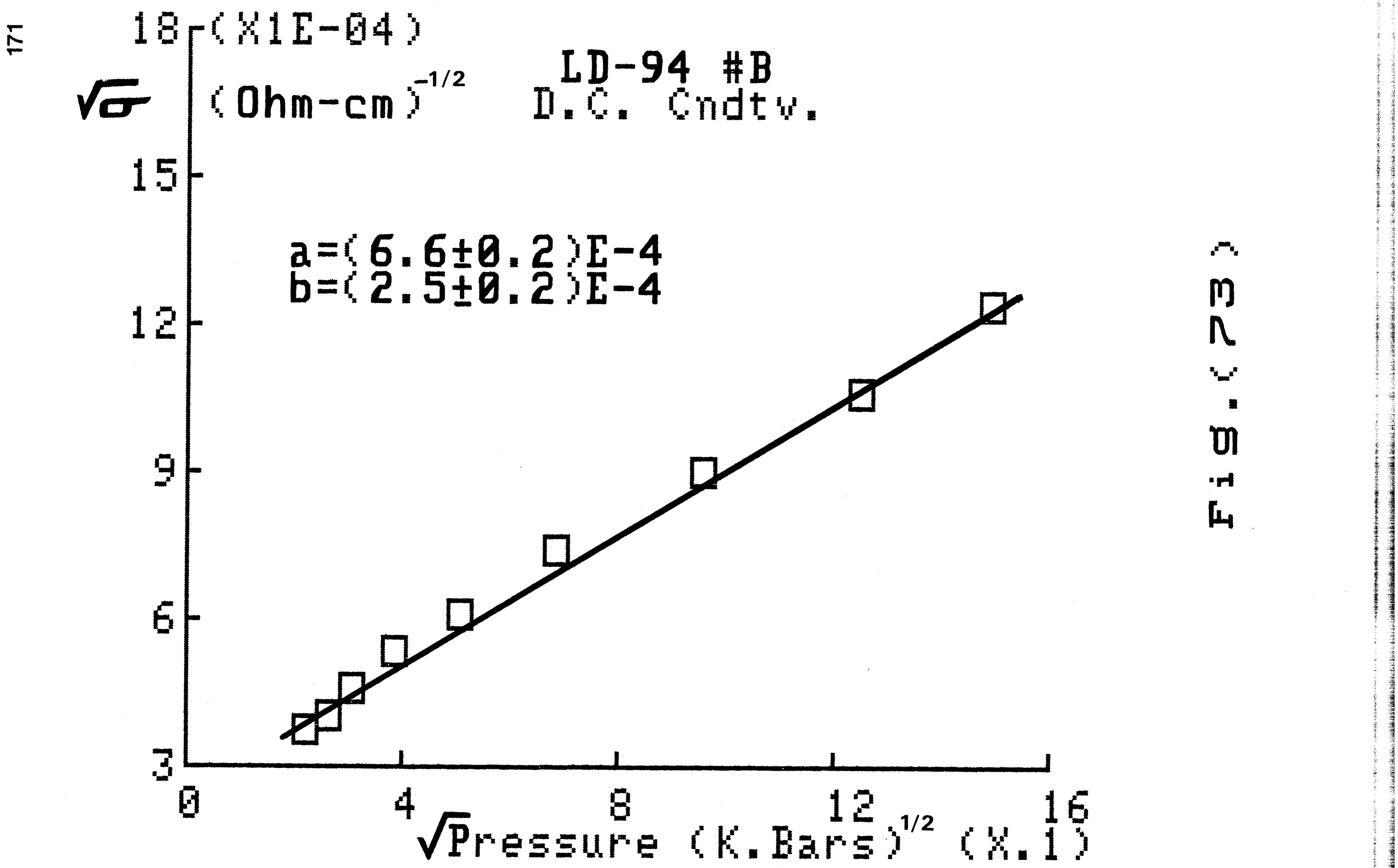
18
(X1E-04)
√σ
(Ohm-cm)^-1/2
LD-94 #B
D.C. Cndtv.
15
a=(6.6±0.2)E-4
b=(2.5±0.2)E-4
12
9
6
3
0
4
8
12
16
√Pressure (K.Bars)^1/2 (X.1)

Fig. (23)

TABLE (3.17)

THE EFFECTS OF PRESSURE ON LD-14A AT 1 KHz.

	<===√PRESSURE (K.Bars)$^{1/2}$===>								
Sample	0.23	0.27	0.31	0.39	0.51	0.69	0.96	1.25	1.49
V : σ'	2.8	6.8	8.4	10.9	13.9	16.5	22	28	36
K	10.6	10.6	10.6	10.2	9.8	9.4	9.0	8.5	7.7
DM	0.47	1.15	1.4	1.9	2.5	3.2	4.4	5.9	8.5
σ	0.33	1.07	2.8	6.0	11.3	13.7	19	26	33
H : σ'	7.9	8.8	9.8	10.6	13.5	19	31	35	47
K	12.5	12.1	12.0	11.8	11.5	11.0	10.5	9.5	8.5

cont'd

TABLE (3.17) Cont'd

	DM	1.1	1.3	1.5	1.6	2.1	3.3	5.4	6.7	10
	σ	1.7	2.4	3.1	5.7	8.7	13.7	21	32	41
F :	σ'	5.5	7.0	7.9	11.0	13.3	21	28	38	48
	K	12.3	12.4	13.0	12.8	12.9	12.7	11.8	11.4	10.9
	DM	0.80	1.1	1.1	1.55	1.85	2.9	4.3	5.9	7.9
	σ	1.0	1.4	3.0	5.8	8.2	13.7	20	33	43

Three Different Samples Are Observed For Verifying The Reproducibility. Note The Curious Decrease Of The Dielectric Constant With Pressure. All Values Of σ' Are (X1E-7), While Those Of σ Are (X1E-9).

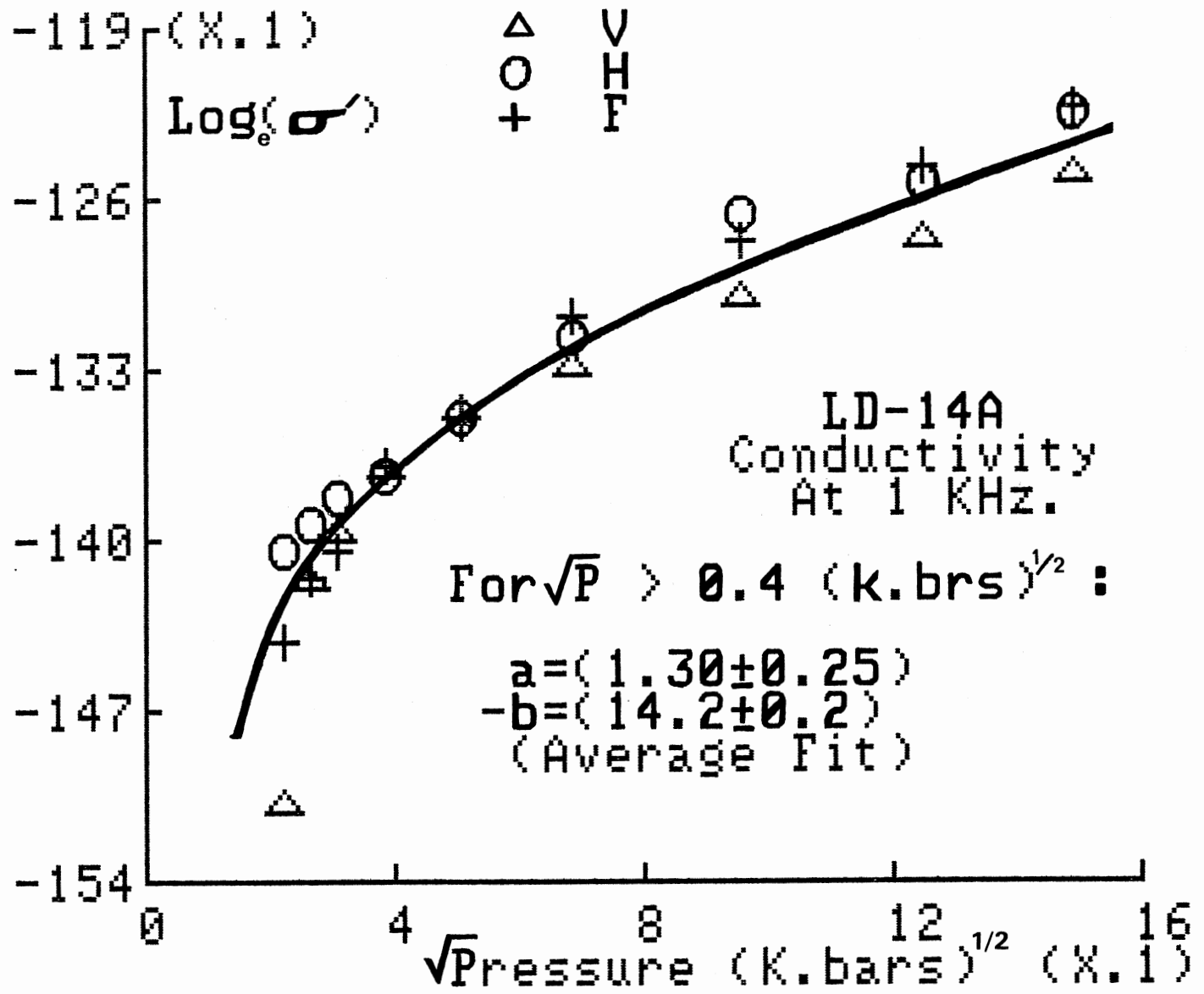
-119
(X.1)
Log$_e$(σ')
△ V
○ H
+ F
-126
-133
-140
-147
-154
LD-14A
Conductivity
At 1 KHz.
For √P > 0.4 (k.brs)^1/2 :
a=(1.30±0.25)
-b=(14.2±0.2)
(Average Fit)
0
4
8
12
16
√Pressure (K.bars)^1/2 (X.1)

Fig. (74)

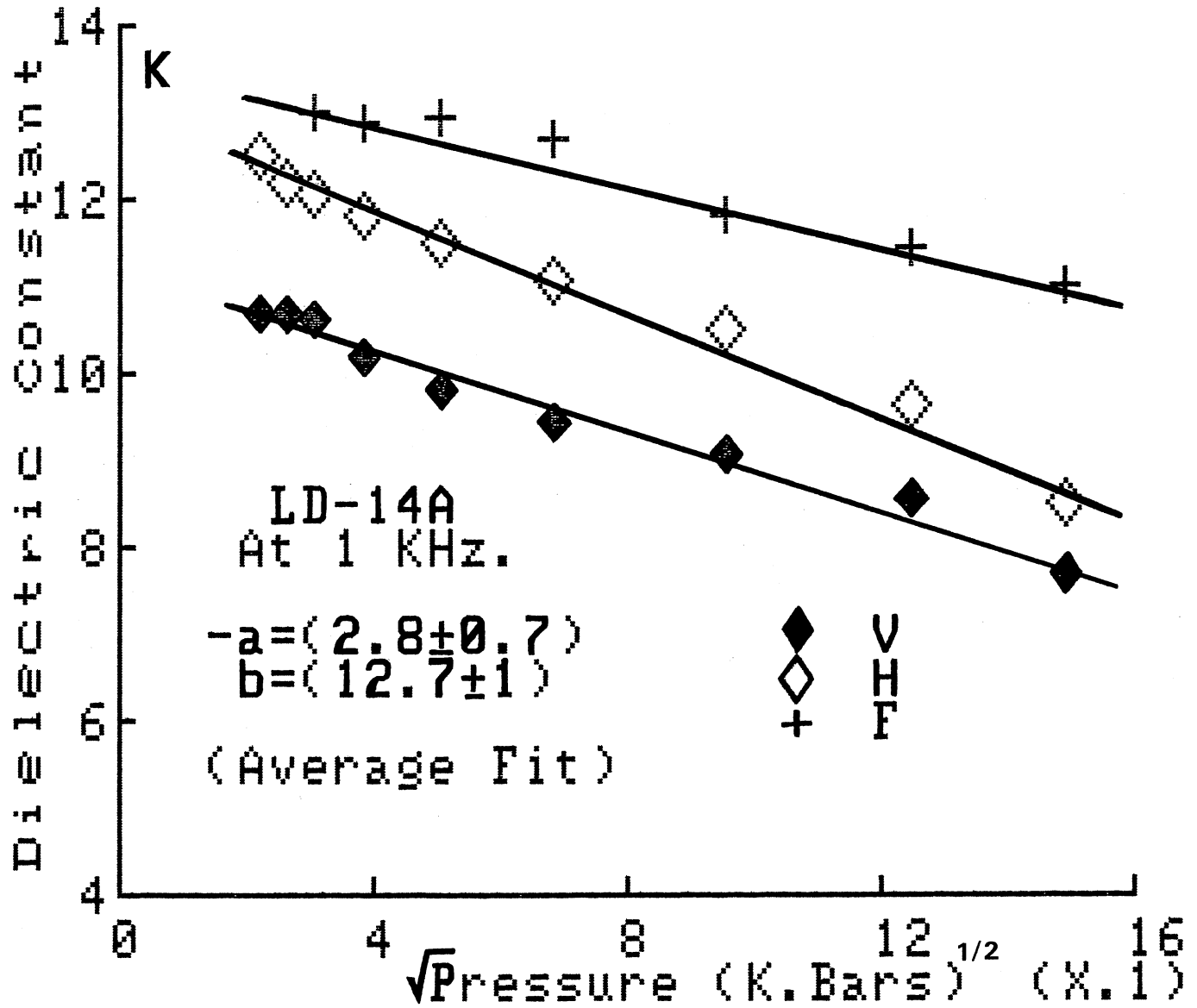
K
Dielectric Constant
14
12
10
8
6
4
0
4
8
12
16
√Pressure (K.Bars)^1/2 (X.1)
LD-14A
At 1 KHz.
-a=(2.8±0.7)
b=(12.7±1)
(Average Fit)
V
H
F

Fig. (25)

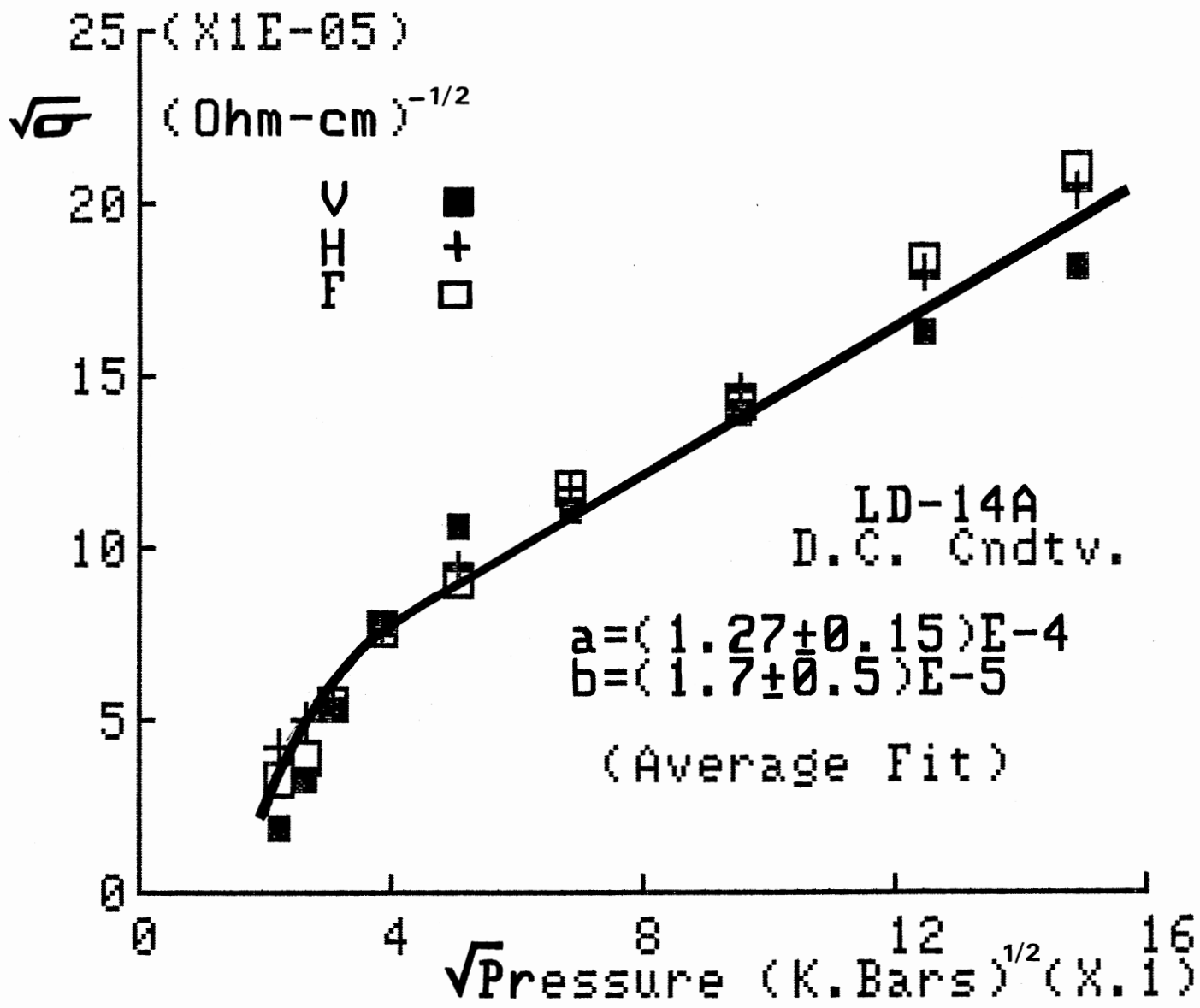
25
(X1E-05)
√σ
(Ohm-cm)^-1/2
20
15
10
5
0
V
H
F
LD-14A
D.C. Cndtv.
a=(1.27±0.15)E-4
b=(1.7±0.5)E-5
(Average Fit)
0
4
8
12
16
√Pressure (K.Bars)^1/2 (X.1)

Fig. (26)

TABLE (3.18)

THE EFFECTS OF PRESSURE ON LD-6A AT 10 KHz.

	<===$\sqrt{P}$RESSURE (K.Bars)$^{1/2}$===>								
Sample	0.23	0.27	0.31	0.39	0.51	0.69	0.96	1.25	1.49
D : σ'	0.69	0.94	1.1	1.4	2.0	3.0	4.8	6.8	9.1
K	15.5	16.0	16.5	17.8	19.6	21.5	22.0	23.0	22.0
DM	0.80	1.05	1.2	1.4	1.9	2.5	3.9	5.3	7.4
σ	1.24	2.60	4.1	8.0	13.7	24	38	60	76

All Values Of σ' Are (X1E-5), While Those Of σ Are (X1E-8).

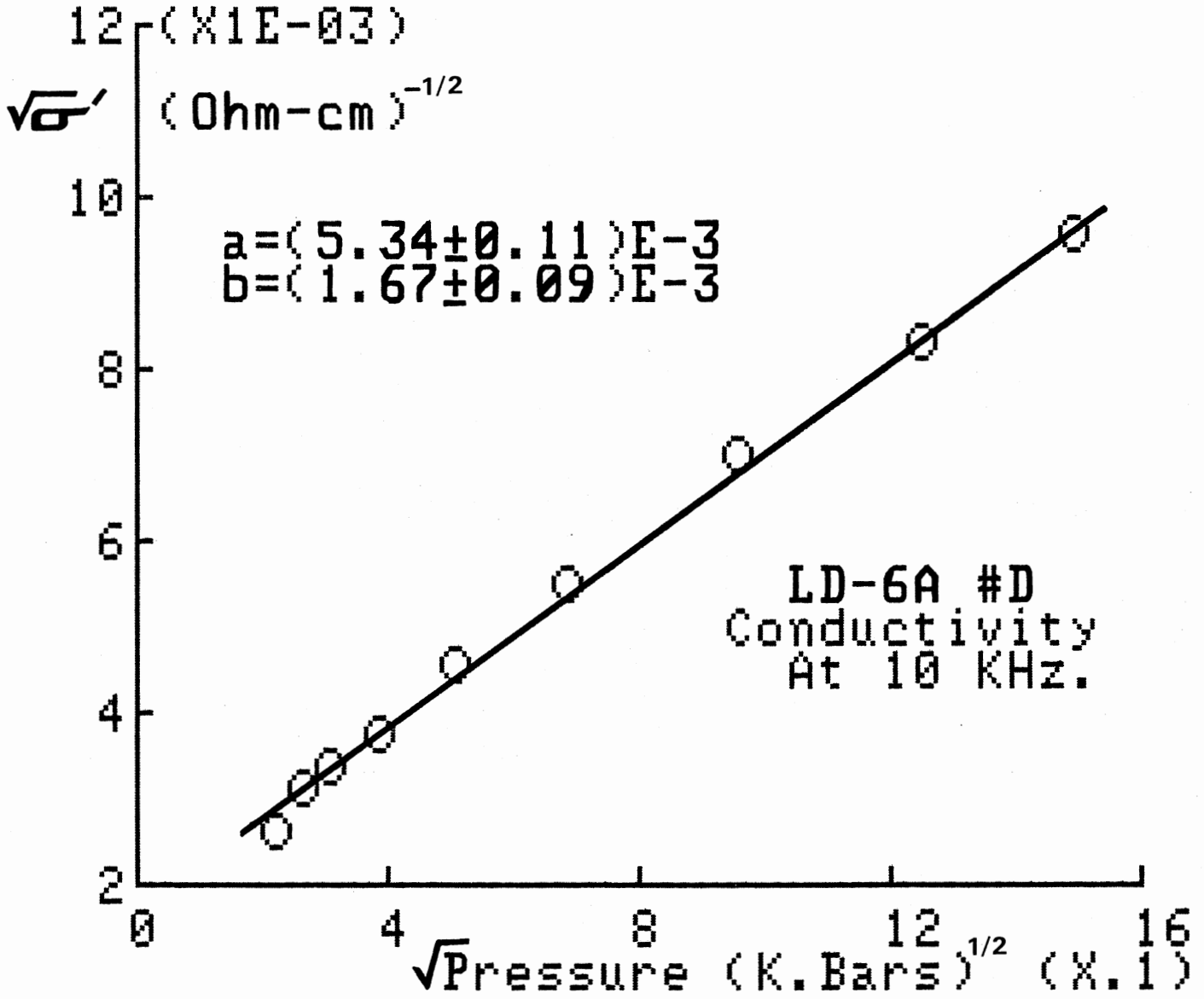
12
(X1E-03)
√σ′
(Ohm-cm)^-1/2
10
8
6
4
2
a=(5.34±0.11)E-3
b=(1.67±0.09)E-3
LD-6A #D
Conductivity
At 10 KHz.
0
4
8
12
16
√Pressure (K.Bars)^1/2 (X.1)

Fig. 27

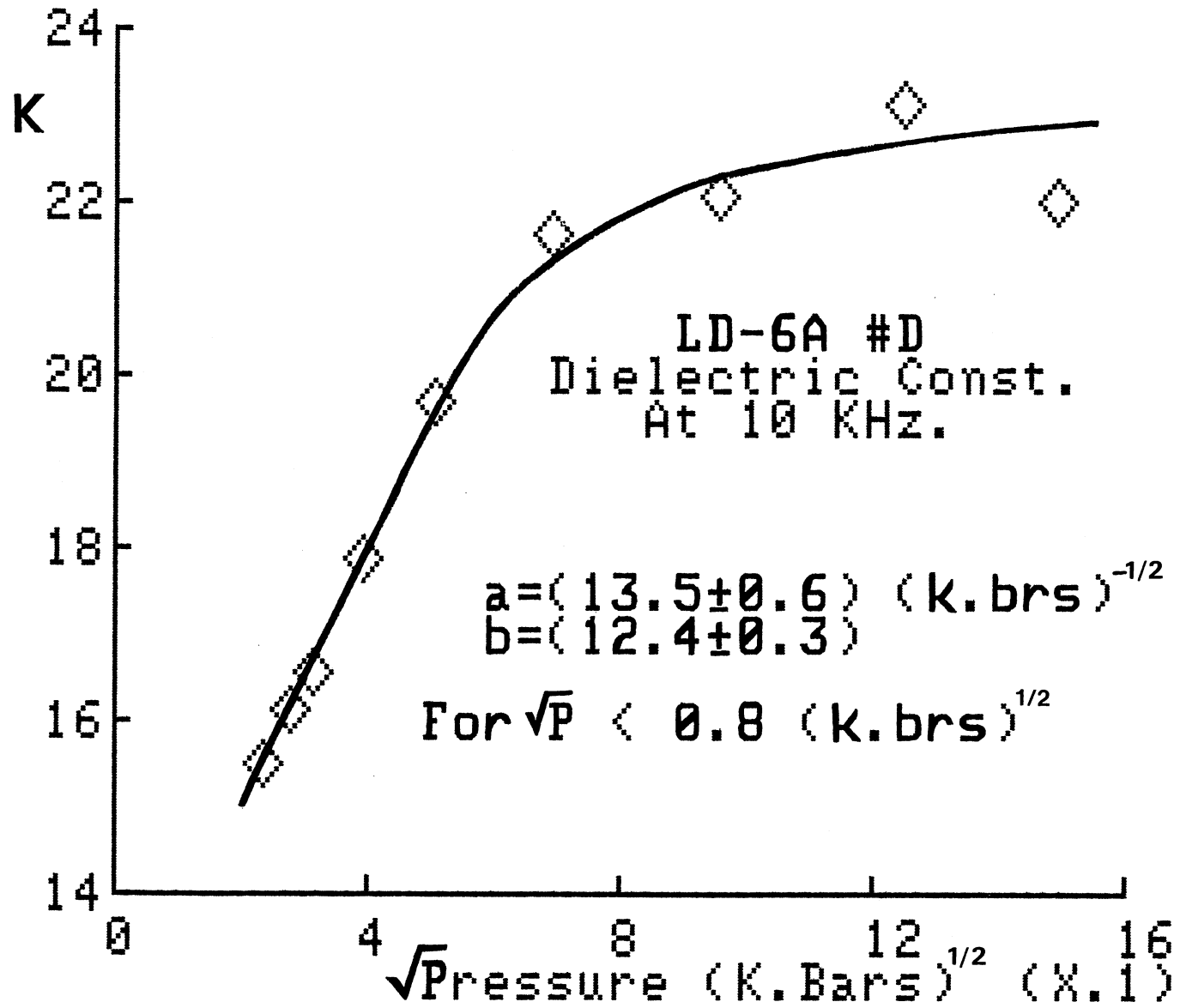
K
24
22
20
18
16
14
0
4
8
12
16
LD-6A #D
Dielectric Const.
At 10 KHz.
a=(13.5±0.6) (k.brs)^-1/2
b=(12.4±0.3)
For √P < 0.8 (k.brs)^1/2
√Pressure (K.Bars)^1/2 (X.1)

Fig. 28)

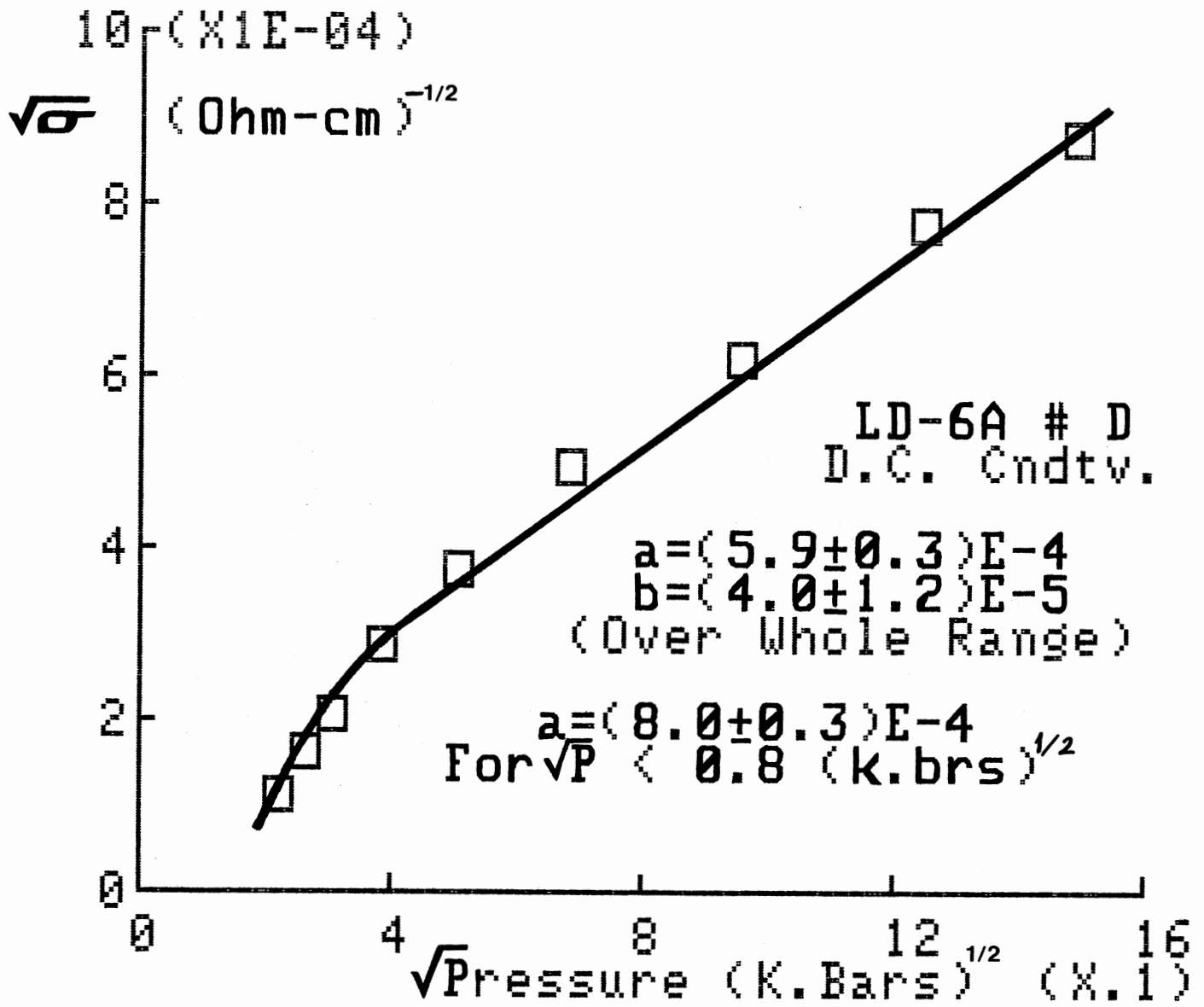
10 (X1E-04)
√σ
(Ohm-cm)^-1/2
8
6
4
2
0
0
4
8
12
16
√P Pressure (K.Bars)^1/2 (X.1)
LD-6A # D
D.C. Cndtv.
a=(5.9±0.3)E-4
b=(4.0±1.2)E-5
(Over Whole Range)
a=(8.0±0.3)E-4
For √P < 0.8 (k.brs)^1/2

Fig. 29

TABLE (3.19)

THE EFFECTS OF PRESSURE ON LD-54 AT 1 KHz.

	<===$\sqrt{P}$RESSURE (K.Bars)$^{1/2}$===>								
Sample	0.23	0.27	0.31	0.39	0.51	0.69	0.96	1.25	1.49
B : σ'	1.3	1.2	1.14	1.2	1.55	1.8	2.1	2.4	2.6
K	4.2	4.5	4.7	4.7	5.0	5.2	5.6	5.7	5.7
DM	0.05	0.05	0.04	0.05	0.06	0.06	0.07	0.08	0.08
σ	0.59	0.83	1.0	1.5	2.2	3.25	4.44	6.1	6.2

All Values Of σ' Are (X1E-8), While Those Of σ Are (X1E-12).

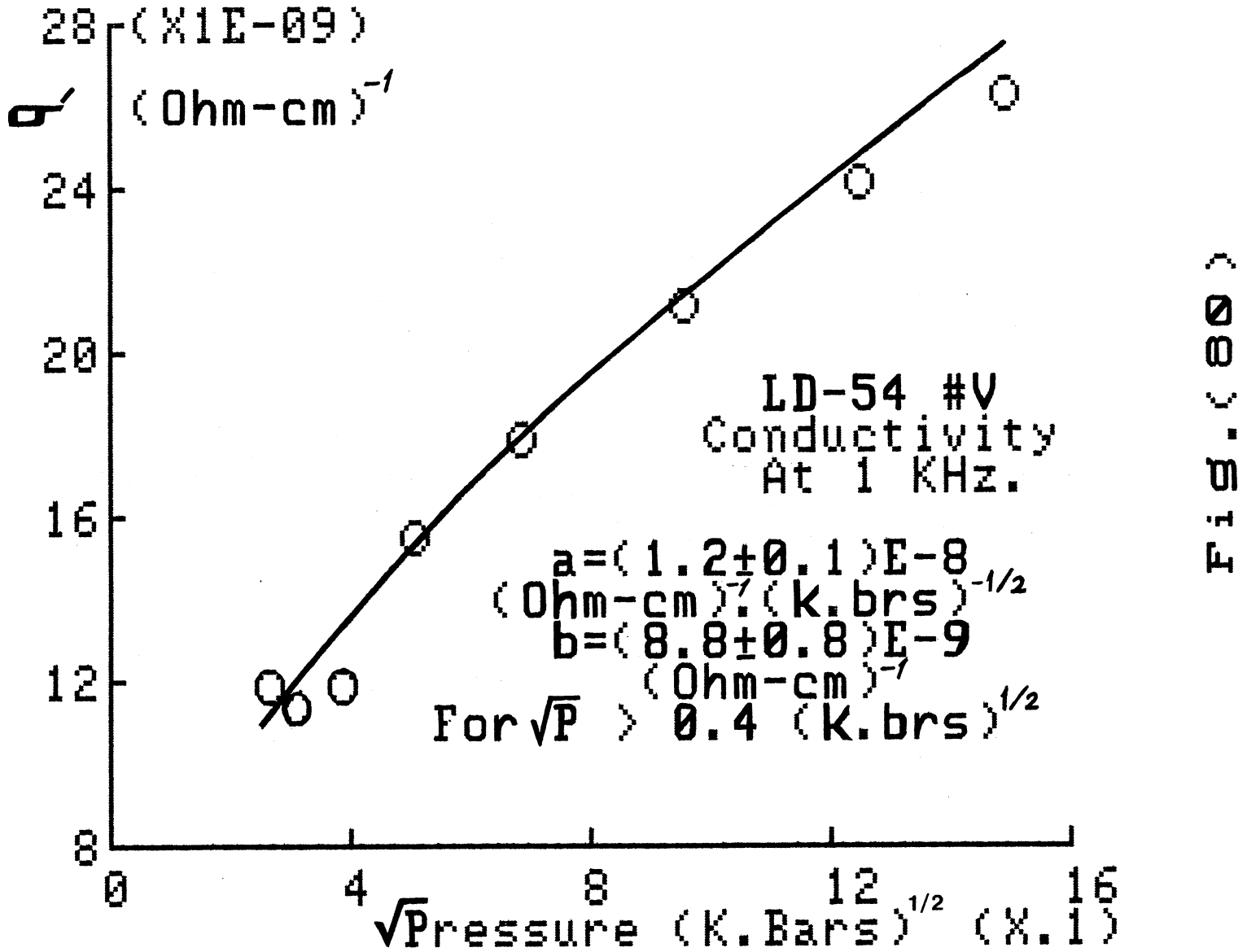
28
24
20
16
12
8
(X1E-09)
σ
(Ohm-cm)$^{-1}$
LD-54 #V
Conductivity
At 1 KHz.
a=(1.2±0.1)E-8
(Ohm-cm)$^{-1}$(k.brs)$^{-1/2}$
b=(8.8±0.8)E-9
(Ohm-cm)$^{-1}$
For $\sqrt{P}$ > 0.4 (k.brs)$^{1/2}$
0
4
8
12
16
$\sqrt{P}$ Pressure (K.Bars)$^{1/2}$ (X.1)

Fig. (80)

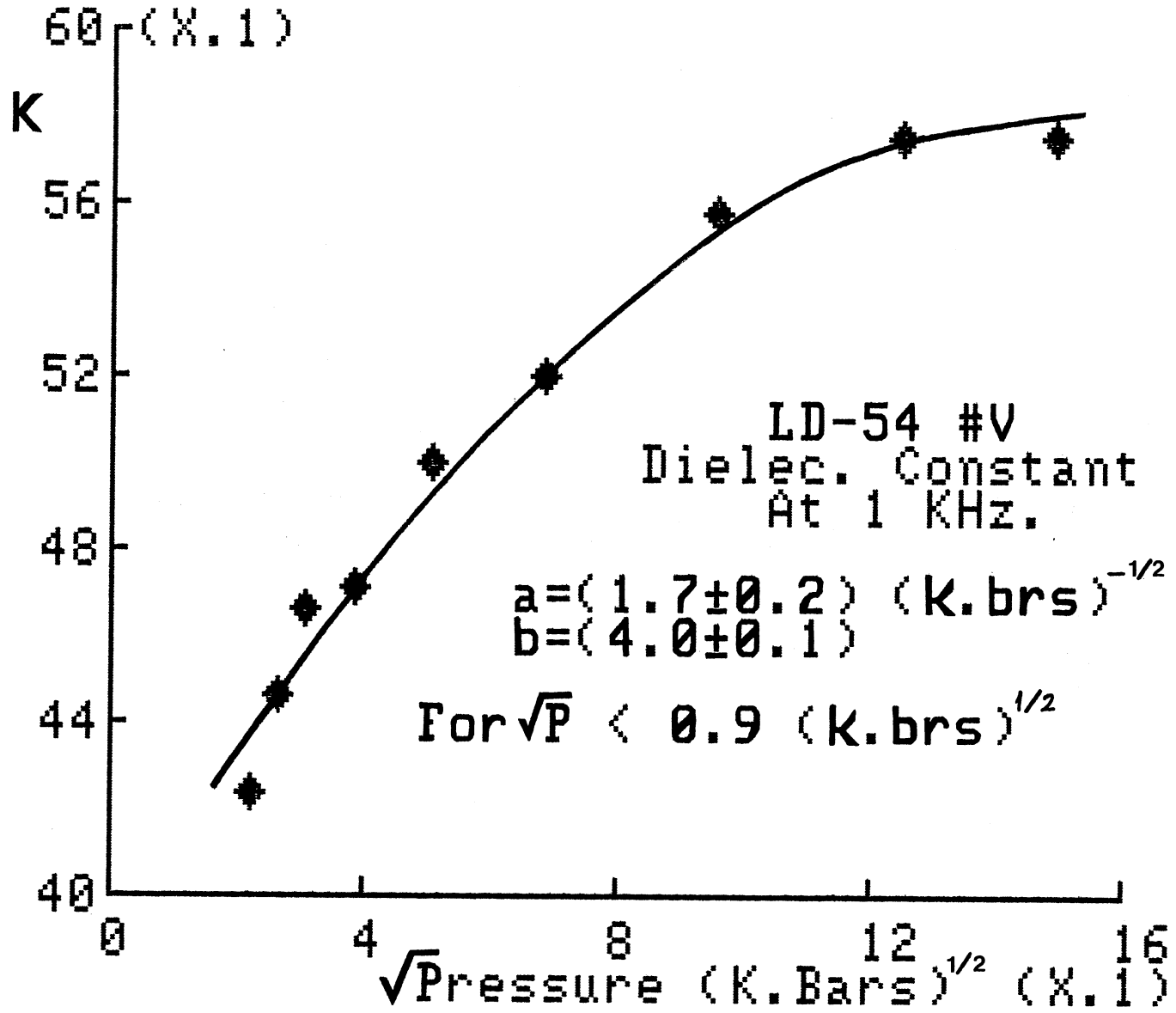
60 (X.1)
K
56
52
48
44
40
0
4
8
12
16
LD-54 #V
Dielec. Constant
At 1 KHz.
a=(1.7±0.2) (K.brs)^-1/2
b=(4.0±0.1)
For √P < 0.9 (K.brs)^1/2
√Pressure (K.Bars)^1/2 (X.1)

Fig. (81)

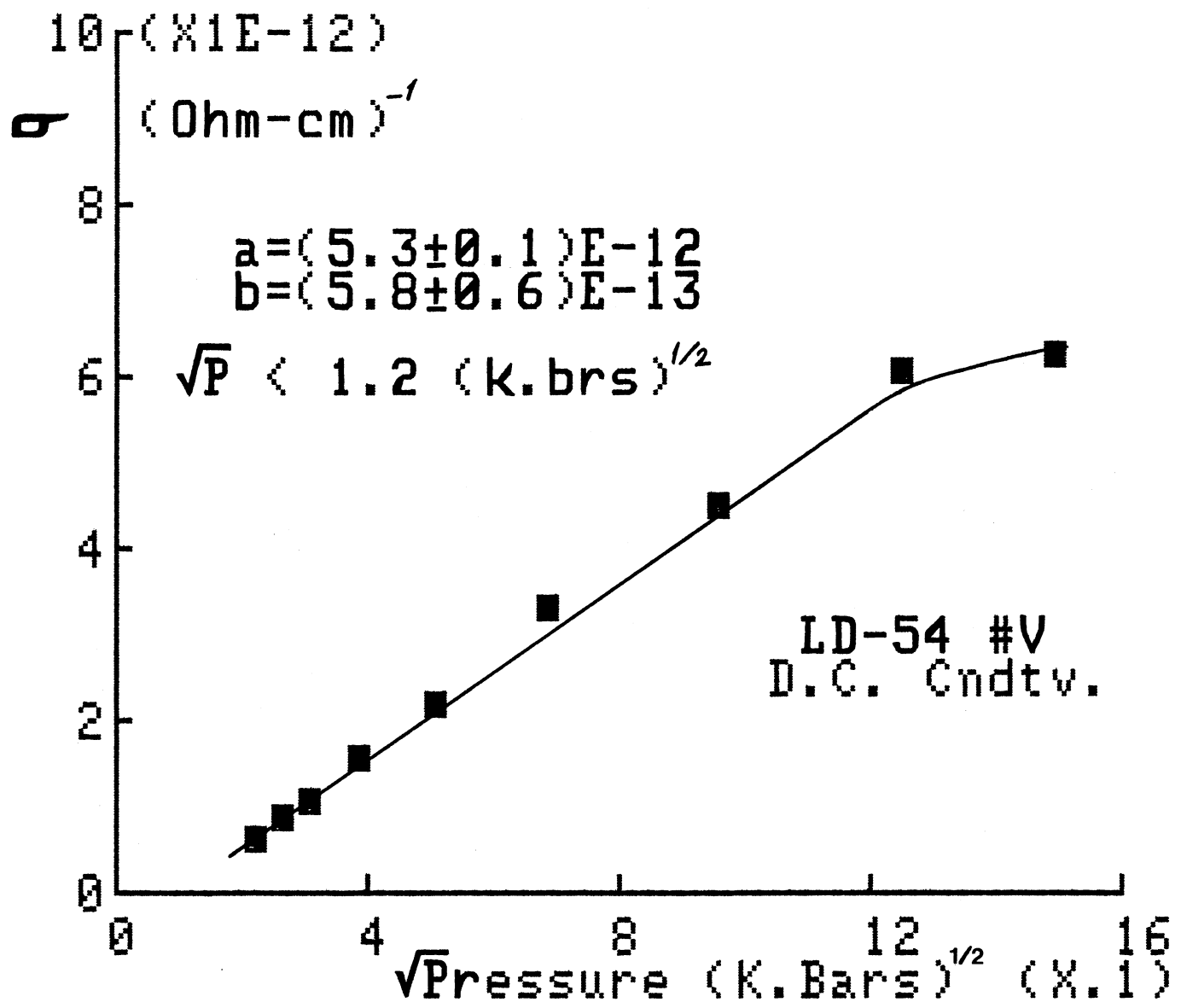
10
(X1E-12)
σ
(Ohm-cm)^-1
8
a=(5.3±0.1)E-12
b=(5.8±0.6)E-13
√P < 1.2 (k.brs)^1/2
6
4
2
0
LD-54 #V
D.C. Cndtv.
0
4
8
12
16
√Pressure (K.Bars)^1/2 (X.1)

Fig.(82)

TABLE (3.20)

THE EFFECTS OF PRESSURE ON LD-52B AT 1 KHz.

	<===$\sqrt{}$PRESSURE (K.Bars)$^{1/2}$===>								
Sample	0.23	0.27	0.31	0.39	0.51	0.69	0.96	1.25	1.49
H : σ'	2.0	2.9	2.9	3.4	3.6	4.0	4.7	5.1	5.7
K	6.0	6.8	6.8	7.4	7.6	7.8	8.3	8.7	8.8
DM	0.06	0.07	0.07	0.08	0.09	0.09	0.10	0.11	0.12
σ	4.9	5.1	5.4	6.0	6.7	8.2	9.97	12.5	14.6

All Values Of σ' Are (X1E-8), While Those Of σ Are (X1E-12).

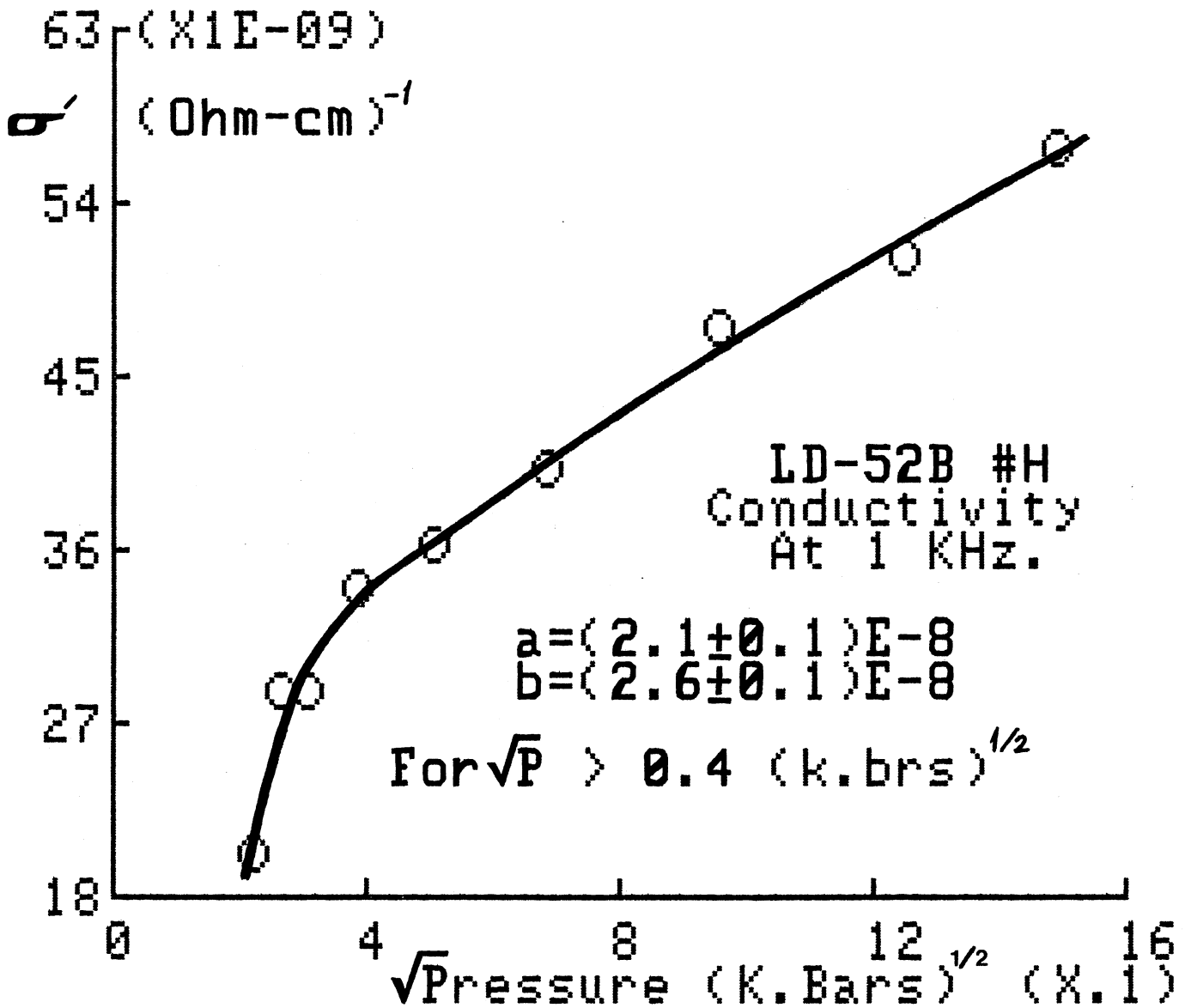
63
54
45
36
27
18
(X1E-09)
σ′
(Ohm-cm)⁻¹
LD-52B #H
Conductivity
At 1 KHz.
a=(2.1±0.1)E-8
b=(2.6±0.1)E-8
For √P > 0.4 (k.brs)^1/2
0
4
8
12
16
√Pressure (K.Bars)^1/2 (X.1)

Fig. (83)

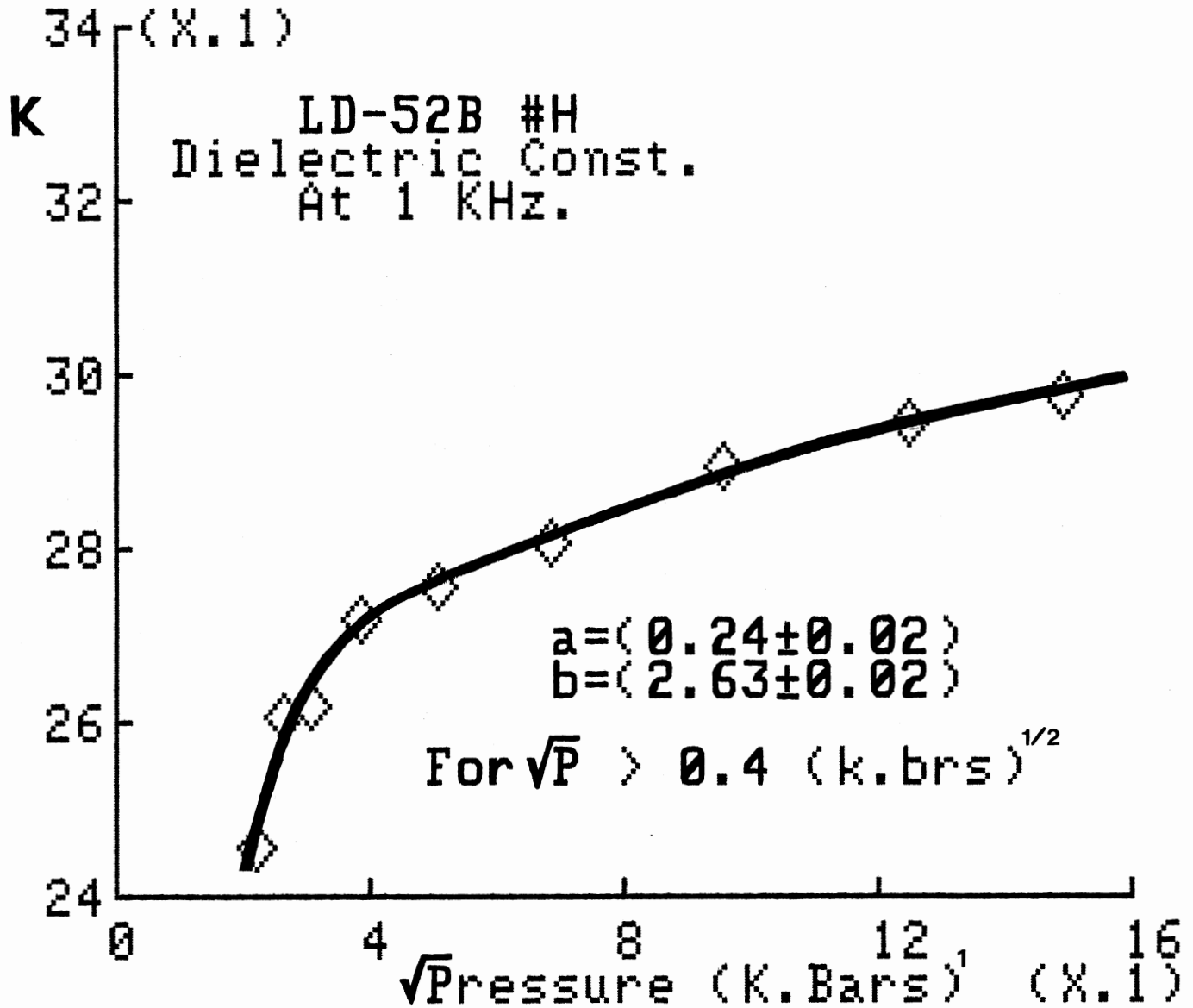
34 (X.1)
K
LD-52B #H
Dielectric Const.
At 1 KHz.
32
30
28
26
24
a=(0.24±0.02)
b=(2.63±0.02)
For √P > 0.4 (k.brs)^1/2
0
4
8
12
16
√Pressure (K.Bars)^1/2 (X.1)

Fig.(84)

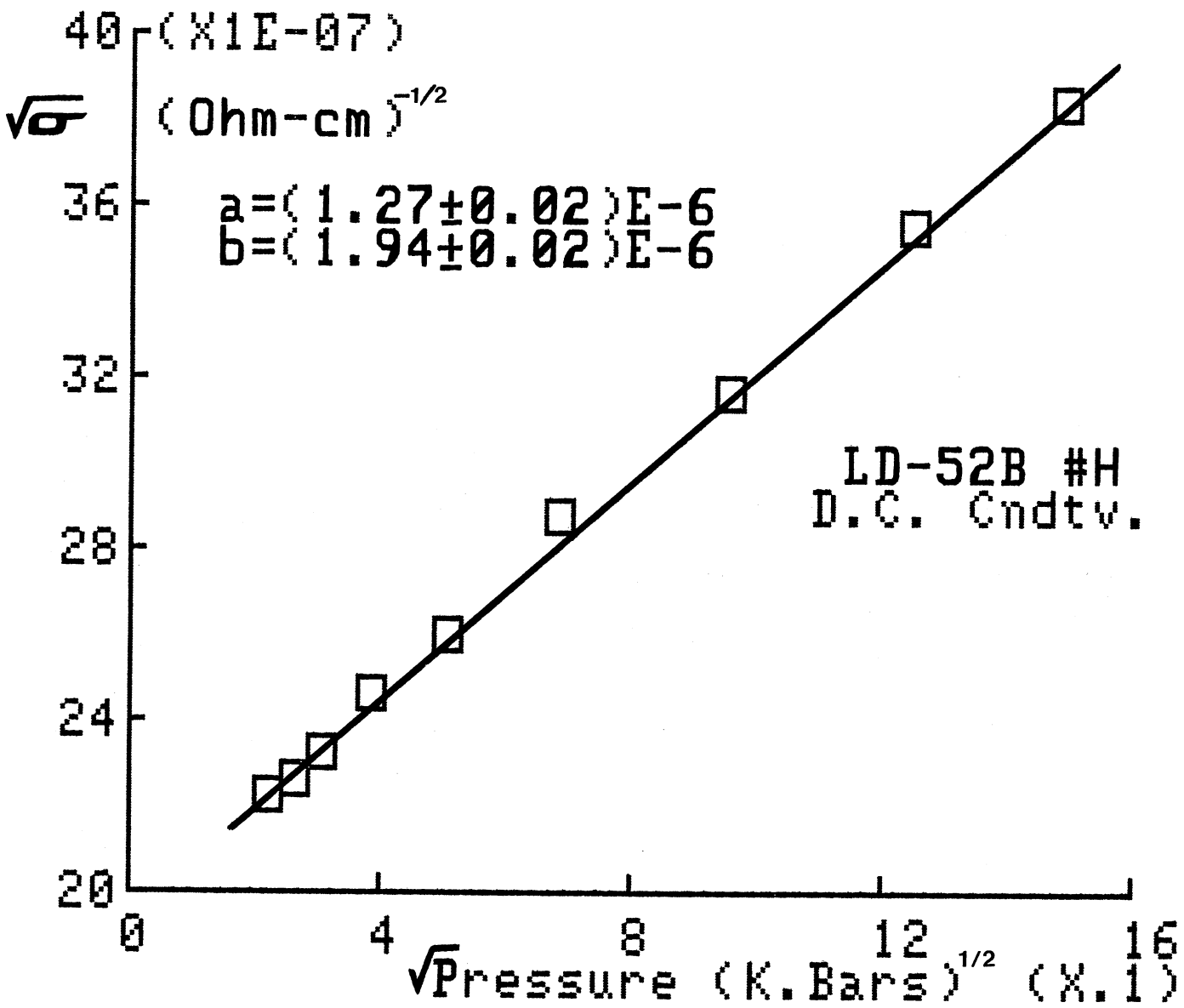
40
(X1E-07)
√σ
(Ohm-cm)^-1/2
36
a=(1.27±0.02)E-6
b=(1.94±0.02)E-6
32
28
24
20
LD-52B #H
D.C. Cndtv.
0
4
8
12
16
√Pressure (K.Bars)^1/2 (X.1)

Fig. C (85)

TABLE (3.21)

THE EFFECTS OF PRESSURE ON LD-106 AT 1 KHz.

	<===√PRESSURE (K.Bars) ===>								
Sample	0.23	0.27	0.31	0.39	0.51	0.69	0.96	1.25	1.49
E : σ'	4.25	4.45	4.77	6.22	7.56	10.5	14.8	18.2	17.9
K	16.4	16.5	16.6	18.0	20.5	22.4	25.6	26.0	25.1
DM	0.47	0.48	0.52	0.62	0.67	0.85	1.04	1.25	1.28
σ	0.44	0.38	0.57	1.47	1.96	2.87	4.13	5.80	6.43

All Values Of σ' Are (X1E-7), While Those Of σ Are (X1E-9).

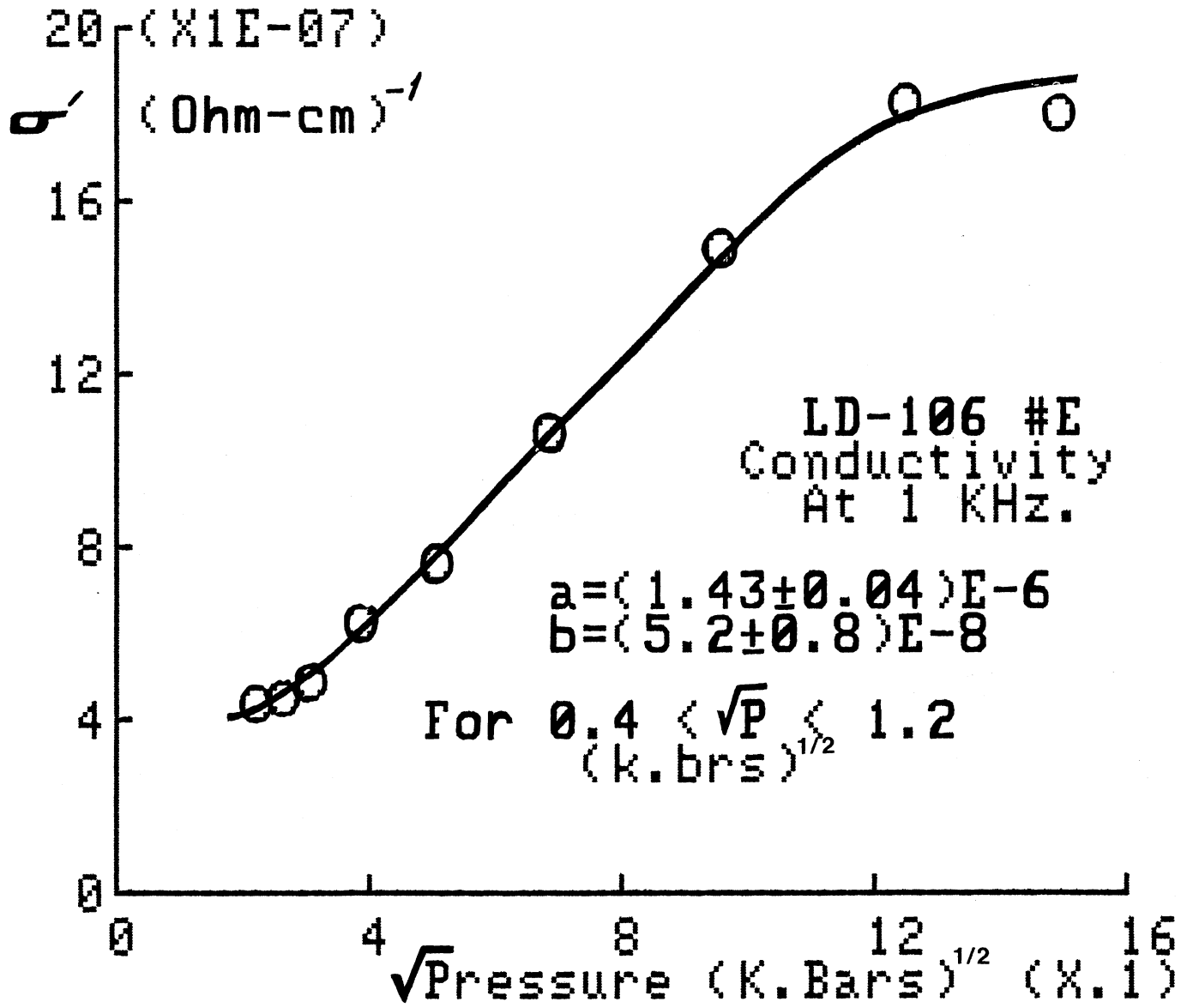
20
(X1E-07)
σ′
(Ohm-cm)⁻¹
16
12
8
4
0
0
4
8
12
16
√Pressure (K.Bars)^1/2 (X.1)
LD-106 #E
Conductivity
At 1 KHz.
a=(1.43±0.04)E-6
b=(5.2±0.8)E-8
For 0.4 < √P < 1.2
(k.brs)^1/2

Fig.(86)

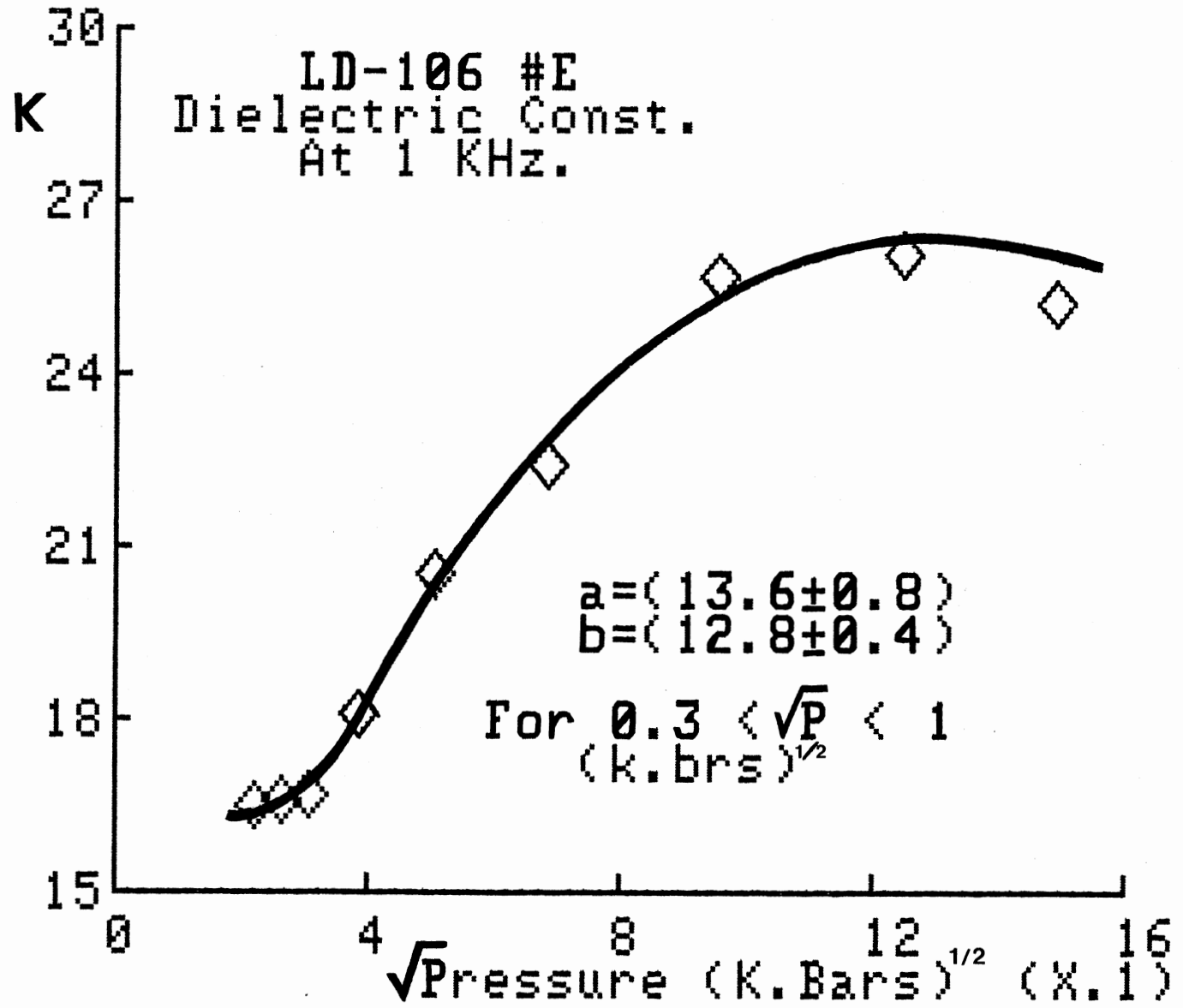
LD-106 #E
Dielectric Const.
At 1 KHz.
K
30
27
24
21
18
15
0
4
8
12
16
a=(13.6±0.8)
b=(12.8±0.4)
For 0.3 < √P < 1
(k.brs)^1/2
√Pressure (K.Bars)^1/2 (X.1)

Fig.(87)

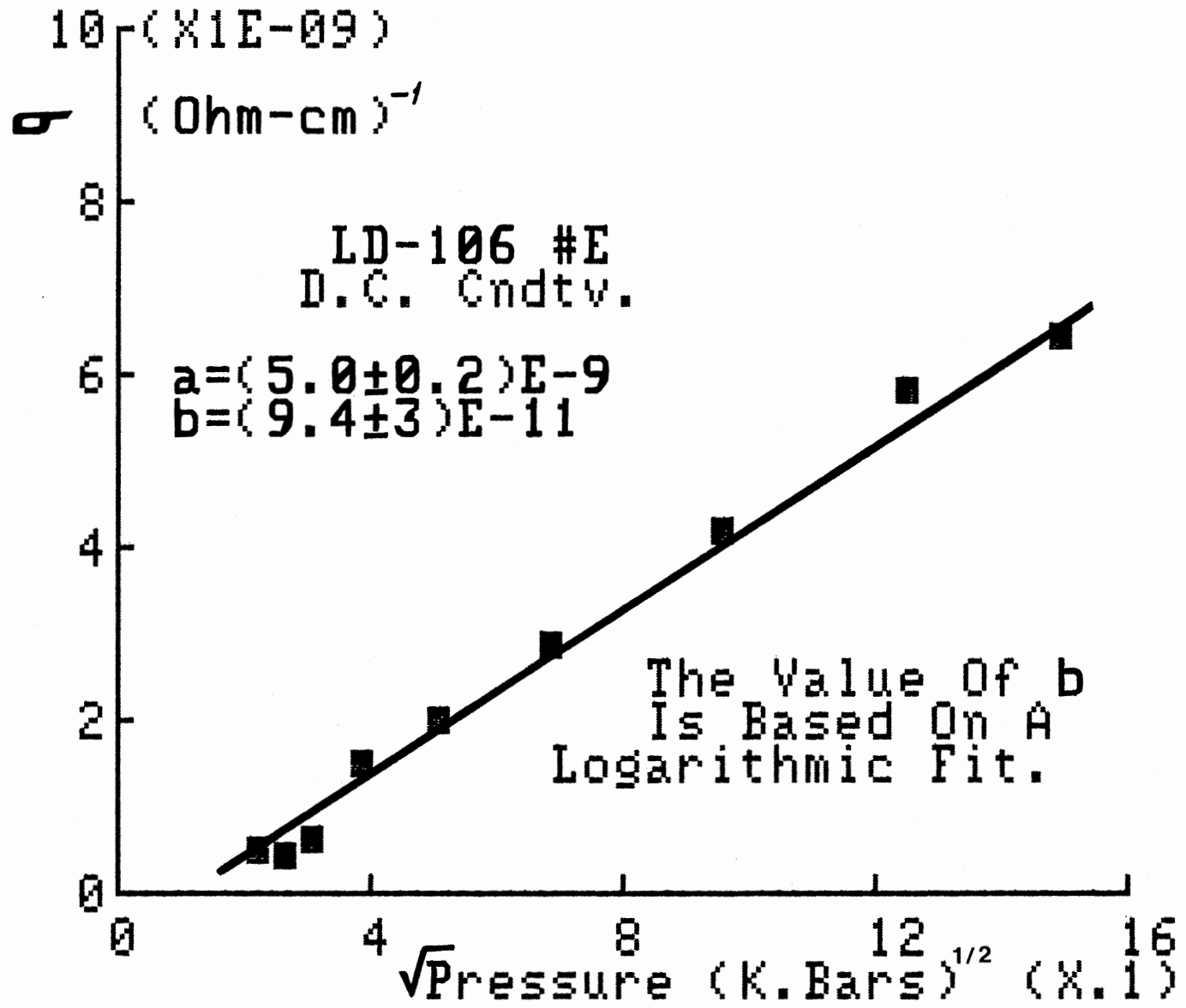
10
(X1E-09)
σ
(Ohm-cm)⁻¹
8
6
4
2
0
LD-106 #E
D.C. Cndtv.
a=(5.0±0.2)E-9
b=(9.4±3)E-11
The Value Of b
Is Based On A
Logarithmic Fit.
0
4
8
12
16
√Pressure (K.Bars)^1/2 (X.1)

Fig. (88)

C) The Effects Of Temperature On The Polymers, Activation Energy Study

Most polymers in this study were observed between -170 °C and room temperature. This provided us with the widest range of temperatures possible. Temperatures above room temperature did not prove to be useful for a variety of reasons, the most important of which was the irreversible increase in the thickness of the compressed pellet, creating excess differential pressure on the sample and thereby altering the true conductivity values. There was also evidence that higher temperatures (above 75 °C) produced irreversible change in the room temperature conductivity values.

Nevertheless we did include one observation on LD-105 #G at 100 KHz. where temperatures up to 75 °C were used. This particular case seemed impervious to the above problems, including the D.C. conductivity study. Another instance involved sample LD-54 #V where a 50 °C Temperature was used in order to obtain a wider range as it was not feasible to carry measurements at -170 °C for this particular polymer.

Tables (3.22)-(3.31) show the dependence of the four basic quantities σ', K, DM, and σ (DC), on the temperature at one or two frequencies. Both conductivities displayed the usual $\sim \exp(-Ea/k_B T)$ law, Ea being an activation energy which can be slightly temperature-dependent. All Ea - values obtained from the plots of $\mathrm{Log_e}(\sigma)$ or $\mathrm{Log_e}(\sigma')$ versus $1/k_B T$, displayed excellent reproducibility in all cases considered - an indication that whatever was behind the unaccountable varia-

tions in some of the frequency and pressure dependent results, does not seem to play an active role with respect to the temperature. This supports the hypothesis that both the length distribution and impurity concentration differences are the main causes of the apparent discrepancies. It will be seen in chap. (4) that the activation energy Ea does not involve these particular quantities.

For the sake of simplification, the Boltzmann constant k_B is written as "k" in the graphs depicting the $1/k_BT$ dependence All measurements in this section were done under the "ambient" pressure conditions described in sec.(3.2A).

TABLE (3.22)

THE TEMPERATURE DEPENDENCE OF LD-105

	<=== TEMPERATURE °C ===>									
Sample	75	50	25	10	-25	-50	-75	-95	-125	-170
G : σ'	10.2	6.8	4.6	3.3	1.6	0.75	0.41	0.18	0.07	0.03
K	16.7	14.4	10.8	8.5	5.4	4.4	3.9	3.7	3.7	3.4
DM	1.1	0.85	0.77	0.70	0.54	0.31	0.19	0.09	0.04	0.02
σ	69.3	38.7	10.8	7.52	1.74	0.54	0.13	0.06	.002	1E-4
G : σ'	--	--	1.2	0.94	0.40	0.22	0.11	0.05	.007	3E-4
K	--	--	24.0	22.0	16.2	11.8	7.45	4.7	3.9	3.4

cont'd

TABLE (3.22) Cont'd

	DM	--	--	3.1	1.8	1.3	0.94	0.75	1.2	0.35	0.02
					T=0 °C		T=-55 °C				
L :	σ'	--	--	4.2	2.5	1.3	0.61	0.34	0.19	0.06	0.03
	K	--	--	10.4	7.2	5.1	4.1	3.6	3.5	3.3	3.4
	DM	--	--	0.73	0.64	0.45	0.27	0.17	0.10	0.03	0.02
	σ	--	--	8.1	2.2	1.2	0.21	0.08	0.02	.001	7E-5

Sample #G Was Observed At 100 KHz And 3.5 KHz Respectively.

Sample #L Was Observed At 100 KHz Only. All Values Of σ' Are (X1E-5), Those Of σ (DC) Are (X1E-8).

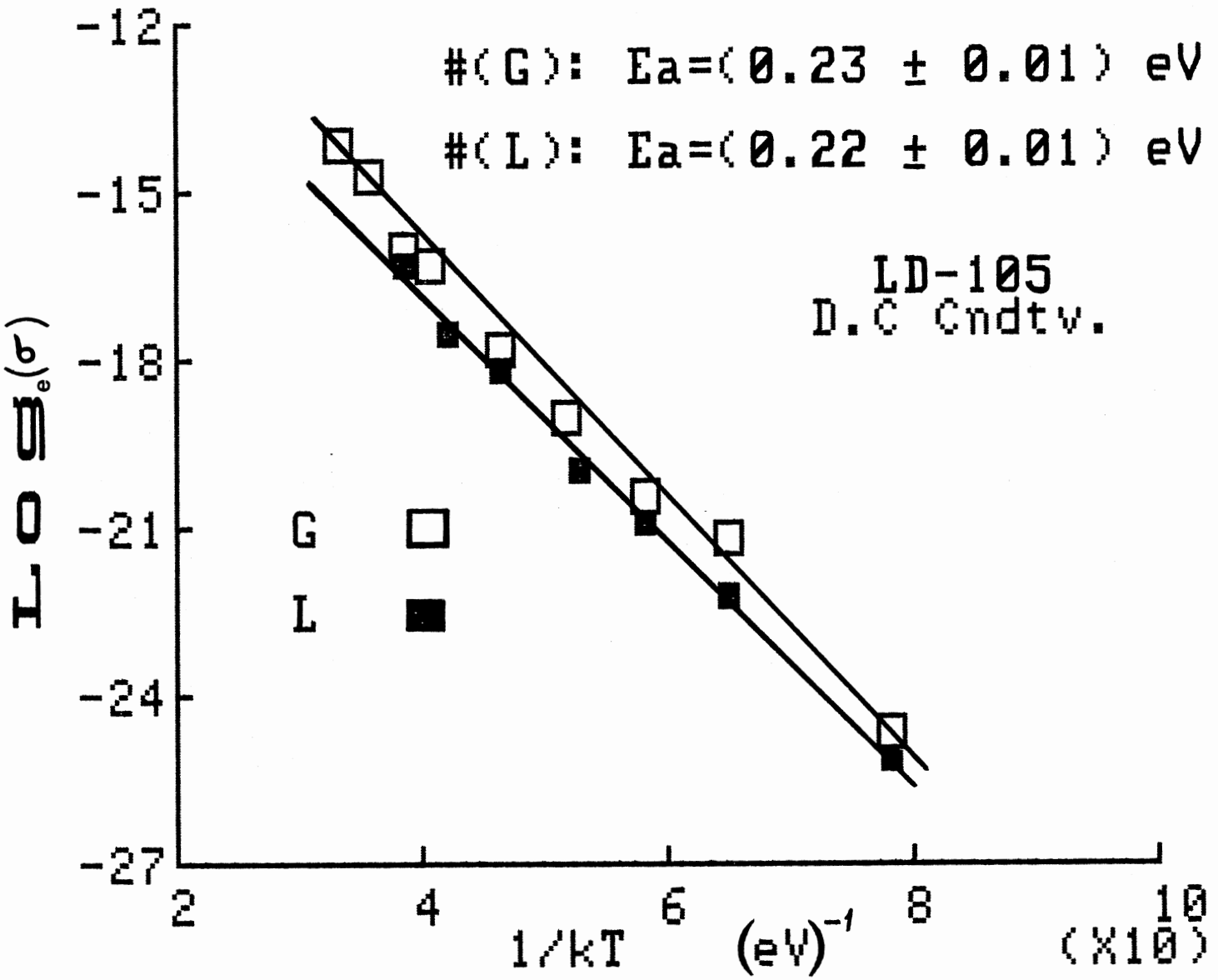
#(G): Ea=(0.23 ± 0.01) eV
#(L): Ea=(0.22 ± 0.01) eV
LD-105
D.C Cndtv.
G
L
Log σ_e(σ)
-12
-15
-18
-21
-24
-27
2
4
6
8
10
1/kT (eV)$^{-1}$
(X10)

Fig.(89)

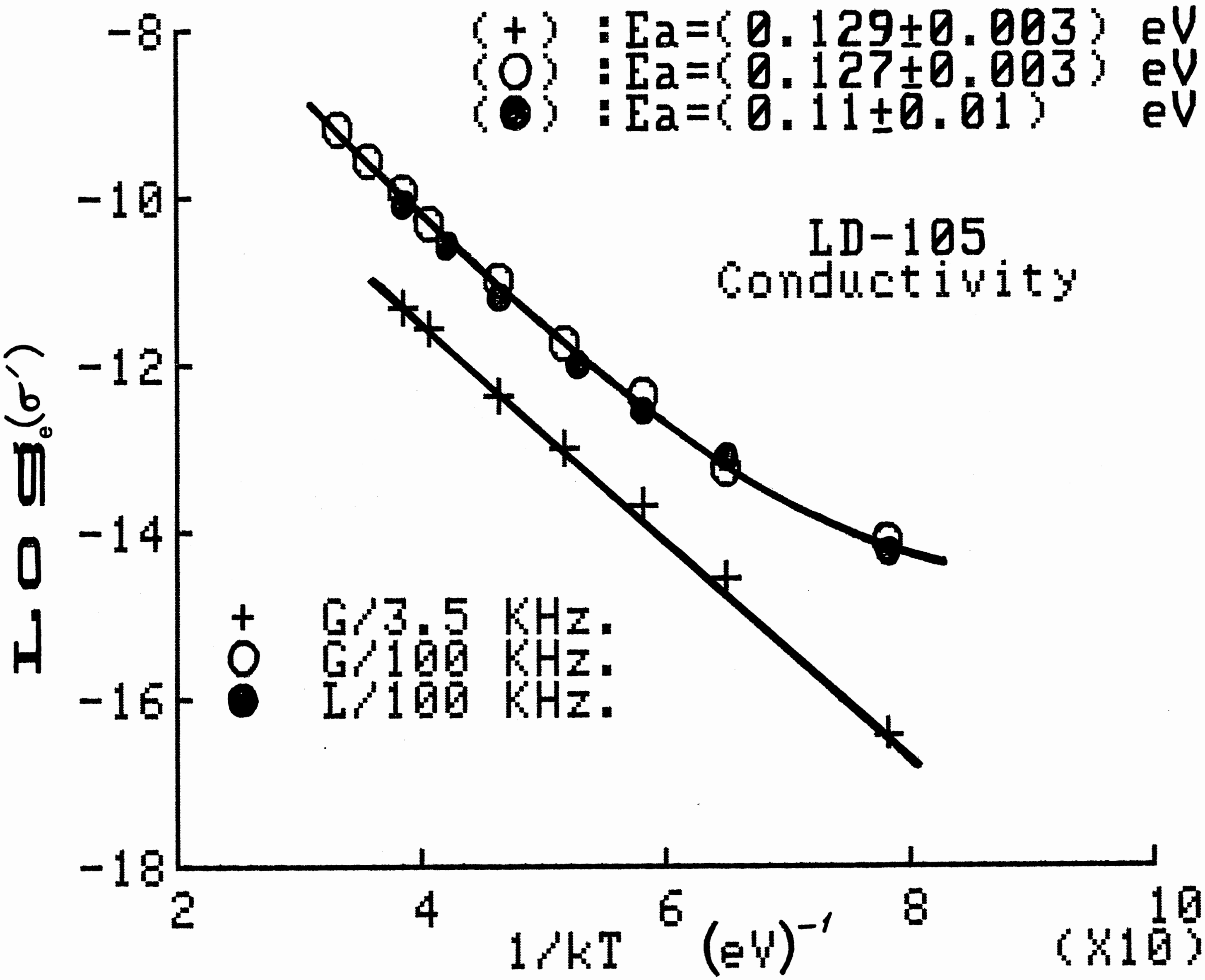
(+) :Ea=(0.129±0.003) eV
(O) :Ea=(0.127±0.003) eV
(●) :Ea=(0.11±0.01) eV
LD-105
Conductivity
+ G/3.5 KHz.
O G/100 KHz.
● L/100 KHz.
-8
-10
-12
-14
-16
-18
2
4
6
8
10
1/kT (eV)^-1
(X10)
Log_e(σ^-1)

Fig.(90)

TABLE (3.23)

THE TEMPERATURE DEPENDENCE OF LD-104

	<=== TEMPERATURE °C ===>							
Sample	25	0	-25	-50	-75	-95	-125	-170
G : σ'	29.4	12.5	3.77	1.68	0.79	0.32	0.11	0.12
K	9.1	6.4	4.2	3.8	3.6	3.4	3.2	3.3
DM	0.58	0.35	0.16	0.08	0.04	0.02	6E-3	6E-3
σ	15.5	7.8	0.90	0.16	.037	.011	.0087	.0074
H : σ'	31.7	12.9	4.80	1.70	0.69	0.35	0.10	0.12
K	8.8	6.3	4.9	4.3	4.0	3.9	3.8	3.8
DM	0.65	0.37	0.18	0.07	0.03	0.02	5E-3	5E-3
σ	16.3	9.6	1.0	0.20	0.04	.011	.0078	.0052

Observed At 10 KHz. For Two Samples G And H. All Values Of σ' Are (X1E-7), Those Of σ (DC) Are (X1E-10).

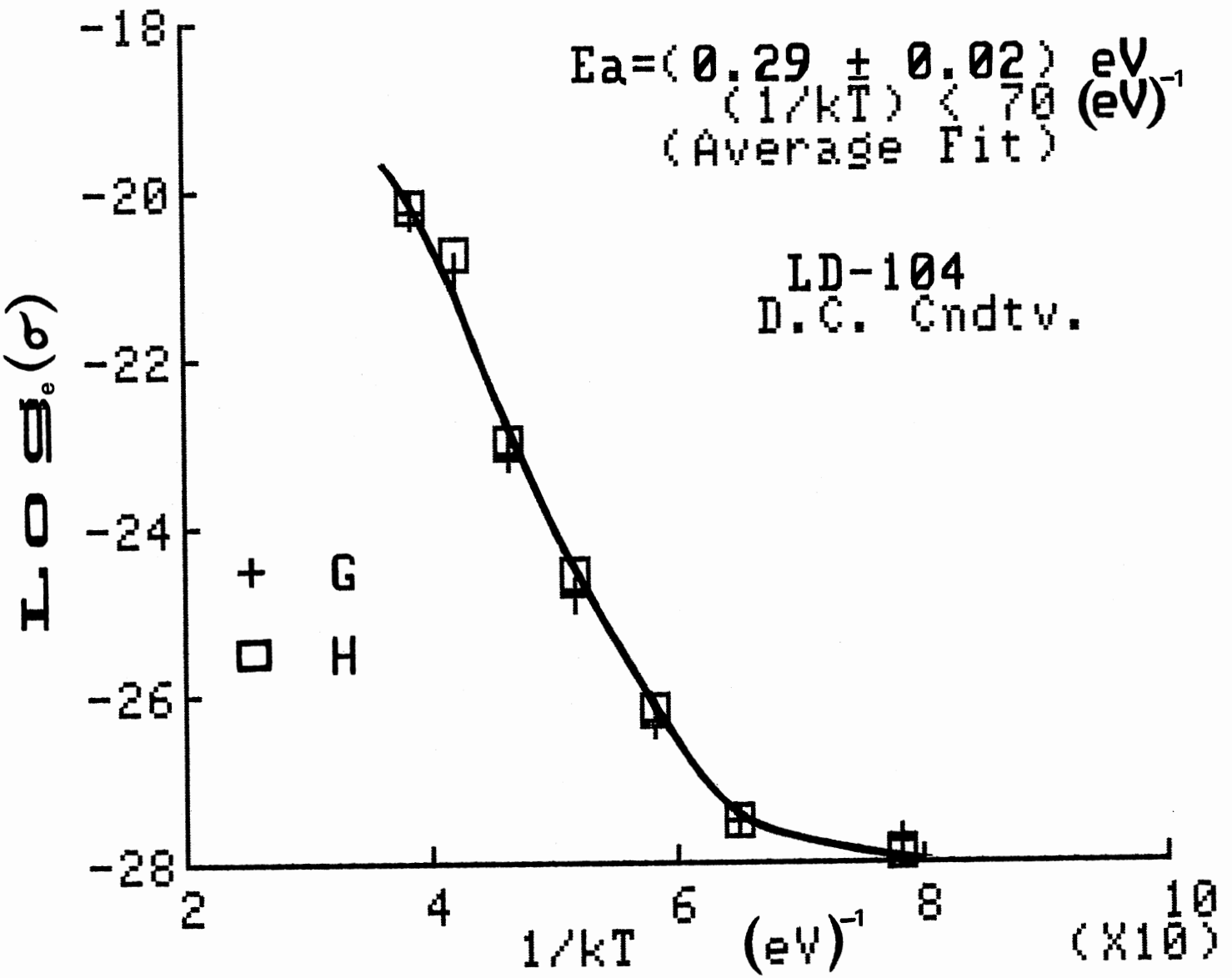
Ea=(0.29 ± 0.02) eV
(1/kT) < 70 (eV)⁻¹
(Average Fit)
LD-104
D.C. Cndtv.
+ G
□ H
Log σe(σ)
-18
-20
-22
-24
-26
-28
2
4
6
8
10
1/kT (eV)⁻¹
(X10)

Fig.(91)

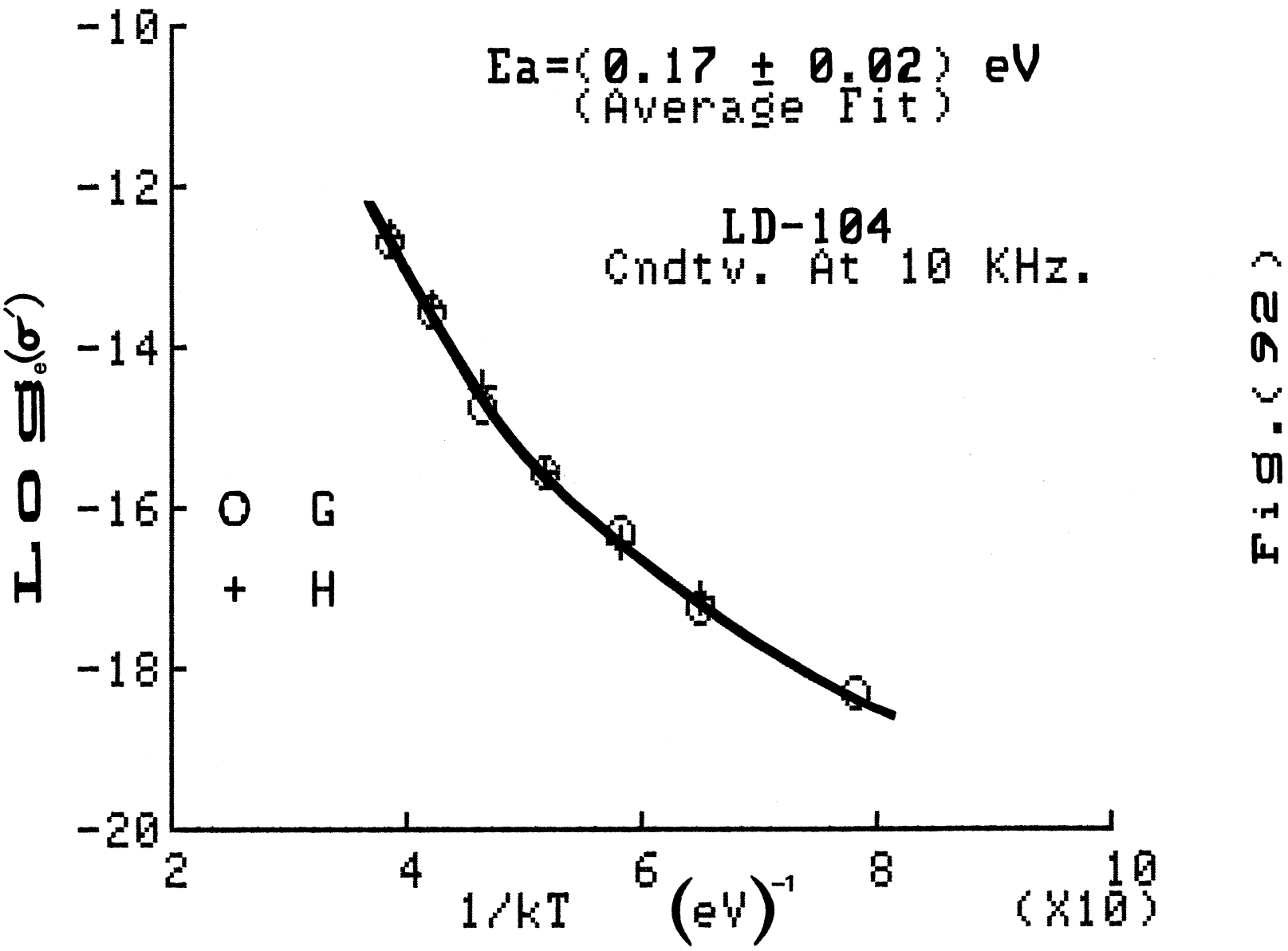
Ea=(0.17 ± 0.02) eV
(Average Fit)
LD-104
Cndtv. At 10 KHz.
O G
+ H
Log σe
-10
-12
-14
-16
-18
-20
2
4
6
8
10
1/kT (eV)-1
(X10)

Fig.(92)

TABLE (3.24)

THE TEMPERATURE DEPENDENCE OF LD-97

	<=== TEMPERATURE °C ===>							
Sample	25	0	-25	-50	-75	-95	-125	-170
S : σ'	46.2	24.1	7.47	2.87	1.02	0.76	0.14	0.19
K	13.9	8.83	6.03	5.2	4.7	4.5	4.2	4.3
DM	0.59	0.49	0.22	0.10	.038	.030	.024	.008
σ	30.7	21.4	2.30	0.45	.069	.025	.017	.011
T : σ'	36.7	15.1	5.42	1.71	0.90	0.45	0.14	0.13
K	10.2	6.98	5.45	4.7	4.4	4.3	4.1	3.9
DM	0.65	0.39	0.18	.065	.037	.019	6E-3	6E-3

cont'd

TABLE (3.24) Cont'd

	σ	43.9	11.4	1.59	0.28	.059	.020	.013	.012
S :	σ'	12.0	7.40	2.3	0.80	0.35	0.17	.011	5E-3
	K	32.2	19.0	9.2	6.7	5.6	5.3	4.8	4.4
	DM	0.67	0.70	0.45	0.21	0.11	.058	.0043	.0020
T :	σ'	8.94	5.62	1.95	0.57	0.23	.095	.023	.0074
	K	22.0	13.7	8.2	6.0	5.3	4.9	4.6	3.9
	DM	0.73	0.74	0.43	0.17	.078	.035	.009	.0034

Observed Respectively At 10 KHz. And 1 KHz. For Each Of Two Samples (S), And (T). All Values Of σ' Are (X1E-7), Those Of σ (DC) Are (X1E-10).

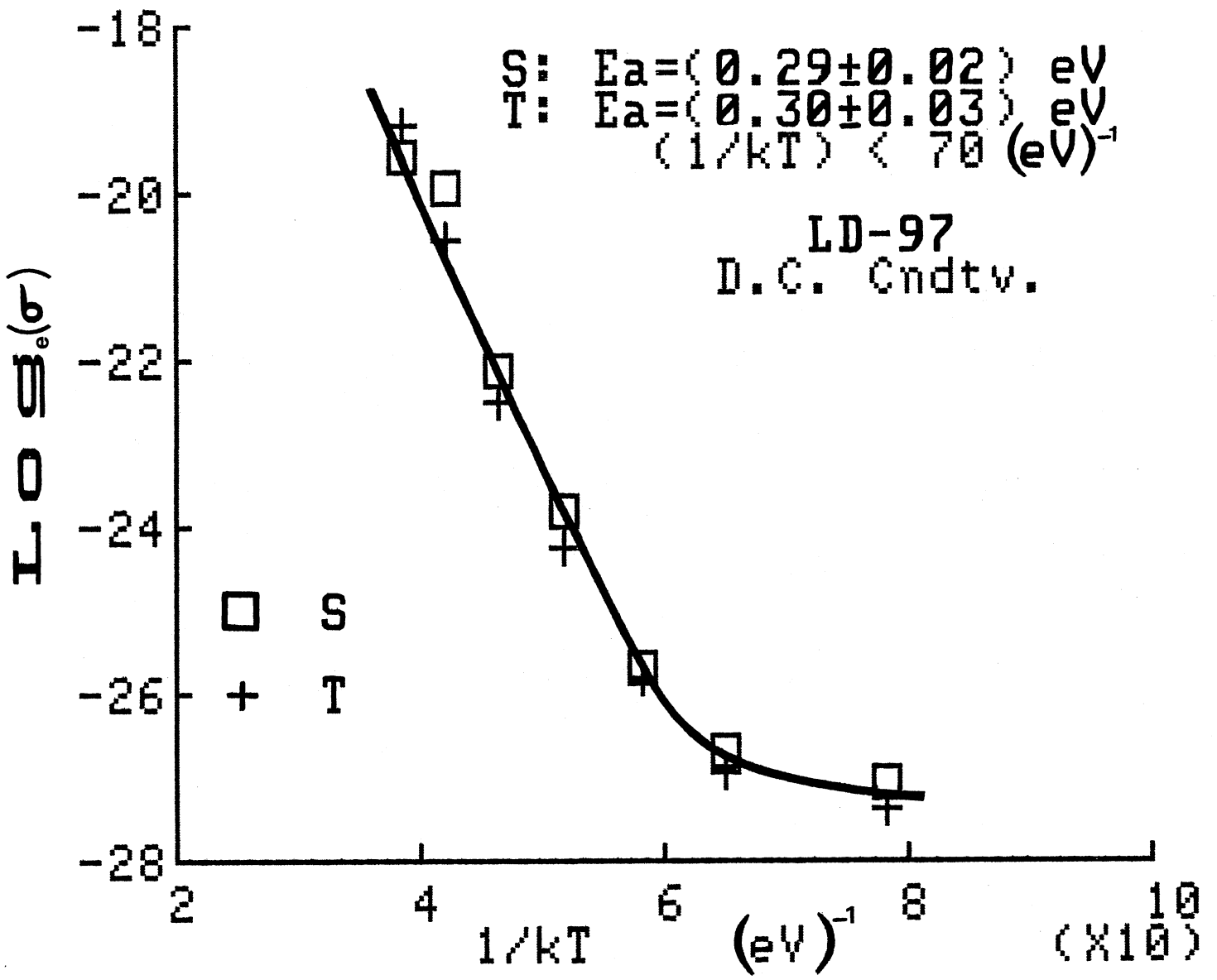
S: Ea=(0.29±0.02) eV
T: Ea=(0.30±0.03) eV
(1/kT) < 70 (eV)⁻¹
LD-97
D.C. Cndtv.
Log σe(σ)
-18
-20
-22
-24
-26
-28
S
T
2
4
6
8
10
1/kT (eV)⁻¹
(X10)

Fig. (93)

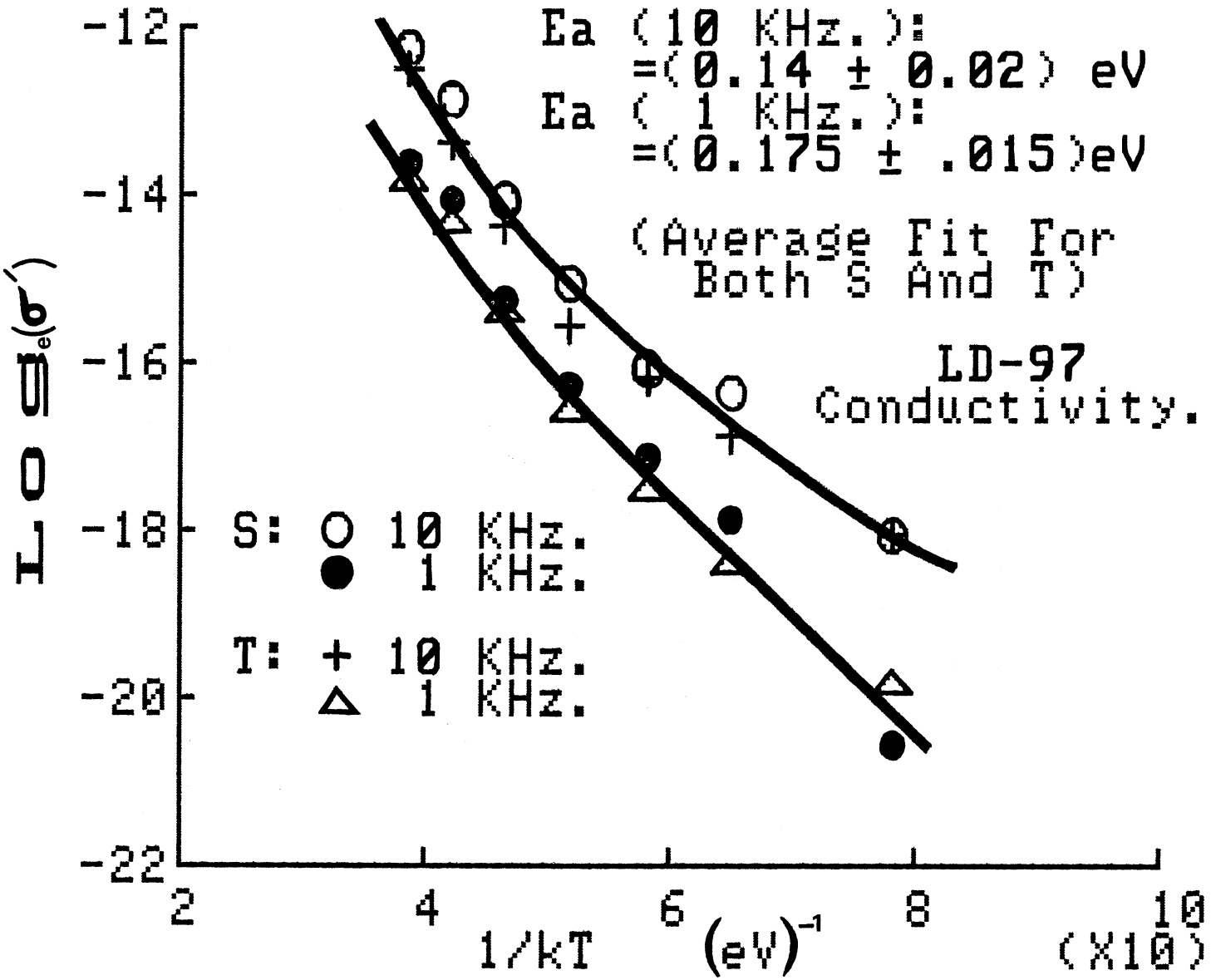
Ea (10 KHz.):
=(0.14 ± 0.02) eV
Ea (1 KHz.):
=(0.175 ± .015)eV
(Average Fit For
Both S And T)
LD-97
Conductivity.
S: O 10 KHz.
● 1 KHz.
T: + 10 KHz.
△ 1 KHz.
-12
-14
-16
-18
-20
-22
2
4
6
8
10
(X10)
1/kT (eV)⁻¹
Log σe(σ')

Fig. (94)

TABLE (3.25)

THE TEMPERATURE DEPENDENCE OF LD-95

	<=== TEMPERATURE °C ===>							
Sample	25	0	-25	-50	-75	-95	-125	-170
B : σ'	24.0	12.6	5.97	1.97	1.05	0.63	0.13	.073
K	7.85	5.70	4.70	4.00	3.96	3.82	3.60	3.68
DM	0.55	0.40	0.23	.088	.048	.030	.007	.004
σ	36.2	13.2	3.92	0.70	0.15	.064	.030	.021
B : σ'	8.94	5.05	2.09	0.74	0.43	0.18	.037	.024
K	17.0	11.0	7.74	5.55	4.77	4.53	4.10	3.82
DM	0.95	0.83	0.48	0.24	0.16	0.07	.016	.011

Observed At 10 KHz. And 1 KHz. Respectively. All Values Of σ' Are (X1E-7), Those Of σ (DC) Are (X1E-10).

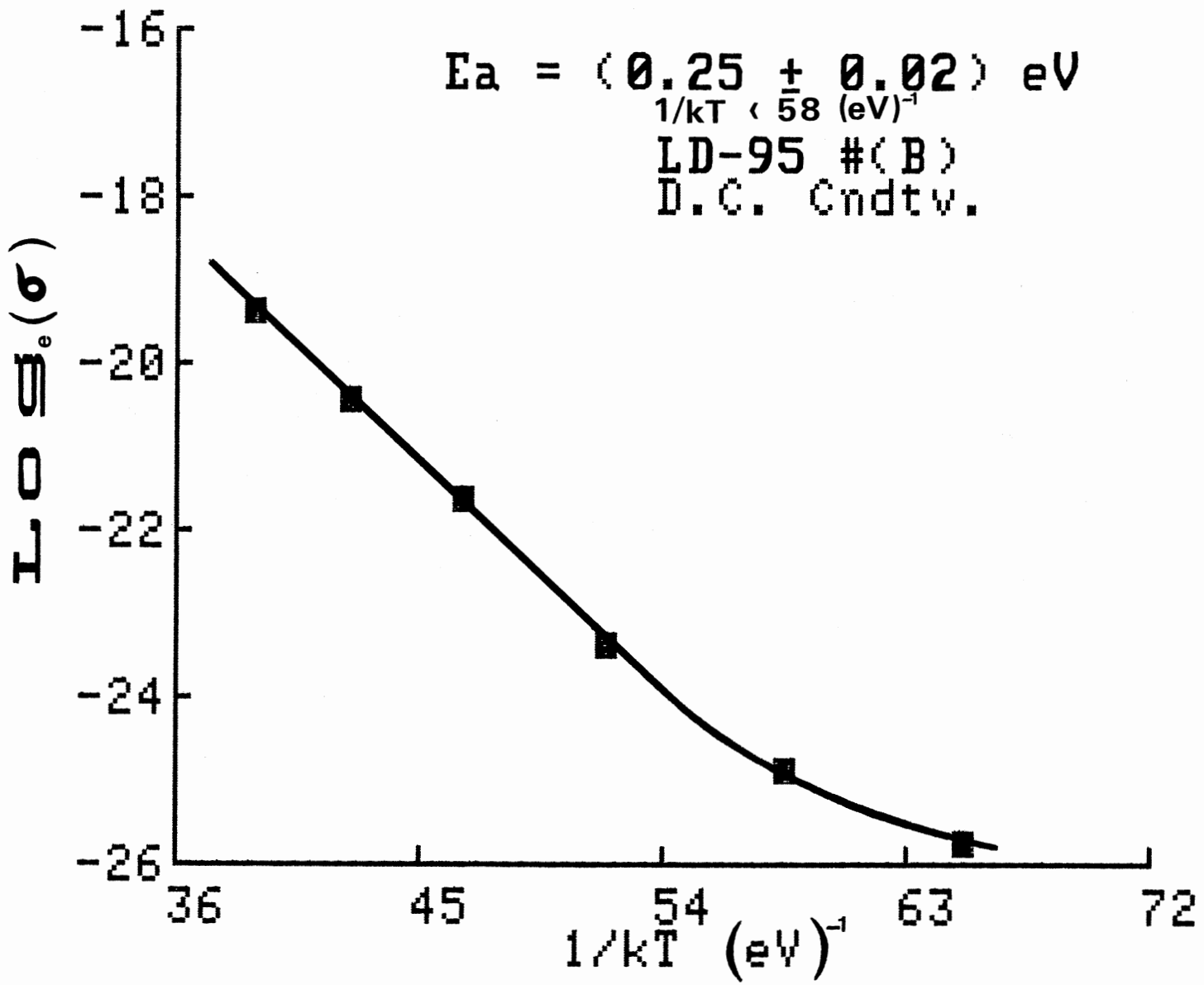
Ea = (0.25 ± 0.02) eV
1/kT ‹ 58 (eV)⁻¹
LD-95 #(B)
D.C. Cndtv.
Log σe
-16
-18
-20
-22
-24
-26
36
45
54
63
72
1/kT (eV)⁻¹

Fig.(95)

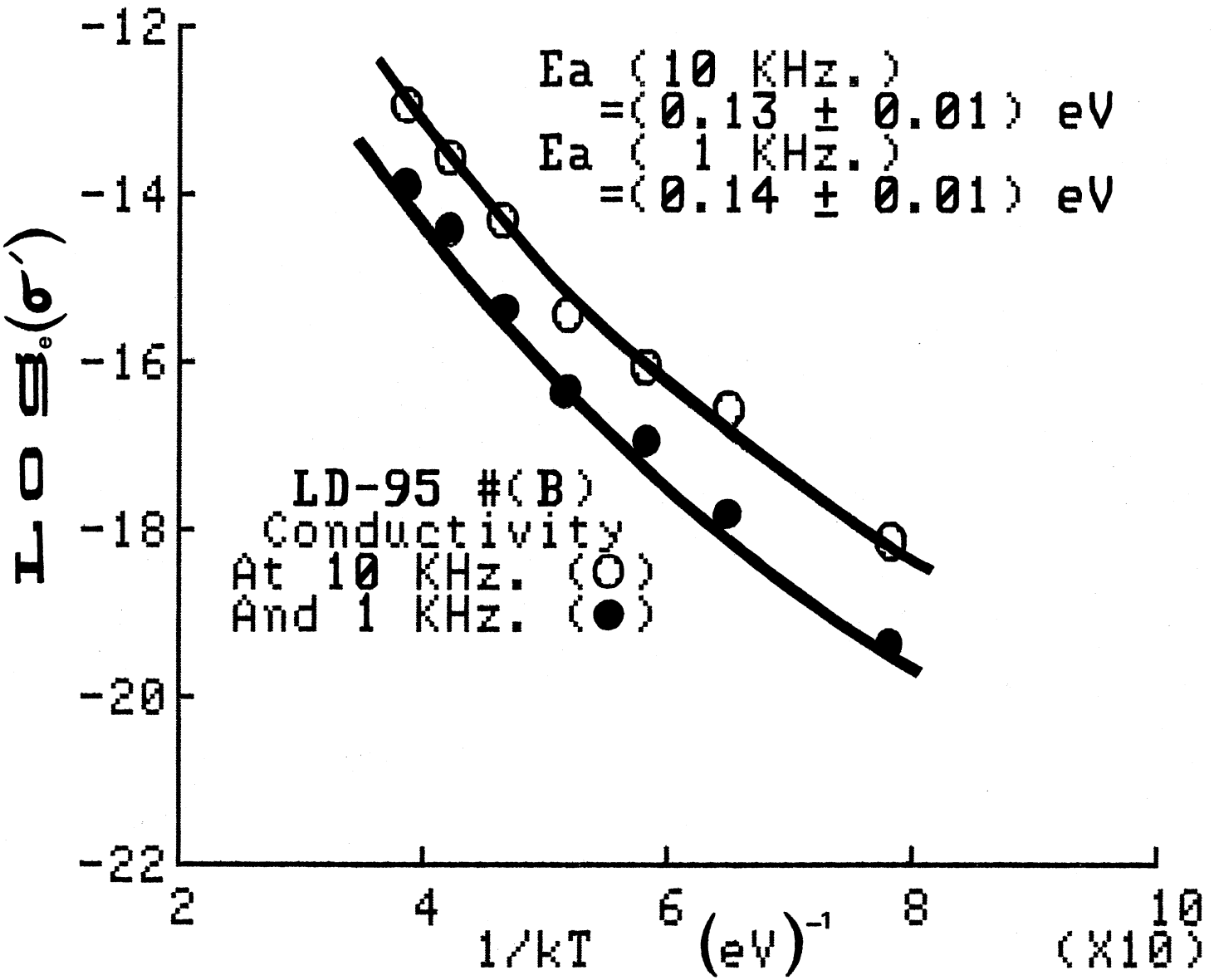
Ea (10 KHz.)
=(0.13 ± 0.01) eV
Ea (1 KHz.)
=(0.14 ± 0.01) eV
LD-95 #(B)
Conductivity
At 10 KHz. (O)
And 1 KHz. (●)
Log σe(σ')
-12
-14
-16
-18
-20
-22
2
4
6
8
10
1/kT (eV)⁻¹
(X10)

Fig. 96)

TABLE (3.26)

THE TEMPERATURE DEPENDENCE OF LD-94

	<=== TEMPERATURE °C ===>							
Sample	25	0	-25	-50	-75	-95	-125	-170
S : σ'	55.2	40.0	19.3	8.50	4.70	1.98	0.55	0.14
K	13.1	9.54	6.82	4.94	4.27	4.00	3.72	3.65
DM	0.76	0.75	0.51	0.31	0.20	.089	.027	.007
σ	24.1	11.9	3.40	0.71	0.24	.074	.0064	.0017
S : σ'	28.1	14.3	6.71	3.15	1.43	0.80	0.19	.024
K	25.3	18.6	14.0	8.85	6.74	5.20	4.42	3.85
DM	2.00	1.38	0.86	0.64	0.38	0.28	.077	.011

Observed At 10 KHz And 1 KHz Respectively. All Values Of σ' Are (X1E-7), Those Of σ (DC) Are (X1E-9).

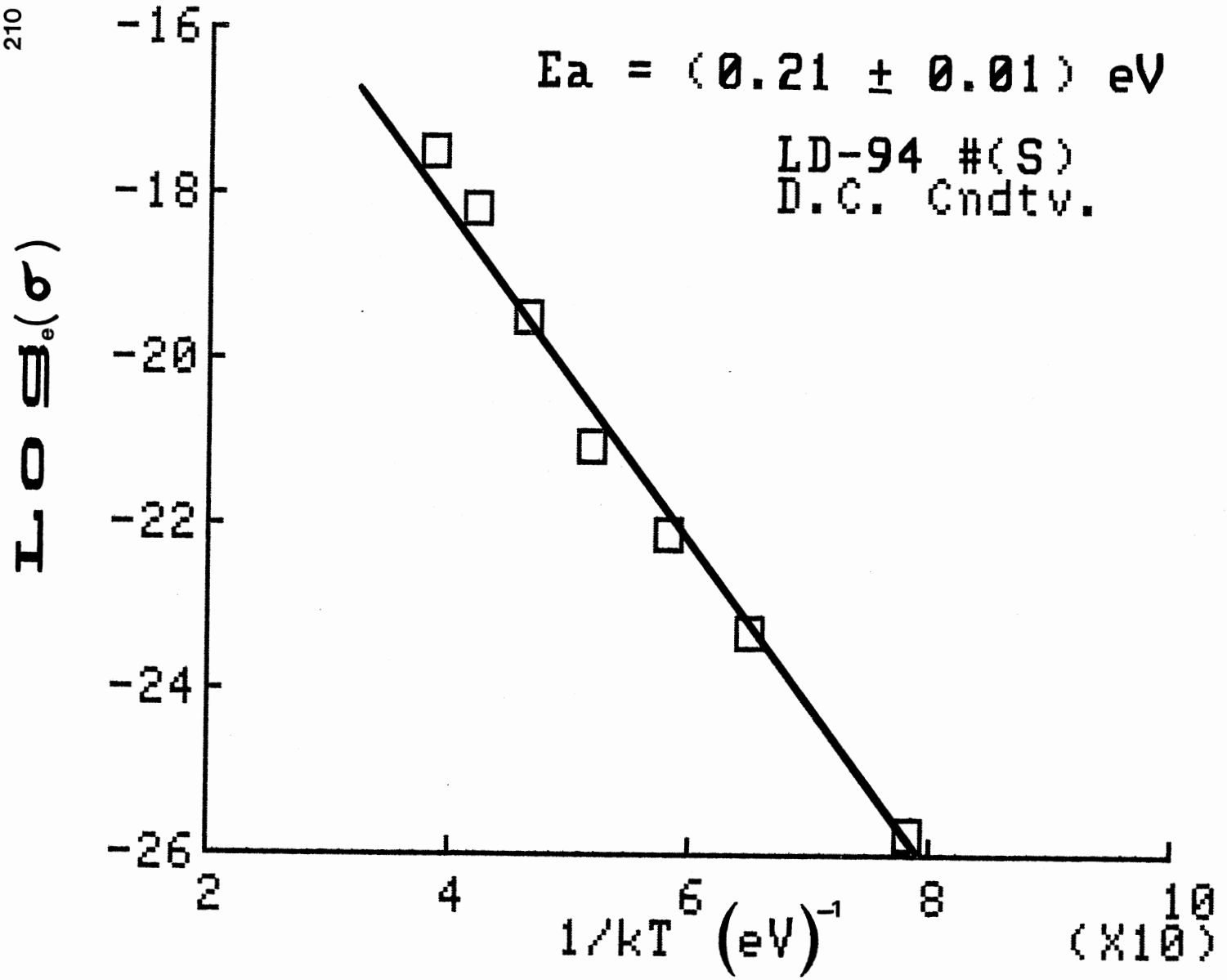
Ea = (0.21 ± 0.01) eV
LD-94 #(S)
D.C. Cndtv.
Log σe
-16
-18
-20
-22
-24
-26
2
4
6
8
10
1/kT (eV)⁻¹
(X10)

Fig. 97

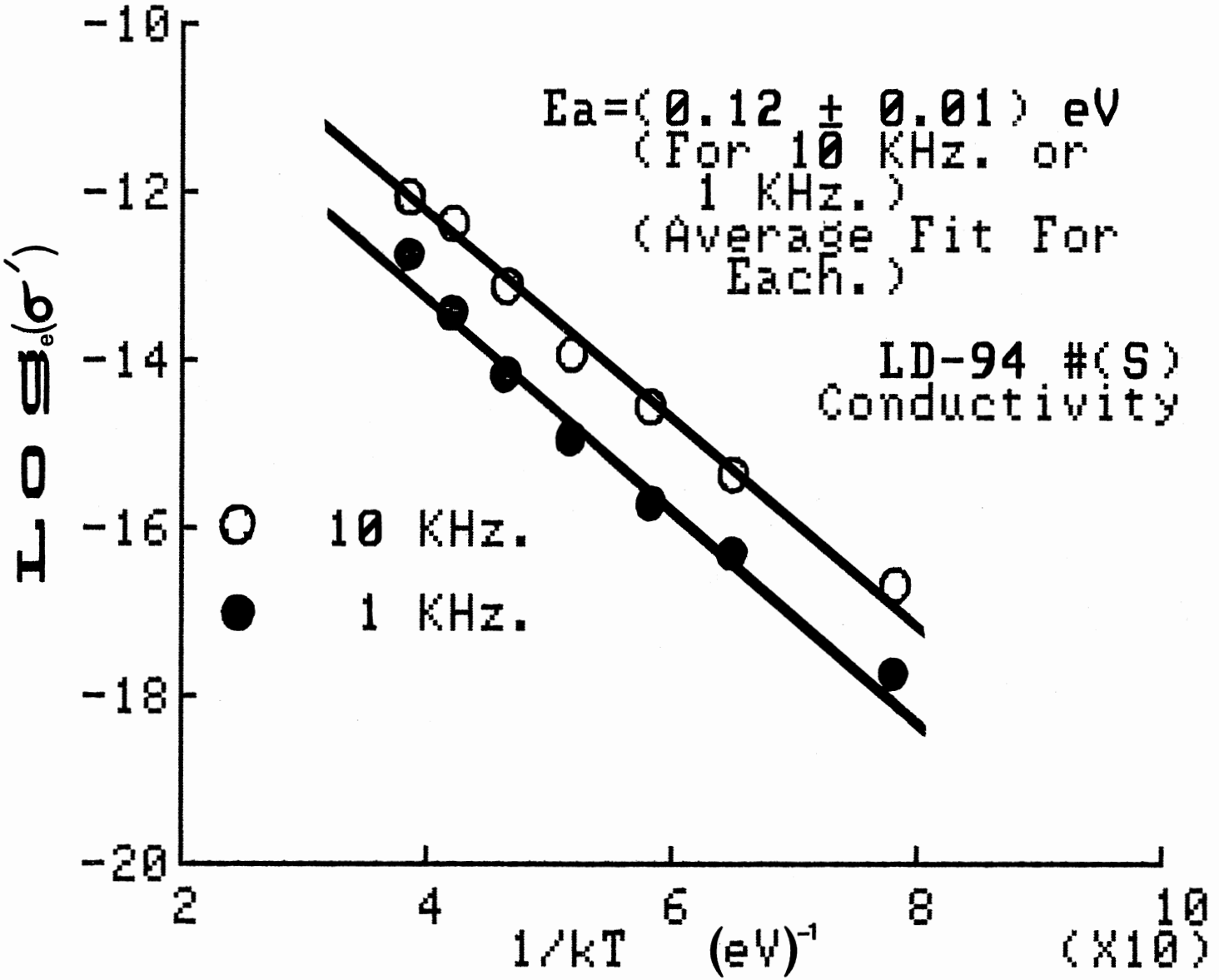
Ea=(0.12 ± 0.01) eV
(For 10 KHz. or
1 KHz.)
(Average Fit For
Each.)
LD-94 #(S)
Conductivity
10 KHz.
1 KHz.
Log σe(σ')
-10
-12
-14
-16
-18
-20
2
4
6
8
10
(X10)
1/kT (eV)-1

Fig.(98)

TABLE (3.27)

THE TEMPERATURE DEPENDENCE OF LD-14A

		<=== TEMPERATURE °C ===>							
Sample		25	0	-25	-50	-75	-95	-125	-170
V :	σ'	11.3	5.70	3.22	1.45	1.04	0.59	0.24	--
	K	5.65	5.11	4.70	4.40	4.23	4.16	4.10	--
	DM	0.36	0.20	0.12	.059	.044	.025	.010	--
	σ	5.97	1.87	0.63	0.16	.045	.018	.010	--
V :	σ'	4.23	2.18	1.02	0.48	0.23	0.16	.054	--
	K	10.4	8.26	6.57	5.68	5.12	4.89	4.62	--
	DM	0.73	0.47	0.28	0.15	.079	.058	.021	--

Observed At 10 KHz. And 1 KHz. Respectively. All Values Of σ' Are (X1E-7), Those Of σ (DC) Are (X1E-10).

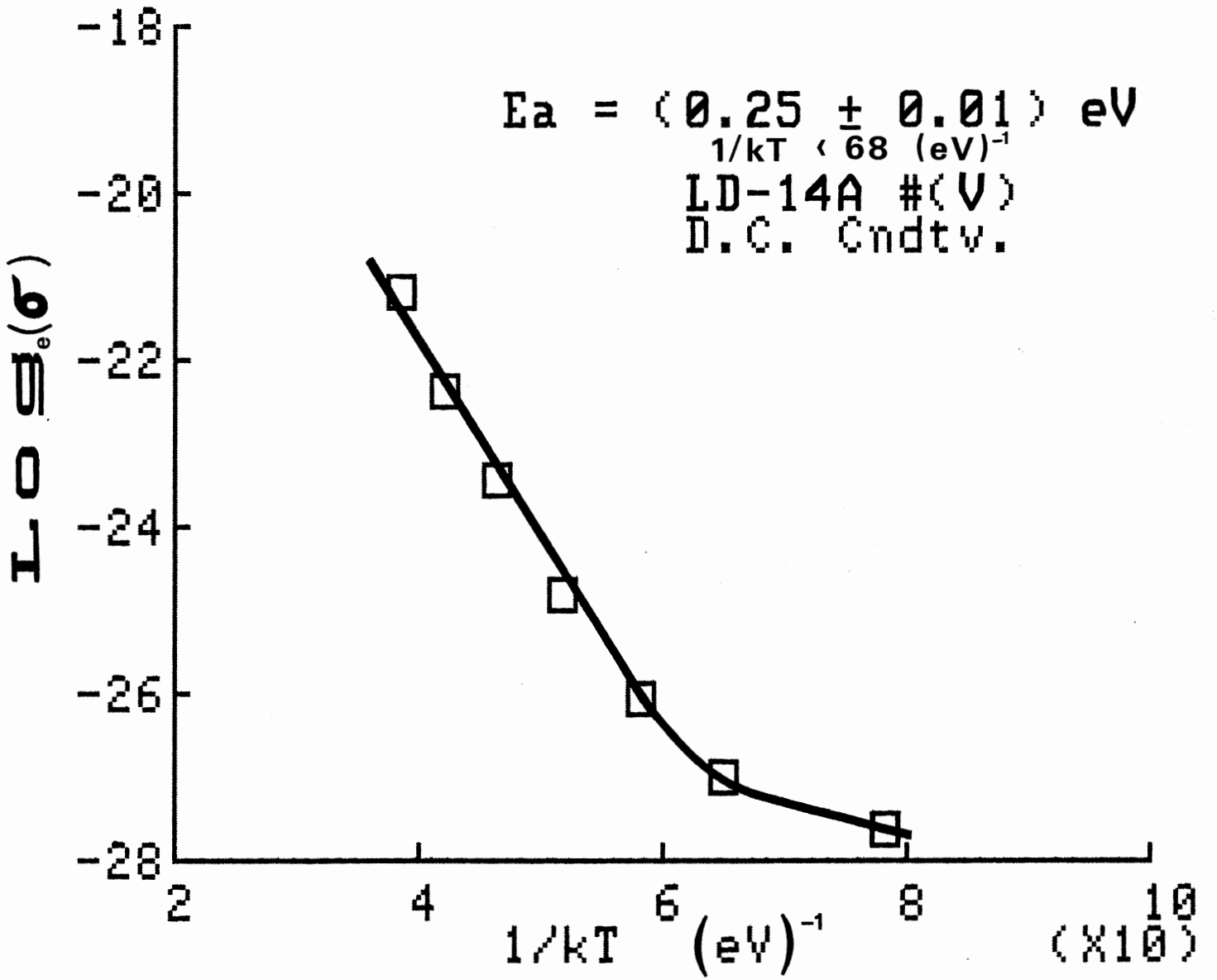
Ea = (0.25 ± 0.01) eV
1/kT < 68 (eV)⁻¹
LD-14A #(V)
D.C. Cndtv.
Log σe
-18
-20
-22
-24
-26
-28
2
4
6
8
10
1/kT (eV)⁻¹
(X10)

Fig. (99)

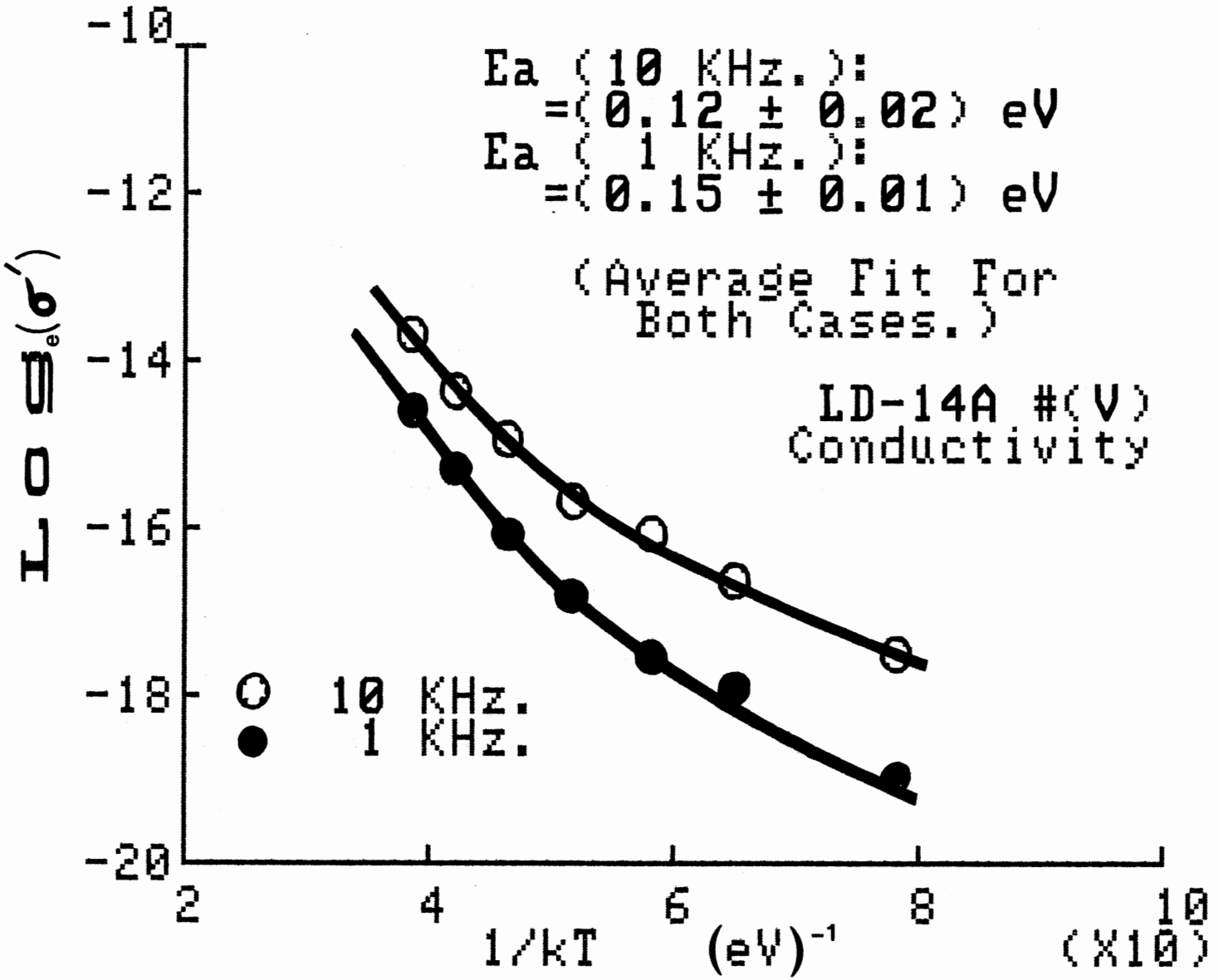
Ea (10 KHz.):
=(0.12 ± 0.02) eV
Ea (1 KHz.):
=(0.15 ± 0.01) eV
(Average Fit For
Both Cases.)
LD-14A #(V)
Conductivity
O 10 KHz.
● 1 KHz.
-10
-12
-14
-16
-18
-20
2
4
6
8
10
1/kT (eV)⁻¹
(X10)
Log σe(σ')

Fig. (100)

TABLE (3.28)

THE TEMPERATURE DEPENDENCE OF LD-6A

	<=== TEMPERATURE °C ===>							
Sample	25	0	-25	-50	-75	-95	-125	-170
F : σ'	8.43	5.83	3.52	2.30	1.70	1.22	0.55	0.18
K	18.7	16.7	13.7	10.5	8.3	6.7	5.3	4.3
DM	0.81	0.63	0.46	0.40	0.37	0.33	0.19	.076
σ	49.2	26.1	9.24	3.63	1.35	0.49	.067	.014

Observed At 1 KHz. All Values Of σ' Are (X1E-7), Those Of σ (DC) Are (X1E-10).

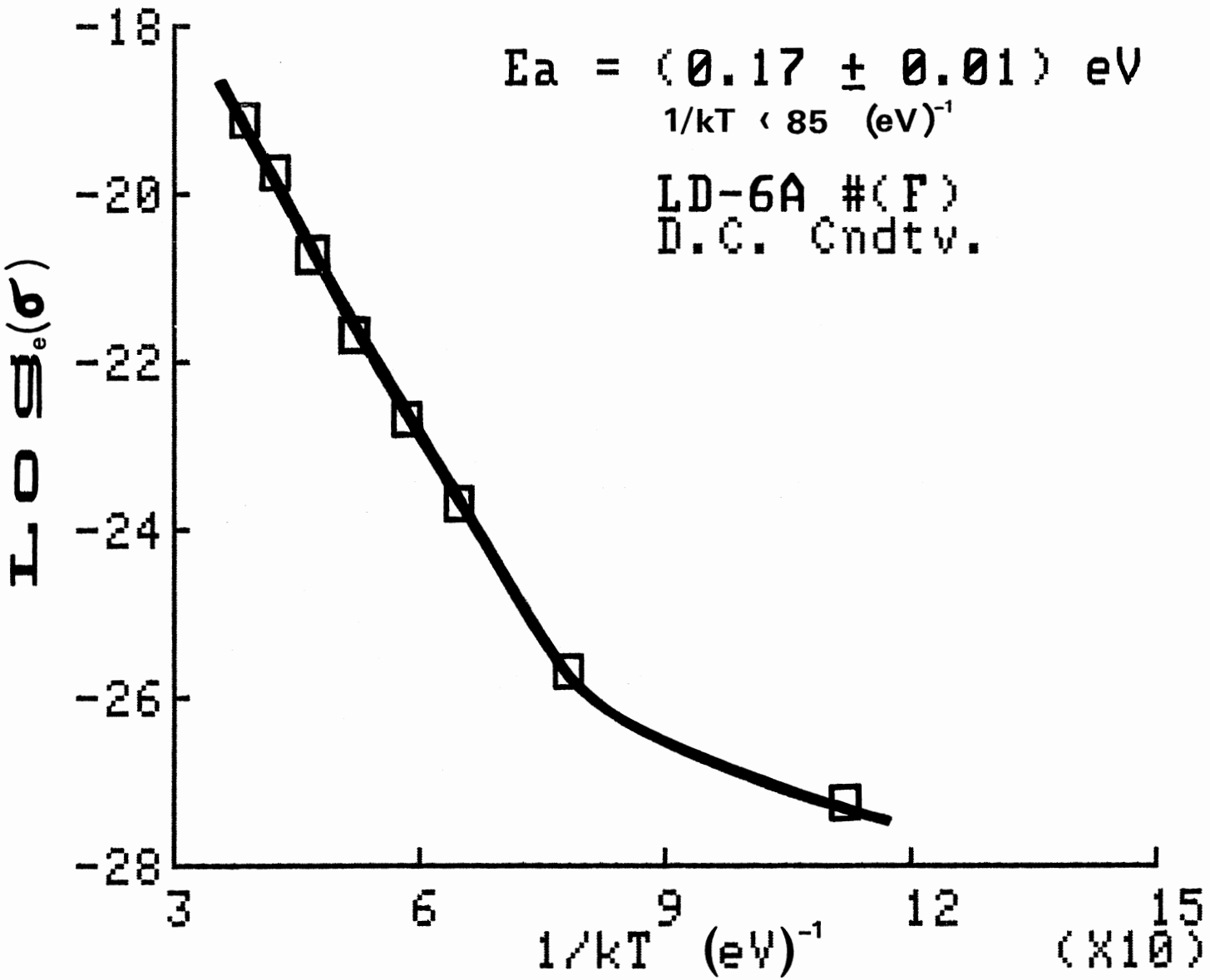
Ea = (0.17 ± 0.01) eV
1/kT < 85 (eV)⁻¹
LD-6A #(F)
D.C. Cndtv.
Log σe
-18
-20
-22
-24
-26
-28
3
6
9
12
15
1/kT (eV)⁻¹
(X10)

Fig.(101)

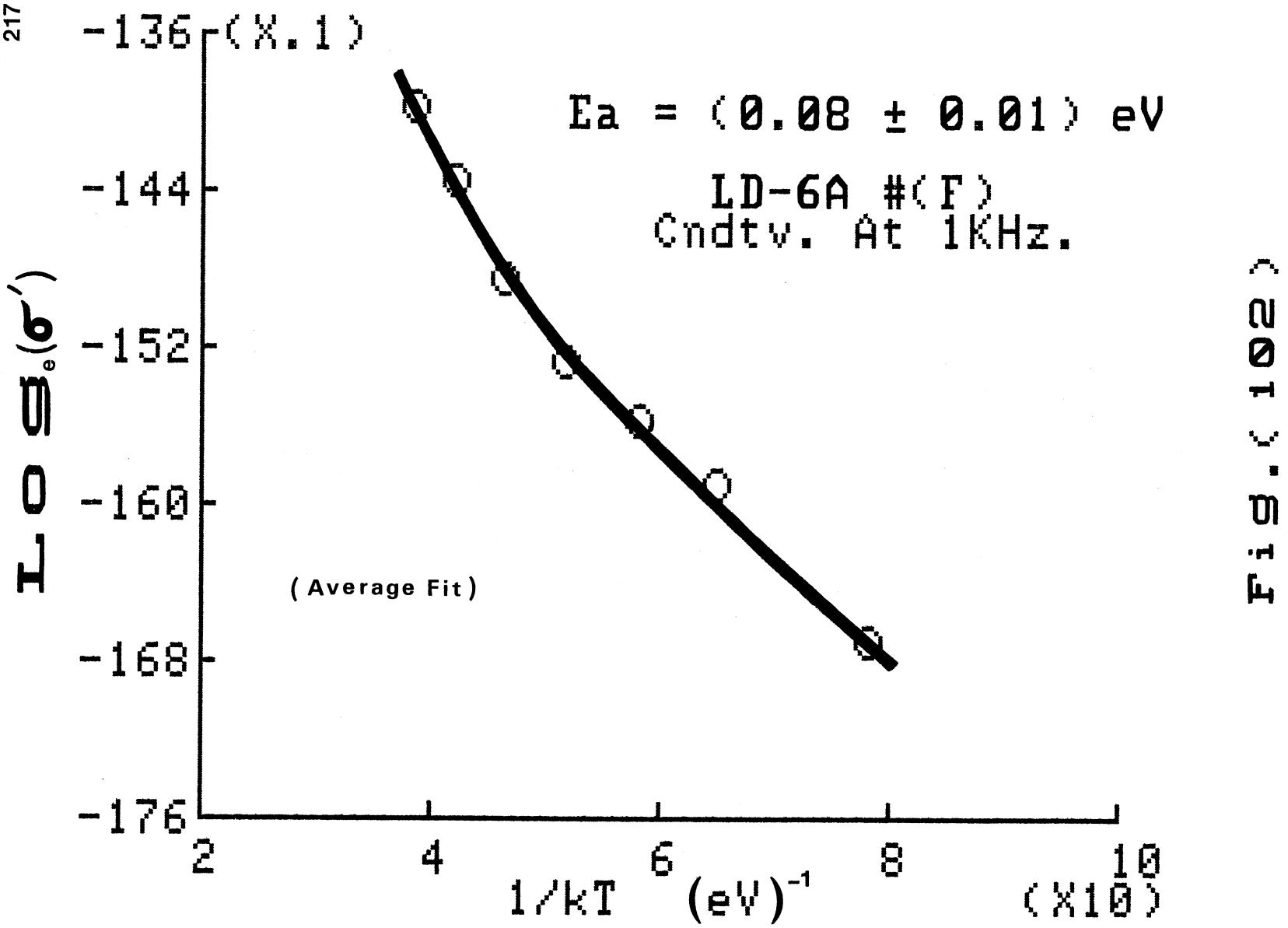
-136 (X.1)
-144
-152
-160
-168
-176
Log $\sigma_e(\sigma')$
Ea = (0.08 ± 0.01) eV
LD-6A #(F)
Cndtv. At 1KHz.
(Average Fit)
2
4
6
8
10
1/kT (eV)$^{-1}$
(X10)

Fig.(102)

TABLE (3.29)

THE TEMPERATURE DEPENDENCE OF LD-54

	<=== TEMPERATURE °C ===>							
Sample	50	25	0	-25	-50	-75	-95	-125
V : σ'	6.68	2.48	1.35	0.65	0.57	0.58	0.57	0.40
K	8.1	6.3	6.2	5.7	5.3	5.2	4.97	4.47
DM	0.15	0.07	0.04	0.02	.019	.020	.021	.016
σ	67.4	5.30	3.28	3.00	2.72	2.44	2.15	1.61

Observed At 1 KHz. All Values Of σ' Are (X1E-8), Those Of σ (DC) Are (X1E-13).

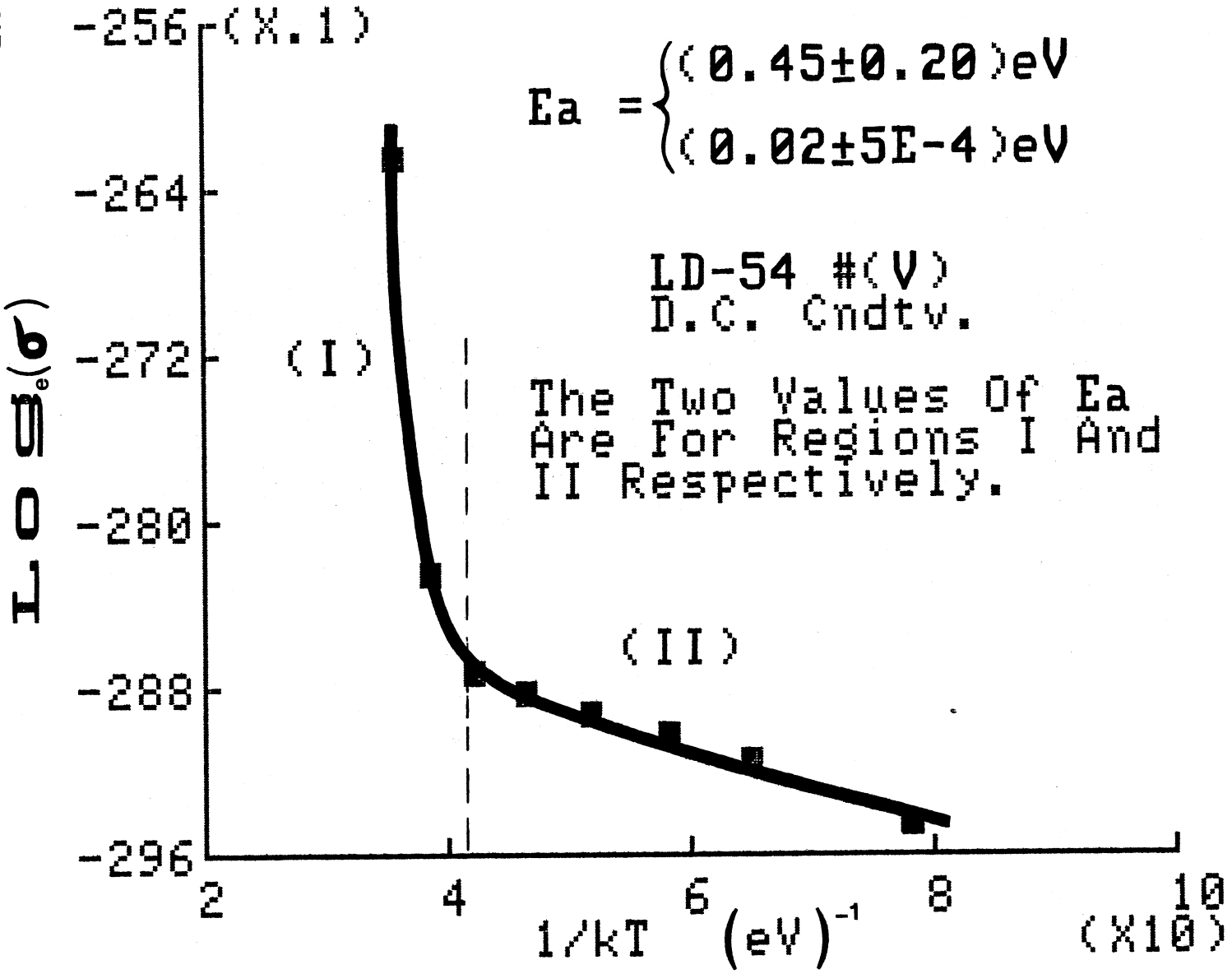
-256 (X.1)
-264
-272
-280
-288
-296
Log σ_e(σ)
(I)
(II)
2
4
6
8
10
1/kT (eV)$^{-1}$
(X10)
Ea = {(0.45±0.20)eV
(0.02±5E-4)eV
LD-54 #(V)
D.C. Cndtv.
The Two Values Of Ea
Are For Regions I And
II Respectively.

Fig. (10)

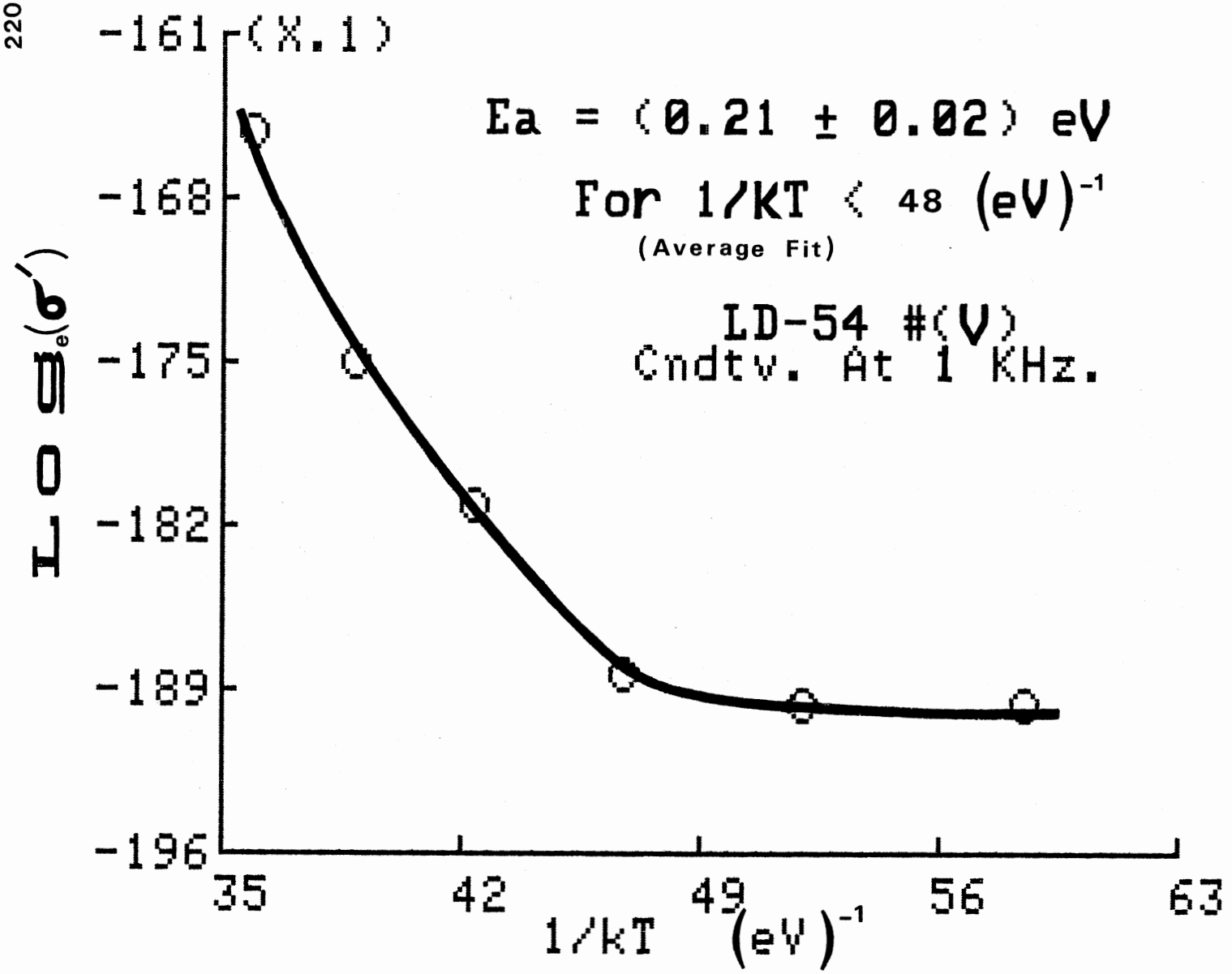
-161 (X.1)
-168
-175
-182
-189
-196
35
42
49
56
63
1/kT (eV)$^{-1}$
Log $\sigma_e(\sigma')$
Ea = (0.21 ± 0.02) eV
For 1/KT < 48 (eV)$^{-1}$
(Average Fit)
LD-54 #(V)
Cndtv. At 1 KHz.

Fig.(104)

TABLE (3.30)

THE TEMPERATURE DEPENDENCE OF LD-52B

Sample	<=== TEMPERATURE °C ===> 25	0	-25	-50	-75	-90	-125	-170
H : σ'	33.1	14.3	9.43	7.16	--	6.47	5.05	--
K	6.58	5.85	5.41	5.07	--	4.77	4.52	--
DM	.090	.044	.032	.025	--	.024	.020	--
σ	5.41	4.45	3.39	2.67	--	2.10	1.29	--

Observed At 1 KHz. All Values Of σ' Are (X1E-9), Those Of σ (DC) Are (X1E-12).

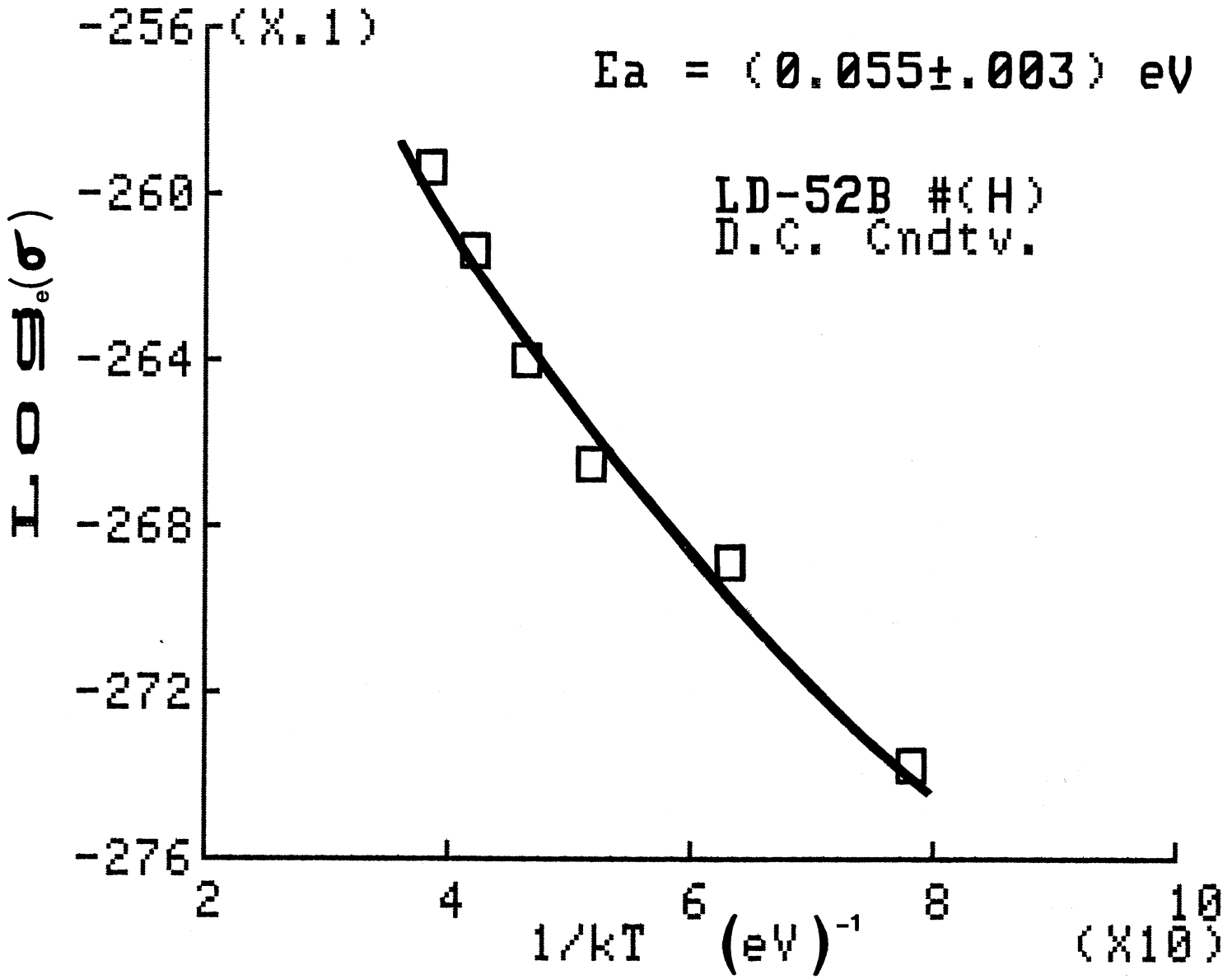
-256 (X.1)
-260
-264
-268
-272
-276
LOG σ_e
Ea = (0.055±.003) eV
LD-52B #(H)
D.C. Cndtv.
2
4
6
8
10
1/kT (eV)$^{-1}$
(X10)

Fig.(105)

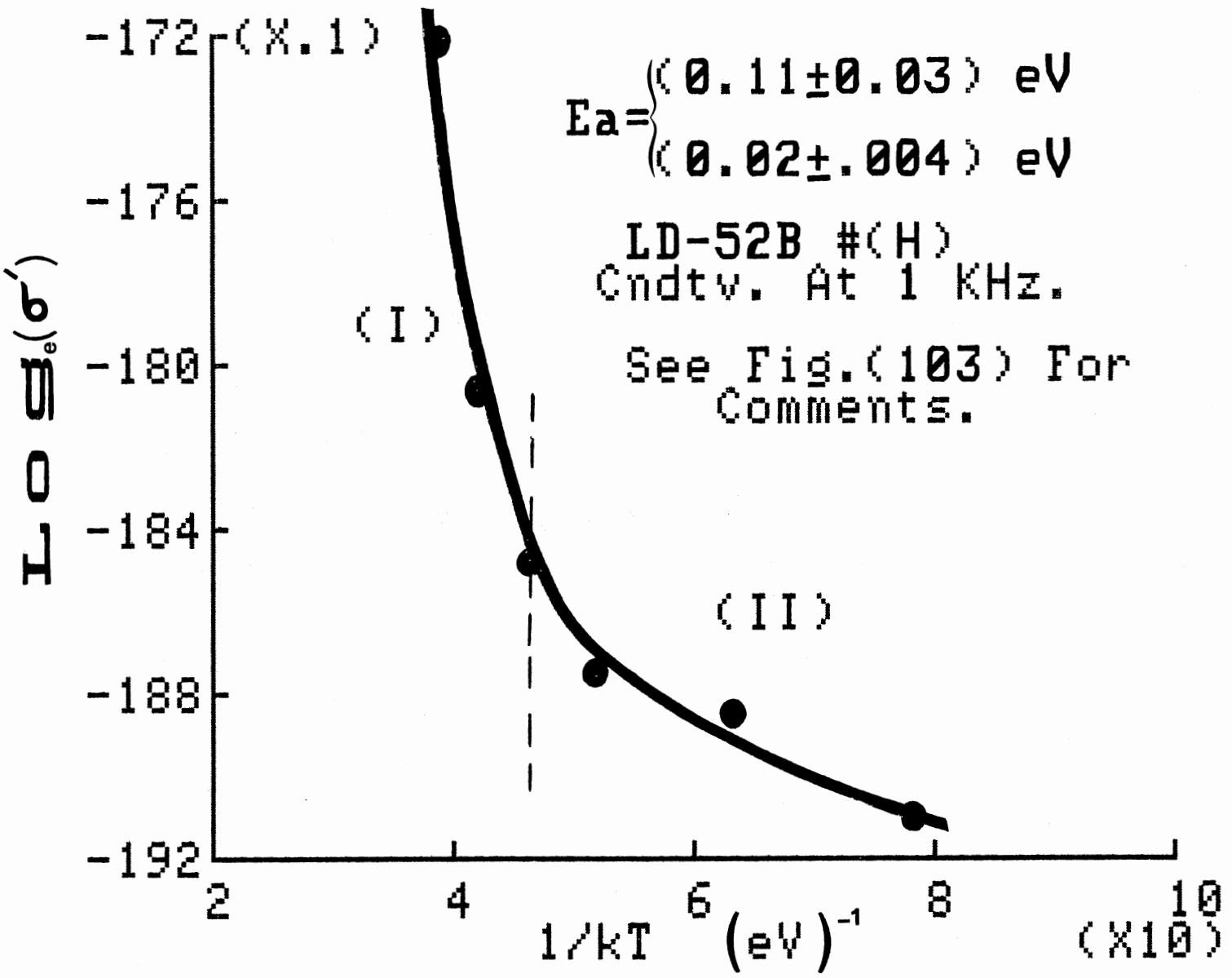
-172
-176
-180
-184
-188
-192
(X.1)
Log σ_e(σ')
Ea={(0.11±0.03) eV
(0.02±.004) eV
LD-52B #(H)
Cndtv. At 1 KHz.
See Fig.(103) For
Comments.
(I)
(II)
2
4
6
8
10
1/kT (eV)$^{-1}$
(X10)

Fig.(106)

TABLE (3.31)

THE TEMPERATURE DEPENDENCE OF LD-106

	<=== TEMPERATURE °C ===>							
Sample	25	0	-25	-50	-75	-95	-125	-170
C : σ'	20.3	9.50	3.47	0.92	0.54	0.25	0.11	--
K	11.5	7.98	6.88	5.74	5.25	4.95	4.54	--
DM	0.32	0.20	.090	.028	.018	9E-3	4E-3	--
H : σ'	12.6	5.23	2.41	0.81	0.45	0.37	0.20	0.18
K	8.02	6.12	5.02	4.70	4.40	4.24	4.07	3.85
DM	0.28	0.15	.086	.030	.018	.016	9E-3	.0085
σ	38.7	7.00	3.80	3.50	3.50	3.72	3.50	3.28

Observed For Two Samples C And H At 1 KHz. All Values Of σ' Are (X1E-8), Those Of σ (DC) Are (X1E-12).

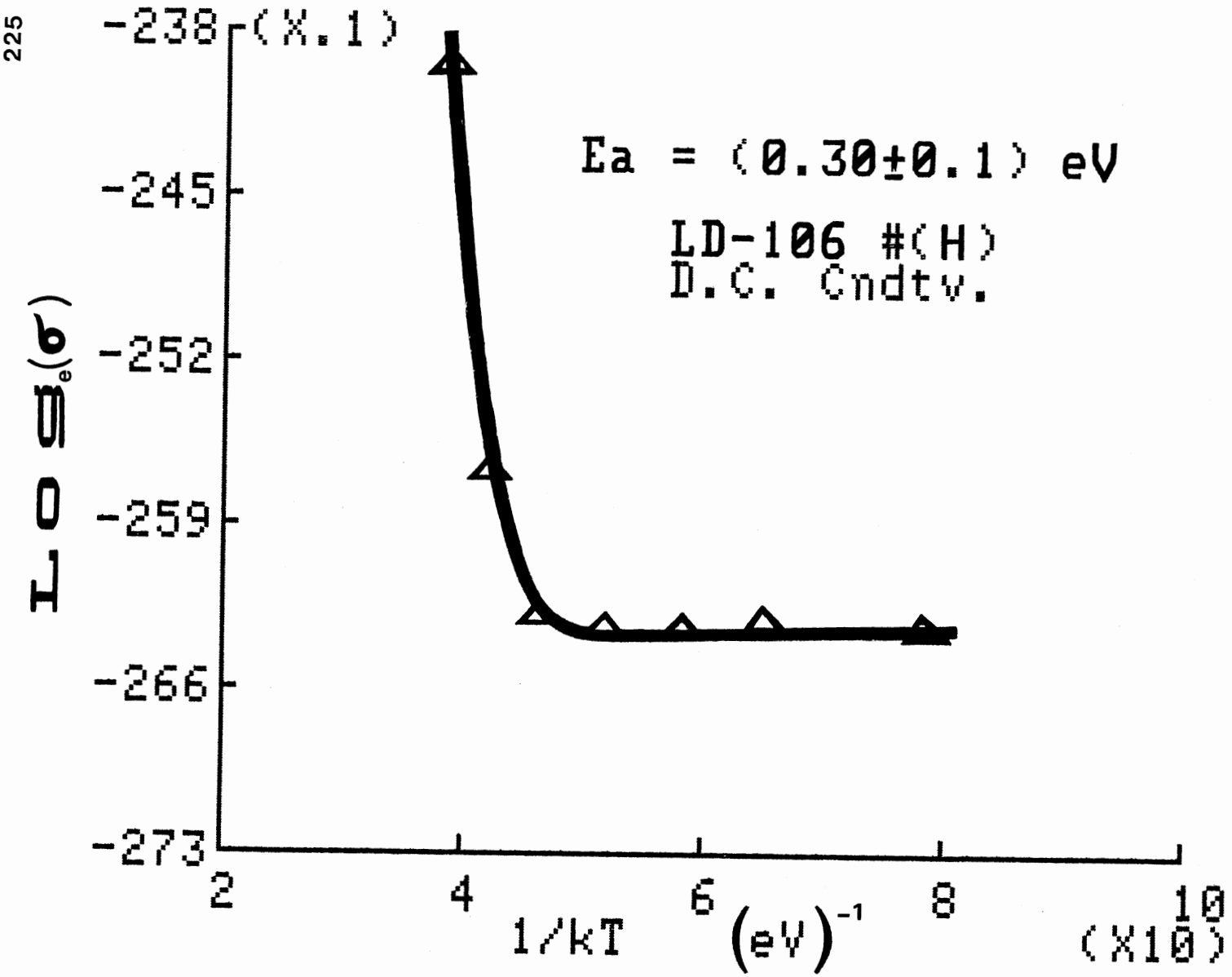
-238
(X.1)
-245
-252
-259
-266
-273
Log σ_e
Ea = (0.30±0.1) eV
LD-106 #(H)
D.C. Cndtv.
2
4
6
8
10
1/kT (eV)$^{-1}$
(X10)

Fig. (107)

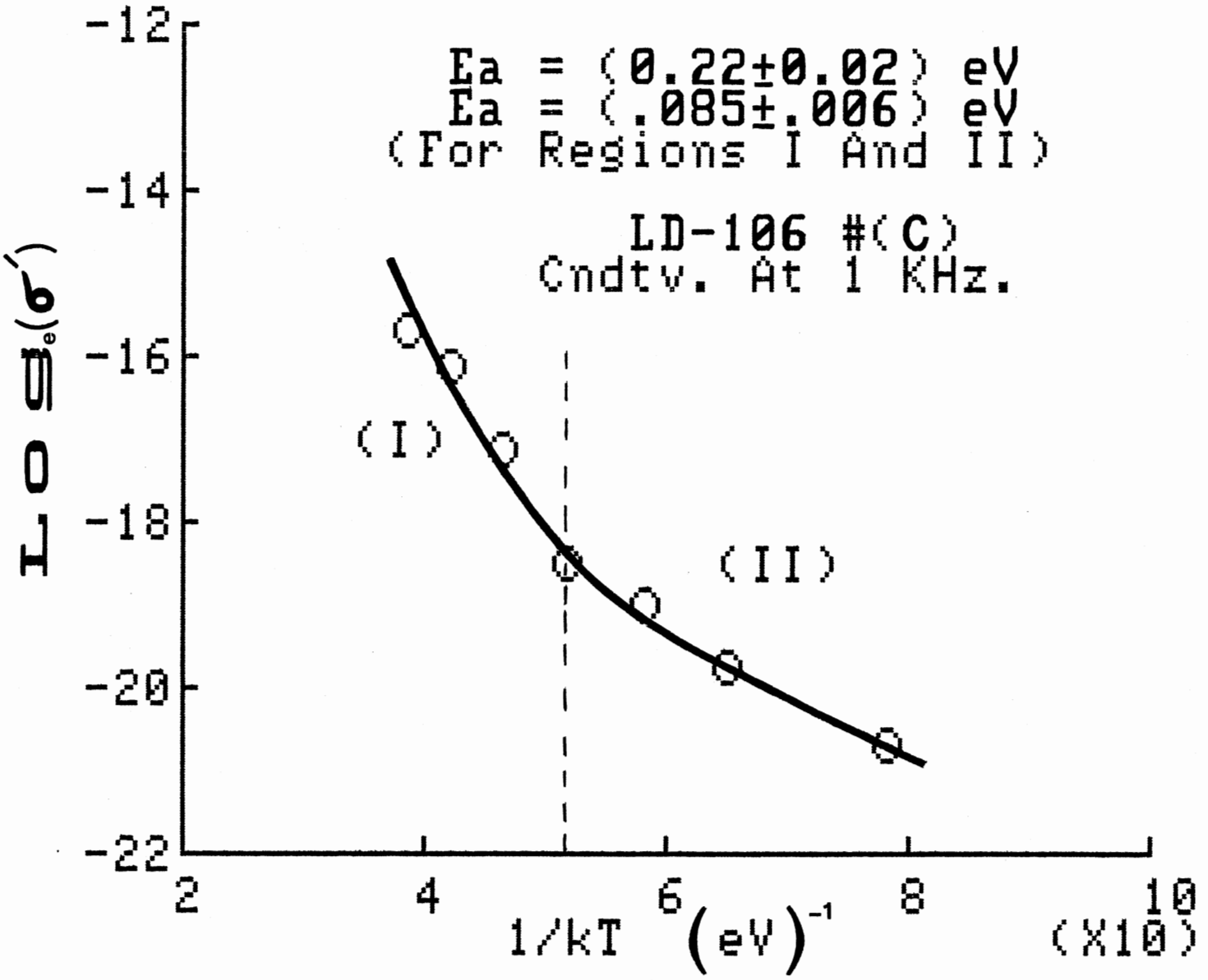
Ea = (0.22±0.02) eV
Ea = (.085±.006) eV
(For Regions I And II)
LD-106 #(C)
Cndtv. At 1 KHz.
(I)
(II)
-12
-14
-16
-18
-20
-22
2
4
6
8
10
(X10)
1/kT (eV)⁻¹
Log σe(σ')

Fig.(108)

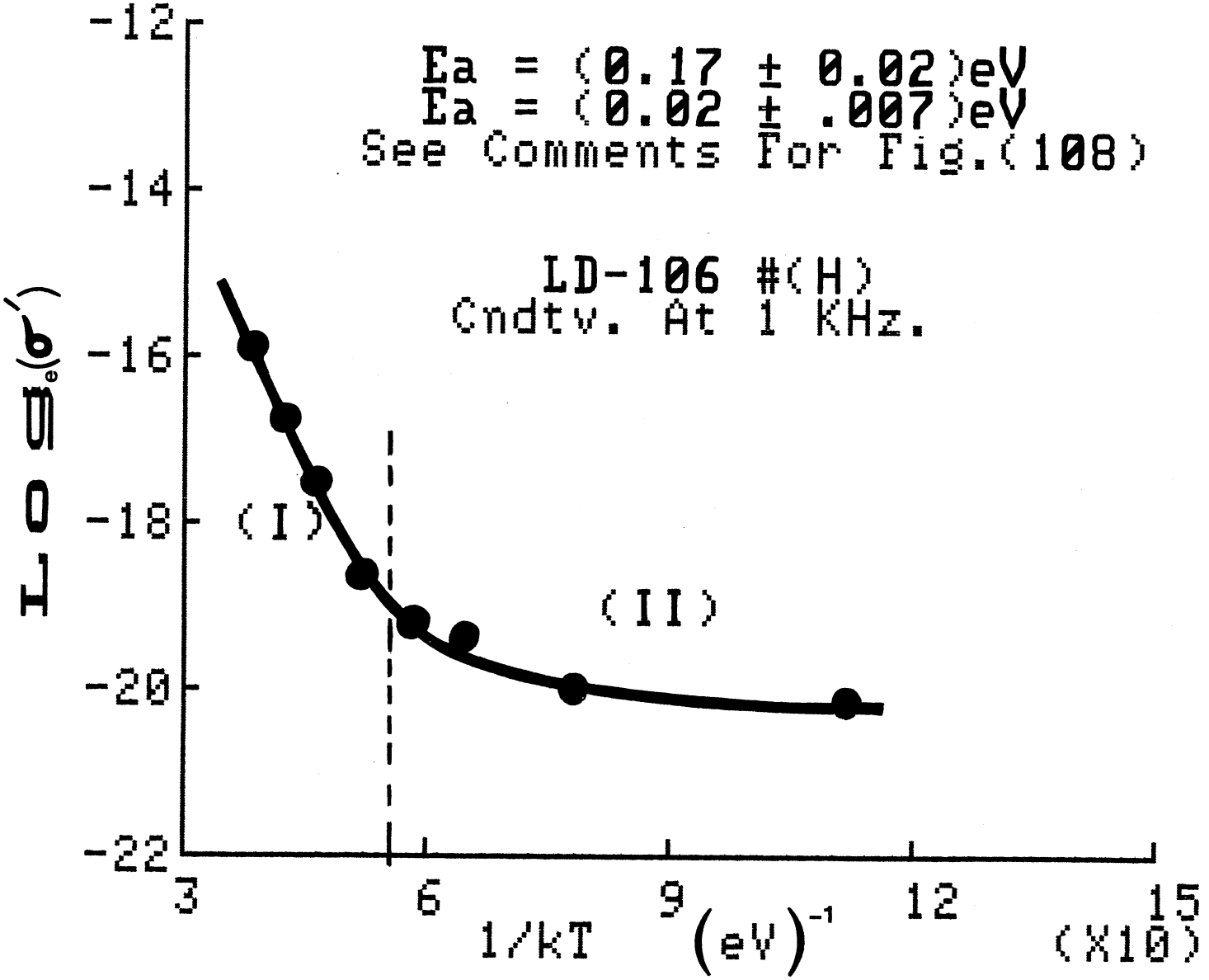
Ea = (0.17 ± 0.02)eV
Ea = (0.02 ± .007)eV
See Comments For Fig.(108)
LD-106 #(H)
Cndtv. At 1 KHz.
Log σ'e
-12
-14
-16
-18
-20
-22
(I)
(II)
3
6
9
12
15
1/kT (eV)-1
(X10)

Fig.(109)

D) The Effect of The D.C. Electric Field Bias on The Conductive and Dielectric Properties

This section examines the behaviour of polymers when subjected to a D.C. electric field bias under room conditions described in Sec.(3.2A). The A.C. quantities were observed at 1 KHz. except for LD-105 which was observed at 3.5 KHz. due to technical reasons. In some cases the DC. electric field had little or no effect on the A.C. characteristics. In most cases the A.C. quantities showed a rather mild dependence, the loss factor displaying the greatest relative increase with the D.C. electric field bias, followed by K which decreased slowly with the bias, and finally by the AC. conductivity which either increased or decreased slightly depending on the way in which DM and K varied.

The DC conductivity displayed the anticipated exponential dependence: $\sigma = \sigma_o [\exp(\eta_+) - 1]/\eta_+$, originally discovered by Rosen & Pohl (1) through an empirical fit of their data. Our results showed perfect agreement with this formula which, can also be used to infer the average characteristic length of the eka-conjugation region (identifiable as the average molecular length) as follows: The equation:

$$Q = [\exp(x) - 1]/x \qquad 3.2.2$$

where $Q = \sigma/\sigma_o$ and x is given by $eELo/2k_BT \equiv A.E$, (E being the D.C. electric field bias, "e" is the absolute elctronic charge, and Lo is the average molecular length), is plotted as a function of E. The value of E for which $Q = \exp(1) - 1 = 1.718$

corresponds to E = 1/A. So by locating this value of E on the graph, Lo can be calculated from:

$$A = eLo/2k_BT \qquad 3.2.3$$

This, however, is a rather simplified way for determining the length Lo since it is usually difficult to obtain an accurate fit for a curved line especially when the data contains appreciable error. To enhance the reliability of our results we developed a modified version of the above in which an iteration procedure was followed. This yielded highly improved and more self-consistent results.

Our method makes use of the fact that according to (3.2.2)

$$\log_e(Q.E + 1/A) = A.E - \log_e(A) \qquad 3.2.4$$

So by plotting the left-hand side of eq.(3.2.4) versus E, the value of A can be read off the graph either from the slope or from the intercept (as $-\log_e(A)$). There is one catch, however to this scheme: the value of A is not known to begin with, so the left-hand side of eq.(3.2.4) cannot be used directly. This problem immediately suggests a solution by an iteration precedure, whereby an initial value of "A" is inserted in the L.H.S of (3.2.4), (most likely the "rough" value calculated from the Rosen-Pohl procedure). As it turned out, only two to three iterations at most were necessary to obtain good convergence. The value of A shown in Figs.(110) - (142) is the average value between the one obtained from the slope, and the value obtained from "$-\log_e(A)$" in the last iteration.

The molecular lengths based on these values of A are given in table (3.42b).

TABLE (3.32)

D.C. ELECTRIC FIELD EFFECT ON LD-105

	<=== DC ELECTRIC FIELD BIAS ===> (1000 V/cm)							
Sample	.050	0.57	1.12	2.24	2.94	3.83	4.57	5.58
G : σ	1.09	1.19	1.20	1.34	1.45	1.64	2.03	3.30
σ'	1.09	1.31	1.39	1.52	1.62	1.80	2.11	--
K	23.9	15.2	14.0	12.0	11.2	9.41	10.8	--
DM	2.35	4.42	5.09	6.50	7.45	9.82	10.0	--

cont'd

TABLE (3.32) Cont'd

	<=== DC ELECTRIC FIELD BIAS ===> (1000 V/cm)							
	.114	0.61	1.19	2.38	3.13	4.04	4.85	6.50
H : σ	0.93	1.11	1.18	1.25	1.39	1.63	1.96	2.34
σ'	1.03	1.22	1.30	1.40	1.55	--	--	--
K	23.7	16.4	15.7	16.4	14.2	--	--	--
DM	2.25	3.82	4.23	4.47	5.61	--	--	--

Observed For Two Samples G And H At 3.5 KHz. All Values Of σ Are (X1E-7), Those Of σ' Are (X1E-5).

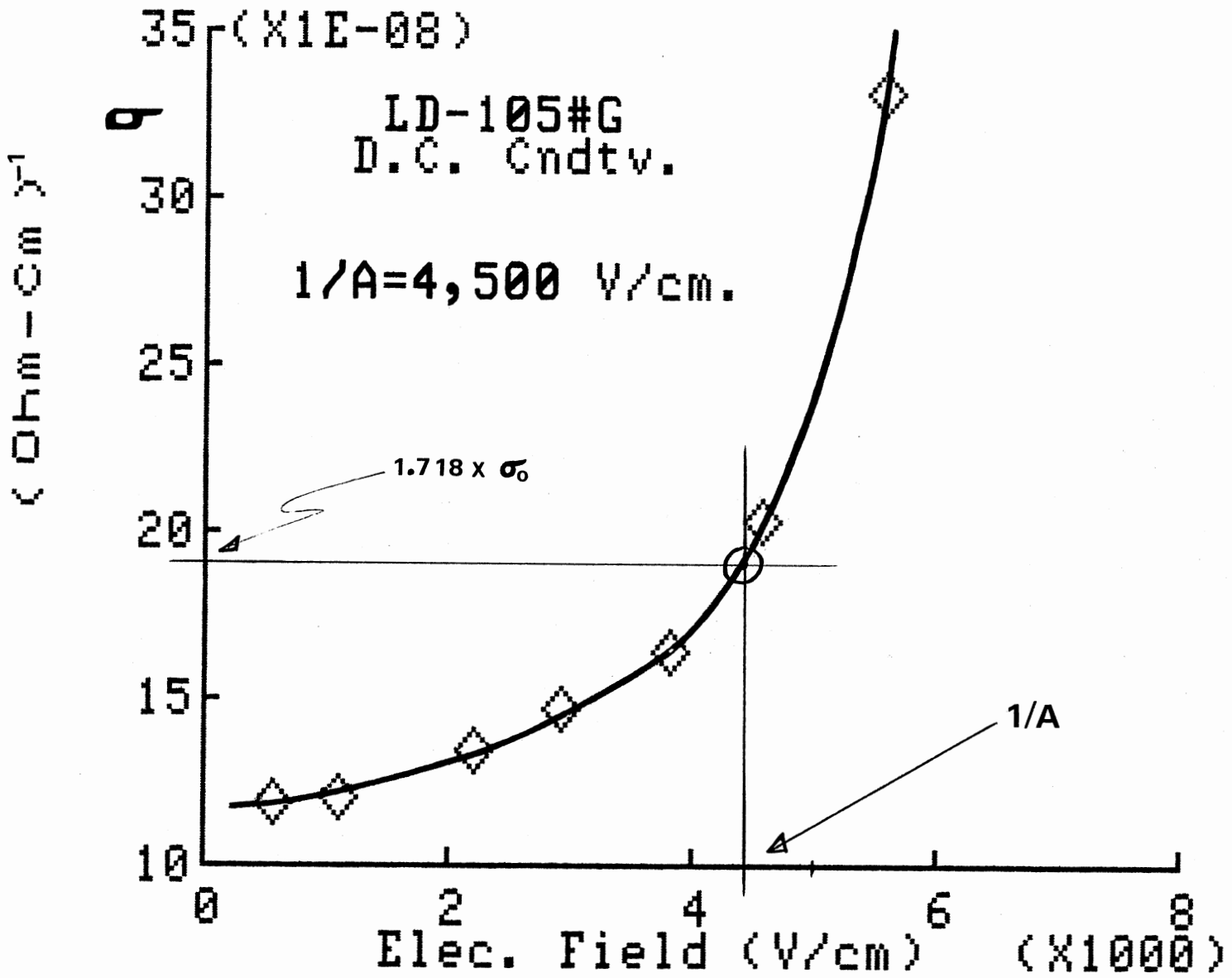
35
(X1E-08)
σ
LD-105#G
D.C. Cndtv.
1/A=4,500 V/cm.
30
25
20
15
10
1.718 x σo
1/A
0
2
4
6
8
Elec. Field (V/cm)
(X1000)
(Ohm-Cm)-1

Fig.(110)

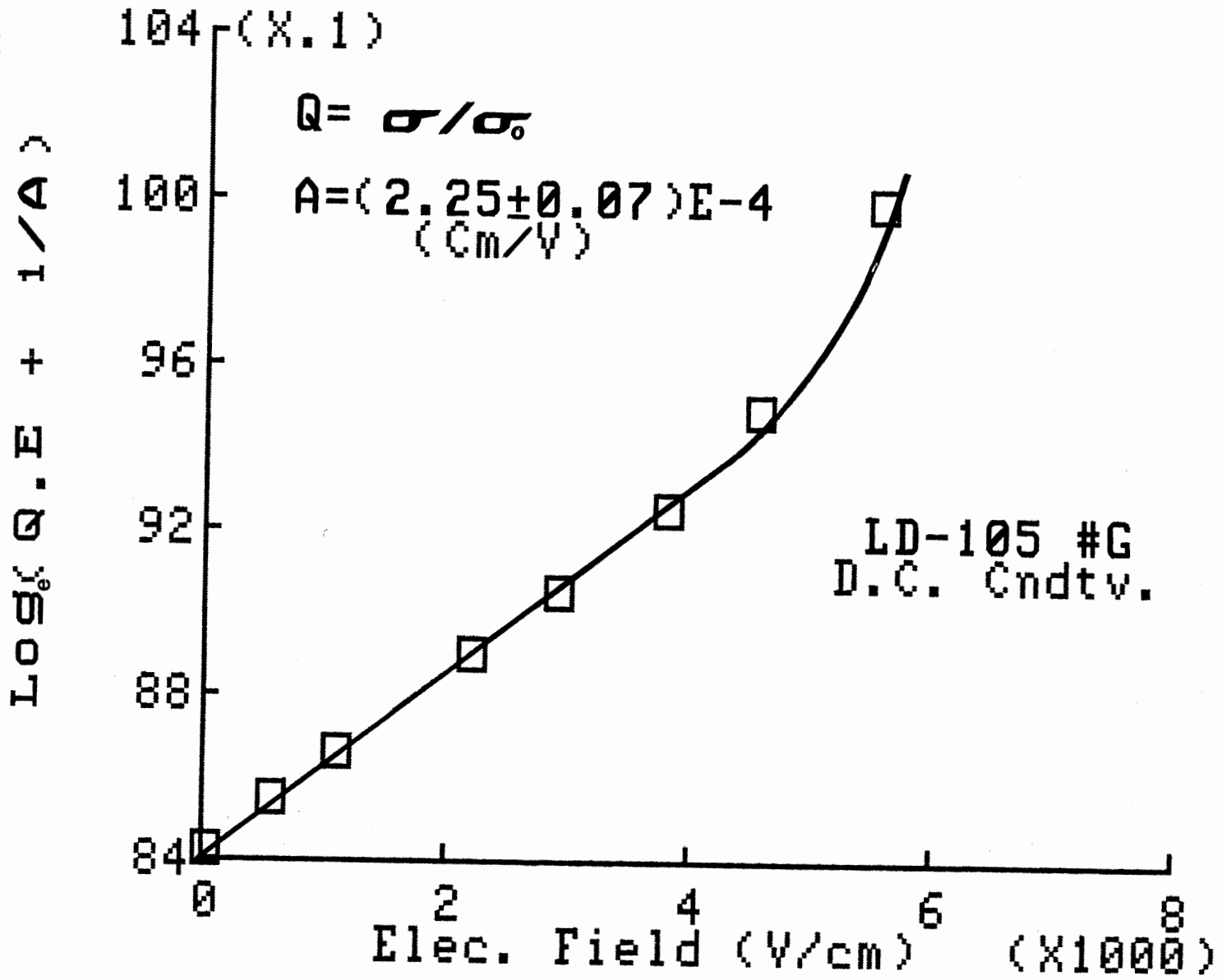
104
100
96
92
88
84
(X.1)
Q= σ/σ₀
A=(2.25±0.07)E-4
(Cm/V)
LD-105 #G
D.C. Cndtv.
Log(Q.E + 1/A)
0
2
4
6
8
Elec. Field (V/cm)
(X1000)

Fig.(111)

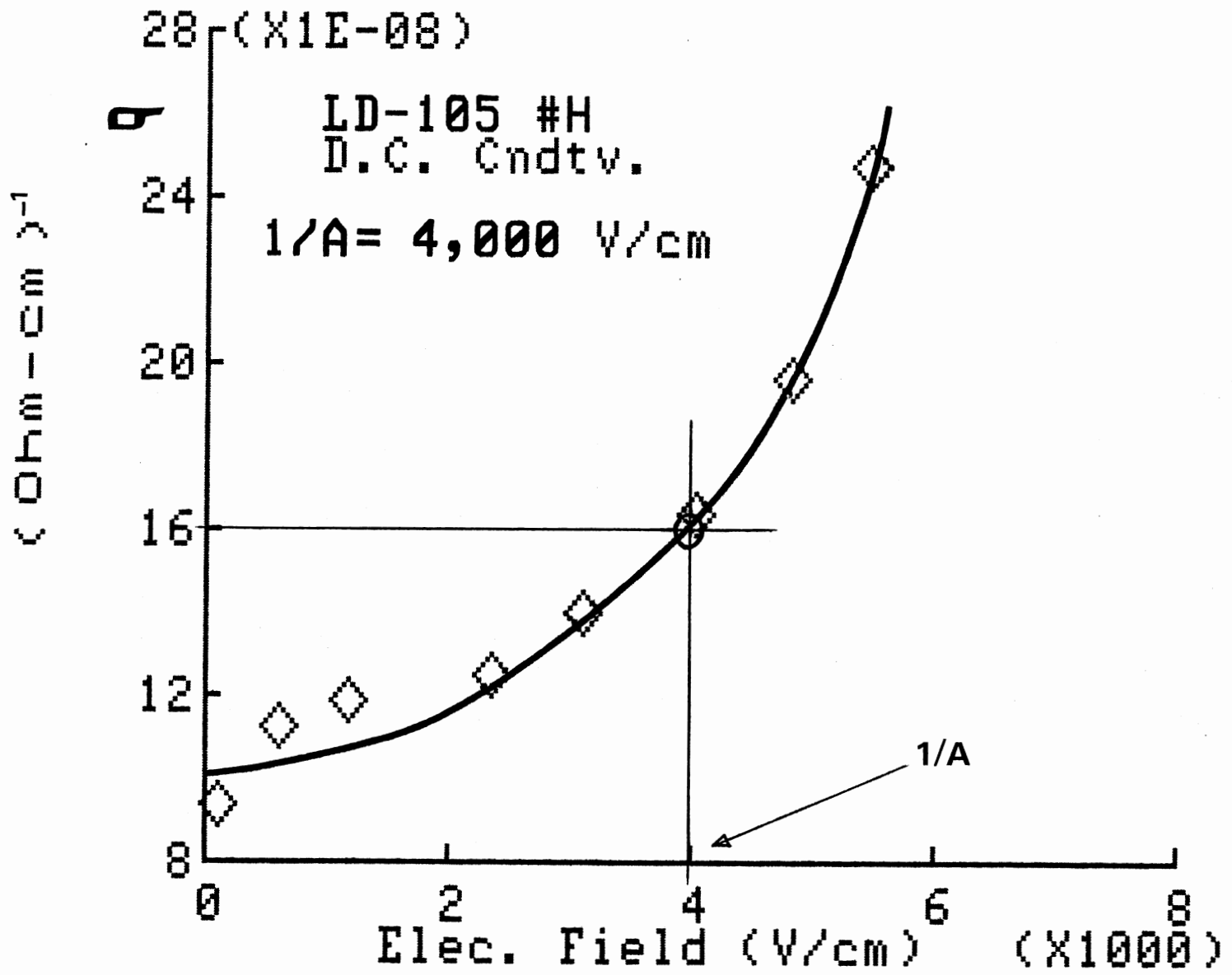
28
(X1E-08)
σ
LD-105 #H
D.C. Cndtv.
1/A= 4,000 V/cm
24
20
16
12
8
(Ohm-cm)⁻¹
1/A
0
2
4
6
8
Elec. Field (V/cm)
(X1000)

Fig.(112)

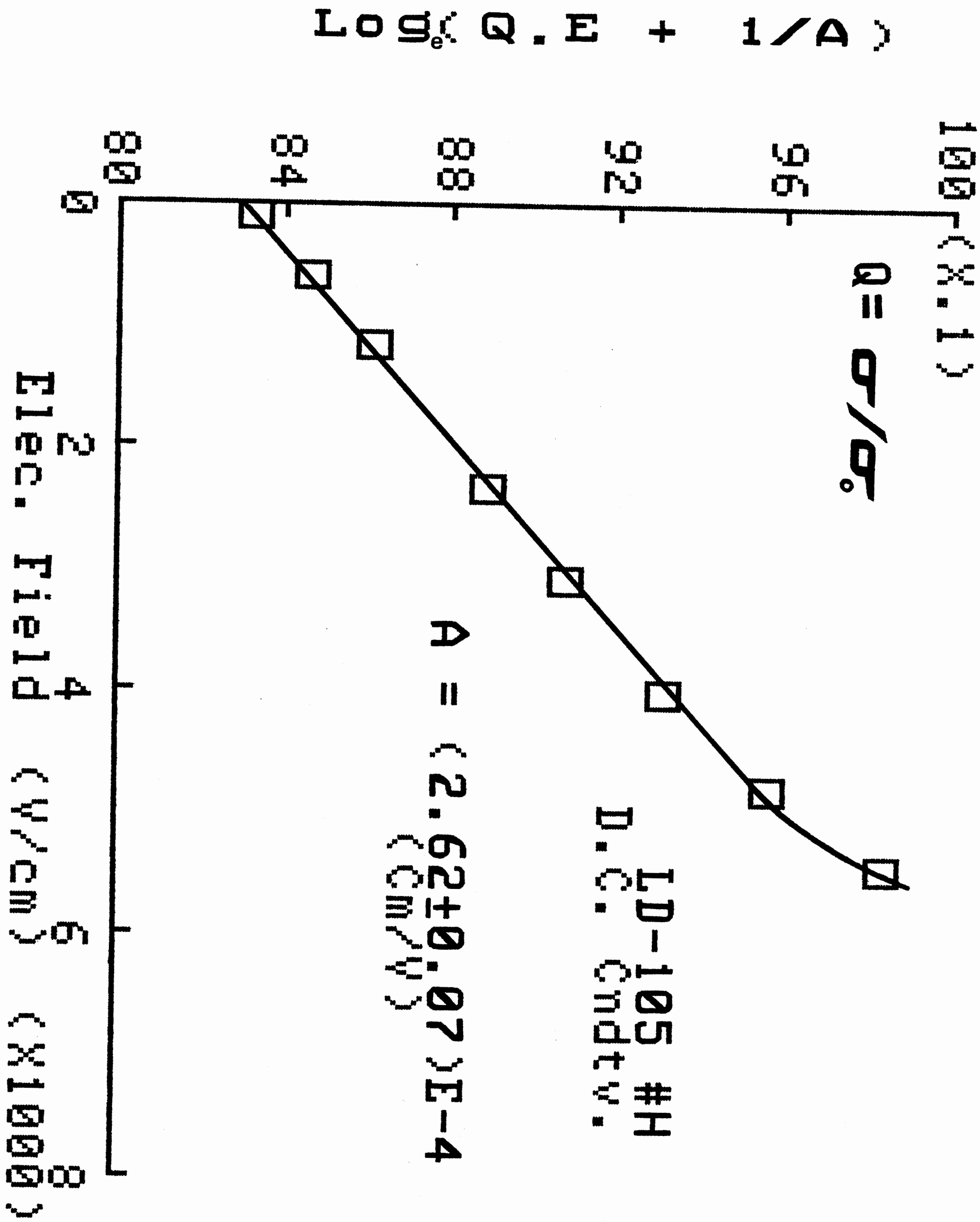
Log_e(Q.E + 1/A)
(X.1)
100
96
92
88
84
80
0
2
4
6
8
Q= σ/σ₀
LD-105 #H
D.C. Cndtv.
A = (2.62±0.07)E-4
(Cm/V)
Elec. Field (V/Cm) (X1000)

Fig.(113)

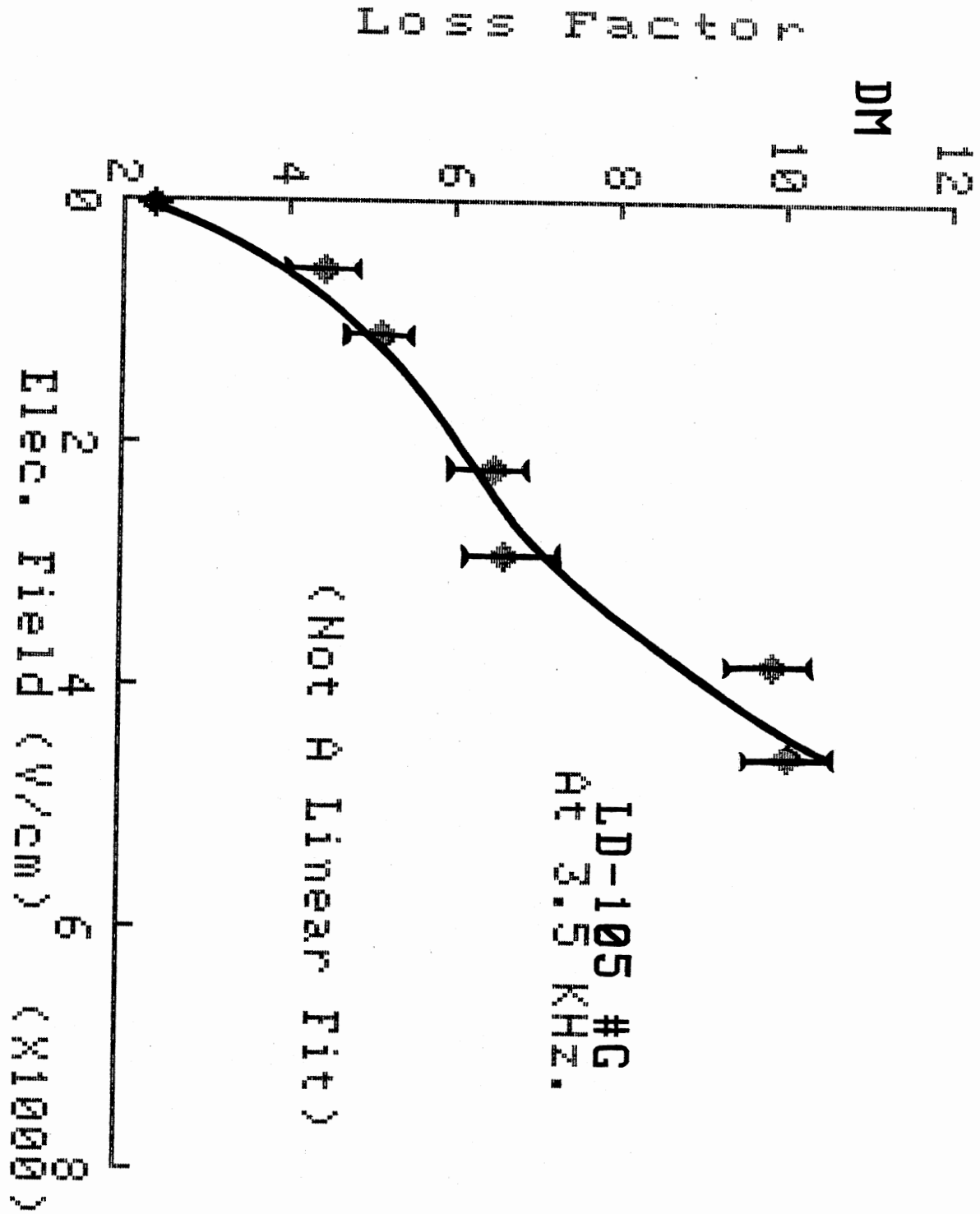
Loss Factor
DM
0
2
4
6
8
10
12
Elec. Field (V/cm) (x1000)
0
2
4
6
8
LD-105 #G
At 3.5 KHz.
(Not A Linear Fit)

Fig. (114)

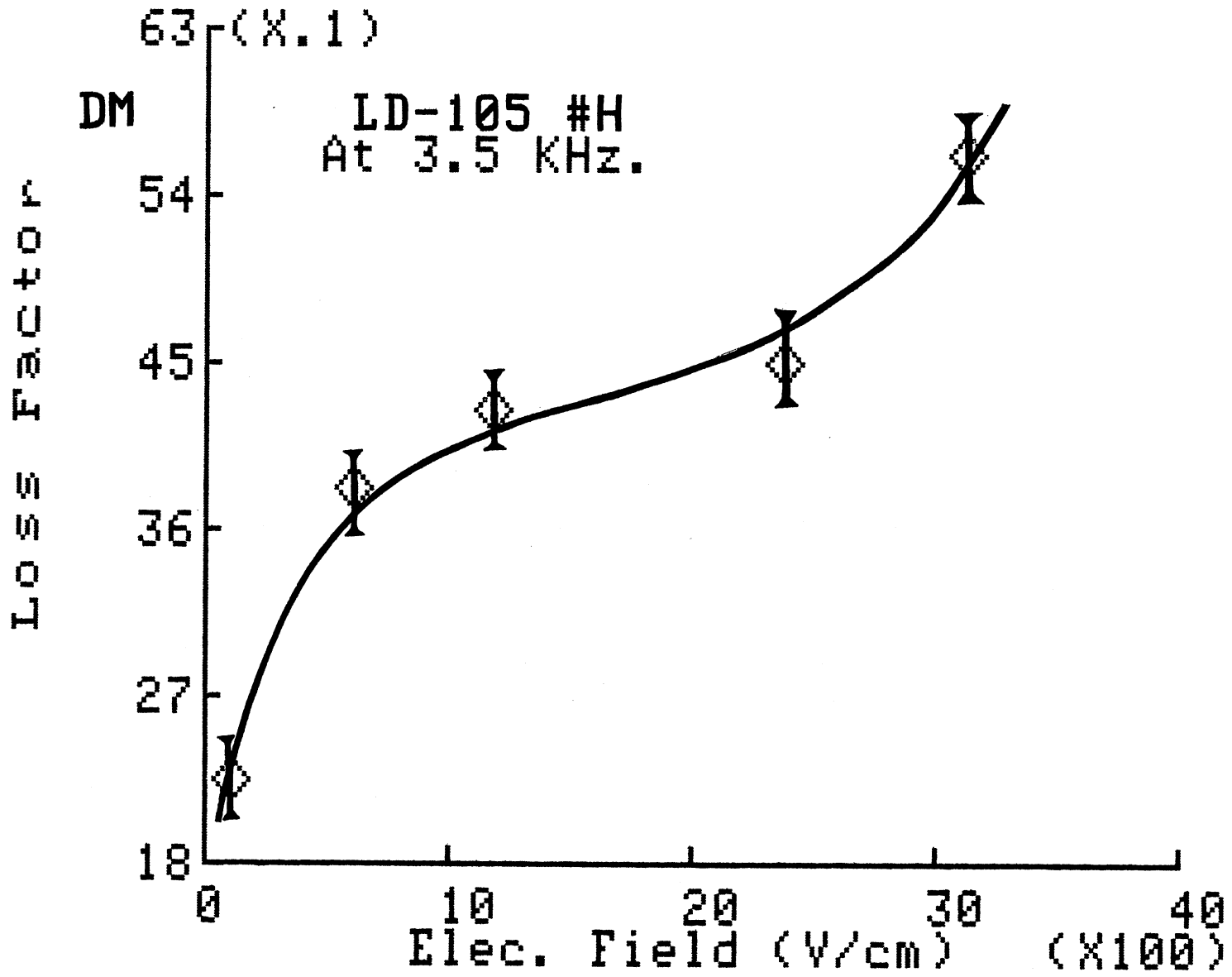
63 (X.1)
DM
LD-105 #H
At 3.5 KHz.
54
45
36
27
18
Loss Factor
0
10
20
30
40
Elec. Field (V/cm) (X100)

Fig.(115)

TABLE (3.33)

D.C. ELECTRIC FIELD EFFECT ON LD-104

	<=== DC ELECTRIC FIELD BIAS ===> (1000 V/cm)							
Sample	.150	0.88	1.74	3.70	5.54	7.33	9.16	12.7
G : σ	1.74	3.42	4.11	5.25	6.65	8.50	10.3	16.5
σ'	8.46	8.74	9.40	11.4	14.7	16.2	--	--
K	23.4	23.3	22.7	21.8	21.7	21.2	--	--
DM	0.65	0.67	0.75	0.94	1.21	1.37	--	--

cont'd

TABLE (3.33) Cont'd

	<=== DC ELECTRIC FIELD BIAS ===> (1000 V/cm)							
	.158	0.95	1.89	4.00	5.97	7.90	9.84	13.6
H : σ	1.50	3.00	3.40	4.84	5.90	8.90	10.5	17.0
σ'	7.64	7.75	7.77	8.12	9.11	9.80	--	--
K	19.0	18.4	18.1	17.9	18.7	18.9	--	--
DM	0.72	0.76	0.77	0.82	0.87	0.93	--	--

Observed For Two Samples G and H At 1 KHz. All Values Of σ Are (X1E-9), Those Of σ' Are (X1E-7).

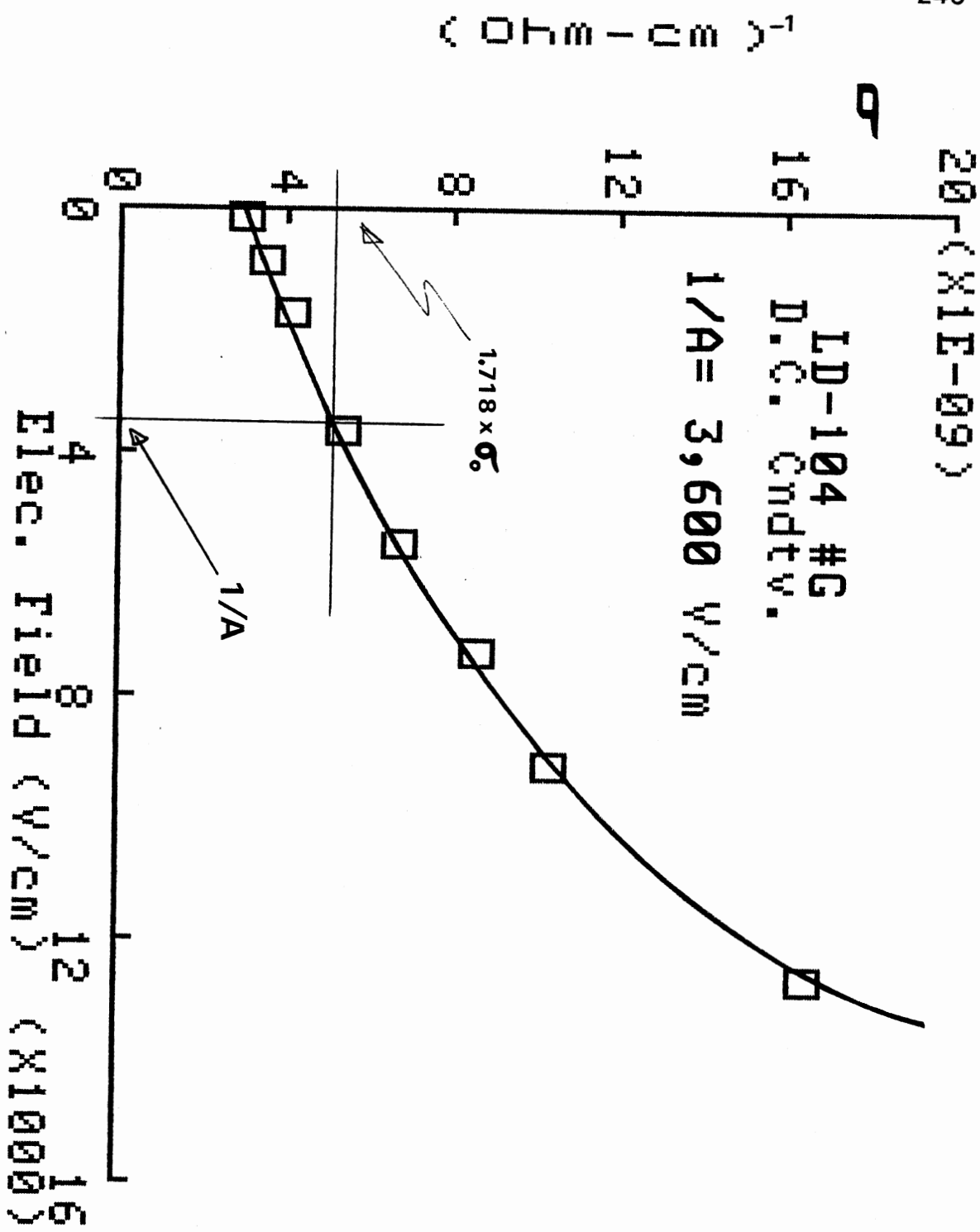
(Ohm-cm)$^{-1}$
9
LD-104 #G
D.C. Cndtv.
1/A= 3,600 Ω/cm
1.718 x 9°
1/A
Elec. Field (V/cm) (X1000)
(X1E-09)
0
4
8
12
16
20

Fig.(116)

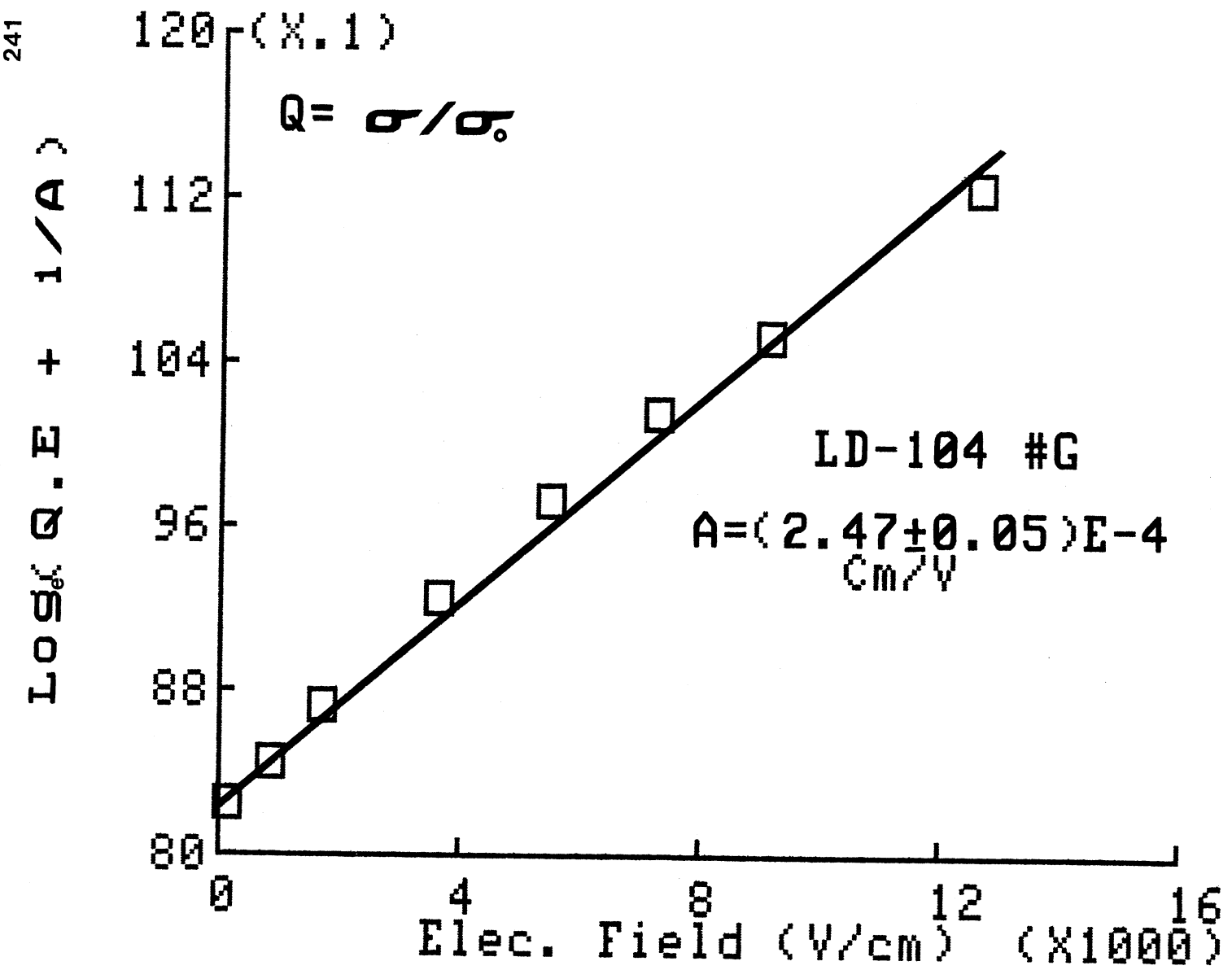
120
(X.1)
Q= σ/σ₀
112
104
96
88
80
Log(Q.E + 1/A)
LD-104 #G
A=(2.47±0.05)E-4
Cm/V
0
4
8
12
16
Elec. Field (V/cm) (X1000)

Fig. (112)

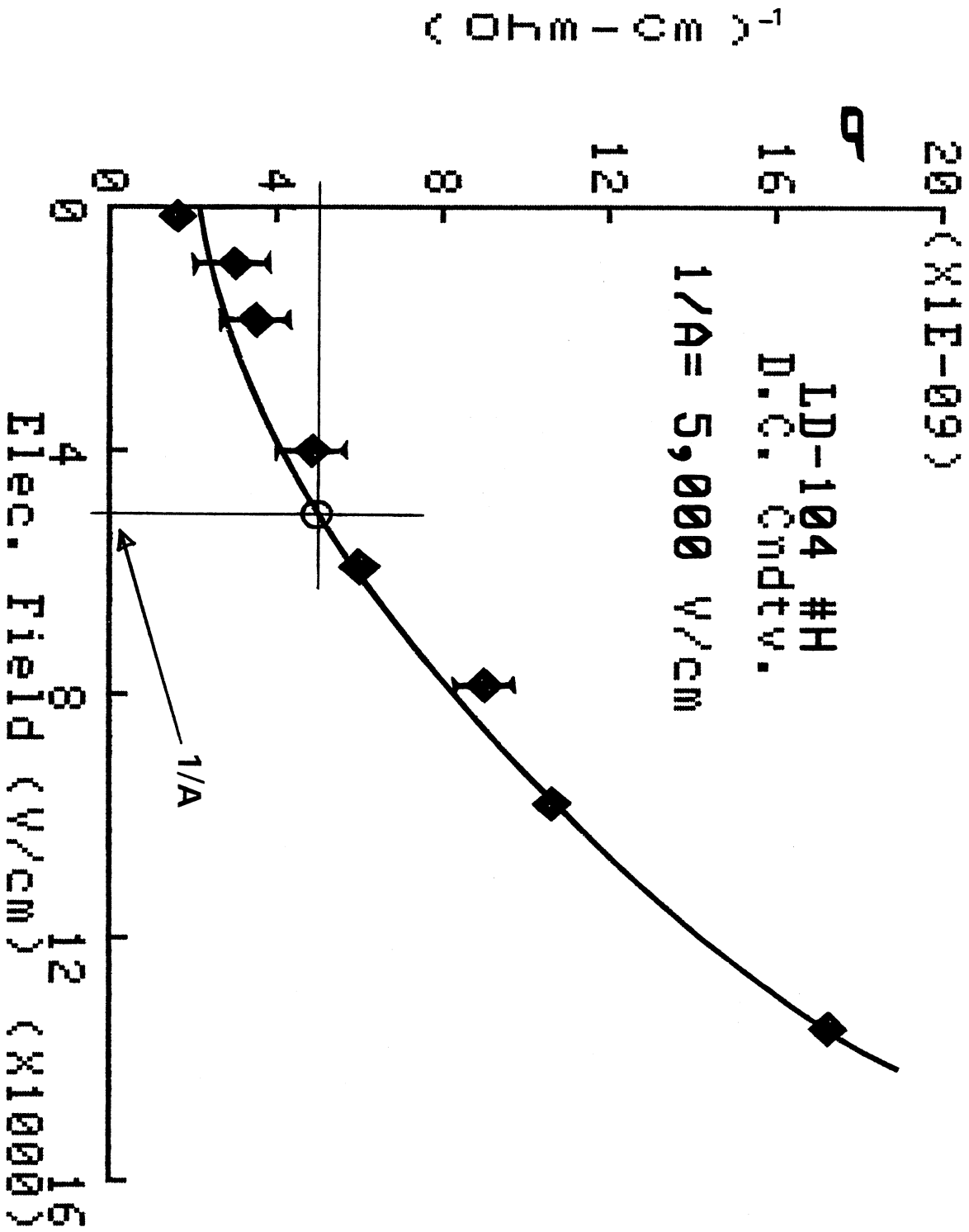
(Ohm-Cm)$^{-1}$
q
(X1E-06)
LD-104 #H
D.C. Cndtv.
1/A= 5,000 V/cm
1/A
Elec. Field (V/cm) (X1000)

Fig.(118)

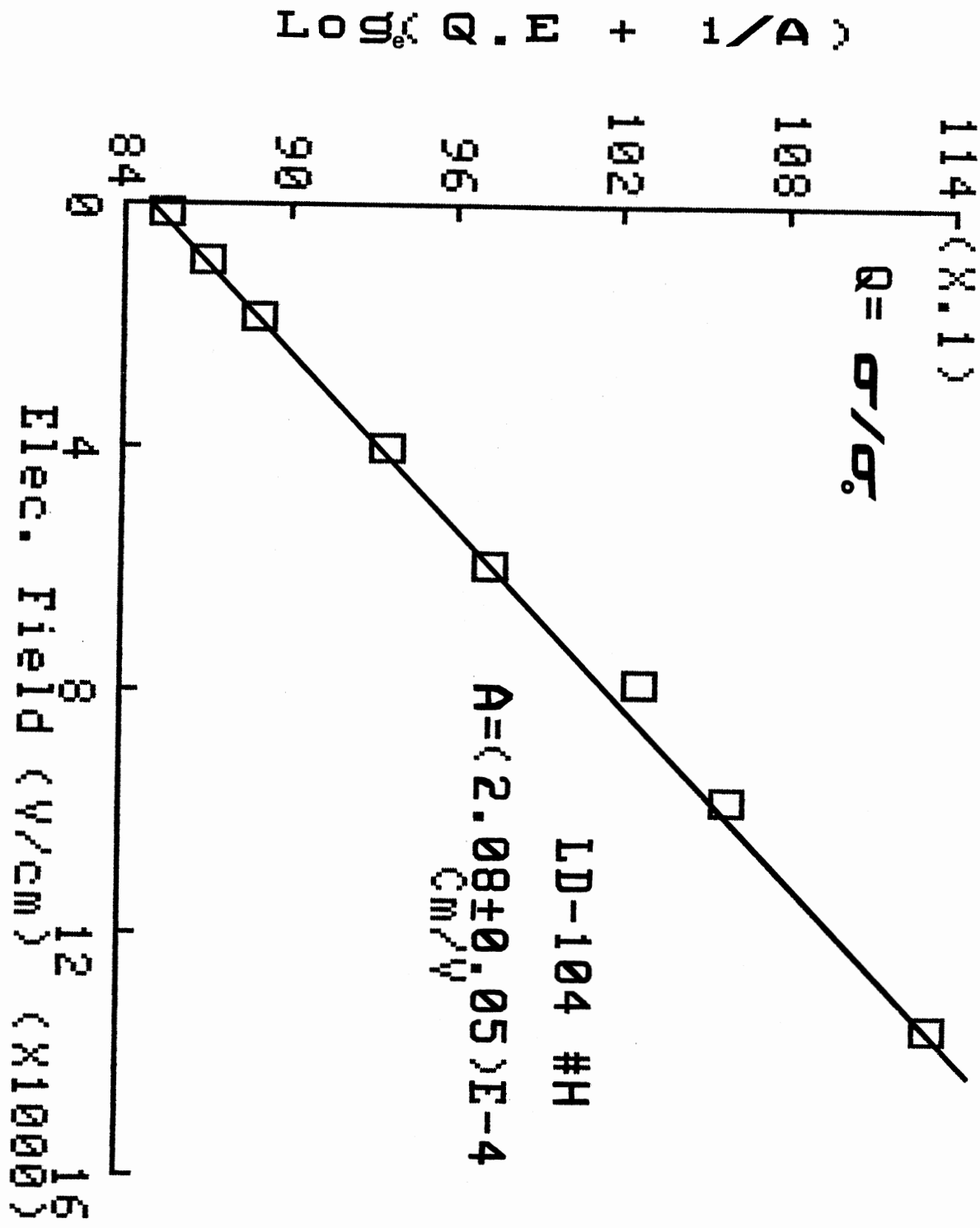
Log$_e$(Q.E + 1/A)
84
96
108
114
(X.1)
Q = Q/Q$_o$
0
4
8
12
16
Elec. Field (V/cm) (X1000)
LD-104 #H
A=(2.08±0.05)E-4
(cm/μJ)

Fig.(119)

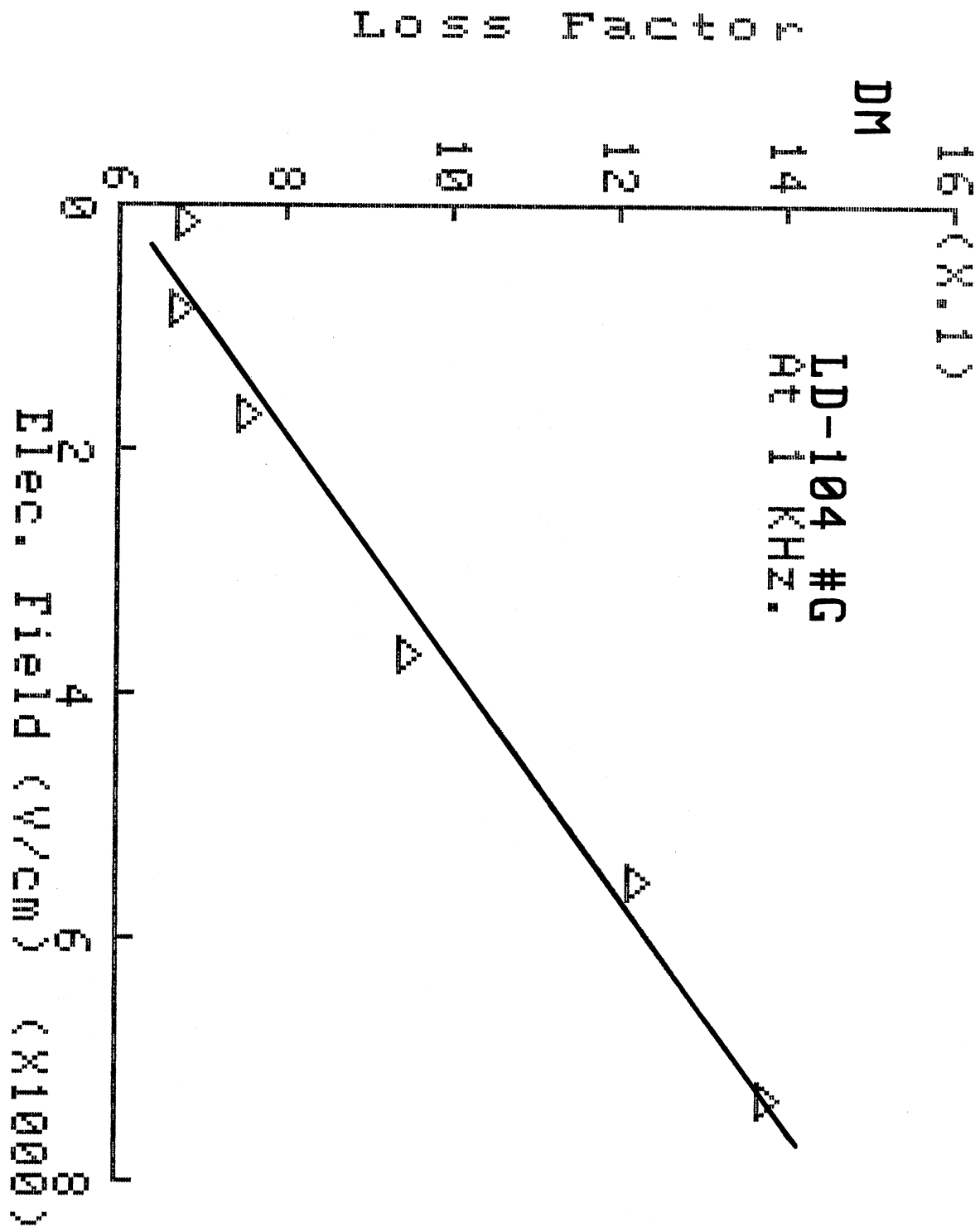
Loss Factor
DM
LD-104 #G
At 1 KHz.
Elec. Field (V/cm) (x1000)
0
2
4
6
8
0
5
10
15
20
25
(x10)

Fig.(120)

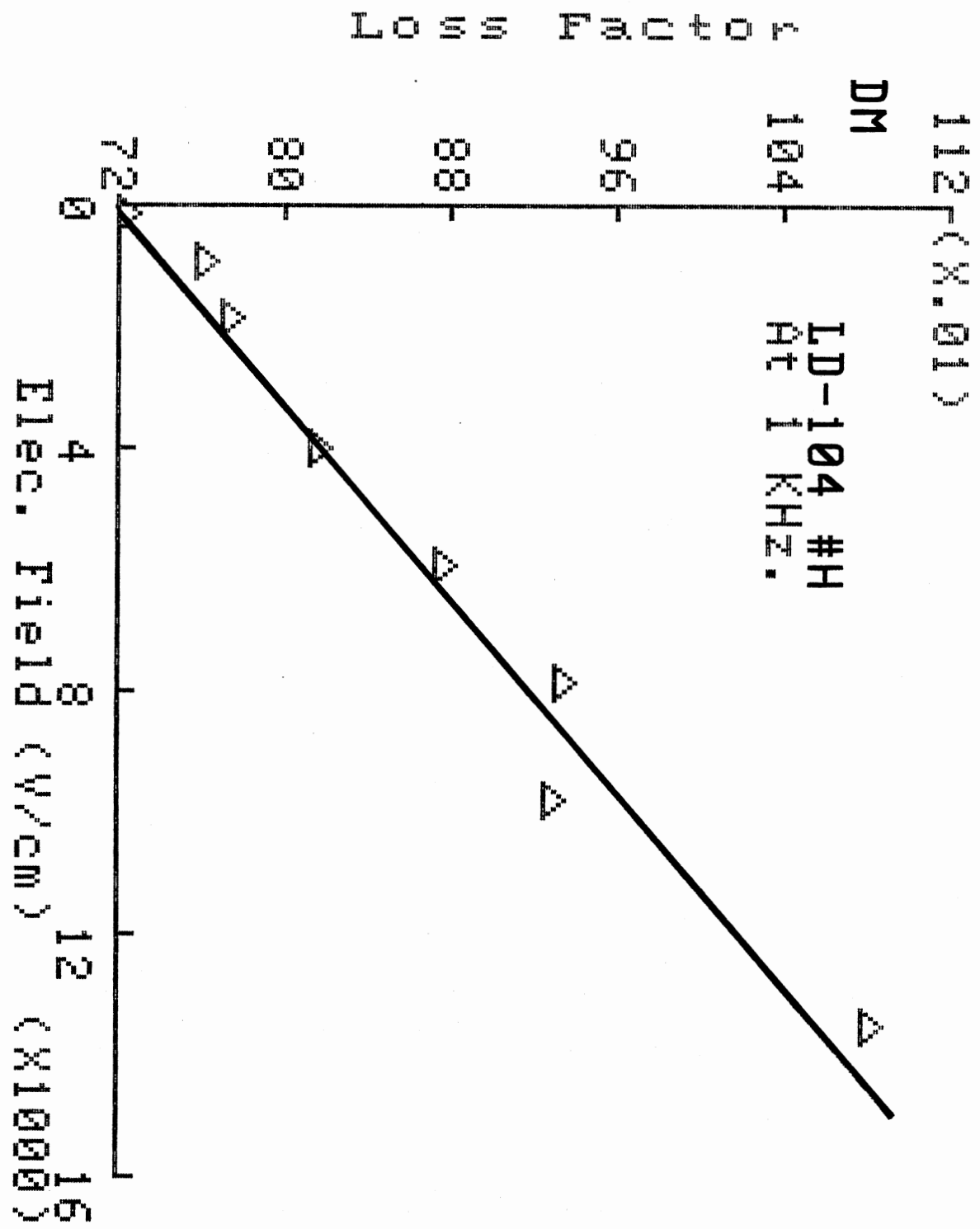
Loss Factor
DM
LD-104 #H
at 1 kHz.
tg δ (x.01)
0
4
8
12
16
Elec. Field (V/cm) (x1000)

Fig.(121)

TABLE (3.34)

D.C. ELECTRIC FIELD EFFECT ON LD-97

	<=== DC ELECTRIC FIELD BIAS ===> (1000 V/cm)							
Sample	.116	0.82	1.72	3.46	5.07	6.77	8.35	11.5
S : σ	3.05	7.12	8.68	13.0	16.1	17.0	20.9	27.6
σ'	1.19	1.38	1.47	1.83	2.05	2.60	--	--
K	32.7	29.3	27.3	26.7	26.3	27.3	--	--
DM	0.65	0.85	0.97	1.23	1.40	1.72	--	--

cont'd

TABLE (3.34) Cont'd

	<=== DC ELECTRIC FIELD BIAS ===> (1000 V/cm)							
	.114	0.81	1.68	3.49	5.22	6.78	--	11.6
T : σ	3.29	4.64	5.31	7.55	13.6	16.5	--	26.2
σ'	.896	1.01	1.34	1.72	2.09	--	--	--
K	21.4	19.4	18.4	19.6	19.7	--	--	--
DM	0.75	0.94	1.31	1.58	1.91	--	--	--

Observed For Two Samples S And T At 1 KHz. All Values Of σ Are (X1E-9), Those Of σ' Are (X1E-6).

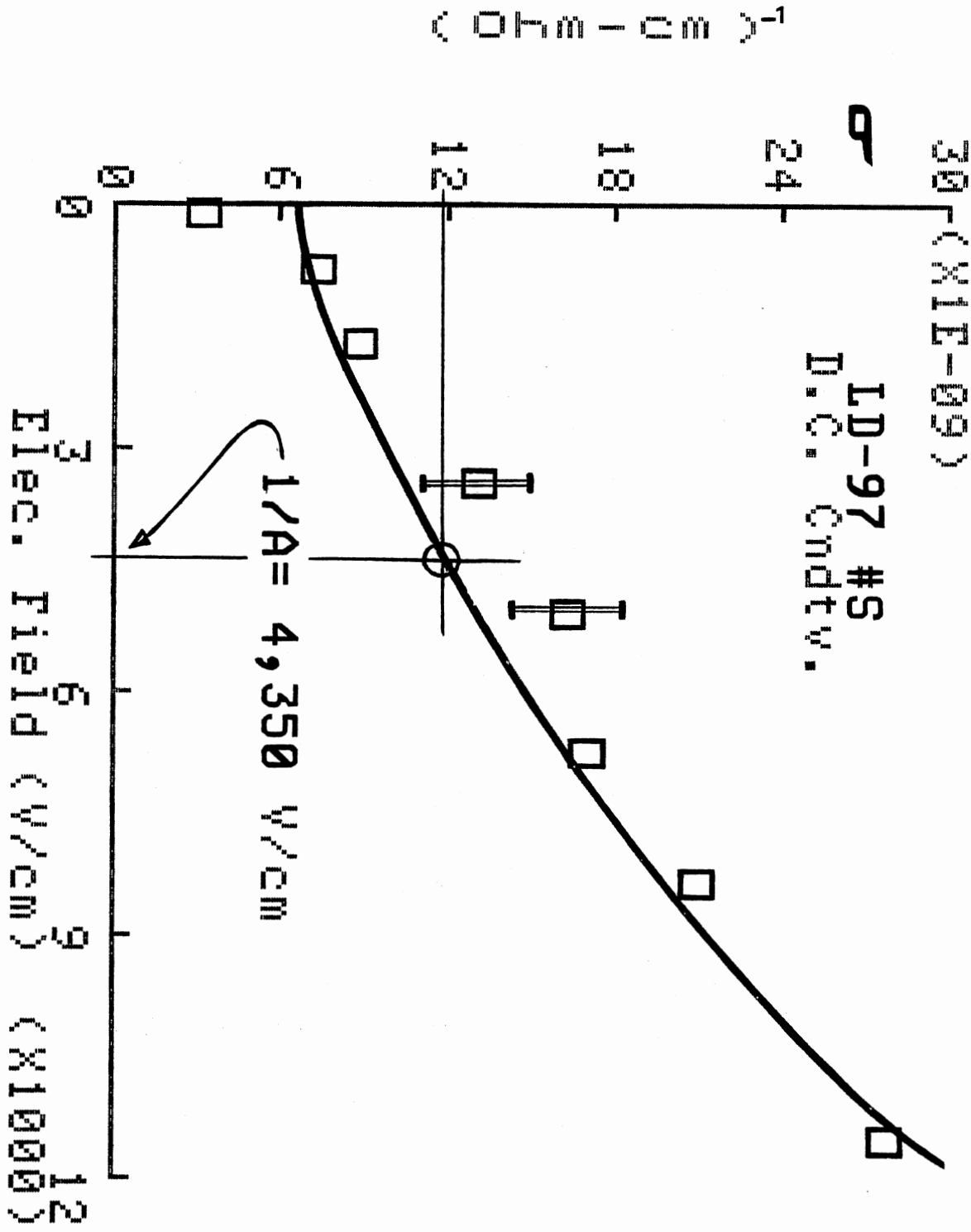
(Ohm-cm)$^{-1}$
9
0
6
12
18
24
30
(60-11-86)
(X1E-09)
LD-97 #S
D.C. Cndtv.
1/A= 4,350 w/cm
Elec. Field (V/cm)
(X10000)
0
3
6
9
12

Fig.(122)

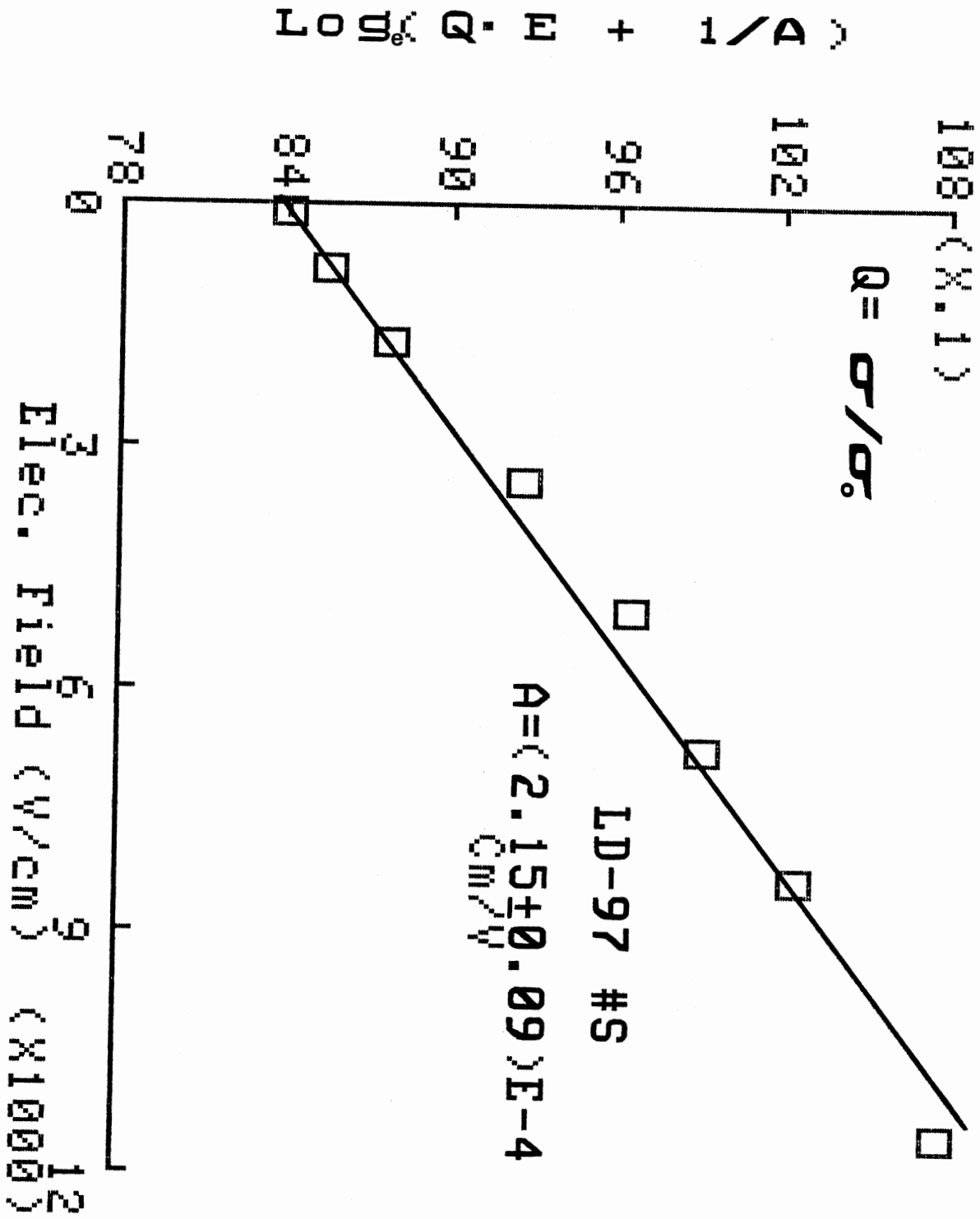
Log$_e$(Q· E + 1/A)
78
84
90
96
102
108
(x 1)
Q = q/q$_o$
0
3
6
9
12
Elec. Field (V/cm) (x10000)
A=(2.15±0.09)E-4
(cm/V)
LD-97 #S

Fig.(123)

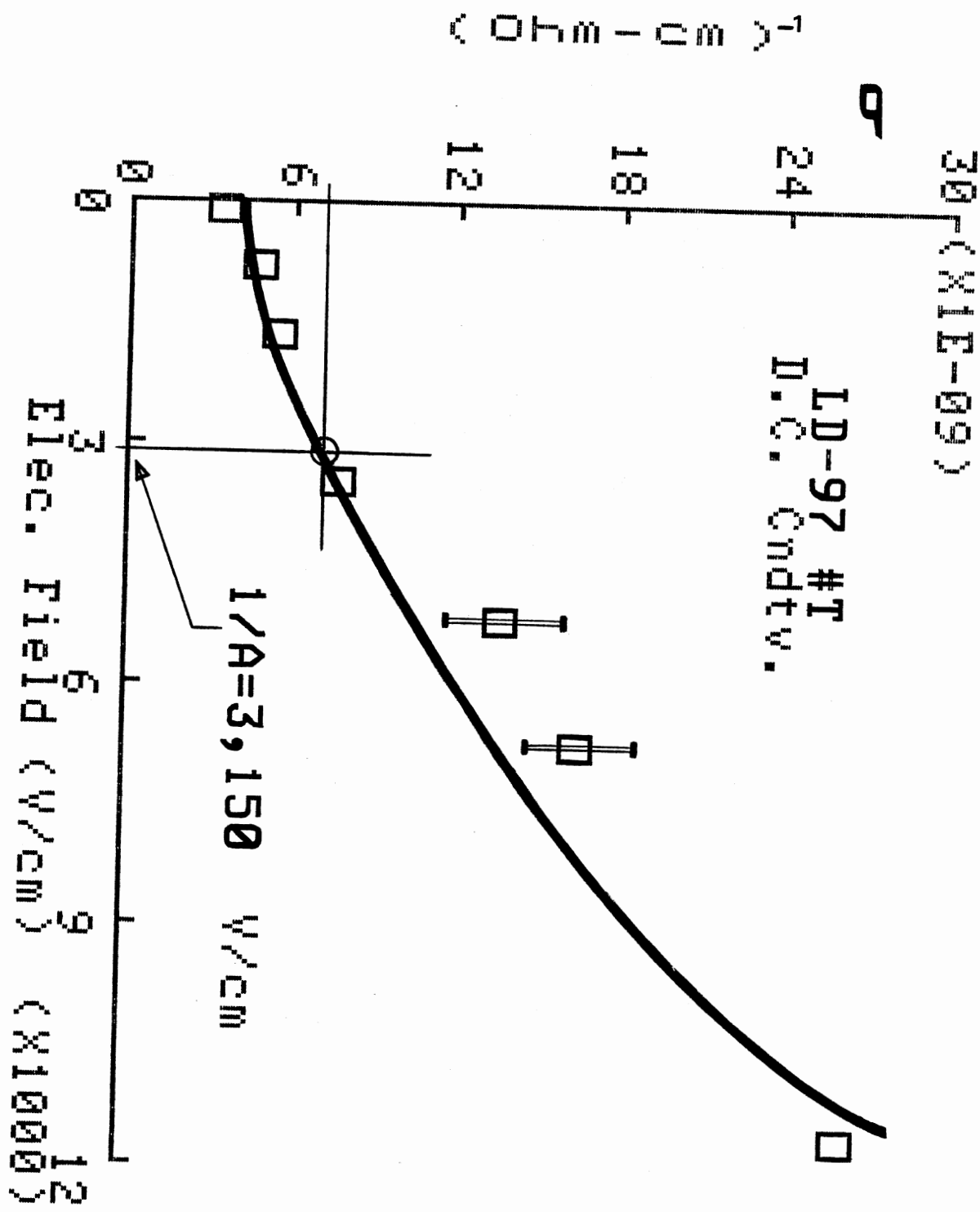
(Ohm-cm)$^{-1}$
9
0
6
12
18
24
30
(X1E-09)
ID-97 #1
D.C. Cndtv.
Elec. Field (V/cm) (X10000)
12
9
6
3
0
1/A=3,150 V/cm

Fig.(124)

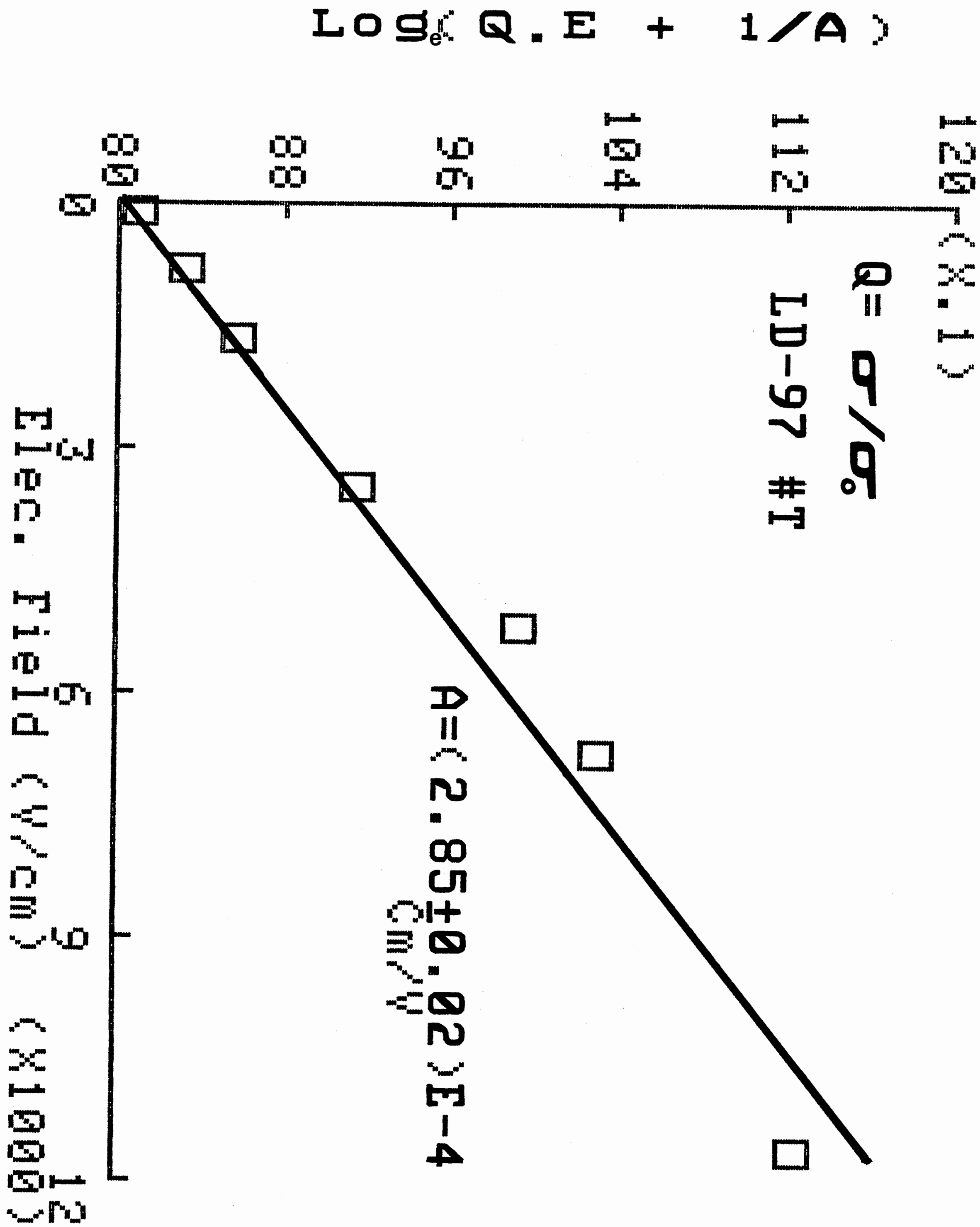
Loge(Q.E + 1/A)
80
88
96
104
112
120
(X.1)
Q= σ/σo
LD-97 #T
A=(2.85±0.02)E-4
(Cm/V)
0
3
6
9
12
Elec. Field (V/Cm) (X1000)

Fig.(125)

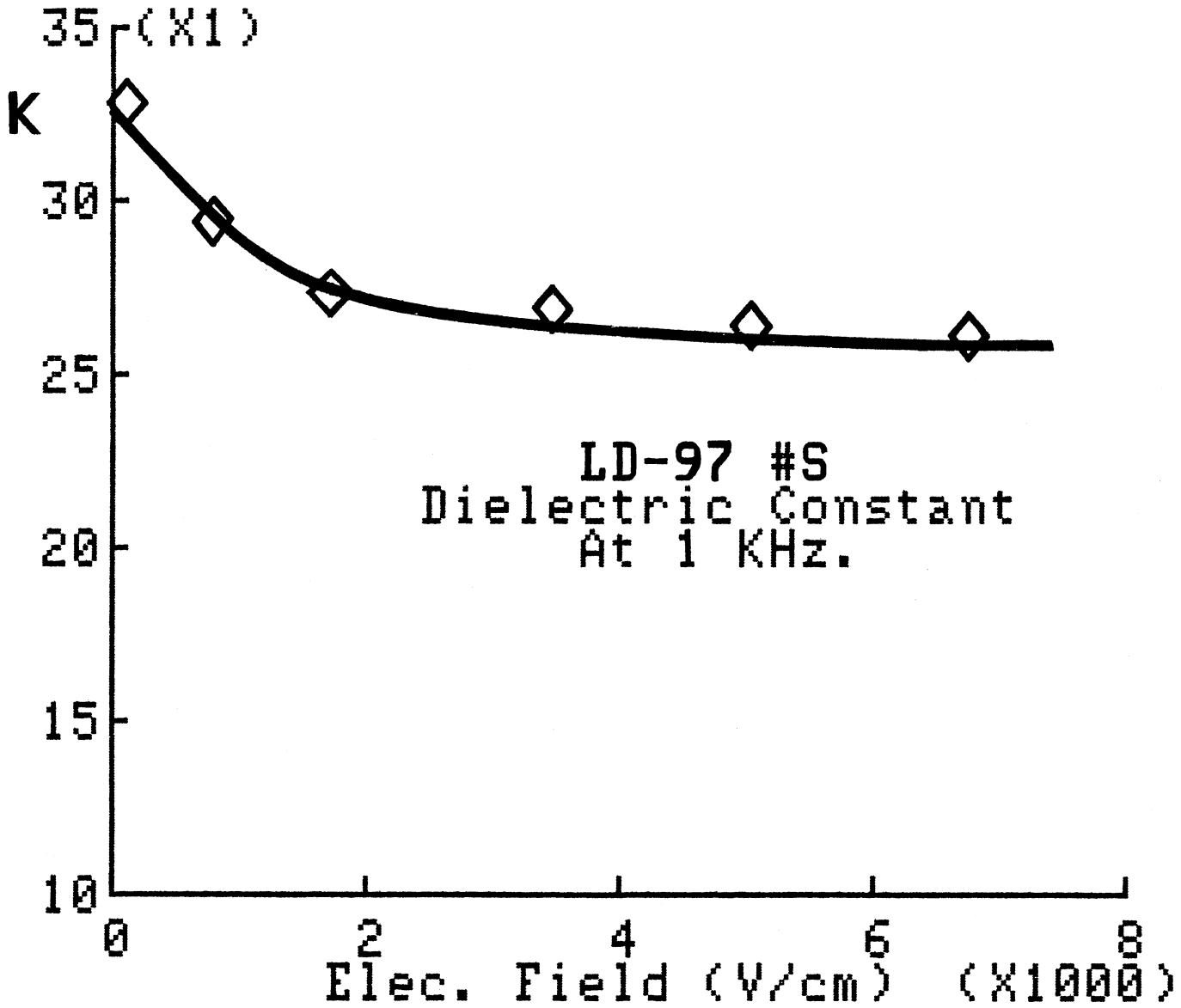
35 (X1)
K
30
25
20
15
10
0
2
4
6
8
Elec. Field (V/cm) (X1000)
LD-97 #S
Dielectric Constant
At 1 KHz.

Fig. (126)

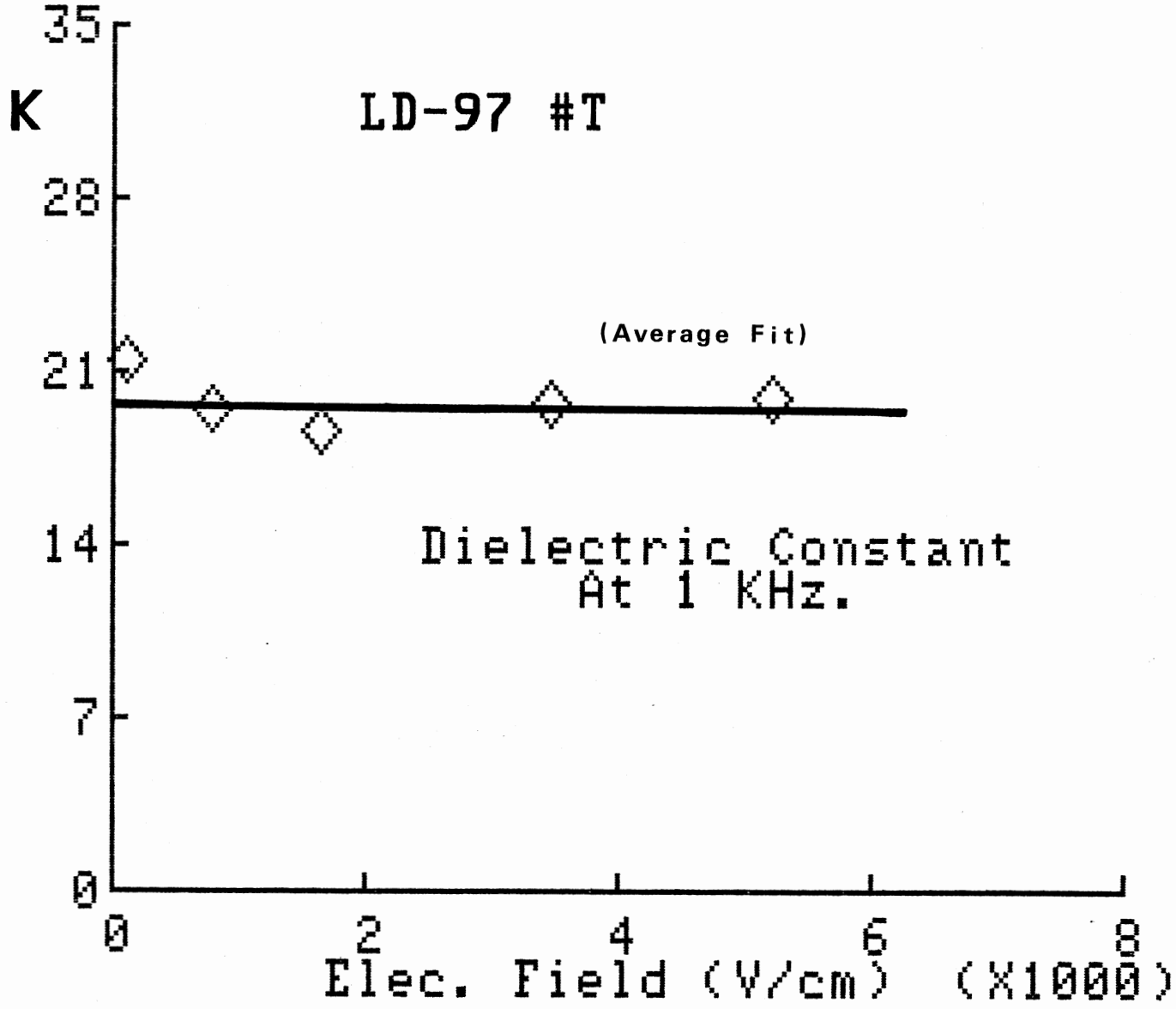
K
LD-97 #T
(Average Fit)
Dielectric Constant
At 1 KHz.
35
28
21
14
7
0
0
2
4
6
8
Elec. Field (V/cm) (X1000)

Fig. (127)

TABLE (3.35)

D.C. ELECTRIC FIELD EFFECT ON LD-95

	<=== DC ELECTRIC FIELD BIAS ===> (1000 V/cm)								
Sample	.101	0.72	1.44	3.08	4.58	6.11	7.63	10.7	13.7
R : σ	3.47	4.21	4.47	4.78	5.13	5.53	5.91	7.17	8.75
σ'	8.94	8.86	8.89	9.29	9.33	9.37	9.40	9.44	--
K	16.3	15.7	15.4	14.9	14.8	14.7	14.6	14.4	--
DM	.987	1.01	1.04	1.12	1.13	1.15	1.16	1.17	--

Observed At 1 KHz. All Values Of σ Are (X1E-9),

Those Of σ' Are (X1E-7).

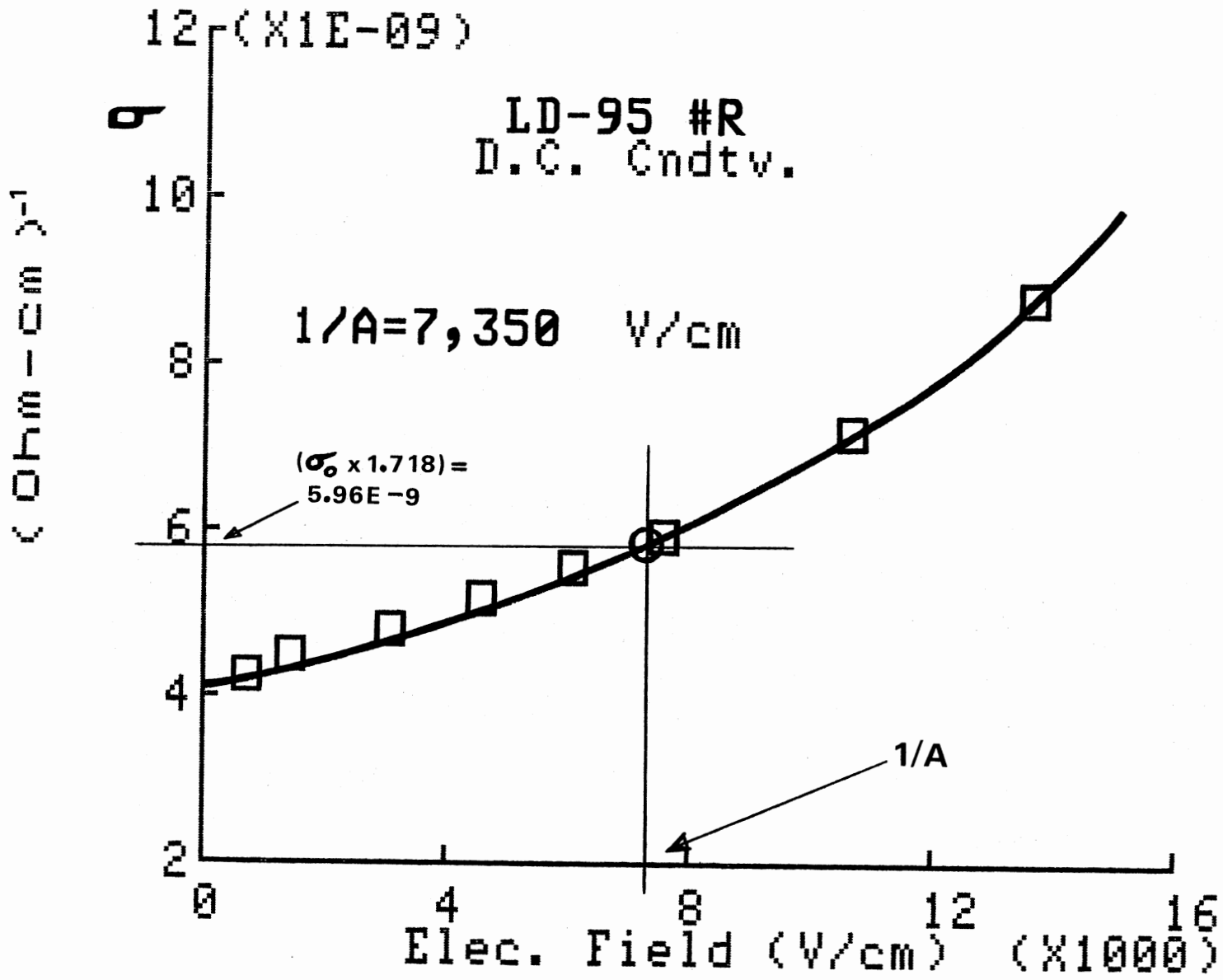
12
(X1E-09)
σ
10
8
6
4
2
(Ohm-cm)$^{-1}$
LD-95 #R
D.C. Cndtv.
1/A=7,350 V/cm
(σ_o x 1.718) =
5.96E-9
1/A
0
4
8
12
16
Elec. Field (V/cm) (X1000)

Fig. (128)

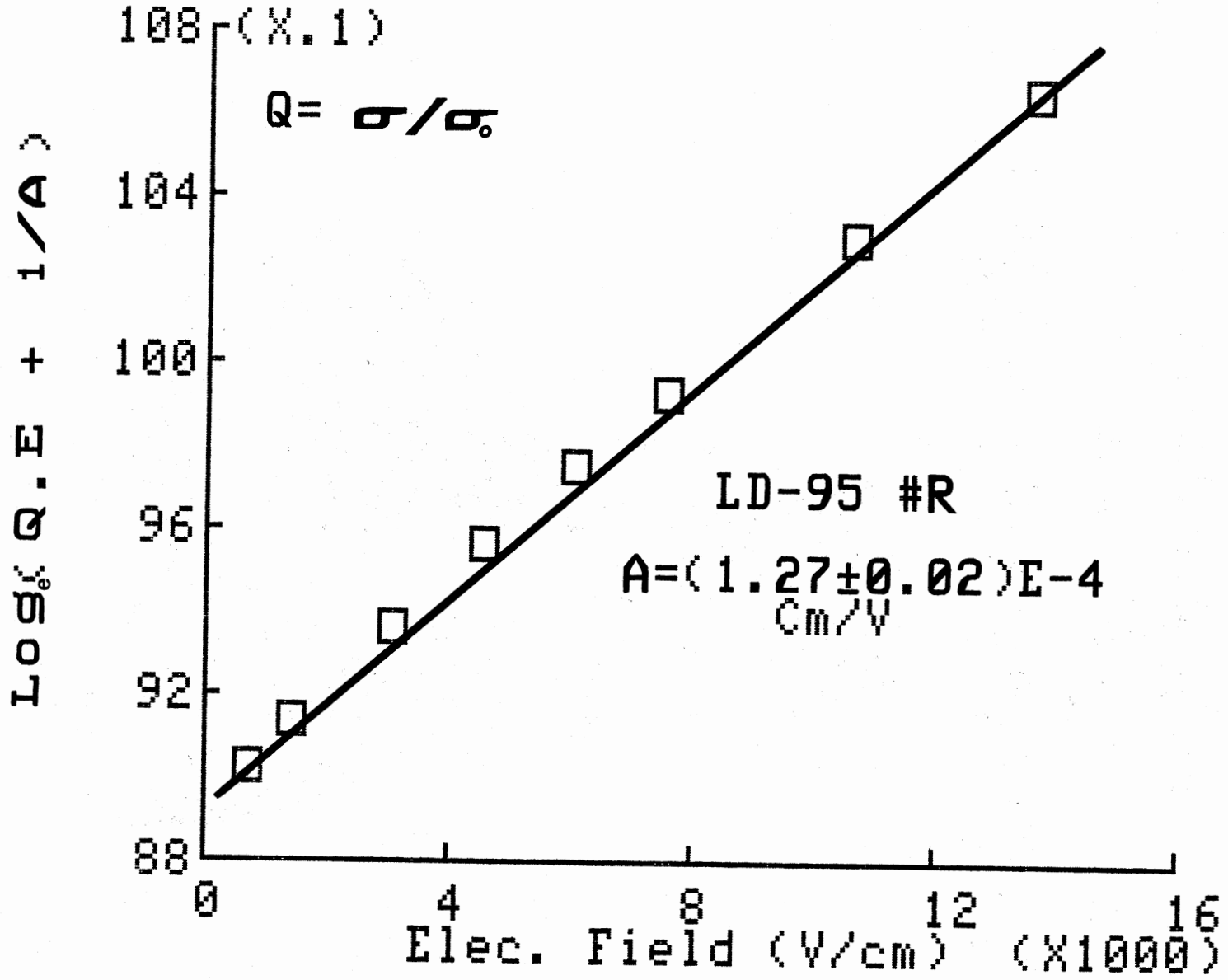
108
(X.1)
Q= σ/σ₀
104
100
96
92
88
Log(Q.E + 1/A)
LD-95 #R
A=(1.27±0.02)E-4
Cm/V
0
4
8
12
16
Elec. Field (V/cm) (X1000)

Fig.(129)

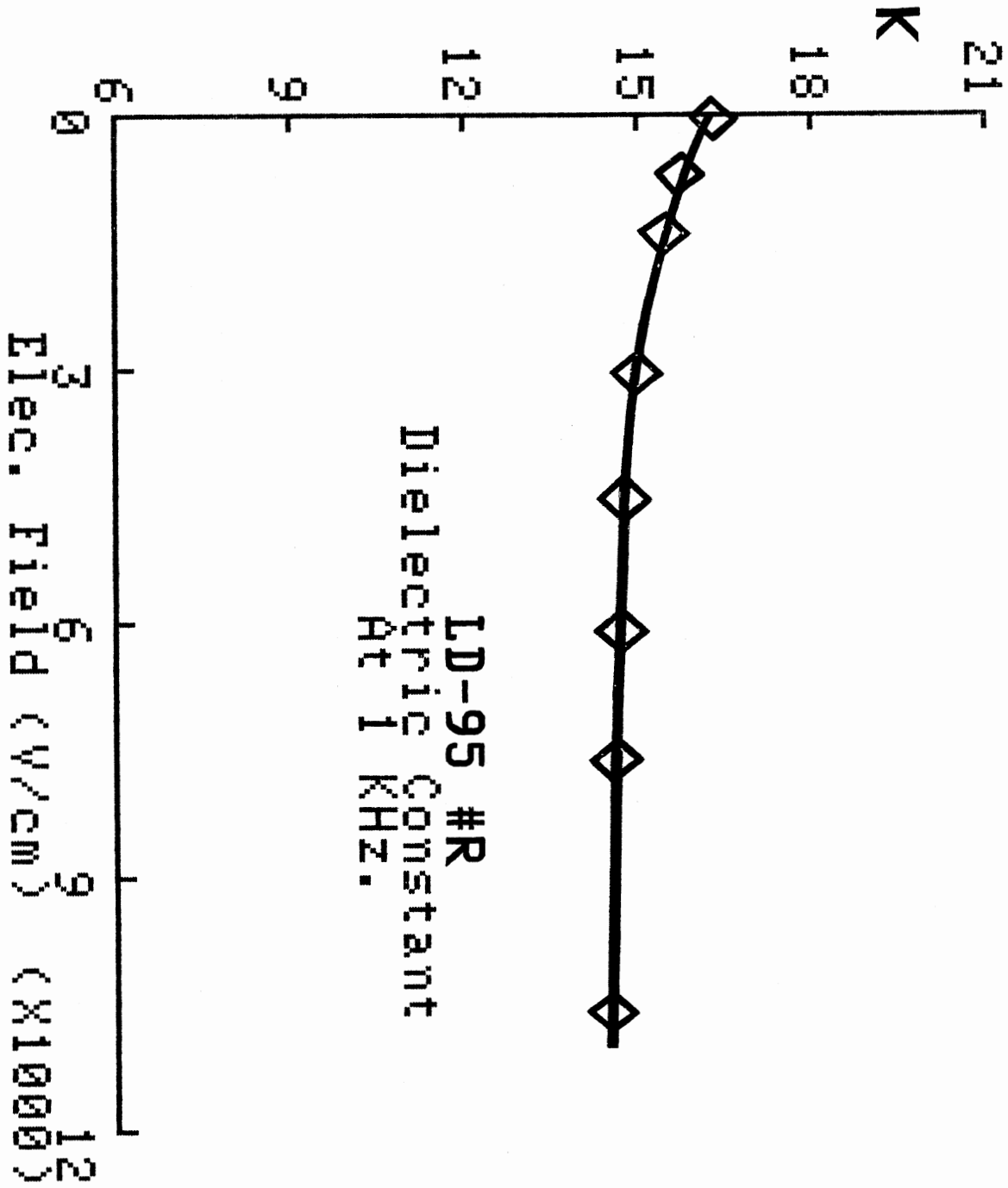
K
21
18
15
12
9
6
0
3
6
9
12
Elec. Field (V/cm) (X1000)
LD-95 #R
Dielectric Constant
At 1 KHz.

Fig.(130)

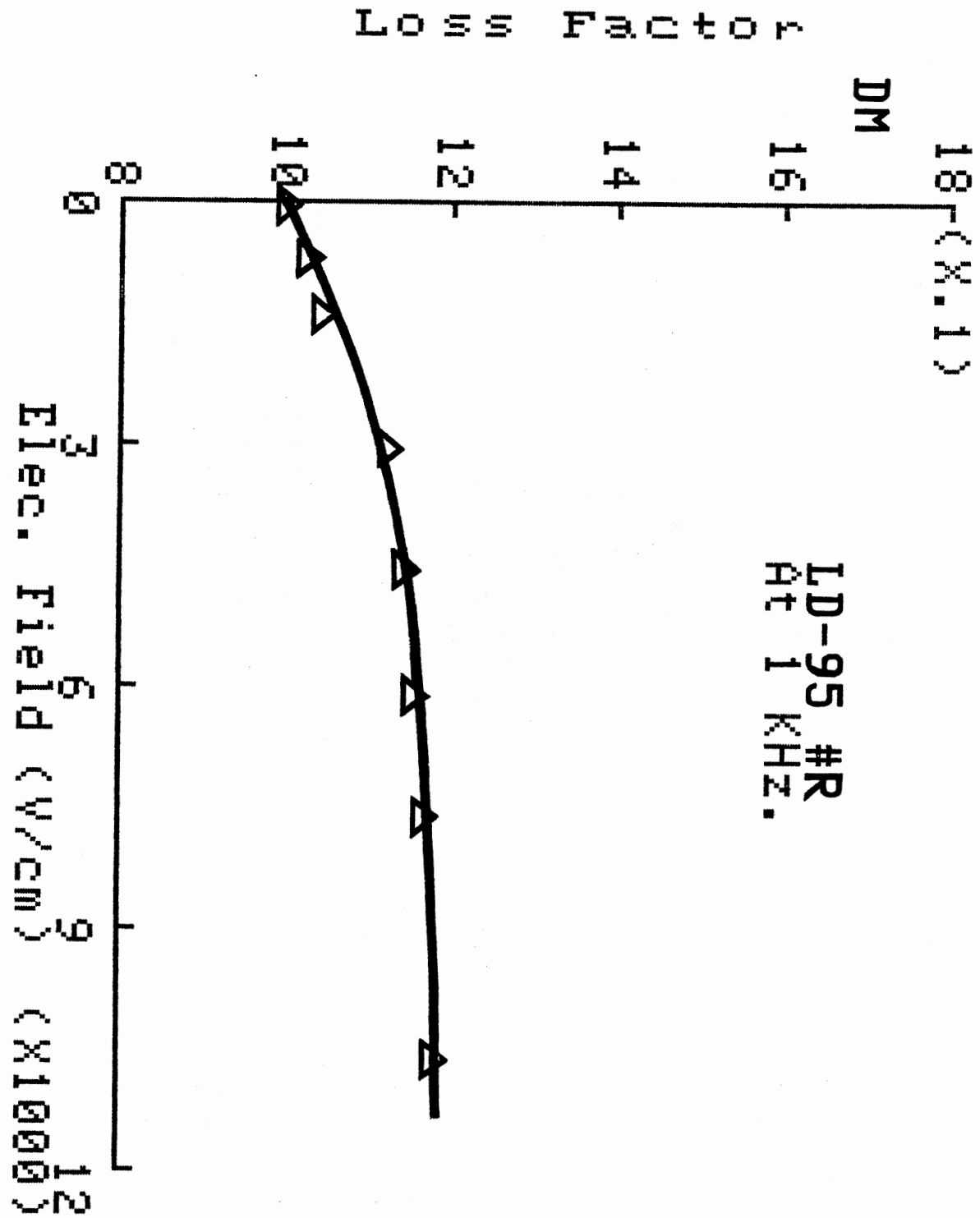
Loss Factor
DM
8
10
12
14
16
18
(x.1)
0
3
6
9
12
Elec. field (V/cm)
(0001X)
(X1000)
LD-95 #R
Pt 1 KHz.

Fig.(131)

TABLE (3.36)

D.C. ELECTRIC FIELD EFFECT ON LD-94

	<=== DC ELECTRIC FIELD BIAS ===> (1000 V/cm)								
Sample	.122	0.84	1.65	3.31	4.74	6.26	8.47	11.8	15.2
S : σ	2.41	3.09	3.12	3.44	3.55	4.03	4.60	5.06	6.56
σ'	5.53	5.44	5.55	5.75	5.80	5.87	6.03	6.37	--
K	13.1	12.9	12.5	12.3	12.2	12.1	12.1	12.1	--
DM	0.76	0.76	0.80	0.84	0.85	0.87	0.90	0.95	--

Observed At 10 KHz. All Values Of σ Are (X1E-8),

Those Of σ' Are (X1E-6).

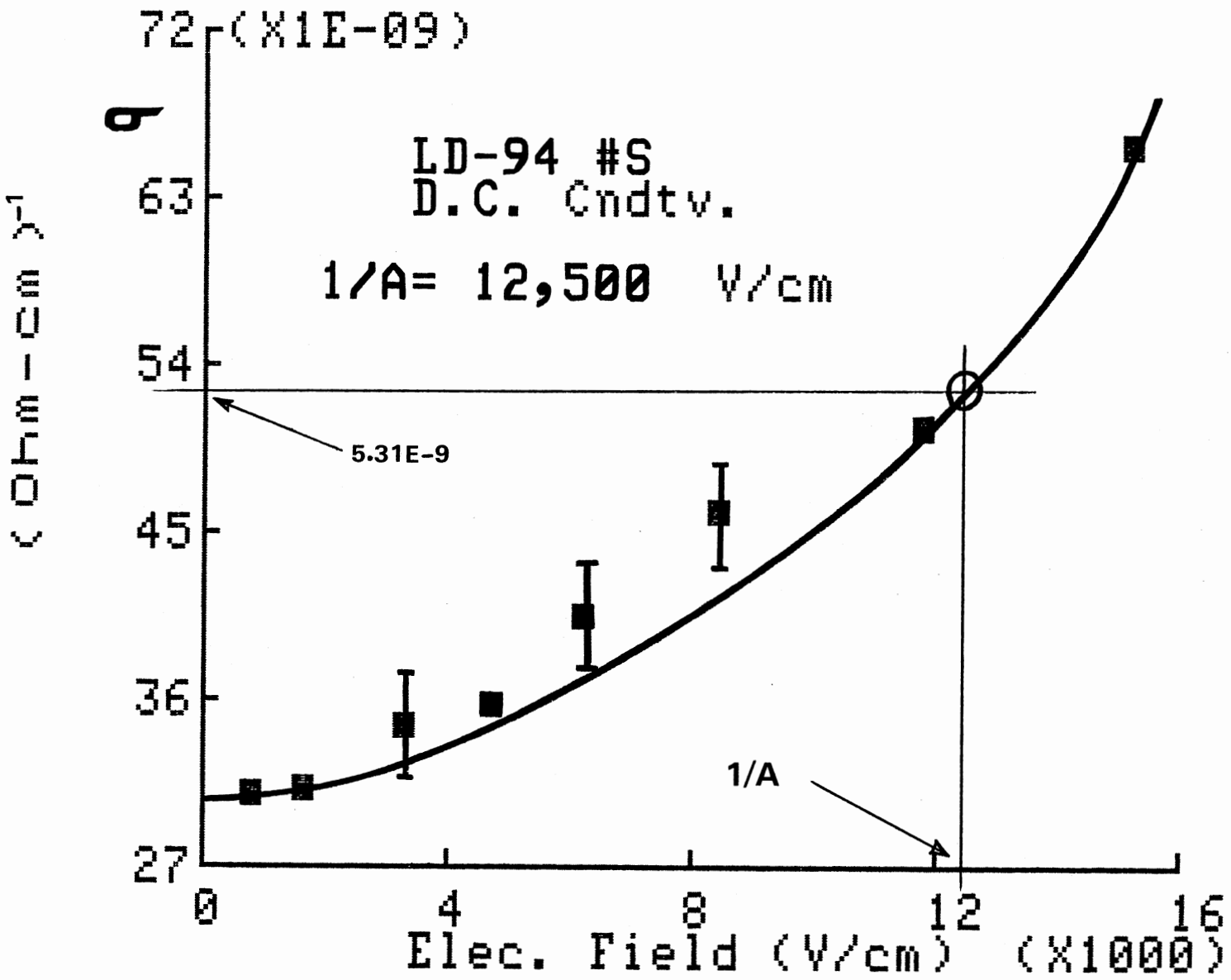
72
(X1E-09)
63
54
45
36
27
σ
(Ohm-Cm)⁻¹
LD-94 #S
D.C. Cndtv.
1/A= 12,500 V/cm
5.31E-9
1/A
0
4
8
12
16
Elec. Field (V/cm) (X1000)

Fig.(132)

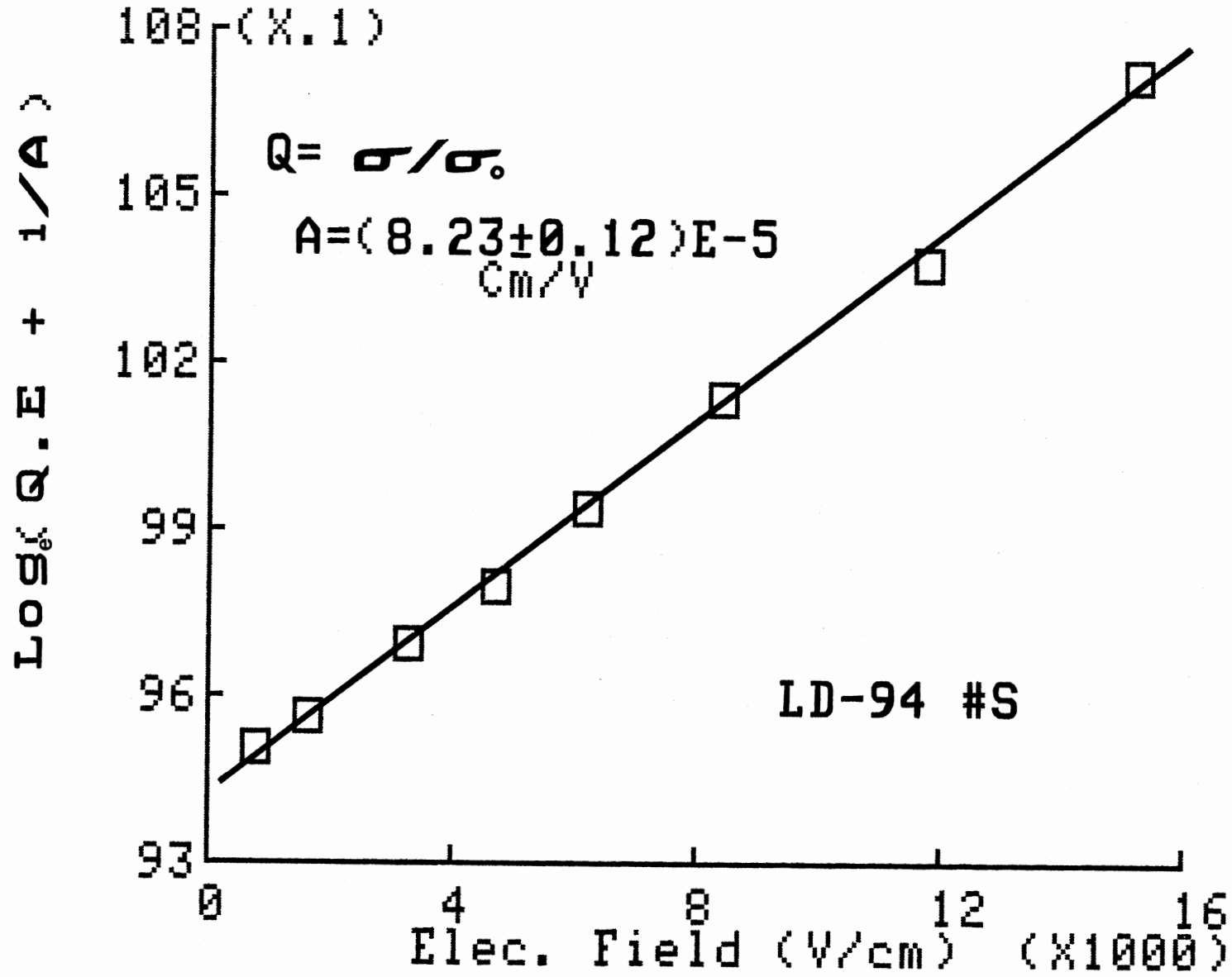
108
105
102
99
96
93
(X.1)
Q= σ/σ₀
A=(8.23±0.12)E-5
Cm/V
LD-94 #S
0
4
8
12
16
Elec. Field (V/cm) (X1000)
Log(Q.E + 1/A)

Fig. (133)

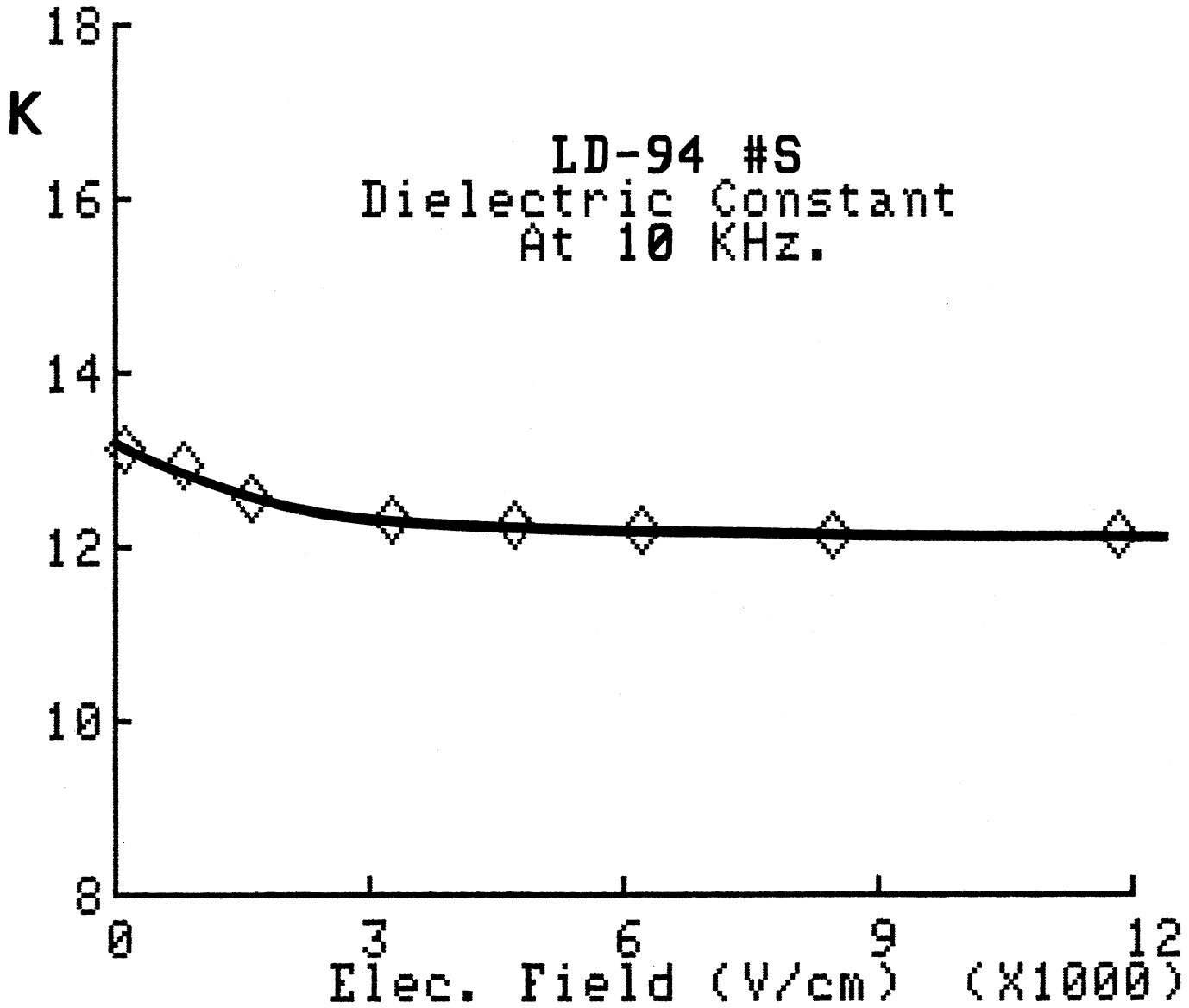
LD-94 #S
Dielectric Constant
At 10 KHz.
K
18
16
14
12
10
8
0
3
6
9
12
Elec. Field (V/cm) (X1000)

Fig.(134)

TABLE (3.37)

D.C. ELECTRIC FIELD EFFECT ON LD-14A

	<=== DC ELECTRIC FIELD BIAS ===> (1000 V/cm)								
Sample	.127	0.89	1.79	3.58	5.09	7.14	8.93	12.5	16.0
V : σ	5.80	5.88	6.47	7.35	8.84	8.98	10.5	14.8	22.7
σ'	4.23	4.29	4.28	4.46	4.51	--	--	--	--
K	10.4	9.80	9.67	9.56	9.35	--	--	--	--
DM	0.79	0.79	0.80	0.84	0.87	--	--	--	--

Observed At 1 KHz. All Values Of σ Are (X1E-10),

Those Of σ' Are (X1E-7).

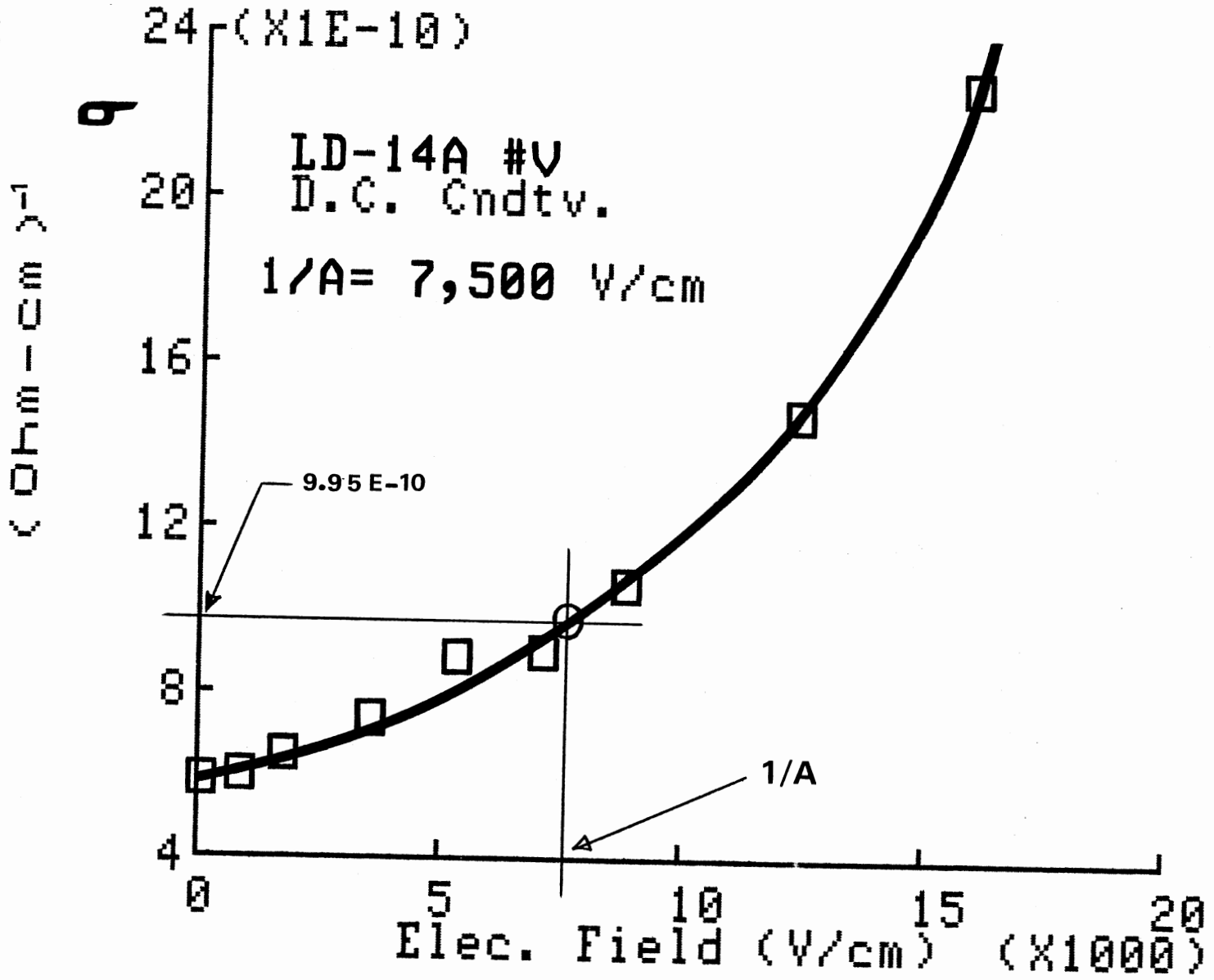
24 (X1E-10)
σ
LD-14A #V
D.C. Cndtv.
1/A= 7,500 V/cm
20
16
12
8
4
9.95 E-10
1/A
0
5
10
15
20
Elec. Field (V/cm) (X1000)
(Ohm-cm)-1

Fig. (135)

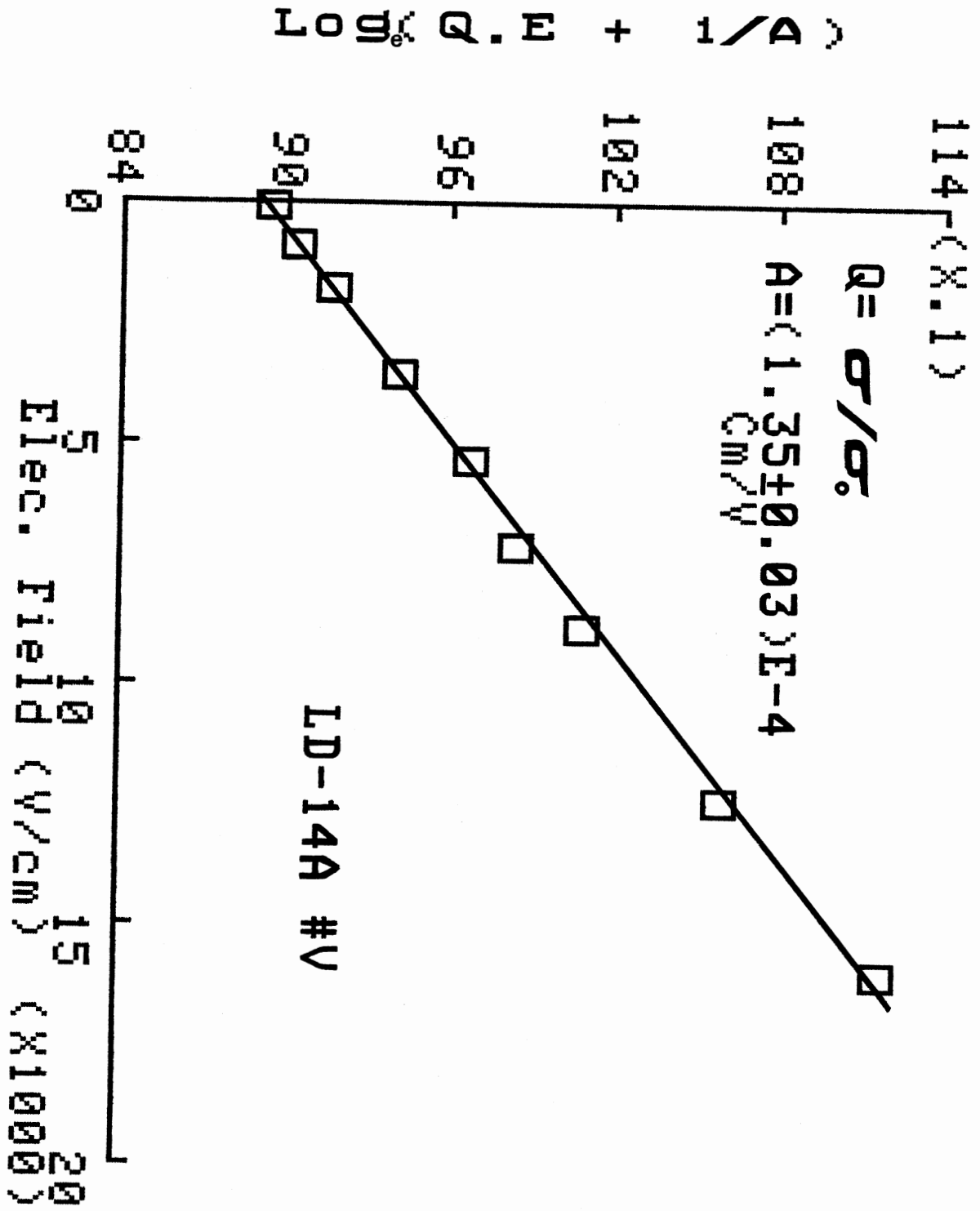
Log$_e$(Q.E + 1/A)
(X.1)
114
108
102
96
90
84
0
5
10
15
20
(0001X)
Elec. Field (V/cm)
LD-14A #V
A=(1.35±0.03)E-4
Cm²/V
Q= Q/Q°

Fig.(136)

TABLE (3.38)

D.C. ELECTRIC FIELD EFFECT ON LD-6A

	<=== DC ELECTRIC FIELD BIAS ===> (1000 V/cm)								
Sample	.070	0.52	1.03	2.70	3.08	4.10	5.12	7.15	9.17
F : σ	5.57	5.73	6.12	7.06	7.58	8.30	9.02	10.6	12.1
σ'	8.63	9.21	9.95	11.2	12.7	14.0	14.1	14.7	--
K	18.9	17.6	17.3	16.9	16.2	16.2	16.1	14.2	--
DM	0.82	0.94	1.03	1.19	1.40	1.55	1.57	1.86	--

Observed At 1 KHz. All Values Of σ Are (X1E-9),

Those Of σ' Are (X1E-7).

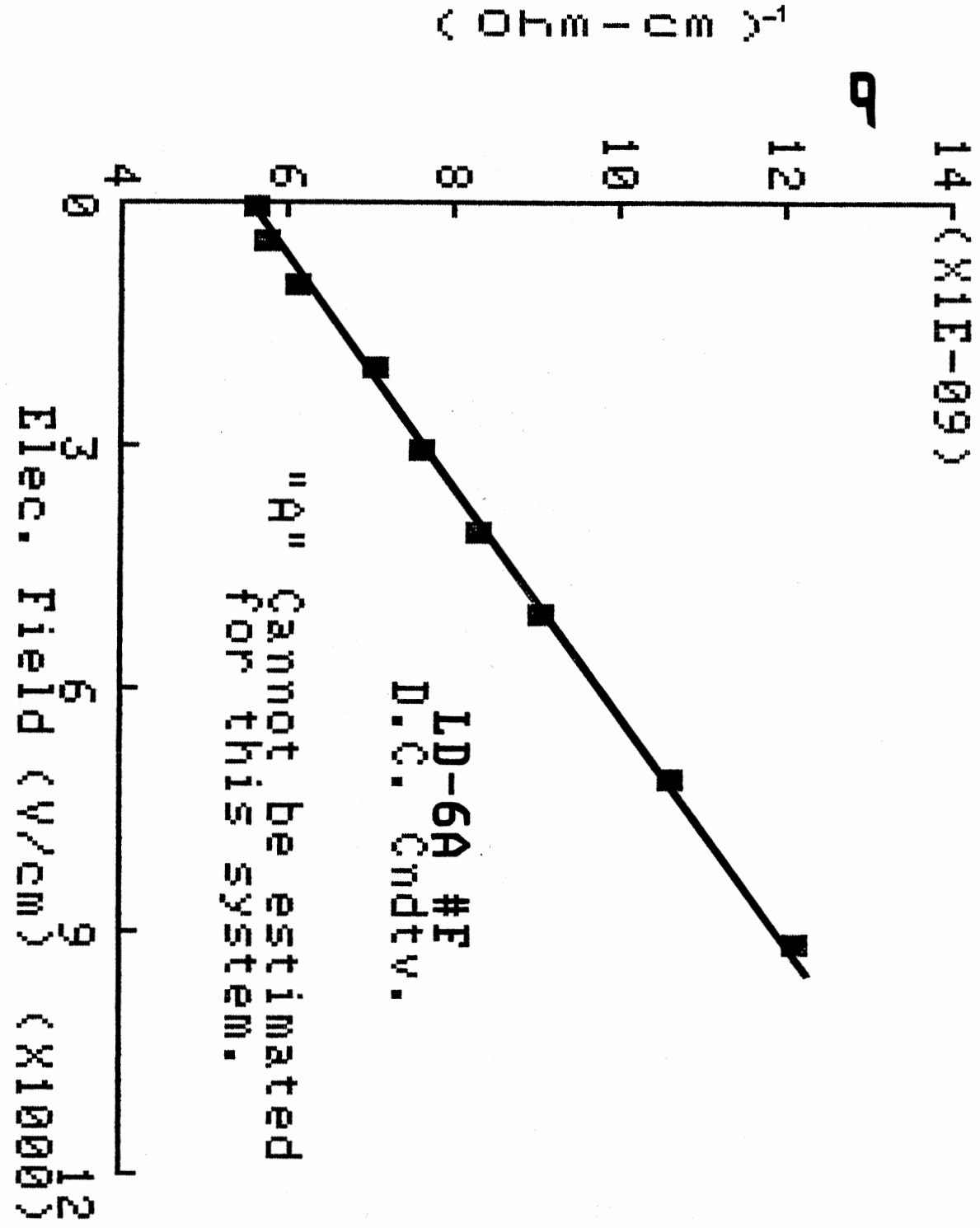
(Ohm-cm)-1
9
14
12
10
8
6
4
(x1E-09)
0
3
6
9
12
Elec. Field (V/cm) (x10000)
LD-6A #F
D.C. Cndtv.
Data was estimated
for this system.
Cannot be estimated

Fig.(137)

TABLE (3.39)

D.C. ELECTRIC FIELD EFFECT ON LD-54

	<=== DC ELECTRIC FIELD BIAS ===> (1000 V/cm)								
Sample	.186	0.81	1.48	2.65	5.18	6.90	18.57	11.8	18.5
V : σ	0.47	0.83	1.40	2.14	4.79	4.80	5.19	5.93	7.26
σ'	1.95	1.98	2.04	2.04	2.05	2.08	2.09	2.12	2.13
K	4.89	4.70	4.70	4.67	4.64	4.64	4.60	4.60	4.60
DM	.072	.075	.078	.078	.079	.080	.082	.083	.083

Observed At 1 KHz. All Values Of σ Are (X1E-12),

Those Of σ' Are (X1E-8).

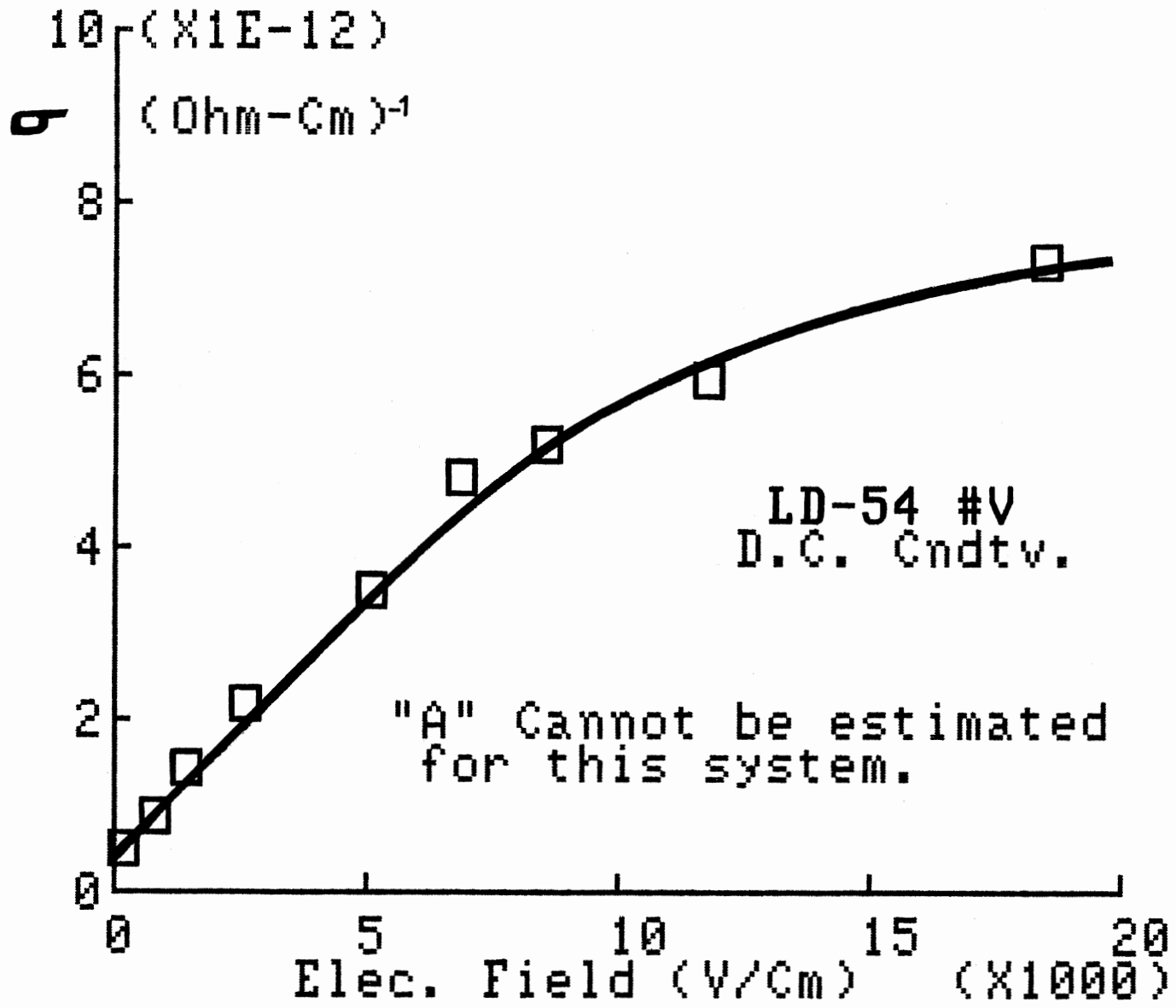
10
(X1E-12)
σ
(Ohm-Cm)-1
8
6
4
2
0
LD-54 #V
D.C. Cndtv.
"A" Cannot be estimated
for this system.
0
5
10
15
20
Elec. Field (V/Cm)
(X1000)

Fig. (138)

TABLE (3.40)

D.C. ELECTRIC FIELD EFFECT ON LD-52B

	<=== DC ELECTRIC FIELD BIAS ===> (1000 V/cm)							
Sample	.200	1.99	3.89	6.72	10.0	12.5	17.3	22.2
H : σ	5.41	8.52	9.85	11.2	14.3	16.4	21.2	21.5
σ'	3.38	2.07	1.83	1.83	2.22	2.26	2.26	2.29
K	6.32	5.11	5.03	5.03	5.03	4.98	4.98	4.94
DM	.096	.073	.065	.065	.080	.082	.082	.084

Observed At 1 KHz. All Values Of σ Are (X1E-12),

Those Of σ' Are (X1E-8).

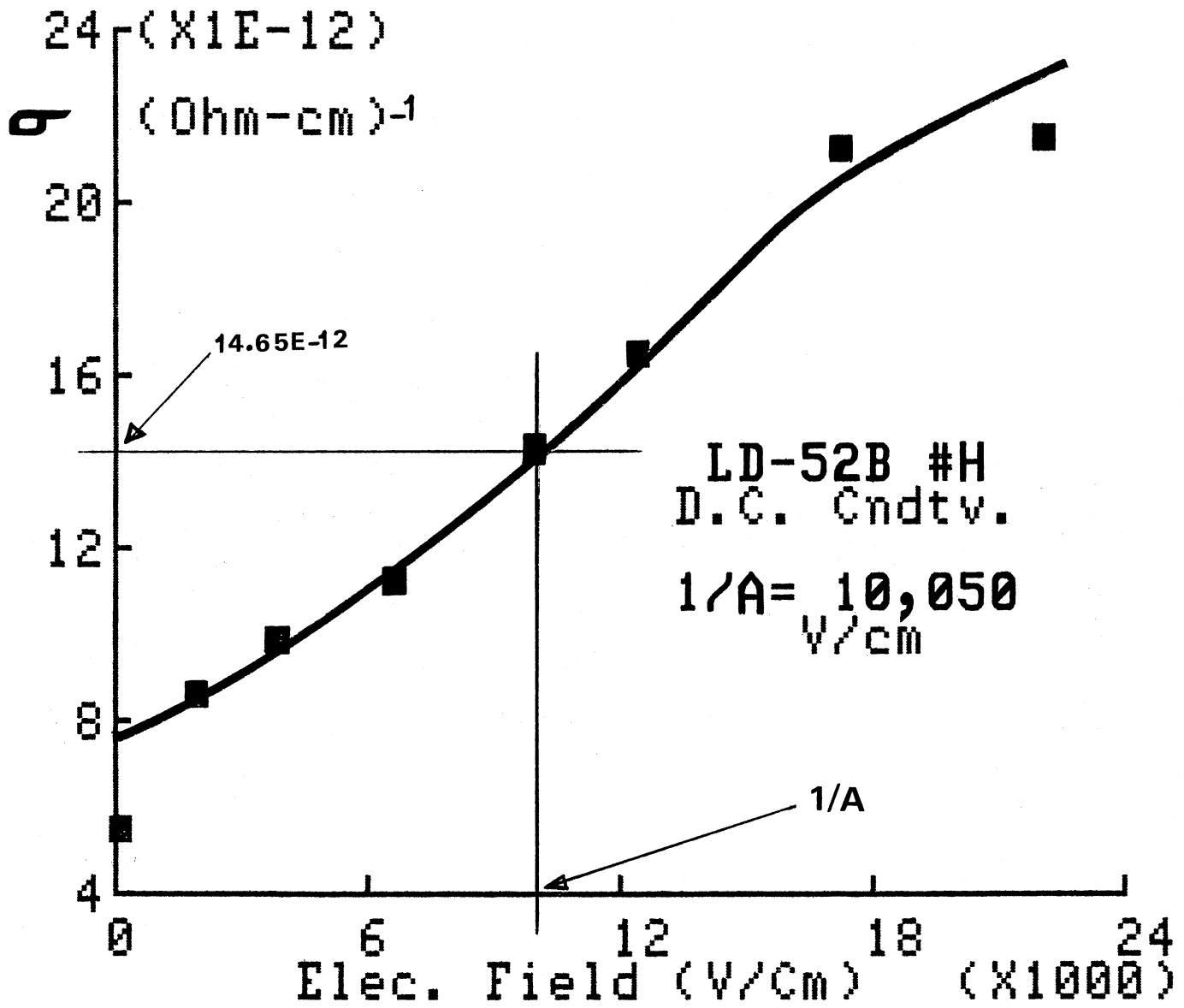
24
(X1E-12)
σ
(Ohm-cm)-1
20
16
12
8
4
14.65E-12
LD-52B #H
D.C. Cndtv.
1/A= 10,050
V/cm
1/A
0
6
12
18
24
Elec. Field (V/Cm) (X1000)

Fig. 139

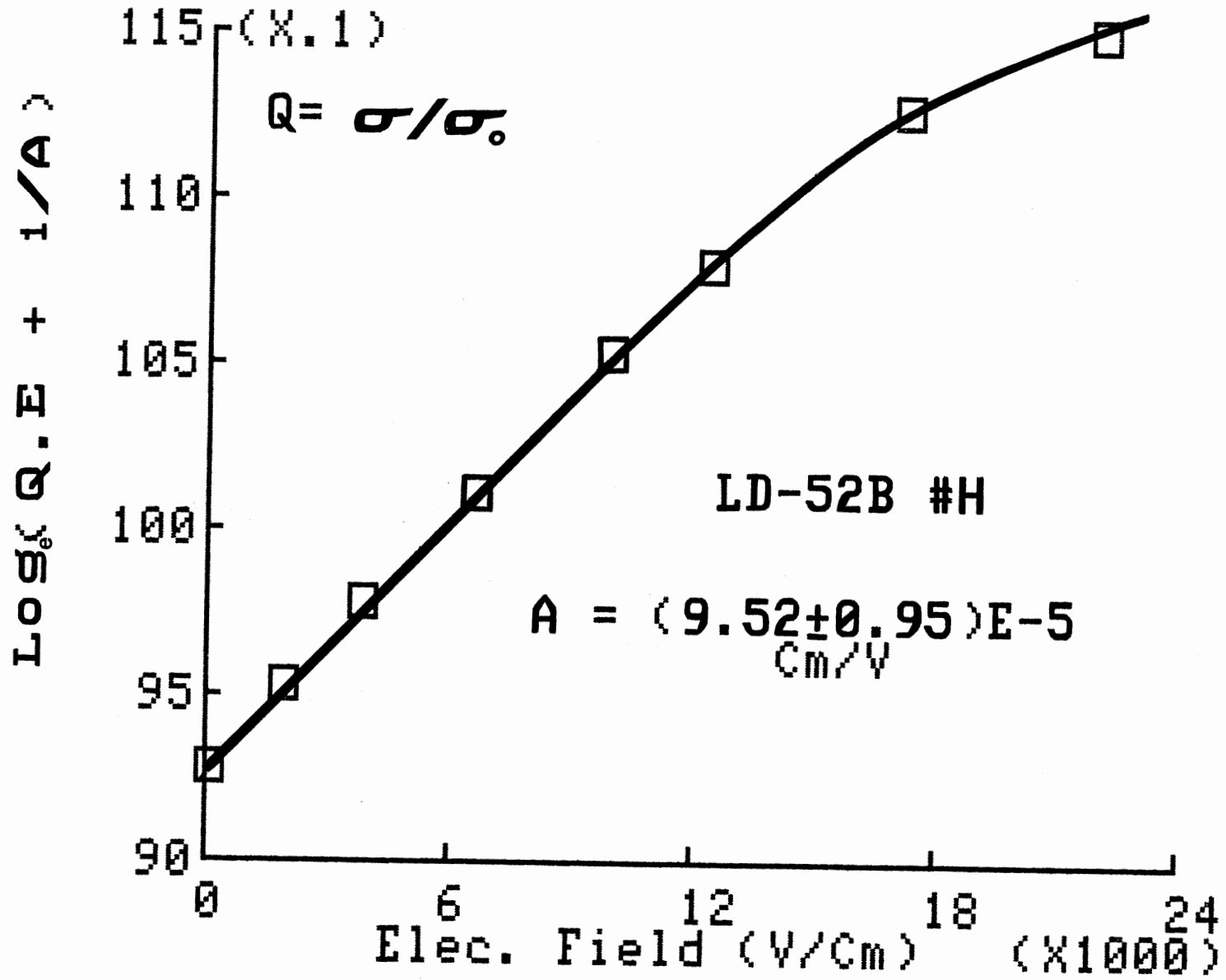
115
(X.1)
Q= σ/σ₀
110
105
100
95
90
Log(Q.E + 1/A)
LD-52B #H
A = (9.52±0.95)E-5
Cm/V
0
6
12
18
24
Elec. Field (V/Cm)
(X1000)

Fig. (140)

TABLE (3.41)

D.C. ELECTRIC FIELD EFFECT ON LD-106

	<=== DC ELECTRIC FIELD BIAS ===> (1000 V/cm)							
Sample	.132	.605	3.36	6.82	9.05	11.9	16.7	21.4
H : σ	.307	1.11	1.60	1.98	2.19	2.27	3.37	5.24
σ'	1.65	1.68	1.69	1.69	1.69	1.64	1.64	1.62
K	9.24	8.55	8.50	8.46	8.46	8.43	8.30	8.30
DM	0.32	0.35	0.36	0.36	0.36	0.35	0.36	0.36

Observed At 1 KHz. All Values Of σ Are (X1E-10),

Those Of σ' Are (X1E-7).

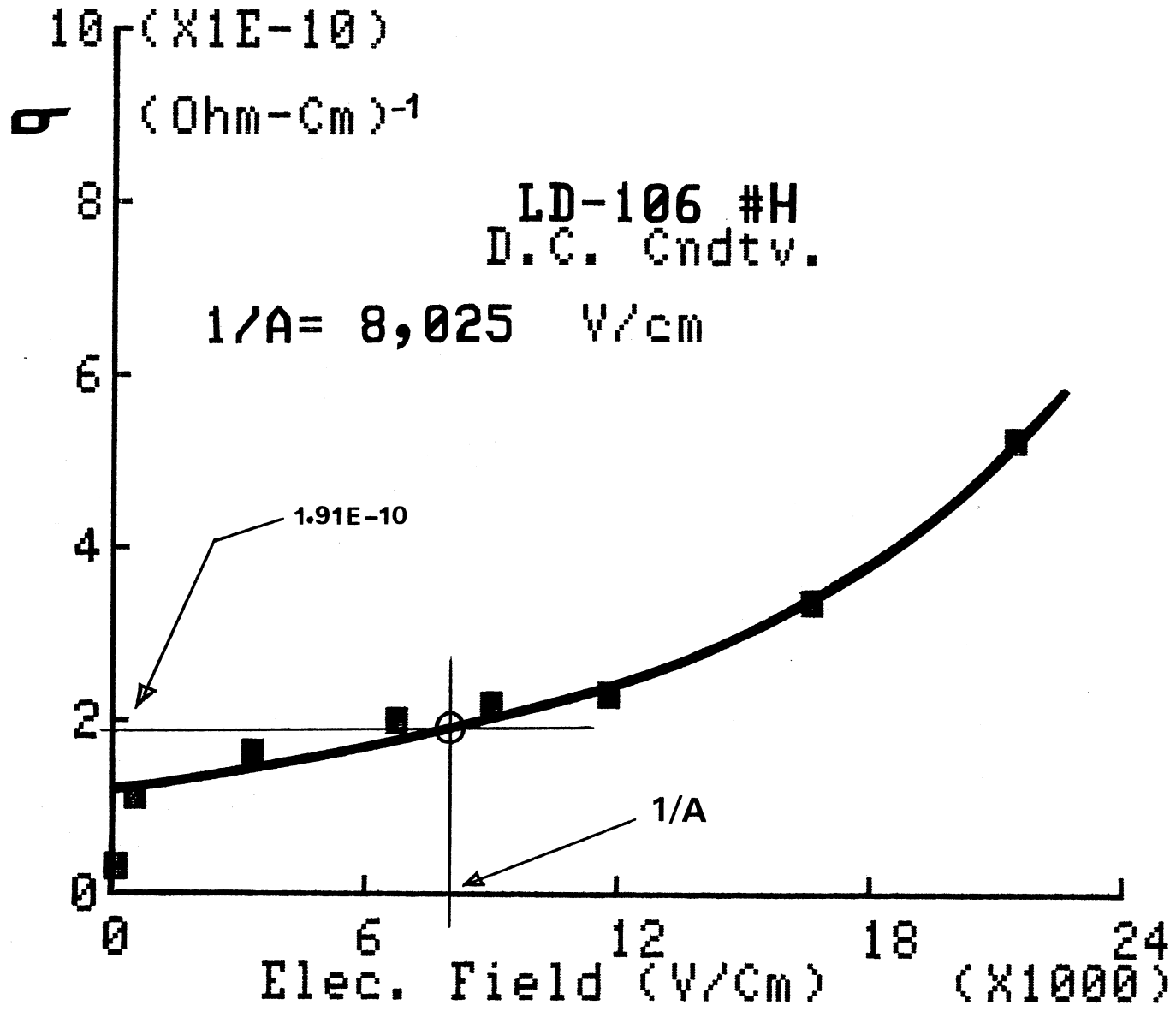
10
(X1E-10)
σ
(Ohm-Cm)-1
LD-106 #H
D.C. Cndtv.
1/A= 8,025 V/cm
8
6
4
2
0
1.91E-10
1/A
0
6
12
18
24
Elec. Field (V/Cm)
(X1000)

Fig. (141)

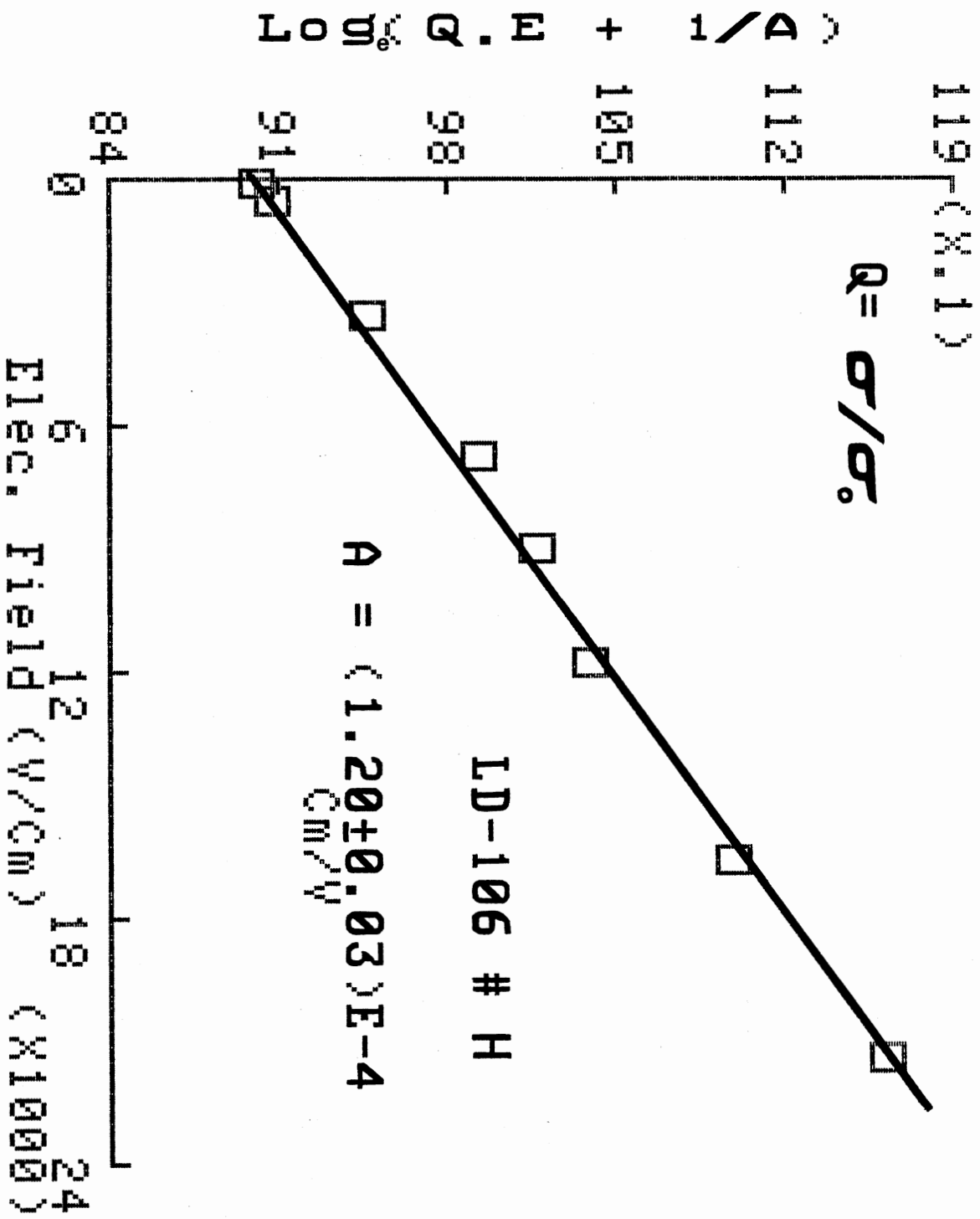
Log$_e$(Q.E + 1/A)
(x 10)
Q = σ/σ$_o$
LD-106 # H
A = (1.20±0.03)E-4 cm/μ
Elec. Field (μ/cm) (x10000)
0
6
12
18
24
84
91
98
105
112
119

Fig.(142)

3.3) Summary of The Main Experimental Results

We give in this section a brief recapitulation of our findings in a tabulated form. The quantities given in table (3.42a) are : 1) The value of the exponent in the relation: $\sigma_{AC} \propto w^{s}$ where w is the frequency. 2) The piezo-conductive and the piezo-capacitive coefficients "C1" and "C2" evaluated from the slopes of the graphical plots in Sec.(3.2B). Table (3.42b) lists: 1) The activation energies for both D.C. and A.C. conduction as reported in Sec.(3.2C). 2) The average molecular lengths as obtained through the procedure outlined in Sec.(3.2D). 3) The four basic quantities K, σ', DM, and σ under room conditions and 1 KHz. (except for LD-105 which was observed at 1.5 KHz.)

For cases where the quantities corresponding to different samples of the same polymer are close to each other, only an average is quoted. Otherwise the distinct values are listed for each sample. A.C. quantities observed at frequencies other than 1 KHz. are preceded by a number corresponding to that frequency in KHz.

The units for the C1 and C2 coefficients can be different depending on whether the most linear data fit is logarithmic or plain, or whether a square-root is involved. Consequently the units are not given in table (3.42a), but can be inferred from the information supplied with each particular case. For example when the "comments" column reads "log" it means that the particular number was obtained from the slope of $\log_e(\sigma)$

versus $\sqrt{P}$, (the plots being always versus $\sqrt{P}$).
The abbreviation "pln" stands for "plain", meaning that the particular quantity was plotted as is, without any transformation. Similarly the $\sqrt{}$ sign means the square-root of that quantity was plotted.

The activation energies are in (eV), while the average molecular length Lo is in Å. The total computational and experimental error in Lo ranges from about 15 - 75 Å.
Unless otherwise noted in the table, the frequency for both C1 and C2 in any given observation is the same. When nothing is mentioned in the left-hand side of the D.C. column for C1, it means that the comment is the same as in the A.C. column, (apart from the frequency).

Finally table (3.43) compares the values of the conductivities as obtained from the zero-pressure intercepts of the pressure plots against the same quantities determined experimentally at 27 PSI and room conditions. It is seen that, in about half the cases the "intercept" values are higher than the corresponding values at 27 PSI, (contrary to what is expected). This however, is mainly due to the fact that the pressure plots are not very linear around the low pressure region, which makes the value of the extrapolation to zero pressure become somewhat higher as the actual curve follows a different path to the one taken by the extrapolation line. In any case, the discrepancies are rather small and should not be regarded as infringing on the certainty of the experimentally determined values.

TABLE (3.42a)

TABULATED SUMMARY OF THE MAIN EXPERIMENTAL RESULTS

POLYMER	S	COMMENT	C1		COMMENT	C2
		A.C		D.C		
LD-105	0.40	log (100)2.05		2.8	log	0.15
-104	0.58	log (G,H) 7.6		8.7	log	2.7 (H)
(G)	--	pln 10.8E-6		5.7E-8		---
(H)	--	pln 14.5E-6		5.7E-8		---
(G,H)	--	log (10)1.15		---	pln	5.5
-97(S)	0.57	log (100)1.05	pln	1.34E-7	log	0.42
	--	pln (10)3.7E-5		--	pln	9.1
(T)	0.47	log (100)2.40	pln	1.94E-7	log	0.62
	--	pln (10)4.3E-5		--	pln	21.7

cont'd

TABLE (3.42a) Cont'd

-95	0.43	√	(10)2.9E-3		2.8E-4	pln	12.9
-94(A)	0.48		----		----		----
(B)	0.34	√	(10)7.2E-3		6.6E-4	pln	17
-14A	0.46	log	1.35	√	1.27E-4	pln	$-(2.8\pm0.70)$
-6A	0.45	√	(10)5.3E-3		5.90E-4	pln	13.5
-54	0.65	pln	1.2E-8		5.3E-12	pln	1.7
-52B	0.83	pln	2.1E-8	√	1.27E-6	√	0.24
-106	0.67	pln	1.4E-6		5.0E-9	pln	13.6

* Only coefficients belonging to the same kind of plot may be compared with each other.

TABLE (3.42b)

TABULATED SUMMARY OF THE MAIN EXPERIMENTAL RESULTS

POLYMER	Ea		Lo	K	DM	σ'	σ
	A.C	D.C					
LD-105	(100)0.12	0.23	1260	64	1.7	8.7E-6	1.0E-7
-104	(10)0.17	0.29	1180	24	0.64	8.5E-7	1.7E-9
-97(S)	(10)0.14	0.29	1114	32	0.58	1.0E-6	3.2E-9
(T)	(10)0.14	0.30	1470	20	0.81	9.1E-7	3.4E-9
(S or T)	0.17	--	--	--	--	---	---
-95	(10)0.13	0.25	670	18	1.0	1.0E-6	3.6E-9
	0.14	--	--	--	--	---	---

cont'd

TABLE (3.42b) Cont'd

-94	(10)0.12	0.21	430	28	1.8	2.8E-6	2.2E-8
	0.12	--	--	--	--	---	---
-14A	(10)0.12	0.25	700	12	0.80	5.5E-7	7.9E-10
	0.15	--	--	--	--	---	---
-6A	0.08	0.17	--	21	0.87	1.0E-6	6.0E-9
-54	0.21	0.45	--	5.0	0.074	2.1E-8	8.4E-13
-52B	0.11/0.02	0.055	490	5.5	0.054	1.8E-8	5.3E-12
-106(C)	0.22/.085	--	--	6.8	0.30	1.1E-7	1.7E-10
(H)	0.17/0.02	0.30	620	--	--	---	---

TABLE (3.43)

COMPARISON OF THE CONDUCTIVITY VALUES AT "ZERO" PRESSURE AS OBTAINED FROM GRAPHICAL EXTRAPOLATION WITH THOSE DETERMINED EXPERIMENTALLY

POLYMER	σ'	σ	σ'	σ
	--- From Intercept -----		--Experimental At 27 PSI-	
LD-105	(100)9.3E-5	4.8E-7	(100)5.4E-5	1.0E-7
-104	1.2E-7	5.5E-10	8.4E-7	1.7E-9
	(10)5.6E-6	---	3.7E-6	---
-97	(100)2.5E-5	1.6E-8	(100)1.2E-5	3.3E-9
	(10)4.5E-6	---	(10)4.1E-6	---
-95	(10)2.5E-6	7.2E-9	(10)3.1E-6	3.6E-9
-94	(10)9.7E-6	6.3E-8	(10)5.5E-6	2.2E-8
-14A	6.8E-7	2.9E-10	5.5E-7	7.9E-10
* -6A	(10)2.8E-6	1.6E-9	(10)3.2E-6	6.0E-9
* -54	8.8E-9	5.8E-13	2.1E-8	8.4E-13
-52B	2.6E-8	3.8E-12	1.8E-8	5.3E-12
-106	5.2E-8	9.4E-11	1.1E-7	1.7E-10

* The experimental values obtained from a different sample to the one used in the pressure plots.

CHAPTER IV

ANALYSIS AND DISCUSSION OF THE EXPERIMENTAL DATA DEVELOPING SOME REALISTIC VIEWS ON ELECTRONIC CONDUCTION

Introduction

This chapter is made up of two main parts, the first is devoted to a theoretical study based on a modified model that takes into account ohmic conduction as an integral part of the conduction process, while the second half deals with the interpretation of the experimental results in light of this model. The study is aimed at understanding the behaviour of polymers with respect to frequency, temperature, and D.C electric field bias. It will not attempt to incorporate a model or theory for the effects of pressure, as this was not within the scope of our study, but was experimentally observed in order to provide us with information about the piezo-capacitive and piezo-conductive coefficients. Pressure theories based on the concept of "overlap" between adjacent π - orbitals (which leads to a decrease in the activation energy) have been only partially successful in explaining the increase of conductivity with the pressure (112-114). Their applicability is mainly limited to low-molecular weight organic materials such as ferrocene, the logarithim of whose conductivity shows a linear increase with

the pressure per unit change in volume (115).

To date, there are no established theories that could account for the effects of pressure on polymers,but the basic trend followed is to attribute the increase in conductivity to an increase in the mobility of the charge carriers due to their greater ability to jump between regions of polyconjugation. Studies on pyrolyzed polyacrylonitrile (116) confirm the aforementioned hypothesis.

4.1) The Hopping Model And Ohmic Conduction

A) Introduction

In most solids (amorphous or crystalline), it has been a generally accepted notion that the ohmic conductivity based on Drude's theory of metallic conduction is frequency independent up to 10^{13} or 10^{14} $sec.^{-1}$ This is because the relaxation times of the scattering process are quite short of the order of (10^{-13} sec.).

However if a hopping process is involved in the bulk transport of charge between molecules (where an electron, has to surmount a potential energy barrier), then it becomes certain that the ohmic conductivity will become frequency - dependent at much lower frequencies, possibly around 10^{7}-10^{9} $sec.^{-1}$ as a consequence of the long relaxation times characteristic of the hopping process across the potential energy barrier separating two molecules.

The conduction process in polymeric materials may be divided into two stages : one involving the motion of the charge carrier within the molecule (eka-conjugation region) and the other involving the motion between adjacent molecules. It has long been debated whether the inter-molecular conduction is mediated by the same type of charge carriers as the intra-molecular conduction. So far, the experimental evidence has not been conclusive, but most observations on A.C and D.C quantities hint at the plausibility of different type of carriers for each of the two stages.

Primarily, the evidence comes from the fact that the total conductivity (ohmic + polarisation) at a given frequency, is generally several orders of magnitude larger than the D.C. conductivity (117-123). Secondly, there is only little or no correlation between the D.C and the A.C components, at least within the intermediate-to-high frequency range (10^2 - 10^8 Hz), (124). Finally, the dependence on the temperature is weaker in the A.C case than the D.C (125-128). Our own results agree very well with the above trends. We shall presently see that by working with an appropriate model which does not compromise ohmic conduction in favour of polarisation conduction, a new light will be shed on the complicated process underlying the electronic transport in polymer structures.

Before we delve into this subject, we shall need a brief exposition of a few concepts borrowed from organic solids.

B) Hopping Model Versus The Band Model

While in the case of inorganic semiconductors charge transport takes place via the strong electron interaction created by the overlap of atomic orbitals, this kind of scheme is generally not favourable in organic solids due to the relatively weak molecular bonding (Van Der Waals type) and the small overlap and exchange orbitals.Thus the ultimate mode of transport is heavily dependent on: 1) How much energy is required to ionize a molecule or atom within an aggregate.
2) Whether the electron affinity is determined by the immediate molecular group or by the polymer molecule as a whole .
3) The type of motion the charge will follow once it becomes freed.

Let us first note that while none of the models proposed is capable of explaining all the observed data on electrical transport, the evidence suggests that choosing a particular model that works is heavily dependent on the relative energies involved in the interaction hamiltonian. The band theory of solids is built around three basic assumptions:
1) The legitimacy of one-electron states in a periodic potential. 2) The neglect of multiplet structure on individual atoms. 3) The treatment of the electron-phonon interaction as a perturbation in comparison with the electron-electron term. It is precisely this last assumption that renders the band model to be an inadequate description in most cases. Ioffe (129), has pointed out that systems with carrier mobilities less than 100 cm2/V-sec. and a mean free path smaller than

that of thermal electrons, the electron-lattice interaction will be so large that a band description is generally unacceptable.

In the case of inorganic crystalline solids, the electron exchange interaction is much stronger than the electron-phonon term. In metals and covalent solids the overlap integral is of the order of 1 eV, while the phonon energy is 0.01 eV ($k_B T$ = 0.025 eV at room temperature). On the other hand, the overlap integral for organic materials (which may also vary from site to site within the solid) is about 0.01-0.1 eV, while the electron-phonon term is not different from the crystalline case; which in effect, makes the electron-phonon interaction equally dominant and thereby default the applicability of perturbation theory.

Systematic calculations of the energy band structure of anthracene were done by Le Blanc (130) using LCAO methods (he places the bandwidth B at $0.56k_B T$). His findings were later amended and modified by Thaxton (131), Katz (132), and Silbey (133), but with not much difference. The conclusion is that the electron-phonon interaction tends to produce narrower band widths which, at the small values quoted, do not allow for the conservation of the phonon energy and wavevector.

Simple arguments based on the uncertainty principle show that for the band model to hold, the mean free path must be greater than the lattice constant (if such a concept can be defined at least locally); and according to Glarum (134) the bandwidth B should be greater than the acoustic waves phonon

energy (Debye frequency).

In long-chain polymers, if we take the molecular length for a "lattice constant", calculations in one dimension will show that the energy bandwidth is of the order of 0.03-0.003 eV for molecular lengths between 100-1000 Å. However, with such a large lattice constant the first condition would not apply except, perhaps, at very low temperatures. Thus, the choice of whether a band model is a more appropriate description than a hopping model should ultimately be decided with respect to the temperature range over which the observations are made.

In short, systems for which the mobility is low are best described in terms of a hopping picture, while in other cases, the effect of temperature on the relative magnitudes of the phonon vibrations, the electron-phonon coupling, and the elec tron exchange term will determine whether a coherent band model should be more favourable (or less) than a random hopping process.

C) <u>The Anderson Localization Theorem</u>

Despite the absence of structural periodicity in amorphous substances, certain concepts related to crystalline solids can still be usefully employed. The most important of these are the density of states, and the energy bands. However the material may no longer possess a Fermi surface since the Bloch wavevector will not in general be a good quantum number. This usually happens when the electron scattering by atomic

centers is strong ($k \sim \Delta k$) $\Longrightarrow$ $kl \simeq 1$, where l is the mean free path. As the interaction gets stronger a new phenomena which is absent in crystalline solids, occurs: The single - particle states become confined around the individual wells falling off with distance like $\exp(-b_\alpha R)$ where $\hbar b_\alpha = \sqrt{2mWo}$, with Wo being the energy of the single particle state and R is the radial distance. What's more important, is that there is no mixing between states: if a state belonging to a given energy level is localized, then all states corresponding to that energy will be localized too. Thus the density of states breaks up into regions of localization (shaded) separated by regions of non-localization Fig.(143). This of course, is possible since the allowed energies are strictly discrete.

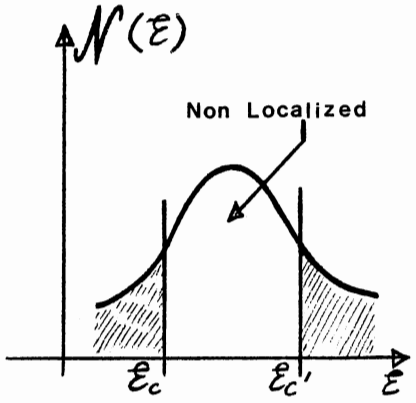

Fig.(143)

The energy separating the different regions is called the mobility edge. Its position relative to the Fermi level(*) and determination is of central importance in the theory of non-crystalline solids, and plays a crucial role in the transport characteristics of the material. The above phenomena was first discovered by Anderson (135) in 1958. The Anderson localization theorem may be considered as a key concept upon which all hopping models are based and its application to polymeric materials will be explored in the next sections.

(*) Defined in the usual way as in crystalline solids.

4.2) A Model For Polymers

A) Basic Assumptions And Postulates

This model is based on the ideas of Frolich (136) concerning a point charge dipole confined to hop between two states with the difference that instead of a single dipole we now have a multitude of them obeying a rate-determining probabilistic process based on the Boltzmann equation in which the number of particles at a given site depends on the number of particles at the two "nearest neighbors" adjacent sites (assuming that particle hopping is between nearest neighbours only).

We shall consider the polymer molecule to consist of S "square-well" potentials corresponding to a uniform potential energy height U1, each of width "a_o" equal to the monomer unit length, so that the molecular length is Lo = a_o.S

At the end terminals of the molecule the potential energy barrier height Uo is assumed to be >> U1, but not infinite, (Fig.(144)), which is realistic of a finite non-zero D.C. conductivity.

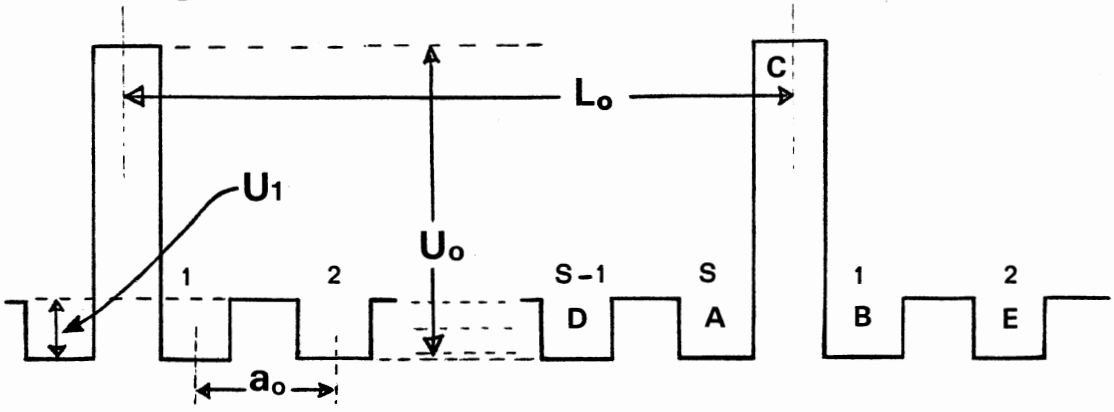

Fig.(144)

Charge carriers in the form of excitons or small-mass polarons hop along the molecular spine from one site to the next with probabilities (per unit time) that depend on the energy difference between the two states. It will be assumed that the system is quasi one-dimensional meaning that in the two dimensions transverse to the molecular spine very little hopping takes place. That is the electron wave-vector's components along the transverse directions are too small to affect transverse hopping, but large enough to allow for the existence of a density of states.

According to the studies of Mott & Davies (137) it is legitimate to assume only nearest neighbor hopping since the "electron" states are Anderson-localized. Furthermore, the Bloch states of an electron in the above described lattice may be written as :

$$\psi_k = \exp(ik.Rn)\,\phi_s(r-Rn) \qquad 4.2.1$$

where ϕ_s are spherically symmetric "S" functions. The corresponding energies are given by (137):

$$Ek = Wo - 2Io.\exp(-b_\alpha R).\cos(k.a) \qquad 4.2.2$$

where $b_\alpha = (\sqrt{2mWo})/\hbar$,and Io is the energy integral which depends on the type of the well being used. Thus the density of states is confined to a bandwidth B of $\simeq 4Io.\exp(-b_\alpha R)$ around Wo and grows narrower and narrower as the localization becomes stronger. The value of Io, (Slater (138)) is typically of the order of 0.001 to 0.05 eV. and without loss of generality

it will be assumed that B is large enough to accommodate many quantum states yet small compared to Wo that the probability of occupation of the states may be assumed not to depend on their energy, but always equal to that corresponding to the state belonging to energy level Wo.

Next, we shall set up the dynamical equations governing the hopping of particles between sites within the molecule and across adjacent molecules, assuming for the time being, that the probabilities per unit time of jumping from site to site are known.

To this end we consider three adjacent sites 1, 2 & 3. We let Nk be the instantaneous number of particles on site k then according to the basic assumptions we have:

$$dN2/dt = -(P21 + P23)N2 + P12N1 + P32N3 \qquad 4.2.3$$

where Pjk is the probability per unit time of jumping from site j to site k. In the case of variable range hopping where distant neighbors are involved the above equation takes the general form :

$$dNj/dt = -\sum_{K}(Pjk)Nj + \sum_{K} PkjNk \qquad 4.2.4$$

This is recognized as Boltzmann's equation governing the rate of transport of particles across cellular membranes by diffusion. For the case of nearest neighbors "k" takes only two values "j-1" & "j+1" giving back eq.(4.2.3) :

$$dNj/dt= -(Pj,j-1 + Pj,j+1)Nj + Pj-1,jNj-1 + Pj+1,jNj+1 \qquad 4.2.5$$

The above is a system of S coupled linear differential equa-

tions whose analytical solution can be formidable even for as few as 3 sites. In sec.(1.4) we have seen that a series solution is possible by invoking boundary conditions at the extremeties of the molecular domains akin to those encountered in crystals i.e. by imagining the macromolecule to be a closed loop so that its right and left endpoints are one and the same. In the Pohl-Pollak theory, the assumption of zero ohmic conduction allowed for a series solution using impedance network methods. However this approach will not work if the ohmic currents are incorporated in the theory.

In order to simplify the problem to a manageable level we shall assume that the hopping between sites within a polymer molecule occurs with relative ease compared to the more difficult hopping across adjacent molecules. In mathematical terms : $P_{jk} \gg P_{S1}$ or P_{1S} for all $j, k \neq 1$ and S . As a consequence of this, the charge carriers within the molecular domain can be legitimately assumed to respond rather instantaneously to the action of an applied electric field . Thus when a D.C electric field is switched on at time $t = 0$, the charge carriers will re-distribute themselves instantly on all sites (except "S" and "1"), according to the static distribution discussed in sec.(1.3D). Consequently we need only to worry about the temporal dependence of the number of charges on sites "S" and "1". This leads to a pair of first order coupled linear differential equations which will be solved in the following sections.

B) An Eigenvalue Problem

To simplify notation we shall denote (see Fig.144) site "S" by "A", and site "1" by "B", site "S-1" by "D" and site "2" by "E". The probabilities per unit time PS1 and P1S for transitions across the barrier will be denoted by "a" and "b" respectively, while PS,S-1 and P12 will be denoted by "a'" and "b'".

Thus eq.(4.2.5) becomes :

$$dNA/dt = -(a + a')NA + bNB + FA \qquad 4.2.6$$

where FA = PDA.ND and is independent of the time (by our previous assumption). Similarly:

$$dNB/dt = aNA - (b + b')NB + FB \qquad 4.2.7$$

with FB = PEB.NE, and is also constant independent of time.

In the absence of electric field the terms "a" and "b" are equal, and also "a'" will be equal to "b'". That is, the "left" and "right" become indistinguishable when $E \longrightarrow 0$. For the calculation of these transition probabilities refer to appendix (D). Eqs.(4.2.6-7) may be cast in matrix form:

$$dN/dt = (\Omega)N + F \qquad 4.2.8$$

where (Ω) is given by :

$$\Omega = \begin{pmatrix} -(a+a') & b \\ a & -(b+b') \end{pmatrix} \qquad 4.2.9$$

In a diagonal representation, eq.(4.2.8) is readily solved according to :

$$N'A = C'1\exp(\lambda_1 t) + F_1'$$

$$N'B = C'2\exp(\lambda_2 t) + F_2'$$

where the C's are constants etc.., and λ_1 ,λ_2 are the eigenvalues of (Ω), and F_1' , F_2' are integration constants

The true number of particles is now found by transforming back to the original basis giving the following :

$$\left.\begin{aligned} NA &= C1\exp(\lambda_1 t) + C2\exp(\lambda_2 t) + NSA \\ NB &= D1\exp(\lambda_1 t) + D2\exp(\lambda_2 t) + NSB \end{aligned}\right\} \qquad 4.2.10$$

The coefficients C ,D ,and NS are best determined from the initial conditions, and the requirement that dNA/dt, dNB/dt as obtained from eq.(4.2.10) conform to eq.(4.2.6-7).

The eigenvalues are determined by solving the secular equation :

$$\lambda^2 + \lambda\,(a+a'+b+b') + (ab'+a'b+a'b') = 0 \qquad 4.2.11$$

The results ,after considerable algebra , are :

$$-\lambda_{1,2} = \begin{cases} (a+a') + ab/[(a+a')-(b+b')] \\ (b+b') - ab/[(a+a')-(b+b')] \end{cases} \qquad 4.2.12$$

Where the above is only valid for non-zero electric field i.e. as long as $a-b \neq 0$ and $a'-b' \neq 0$. Also the condition

$$4ab << [\,(a+a') - (b+b')\,]^2 \qquad 4.2.13$$

has been assumed to hold. This is legitimate on account of the relative magnitudes of a, a', and b, b' (consult appendix D). Finally upon inserting the explicit values of a, b, a'.. from appendix (D), we obtain:

$$-\lambda_{1,2} = \begin{cases} a.\left(1 + \exp(-\eta') + \exp(W-)/[1 + \exp(\eta')]\right) - \xi \\ a.\ 1 + \exp(-\eta') + \exp(W+)/[1 + \exp(\eta')] + \xi \end{cases} \qquad 4.2.14$$

where $\xi = -ab/[(a+a')-(b+b')]$

$$= a.\exp\left[-(U/k_BT + \eta')\right] /\tanh(\eta'/2) \qquad 4.2.15$$

and $W\pm = U/k_BT \pm \eta'$ 4.2.16

Further simplification of eq.(4.2.14) may be obtained by inserting the value of "a" as determined from appendix (D).

Next we define two characteristic times τ_1 and τ_2 :

$$\tau_1 = 1/w1 \quad , \quad \tau_2 = 1/w2$$

where $w1 = -\lambda_1$ and $w2 = -\lambda_2$ 4.2.17

Then we rewrite eq.(4.2.10) as :

$$\left.\begin{aligned} NA &= C1\exp(-w1t) + C2\exp(-w2t) + NSA \\ NB &= D1\exp(-w1t) + C2\exp(-w2t) + NSB \end{aligned}\right\} \qquad 4.2.18$$

At t=0 when the electric field is zero the following initial conditions must hold:

NA(0) = NB(0) = No (this value is determined later).

Also at any other time > 0 we must have :

dNA/dt and dNB/dt as obtained from eq.(4.2.18) conform

to eq.(4.2.6-7). This yields the following sets of equations

$$\left.\begin{aligned} w_1C_1 &= (a+a')C_1 - bD_1 \\ w_2C_2 &= (a+a')C_2 - bD_2 \\ w_1D_1 &= (b+b')D_1 - aC_1 \\ w_2D_2 &= (b+b')D_2 - aC_2 \end{aligned}\right\} \qquad 4.2.19$$

Also :

$$FA = (a+a')NSA - bNSB$$

$$FB = (b+b')NSB - aNSA$$

It should be noted that eqs.(4.2.19) are self-consistent by virtue of the fact that the w's satisfy the secular equation (4.2.11) .

Finally making use of eq.(4.2.12-13) we have :

$$D_1 = (\xi/b)C_1 \quad , \quad D_2 = (-a/\xi)C_2 \qquad 4.2.20$$

Which, when combined with the initial conditions yield:

$$\left.\begin{aligned} C_1 + C_2 &= No - NSA \equiv q_1 \\ (\xi/b)C_1 - (a/\xi)C_2 &= No - NSB \equiv q_2 \end{aligned}\right\} \qquad 4.2.21$$

Whose solution is :

$$C_1 = q_1 + (\xi/a)q_2 \qquad C_2 = -(\xi/a)q_2 \qquad 4.2.22$$

$$D_1 = (\xi/b)q_1 \qquad D_2 = q_2 - (\xi/b)q_1 \qquad 4.2.23$$

Where again, the approximation $\xi^2 << ab$ has been used.

We are now in a position to calculate the ohmic current across the gap, as well as the polarisation currents within the molecules. This will be taken up in the next section.

4.3) Calculation Of The Currents

A) The D.C. Response

We begin this section by calculating the ohmic and the polarisation currents under the influence of a D.C. electric field switched on at time t = 0, and in the positive x-direction. Using the results of sec.(4.2B), the D.C. current across the gap may be written as follows:

The net number of particles flowing across the gap is equal to the number flowing to the right (out of site A) less the number flowing to the left (out of site B). Also if we assume a common cross-sectional area of (πa_o^2), where $2a_o$ is the cross-sectional diameter of a single polymer molecule aligned with the field, then the net flux across the barrier is :

$$[\ a.N_A(t) - a.\exp(-\eta').N_B(t)\ ]/\pi a_o^2$$

where "a" is the probability per unit time of jump from site A to site B. The electric current density is "e" times the above, thus:

$$J_\Omega(t) = \left(N_A(t) - \exp(-\eta').N_B(t) \right).(ea/\pi a_o^2) \qquad 4.3.1$$

By making use of eqs.(4.2.22-23), the current density may be written in a more instructive form as follows:

$$J_\Omega(t) = \left[h_1 \exp(-t/\tau_1) + h_2 \exp(-t/\tau_2) + h_\Delta \right](ea/\pi a_o^2) \qquad 4.3.2$$

where:

$$h_1 = q1(1 - \xi e^{-\eta'}/b) + q2(\xi/a)$$

$$h_2 = q1(\xi/b)e^{-\eta'} - q2(e^{-\eta'} + \xi/a) \qquad 4.3.3$$

$$h_\Delta = N_{SA} - N_{SB}\exp(-\eta')$$

with:

$$\xi/a = \exp[-(W+)]/\tanh(\eta'/2) \quad \text{and} \quad \xi/b = e^{\eta'}.(\xi/a) \qquad 4.3.4$$

So that:
$$\left.\begin{aligned} h_1 &= q1(1 - \xi/a) + q2(\xi/a) \\ h_2 &= q1(\xi/a) - q2(e^{-\eta'} + \xi/a) \end{aligned}\right\} \qquad 4.3.5$$

At time t = 0+ the ohmic current density is:

$$J_\Omega(0) = [(q1 - q2.e^{-\eta'}) + h_\Delta].(ea/\pi a_o^2)$$

$$= \left((No - N_{SA}) - (No - N_{SB})e^{-\eta'} + (N_{SA} - N_{SB}e^{-\eta'})\right).(ea/\pi a_o^2)$$

$$J_\Omega(0) = No(1 - e^{-\eta'}).(ea/\pi a_o^2) \qquad 4.3.6$$

Worth noting is the fact that $h_1 + h_2$ is < 0 (refer to eq. (4.3.5), while h_Δ is positive. This implies that $J_\Omega(t)$ is a monotone increasing function starting from an initial value given by (4.3.6) to a final value of:

$$J_{D.C.} = [\, N_{SA} - N_{SB}.e^{-\eta'}\,](ea/\pi a_o^2) \qquad 4.3.7$$

as t approaches "infinity".

The quantities N_{SA} and N_{SB} may be expressed in terms of the D.C. field using the static distribution of charge along the molecular length of the polymer according to the analysis of sec.(1.3D), we find:

$$N_{SA} = Nm.e^{\eta}(1 - e^{-\eta'})/2\sinh(\eta)$$

$$N_{SB} = e^{-2\eta}.N_{SA} \qquad 4.3.8$$

Where Nm is the average number of charge carriers on a given polymer molecule, (Nm can be < 1), and $\eta = (eELo/2k_BT)$. Hence we may write:

$$J_{D.C.} = Nm[\, 1 - e^{-\eta'}\,].(ea/\pi a_o^2) \qquad 4.3.9$$

Finally the expression for "a" from appendix (D) is inserted in (4.3.9) to give: (assuming $[1+\exp(-\eta')] \ll \exp(U/k_BT)$)

$$J_{D.C.} = Nm.(eC'_B/\pi a_o^2).[\, 1 - \exp(-\eta')\,] \qquad 4.3.10$$

where C'_B is $[\nu_{ph}.\exp(-b_\alpha R)].\exp(-U/k_BT)$, (see Appendix D). Further, since η' may be considered << 1 for all practical purposes, (recall that η' is << η for any value of electric field), then $\exp(x) \simeq 1 + x$, and consequently:

$$J_{D.C.} = Nm.(e^2 C'_B / \pi a_o \cdot k_B T).E \qquad 4.3.11$$

Thus the electric field dependence of the conductivity J/E is controlled by Nm, like in the Rosen-Pohl formula of sec.(3.2D) According to appendix (C), we may therefore write:

$$\sigma_{D.C.} = (2\pi N_i e^2 a_o L_o \cdot C_B/k_B T).\exp(-Ea/k_B T).(e^{\eta_+} - 1)/\eta_+ \qquad 4.3.12$$

Where: Ea = Eg/2 + U , and $C_B = \nu_{ph} e^{-b_\alpha R}$. The (average) molecular volume being taken as $(\pi a_o^2 Lo)$, so that $Nm = Nc.(\pi a_o^2 Lo)$ and Nc is given by eq.(C.10).

Eq.(4.3.12) predicts the observed behaviour of the D.C. conductivity with respect to electric field and temperature. It shows among other things that the pre-exponential factor can be temperature-dependent, depending on how $Ni \cdot C_B$ varies with temperature. This implies that in a logarithmic plot of eq.(4.3.12) versus $(1/k_BT)$, the slope of the resulting "straight" line is not always controlled by the value of Ea. Another important prediction of (4.3.12) is the fact that the activation energy Ea is really made up of two contributions: one coming from the energy gap between the top of the valence band and the bottom of the conduction band (this usually has a weak temperature-dependence), while the other comes from

the term (U) which is related to the height of the potential energy barrier Uo at the end of the molecule by: U = Uo - U1, (see Appendix D). Note also that $\sigma_{D.C.}$ becomes very small as Uo becomes larger and larger. Finally the expression in eq.(4. 3.12) reveals the dependence of the conductivity on the phonon frequency as well as the probabilities of the transition.

We remark at this stage that for D.C conduction there is no steady-state contribution from the polarisation current density Jp, the reason being that Jp exists only as a transient and tends to zero as $t \longrightarrow \infty$, as we shall see in the next section. The total current density during the transient time is $J(t) = J_{\Omega}(t) + Jp(t)$.

The implication of this is that these two currents are in "parallel" with each other rather than in "series", meaning that if we consider site "A" for example, as a node, then the rate of change dN_A/dt is not equal to $J_{\Omega}(t) - Jp(t)$ as may be easily verified from the differential equations and the fact that $Jp(t) = dN_A/dt - dN_B/dt$.

B) The A.C. Response

We shall first obtain the polarisation expression under D.C. electric field conditions as in part (A). From what has been explained already, the dipole moment of a single polymer molecule may be written as:

$$Pm = P_{\infty} + (eLo/2).[\ N_A(t) - N_B(t)\ ] \qquad 4.3.13$$

where Lo is the (average) length of the molecule, N_A & N_B are the instantaneous number of charge carriers on sites "A", "B" and P_{∞} is the static dipole moment associated with a molecule of length $(Lo - 2a_o)$. This is in accordance with the basic assumptions outlined in sec.(4.2A). Assuming all molecules to be aligned with the field, the total polarisation of the system would be Pm/Zo where Zo is the molecular volume and is given by $(\pi a_o^2)Lo$.

The quantities N_A and N_B have been calculated in sec.(4.2 B), we therefore have, similar to the procedure in eq.(4.3.3):

$$N_A - N_B = g_1 \exp(-t/\tau_1) + g_2 \exp(-t/\tau_2) + g_{\Delta} \qquad 4.3.14$$

where: $g_1 = q1(1 - e^{\eta' \xi/a}) + q2(\xi/a)$

$$g_2 = q1(e^{\eta' \xi/a}) - q2(1 + \xi/a) \qquad 4.3.15$$

$$g_{\Delta} = Ns_A - Ns_B$$

As before, at $t = 0+$, the dipole moment is P_{∞}, since $g_1 + g_2 + g_{\Delta} = 0$, and as $t \longrightarrow \infty$, the dipole moment reaches a final value of: $Ps = P_{\infty} + (eLo/2)(\ Ns_A - Ns_B\ ).$ 4.3.16

The term $Ns_A - Ns_B$ is calculated as before to be:

$$Nm(1 - e^{-\eta'}) \quad \text{where } \eta' = (ea_oE/k_BT) \qquad 4.3.17$$

We note at this stage that since Ns_A and Ns_B are both linear with Nm, the D.C polarisation will follow the same electric

field dependence as the conductivity: i.e. it diverges rather than tends to the experimentally observed saturation limit. This supports the speculation that the charge carriers responsible for the polarisation cannot be the same as those mediating D.C. conduction. In view of this we shall assume that the charge carriers responsible for the polarisation cannot exist outside the polymer molecule, (i.e. they do not participate in D.C. ohmic conduction), and that their number density Np is different to that of the ohmic current carriers No, together with the possibility of a lower activation energy: thus we write:

$$Np = Ni'.\exp(-Ep/2k_BT) \qquad 4.3.18$$

where $Ni' \neq Ni$ (possibly greater), and Ep is smaller than Eg of the D.C. carriers. The above assumptions are strongly supported by the experimental facts that the A.C. conductivity is several orders of magnitude higher than the D.C. case, and that the A.C. activation energy is about one half that of the D.C. case. However, because this issue is highly debatable at the present and because our model is somewhat simplified, we shall not attempt to propose a specific D.C. electric field dependence for Np, the reason being that for A.C. conduction, small field amplitudes are used, and in this regard (4.3.16) may be considered legitimate in as much as Nm will be independent of the electric field amplitude at small fields, while $(1 - e^{-\eta'})$ becomes $\simeq \eta'$ making Ps to vary linearly with E.

Coming to the A.C. response of the system we note that it can be obtained by one of two methods: Since the response

to a unit-step function is known, the response to a harmonic excitation can be obtained by performing a Laplace transform on the D.C. response. However the mathematics is not trivial and requires contour integration. A more realistic method is to observe that a system with two relaxation times is equivalent to a second order differential equation of the form:

$$\tau_1 \tau_2 \ddot{Y} + (\tau_1 + \tau_2)\dot{Y} + Y = F \qquad 4.3.19$$

where Y stands for either the ohmic current density, or the polarisation. In the first case, F is given by: $h_\Delta \cdot (ea/\pi a_o^2)$, which is simply $\sigma_{DC} \cdot E$ (for small fields), see eqs.(4.3.11-12) while in the second case, F is given by: Qp.E , where Qp = (eLo) $Np/4k_BT$ (obtained from eq.(4.3.16) again assuming small fields). The above assumptions are legitimate for the case of A.C. studies where only a small-amplitude signal is used. Moreover the time-dependence of the relaxation times τ_1 and τ_2 through their electric field dependence has been ignored in view of the fact that for small amplitudes ($\eta \ll 1$) the dependence of τ_1 and τ_2 on "E" is not strong, we have referring to eqs.(4.2.14) and eqs.(D.9 - D.15) in the appendix:

$$1/\tau_1 = P'[\exp(U/k_BT)/(2+\eta')]/\exp(U/k_BT) \qquad 4.3.20$$

$$= P'/(2+\eta') \qquad 4.3.21$$

Under the same assumptions we also find that $1/\tau_2$ is also given by (4.3.21). Therefore :

$$(\tau_1 + \tau_2) = 2(2+\eta')/P' \quad , \text{ and}$$

$$\tau_1 \tau_2 = 4(1+\eta')/(P')^2 \text{ (neglecting terms of order } \eta'^2)$$

The solution to (4.3.19) with F = Foexp(iwt) is:

$$Y = F/[\ 1 - w^2 \tau_1 \tau_2 + iw(\tau_1 + \tau_2)\ ] \qquad 4.3.22$$

From which the real and imaginary parts for the amplitudes of J_Ω and $Jp = iwP$ are obtained. We find :

$$Re(J) = (\sigma\ [1 - w^2\tau_1\tau_2] + Qp.w^2(\tau_1 + \tau_2)).E/D^2 \qquad 4.3.23$$

where: $D^2 = (1 - w^2\tau_1\tau_2)^2 + w^2(\tau_1 + \tau_2)^2$

For our purposes we may suppose $w^2\tau_1\tau_2$ is $<<$ 1 , since from (4.3.20-21) the value of $(\tau_1\tau_2)$ is $\sim 10^{-7} - 10^{-9}$ s.

Hence the total conductivity may be written as:

$$\sigma' = [\sigma + Qp.w^2(\tau_1 + \tau_2)]/[1 + w^2(\tau_1 + \tau_2)^2\ ] \qquad 4.3.24$$

The implications of eq.(4.3.24) are very much in agreement with the experimentally observed results:

σ' increases with frequency from its D.C.value of $\sigma \equiv \sigma_{D.C.}$ to its "final" value of $Qp/(\tau_1 + \tau_2)$. The rate of increase actually depends on the values of the relaxation times τ_1 & τ_2 Moreover it is seen that the dominant term in (4.3.24) comes from the polarisation current and not from the ohmic current.

The relative magnitudes of these two terms in the high - frequency limit is given by:

$$\sigma'/\sigma = (Lo/8\pi a_o)(Ni'/Ni)\exp(W_\Delta/k_BT)/(C_B.[\tau_1 + \tau_2]) \qquad 4.3.25$$

where $W_\Delta = U + (Eg - Ep)/2$, and $C_B = P' = \nu_{ph.}e^{-b\alpha R} \cong 10^{11}\ s^{-1}$

By inserting typical values of these parameters say: $Lo \simeq 1000$ Å, $a_o \simeq 1$ Å, $Ep \simeq Eg/2$, $U \simeq Eg \simeq 10k_BT$, and $(\tau_1 + \tau_2) \simeq 10^{-4}$ s ; we find:

$$\sigma'/\sigma \approx Ni'/Ni \qquad 4.3.26$$

Thus ratio of the total conductivity to the D.C. conductivity

is on the order of the ratio of the polarisation charge carrier concentration to the ohmic charge carrier concentration.

According to Vlasova(139,140), EPR and thermal emf studies on polypyridines and polyacrylonitrile at temperatures of 300 °K - 370 °K reveal that the concentration of free charge carriers (ohmic, that is) is about one to two orders of magnitude lower than that of the paramagnetic charge centers, which are believed to be the impurity sites where the donor and/or the acceptor complexes reside (141-143). It is therefore very plausible to assume that Ni'/Ni could be as much as 1000, or more, since a given charge complex site may contribute more than just one carrier. Of course the experimentally observed conductivities are in strong support of the above conjecture.

The dielectric constant is likewise found to be:

$$K' = 1 + (Npe^2 Lo^2 / 4\epsilon_o k_B T) / [1 + w^2 (\tau_1 + \tau_2)^2] \qquad 4.3.27$$

which follows a Debye-type relaxation with a relaxation time of $(\tau_1 + \tau_2)$. The interesting thing to note is that as in the Pohl-Pollak model, K' is proportional to the square of the molecular length.

4.4) Discussion Of The Experimental Results In Light Of Our Simplified Two-Site Model

Before we begin to examine how well our simplified model fairs in accounting for the experimentally observed results, let us note that our model was based on many idealizations in order to keep the mathematics as simple as possible. Thus, at best, our model is meant to be a rough approximation for the purpose of illustrating the mechanisms behind the observed behaviour, and is in no way a true description of reality. Some important compromises were made among which:

1) The assumption that all the potential energy barriers between molecules have the same height. This of course is not true. A more realistic expression can be obtained by assuming a Gaussian distribution, or even a uniform distribution over some range of energies (Frolich (144), Mott & Davis (145)). This will give rise to a corresponding distribution of relaxation times since according to appendix (D) the relaxation times depend on the barrier height.

2) The mathematics can be further complicated by assuming a variable-range hopping, in which the most probable hops are those for which the range R causes $w\tau$ to be $\simeq 1$ $\Rightarrow$

$$b_\alpha R \simeq \ln(\nu_{ph}/w) \qquad 4.4.1$$

Mott & Davis (146) applied this for amorphous organic materials). However, to follow up on this scheme for the case of polymers requires the re-writing of the basic dynamical equations. For the sake of reference, Mott & Davis derived an ex-

pression for the A.C conductivity in amorphous silicon based on the above assumptions, and found it to vary like:

$\sim w\{\ln(\nu_{ph}/w)\}^4$, which when plotted on a log-log scale does give a linear plot having a slope of about 0.8 if ν_{ph} is taken to be $\sim 10^{12}$ s^{-1}.

3) Other refinements such as taking into account the polaron effective mass, the location of the mobility edge with respect to the Fermi level, and the compensation effects in the high impurity concentration systems, can enhance the accuracy of the theory. But the computational labour becomes extremely tedious.

4) Finally, our model ignored intra-molecular motion, and concentrated only on inter-molecular conduction. Thus the relaxation times came out independent of the molecular length Lo. The implication of this is that it will not predict the observed behaviour of the loss factor under large D.C bias. For the very same reasons, our system is described by only two relaxation times as compared to the infinite set given in the Pohl-Pollak model.

With the above in mind, we now assess how our model compares with previously established theories in accounting for the experimental data. To start with, the frequency dependence of the A.C. quantities follows a Debye-type behaviour according to eqs.(4.3.24 & 27). As seen from the theoretical plots in Fig.(145) for the conductivity versus frequency, the slope is greater than the observed values which are in the range of (0.4-0.8). The reason for this is obvious: a single

relaxation time cannot account for slopes below one, because of the nature of the Debye curve. However by employing a superposition of Debye-like functions corresponding to a series of relaxation times, each contributing a certain percentage , we find that it is possible to simulate the experimental data as Fig.(146) indicates. The greater the range of the superposition, the smaller will be the slope of the resulting plot

Similarly the dielectric constant plot (A) shown in Fig. (147) based on eq.(4.3.27) indicates a similar problem. Curve (B), however, which is made up of a superposition of two relaxation times is pretty close the observed shapes. The fact that the observed exponent "s" in the relation : $\sigma' \propto w^s$ is below one (actually lower than the (0.7-0.8) value characteristic of low-molecular weight organic substances), has always been taken as an indication to the existence of a wide distribution of relaxation times (127).

Next we look at conductivity as a function of the temperature as given by (4.3.12) and (4.3.24). Inspection of the experimental results of sec.(3.3C) show that range of variation of the D.C conductivity cannot be accounted for on the basis of the single form (A.x)exp(-B.x), where B is taken equal to the activation energy Ea as determined from the experimental plot, and "A" is chosen to fit the value of σ at the lowest value of x = 1/kT. Thus the function (A.x)exp(-B.x) does not reproduce the same "steepness" of the observed slopes, unless B is chosen greater than "Ea", in which case the fit loses its purpose. In order to achieve more flexibility in the slope

adjustment of the linear fit, we have to allow for some dependence on "x" of both the pre-exponential factor "A", and the parameter "B". As the experimental evidence suggests, we know there is some very slow decrease of "Ea" with x, it is therefore reasonable to let "B" —> $B/(\ln(x))^{\beta}$, where β is a parameter whose value ranges from 0 to 1 (inclusive).
We shall also let "A" --> A/x^{α} , where "α" is a real number positive, negative, or zero. This choice simulates the possibility that in some systems, "C_B" and "Ni" (perhaps), of eq. (4.3.12) can be temperature-dependent.

Fig.(148) shows how different choices for "α" and "β" can affect the slope as well as the range of the variation of the logarithmic plot. Values of $\alpha < 1$ and values of $\beta > 0$ will tend to decrease the slope and the range of the plot, as in case (A), while values of $\alpha \geqslant 1$ and those of β close to 0 will result in much steeper slopes (case C). The plot in (B) corresponds to an intermediate set of values: $\alpha = 0.5$, $\beta = 0.5$ The striking thing about Fig.(148) is that all the plots look extremely linear despite the fact that the actual expression plotted is strictly not a straight line. The reason of course is due to the very small range over which "x" varies: from 38 to 120. In any case the above observations should enable us to realize that even though a logarithmic plot may appear perfectly linear, it does not necessarily correspond to a behaviour like A.exp(B.x), (where A and B are constants). In other words, logarithmic plots cannot be considered reliable enough to deduce the true functional form of a given quantity

because of their extreme insensitivity over the limited range of variation in "x".

A major question that arises naturally, is whether the choice of the parametrs that reproduce a particular slope is unique. The answer, in general (i.e under un-restricted parameter variation), is obviously no. However once the parameters are confined to a specific range justified on physical grounds then the choice for the parameters becomes (almost) unique. For example, in the case of the D.C conductivity plot for LD-105 G, any value of $\beta > 0$ would require values of $\alpha > 1$ in order to produce the same slope of the plot in Fig.(89): For $\beta = 0.1$ we find $\alpha = 1.35$; however this implies that $C_B Ni \simeq$ varies like $(kT)^{1.35}$ which may not reflect a physically acceptable law. The choice $\beta = 0$, gave $\alpha = 0.45$, ($\Longrightarrow$ $C_B Ni \simeq (kT)^{0.45}$ which is not unreasonable considering the short-cuts in our model). Next, since the A.C. conductivity in eq.(4.3.24) follows the same temperature dependence as the D.C case, the foregoing arguments apply. For illustration, we've reproduced a fit for LD-95 (B) at 1 KHz. in Fig.(150), using $\alpha = 1$, and $\beta = 0$. It is seen that the agreement is perfect. The fact that for A.C conduction the intrinsic number density Ni' varies with (kT) possibly differently than Ni does, is another indication supporting the hypothesis that A.C conduction is mediated by a different type particle than in the D.C. case.

Before closing we remark that the plots for the dielectric constant (vs. frequency) and the D.C conductivity (vs.temperature) are self-consistent in the sense that for the 1.114E-4

value selected for the pre-exponential coefficient (==> Ni 1.4×10^{16} $cm.^{-3}$), the value for the dielectric constant came out to be around 88 (at DC) by chosing N_i' to be 0.5×10^{19} $cm.^{-3}$, in good agreement with what has already been discussed in section (4.3B).

Finally there is no need to make theoretical plots for the electric field dependence, since the experimental curves have already been fitted to the theoretical plot of the Rosen-Pohl formula and the agreement is excellent.

FIGURE CAPTIONS

Fig.(145): Debye-type plots for the conductivity based on eq.(4.3.24).

Fig.(146): Effect of the superposition of three Debye-type functions using 60% of the curve corresponding to relaxation time τ = 2E-3 s. , 25% of the one corresponding to 2E-4 s , and 15% of the 2E-5 s. curve. Note the almost perfect linearity, and lowering of the slope value.

Fig.(147): Dielectric constant for: (A) Single relaxation time of 2E-4 s . (B) Superposition using 60% of the curve corresponding to 2E-3 s , and 30% of the 2E-5 s curve.

Fig.(148): Effect of different values of the parameters α & β on the logarithmic plots for the D.C conductivity:

(A) $\alpha = 0.5$, $\beta = 1$ ($\Longrightarrow C_B Ni \propto (k_B T)^{1/2}$ and $Ea \propto 1/\log_e(1/k_B T)$).

(B) $\alpha = 0.5$, $\beta = 0.5$ ($\Longrightarrow C_B Ni \propto (k_B T)^{1/2}$ and $Ea \propto 1/\sqrt{\log_e(1/k_B T)}$).

(C) $\alpha = 1$, $\beta = 0.11$ ($\Longrightarrow C_B Ni \propto k_B T$ and $Ea \propto 1/[\log_e(1/k_B T)]^{0.11}$

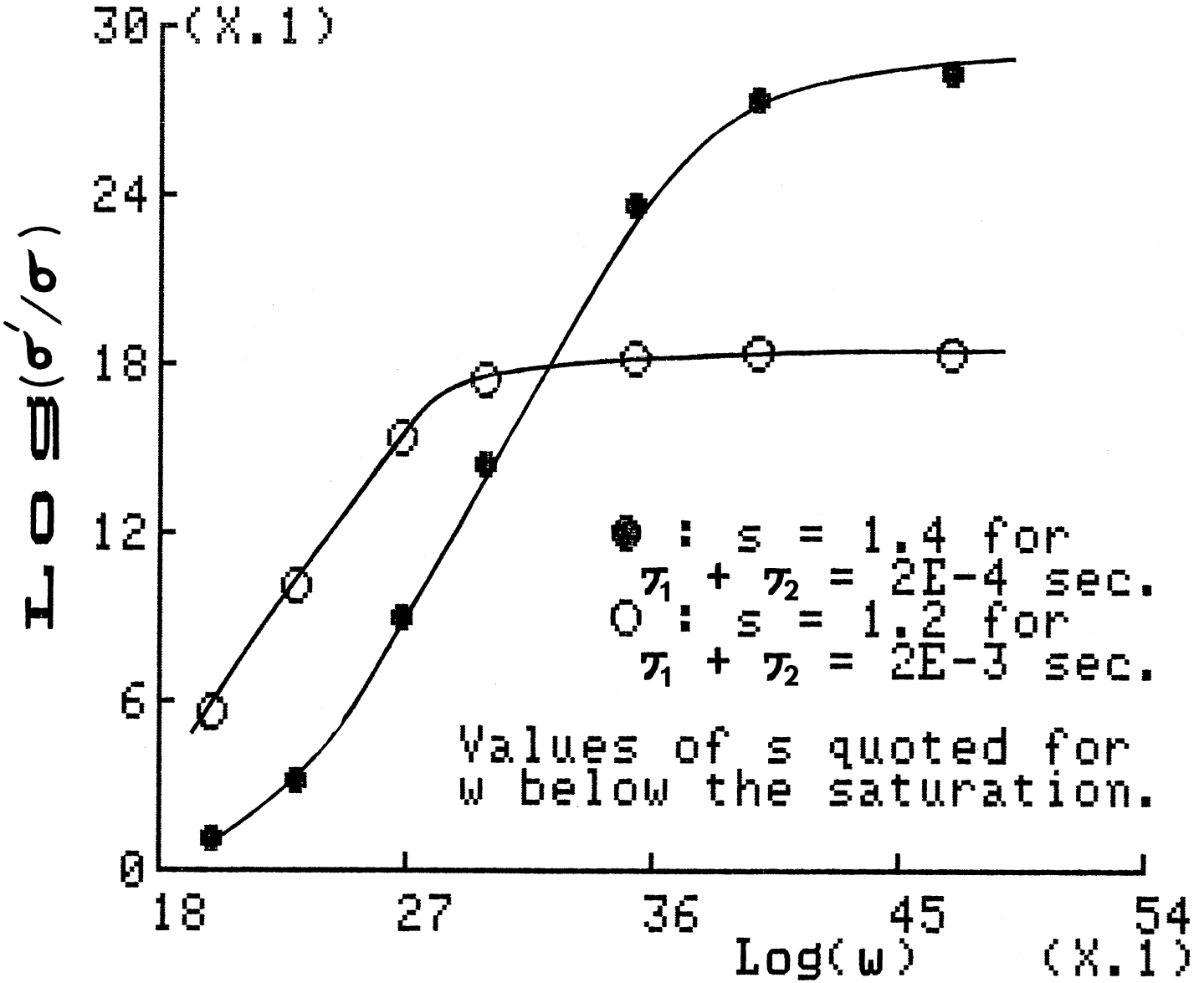
30 (X.1)
24
18
12
6
0
Log(σ'/σ)
● : s = 1.4 for
τ1 + τ2 = 2E-4 sec.
○ : s = 1.2 for
τ1 + τ2 = 2E-3 sec.
Values of s quoted for
w below the saturation.
18
27
36
45
54
Log(w) (X.1)

Fig.(145)

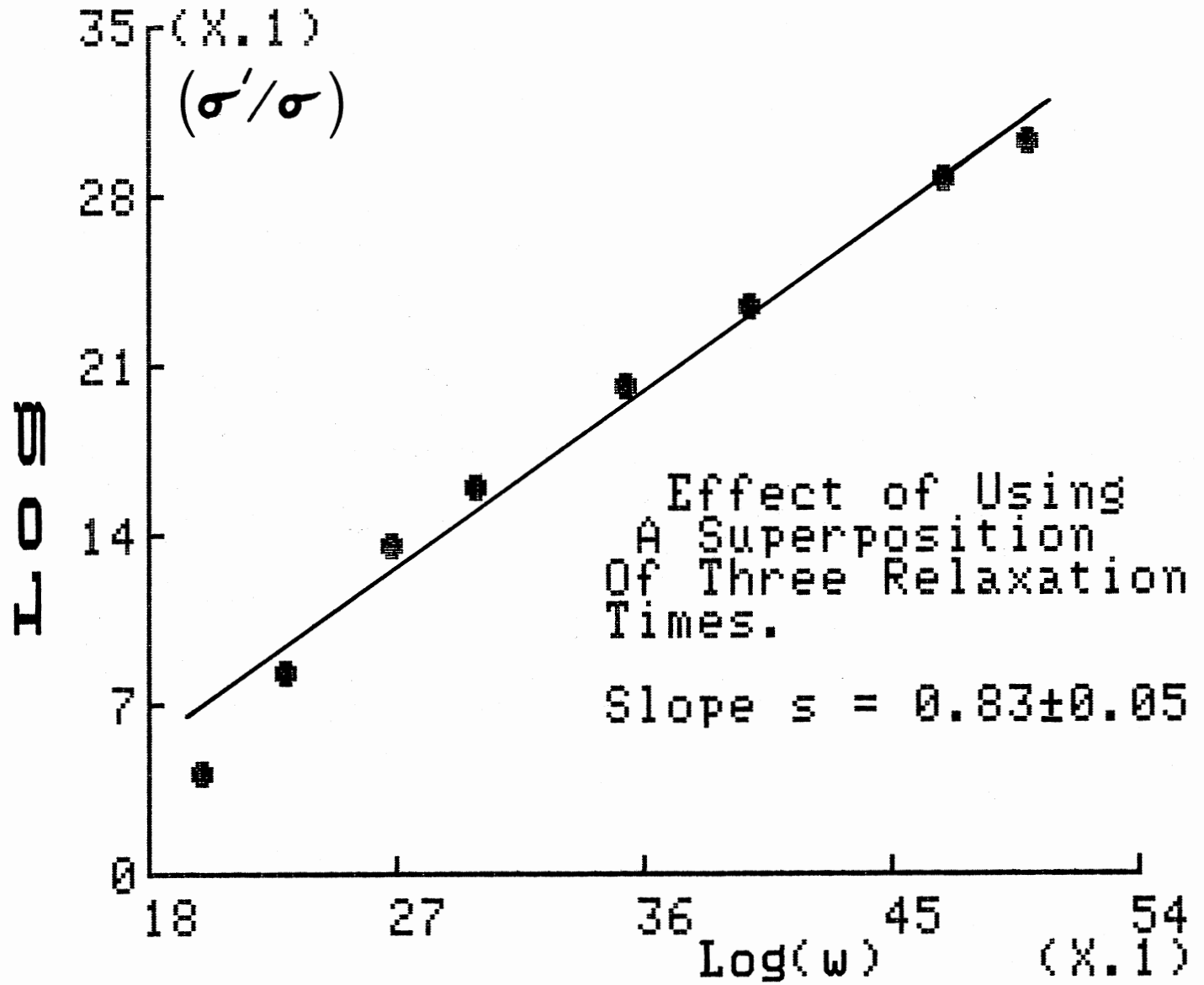
35 (X.1)
(σ'/σ)
28
21
14
7
0
Log
18
27
36
45
54
Log(w) (X.1)
Effect of Using
A Superposition
Of Three Relaxation
Times.
Slope s = 0.83±0.05

Fig.(146)

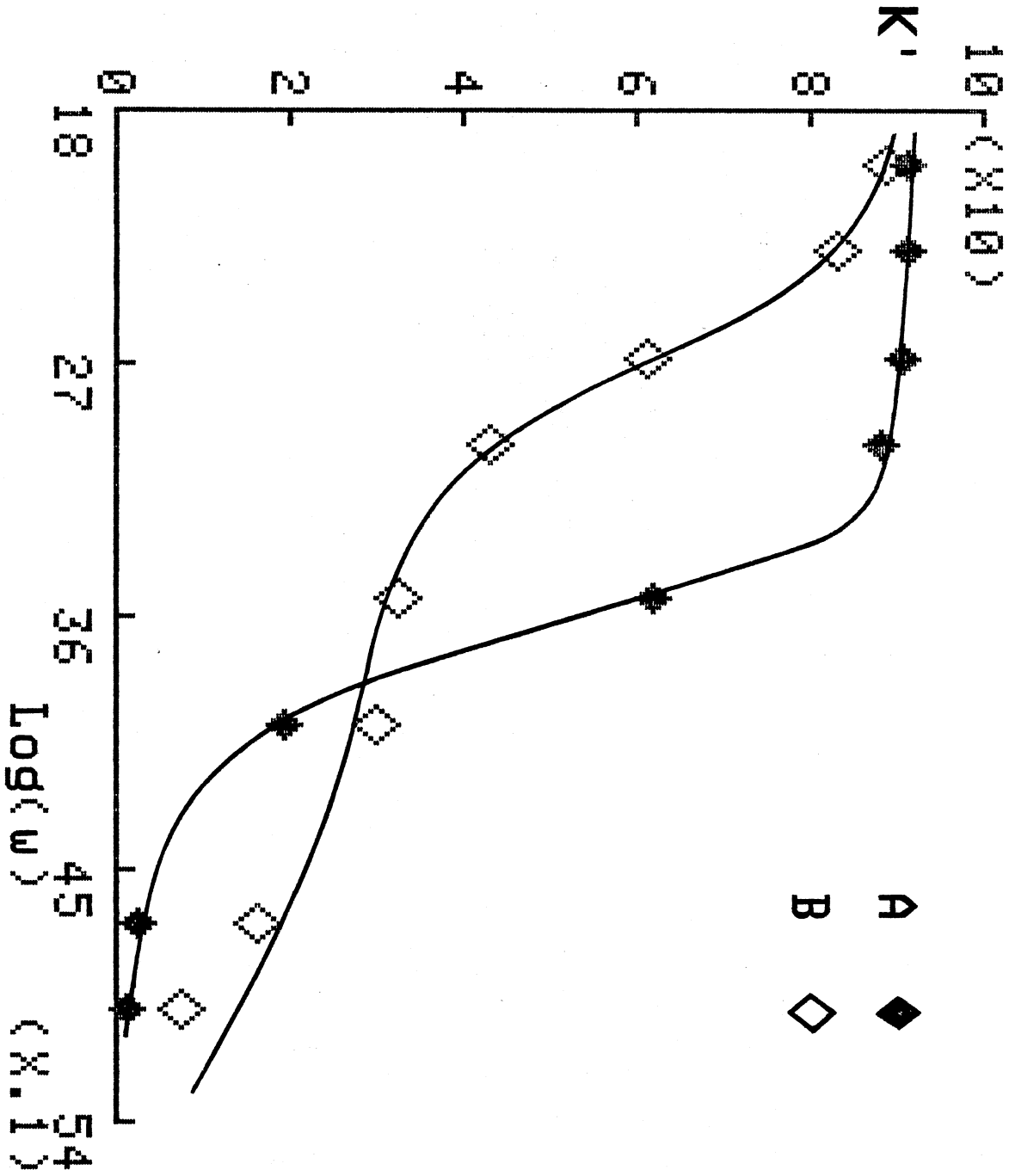

Fig.(147)

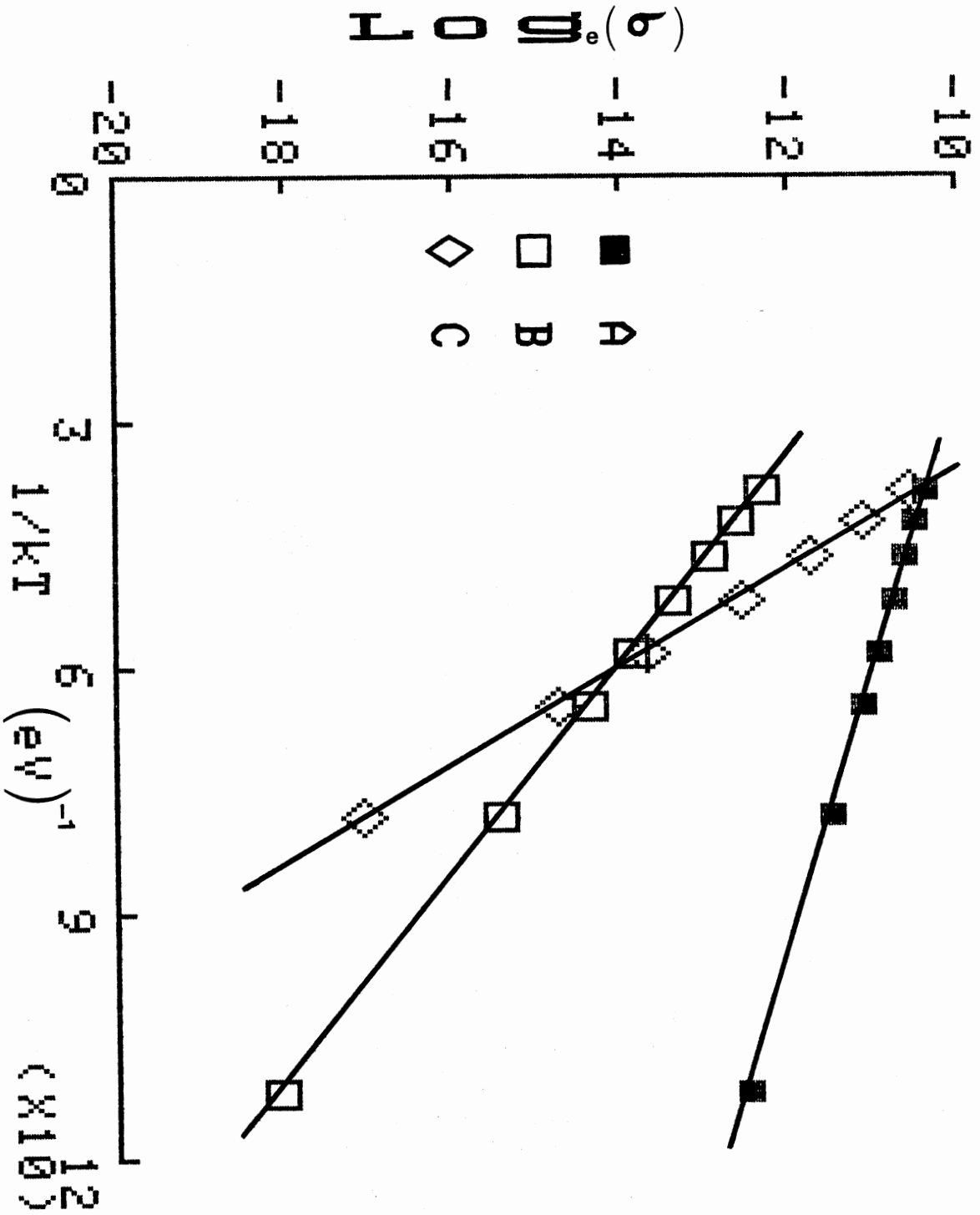

Fig.(148)

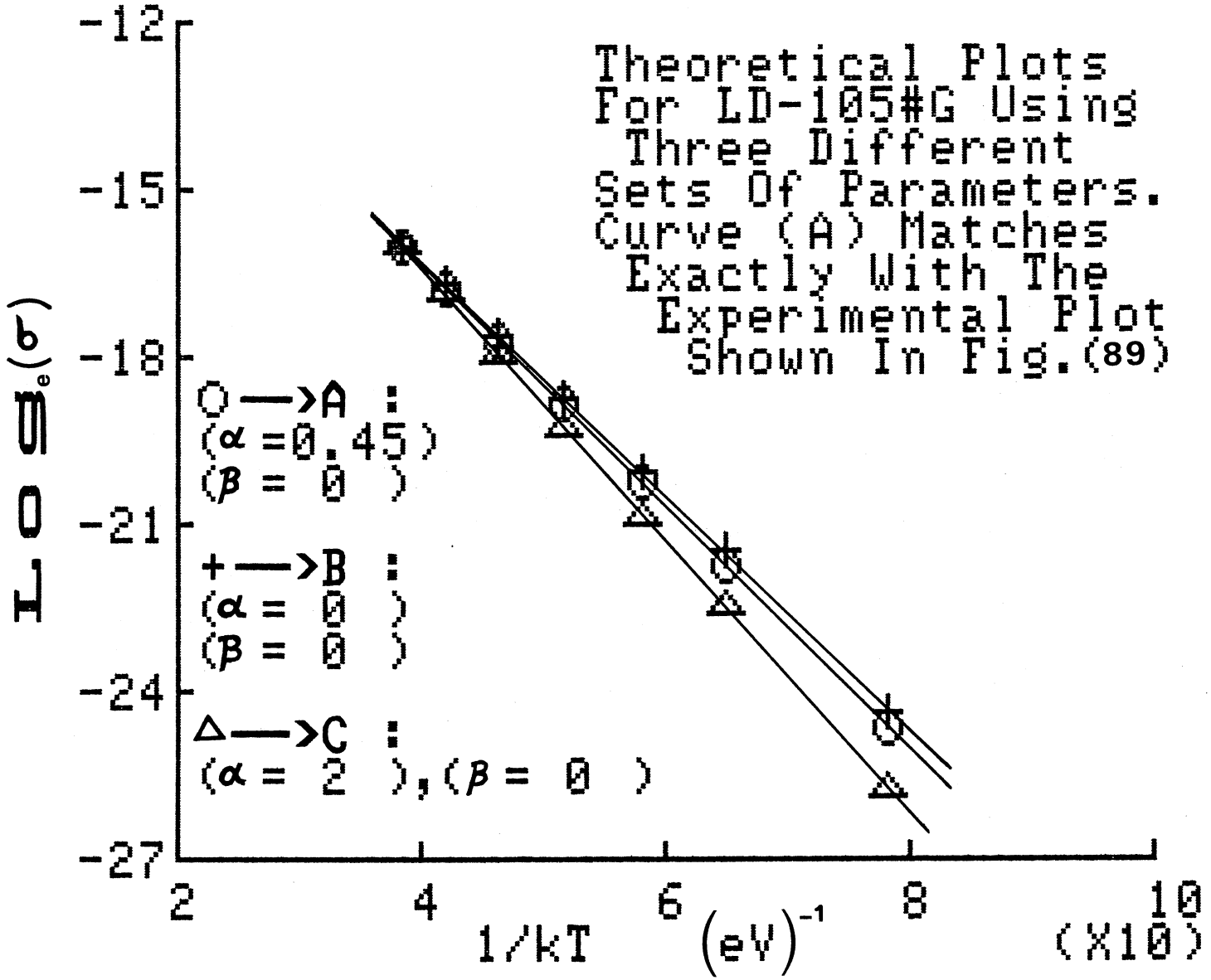
Theoretical Plots
For LD-105#G Using
Three Different
Sets Of Parameters.
Curve (A) Matches
Exactly With The
Experimental Plot
Shown In Fig.(89)
O —>A :
(α =0.45)
(β = 0)
+ —>B :
(α = 0)
(β = 0)
Δ —>C :
(α = 2),(β = 0)
-12
-15
-18
-21
-24
-27
Log σe(σ)
2
4
6
8
10
1/kT (eV)-1
(X10)

Fig.(149)

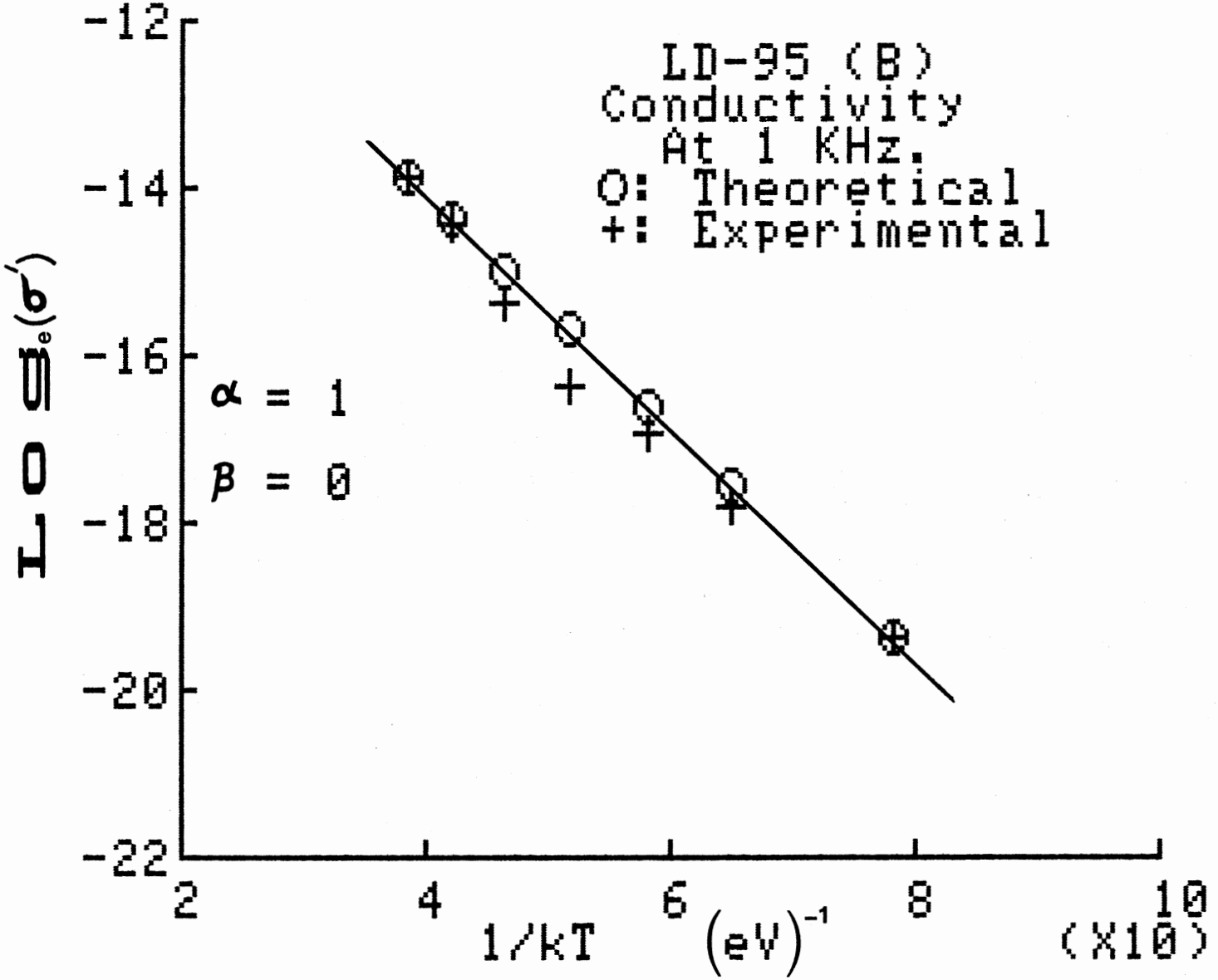
LD-95 (B)
Conductivity
At 1 KHz.
O: Theoretical
+: Experimental
α = 1
β = 0
LOG$_e$(σ')
-12
-14
-16
-18
-20
-22
2
4
6
8
10
1/kT (eV)$^{-1}$
(X10)

Fig.(150)

4.5) Conclusion And Recommendations

The previous sections have shown that electrical conduction and polarisation in polymeric materials can be fairly understood on the basis of a hopping model that ignores the intra-molecular motion, but at the same time takes into account the polarisation of the whole molecule. Certain bold assumptions were required to explain the drastic differences between the D.C and the A.C behaviour. These assumptions were legitimized on the basis of the findings of other authors in this field (117-128,139-141).

As we saw in sec.(4.4), the two-site model is not very successful in the areas of frequency-domain analysis, however it does give us a clear picture as to what is really needed to construct a satisfactory model that will account for all the descripancies. In this regard we feel that the two-site model has served its purpose in the understanding of the phenomena of hyper-electronic polarisation.

This project was primarily undertaken to find means that will help in the synthesis of polymers having negligible loss. From what has been learned it seems that the very quantities that produce larger polarisation (namely Ni' and Lo) also give rise to a higher A.C conductivity and hence larger losses. It looks as though the dielectric constant and the conductivity do not "commute" in the sense that we cannot enhance one property without destroying the better characteristics of the other. Although it does sound like a hopeless situation, there are other quantities that can affect the loss factor but are

not in the picture yet. To see what's involved let us write the expression for the loss factor DM based on the two-site model of sec.(4.2-3). We have according to eqs.(4.3.24 & 27)

$$DM = (Qp/[Qp+\epsilon_o]) \frac{w\tau}{1 + (\epsilon_o/[Qp+\epsilon_o])(w\tau)^2} \qquad 4.5.1$$

where $\tau = \tau_1 + \tau_2$. This is a Debye-type behaviour displaying a "peak" at : $w = (1 + Qp/\epsilon_o)^{1/2}/\tau$ 4.5.2

Consequently by restricting our operational frequency to the "left side" of the peak (i.e. for values of $w << 1/\tau$), we can insure the highest dielectric quality possible since K is greatest in this region while DM is smallest. To be of any practical value, however, τ must be small enough so that $1/\tau$ will be "pushed" farther out along the frequency axis so as to provide a wider operating range. In essence, this means that the probability P', (where $P' = \nu_{ph.}\exp(-b_\alpha R)$), has to be maximized. Which in turn means that a higher phonon frequency is desirable, and a more extended wavefunction (smaller b_α) would be essential.

Physically, this corresponds to lower impurity levels and more order in the lattice, also more "rigid" molecular side groups are needed that will exhibit higher natural frequencies of vibration in order to increase $\nu_{ph.}$

An important piece of correlation is provided between the the total conductivity and the loss factor, by examining the results shown in table (4.1):

It is observed from the table and the corresponding plot in Fig.(151) that there is quite a strong correlation between the ratio σ'/σ and the loss factor DM: The greater the ratio of σ' to σ , the lower will be the loss factor. Which again supports the hypothesis that the A.C. conduction is really a different type of conduction as compared to the conventional ohmic type which is expected to produce higher losses for larger values of the conductivity.

TABLE (4.1)

CORRELATION EFFECTS BETWEEN THE CONDUCTIVITY THE DIELECTRIC PARAMETERS

Polymer	DM	σ'/σ	K	Q
LD-105	1.70	87	64	38
-104	0.64	500	24	38
-97	0.70	290	26	38
-95	1.00	280	18	18
-94	1.80	130	28	16
-14A	0.80	695	12	15
-6A	0.87	170	21	24
-54	0.074	25000	5	68
-52B	0.054	3500	5.5	102
-106	0.30	670	6.8	23

* Q is the "Quality Factor" , which is K/DM

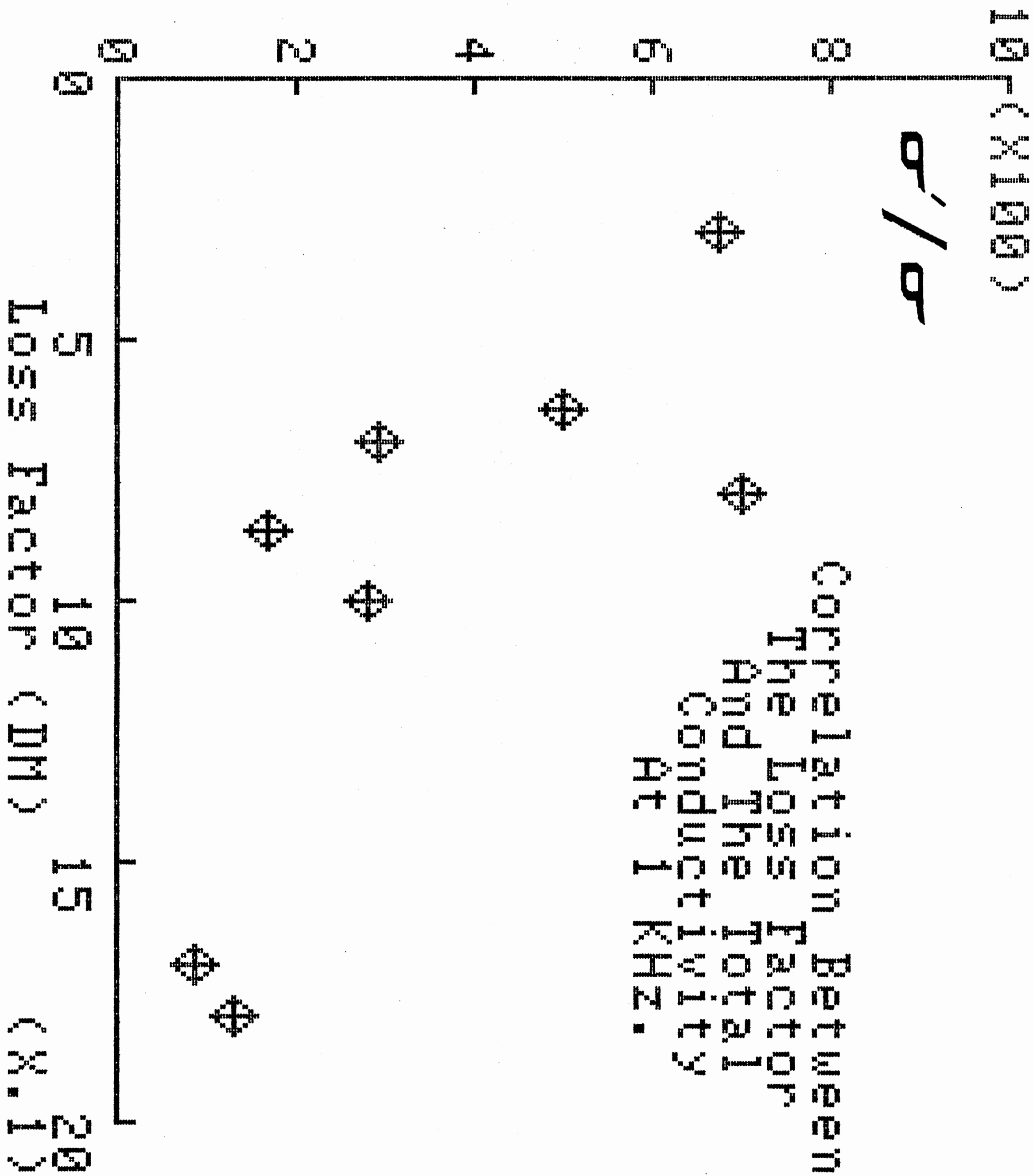
Correlation Between
The Loss Factor
And The Total
Conductivity
At 1 KHz.
σ'/σ
(X100)
Loss Factor (DM)
(X.1)
0
2
4
6
8
10
0
5
10
15
20

Fig.(151)

In closing we mention that in order to obtain promising results in this field of polymers, many other channels of investigation have to be pursued concurrently. Thus in addition to dielectric studies, one must carry more extensive research in the areas of Hall effect and thermo-emf measurements, NMR and EPR spectroscopy, photo-conduction and ionization, also band theory studies for the case of crystalline structures.

As to future recommendations regarding the dielectric studies, we note that a more controlled method for pre-fabricating the polymer samples into thin solid discs instead of powdered samples, will help eliminate many of the reproducibility problems we encountered. Moreover, extensive study of the effects of pressure must be carried to determine whether subjecting the polymer to high pressures does affect its molecular cross-link character. This point is extremely crucial in ascertaining whether two pellets molded from the same powdered material can be regarded as identical systems.

Finally, there are other areas of study that can provide vital information if carried successfully. These are:

1) The dependence of the activation energy (D.C & A.C) on other parameters such as pressure, and D.C electric field.

2) Investigating the same properties we studied at much lower temperatures, and a wider frequency range up to microwaves region.

3) A thorough study of the dependence of the relaxation time(s) on temperature, D.C electric field, and pressure. An analysis of the various distributions employing time-of-flight

technique can be a powerful method in determining the Fourier components, and hence the relaxation time modes.

4) Intensive correlation studies related to the chemical aspect of the polymers, such a systematic study of the effects of impurities, replacement of the side groups, and compensation effects between donors / acceptors ratios, can provide useful information to help optimize the features of a given species.

5) Investigative study of a wide variety of monomers to select the best possible candidates that comply with what has been recommended for lowering the loss factor. This last point is perhaps the most basic of all the others, and we feel that it should be pursued first, or at least concurrently with (4).

Despite the fact that our own undertaking was not supplemented by any of the above topics, we have managed to compile a good deal of very informative data which as we have seen, did show relatively good agreement with existing models. And although we have barely "scratched the surface" of this multidisciplinary field, we do believe our attempt was worthwhile.

REFERENCES

1. R. Rosen and H. Pohl, J. Poly. Sci. 4-A1, 1135 (1966).

2. R. Hartman and H. Pohl, J. Poly. Sci. 6-A1, 1135 (1968).

3. H. Pohl and E. Englehardt, J. Phys. Chem. 66,2085 (1962)

4. M. Kaplan, P. Schmidt, C. Chen, and W. Walsh, J. Appl. Phys. Letters 36 (10), 867 (1980).

5. R. Greene, G. Street and L. Suter, Phys. Letters 34, 577 (1975).

6. A. Garito and A. Heeger, Accts. Of Chemical Research 7, 232 (1974).

7. J. Wyhof and H. Pohl, J. Poly. Sci. 8-A2, 1741 (1970).

8. H. Pohl and M. Pollak, J. Chem. Phys. 63 (7), 2980 (1975).

9. H. Pohl And M. Pollak, J. Chem. Phys. 66 (9), 4931 (1977).

10. A. Pocchetino, Acad. Kinei. Rendiconti 15, 355 (1906).

11. A. Szent-Gyorgi, Science 93, 609 (1941).

12. R. Fuoss, "The Chemistry Of Large Molecules" Eds. R. Burks and O. Grummitt, Interscience, N.Y., 1943.

13. R. Fuoss and J. Kirkwood, Amer. Chem. Soc. 63, 385 (1941).

14. J. Kirkwood and R. Fuoss, J. Chem. Phys. 9, 329 (1941).

15. R. Fuoss, J. Amer. Chem. Soc. 63, 378 (1941).

16. R. Fuoss, J. Amer. Chem. Soc. 63, 2401 (1941).

17. R. Fuoss and J. Kirkwood, J. Amer. Chem. Soc. 63, 369 (1941).

18. M.I.T, "Tables Of Dielectric Materials" Vol.1 (1944), Vol.2 (1945), Vol.3 (1948).

19. R. Fujishiro And A. Kotera, J. Chem. Phys. (Japan) 70, 114 (Pure Chemistry Section), (1949).

20. F. Wurstlin, Kolloid-Z 120, 84 (1951).

21. H. Akamatsu and H. Inokuchi, J. Chem. Phys. 18, 810 (1950).

22. A. Many, E. Harnik, and D. Gerlich, J. Chem. Phys. 23, 1733 (1955).

23. G. Cardwell and D. Eley, Disc. Faraday Soc. 27, 115 (1959).

24. D. Eley and D. Spivey, Trans. Fraday Soc. 156, 1432 (1960).

25. A.J. Curtis "Progress In Dielectrics" Vol. II Eds. J. Birks and J. Schulman, John Wiley & Sons, N.Y., 1960, p.31.

26. G. Mikhailov, A. Lobanov, and B. Sazhin, Zhur. Tekh. Fiz. 24, 1553 (1954).

27. G. Mikhailov, J. Poly. Sci. 30, 605 (1958).

28. G. Mikhailov and T. Borisova, Zhur. Tekh. Fiz. 23, 2159 (1953).

29. G. Mikhailov, S. Kabin, and B. Sazhin, Zhur. Tekh. Fiz. 25, 590 (1955).

30. G. Mikhailov, B. Sazhin, and N. Kuprianchik, Zhur. Tekh. Fiz. 27, 948 (1957).

31. E. Hoff, D. Robinson, and A. Willbourn, J. Poly. Sci. 18, 161 (1955).

32. T. Nakajima and S. Saito, Bull. Electrotech Lab. (Japan) 21, 161 (1957).

33. T. Nakajima and S. saito, Bull. Electrotech Lab. (Japan) 21, 802 (1957).

34. J. Gibbs and E. De Marzio, J. Chem. Phys. 28, 378 (1958).

35. W. Reddish, Trans. Faraday Soc. 46, 459 (1950).

36. H. Pohl, "Proc. Fourth Conference On Carbon" Ed. S. Mrozowski, Pergamon Press, 1960, p.241.

37. H. Pohl and J. Laherrere, "Semiconduction In Molecular Solids" Ed. H.Pohl, Ivy-Curtis Press, Phila., 1960, p.93

38. H. Pohl, Chem. Engineering 68, 104 (1961).

39. H. Pohl, Electro - Technology 67, 85 (1961).

40. H. Pohl, J. Bornman and W. Itoh, "Organic Semiconductors" Eds. J.Brophy and J. Buttrey, Macmillan, N.Y, 1962, p.142

41. op. cit #40, p.134.

42. H. Pohl, A. Rembaum, and A. Henry, J. Amer. Chem. Soc. 84, 2699 (1962).

43. H. Pohl and D. Opp, J. Phys. Chem. 66, 2121 (1962).

44. H. Pohl and R. Rosen, "Proc. Fifth Conf. On Carbon" Ed. S. Mrozowski, Pergamon Press, N.Y, 1963, p.113.

45. H. Pohl, C. Gogos, and C. Cappas, J. poly. Sci. 1A, 2207 (1963).

46. H. Pohl, "Prog. Solid State Chemistry" Vol.1 Ed. H.Reiss, Pergamon Press, N.Y., 1964, p.316.

47. H. Pohl and R. Chartoff, J. Poly. Sci. 2A, 2728 (1964).

48. H. Pohl, "Electronic Aspects Of Biochemistry", Academic Press, N.Y., 1964.

49. R. Kepler, P. Bierstedt, and R. Merrifield, Phys. Rev. letters 5, 503 (1960).

50. R. Kepler, J. Chem. Phys. 39, 3528 (1963).

51. H. Akamatsu, H. Inokushi, and Y. Matsunaga, Bull. Chem. Soc. Japan 29, 213 (1956).

52. H. Akamatsu, H. Inokushi, and Y. Matsunaga, Nature 175, 168 (1954).

53. I. Shirotani, H. Inokushi, and S. Minomura, Bull. Chem. Soc. Japan 39, 386 (1966).

54. R. Hartman, "Hyper-Electronic Polarization And Related Electronic Properties Of Macro-Molecular Solids: Organic Semi-Conduction", Ph.D. Thesis, Oklahoma State University Stillwater, Oklahoma 1968.

55. H. Pohl and J. Wyhof, J. Non-Cryst. Solids 11, 137 (1972).

56. H. Pohl, J. Biol. Phys. 2, 113 (1974).

57. R. Pethig and H. Pohl, "Workshop Of The National Founda-

tion For Cancer Research Marine Biological Laboratory", Oklahoma State Research Note # 65, (1976).

58. P. Vijaykumar and H. Pohl, J. Poly. Sci. 22, 1439 (1984).

59. P.S. Vijaykumar, "Giant Polarization In Stable Polymeric Dielectrics", Ph.D Thesis, Oklahoma State University,1984

60. A. Charlesby, Proc. Phys. Soc. 57, 496 and 514 (1945), and A215, 187 (1952).

61. P. Alexander, A. Charlesby, and M. Ross, Proc. Roy. Soc. 223, 392 (1954).

62. P. Alexander and A. Charlesby, J. Poly. Sci. 23, 355 (1957)

63. R. Black and B. Lyons, Nature Lond.180, 1346 (1957).

64. O. Sissman and C. Bopp, "Physical Properties Of Irradiated Plastics", ORNL 928 (1951).

65. J. Fowler and F. Farmer, Nature Lond. 171, 1020, (1953).

66. ibid 173, 317 (1954).

67. ibid 174, 136 And 800 (1954).

68. ibid 175, 516, 590 , And 648 (1955).

69. J. Fowler and F. Farmer, Brit. J. Radiology, N.S. 24, 118 (1956).

70. A. Chapiro, J. Chem. Phys. 47, 747 (1950).

71. A. Chapiro, M. Magat, J. Sebban, and P. Wahl, "Symposium On Macromolecular Chemistry", Milan (1954).

72. A.Chapiro and E. Migirdycyan, J. Chem.Phys. 52, 439 (1955).

73. W.A. Little, Phys. Rev. 134, A1416 (1964).

74. W.A. Little, Sci. Amer. 212, 21 (1965).

75. W.A. Little, J. Poly. Sci. 17C, 3 (1967).

76. M.L. Cohen, Rev. Mod. Phys. 36, 240 (1964).

77. A.K. Jonscher, "Physics Of Dielectrics" Ed. C.H. Goodman, Institute Of Physics, Bristol, 1980, p.22.

78. R.H. Cole, "Physics Of Dielectrics" Ed. C.H. Goodman, Institute Of Physics, Bristol, 1980, p.1.

79. L.A. Dissado and R.M. Hill, Nature 279, 685 (1978).

80. R.M. Hill and L.A. Dissado, Nature 281, 286 (1979).

81. L.K. Ngai, A.K. Jonscher, and C.T. White, Nature 277, 185, (1979).

82. H. Pohl and J. Laherrere, "Proc. Fourth Conf. On Carbon" Ed. S. Mrozowski, Pergamon Press, 1960, p.259.

83. P. Debye, "Polar Molecules", Chemical Catalog Co., N.Y., 1929; (And Dover, 1947).

84. K.S. Cole and R.H. Cole, J. Chem. Phys. 9, 341 (1949).

85. D.W. Davison and R.H. Cole, J.Chem. Phys. 18, 1417 (1951)

86. A.G. MacDiarmid and A.J. Heeger, " Organic Metals And Semiconductors: The Chemistry Of Polyacetylene, (CH)x, And Its Derivatives", Synthetic Metals 1, 101 (1979-80)

87. K. Chiang, A. Heeger and A.G. Macdiarmid, Ber. Bunsenges. Phys. Chem. 83, 407 (1979).

88. A.S. Davydove, "Theory Of Molecular Excitons", McGraw Hill, N.Y., 1962.

89. V.M. Kenkre and P. Reineker, "Exciton Dynamics In Molecular Crystals", Springer Verlag N.Y., 1982.

90. R.S. Knox, "Theory Of Excitons", Academic Press, N.Y., 1963.

91. C. Kittel, "Solid State Physics" 5th. ed., John Wiley & Sons, N.Y., 1976, p.370

92. J. Wyhof and H. Pohl, J. Poly. Sci. 10-A1, 387 (1972).

93. Von Hippel, "Dielectrics And Waves", M.I.T Press 3rd.ed. John Wiley & Sons, N.Y., 1962, p.93-100

94. H. Frohlich, "Theory Of Dielectrics" 2nd. ed., Clarendon Press, Oxford, 1958, p.22-61.

95. B. Scaife, "Complex Permittivity", English Univ. Press, 1971, p.25

96. M. Pollak, Proc. Royal Soc. Lond. A-325, 383 (1971).

97. A. Miller and E. Abrahams, Phys. Rev.120 (3),745 (1960).

98. R. Boyd, "Methods Of Experimental Physics" Vol.16 part C Ed. R. Fava, Academic Press, N.Y, 1980, p.379.

99. G. Williams, Polymers 4, 27 (1963).

100. J. Hopkinson, "Original Papers", Vol.2, Cambridge Univ. Press, 1901, p.119.

101. W. Reddish, "Pure And Applied Chemistry", Vol.5, Butterworth, London, 1962, p.723.

102. B. Hamon, "Proc. Instn. Elect. Engrs.", 99, part IV, Monograph 27, (1952).

103. R. McIntosh, "The Dielectric Behaviour Of Physically Adsorbed Gases", Marcel Dekker, N.Y, 1966. p.88-103 & 111-120.

104. W. Reddish, Trans. Faraday Soc. 46, 459 (1950).

105. S. Ono, T. Kuge, and N. Koizumi, Bull. Chem. Soc. Japan, 31, 34 (1958).

106. S. Hottman and H. Pohl, Rev. Sci. Instr. 42 (3), 387 (1971).

107. P.Chester and G.Jones, Phil. Magazine 44, 1281 (1953).

108. H. Wintle and S. Kurylowicz, IEEE Trans. Instr. Measur. IM-34 (1), 41 (1985).

109. American Institute Of Physics Handbook 3rd. edition, McGraw Hill Co., N.Y. (1972), p.5-131/2.

110. Handbook Of Plastics & Elastomers, C.Harper ed., McGraw-Hill Co., N.Y. (1975), p.2-12/13 & 16.

111. L. Dunn, W. Ford, N. Hilal, P.S. Vijayakumar,and H. Pohl J. Poly.Sci. 22 (Polymer Physics Edition), 2243 (1984).

112. G. Samara and H. Drickamer, J. Chem. Phys.37, 474 (1962).

113. R. Aust, W. Bentley, and H. Drickamer, J. Chem. Phys. 41, 1856 (1964).

114. W. Bentley and H. Drickamer, J. Chem. Phys. 42, 1573 (1965).

115. Y. Okamoto, I. Chang, and M. Kantor, J. Chem. Phys. 41, 4010 (1964).

116. A.V. Airapetyants and R.M. Vlasova, Elektrokhimiya 1, 1400 (1965).

117. A. Berlin, L. Boguslavski, R. Burshtein, N. Mateeva, A. Sherle, and N. Shurmovskaya, Dokl. Akad. Nauk. SSSR. 136,

1127 (1961).

118. C. Higgins and A. Sharnaugh, J. Chem. Phys. 38, 393 (1963).

119. A. Vannikov, L.P. Sidorova, V.I. Yakovenko and N.A. Bakh, Elektrokhimiya 2, 1474 (1966).

120. I. Storbeck and M. Starke, Ber. Bunsenges. Phys.Chem. 89, 343 (1965).

121. D. Eley and G. Parfitt, Trans. Faraday Soc. 51, 1529 (1965).

122. C. Garrett, "Organic Semiconductors", Radiation Research Supplement 2, 340 (1960).

123. C. Huggins and A. Sharnaugh, "Dielectric Properties Of Some Powdered Organic Semiconductors", J. Chem.Phys. 38, 393 (1963).

124. K.C. Kao and W. Hwang, "Electrical Transport In Solids", Pergamon Press, 1981, p.39-41.

125. S. Kabashima and T.Kawakubo, J. Phys. Soc. Japan 24, 493, (1968).

126. L. Boguslavski and A. Vannikov, J. Electrochem. Soc. 111, 755 (1964).

127. op. cit. #(124), p.41

128. A.K. Jonscher, J. Non-Cryst. Solids 8-10, 239 (1972).

129. A. Ioffe, "Proc. Int. Conf. Electron Transport", Can. J. Of Phys. 34, 1342 (1956).

130. O.H. Le Blanc Jr., J. Chem. Phys. 35, 1725 (1961); erratum J. Chem. Phys. 36, 1082 (1962).

131. G. Thaxton, R. Jarnagin, and M. Silver, J. Phys. Chem. 66, 2461 (1962).

132. J. Katz, S. Rice, S. Choi, and J. Jortner, J. Chem. Phys. 39, 1683 (1963).

133. R. Silbey, J. Jortner, and S. Rice, J. Chem. Phys. 42, 733 (1965); errata J. Chem. Phys. 43, 2925 (1965).

134. S. Glarum, J. Phys. Chem. Solids 24, 1577 (1963).

135. P.W. Anderson, " On The Absence Of Diffusion In Certain

Random Lattices", Phys. Rev. 109, 1492 (1958).

136. op. cit. #(94), p.68-73.

137. N. Mott and E. Davis, "Electronic Processes In Non - Crystalline Materials", Clarendon Press, Oxford, 1979, p.16-25.

138. J. Slater, "Quantun Theory Of Molecules And Solids", Vol.1, McGraw-Hill, N.Y., 1963.

139. R.M. Vlasova and A.V. Airapetyants, Fiz. Tverd. Tela. 7, 3079 (1965).

140. R. Vlasova, S. Gasparyan, V. Kargin, L. Rozenshtein, and V. Kholmogorov, Dokl. Akad. Nauk SSSR. 156, 647 (1964).

141. N. Bakh, A. Vannikov, A. Grishina, and S. Nizhinii, Usp. Khim. 34, 1733 (1965).

142. A. Dulov, A.Slinkin, A. Rubinshtein, and I. Kotlyarevskii Dokl. Akad. Nauk SSSR. 143, 1355 (1962).

143. A. Dulov, A. Slinkin, and A. Rubinshtein, Izv. Akad. Nauk SSSR., 26 (1964).

144. op. cit. #(94), p.90-98.

145. op. cit. #(137), p.32-37.

146. op. cit. #(137), p.59-61.

147. P. Le Comber and J. Mort, " Electronic And Structural Properties Of Amorphous Semiconductors.", Academic Press London, 1973, p.47.

148. M. Cohen, J. Non-Cryst. Solids 4, 391 (1970).

149. H. Fritzsche, J. Non-Cryst. Solids 6, 49 (1971).

150. A. Gubanov, "Quantum Theory Of Amorphous Conductors.", Consultants Bureau, N.Y., 1965.

151. J. Marshall and A. Owen, Phil. Mag. 24, 1281 (1971).

SELECTED BIBILIOGRAPHY

Boguslavskii, L.I, and Vannikov, A.V, "Organic Semiconductors And Biopolymers.", Plenum Press, N.Y., 1970.

Coelho, R., "Physics Of Dielectrics For The Engineer.", Elsevier, 1979.

Daniel, V., "Dielectric Relaxation." Academic Press, N.Y., 1967.

Hill, N., Vaughan, W., Price, A., and Davis, M., "Dielectric Properties And Molecular Behaviour." Van Nostrand Reinhold Co., London - New York, 1969.

Kao, K.C, and Hwang, W., "Electrical Transport In Solids.", Pergamon Press, Oxford, 1981.

Mott, N., and Davis, E., "Electronic Processes In Non-Crystalline Materials.", Clarendon Press, Oxford, 1979.

Le Comber, P., and Mort, J., "Electronic And Structural Properties Of Amorphous Semiconductors.

APPENDIX (A)

CALIBRATION PROCEDURES AND RESULTS

1) Calibration Of The Schering Bridge Loss Factor Dial

Let us consider a purely resistive element Rp whose value has been accurately determined, and with high precision (refer to part "2"). The resistor Rp is chosen from a material that obeys Drudes theory of ohmic conduction so that there is no need to worry about its frequency dependence over the range of frequencies we are interested in, namely (0.1 - 100) KHz.

If (C_L, D_L) are the open-terminal readings of the bridge when balanced at frequency "w",we may think of the loss factor D_L as arising from a fictitious resistor Ro across the bridge terminals, in parallel with the lead capacitance C_L , Ro will be given by:

$$Ro = 1/(wD_L C_L) \qquad A.1$$

Consequently when the resistor Rp is connected to the bridge terminals the equivalent resistance across the bridge's terminals will be:

$$Rx = RoRp/(Ro + Rp) \qquad A.2$$

This means that under ideal conditions (i.e. assuming Rp does not have any intrinsic capacitance of its own), the readings of the bridge dials (at balance) will become: (Cx,Dx) where:

$$Cx = C_L \quad \text{and} \quad Dx = 1/(wCxRx) \qquad A.3$$

It follows from eq.(A.2 & 3) , that :

$$Dx.Cx = D_L.C_L + 1/(wRp) \qquad A.4$$

$$\text{or : } Dx = D_L + Dm \quad \text{where } Dm = 1/(wRpC_L) \qquad A.5$$

Consequently, if the bridge dials are accurate, a plot of Dx versus Dm (corresponding to different values of Rp), should reveal a straight line having a slope of unity and an intercept equal to D_L. Otherwise, the dial readings have to be corrected accordingly. We note that for the above reasoning to be valid, it is implicitly assumed that the capacitance dial readings are correct and true. For our system this was indeed the case: the capacitance dial was checked against standard air capacitors having better than 0.1% precision, and almost zero loss-factor (so as not to be dependent on the loss-dial reading no matter what its condition might be). The readings always came out to be within (0.2-0.5)% of the air standard values. Of course at higher losses the capacitance readings will have more error due to the inter-dependence between the loss-factor dial and the capacitance dial, especially if the loss-factor dial is already in error.

In principle, the value of the "Y"-intercept in the plot of Dx versus Dm should agree with the (un-calibrated) open - terminal reading D_L. However, this is not the case, possibly due to an accumulation of errors from the calibration of the high-value resistors (in the range of (50 - 1000)MΩ) which are used in the low-loss reading range. Whatever the case might be, the graphical plot is considered accurate enough

to give a reliable value of the intercept, since most of the graph points are from high-loss values (Dm >> D_L). We note that the value of D_L as determined from the plot and from the open-terminals readings are really not that much different, for example at 100 Hz. D_L = 0.043 from direct reading, while from the graphical plot D_L = 0.03 . Yet we have to accept the intercept value of D_L as the "true" (un-calibrated) value in order that the graphical analysis be self-consistent. Finally the true (corrected) value of D_L , or any other nominal dial value, is obtained through the graphical plot:

$$Dx(\text{nominal}) = a.Dm(\text{true}) + b \qquad \text{A.6}$$

Where "a" and "b" are determined from the graph.

At frequencies higher than 100 Hz., it was found necessary to divide the range of Dx into "low" and "high" values, since the plots were not extremely linear but showed a consistently repeated pattern whereby the high values have slopes close to one, while the low values are about 20% greater.

Figs.(152-163) show the calibration plots at the frequencies indicated. The errors quoted reflect the uncertainties in both the computational linear fit and the uncertainties in reading the loss-dial divisions as well as the error estimates on the values of Rp (listed in part "2").

Finally we note that all readings were taken under guarded circuit conditions. The resitors Rp themselves being housed in a special, guarded box holder whose capacitance with and without the resistors Rp was carefully checked for any variation

before its value was included as part of the lead capacitance C_L. A sample of the programs used in the processing of the raw data for calibration is given at the end of the appendix (A) for the 0.50 and the 1 KHz. cases. Also included is a sample of the 25 programs used in the processing of the measurements data under different macroscopic conditions.

2) Determination Of The Resistors Rp Used In The Bridge Loss-Dial Calibration, And In The Calibration Of The Internal Resistance Rg Of The D.C. Electrometer

All the resistors used in the calibration were chosen to be either the four-color ceramic or metal film types, or the sealed-in-glass ultra precision wire type. Resistors under the 10 MΩ range were determined to within 0.1% using a Hewlett-Packard model HP-3468A digital multimeter. Those above the 10 MΩ range were determined to within (1-3)%. These resistors were then employed in the calibration of the internal resistance Rg of the Keithly model 610-B DC electrometer at various settings of its "amperes" selection dial. The method consists of using a known voltage source in series with the electrometer and the pre-determined resistor Rp. From the reading of the current in the loop, the total resistance is computed and the internal resistance Rg is accounted for as the difference between the total and Rp. The results of these measurements are given in table (A.1)

TABLE (A.1)

ELECTROMETER CALIBRATION

Electrometer Setting		Rg
10^{-11}	(MΩ)	100,700 ± 800
10^{-10}		10,800 ± 200
10^{-9}		995 ± 12
10^{-8}		98.5 ± 1.5
10^{-7}		9.6 ± 0.7
10^{-6}		1.02 ± 0.05
10^{-5}	(KΩ)	97 ± 2
10^{-4}		9.98 ± 0.08
10^{-3}	(Ω)	995 ± 5

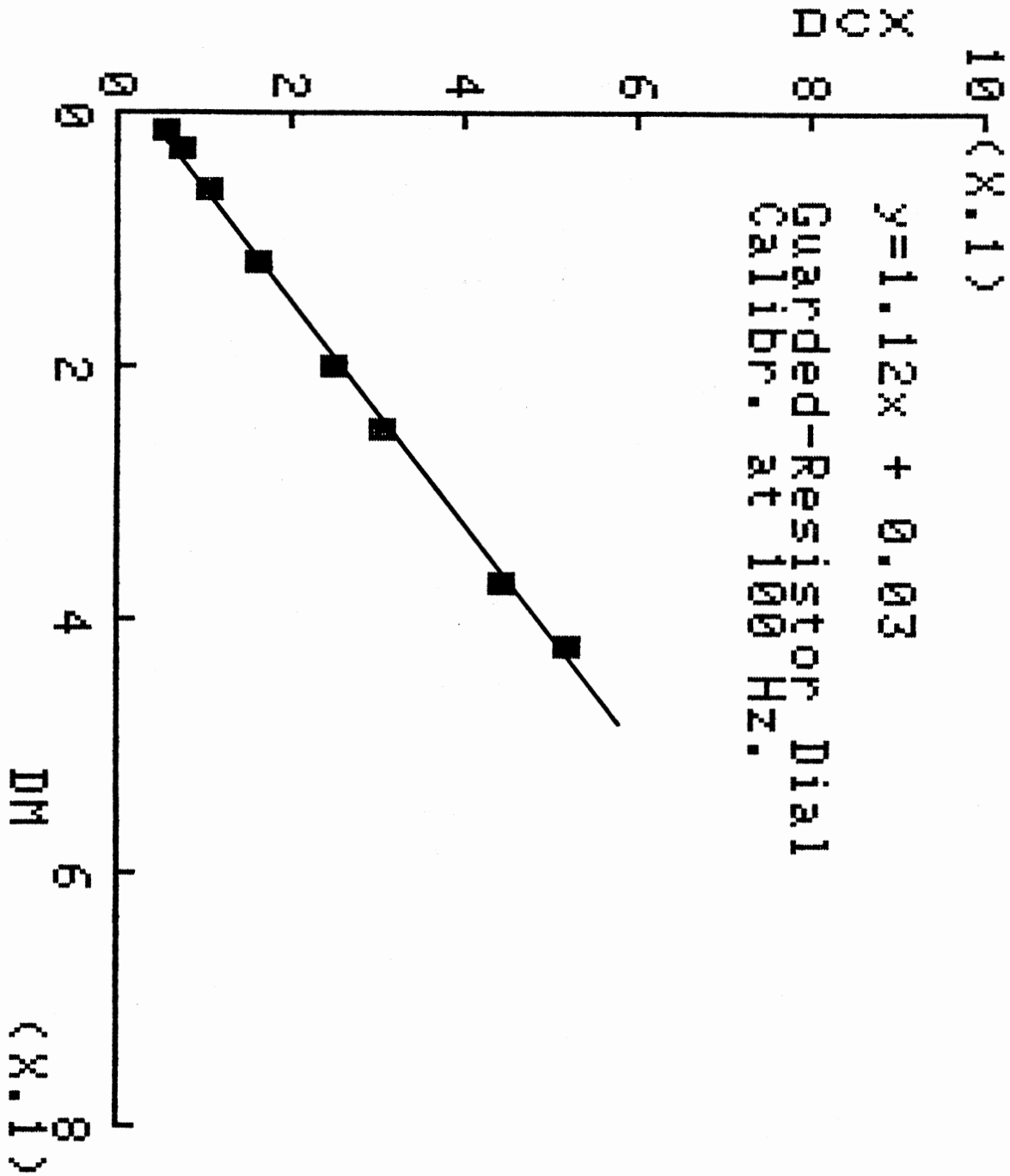
DCX
0
2
4
6
8
10
(X.1)
DM
0
2
4
6
8
(X.1)
Y=1.12X + 0.03
Guarded-Resistor Dial
Calibr. at 100 Hz.

Fig.(152)

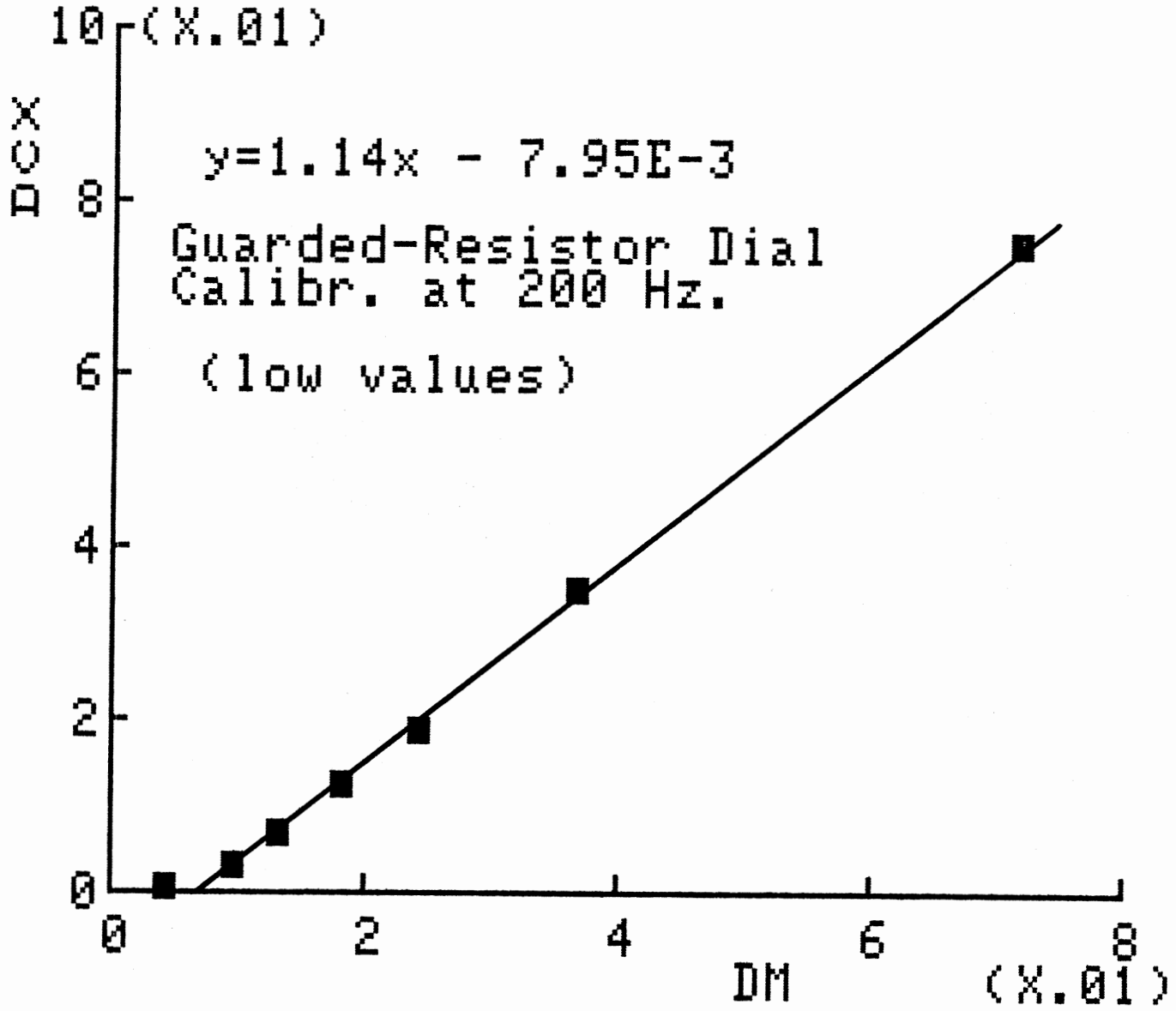
10 (X.01)
DCX
y=1.14x - 7.95E-3
Guarded-Resistor Dial
Calibr. at 200 Hz.
(low values)
8
6
4
2
0
0
2
4
6
8
DM
(X.01)

Fig. (15)

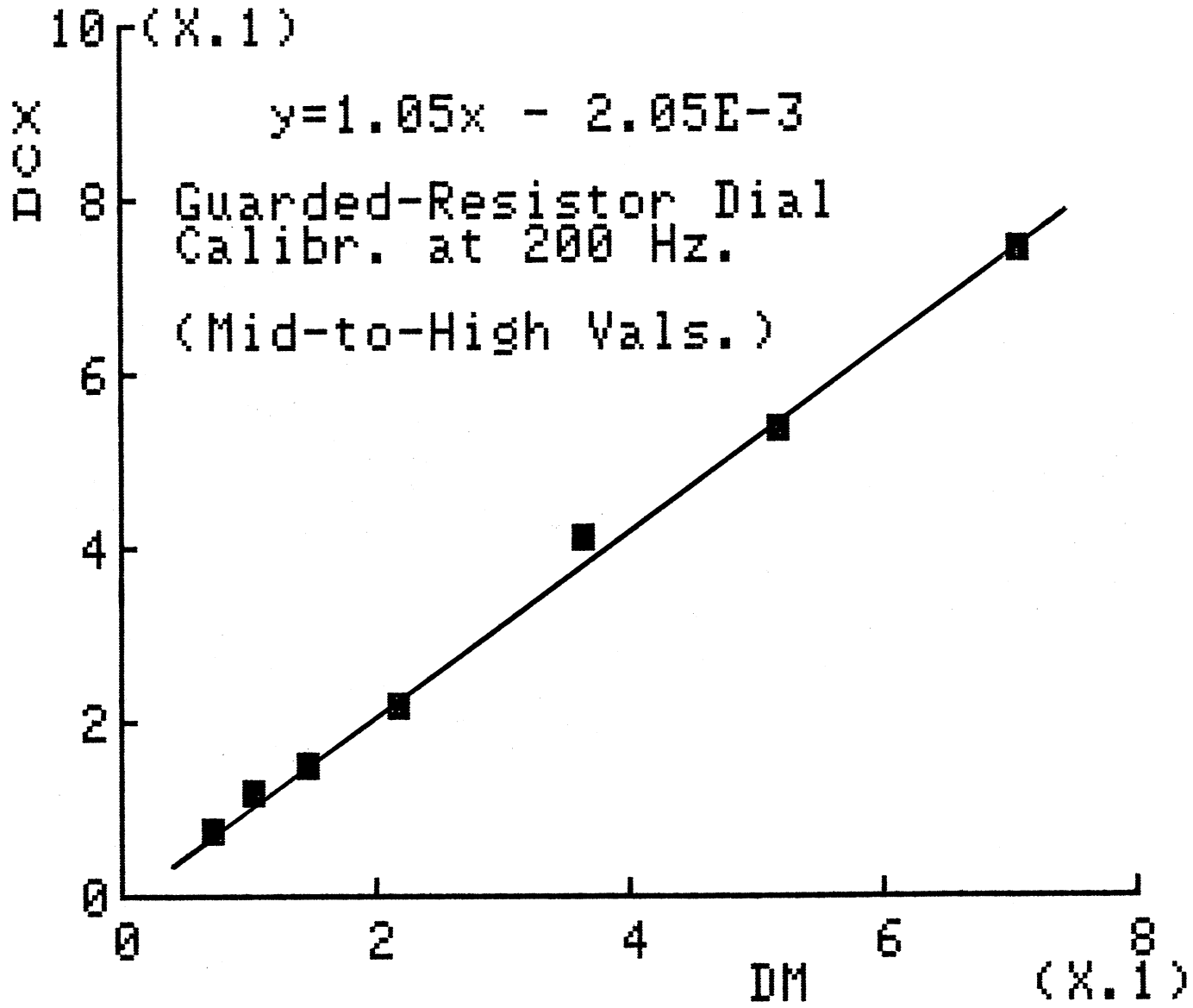
10 (X.1)
y=1.05x - 2.05E-3
DCX
8
Guarded-Resistor Dial
Calibr. at 200 Hz.
(Mid-to-High Vals.)
6
4
2
0
0
2
4
6
8
DM
(X.1)

Fig. (154)

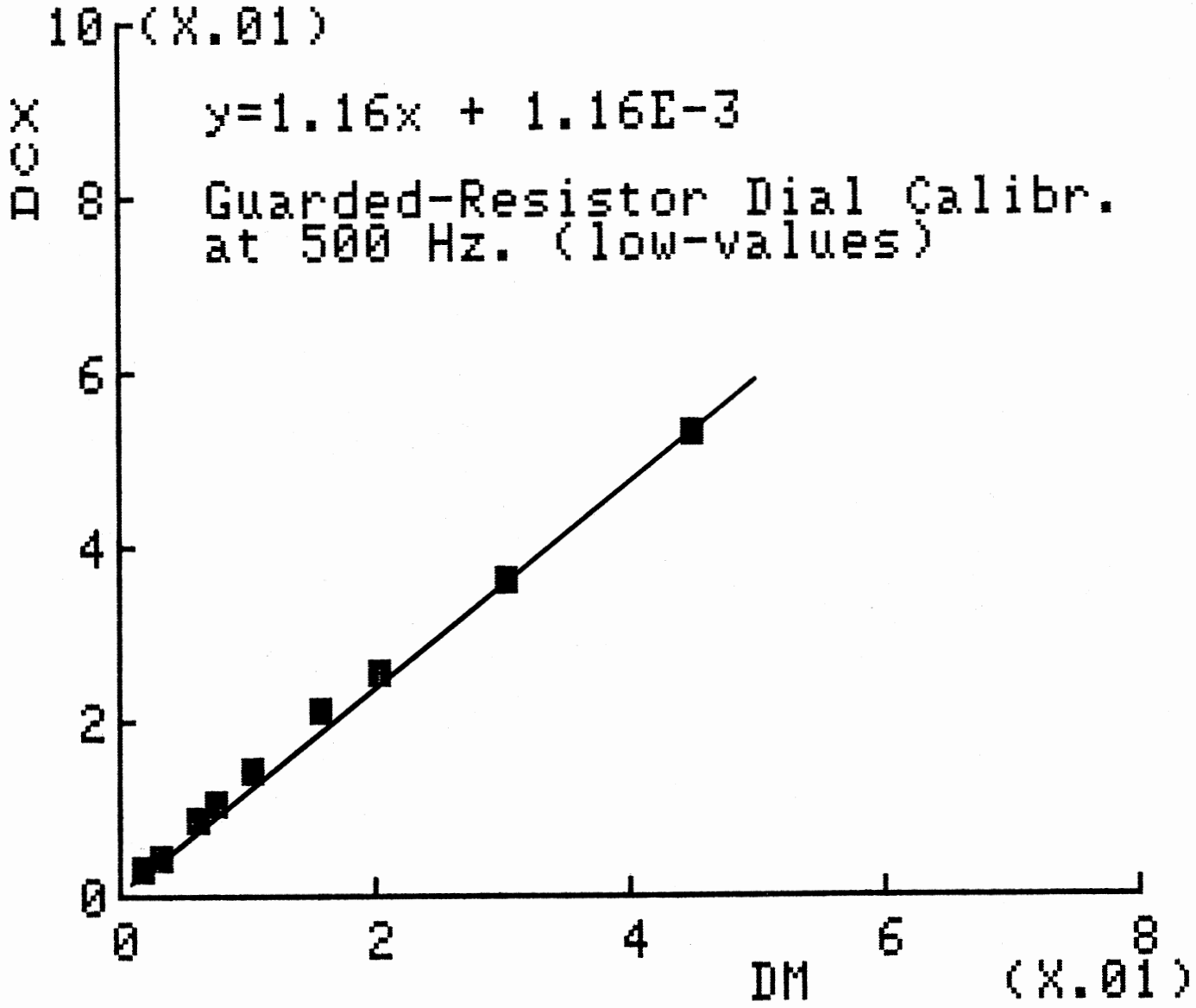
10 (X.01)
DCX
8
6
4
2
0
y=1.16x + 1.16E-3
Guarded-Resistor Dial Calibr.
at 500 Hz. (low-values)
0
2
4
6
8
DM
(X.01)

Fig. (155)

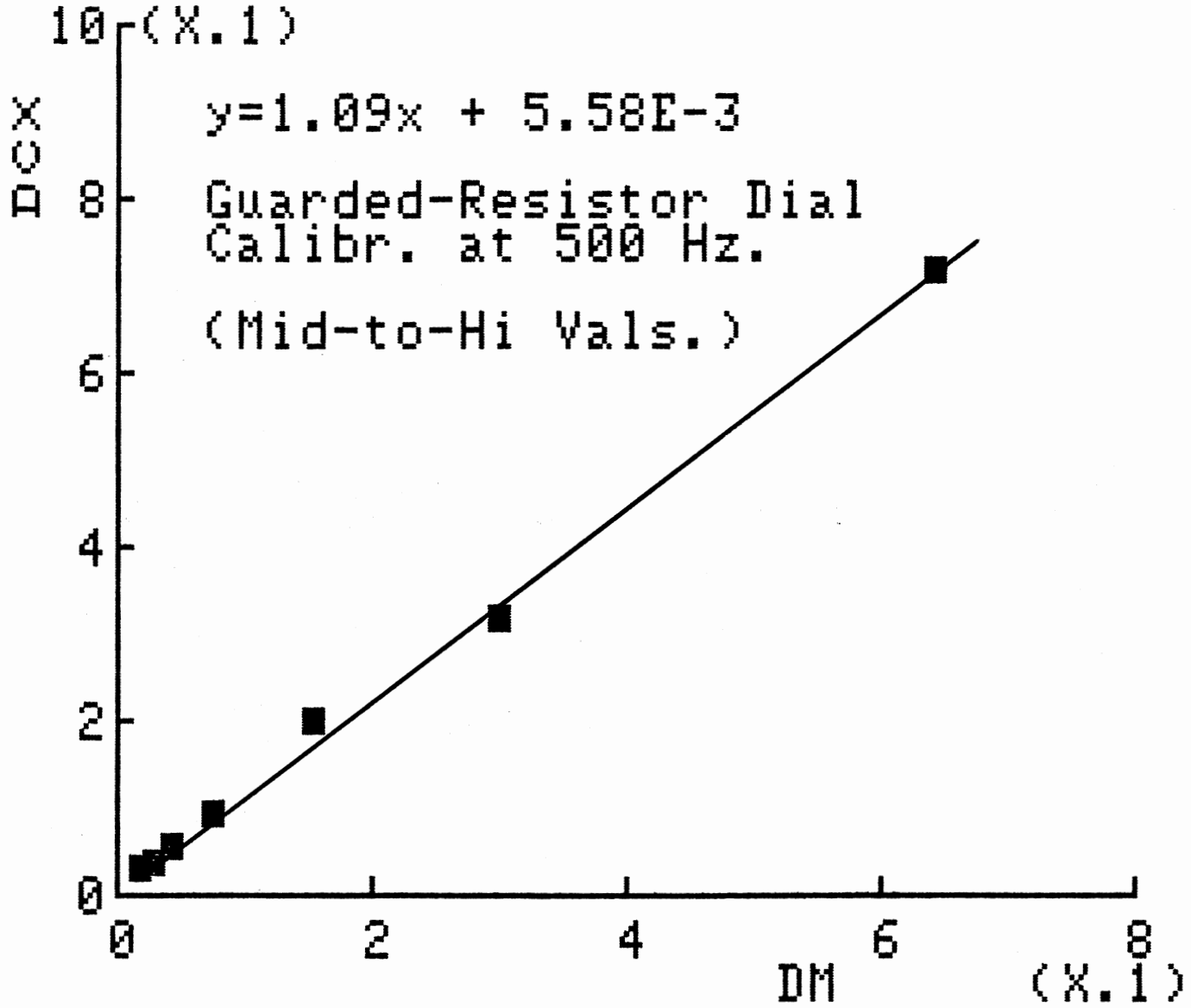
10 (X.1)
DCX
8
6
4
2
0
y=1.09x + 5.58E-3
Guarded-Resistor Dial
Calibr. at 500 Hz.
(Mid-to-Hi Vals.)
0
2
4
6
8
DM
(X.1)

Fig. (156)

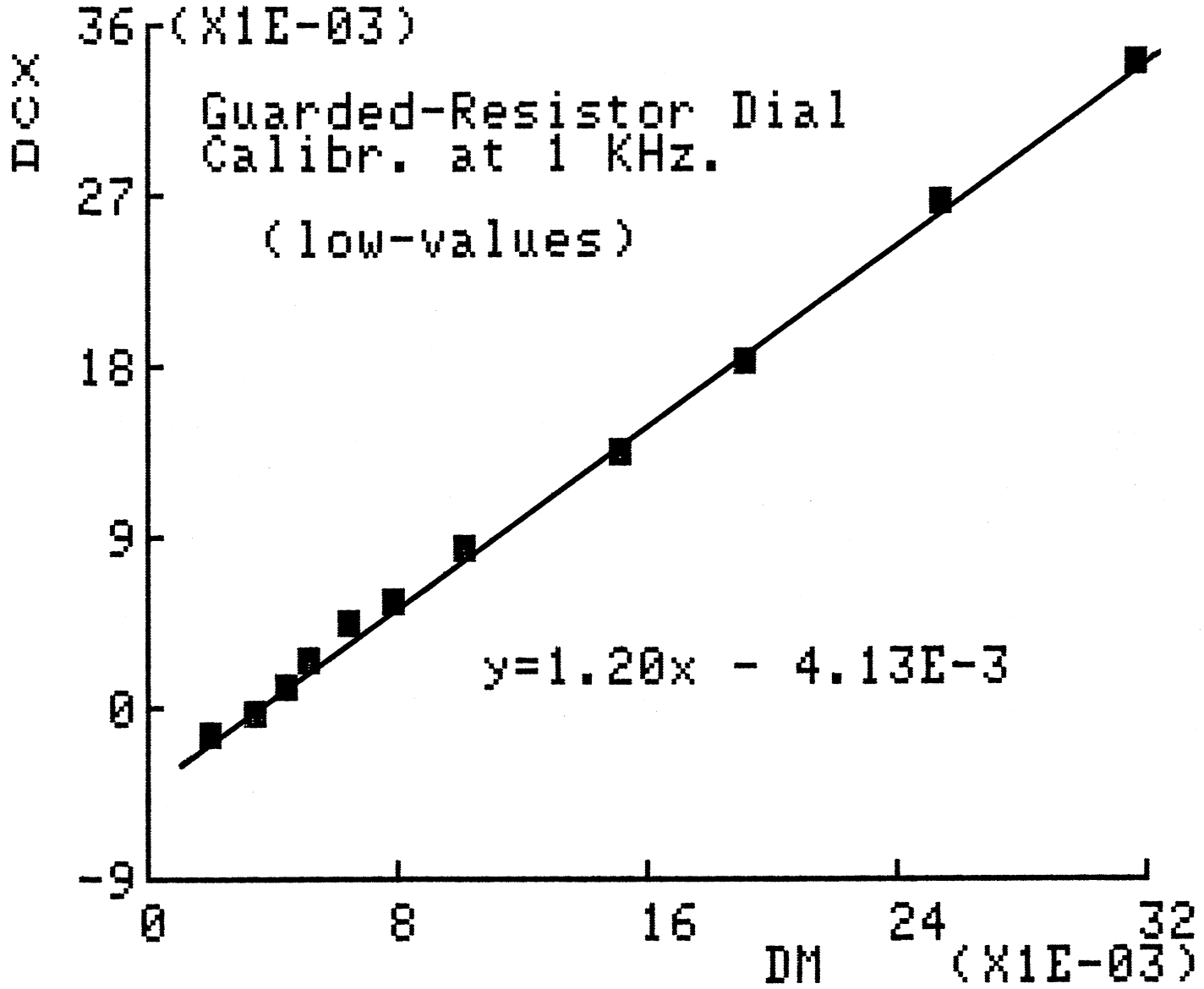
ΔCx
36 (X1E-03)
27
18
9
0
-9
Guarded-Resistor Dial
Calibr. at 1 KHz.
(low-values)
y=1.20x - 4.13E-3
0
8
16
24
32
DM (X1E-03)

Fig. (15)

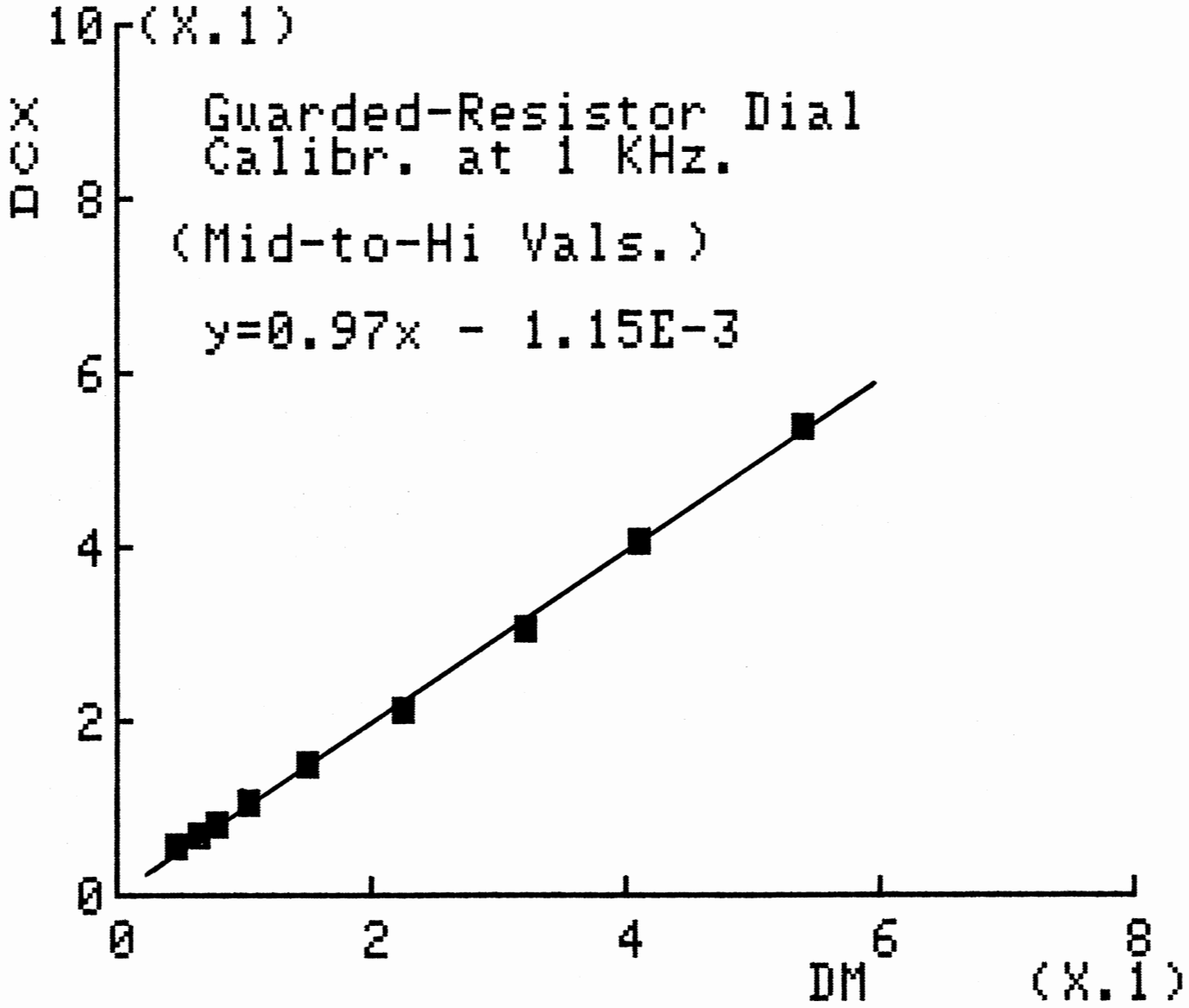
10 (X.1)
DCX
8
6
4
2
0
Guarded-Resistor Dial
Calibr. at 1 KHz.
(Mid-to-Hi Vals.)
y=0.97x - 1.15E-3
0
2
4
6
8
DM
(X.1)

Fig. (158)

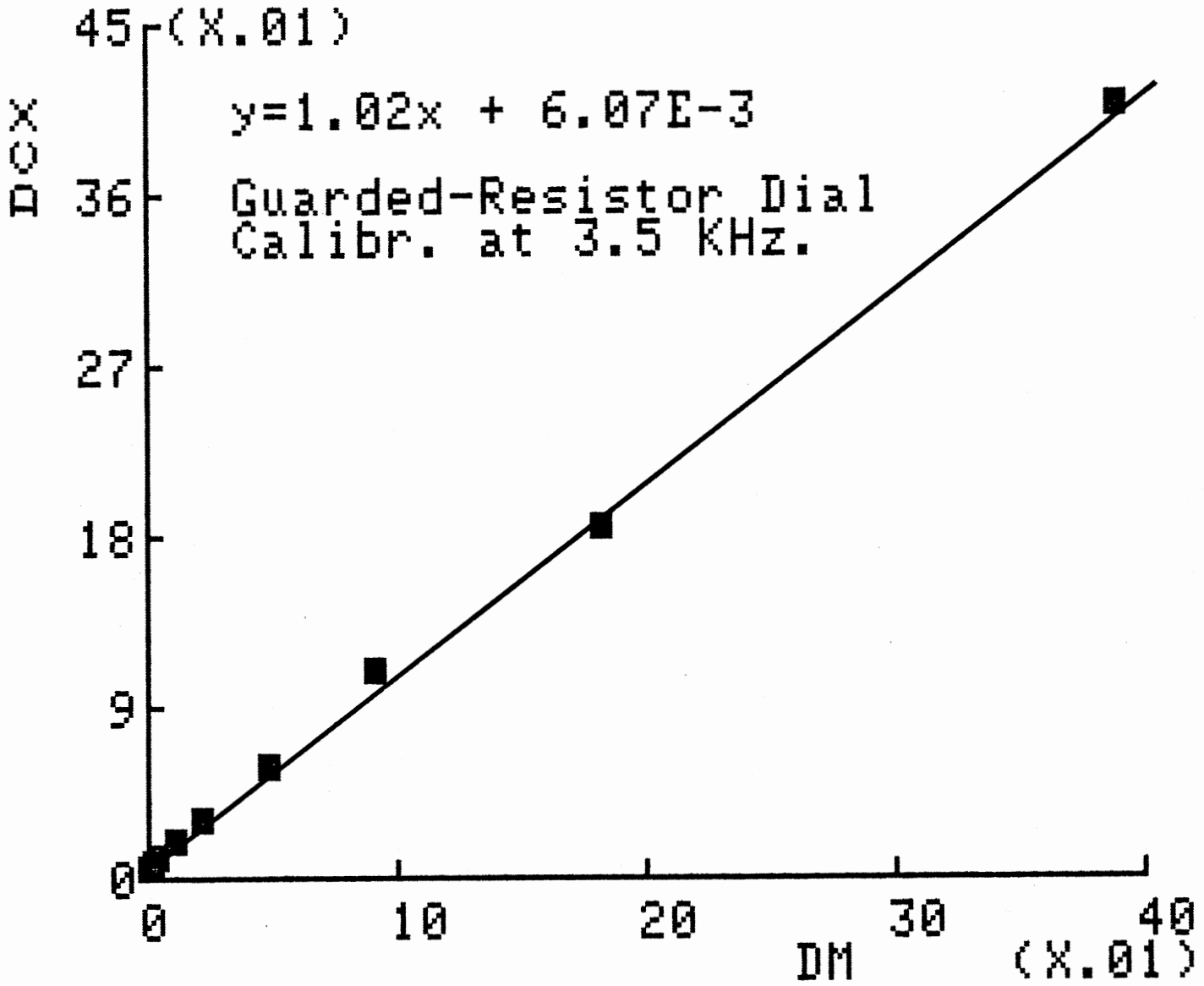
45
(X.01)
y=1.02x + 6.07E-3
Guarded-Resistor Dial
Calibr. at 3.5 KHz.
DX
36
27
18
9
0
0
10
20
30
40
DM
(X.01)

Fig.C (15A)

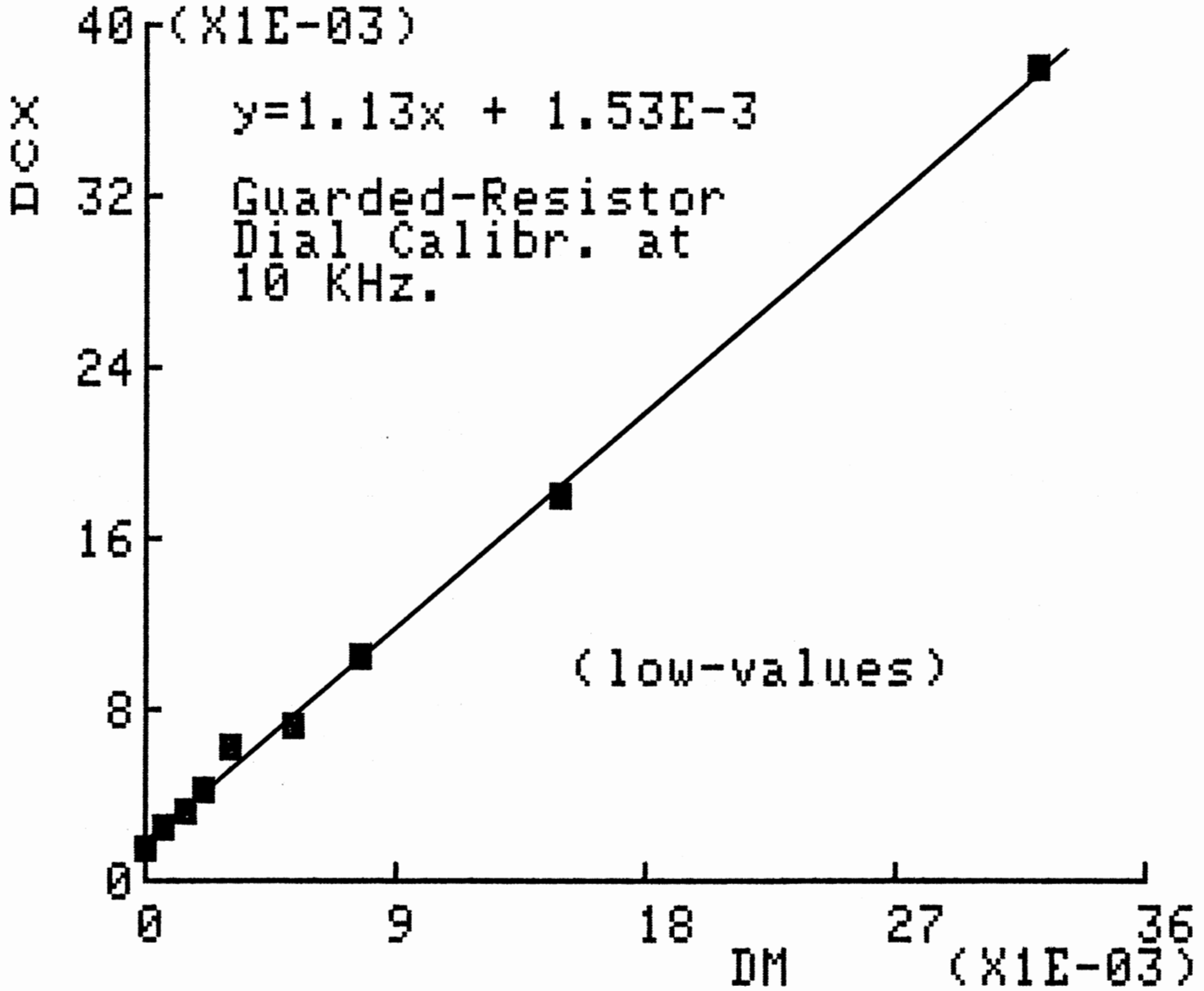
40
(X1E-03)
y=1.13x + 1.53E-3
Guarded-Resistor
Dial Calibr. at
10 KHz.
32
24
16
8
0
(low-values)
0
9
18
27
36
DM
(X1E-03)

Fig.(160)

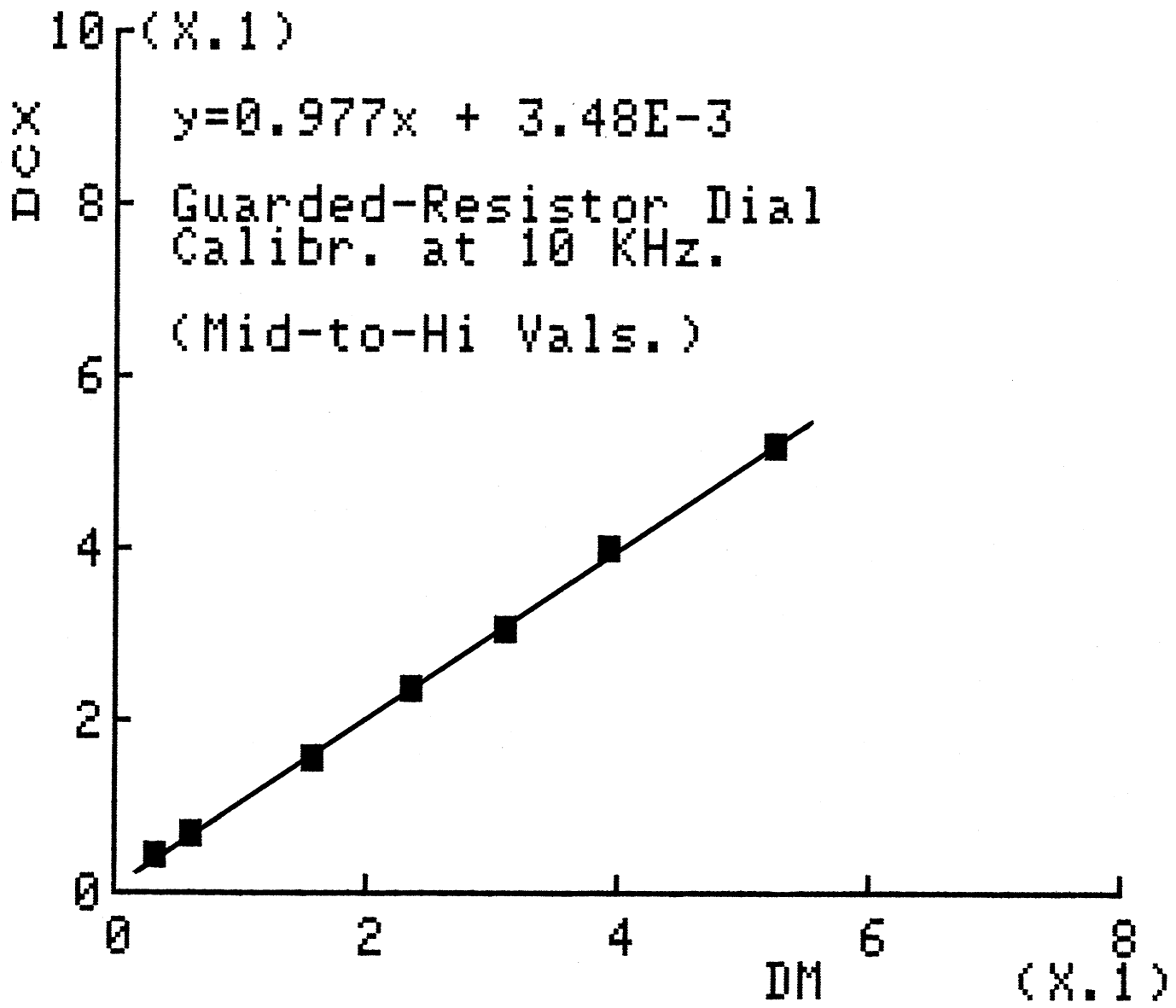
10 (X.1)
y=0.977x + 3.48E-3
Guarded-Resistor Dial
Calibr. at 10 KHz.
(Mid-to-Hi Vals.)
DUT X
8
6
4
2
0
0
2
4
6
8
DM
(X.1)

Fig. (161)

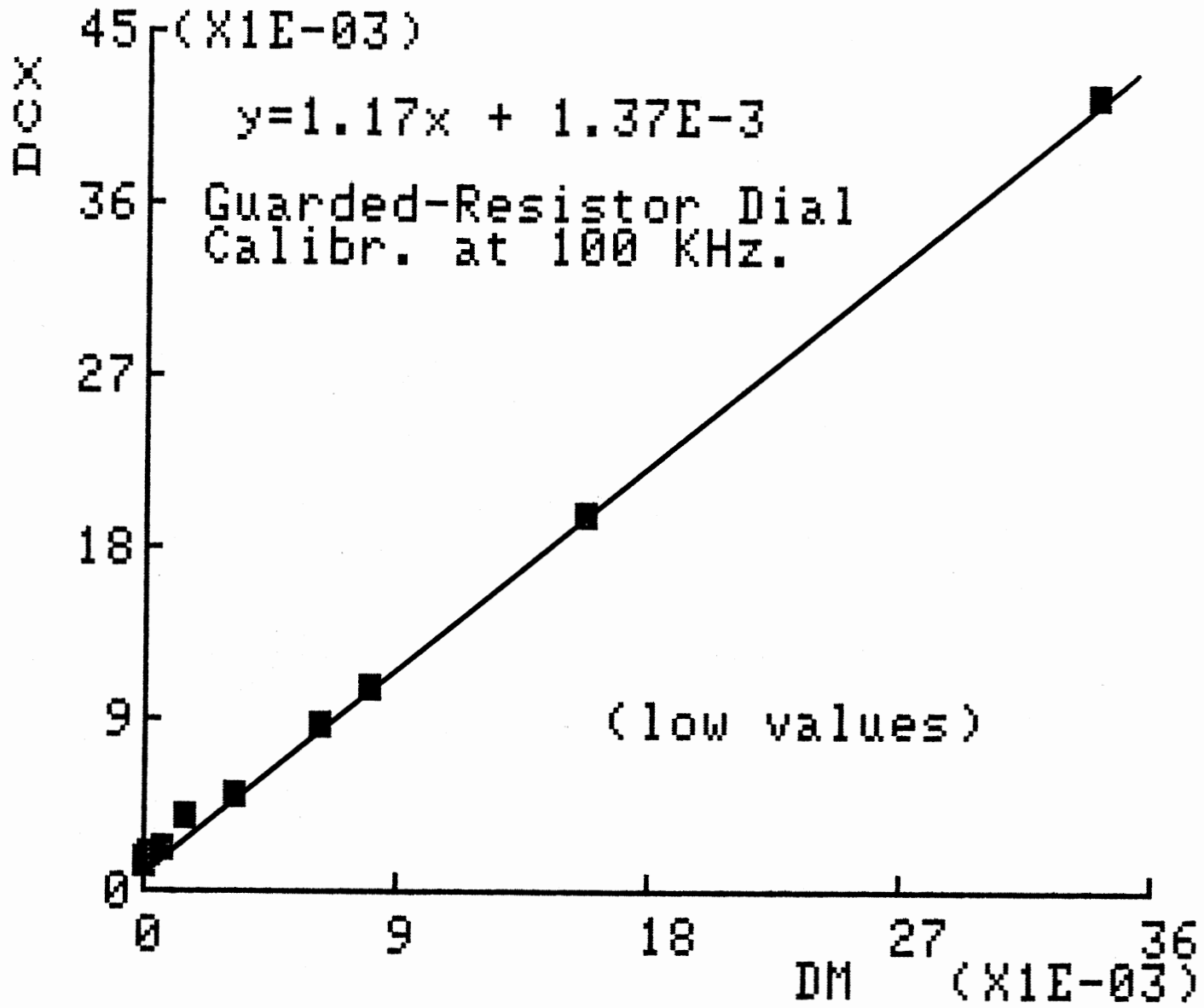
45 (X1E-03)
DCX
y=1.17x + 1.37E-3
36
Guarded-Resistor Dial
Calibr. at 100 KHz.
27
18
9
(low values)
0
0
9
18
27
36
DM (X1E-03)

Fig.(162)

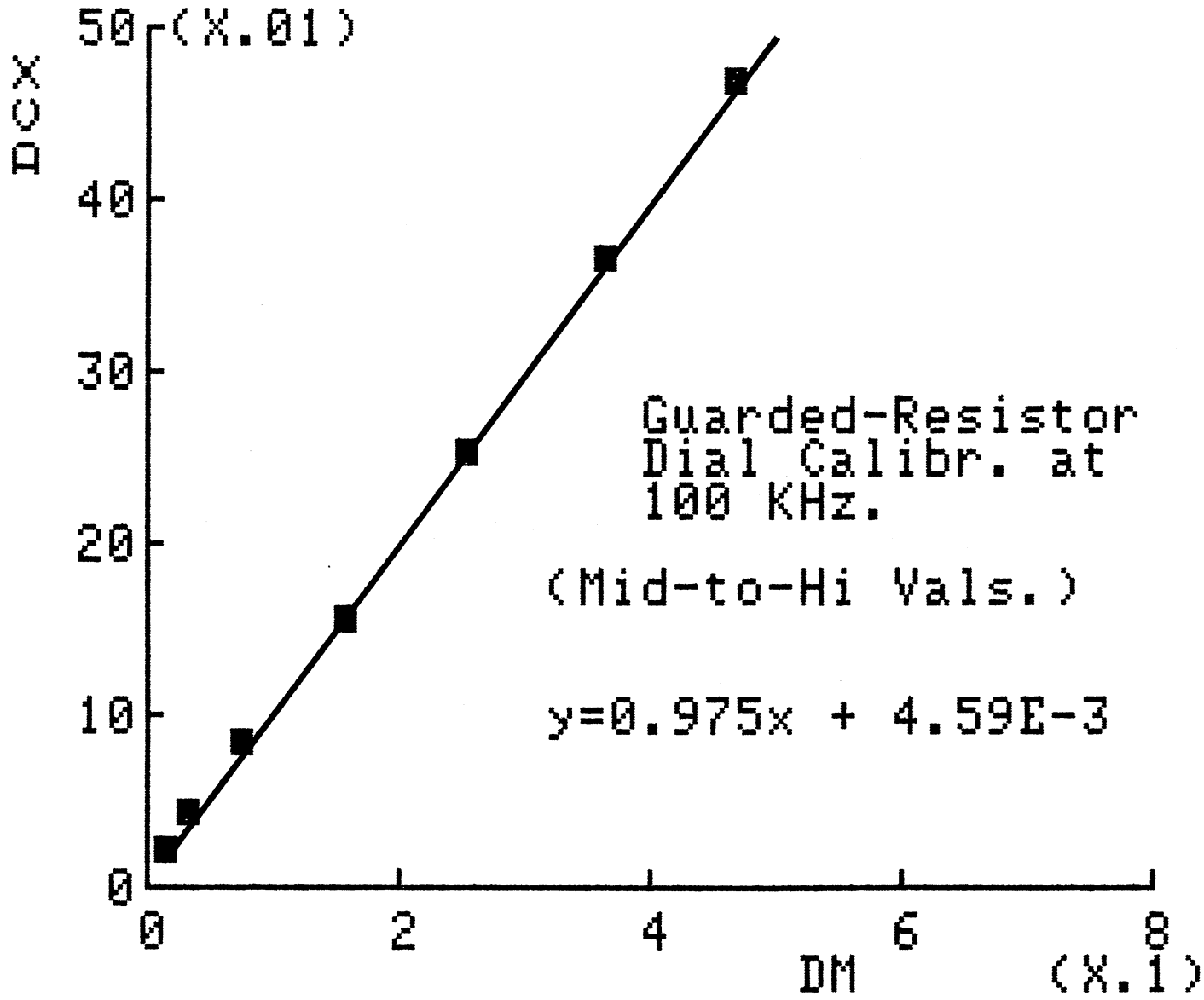
DCX
50 (X.01)
40
30
20
10
0
0
2
4
6
8
DM (X.1)
Guarded-Resistor
Dial Calibr. at
100 KHz.
(Mid-to-Hi Vals.)
y=0.975x + 4.59E-3

Fig. 6 (cont.)

```
5  PRINT  CHR$ (4)"PR#1": PRINT
    CHR$ (9)"15L": PRINT "DIAL
   CALIBR. FOR GUARDED SCHERING
    BRIDGE AT 500 HZ. BY N. A.
   HILAL": PRINT  CHR$ (4)"PR#0
   "
7  PRINT  CHR$ (4)"PR#1": PRINT
    CHR$ (9)"15L": PRINT "    D
   M          DCX          CPX
         %ERR D          %ERR C
         ": PRINT  CHR$ (4)"PR#
   0"
10  DIM C(25),D(25),R(25)
20  FOR I = 1 TO 14
30  READ C(I),D(I),R(I)
35 DF = 0.05 * (D(I) + 0.099)
40  IF DF > 0.01 THEN 180
50 CS = C(I)
60 DCX = DF
70 CPX = CS / (1 + (DF ^ 2))
75  GOTO 80
77 CPX = CS / (1 + (DCX ^ 2))
80 CT = 200.1
90 G = 1 / (6.29575 * R(I) * 5 *
   (10 ^  - 4))
95 DM = G / CT
110 CE = CPX - CT
130 ERRC = (CE / CT) * 100
150  PRINT  CHR$ (4)"PR#1": PRINT
    CHR$ (9)"14L": PRINT DM,DCX
   ,CPX,PCERD,ERRC: PRINT  CHR$
   (4)"PR#0"
160  NEXT I
170  GOTO 225
180 CS = C(I) * (1 - 0.026 * 5 *
   DF)
190  IF DF > 0.1 THEN 210
200  GOTO 60
210 DCX = DF * (1 - 0.026 * 5 *
   DF)
220  GOTO 77
225  DATA  201,-0.047,856.75,200
   .5,-0.018,454.54,201.4,0.067
   5,255.41
230  DATA  201.7,0.11,203.41,201
   .5,0.178,153,201.8,0.32,101

235  DATA  202,0.41,77.25,202.8,
   0.62,52,203.2,0.96,35.25
237  DATA  206.7,1.73,20.365,213
   .8,4,10.25,235,6.44,5.265
240  DATA  323.3,15.81,2.46,476,
   26.08,1.737
250  END
```

```
5  PRINT  CHR$ (4)"PR#1": PRINT
    CHR$ (9)"15L": PRINT "DIAL
   CALIBR. FOR GUARDED SCHERING
    BRIDGE AT 1 KHZ. BY N. A. H
   ILAL": PRINT  CHR$ (4)"PR#0"

7  PRINT  CHR$ (4)"PR#1": PRINT
    CHR$ (9)"15L": PRINT "    D
   M          DCX          CPX
         %ERR D          %ERR C
         ": PRINT  CHR$ (4)"PR#
   0"
10  DIM C(23),D(23),R(23)
20  FOR I = 1 TO 23
30  READ C(I),D(I),R(I)
35 DF = 0.01 * (D(I) + 0.15)
40  IF DF > .01 THEN 180
50 CS = C(I)
60 DCX = 0.01 * D(I)
70 CPX = CS / (1 + (DF ^ 2))
75  GOTO 80
77 CPX = CS / (1 + (DCX ^ 2))
80 CT = 200
90 G = 1 / (6.29575 * R(I) * (10
    ^  - 3))
95 DM = G / CT
110 CE = CPX - CT
130 ERRC = (CE / CT) * 100
150  PRINT  CHR$ (4)"PR#1": PRINT
    CHR$ (9)"14L": PRINT DM,DCX
   ,CPX,PCERD,ERRC: PRINT  CHR$
   (4)"PR#0"
160  NEXT I
170  GOTO 225
180 CS = C(I) * (1 - 0.026 * DF)

190  IF DF > 0.1 THEN 210
200  GOTO 60
210 DCX = 0.01 * D(I) * (1 - 0.0
   26 * DF)
220  GOTO 77
225  DATA  200.1,-.145,381.7,200
   .2,-.031,230.25,200.2,.11,17
   8.25
230  DATA  200.78,.25,153,200.8,
   .44,121.88,200.4,.54,101
235  DATA  201,.82,77.25,200.6,1
   .34,52,200.95,1.82,41.25
237  DATA  200.8,2.67,31.13,201.
   4,3.4,25,202.4,4.19,20.88
   = = = = = = = = = = = = =
247  DATA  235.6,40.54,1.922,260
   .35,54.05,1.472
250  END
```

The following program was used to obtain the results of the frequency-response measurements from the raw data at 1 KHz corresponding to the different polymers and their multiple "trial" samples. There are some 25 other similar programs corresponding to different frequencies, pressures, temperatures and electric fields.

```
5  PRINT  CHR$ (4)"PR#1": PRINT
     CHR$ (9)"80N": PRINT  CHR$
    (9)"17L": PRINT  CHR$ (9)"70
    R": PRINT "PARAMETERS EVALUA
    TION AT 1 KHZ. UNDER ROOM CO
    NDS. OF TEMP. AND PRESSURE B
    Y N.A.HILAL @ 1987 ": PRINT
     CHR$ (4)"PR#0"
7  PRINT  CHR$ (4)"PR#1": PRINT
     CHR$ (9)"17L": PRINT "
     K          DM         ACC
        KI          SG ": PRINT  CHR$
    (4)"PR#0"
10  DIM C(32),D(32),A(32),TH(32)
    ,CL(32),DL(32),G(32)
20  FOR I = 1 TO 12
25  READ C(I),D(I),A(I),TH(I),CL
    (I),DL(I),G(I)
30 CA = 8.854 * A(I) * 10 / (TH(
    I) * 2.54)
35 CV = 8.854 * (1.22718 - A(I))
     * 10 / (2.54 * TH(I))
45  IF D(I) > 1 THEN 125
50 CS = C(I)
60 DT = 0.8333 * 0.01 * D(I) + 0
    .00344
62 DLC = 0.8333 * 0.01 * DL(I) +
    0.00344
70  GOTO 80
75 DT = 1.0325 * DX + 1.08E - 3
80 CP = CS / (1 + (DT ^ 2))
90 CM = CP - CL(I) - CV + 0.81
100 K = CM / CA
105 PDC = CP * DT - DLC * CL(I)
107 DM = PDC / CM
110 GX = G(I) / (6283.2 * CA * (
    1E - 12))
114 KI = K * DM - GX
115 ACC = (8.854E - 12) * 6283.2
     * K * DM
117 SG = G(I) * TH(I) * 2.54E -
    3 / A(I)
120  GOTO 157
125 CS = C(I) * (1 - .026 * D(I)
     * .01)
130  IF D(I) > 10 THEN 150
135  IF D(I) < 2.5 THEN 60
140 DX = .01 * D(I)
145  GOTO 75
150 DX = D(I) * (1 - .026 * D(I)
     * .01) * .01
```

```
155  GOTO 75
157  PRINT  CHR$ (4)"PR#1": PRINT
     CHR$ (9)"17L": PRINT K,DM,A
    CC,KI,SG: PRINT  CHR$ (4)"PR
    #0"
170  NEXT I
200  DATA  209.7,7.71,0.9574,29,
    188.45,-0.011,2.6364E-8
205  DATA  248.7,23.85,0.9852,25
    ,191.4,0.015,1.61E-7
210  DATA  253.5,20.85,0.9852,25
    ,191.4,0.015,1.5E-7
215  DATA  249.4,25.67,1.0387,27
    ,191.4,0.015,1.8168E-7
217  DATA  249.8,22.75,0.940124,
    26.5,191.4,0.015,1.9133E-7
221  DATA  207.1,6.4,0.93314,24.
    5,188.5,0.02,1.35294E-8
225  DATA  202.7,5.85,0.87965,26
    .5,188.5,0.02,0.6949E-8
227  DATA  206,7.25,0.9244,26.8,
    188.5,0.02,1.3809E-8
228  DATA  211.5,8.35,0.8659,18.
    7,188.5,0.02,1.38095E-8
234  DATA  208.6,7.58,1.0207,40,
    188.5,0.02,6.12903E-8
235  DATA  210.8,8.0,0.9032,40,1
    88.5,0.02,6.94915E-8
240  DATA  213.1,10,0.97625,33,1
    88.5,0.02,8.86793E-8
250  DATA  199.2,0.28,1.0207,16.
    1,188.9,0.018,1.2882E-11
255  DATA  197.75,0.175,0.99353,
    18,188.4,-0.028,0.88747E-11
257  DATA  196,0.16,0.97625,22,1
    88.4,-0.028,0.65719E-11
260  DATA  200.3,0.41,0.95033,15
    .5,188.4,-0.028,1.15242E-11
265  DATA  199.8,0.34,0.95033,15
    .2,188.4,-0.028,0.77199E-11
270  DATA  201.4,0.49,0.95033,16
    ,188.4,-0.028,0.90909E-11
273  DATA  199.8,1.12,0.899204,1
    5.5,188.4,-0.028,0.32344E-10

275  DATA  202.7,1.78,0.899204,1
    6.75,188.4,-0.028,0.33670E-1
    0
280  DATA  312.4,33.55,0.914125,
    23,188.5,0.02,6.1290E-7
295  END
```

APPENDIX (B)

CORRECTIONS DUE TO IMPERFECT GEOMETRY OF THE SAMPLE

1) Case Of The Uniform Dielectric Slab That Does Not Fill The Whole Space Between The Plates

Consider a parallel plate capacitor of plate area A and plate separation "s", and let "b" denote the thickness of the uniform dielectric slab having a dielectric constant K, but which does not fill the whole space.

By choice: $b \leqslant s$, Fig.(164).

From elementary electrostatics we find the capacitance of the system to be:

$$C' = C/(1-\Delta/s).[1+\Delta\cdot K/b] \qquad B.1$$

where C is the capacitance when the dielectric material fills the whole space. If Co is the capacitance of the system in the absence of the dielectric (b = 0), then Co = C/K.

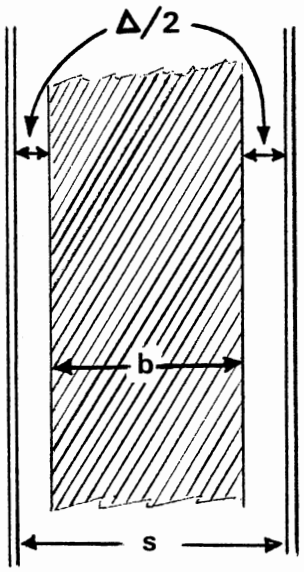

Fig.(164)

The experimental dielectric constant that is measured is C'/Co, we shall denote this by K', so that :

$$K' = K/(1-\Delta/s).[1+\Delta\cdot K/b] \qquad B.2$$

We shall introduce a new parameter **q** defined by $q = 1 - \Delta/s = b/s$, so that eq.(B.2) becomes:

$$K' = K/[\, q + K(1-q) \,] \qquad B.3$$

It is seen from the above expression that $K' \leqslant K$, since for any **q** we have: $q + (1-q) = 1$, hence $q + K.(1-q) \geqslant 1$, as K is $\geqslant 1$ always. For $K = 10$ and $q = 0.96$, $K' = 7.35$. Thus there is 25% error caused by only 2% gap on each side between the plates and the dielectric. Obviously the amount of error depends on the actual value of K. The correct value of the dielectric constant can be obtained if the proper value of **q** is known, by inverting eq.(B.3):

$$K = q\,K'/[\, 1 - K'(1-q) \,] \qquad B.4$$

Of course, the above description is a bit exaggerated for the sake of illustration. In a real situation the dielectric piece may look as shown in Fig.(165 a & b). These are called the central bulge and the wedge respectively, they have more complicated geometry, but the corrections can be obtained despite the lengthy algebra. This is done in part (2).

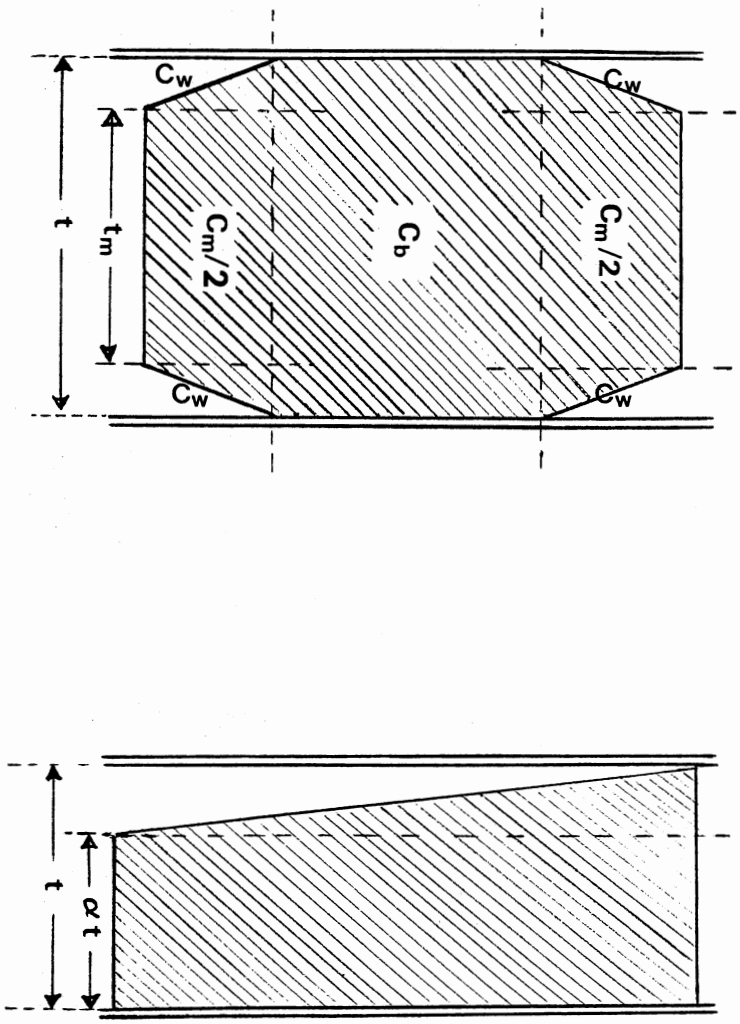

Fig.(165)

2) Case Of Non-Uniform Dielectric Geometry

Consider the situation shown in Fig.(165a), we shall use a series of approximations as follows:

The capacitor in Fig.(165a) can be thought of as a series and parrallel combinations of the individual capacitors shown by the dotted lines. Thus for example, the total capacitance C' may be written as:

$$C' = Cb + CwCm/(Cw+Cm) \qquad B.5$$

The only sub-section whose capacitance is not known is Cw. So we first need to calculate that:

If we divide the capacitor into thin slabs of thickness dx as shown in Fig.(165c), then we may write for a single slab:

$$Cx = (\epsilon_1 . A1 + \epsilon_2 . A2)/dx \qquad B.6$$

(law of parallel combinations)

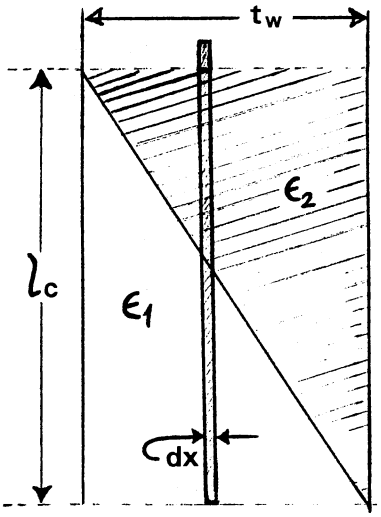

Fig.(165c)

The areas A1 & A2 are given by: $A1 = lc.(-ax + lc)$, $A2 = lc.(ax)$, where "-a" is the slope ($a = lc/t_w$), lc being the side length of the plate ($lc^2 = A$), and t_w is the plate separation. Also note that $A1 + A2 = lc^2 = A$ (as expexted).

Since 1/Cx is the infinitesimal quantity, we shall denote it by d(1/Cw), so that an integration over "x" from 0 to t_w will give us the inverse of the series equivalent combination of all the slabs, namely (1/Cw).

Thus we have:

$$1/Cw = \int_0^{t_w} \frac{dx}{alc(\epsilon_2 - \epsilon_1)x + \epsilon_1 lc^2}$$

From which : $Cw = alc[\epsilon_2 - \epsilon_1]/\log_e(\epsilon_2/\epsilon_1)$ B.7

Of importance to note, is the fact that eq.(B.7)is symmetric in ϵ_1 and ϵ_2, which is expected of course on physical grounds. The above expression also has the correct limit as $\epsilon_1 \longrightarrow \epsilon_2$.

This can be seen by setting $\epsilon_2 = \epsilon_1 + \delta$, then using the approximation: $\log_e(1 + x) \simeq x$ when $x << 1$.

In a typical situation the plate area belonging to the central portion Cb is about 40% of the total. Hence we shall take the areas corresponding to the various sub-sections to be as follows:

Ab = 0.4A , Aw = 0.3A (for each of the top and bottom portions), Am = 0.6A (for the top and bottom portions combined, corresponding to a total capacitance Cm). The various "plate separations" are similarly taken as follows:

tb = t , tm = α t , and 2.tw = (1 - α) t , where the value of α is to be determined on an individual basis for each particular case.

Consequently we find for the total capacitance, (setting $\epsilon_1 = \epsilon_o$, and $\epsilon_2 = \epsilon$ in eq.(B.7)):

$$C' = Cb + 0.6(\epsilon - \epsilon_o)(A/t)/[(1-\alpha)\log_e(K) + \alpha(K-1)/K] \quad B.8$$

where : $Cb = 0.4\epsilon(A/t)$ B.9

Again, the experimental value of the dielectric constant is $K' = C'/Co$ where $Co = \epsilon_o A/t$, so that the relationship between the experimentally measured "K" (namely K') and the real "K", is :

$$K' = 0.4K + 0.6(K-1)/[(1-\alpha)\log_e(K) + \alpha(K-1)/K \,] \qquad B.10$$

We note the following limiting cases: When $\alpha \longrightarrow 1$ (which corresponds to the case when the dielectric fills the whole space), then $K' \longrightarrow K$ (as required). When $K = 1$ (corresponding to no dielectric at all), then $K' \longrightarrow K = 1$. This may be seen by working out the proper limits, letting $K = 1 + x$ where x is a small number $\longrightarrow 0$, then using $\log_e(1+x) \simeq x$ and performing the appropriate cancellations before letting $x \longrightarrow 0$, etc...

In a typical situation, t is $\sim$ 27 mils, and t - 2.tw is $\sim$25.5 mils, which corresponds to $\alpha = 0.94$. Hence taking $K = 10$ again in eq.(B.10) we find :

$K' = 9.2$ which is 0.92 K $\Longrightarrow$ 8% relative error.

In general, the actual amount of error will depend on the value of K which is not known a priori. Hence it will be necessary to solve eq.(B.10) for K in terms of the measured quantity K'. As seen from the above an analytical solution is not feasible and a graphical procedure must be used. Thus by plotting the function K'(K) versus K over the range of K which is of interest, see Fig.(166), we can locate the proper value of K by drawing a horizontal line at the specific value of K' and determining the abcissa of the intersection point.

Finally, the "wedge" dielectric in Fig.(165b) is treated

similarly, by dividing it into a wedge and a rectangle,then working out the equivalent combination. The result is :

$$K' = (K-1)/[(1-\alpha)\log_e(K) + \alpha(K-1)/K \,] \qquad B.11$$

All previous comments remaining applicable.

In conclusion, we believe that the error in the measured dielectric constant could not have been more than 10% at the worst since in most cases α was practically unity (no more than 0.5 mil difference could be detected in a typical disc thickness of 30 mils ($\Longrightarrow \alpha = 0.98$). The handful of cases where α was 0.95 or lower were corrected for accordingly by using the graphical technique discussed above.

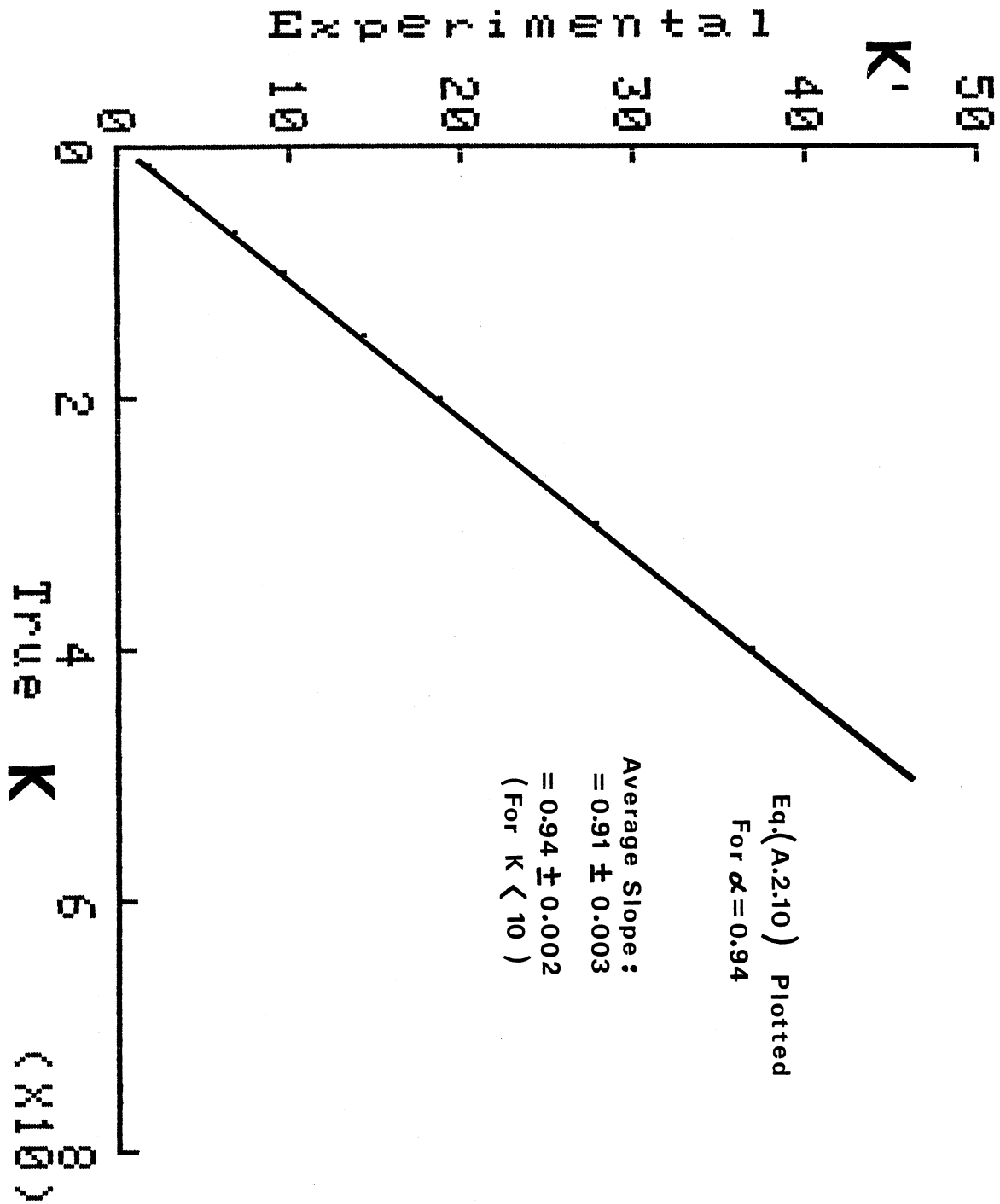
Experimental K
0
10
20
30
40
50
True K (x10)
0
2
4
6
8
Eq.(A.2.10) Plotted For α = 0.94
Average Slope : = 0.91 ± 0.003 = 0.94 ± 0.002 (For K < 10)

Fig.(166)

APPENDIX (C)

THEORETICAL BASIS OF THE ROSEN-POHL FORMULA FOR THE D.C. CONDUCTIVITY UNDER LARGE D.C. ELECTRIC FIELD

We have seen in sec.(1.3B) that the number density of thermally activated charge carriers available for D.C. conduction may be written as:

$$No = Ni.\exp(-Eg/2k_BT) \qquad C.1$$

where Ni is the intrinsic number density (which may be temperature dependent for some systems), and Eg can be thought of as an energy gap between the top of the "valence band" and the bottom of the "conduction band" in the sense discussed in sec.(1.3B).

When a D.C. electric field is switched on, the charge carriers will gain potential energy (if they are negative), and lose potential energy (if they are positive), see sec.(1.3C). In either case, this means that the effective energy gap that must be surmounted will be decreased by the amount of potential energy gained or lost. (Recall that "holes" act as free (positive) charge carriers in the valence band.)

For electrons or holes, we therefore have:

$$Eg \longrightarrow Eg - |e.\phi(x)| \qquad C.2$$

where : $\phi(x)$ is the potential energy function at position

site (x) where the charge carrier is, (refer to eq.(1.3..13)) and "e" is the charge of the carrier (negative or positive). Note also that $\phi(x)$ is positive for holes and negative for electrons over most of the range of "x", (refer to Fig.(10)).

Next we ask ourselves what is the most probable value for "x" ? The answer to this can be found as follows:
Since the electron is most likely to be found at the position of maximum potential energy (minimum P.E. for holes), then it is very legitimate to use the value of ϕ at the position of extremum, found by setting the derivative of eq.(1.3.13) equal to zero. We get:

$$Xo = - L'/(1 + Eh/E) \quad (\text{ for electrons }) \qquad C.3$$

where L' is given by eq.(1.3.11), and is identified as one-half the molecular length, which, we denote by Lo here. That is: $L' = Lo/2$. For holes, $Xo \longrightarrow + L'/(..)$ etc..

The value of $\phi(Xo)$ is therefore:

$$\phi(Xo) = EL'/(1 + Eh/E) + Eh.[\, L'/(1 + Eh/E) + L'.\log_e\{(Eh/E)/(1 + Eh/E)\}\,] \qquad C.4$$

For small electric fields << Eh , and for large electric fields >> Eh , eq.(C.4) yields the same limit namely:

$$\phi(Xo) \simeq EL' \quad (- EL' \text{ for holes }). \qquad C.5$$

Hence we are justified in taking the magnitude of the energy gap in the presence of the electric field to be :

$$Eg' = Eg - |e|.EL' \qquad C.6$$

Now let us go back to the expression in eq.(1.3.2):

$$N(w) = \frac{Z(w)}{\exp[(Eg-u)/k_BT] + 1}$$

where u is the Fermi level, and Eg is the activation energy. In the presence of a D.C electric field, the argument of the exponential term becomes (using eq.(C.6)):

$$((Eg - |e|.EL') - u)/k_BT$$

which, upon substituting u = Eg/2 , (refer to sec.(1.3.B)) becomes:

$$(Eg/2 - |e|.EL')/k_BT = (Eg/2 - |e|.ELo/2)/k_BT$$

So that effectively, the population of the energy levels is now given by:

$$N'(w) = \frac{Z(w)}{\exp[(Eg - |e|.ELo)/2k_BT] + 1} \qquad C.7$$

Next we must account for the fact that not all the polymer molecules are oriented parallel to the field. If we assume a random distribution (which is legitimate for long-chain molecules), then "Eg - |e|.ELo" in eq.(C.7) will have to be replaced by:

$$E(\theta) = Eg - e.ELo.\cos(\theta) \qquad C.8$$

where from now on "e" denotes the absolute value of the electronic charge, and "θ" takes on all values from 0 to $\pi/2$.

Finally we may assume that the number density for intrinsic

charge carriers is uniform (i.e. each polymer molecule contributes the same number of particles), this means that the contribution to the intrinsic number density of the carriers generated by those molecules within a solid angle $d\Omega$ is :

$$dNi = Ni.d\Omega \qquad C.9$$

Consequently, the number density for thermally, and field-activated charge carriers is:

$$Nc = \int_{\Omega} dNi.\exp(-E(\theta)/2k_BT) \qquad C.10$$

Upon performing the integration between the proper limits on θ , we obtain :

$$Nc = 2\pi Ni.\exp(-Eg/2k_BT) \int_0^{\pi/2} \exp[-eELo.\cos(\theta)/2k_BT]\sin(\theta).d\theta$$

or :

$$Nc = 2\pi No.[\ \exp(\eta_+) - 1\ ] / \eta_+ \qquad C.11$$

where $\eta_+ = eELo/2k_BT$. Eq.(C.11) was first determined emperically by Rosen & Pohl (1), but their derivation did not justify the use of eq.(C.6), the reason for which we presented our own side of the argument.

APPENDIX (D)

CALCULATION OF THE TRANSITION PROBABILITIES

Throughout this section all probabilities encountered are per unit time unless otherwise stated. For the sake of brevity the "per unit time" phrase is usually omitted unless there is reason for ambiguity.

Let us consider hopping between two states "A" and "B" separated by a potential barrier represented by an intermediate state "C" ,Fig.(167).

The probability per unit time of hopping from "A" to "B" via "C" as an intermediate stage is derived as follows:

The probability Pxy of hopping between two consecutive states "X" and "Y" is really the conditional probability that state "Y" gets occupied given that "X" is occupied; and we write it as P(Y|X). If P(X) and P(Y) are the probabilities of occupation of states "X" and "Y" then by its very definition: P(Y|X) = P(Y)/P(X) , that is: P(Y|X) is the probability of occupying "Y" per unit probability of occupying "X". It follows from the above reasoning that the probability

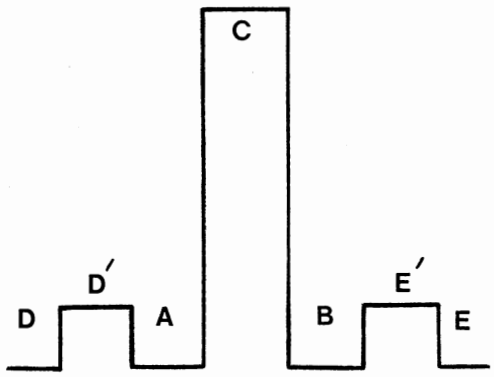

Fig.(167)

of jumping from "X" to "Y", PXY should be proportional to the factor $\exp[-(Wy-Wx)/k_BT]$, where Wx and Wy are the energies of the states involved in the transition. The above assumes implicitly that the energies are remote enough from the Fermi level to justify using the Maxwell-Boltzmann distribution in place of the Fermi-Dirac expression.

Now the probability of jumping from "A", namely Pa, is equal to:

Pa = PAC + PAD (since only nearest-neighbour hops are assumed). Similarly Pc = PCA + PCB. According to Mott & Davis (146), Px should be proportional to the phonon frequency and to a factor describing the degree of localization of the wave function around a given site. The reason being that for non-crystalline solids it is assumed that the hopping is thermally activated, phonon-induced, and that it is field-assisted in the sense that a D.C. electric field bias would give the electron a preferable direction to follow after it scatters by a phonon. Thus Pa should be given by:

$$Pa = \nu_{ph} \exp(-b_\alpha . R) \qquad D.1$$

where ν_{ph} is the phonon frequency (typically $\sim 10^{12}$ s^{-1}), and "b_α" is a parameter depending on the energy of the state:

$$b_\alpha = bo\alpha\ (Ec - Wa)^n \qquad D.2$$

Ec being the mobility edge (sec.(4.1)), and n is around 0.62
$bo\alpha$ is a parameter of the order of the inverse distance between scattering centers (sites).
Since by assumption, the electron states involved in hopping are deep-lying states below the mobility edge (Ea << Ec) then

it is not difficult to see that all the Pa's are approximately the same. In other words the energies Wa are far removed from both the Fermi-level as well as the mobility edge on the scale of k_BT. Typical density of states diagrams for amorphous semi-conductor materials (not necessarily polymers) might look something like the ones shown in Fig.(168).

We may write explicitly, (suppressing the k_BT factor):

$$Pa = ka(\exp[-(Uo-Wa)] + \exp[-(U1-Wa)]) \qquad D.3$$

$$Pc = kc(\exp[-(Wa-Uo)] + \exp[-(Wb-Uo)]) \qquad D.4$$

The normalization constants ka and kc are detrmined from the above pair of equations. Hence it follows that:

$$PAC = Pa.\exp(-Wa).\exp(-(Uo-Wa)/[\ \exp(-Uo) + \exp(-U1)\ ]$$

$$= Pa/[\ 1 + \exp(Uo-U1)\ ] \qquad D.5$$

$$\text{Similarly } PCB = Pc/[\ 1 + \exp(Wb-Wa)\ ] \qquad D.6$$

We leave it as an exercise in probability computing to show that the probability for the compounded process A —> C and C —> B is given by:

$$PAB = PAC.PCB/(PAC + PCB) \qquad D.7$$

From which we obtain:

$$PAB = Pa.Pc/\{\ Pa[1+\exp(Wb-Wa)] + Pc[1+\exp(Uo-U1)]\ \} \qquad D.8$$

In the absence of electric field, Wa = Wb, and so PAB = PBA as they should for reasons of symmetry. Further since Uo-U1 ≡ U is >> 1, then we may neglect "1" in comparison to the exponential term. Also we shall assume that Pa = Pc = P', also setting $(Wb-Wa)/k_BT = -eE.lg/k_BT \equiv -\eta'$ (where lg is the gap width separating two molecules, usually taken equal to "a_o")

Fig.(168) CAPTIONS

Four possible forms of the density of states $N(E)$ for amorphous semi-conductors, localized states are shown shaded. (After Le Comber & Mort (147), and Mott & Davis (137) p.211).

a) Overlapping band tails proposed by Cohen et al.(148). This is considered unlikely to apply for materials that are transparent in the visible and infra-red regions.

b) "Mobility Gap" in the region of the localized states created by non-overlapping bands for which the Fermi level lies around the center of the gap, (Fritzsche (149).

c) Introduction of impurity levels due to partially compensated dopants (as in chalcogenides glasses).

d) Same as "c" but with donor and acceptor levels (D & A) split, (Gubanov (150). This results in the pinning of the Fermi energy $\mathcal{E}_F$ at a fixed value over a wide temperature range, if the "D" & "A" bands partially overlap.
When the "D" & "A" bands are completely separate, the position of the Fermi energy does not have to be symmetrically located between the two bands, (Marshall & Owen (151)).

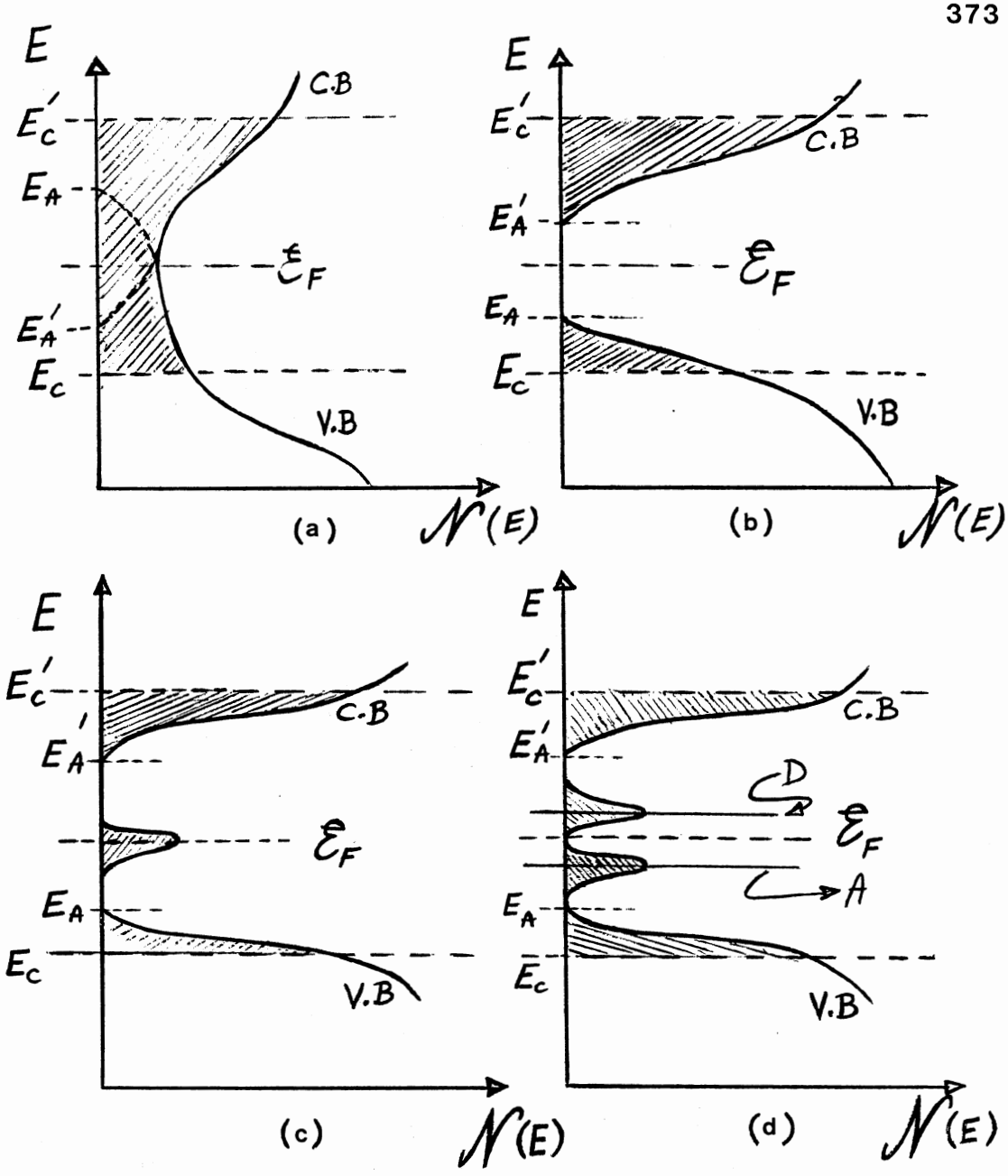
E
E'c
EA
εF
E'A
Ec
C.B
V.B
(a)
N(E)
E
E'c
C.B
E'A
εF
EA
Ec
V.B
(b)
N(E)
E
E'c
C.B
E'A
εF
EA
Ec
V.B
(c)
N(E)
E
E'c
C.B
E'A
D
εF
A
EA
Ec
V.B
(d)
N(E)

Fig. (168)

we finally get:

$$PAB = P'/[\ 1 + \exp(-\eta') + \exp(U/k_BT)\ ] \qquad D.9$$

Note that η' is positive for positive charge and negative for negative charge. Likewise, it follows that PBA is just what PAB would be for a charge of the opposite sign. Therefore :

$$PBA = P'/[\ 1 + \exp(\eta') + \exp(U/k_BT)\ ] \qquad D.10$$

In as much as $|\eta'| << U/k_BT$ for most electric field values (which is reasonable for electric fields below the voltage breakdown threshold), then it is easy to show that:

$$PBA = PAB.\exp(-\eta') \qquad D.11$$

Which says that it is more difficult to jump against the field than with the field. The expressions for PAD and PBE are calculated in a similar fashion:

$$PAD = P'/[\ 1 + \exp(\eta') + \exp(-U/k_BT\ ] = PBE.\exp(-\eta') \qquad D.12$$

Also of interest are the "cross" relations linking PAB to PBE and PBA to PAD, we find (using the assumption $|\eta'| << U/k_BT$):

$$PBE = PAB.\{\ 1 + \exp(U/k_BT)/[\ \exp(-\eta') + 1]\ \}$$
$$= PAB.\exp(U/k_BT)/[\ \exp(-\eta') + 1\ ] \qquad D.13$$

While :

$$PAD = PBA.\{\ 1 + \exp(U/k_BT)/[\ \exp(\eta') + 1]\ \}$$
$$= PBA.\exp(U/k_BT)/[\ \exp(\eta') + 1\ ] \qquad D.14$$

The above expressions can be further simplified under varied conditions such as: $1 << \eta' << U/k_BT$, and $\eta' << 1 << U/k_BT$ etc. These possibilities are explored in the text in chap.(4).

VITA

Nabil Amin-Peter Hilal

Candidate for the Degree

of

Doctor of Philosophy

Thesis: ELECTRONIC TRANSPORT PROCESSES IN SOME HIGHLY INSULATING AND SEMI-CONDUCTING POLYMERS

Major Field: Physics

Biographical:

Personal Data: Born in Aleppo, Syria, the son of Amin Peter Hilal and Nuha Milhem Shabshab (Lebanese).

Education: Bachelor of Science in Physics, from The American University of Beirut, Lebanon, 1970. Master of Science in Low-Temperature Physics, from The American University of Beirut, Lebanon, 1973. Completed the requirements for the degree of Doctor of Philosophy at Oklahoma State University, Stillwater, Oklahoma, May, 1988.

Professional Experience: Senior Physics Lab. Instructor, Amer. Univ. of Beirut, Beirut, Lebanon, 1971-75. Lecturer in Quantum Mechanics and Special Theory of Relativity, The Lebanese University at Mansourieh College of Science, Lebanon, 1976. Adjunct Lecturer in Physics, Mathematics and Astronomy at Queens College and Hunter College of the City University of New York, 1977-1980. Research Associate and Physics Lab. instructor at Oklahoma State University, Stillwater, 1981-1987.

Honors and Other Achievements: Prize winner of several world contests in color photography (1968, 1971). World renowned musicologist and expert record collector (one of the World's largest and rarest personal collections). Expert philatelist of unsurpassed caliber and knowledge. Honors in Jazz percusssion ensembles, member Oklahoma State University Marching Band & Concert Band (1982-83).